

UC San Diego

UC San Diego Electronic Theses and Dissertations

Title

Investigations into novel modes of reactivity and stereoselectivity for the cycloaromatization of conjugated enediynes and dienynes

Permalink

<https://escholarship.org/uc/item/14v6v6gz>

Author

Hitt, David M.

Publication Date

2011

Peer reviewed|Thesis/dissertation

UNIVERSITY OF CALIFORNIA, SAN DIEGO

Investigations into Novel Modes of Reactivity and Stereoselectivity for the Cycloaromatization of
Conjugated Enediynes and Dienynes

A dissertation submitted in partial satisfaction of the requirements for the degree of Doctor of
Philosophy

in

Chemistry

by

David M. Hitt

Committees in charge:

Professor Joseph M. O'Connor, Chair
Professor William H. Gerwick
Professor Arnold L. Rheingold
Professor Emmanuel A. Theodorakis
Professor Jerry Yang

2011

Copyright

David M. Hitt, 2011

All rights reserved.

The Dissertation of David M. Hitt is approved, and it is acceptable in quality and form for publication on microfilm and electronically:

Chair

University of California, San Diego

2011

DEDICATION

To my fiancée and family.

TABLE OF CONTENTS

| | |
|---|-------|
| Signature Page..... | iii |
| Dedication..... | iv |
| Table of Contents..... | v |
| List of Schemes..... | ix |
| List of Figures..... | xv |
| List of Tables..... | xxi |
| List of Abbreviations..... | xxiii |
| Acknowledgments..... | xxvi |
| Curriculum Vitae..... | xxvii |
| Abstract of Dissertation..... | xxx |
| CHAPTER 1: Methods of Acceleration for Conjugated Dienyne Cycloaromatization..... | 1 |
| I. Introduction..... | 2 |
| II. Photolytic Triggering..... | 5 |
| III. Alkyne – Allene Isomerization Induced..... | 11 |
| IV. Nucleophilic Attack of Alkyne..... | 15 |
| V. Umpolung Activation of Alkyne..... | 20 |
| VI. Metal Vinylidene Triggered..... | 38 |
| VII. η^6 -Coordination of π System..... | 47 |
| VIII. Metal Carbene Induced..... | 50 |
| IX. Conclusions and Future Outlook..... | 52 |
| X. References..... | 54 |
| XI. Acknowledgements..... | 58 |
| CHAPTER 2: Dienyne Cycloaromatization Triggered by Ruthenium C-H Bond Activation | 59 |

| | |
|--|-----|
| I. Introduction..... | 60 |
| II. Initial Observation and Optimization..... | 63 |
| III. Structure of Transient Complexes..... | 69 |
| IV. Attempts to Increase Catalytic Activity of System..... | 73 |
| V. Mechanistic Studies and Discussion..... | 76 |
| VI. Conclusions and Future Outlook..... | 86 |
| VII. Experimental..... | 87 |
| i. General Procedures..... | 87 |
| ii. Materials..... | 87 |
| iii. Instrumentation..... | 88 |
| iv. Preparation and characterization data for dienyne substrates and synthetic intermediates..... | 88 |
| v. Preparation and characterization data for cycloaromatized products. | 96 |
| vi. Procedures for VT, kinetic, and exploratory experiments..... | 101 |
| vii. ¹ H and ¹³ C NMR spectra for unknown compounds..... | 107 |
| VIII. References..... | 139 |
| IX. Acknowledgments..... | 141 |
| CHAPTER 3: Stereoselective η^6 -Arene Complexation during Ruthenium Mediated | |
| Dienyne and Eneidyne Cycloaromatization Reactions..... | |
| I. Introduction..... | 142 |
| II. Dienyne Stereoselectivity: Discovery and Substrate Scope..... | 143 |
| III. Solid State Structure Determination of the η^6 -Arene Products..... | 156 |
| IV. Eneidyne Stereoselectivity: Discovery and Substrate Scope..... | 159 |
| V. Stereoselective 5- <i>exo-trig</i> cyclization..... | 159 |
| VI. Arene Binding Experiments..... | 163 |
| | 167 |

| | |
|--|-----|
| VII. Models for Stereoselectivity..... | 170 |
| VIII. Conclusions and Future Outlook..... | 177 |
| IX. Experimental..... | 178 |
| i. General Procedures..... | 178 |
| ii. Materials..... | 179 |
| iii. Instrumentation..... | 179 |
| iv. Preparation and characterization data for synthetic intermediates, dienyne, enediyne, and arene substrates..... | 180 |
| v. Procedures for NMR scale reactions..... | 195 |
| vi. Preparation and characterization data for Ru-arene complexes..... | 197 |
| vii. ¹ H and ¹³ C NMR spectra for characterized compounds..... | 205 |
| viii. X-ray crystallographic summary and ORTEPS for characterized structures..... | 272 |
| X. References..... | 287 |
| XI. Acknowledgments..... | 290 |
| CHAPTER 4: A Novel Route of Cycloaromatization for Conjugated Ene-diyne..... | 291 |
| I. Introduction..... | 292 |
| II. Results..... | 293 |
| III. Discussion..... | 299 |
| IV. Conclusions and Future Outlook..... | 303 |
| V. Experimental..... | 304 |
| i. General Procedures..... | 304 |
| ii. Materials..... | 304 |
| iii. Instrumentation..... | 305 |
| iv. Preparation and characterization data for synthetic intermediates and enediyne substrates..... | 305 |

| | |
|--|-----|
| v. Procedures for NMR scale reactions..... | 307 |
| vi. Preparation and characterization data for cycloaromatized products..... | 308 |
| vii. ¹ H and ¹³ C NMR spectra for unknown compounds..... | 310 |
| viii. X-ray crystallographic summary and ORTEPS for characterized structures..... | 321 |
| VI. References..... | 325 |
| VII. Acknowledgements..... | 326 |

LIST OF SCHEMES

| | |
|--|----|
| Scheme 1-1. Intermediates believed to be involved in the thermal cycloaromatization of dienyne..... | 2 |
| Scheme 1-2. General mechanism for a thermal dienyne [1,7]-hydrogen shift / cycloaromatization..... | 3 |
| Scheme 1-3. Retrosynthesis of aromatic products deriving from dienyne..... | 4 |
| Scheme 1-4. Mechanistic pathways of conversion for photolytically generated cyclic allene 10 | 7 |
| Scheme 1-5. High yielding photocycloaromatization of 2,4-substituted phenanthrene 19 from readily available 2-naphthylcarboxaldehyde 21 | 11 |
| Scheme 1-6. General mechanism for dienyne cycloaromatization through base-catalyzed allene formation..... | 11 |
| Scheme 1-7. Allene isomerization for the formation of a naphthylidiphenylmethyl radical. | 12 |
| Scheme 1-8. Deuterium labeling supports a competition between concerted and base-assisted conversion of <i>o</i> -quinodimethane 23 | 13 |
| Scheme 1-9. Use of propargyl sulfides for ambient temperature cycloaromatization... | 14 |
| Scheme 1-10. 6π Electrocyclization from a 1,3-stannane shift..... | 14 |
| Scheme 1-11. Base-induced cycloaromatization of Freelingyne (35) proceeding through allene intermediate..... | 15 |
| Scheme 1-12. Use of vinyl triflate dienyne to trigger cycloaromatization via nucleophilic attack of the alkyne..... | 16 |
| Scheme 1-13. Improved cyclization yields by use of strained cyclic dienyne..... | 17 |
| Scheme 1-14. Activation of dienynyl ketones under Lewis acidic conditions..... | 18 |
| Scheme 1-15. Proposed intramolecular bond rearrangements for the formation of 46 – 49 | 19 |
| Scheme 1-16. General mechanism for umpolung activation of alkyne..... | 20 |

| | |
|--|----|
| Scheme 1-17. In-situ generation of dienyne resulting in cycloaromatized product..... | 21 |
| Scheme 1-18. Metal catalyzed cycloaromatization of dienynes possessing nucleophilic terminal alkene components..... | 22 |
| Scheme 1-19. Ambient temperature gold catalyzed cycloaromatization of geminal and tri-substituted terminal alkene Type II-internal dienynes..... | 23 |
| Scheme 1-20. Complementary methods for synthesis of stereoisomeric pairs of biaryl complexes..... | 24 |
| Scheme 1-21. Acid catalyzed tautomeric dienyne 71-A cycloaromatization..... | 25 |
| Scheme 1-22. TFA and I(py) ₂ BF ₄ triggered cycloaromatizations in the formation of extended polyaromatic platforms..... | 26 |
| Scheme 1-23. Expanded alkyne substituent scope via use of ICl as the cyclization triggering reagent..... | 27 |
| Scheme 1-24. Photolytic activation of cycloaromatization with iodine electrophilic triggering..... | 28 |
| Scheme 1-25. Use of iron catalysis for dienyne cycloaromatization..... | 31 |
| Scheme 1-26. One pot 6- <i>endo</i> cycloaromatization / Heck coupling..... | 32 |
| Scheme 1-27. Capture of activated alkyne by tethered nucleophile coupled with Heck coupling to give cycloaromatized product..... | 33 |
| Scheme 1-28. Intermolecular capture of coordinated alkyne leading to aromatized product..... | 34 |
| Scheme 1-29. Gold catalyzed cycloaromatization of the <i>Z,Z</i> -dienyne 98 | 35 |
| Scheme 1-30. [1,7]-H shift facilitated by η^2 -complexation..... | 36 |
| Scheme 1-31. Formal [1,7]-H shift cycloaromatization pathway catalyzed by base..... | 37 |
| Scheme 1-32. General mechanism of dienyne cycloaromatization involving a metal vinylidene intermediate..... | 39 |
| Scheme 1-33. First example of metal vinylidene dienyne cycloaromatization..... | 40 |

| | |
|--|----|
| Scheme 1-34. Applications of metal vinylidene dienyne cycloaromatizations..... | 41 |
| Scheme 1-35. Vinylidene cycloaromatizations resulting in 1,2-shift of non-hydrogen substituents..... | 42 |
| Scheme 1-36. Isotopic labeling experiments probing mechanism of [TpRu(PPh ₃)(NCMe) ₂]PF ₆ (123) catalyzed cycloaromatization / formal 1,2-substituent shifts..... | 43 |
| Scheme 1-37. Proposed mechanistic pathways for formation of the 1,2-halide and aryl shift products..... | 44 |
| Scheme 1-38. Dependence of electronic nature of alkene of reaction pathway..... | 45 |
| Scheme 1-39. Changing reactivity of alkylidenyl substituted dienynes as the carbon tether size increases..... | 45 |
| Scheme 1-40. Proposed mechanism for 1,3-methylene migration. | 46 |
| Scheme 1-41. NMR observation of transient species in [Cp* <i>Ru</i> (NCMe) ₃]PF ₆ (142) triggered cycloaromatization of 1-chlorodienynes..... | 48 |
| Scheme 1-42. X-ray characterization of η^6 -dienyne..... | 49 |
| Scheme 1-43. Reaction of a metal carbene with the dienynyl alkyne resulting in an overall cycloaromatization..... | 51 |
| Scheme 1-44. Use of pendent Fischer carbenes for metathesis cycloaromatization.... | 52 |
| Scheme 2-1. The Hopf cycloaromatization..... | 60 |
| Scheme 2-2. Triggering the formal Hopf cycloaromatization with [Cp* <i>Ru</i> (NCMe) ₃]PF ₆ 3 | 61 |
| Scheme 2-3. Cycloaromatization resulting from allylic alkyl addition to internal alkyne carbon..... | 62 |
| Scheme 2-4. Metal catalyzed cycloaromatization via [1,7]-H shift..... | 62 |
| Scheme 2-5. Acid catalyzed cycloaromatization of <i>in situ</i> generated dienyne 12 | 63 |
| Scheme 2-6. Synthesis of dienynes with varying alkyne substitution..... | 63 |

| | |
|--|-----|
| Scheme 2-7. Synthesis of 15-TMS-Z enriched sample..... | 66 |
| Scheme 2-8. Synthetic route to geometrically pure 15-TMS-E | 68 |
| Scheme 2-9. Additional experiments designed to produce a metal catalyzed cycloaromatization..... | 75 |
| Scheme 2-10. Proposed metal hydride C-H activation mechanism..... | 82 |
| Scheme 2-11. Proposed mechanism for conversion of the observable transient complexes, I and II to aromatized products..... | 83 |
| Scheme 2-12. Possible thermodynamic explanation for hydrogen shuttling from VIII-η^4 to II | 84 |
| Scheme 2-13. Intramolecular competition study showing selective CH activation of the <i>cis</i> - allylic methyl with [CpRu(NCMe) ₃]PF ₆ (25)..... | 85 |
| Scheme 2-14. π - σ - π isomerization..... | 85 |
| Scheme 3-1. Use of cationic CpRu-arene complexes in the synthesis of core structure of peptidomacrocyclic antibiotics..... | 144 |
| Scheme 3-2. Stereoselective alkylation via benzylic deprotonation of a CpRu-arene... | 145 |
| Scheme 3-3. Ruthenium triggered Hopf cycloaromatization..... | 147 |
| Scheme 3-4. Proposed intermediates for the ruthenium triggered Bergman cyclization. | 148 |
| Scheme 3-5. Alternative intermediates not involving coordination of the central alkene. | 149 |
| Scheme 3-6. Potential chiral relay system for a hydroboration / oxidation sequence created upon prior stereoselective binding of Cp* Ru ⁺ induced by chiral substituent R*..... | 150 |
| Scheme 3-7. Stereoselective CpRu η^6 -complexation of chiral arene..... | 151 |
| Scheme 3-8. Accepted mechanism of the Dötz reaction..... | 152 |
| Scheme 3-9. Incorporation of alkyne stereocenter as secondary propargylic ethers for facially selective benzannulation..... | 153 |

| | |
|--|-----|
| Scheme 3-10. Stereoselectivity by facial steric differentiation of a rigid bicyclic substrate..... | 154 |
| Scheme 3-11. Chiral auxiliary approach to stereoselective η^6 -complexation..... | 154 |
| Scheme 3-12. Diastereoselective formation of an η^6 -bound naphthalenophane complex..... | 155 |
| Scheme 3-13. Synthetic route to dienynes 39 and 40 | 156 |
| Scheme 3-14. Initial observation of stereoselectivity for the dienyne cycloaromatization reaction..... | 157 |
| Scheme 3-15. Probing the effect of the metal-ligand environment on the stereoselectivity..... | 158 |
| Scheme 3-16. Synthetic route to model enediyne substrates for initial studies..... | 160 |
| Scheme 3-17. Initial studies on enediyne cycloaromatization stereoselectivity..... | 161 |
| Scheme 3-18. Probing the effect of alkyne substitution on the stereoselectivity..... | 162 |
| Scheme 3-19. Probing the effect of the metal-ligand environment on the stereoselectivity..... | 163 |
| Scheme 3-20. Capture of the <i>p</i> -benzyne radical by 5- <i>exo-trig</i> cyclization..... | 164 |
| Scheme 3-21. Proposed method of stereocontrol for 5- <i>exo</i> capture of the <i>p</i> -benzyne radical..... | 165 |
| Scheme 3-22. Synthetic route to enediyne substrate 64 with tethered alkene..... | 166 |
| Scheme 3-23. Demonstration of Cp* <i>Ru</i> mediated enediyne cycloaromatization in combination with a 5- <i>exo</i> radical cyclization..... | 167 |
| Scheme 3-24. Basic mechanistic scenarios for formation of the ruthenium arene complex..... | 168 |
| Scheme 3-25. Proposed pathways for conversion of diastereomeric η^4 -diyne complexes involving η^6 -enediyne intermediates..... | 171 |

| | |
|---|-----|
| Scheme 3-26. Proposed models of stereoselectivity based on equilibrium effects of the η^4 -diyne intermediate..... | 173 |
| Scheme 3-27. Proposed model of stereoselectivity based on a post rate-limiting step equilibrium between the two diastereomeric η^6 -enediyne intermediates..... | 175 |
| Scheme 3-28. η^4 -Diene stereochemical model..... | 176 |
| Scheme 3-29. η^6 -Dienyne stereochemical model..... | 177 |
| Scheme 4-1. Thermal cycloaromatization of conjugated enediyne 1 to atom abstraction products 2 through intermediacy of <i>para</i> -benzyne 3 | 292 |
| Scheme 4-2. Novel enediyne cycloaromatization pathway of 4 to 5-chloro-8-ethyl-tetraline 5 | 293 |
| Scheme 4-3. Synthetic route and ORTEP of model enediyne 4 | 294 |
| Scheme 4-4. Expected and unexpected cycloaromatization of enediyne 4 | 295 |
| Scheme 4-5. Absolute structure determination of 5 through formation of crystalline Cp*Ru-arene complex 9 | 295 |
| Scheme 4-6. HCl promoted cycloaromatization of 4 and possible observation of addition product 12 | 298 |
| Scheme 4-7. ^{13}C labeling experiment demonstrating bond formation between the propargylic and internal alkyne carbon atoms..... | 299 |
| Scheme 4-8. Proposed mechanism for thermal cycloaromatization of enediyne 4 in CDCl_3 | 300 |
| Scheme 4-9. Enediyne cycloaromatization resulting from double HCl addition..... | 301 |
| Scheme 4-10. Dienyne cycloaromatization triggered by [1,7]-H shift..... | 301 |
| Scheme 4-11. Intimate ion-pair rationalization for preference of kinetic <i>syn</i> addition product formation..... | 302 |

LIST OF FIGURES

| | |
|---|-----|
| Figure 1-1. Classification of dienyne substrates..... | 5 |
| Figure 1-2. Pictorial representation of fluorescent linear single state 16-S_Q and non-fluorescent <i>trans</i> -stilbene “like” singlet state 16-S_{tS} | 10 |
| Figure 2-1. HSQC / HMBC correlations and proposed structure for II | 71 |
| Figure 2-2. Possible structures for I and comparison with analogous known compounds..... | 72 |
| Figure 2-3. Possible structures for III | 73 |
| Figure 2-4. Dienyne substrates used for Liu’s metal-catalyzed dienyne cyclization.... | 76 |
| Figure 2-5. Plots for the formation of II vs. time and regression trend lines for the reaction of 15-TMS and 3 | 79 |
| Figure 2-6. Comparison of X-ray characterized enediyne and dienyne Cp*RuL _n complexes to possible intermediate structures for a [1,7]-H shift..... | 81 |
| Figure 2-7. 14-Me ¹ H NMR spectrum (500 MHz, CDCl ₃)..... | 108 |
| Figure 2-8. 14-Me ¹³ C NMR spectrum (100 MHz, CDCl ₃)..... | 109 |
| Figure 2-9. 15-Me (75:25 <i>E</i> / <i>Z</i>) ¹ H NMR spectrum (400 MHz, CDCl ₃)..... | 110 |
| Figure 2-10. 15-Me (75:25 <i>E</i> / <i>Z</i>) ¹³ C NMR spectrum (100 MHz, CDCl ₃)..... | 111 |
| Figure 2-11. 15-Pr (6:4 <i>E</i> / <i>Z</i>) ¹ H NMR spectrum (400 MHz, CDCl ₃)..... | 112 |
| Figure 2-12. 15-Pr (6:4 <i>E</i> / <i>Z</i>) ¹³ C NMR spectrum (100 MHz, CDCl ₃)..... | 113 |
| Figure 2-13. 15-TMS (92:8 <i>Z</i> / <i>E</i>) ¹ H NMR spectrum (500 MHz, CDCl ₃)..... | 114 |
| Figure 2-14. 15-TMS (92:8 <i>Z</i> / <i>E</i>) ¹³ C NMR spectrum (100 MHz, CDCl ₃)..... | 115 |
| Figure 2-15. 15-TMS-E ¹ H NMR spectrum (400 MHz, CDCl ₃)..... | 116 |
| Figure 2-16. 15-TMS-E ¹³ C NMR spectrum (100 MHz, CDCl ₃)..... | 117 |
| Figure 2-17. 86:14 16-Me / 17-Me ¹ H NMR spectrum (500 MHz, CDCl ₃)..... | 118 |
| Figure 2-18. 86:14 16-Me / 17-Me ¹³ C NMR spectrum (125 MHz, CDCl ₃)..... | 119 |
| Figure 2-19. 69:31 16-Pr / 17-Pr ¹ H NMR spectrum (500 MHz, CDCl ₃)..... | 120 |

| | |
|--|-----|
| Figure 2-20. 69:31 16-Pr / 17-Pr ¹³ C NMR spectrum (125 MHz, CDCl ₃)..... | 121 |
| Figure 2-21. 17-TMS ¹ H NMR spectrum (400 MHz, CDCl ₃)..... | 122 |
| Figure 2-22. 17-TMS ¹³ C NMR spectrum (100 MHz, CDCl ₃)..... | 123 |
| Figure 2-23. 18-TMS ¹ H NMR spectrum (300 MHz, CDCl ₃)..... | 124 |
| Figure 2-24. 18-TMS ¹³ C NMR spectrum (100 MHz, CDCl ₃)..... | 125 |
| Figure 2-25. 89:7:2:2 19 / 39 / 40 / 14-Me ¹ H NMR spectrum (500 MHz, CDCl ₃)..... | 126 |
| Figure 2-26. 89:7:2:2 19 / 39 / 40 / 14-Me ¹³ C NMR spectrum (125 MHz, CDCl ₃)..... | 127 |
| Figure 2-27. 20 ¹ H NMR spectrum (400 MHz, CDCl ₃)..... | 128 |
| Figure 2-28. 20 ¹³ C NMR spectrum (100 MHz, CDCl ₃)..... | 129 |
| Figure 2-29. 26 ¹ H NMR spectrum (500 MHz, CDCl ₃)..... | 130 |
| Figure 2-30. 26 ¹³ C NMR spectrum (100 MHz, CDCl ₃)..... | 131 |
| Figure 2-31. 41 ¹ H NMR spectrum (400 MHz, CDCl ₃)..... | 132 |
| Figure 2-32. 41 ¹³ C NMR spectrum (100 MHz, CDCl ₃)..... | 133 |
| Figure 2-33. I / II ¹ H NMR spectrum (400 MHz, CDCl ₃)..... | 134 |
| Figure 2-34. II ¹³ C NMR spectrum (100 MHz, CDCl ₃)..... | 135 |
| Figure 2-35. III ¹ H NMR spectrum (400 MHz, CDCl ₃)..... | 136 |
| Figure 2-36. II HSQC spectrum (500 MHz, CDCl ₃)..... | 137 |
| Figure 2-37. II HMBC spectrum (500 MHz, CDCl ₃)..... | 138 |
| Figure 3-1. Comparison of the two stereochemical assignment conventions for planar chiral metal η^6 -arene complexes..... | 146 |
| Figure 3-2. Conserved relative stereochemistry for the major and minor diastereomers from the metal-triggered dienyne cyclization reactions..... | 159 |
| Figure 3-3. X-ray determined stereochemical assignments for 57-ma / 57-mi and inferred assignments for 56-ma / 56-mi | 162 |
| Figure 3-4. Eneidyne structural changes induced by η^4 -coordination of the alkynes... | 174 |
| Figure 3-5. 75 ¹ H NMR spectrum (500 MHz, CDCl ₃)..... | 206 |

| | |
|--|-----|
| Figure 3-6. 75 ¹³ C NMR spectrum (100 MHz, CDCl ₃)..... | 207 |
| Figure 3-7. 39 ¹ H NMR spectrum (400 MHz, CDCl ₃)..... | 208 |
| Figure 3-8. 39 ¹³ C NMR spectrum (100 MHz, CDCl ₃)..... | 209 |
| Figure 3-9. 40 ¹ H NMR spectrum (400 MHz, CDCl ₃)..... | 210 |
| Figure 3-10. 40 ¹³ C NMR spectrum (100 MHz, CDCl ₃)..... | 211 |
| Figure 3-11. 42 ¹ H NMR spectrum (400 MHz, CDCl ₃)..... | 212 |
| Figure 3-12. 42 ¹³ C NMR spectrum (75 MHz, CDCl ₃)..... | 213 |
| Figure 3-13. 42-ma ¹ H NMR spectrum (300 MHz, CDCl ₃)..... | 214 |
| Figure 3-14. 42-mi ¹ H NMR spectrum (400 MHz, CDCl ₃)..... | 215 |
| Figure 3-15. 42-mi ¹³ C NMR spectrum (100 MHz, CDCl ₃)..... | 216 |
| Figure 3-16. 43 ¹ H NMR spectrum (400 MHz, CDCl ₃)..... | 217 |
| Figure 3-17. 43 ¹³ C NMR spectrum (75 MHz, CDCl ₃)..... | 218 |
| Figure 3-18. 48-ma ¹ H NMR spectrum (400 MHz, CDCl ₃)..... | 219 |
| Figure 3-19. 48-ma ¹³ C NMR spectrum (100 MHz, CDCl ₃)..... | 220 |
| Figure 3-20. 48-mi ¹ H NMR spectrum (CDCl ₃ , 400MHz)..... | 221 |
| Figure 3-21. 48-mi ¹³ C NMR spectrum (CDCl ₃ , 75 MHz)..... | 222 |
| Figure 3-22. 44 ¹ H NMR spectrum (CDCl ₃ , 400 MHz)..... | 223 |
| Figure 3-23. 44 ¹³ C NMR spectrum (CDCl ₃ , 100 MHz)..... | 224 |
| Figure 3-24. 49-ma > 49-mi ¹ H NMR spectrum (CDCl ₃ , 400 MHz)..... | 225 |
| Figure 3-25. 49-ma > 49-mi ¹³ C NMR spectrum (CDCl ₃ , 100 MHz)..... | 226 |
| Figure 3-26. 49 ¹ H NMR spectrum (CDCl ₃ , 400 MHz)..... | 227 |
| Figure 3-27. 49 ¹³ C NMR spectrum (CDCl ₃ , 100 MHz)..... | 228 |
| Figure 3-28. 45 ¹ H NMR spectrum (CDCl ₃ , 500 MHz)..... | 239 |
| Figure 3-29. 45 ¹³ C NMR spectrum (CDCl ₃ , 100 MHz)..... | 230 |
| Figure 3-30. 50-ma ¹ H NMR spectrum (CDCl ₃ , 400 MHz)..... | 231 |
| Figure 3-31. 50-ma ¹³ C NMR spectrum (CDCl ₃ , 100 MHz)..... | 232 |

| | |
|--|-----|
| Figure 3-32. 50-mi ^1H NMR spectrum (CDCl_3 , 400 MHz)..... | 233 |
| Figure 3-33. 50-mi ^{13}C NMR spectrum (CDCl_3 , 100 MHz)..... | 234 |
| Figure 3-34. 46 ^1H NMR spectrum (CDCl_3 , 400 MHz)..... | 235 |
| Figure 3-35. 46 ^{13}C NMR spectrum (CDCl_3 , 100 MHz)..... | 236 |
| Figure 3-36. 47 ^1H NMR spectrum (CDCl_3 , 400 MHz)..... | 237 |
| Figure 3-37. 47 ^{13}C NMR spectrum (CDCl_3 , 100 MHz)..... | 238 |
| Figure 3-38. 52-ma ^1H NMR spectrum (CDCl_3 , 300 MHz)..... | 239 |
| Figure 3-39. 52-ma ^{13}C NMR spectrum (CDCl_3 , 75 MHz)..... | 240 |
| Figure 3-40. 52-mi ^1H NMR spectrum (CDCl_3 , 400 MHz)..... | 241 |
| Figure 3-41. 52-mi ^{13}C NMR spectrum (CDCl_3 , 100 MHz)..... | 242 |
| Figure 3-42. 53 ^1H NMR spectrum (CDCl_3 , 400 MHz)..... | 243 |
| Figure 3-43. 53 ^{13}C NMR spectrum (CDCl_3 , 100 MHz)..... | 244 |
| Figure 3-44. 54 ^1H NMR spectrum (CDCl_3 , 400 MHz)..... | 245 |
| Figure 3-45. 54 ^{13}C NMR spectrum (CDCl_3 , 100 MHz)..... | 246 |
| Figure 3-46. 56-ma ^1H NMR spectrum (CDCl_3 , 400 MHz)..... | 247 |
| Figure 3-47. 56-ma ^{13}C NMR spectrum (CDCl_3 , 100 MHz)..... | 248 |
| Figure 3-48. 57 ^1H NMR spectrum (CDCl_3 , 400 MHz)..... | 249 |
| Figure 3-49. 57 ^{13}C NMR spectrum (CDCl_3 , 100 MHz)..... | 250 |
| Figure 3-50. 57-ma ^1H NMR spectrum (CDCl_3 , 300 MHz)..... | 251 |
| Figure 3-51. 57-mi ^1H NMR spectrum (CDCl_3 , 300 MHz)..... | 252 |
| Figure 3-52. 57-mi ^{13}C NMR spectrum (CDCl_3 , 100 MHz)..... | 253 |
| Figure 3-53. 58 ^1H NMR spectrum (CDCl_3 , 300 MHz)..... | 254 |
| Figure 3-54. 58 ^{13}C NMR spectrum (CDCl_3 , 125 MHz)..... | 255 |
| Figure 3-55. 67 ^1H NMR spectrum (CDCl_3 , 400 MHz)..... | 256 |
| Figure 3-56. 67 ^{13}C NMR spectrum (CDCl_3 , 100 MHz)..... | 257 |

| | |
|---|-----|
| Figure 3-57. 68 ^1H NMR spectrum (CDCl_3 , 400 MHz)..... | 258 |
| Figure 3-58. 68 ^{13}C NMR spectrum (CDCl_3 , 100 MHz)..... | 259 |
| Figure 3-59. 77 ^1H NMR spectrum (CDCl_3 , 400 MHz)..... | 260 |
| Figure 3-60. 77 ^{13}C NMR spectrum (CDCl_3 , 100 MHz)..... | 261 |
| Figure 3-61. 69 ^1H NMR spectrum (CDCl_3 , 400 MHz)..... | 262 |
| Figure 3-62. 69 ^{13}C NMR spectrum (CDCl_3 , 75 MHz)..... | 263 |
| Figure 3-63. 78 ^1H NMR spectrum (CDCl_3 , 300 MHz)..... | 264 |
| Figure 3-64. 78 ^{13}C NMR spectrum (CDCl_3 , 100 MHz)..... | 265 |
| Figure 3-65. 64 ^1H NMR spectrum (CDCl_3 , 400 MHz)..... | 266 |
| Figure 3-66. 64 ^{13}C NMR spectrum (CDCl_3 , 100 MHz)..... | 267 |
| Figure 3-67. 71 ^1H NMR spectrum (CDCl_3 , 400 MHz)..... | 268 |
| Figure 3-68. 71 ^{13}C NMR spectrum (CDCl_3 , 75 MHz)..... | 269 |
| Figure 3-69. 79 ^1H NMR spectrum (CDCl_3 , 400 MHz)..... | 270 |
| Figure 3-70. 79 ^{13}C NMR spectrum (CDCl_3 , 100 MHz)..... | 271 |
| Figure 3-71. ORTEP of 42-mi | 272 |
| Figure 3-72. ORTEP of 48-mi | 274 |
| Figure 3-73. ORTEP of 50-ma | 276 |
| Figure 3-74. ORTEP of 50-mi | 278 |
| Figure 3-75. ORTEP of 52-ma | 280 |
| Figure 3-76. ORTEP of 52-mi | 282 |
| Figure 3-77. ORTEP of 57-ma | 284 |
| Figure 3-78. ORTEP of 57-mi | 286 |
| Figure 4-1. 4 ^1H NMR spectrum (CDCl_3 , 400 MHz)..... | 311 |
| Figure 4-2. 4 ^{13}C NMR spectrum (CDCl_3 , 75 MHz)..... | 312 |
| Figure 4-3. 4-^{13}C ^1H NMR spectrum (CDCl_3 , 400 MHz)..... | 313 |
| Figure 4-4. 4-^{13}C ^{13}C NMR spectrum (CDCl_3 , 75 MHz)..... | 314 |

| | |
|---|-----|
| Figure 4-5. 5 ^1H NMR spectrum (CDCl_3 , 400 MHz)..... | 315 |
| Figure 4-6. 5 ^{13}C NMR spectrum (CDCl_3 , 100 MHz)..... | 316 |
| Figure 4-7. 8 ^1H NMR spectrum (CDCl_3 , 400 MHz)..... | 317 |
| Figure 4-8. 8 ^{13}C NMR spectrum (CDCl_3 , 100 MHz)..... | 318 |
| Figure 4-9. 9 ^1H NMR spectrum (CDCl_3 , 400 MHz)..... | 319 |
| Figure 4-10. 9 ^{13}C NMR spectrum (CDCl_3 , 100 MHz)..... | 320 |
| Figure 4-11. ORTEP of 4 | 321 |
| Figure 4-12. ORTEP of 9 | 323 |

LIST OF TABLES

| | |
|---|-----|
| Table 1-1. Comparison of fluorescent singlet state lifetime (τ_s) and quantum yield of fluorescence (Φ_f) and reaction (Φ_{rxn}) for dienyne of differing terminal alkene substitution.to be continued..... | 9 |
| Table 1-2. Summary of Fürstner and coworkers study of metal catalysis for the formation of phenanthrenes from dienyne cycloaromatization..... | 29 |
| Table 1-3. Organization of references covered in this review for dienyne cycloaromatization activation methodologies classified by dienyne Type (see Figure 1-1) and promoter / catalytic reagent..... | 54 |
| Table 2-1. Initial screening of dienyne substrates with varying alkyne substitution for reaction with $[\text{Cp}^*\text{Ru}(\text{NCMe})_3]\text{PF}_6$ 3 | 66 |
| Table 2-2. Exploratory experiments with <i>Z</i> enriched sample of 15-TMS | 67 |
| Table 2-3. Yields of transient species and 17-TMS for the reaction <i>trans</i> -dienyne 15-TMS-E | 69 |
| Table 2-4. NMR chemical shift values for known $[\text{Cp}^*\text{Ru}(\eta^4\text{-diene})\text{NCMe}]\text{X}$ complexes. | 71 |
| Table 2-5. Performance of 15-TMS under previously reported literature conditions.... | 77 |
| Table 2-6. Relative rates and calculated reaction orders for the conversion of 15-TMS and 3 to II | 79 |
| Table 2-7. Observed change in the II TMS resonance integral at different times for normalized kinetic run..... | 104 |
| Table 2-8. Observed change in the II TMS resonance integral at different times for kinetic run with increased CD_3CN concentration..... | 105 |
| Table 2-9. Observed change in the II TMS resonance integral at different times for kinetic run with decreased 3 concentration..... | 106 |
| Table 2-10. Observed change in the II TMS resonance integral at different times for kinetic run with decreased 15-TMS concentration..... | 107 |

| | |
|--|-----|
| Table 3-1. Exploring substrate scope with dienynes containing an allylic stereocenter. | 158 |
| Table 3-2. Arene binding experiments..... | 169 |
| Table 3-3. Crystal data and structure refinement for 42-mi | 273 |
| Table 3-4. Crystal data and structure refinement for 48-mi | 274 |
| Table 3-5. Crystal data and structure refinement for 50-ma | 276 |
| Table 3-6. Crystal data and structure refinement for 50-mi | 278 |
| Table 3-7. Crystal data and structure refinement for 52-ma | 280 |
| Table 3-8. Crystal data and structure refinement for 52-mi | 282 |
| Table 3-9. Crystal data and structure refinement for 57-ma | 284 |
| Table 3-10. Crystal data and structure refinement for 57-mi | 286 |
| Table 4-1. Screening different reaction conditions to determine the role of solvent and hydrogen atom donor for the reaction of 4 | 297 |
| Table 4-2. Crystal data and structure refinement for 4 | 321 |
| Table 4-3. Crystal data and structure refinement for 9 | 323 |

LIST OF ABBREVIATIONS

Alphabetical within Category

Chemical Abbreviations

(– Indicates covalent substituent)

| | |
|--|---|
| –Ac: acetyl, $-\text{C}(\text{O})\text{CH}_3$ | LAH: lithium aluminum hydride |
| –Ar: aryl group | LHMDS: lithium <i>bis</i> -(trimethylsilyl)amide |
| –Bn: benzyl, $-\text{CH}_2\text{C}_6\text{H}_5$ | –Me: methyl, $-\text{CH}_3$ |
| –Boc: <i>tert</i> -butyl carbamyl, $-\text{C}(\text{O})\text{OC}(\text{CH}_3)_3$ | NMP: <i>N</i> -Methyl-2-pyrrolidone |
| – ⁿ Bu: <i>n</i> -butyl, $-\text{CH}_2(\text{CH}_2)_2\text{CH}_3$ | Pet. ether: petroleum ether |
| – ^t Bu: <i>tert</i> -butyl, $-\text{C}(\text{CH}_3)_3$ | –Ph: phenyl, $-\text{C}_6\text{H}_5$ |
| 1,4-CHD: 1,4-cyclohexadiene | –PMP: <i>para</i> -methoxyphenyl, $-(4\text{-C}_6\text{H}_4\text{OCH}_3)$ |
| cod: 1,5-cyclooctadiene | – ^o Pr: cyclopropyl |
| Cp: cyclopentadienyl | – ⁱ Pr: <i>iso</i> -propyl, $-\text{CH}(\text{CH}_3)_2$ |
| Cp*: pentamethylcyclopentadienyl | – ⁿ Pr: <i>n</i> -propyl, $-\text{CH}_2\text{CH}_2\text{CH}_3$ |
| CSA: camphorsulfonic acid | py: pyridine |
| D / -d: deuterium | TBAF: tetrabutylammonium fluoride |
| DABCO: 1,4-diazabicyclo[2.2.2]octane | –TBDMS: <i>tert</i> -butyl-dimethylsilyl, $-\text{Si}(\text{CH}_3)_2\text{C}(\text{CH}_3)_3$ |
| DBU: 1,8-diazabicyclo[5.4.0]undec-7-ene | –TES: triethylsilyl, $-\text{Si}(\text{CH}_2\text{CH}_3)_3$ |
| DCE: 1,2-dichloroethane | –Tf: triflyl, $-\text{SO}_2\text{CF}_3$ |
| DMF: <i>N,N</i> -dimethylformamide | TFA: trifluoroacetic acid |
| DMSO: dimethylsulfoxide | TFE: 2,2,2-trifluoroethanol |
| DNA: deoxyribonucleic acid | THF: tetrahydrofuran |
| –Et: ethyl, $-\text{CH}_2\text{CH}_3$ | –THP: 5-(3,4-dihydropyryl) |
| – ⁿ Hex: <i>n</i> -hexyl, $-\text{CH}_2(\text{CH}_2)_4\text{CH}_3$ | –TIPS: tri- <i>iso</i> -propylsilyl, $-\text{Si}(\text{CH}(\text{CH}_3)_2)_3$ |
| IBX: 2-iodoxybenzoic acid | –TMS: trimethylsilyl, $-\text{Si}(\text{CH}_3)_3$ |
| L: metal ligand (e.g. AuL^+) | Tp: <i>tris</i> -pyrazolylborate |

-Ts: tosyl, $-\text{SO}_2(4\text{-C}_6\text{H}_4\text{CH}_3)$

Experimental / Spectroscopic

$\Delta H^\circ_{\text{rxn}}$: standard reaction enthalpy

δ : chemical shift

η^x : x atoms π bound to metal

κ^x : x atoms σ bound to metal

Φ : quantum yield

τ : lifetime

A: pre-exponential term (Arrhenius equation)

app.: apparent

CIP: Cahn-Ingold-Prelog

d: doublet

d.r.: diastereomeric ratio

E/Z: alkene stereochemical assignment

E_a : activation energy

EI: electron ionization

EPR: electron paramagnetic resonance

eq / eq.: equivalent

ESI: electron spray ionization

FT: Fourier transform

GC/MS: gas chromatography / mass spectrometry

$h\nu$: visible or ultraviolet radiation

HMBC: heteronuclear multiple bond correlation

HRMS: high resolution mass spectrometry

HSQC: heteronuclear single quantum coherence

IR: infrared spectroscopy

J: coupling constant

KIE: kinetic isotope effect

m: multiplet

MNDO: modified neglect of differential overlap

mp / m.p. melting point

m/z: mass to charge ratio

NMR: nuclear magnetic resonance

nOe: nuclear Overhauser effect

oct: octet

p: pentet

PM3: parameterized model number 3

PTLC: preparative thin layer chromatography

R^2 : correlation coefficient squared (linear regression)

q: quartet

R/S: carbon stereocenter assignment

R_p/S_p : η^6 -complexation stereochemical assignment

rt: room temperature
s: singlet
S_NAr: nucleophilic aromatic substitution
sp: septet
sx: sextet
t: triplet
VT: variable temperature

Parameter Units

(Conventional SI prefixes were used)

Å: Angstrom
°C: degree Celsius
h / hr: hour
Hz: Hertz
cal: calorie
cm⁻¹: wavenumber
K: Kelvin
L: liter
M: molar
m: meter
min: minute
mol: mole
ppm: parts per million
s: second
torr: millimeter of mercury

ACKNOWLEDGEMENTS

I would like to thank my advisor, Joseph M. O'Connor, for his instruction and guidance and being a wonderful person to work with. I would also like to acknowledge my committee members, Professor Charles L. Perrin, and past and present members of the O'Connor, Perrin, and Yang labs for insightful discussions and suggestions in addition to their support throughout my studies here at UCSD. I must also give thanks to my fiancée Stefanie and my family. Only through their love and support was this work possible.

Antonio G. DiPasquale, Curtis E. Moore, Ryan L. Holland, and Professor Arnold L. Rheingold are thanked for their helpful instruction in the acquisition of X-ray crystallographic data. Anthony Mrse and Xuemei Huang are acknowledged for their assistance in conducting and acquiring data for specialized NMR experiments. Yongxuan Su is acknowledged for acquisition of HRMS data.

The material of Chapter 1, in full, is currently being prepared for submission for publication with the following authors: Hitt, D.M.; O'Connor, J.M. The dissertation author was the primary investigator and author of this material.

The material of Chapter 2, in part, is currently being prepared for submission for publication with the following authors: Hitt, D.M.; O'Connor, J.M. The dissertation author was the primary investigator and author of this material.

The material of Chapter 3, in part, is currently being prepared for submission for publication with the following authors: Hitt, D.M.; Holland, R.L.; O'Connor, J.M. The dissertation author was the primary investigator and author of this material.

The material of Chapter 4, in part, is currently being prepared for submission for publication with the following authors: Hitt, D.M.; Raub, A.G.; O'Connor, J.M. The dissertation author was the primary investigator and author of this material.

CURRICULUM VITAE

Education

- 2007 – 2011 University of California, San Diego
Doctor of Philosophy, Chemistry
- 2005 - 2007 University of California, San Diego
Master of Science, Chemistry
- 2001 – 2005 North Carolina State University
Bachelor of Science, Chemistry with emphasis in Biochemistry
Valedictorian, Summa Cum Laude

Teaching Experience

January 2006 – 2011

Teaching Assistant: Organic Chemistry I & II, UC San Diego

Served as discussion section leader for 90 - 100 students enrolled in a larger 200 - 400 student class of organic chemistry. Primary responsibility was to hold weekly problem-solving sessions designed for open discussion of topics covered in lecture and difficulties encountered during assigned text problems. Secondary responsibilities included midterm / final exam proctoring, quiz writing, and grading. Employed for 10 quarters during the academic year and 6 summer sessions.

September - December 2005 & 2006

Teaching Assistant: Organic Chemistry Laboratory I, UC San Diego

Employed as in-lab instructor for one class per quarter ranging from 20 - 25 students. Primary responsibilities included teaching students in introductory organic laboratory techniques, skills, and instrumentation in addition to writing quizzes and grading laboratory reports / quizzes. Obtained congratulatory letter from department during the Fall 2006 quarter.

August 2002 – May 2004

Supplemental Instruction Leader / Tutor: NC State University

Served as discussion section leader for a 200 - 250 student class of organic chemistry I & II. Also participated in an individual student tutoring system and tutoring walk-in center for general chemistry and organic chemistry run by the university. Earned Master Tutoring Certification from the College Reading and Learning Association (2004) and presented "Synthetic Shortcuts: Strategies for Chemical Synthesis in Organic Chemistry" at the 2004 North Carolina Supplemental Instruction Conference (February 28, 2004 at NC State University).

Research Experience

December 2005 – June 2011

Ph.D. Student: UC San Diego, Advisor: Joseph M. O'Connor

Investigated transition metal mediated and catalyzed enediyne and dienyne cycloaromatizations. The main areas of study were on the stereoselective η^6 – metal complexation of arenes formed during the metal triggered Bergman and Hopf cyclizations and metal catalyzed cyclizations resulting from the allylic CH activation / intramolecular insertion of dienyne. In addition to metal influenced reactivity, a novel thermal mode of enediyne cycloaromatization was also studied in the presence of halogenated solvents.

June 2005 – September 2005

Research Assistant: UC San Diego, Advisor: Michael S. VanNieuwenhze

Assisted in the synthesis of a bacteria cell wall peptidoglycan monomer (Lipid I) for purpose of an antibiotic NMR binding study. Key successes were implementation of an improved reductive opening of a benzylidene protecting group and coupling of monomer carbohydrate units to form the core disaccharide structure of Lipid I.

January 2003 – May 2005

Intern Research Assistant: Inspire Pharmaceuticals, Advisor: Paul Watson

Planned and performed syntheses of various nucleotide and nucleoside drug targets for assay screens. Assisted in initial stages of synthesis for a natural product target. Other responsibilities included general laboratory upkeep, troubleshooting and repairing broken equipment, and management of chemical inventory.

June 2004 – August 2004

Undergraduate Research Assistant: University of Virginia, Advisor: Milton Brown

Designed and synthesized three α -biphenyl- β -lactam based compounds for a binding assay with tubulin, an important protein for cell division and transport. Results were used in a structure-activity relationship study for determining compounds of high anti-cancer activity. Requirements of position included submission of a final progress report and oral presentation to the chemistry department on findings.

Laboratory Technical Expertise

Synthetic organic chemistry in the construction of organic small molecules; Air free techniques (Schlenk line and glove box manipulations) for handling oxygen and water sensitive solids and reaction mixtures; NMR and IR spectroscopy; X-ray crystallography under supervision of the UCSD X-ray facility (performed crystal preparation, data collection, and structure solution for 7 samples).

Organizations

2006 – Present

American Chemical Society

2002 – 2005

Alpha Chi Sigma Chemistry Fraternity, Gamma Xi chapter

- Master Alchemist (president), 2004 – 2005
- Treasurer, 2002 – 2003

Awards and Honors

| | |
|---------|---|
| 2001-05 | NC State University Dean's List |
| 2004 | Research Experience for Undergraduates (REU) Fellow |
| 2004 | Phi Lambda Upsilon, Honorary Chemical Society |
| 2003 | Phi Kappa Phi Honor Society |
| 2003 | Phi Beta Kappa Honor Society |
| 2002-03 | National Dean's List Recipient |
| 2002 | CRC Press LLC Freshman Chemistry Achievement Award |

Publications

D. M. Hitt, J. M. O'Connor, "Methods of Acceleration for Conjugated Dienyne Cycloaromatization" *Manuscript in preparation*.

D. M. Hitt, J. M. O'Connor, "Dienyne Cycloaromatization Triggered by Ruthenium C-H Bond Activation" *Manuscript in preparation*.

D. M. Hitt, R. L. Holland, J. M. O'Connor, "Stereoselective η^6 -Arene Complexation during Ruthenium Mediated Dienyne and Eneidyne Cycloaromatization Reactions" *Manuscript in preparation*.

D. M. Hitt, A.R. Raub, J. M. O'Connor, "A Novel Route of Cycloaromatization for Conjugated Eneidyne" *Manuscript in preparation*.

Presentations

D. M. Hitt, R. L. Holland, J. M. O'Connor, "Stereoselective η^6 -arene complexation in ruthenium mediated enediene and diene cycloaromatization reactions" *Abstracts*, 241st National Meeting of the American Chemical Society, Anaheim, CA, March 27-31, **2011**; ORGN-722

J. M. O'Connor, **D. M. Hitt**, "Metal-catalyzed cycloaromatizations of dienyne" *Abstracts*, 241st National Meeting of the American Chemical Society, Anaheim, CA, March 27-31, **2011**; ORGN-405

J. M. O'Connor, **D. M. Hitt**, A. L. Rheingold, "Diastereoselective Metal-Triggered Bergman Cycloaromatization Reactions" *Abstracts*, 42nd Western Regional Meeting of the American Chemical Society, Las Vegas, NV, September 23-27, **2008**; WRM-251.

ABSTRACT OF DISSERTATION

Investigations into Novel Modes of Reactivity and Stereoselectivity for the Cycloaromatization of
Conjugated Ene-diyne and Dienynes

by

David M. Hitt

Doctor of Philosophy in Chemistry

University of California, San Diego, 2011

Professor Joseph M. O'Connor, Chair

This work begins with a review of practical cycloaromatization methodologies utilizing 1,3-dien-5-yne subunits. As a valuable addition to this body of literature, an ambient temperature diene cycloaromatization pathway resulting from the formal CH activation of an allylic methyl group and subsequent alkyne 1,2-insertion triggered by cationic cyclopentadienyl ruthenium complexes (CpRu) has been discovered. This cyclization route is fundamentally different to previous studies with CpRu that resulted in the formal Hopf product and the new reactivity appears to be correlated with the bulk of the alkyne substituent. Mild levels of catalysis and selectivity have been observed for *cis*-1-allylic substituted dienynes, although *trans*-allylic dienynes were also found to be viable substrates for the stoichiometric reaction. Three transient ruthenium-diene complexes have been identified from the reaction of a TMS substituted diene, one of which is derived from the *trans*-1-allylic diene and the other two appear to be in equilibrium by ligand exchange as supported by VT NMR studies. Kinetic investigations have ruled out metal η^2 -alkyne coordination as the reaction-triggering event as

previously proposed in similar transformations. Two reaction pathways currently being considered are a [1,7]-hydrogen shift mechanism and a metal C-H insertion mechanism.

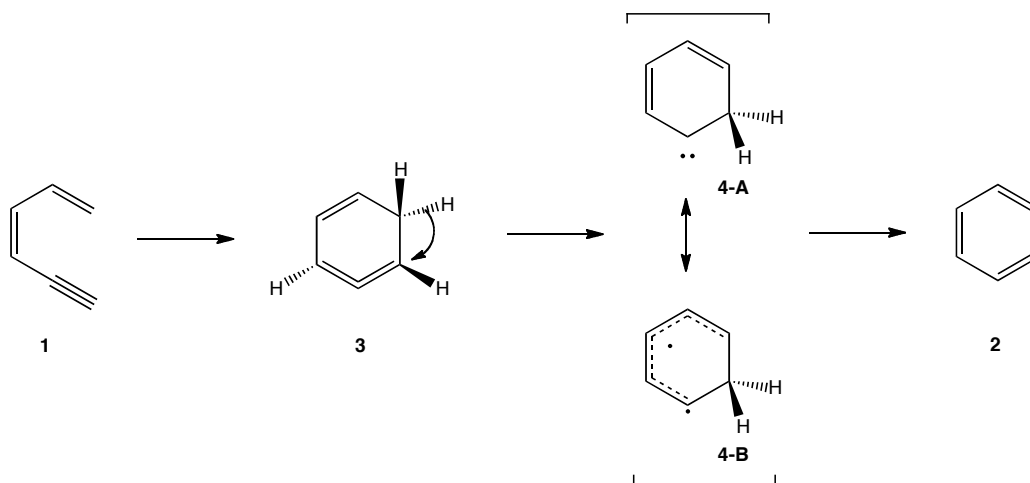
In continuation of previously described metal-triggered cycloaromatizations of dienyne and enediyne, we have investigated *in situ* stereoselective η^6 -complexation of the products from these reactions by use of chiral substrates. Use of allylic or propargylic stereocenters led to diastereomeric ratios (d.r.) as high as 8:2. The highest stereoselectivities were found by use of a Cp* versus a Cp ligand and the relative stereochemistry for the major and minor products for both reactions were found to be consistent by X-ray structure characterization. Arene binding experiments have ruled out a mechanism in which the selective binding step occurs by complexation of the free arene.

Finally we have uncovered a mode of cycloaromatization for enediyne unrelated to the *Bergman* mode. The reaction occurs predominately in CDCl₃ and is promoted by 1,4-cyclohexadiene and HCl. Intermediacy of a *cis,cis*-dienyne is suspected and the current mechanistic hypothesis involves a cascade of pericyclic reactions leading to product initiated by a [1,7]-hydrogen shift from the dienyne.

CHAPTER 1: Methods of Acceleration for Conjugated Dienyne Cycloaromatization

I. Introduction

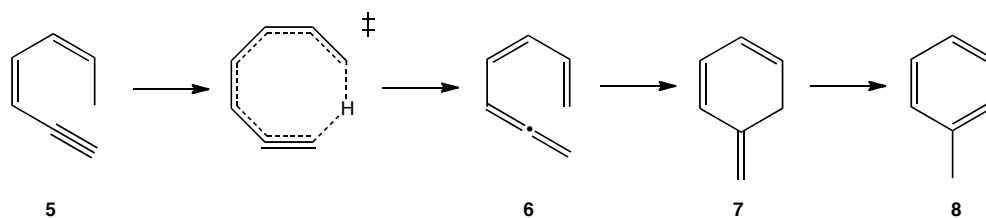
The thermal cycloaromatization of conjugated 1,3-dien-5-yne has long been an area of intense interest among physical organic and computational chemists.¹ Hopf and Musso initially reported that heating (*Z*)-1,3-hexadien-5-yne (**1**) at temperatures in excess of 274°C resulted in conversion to benzene (**2**, Scheme 1-1).² At temperatures greater than 550°C several mechanisms may be active, however computational and experimental studies provide strong support for the mechanism shown in Scheme 1-1 as the most dominant one at lower temperatures.³ From **1**, electrocyclicization leads to cyclic allene intermediate **3** that then proceeds through an initial [1,2]-H shift to afford intermediate **4** which can be represented as a carbene **4-A** or diradical **4-B** resonance form. A final [1,2]-H shift leads to the aromatized product **2**.



Scheme 1-1. Intermediates believed to be involved in the thermal cycloaromatization of dienyne.³

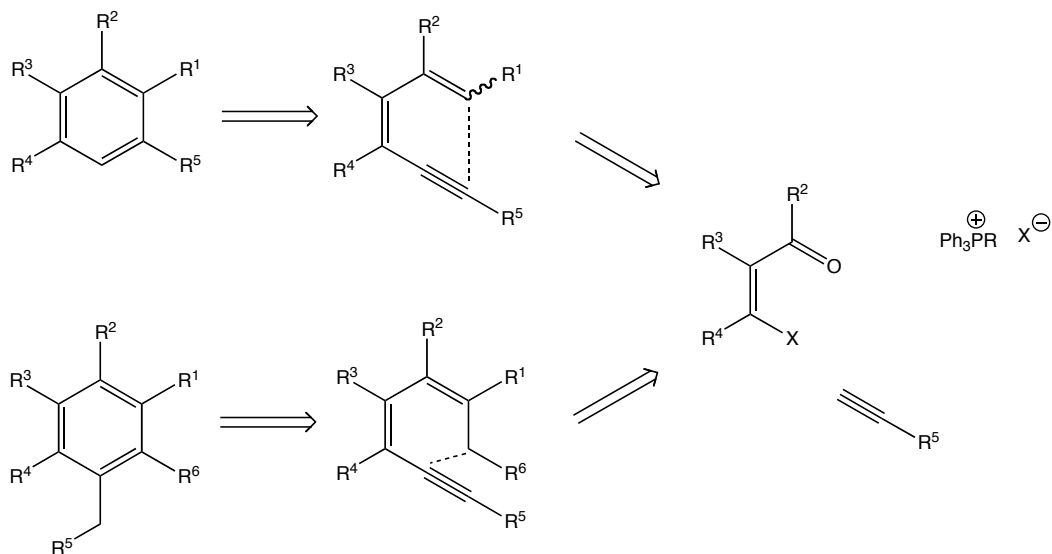
While the electrocyclicization pathway shown in Scheme 1-1 represents the most well studied thermal dienyne cycloaromatization, a lesser-known variant initiates via a [1,7]-H shift

from an *cis*-allylic substituted dienyne **5** to give allene intermediate **6** (Scheme 1-2). 6π Electrocyclization of this species gives *o*-quinodimethane **7**, which in turn isomerizes to aromatized **8**. While thermal [1,7]-H shifts are well known for 1,3,5-hexatrienes,⁴ examples with dienyne are rare and generally occur at high temperature ($> 200^\circ\text{C}$).^{5,6}



Scheme 1-2. General mechanism for a thermal dienyne [1,7]-hydrogen shift / cycloaromatization.

Synthetically, dienyne cycloaromatization provides a reliable way to construct highly substituted aromatic systems from readily available starting materials as depicted in Scheme 1-3. A major drawback of the thermal mode of cyclization is the exceedingly high temperatures required to effect cyclization thus limiting the substrate scope.



Scheme 1-3. Retrosynthesis of aromatic products deriving from dienes.

The motivation behind this review is to highlight the discovery, mechanism and synthetic utility of methodologies that use either catalytic or stoichiometric activators to promote diene cycloaromatizations at temperatures less than 200°C. The review is organized by mechanism of activation and covers cyclizations resulting in a carbon-based aromatic systems (e.g. benzenoid, naphthalenoid). Heterocyclic aromatic systems are not reviewed unless a mechanistic discussion is warranted. In order to decrease redundancy throughout the discussion, diene substrates have been classified according to the presence and location of aromatic alkene subunits as shown in Figure 1-1.

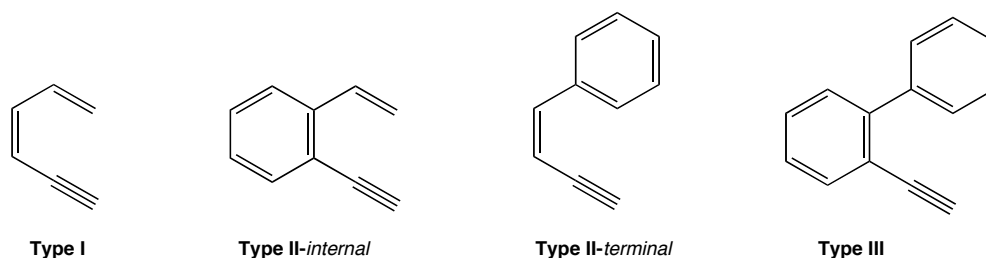


Figure 1-1. Classification of dienyne substrates.

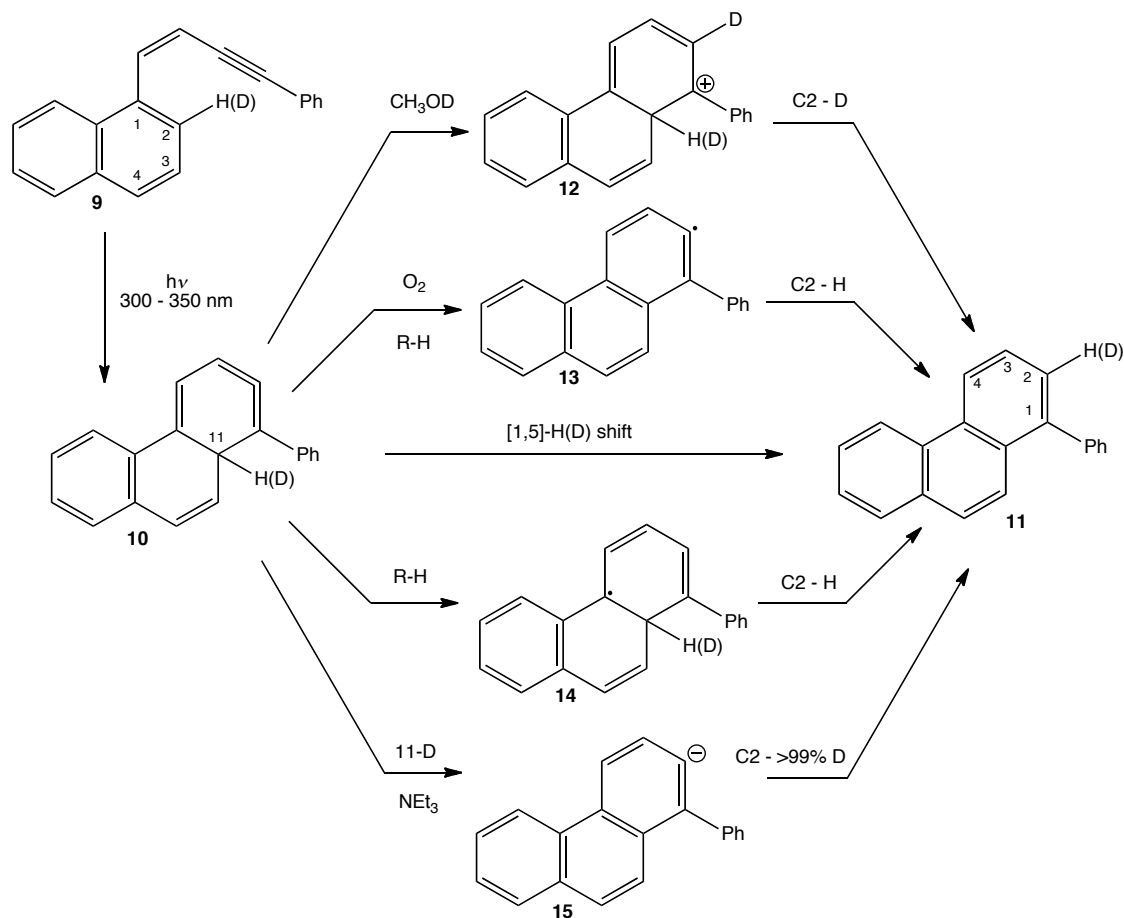
II. Photolytic Triggering

The earliest observation of photolytic dienyne cycloaromatization was demonstrated by Kaplan and coworkers, who showed that irradiation of dienyne **1** at 254 nm resulted in slow ($\Phi = \sim 0.01$) but quantitative conversion to a 2:1 mixture of benzene and fulvene.⁷ This single example actually predates the thermal cycloaromatization, but no mechanistic rationale was provided for the reaction. In later studies, Laarhoven and coworkers, demonstrated the utility of photolyzing substituted enynyl-naphthalenes (e.g. **9**, Scheme 1-4) and phenanthrenes to form cycloaromatized polyaromatic systems in good to moderate yields.⁸ Although alternative mechanisms were proposed in earlier papers, these researchers now favor a mechanism proceeding through cycloallene intermediate **10**, similar to the thermal reaction.^{8d} Intermediate **10** was proposed to convert to product **11** by a variety of pathways depending on the reaction conditions. In protic solvents, **10** acquires a proton from solvent to form cation **12** that then aromatizes to form **11**. This mechanism was consistent with use of CH₃OD that gave >95% deuterium incorporation at the C2 position of **11**. In general, use of protic solvents leads to higher quantum yields when compared to non-polar aprotic solvents because the protonation of **10** represents the lowest energy pathway to product.

Rate acceleration in the presence of air was also observed, particularly in aprotic solvents. Based on this observation, oxygen was proposed to trigger the conversion of **10** by

hydrogen abstraction resulting in the formation of intermediate **13**. In the absence of oxygen, the predominate mechanism results from **10** abstracting a hydrogen atom from solvent to form **14**. This was supported by faster rates in hexanes versus benzene (weaker CH bonds for the former), formation of small amounts of biphenyl when the reaction was conducted in benzene (presumably from attack of the resulting phenyl radical on another molecule of benzene) and incorporation of iodine at the C-2 position of the product **11** when the reaction was conducted in the presence of I₂. Also occurring under air-free conditions is a formal intramolecular [1,5]-H shift. This was confirmed by deuterium labeling at the C-2 position of **9** that gave, albeit diminished, incorporation of D at the C-2 position of **11**.

The most surprising observation was the high degree of rate acceleration in the presence of amine bases, which was determined to be an order of magnitude higher than molecular oxygen acceleration and four orders of magnitude higher than hydrogen abstraction from solvent. Use of C-2 deuterium enriched **9** with amine showed high levels of D incorporation in the C-2 position of **11** under all conditions. Furthermore, without added amine under identical open-air conditions, negligible deuterium incorporation in **11** was observed, ruling out an intramolecular [1,5]-H transfer. Based on these results, a deprotonation / reprotonation mechanism was proposed to proceed through aryl anion **15**. Laarhoven and coworkers have also obtained similar findings for the photocycloaromatizations of **Type II-internal** dienyne.⁹

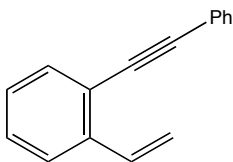
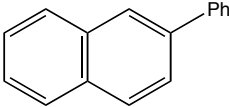
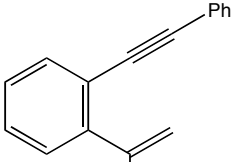
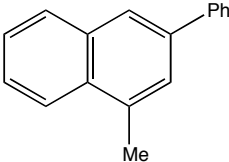
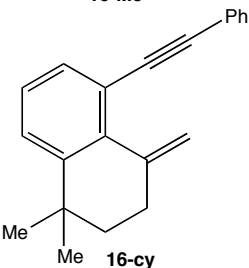
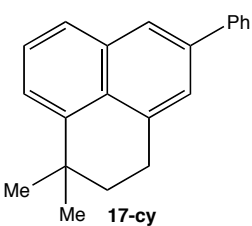


Scheme 1-4. Mechanistic pathways of conversion for photolytically generated cyclic allene **10**.⁸

Key insight into the reactive excited state of the photocycloaromatization came through the work of Lewis and Sajimon who studied the reactivity of various **Type II-internal** dienynes with varying substitution at the terminal alkene.¹⁰ These researchers hypothesized that the efficiency of the cyclization would increase if a higher proportion of the terminal alkene existed in the less stable *syn* conformation **16-syn** versus the *anti* conformation (**16-anti**). To test this prediction, dienynes **16-Me** and **16-cy** were prepared with the expectation that **16-Me** would increase the concentration of rotomer **16-syn** and **16-cy** would lock the diene in the *syn* conformation. As expected, the quantum yield for the formation of **17** (Φ_{rxn}) increased along the series **16-cy** > **16-Me** > **16-H**, but with an unexpected identical trend in quantum yield of

fluorescence (Φ_f) and lifetime of the excited fluorescent singlet state (τ_s). The Φ_f and τ_s trend was rationalized by a *slower* decay of the fluorescent linear single state **16-S₀** to a non-fluorescent *trans*-stilbene “like” singlet state **16-S_{f,s}** for **16-Me / 16-cy** compared to **16-H** which exhibited decay similar to the well-studied diphenylacetylene (Figure 1-2). This explanation was consistent with calculations that showed the activation for **16-S₀** to **16-S_{f,s}** conversion was 6 kcal·mol⁻¹ higher for the respective states of **16-Me / 16-cy** compared to **16-H**. Furthermore, a temperature dependence on the τ_s was observed for **16-Me / 16-cy** that allowed for measurement of the radiation-less decay Arrhenius parameters. While the E_a for **16-Me / 16-cy** was similar to the decay of diphenylacetylene (model for **16-H**), the pre-exponential term ($\log A$) was lower. These authors correlate the decrease in A to the ordered transition state leading to cyclic allene **18** and therefore, at least for **16-Me / 16-cy**, the reactive excited state appears to be the lowest energy fluorescent state of **16-S₀**. Similar conclusions were made in later studies from **Type III** dienyne although Φ_{rxn} was lower in these cases.¹¹

Table 1-1. Comparison of fluorescent singlet state lifetime (τ_s) and quantum yield of fluorescence (Φ_f) and reaction (Φ_{rxn}) for dienynes of differing terminal alkene substitution.¹⁰

| Substrate | Product | Φ_f | τ_s (ns) | Φ_{rxn} |
|---|---|----------|---------------|--------------|
|  16-H |  17-H | 0.1 | < 0.1 | < 0.02 |
|  16-Me |  17-Me | 0.17 | 5.9 | 0.21 |
|  16-cy |  17-cy | 0.21 | 6.8 | 0.47 |

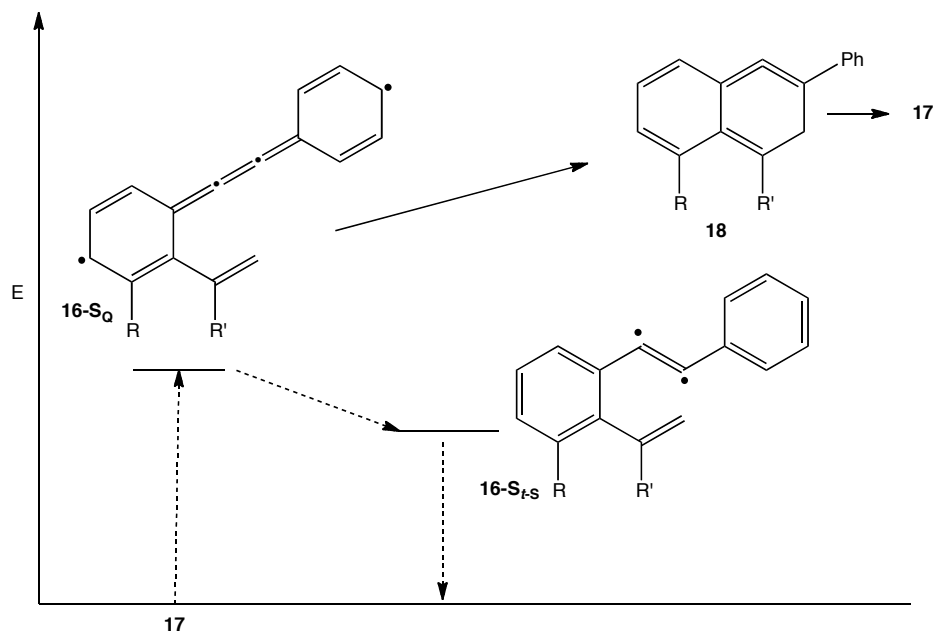
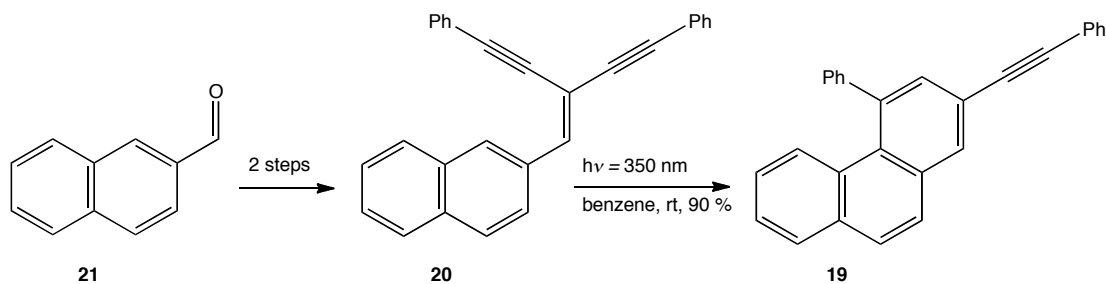


Figure 1-2. Pictorial representation of fluorescent linear single state **16-S_Q** and non-fluorescent *trans*-stilbene “like” singlet state **16-S_{tS}**.¹⁰

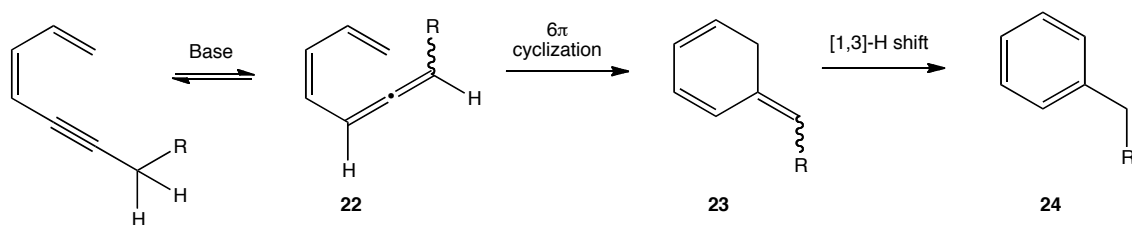
The applicability of the photocycloaromatization for synthesis may be limited. While reactions conditions are mild, isolated yields are in many cases low and by-product formation stemming from radical processes can be problematic.^{8c,12} Despite these difficulties some photocycloaromatization successes have been reported. Neckers and coworkers were able to prepare 2,4-substituted phenanthrene **19** in excellent yield from diendiyne **20** for use in the synthesis of polyaromatic compounds for optical applications (Scheme 1-5).¹³



Scheme 1-5. High yielding photocycloaromatization of 2,4-substituted phenanthrene **19** from readily available 2-naphthylcarboxaldehyde **21**.¹³

III. Alkyne – Allene Isomerization Induced

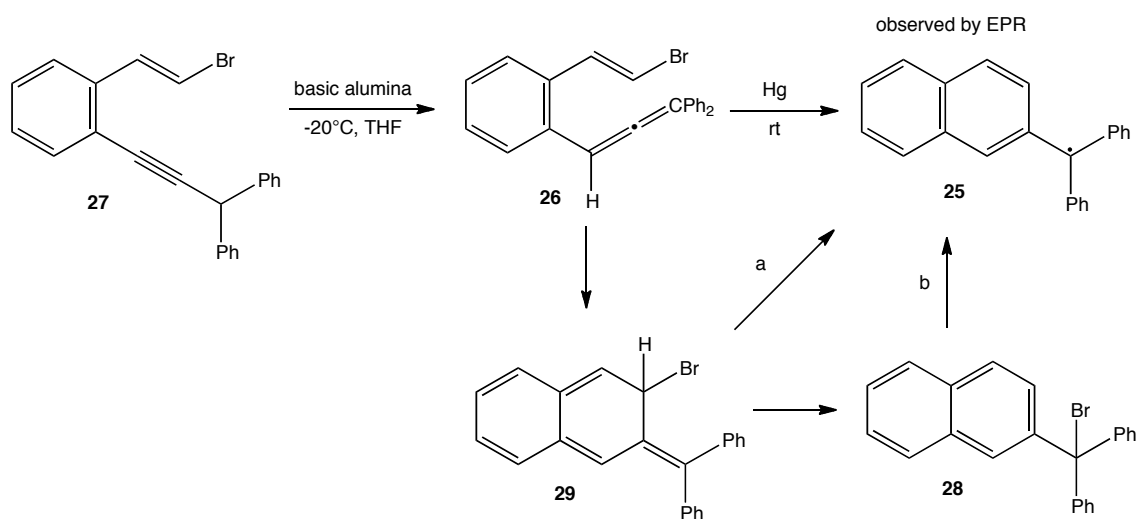
Depending on the electronic nature of the dienyne, it may be possible to thermally isomerize the alkyne portion of the molecule to an allene **22** under basic conditions (Scheme 1-6). From **22**, 6π electrocyclization to afford **23** followed by a formal [1,3]-H shift provides a reasonable pathway for production of aromatic product **24**.¹⁴



Scheme 1-6. General mechanism for dienyne cycloaromatization through base-catalyzed allene formation.

The first application of this dienyne cyclization route was demonstrated by Porter and coworkers who were able to perform the cycloaromatization of halo-substituted dienynes in conjunction with a one-electron reduction to form naphtyldiphenylmethyl radical **25** (Scheme 1-7).¹⁵ Key mechanistic insight came from isolation of the reactive allene **26** that was prepared at

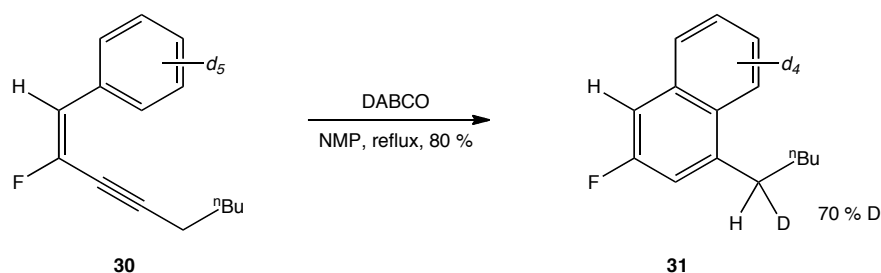
low temperature by treatment of **27** with activated basic alumina and structurally supported by the allenic ^{13}C NMR resonance at δ 209.5. When **26** was warmed to ambient temperature, the benzylic halide **28** was cleanly formed, presumably through initial formation of *ortho*-quinodimethane **29**. The reduction of **26** to **25** with Hg was confirmed by EPR, though, it was unclear if the pathway to **25** was directly from **29** (path a) or **28** (path b).



Scheme 1-7. Allene isomerization for the formation of a naphthyl-diphenylmethyl radical.¹⁵

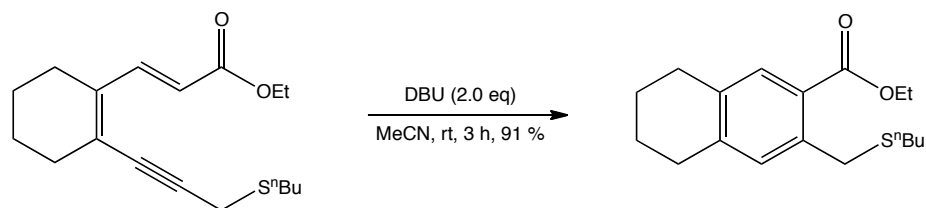
Burton and coworkers have developed conditions to prepare a variety of 1,3-disubstituted naphthalenes using the alkyne isomerization approach.¹⁶ Under optimized conditions, allowing dienynes to react with a nitrogen base such as DABCO or DBU in refluxing *N*-Methyl-2-pyrrolidone (NMP) gave arenes in yields ranging from 60 to 95%. In line with the base-catalyzed isomerization to **22** (Scheme 1-6), only use of **Type II-terminal** dienynes containing a central alkene with an electron withdrawing substituent (e.g. F, CO_2R , CHO) or **Type III** dienynes were effective for the cyclization due to the increased acidity of the propargyl proton.¹⁷ Another interesting observation came when d_5 -dienyne **30** was treated under optimized conditions to give the cyclized naphthalene **31** with partial incorporation of deuterium into the

benzylic position (Scheme 1-8). This result was rationalized by hypothesizing that a base-assisted conversion may compete with an intramolecular [1,3]-H shift for this step in the mechanism (see **23** to **24**, Scheme 1-6). A deprotonation / reprotonation would require acquisition of protons from the bulk media and explains the loss of deuterium in the benzylic position.



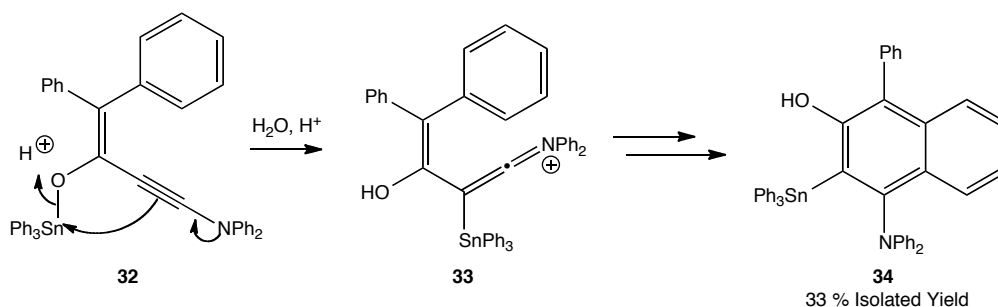
Scheme 1-8. Deuterium labeling supports a competition between concerted and base-assisted conversion of *o*-quinodimethane **23**.^{16a}

More recent work by Zhou and coworkers has shown much milder cyclization conditions can be effected by use of **Type I** and **Type II-internal** dienynes containing propargyl sulfides with an ester or amide off the terminal alkene position (Scheme 1-9).¹⁸ Although the authors do not provide an exact explanation, the decreased pK_a of the propargylic hydrogen atoms resulting from the combined resonance and inductive effects of the carbonyl and sulfide may rationalize the rate acceleration compared to dienynes not containing these substituents.



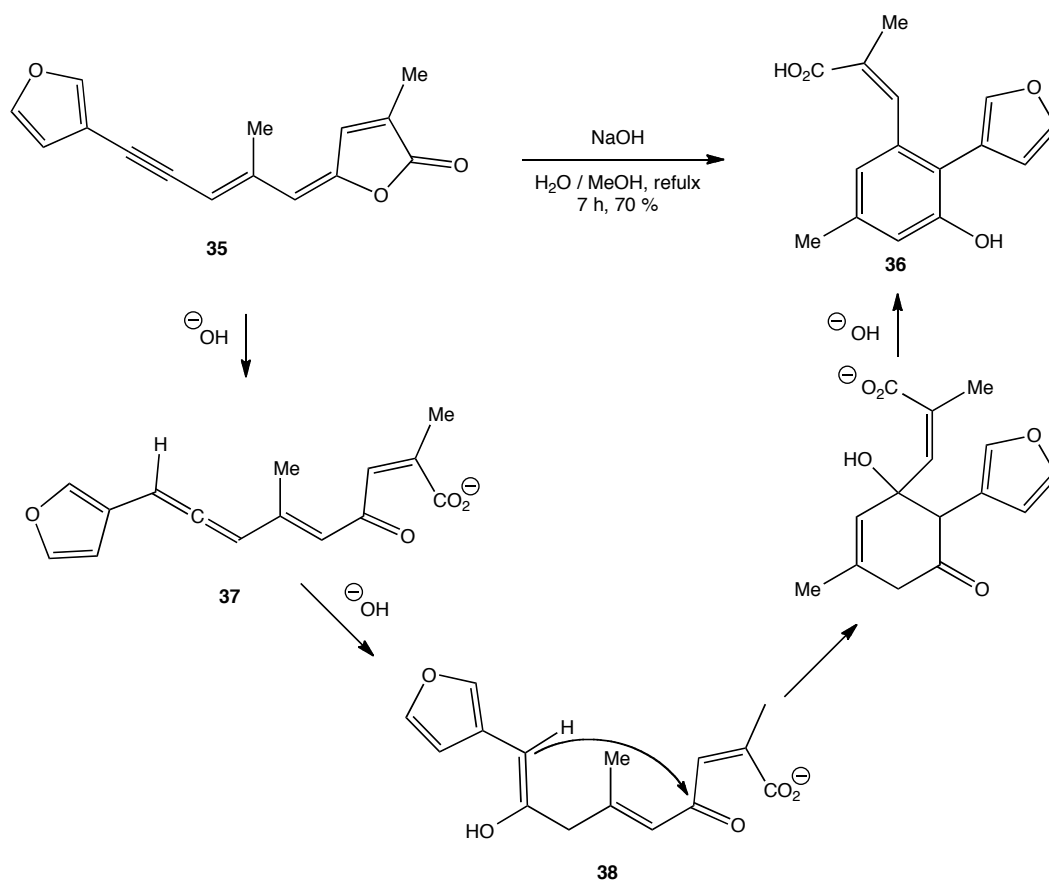
Scheme 1-9. Use of propargyl sulfides for ambient temperature cycloaromatization.¹⁸

While the base-induced isomerization pathway represents the most common way to bring about a 6π electrocyclization, it is not the only possible route. Himbert and coworkers have used alkoxy-stannane dienynes (**32**) with a highly nucleophilic amino alkyne substituent to induce a [1,3]-shift of the tin moiety resulting in the formation of the iminiumene **33** (Scheme 1-10). Compound **33** then follows through cyclization and tautomerization to give product **34**.¹⁹



Scheme 1-10. 6π Electrocyclization from a 1,3-stannane shift.¹⁹

Finally, although not a 6π electrocyclization, treatment of the diyne natural product, Freelingyne (**35**), with base was observed to proceed through a cycloaromatization to give the tri-substituted phenol **36** (Scheme 1-11).²⁰ The proposed mechanism involves hydrolysis of the lactone to give allene **37**. Conjugate addition of hydroxide to **37** gives enol / enolate **38** that then cyclizes and aromatizes to form **36**.

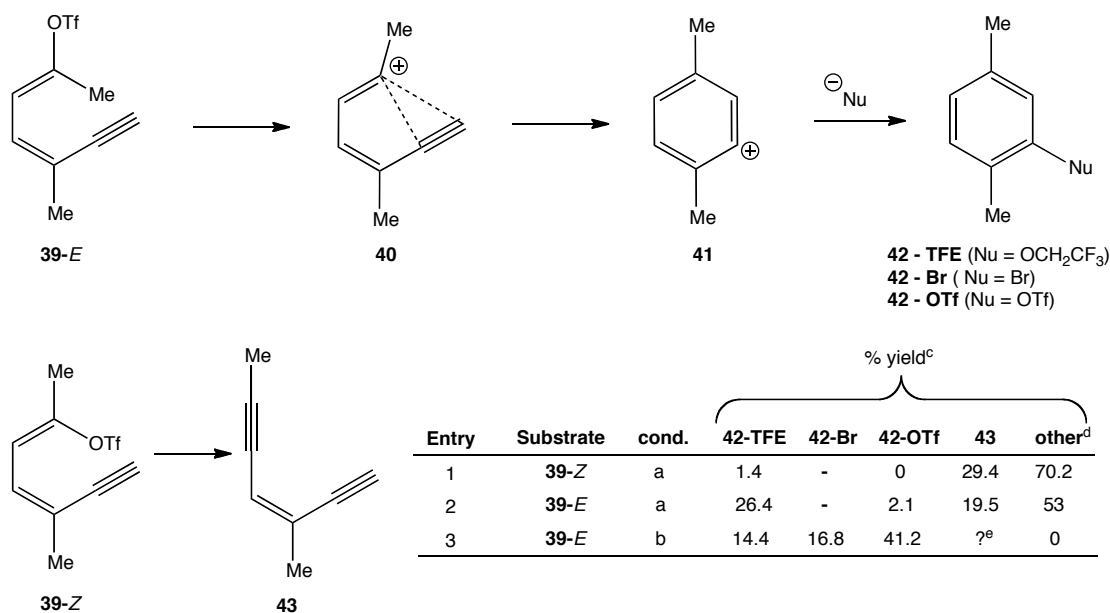


Scheme 1-11. Base-induced cycloaromatization of Freelingyne (**35**) proceeding through allene intermediate.²⁰

IV. Nucleophilic Attack of Alkyne

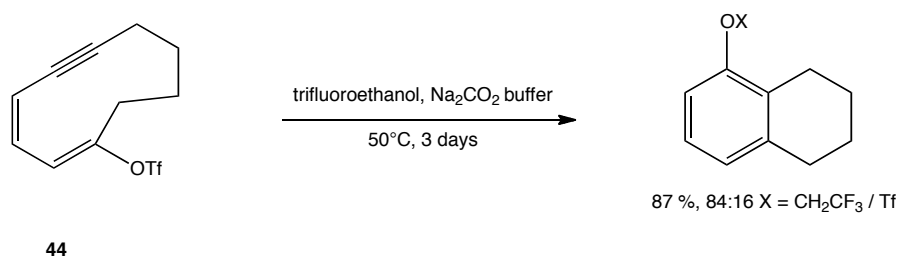
In some instances, the π system of the alkyne can act as a nucleophile if the terminal alkene is sufficiently activated. The most fundamental example of this type of reactivity is demonstrated by the work of Hanack and coworkers who have studied the cycloaromatization of vinyl triflate dienyne **39** (Scheme 1-12).²¹ Upon heating in a basic buffered media, **39** was proposed to ionize to alkyne-stabilized vinyl cation **40**. Attack of the alkyne to give aryl cation **41** followed by trapping with a nucleophile gives cycloaromatized product **42**. It is unclear whether **40** is an actual intermediate or transition state to **41**, but the alkyne is thought to assist in the

departure of the leaving group based on the higher proportion of **42** formed when the *E* stereoisomer (**39-E**) was employed versus the *Z* stereoisomer (**39-Z**). The latter favors formation of the elimination product **43**. The *anti* relationship of the triflate and alkyne in **39-E** was postulated to provide anchimeric assistance of the π electrons. The reaction performs well in weakly nucleophilic polar solvents supporting the formation of ionic intermediates. Although a large proportion of the starting material was observed to polymerize, this problem can be minimized if added bromide nucleophile was used (entry 3). Formation of **42-Br** also suggests that **39** proceeds through intermediate aryl cation **41** during conversion to product, thus ruling out other cyclization mechanisms. In later studies, Hanack in collaboration with Schwarz was able to observe a species consistent with **41** by collisional activation mass spectrometry.²²



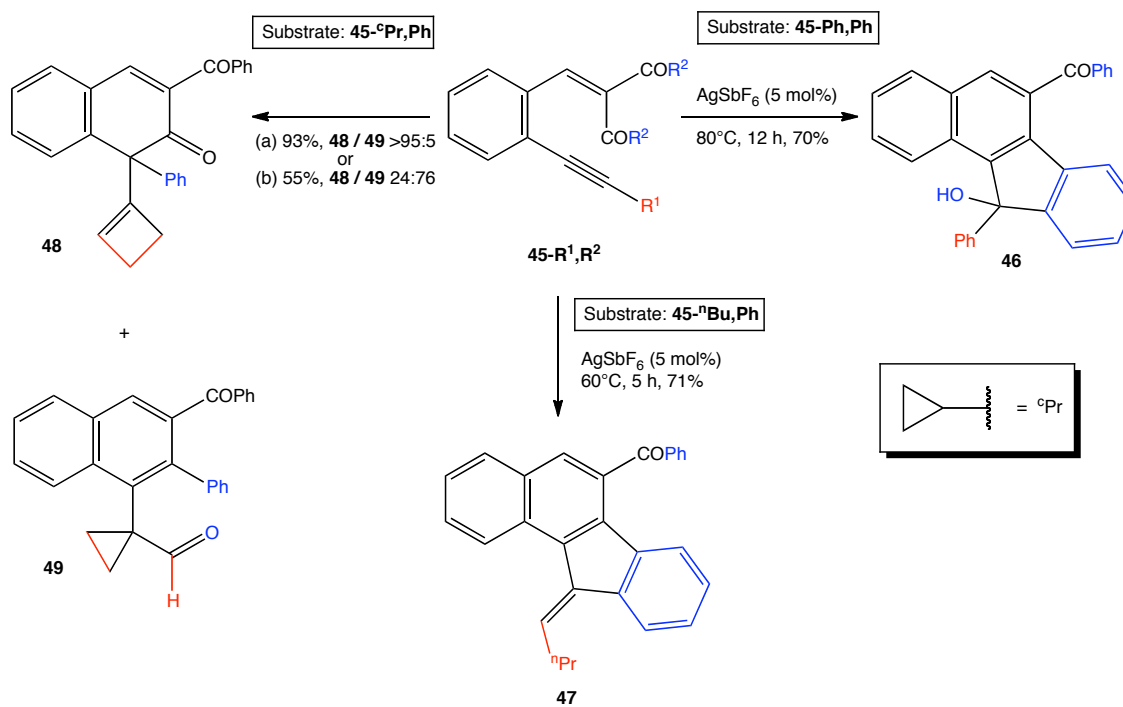
Scheme 1-12. Use of vinyl triflate dienynes to trigger cycloaromatization via nucleophilic attack of the alkyne. Conditions: (a) trifluoroethanol, Na₂CO₃ buffer, 100°C, 5 days; (b) trifluoroethanol / water / dioxane, Na₂CO₃ buffer, LiBr (excess), 100°C, 5 days. (c) determined by capillary g.l.c. (d) mostly polymer (e) undetermined because of overlap with solvent peak.^{21b}

Yields of the substitution products were greatly improved by use of cyclic dienyne **44** (Scheme 1-13).²³ The strained-ring system raises the ground state energy of **44** as compared to **39** and favors the cyclization pathway over elimination.



Scheme 1-13. Improved cyclization yields by use of strained cyclic dienyne.^{23a}

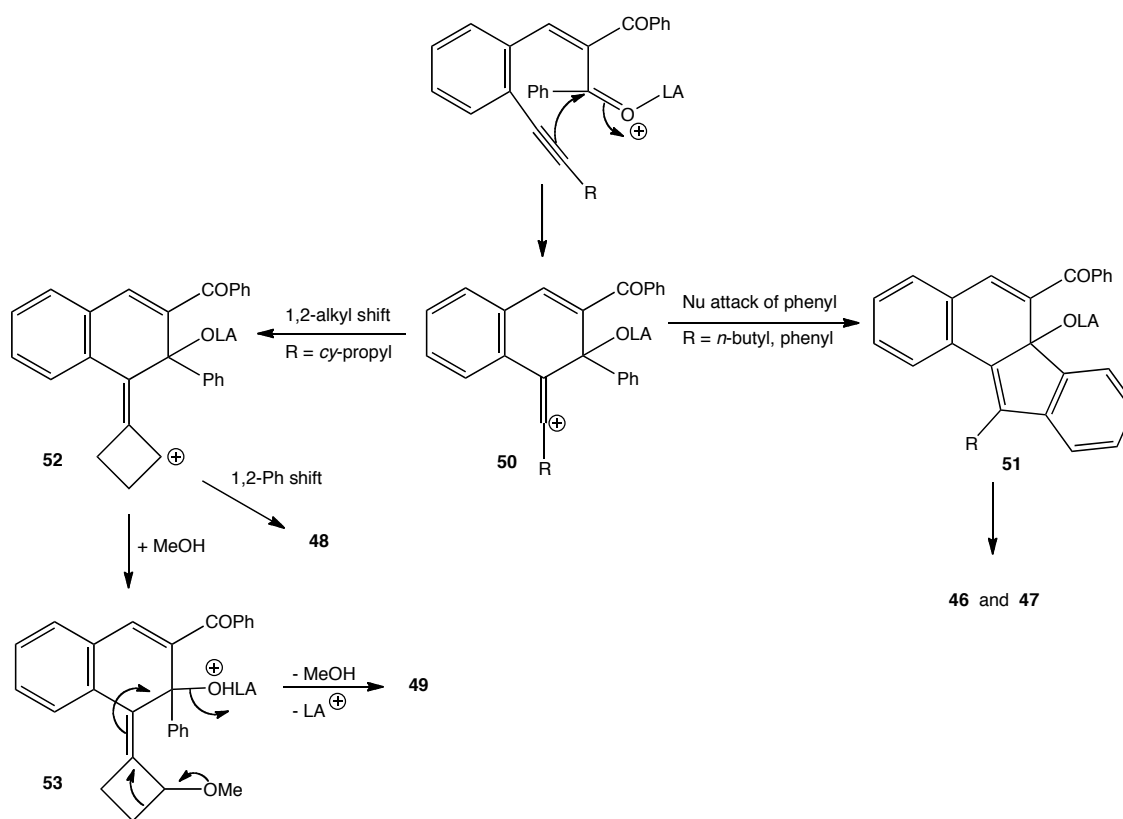
Zhang and Liu have utilized Lewis acids to activate dienyne ketones **45** for intramolecular nucleophilic attack to form several cyclized products depending on the alkyne substituent (Scheme 1-14).²⁴ Reaction of **45-Ph,Ph** or **45-ⁿBu,Ph** in the presence of a catalytic amount of AgSbF₆ resulted in the formation of cycloaromatized products **46** and **47**, respectively, in good yields. Use of cyclopropyl substituted alkyne **45-^cPr,Ph** afforded a mixture of naphthalen-2(1*H*)-one (**48**) and naphthalene (**49**) products in varying ratios depending upon the conditions. In general, it was found to be more difficult to obtain higher ratios of the aromatized product **49**, but it was favored by excess use of methanol under the optimized conditions with In(III) catalyst. Formation of **49** was limited to use of unsubstituted cyclopropyl substituents in substrate **45**. Any substitution on the cyclopropyl ring results in exclusive formation of **48**.



Scheme 1-14. Activation of dienynyl ketones under Lewis acidic conditions. Conditions: (a) AgOTf (5 mol %), 1,2-dichloroethane, 80°C, 12 h (b) In(OTf)₃ (5 mol %), 1,2-dichloroethane, MeOH (4 eq), 50°C, 48 h.²⁴

The proposed mechanisms for these transformations begin with Lewis acid coordination of the carbonyl that induces attack of the internal alkyne carbon to give **50** (Scheme 1-15). Intermediate **50** can then proceed through several pathways depending upon the alkyne substituent. For simple alkyl or aryl substitution, nucleophilic attack of the phenyl gives intermediate **51** that then isomerizes to aromatized products **46** and **47**. For cyclopropyl substitution, **50** proceeds through a 1,2-alkyl shift resulting in the formation of cyclobutyl cation **52**. Two pathways were proposed for **52** that lead to the two observed products, **48** and **49**. One pathway involves a pinacol rearrangement where the carbinol substituent undergoes a 1,2-shift to form cyclobutenyl substituted **48**. In the other pathway, cation **52** is trapped by an oxygen nucleophile before the pinacol can occur to form **53** (Nu = MeOH). Intermediate **53** is

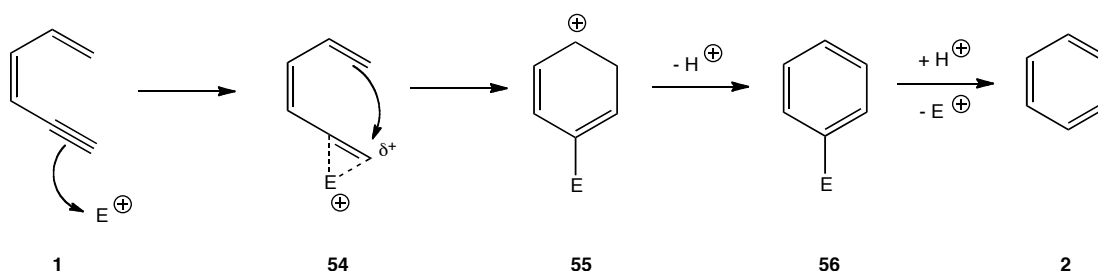
then proposed to proceed through a cascade of bond rearrangements to give the cyclopropyl substituted aromatized product **49**. In support of this latter pathway was the observation that formation of **49** was favored by use of added methanol, which would be expected to accelerate the formation of **53**. There appears to be a very interesting trend of the migratory ability of the transferring substituent (Ph in Scheme 1-15) from conversion of **52** to **48**. For example, reaction of methyl ketone **45-^cPr, Me** under the In(III) optimized conditions resulted in a > 20:1 ratio of **49** / **48**. The methyl group apparently has a lower ability to proceed through a 1,2-shift and therefore increases the rate of formation of **49**.



Scheme 1-15. Proposed intramolecular bond rearrangements for the formation of **46 – 49**.²⁴

V. Umpolung Activation of Alkyne

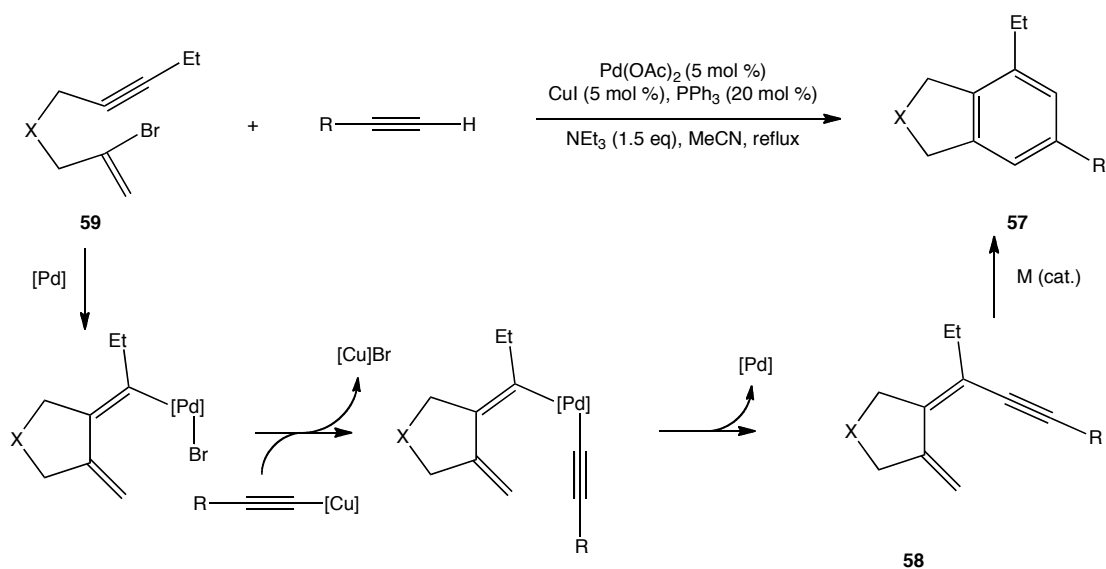
The higher energy π system of the alkyne makes an easy target for metal and non-metal Lewis and Brønsted acids and represents a well-studied mode of initiation for cycloaromatization of conjugated dienyne. The most general form of activation begins with formation of an alkyne complex (**54**) from reaction of dienyne **1** and an electrophile (Scheme 1-16). Formation of **54** results in a deficiency of electrons on the sp-hybridized carbon atoms and induces a 6-*endo-dig* attack of the terminal alkene leading to the cyclized product **55**. Subsequent aromatization by loss of proton gives **56**. If the electrophile is a metal (e.g. Pd, Pt, Au, In), proton exchange usually follows to give the formal Hopf product **2**. In line with the nucleophilic role of the terminal alkene, most reactions proceeding through this mechanism utilize electron-donating terminal alkene substituents to facilitate the cyclization.



Scheme 1-16. General mechanism for umpolung activation of alkyne.

The presumed first example of umpolung activation was by Torii and coworkers who were able to obtain cycloaromatized product **57** in moderate to high yield by *in situ* generation of dienyne **58** under a Sonogashira coupling platform (Scheme 1-17).²⁵ In support of a mechanism involving **58**, the reaction was slowed at room temperature with **59** ($\text{X} = \text{C}(\text{CO}_2\text{Me})_2$, $\text{R} = \text{C}(\text{OH})\text{Me}_2$) thereby permitting isolation of dienyne intermediate **58**. Refluxing the isolated intermediate in MeCN resulted in the formation of **57**. Although the [Pd] / [Cu] catalytic cycle

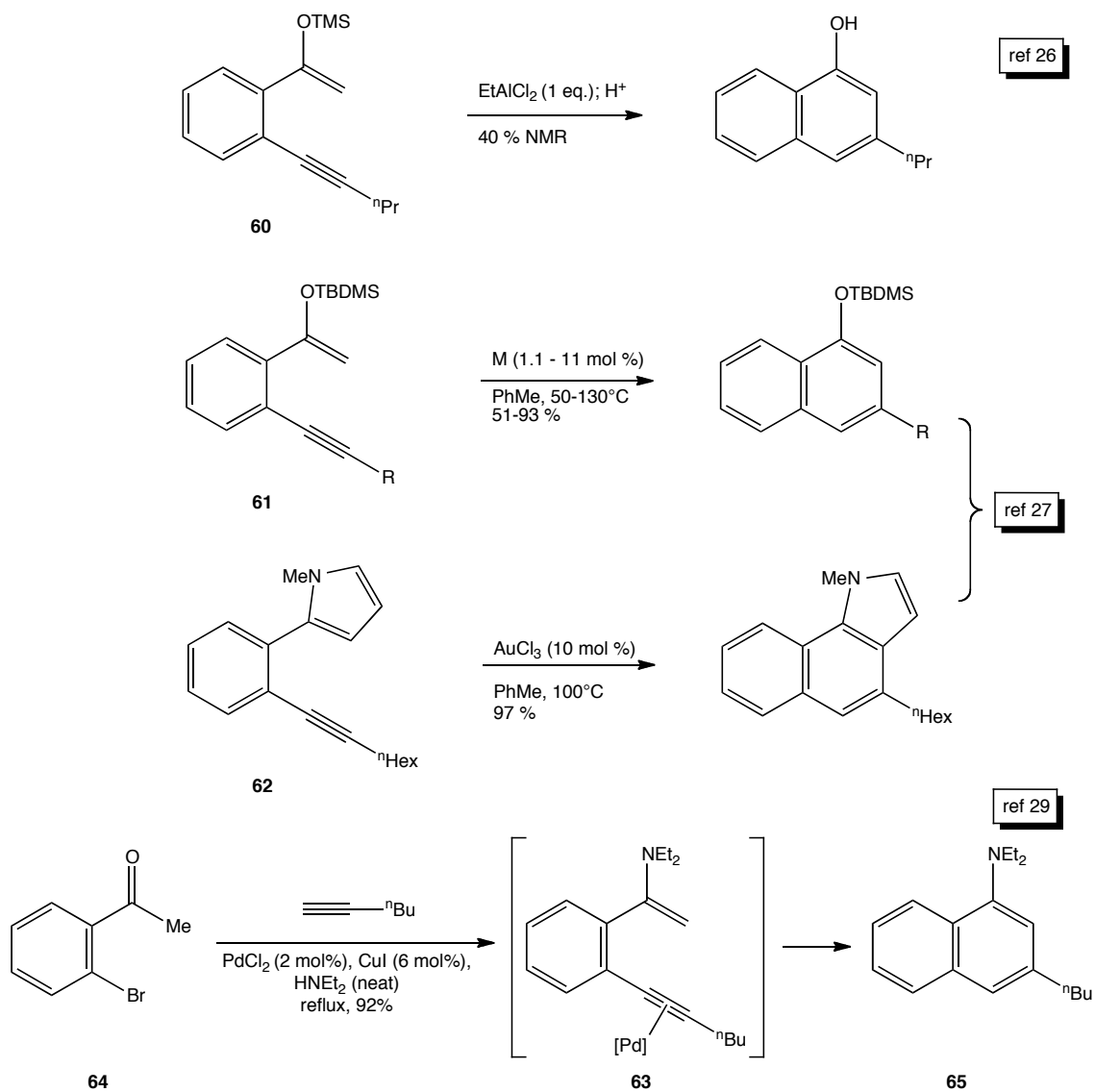
was hypothesized as the mechanism for formation of **58**, the pathway responsible for conversion of **58** to **57** was not discussed.



Scheme 1-17. In-situ generation of dienyne resulting in cycloaromatized product. $X = C(CO_2Me)_2$, NBn ; $R = C(OH)Me_2$, 1-hydroxycyclohexyl, CH_2OTHP , C_6H_{13} .²⁵

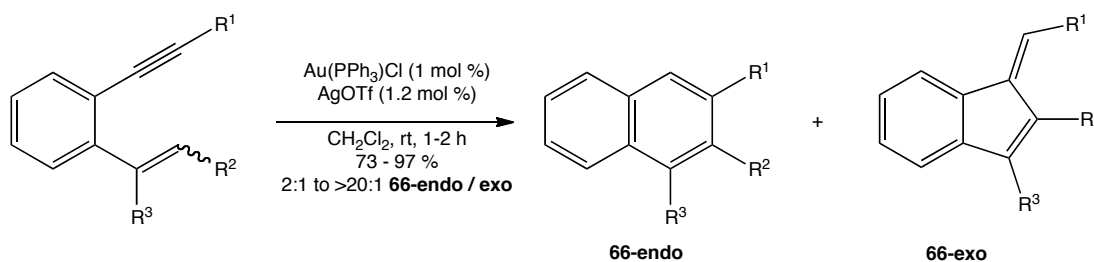
Towards synthesis of naphthalene derivatives by using **Type II**–*internal* dienynes, Yamamoto and coworkers reported cyclization of a silyl enol ether **60** as a single example in extension of their enyne cyclization methodology promoted by ethylaluminum dichloride (Scheme 1-18).²⁶ Dankwardt later published an extensive screen of metal catalysts able to thermally cyclize various silyl enol ethers **61**.²⁷ Among the many significant findings, he found that the cyclization could be conducted at room temperature using stoichiometric silver (I) trifluoroacetate ($AgOC(O)CF_3$) in nitromethane. The methodology was also applied to a series of pyrrole containing dienynes (e.g. **62**), giving cyclized product in excellent yield. Belmont and coworkers have used a similar procedure for the synthesis of acridine derivatives.²⁸ Herndon and coworkers have also made progress towards the use of dienynes for synthesis of nitrogen substituted naphthalenes by *in situ* generation of an enamine **63** from Sonogashira coupling of

bromide **64**. The transient **63** was then proposed to proceed through a 6-*endo* cyclization to give the 1-naphthalenamine product **65** in high yield. While the formation of **65** was high yielding, the methodology seems to be limited in scope as use of non-alkyl substituted alkynes (e.g. phenylacetylene, trimethylsilylacetylene) or increasing the alkyl substitution of the ketone α -carbon only resulted in isolation of the *ortho*-alkynyl arene product.

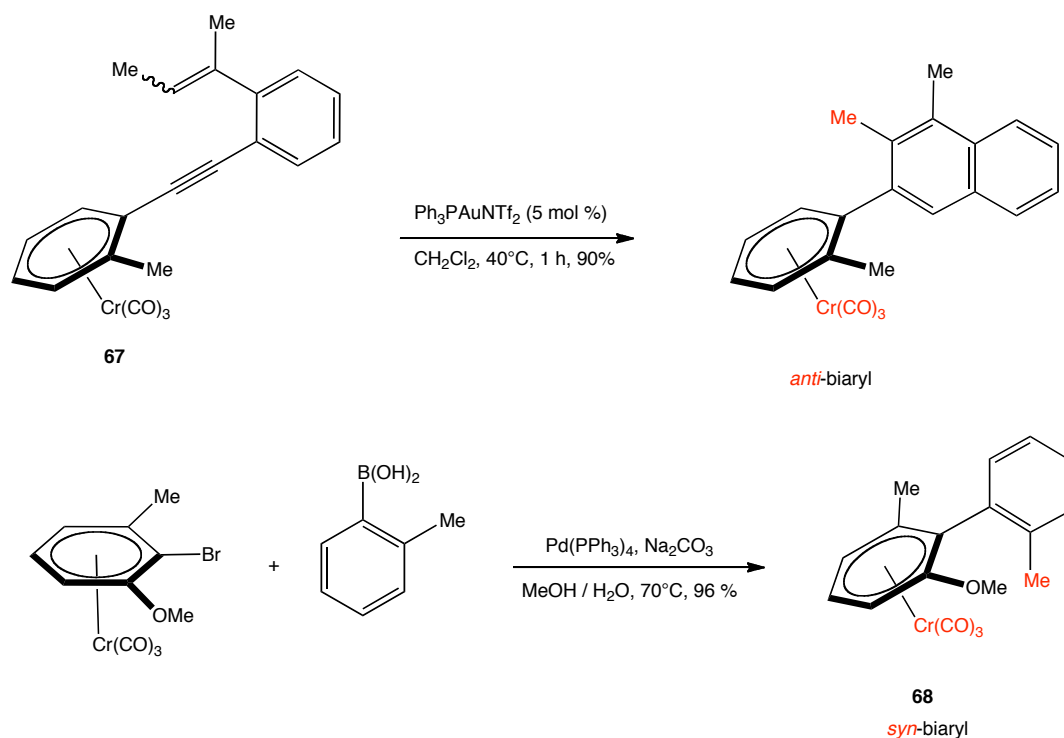


Scheme 1-18. Metal catalyzed cycloaromatization of dienynes possessing nucleophilic terminal alkene components. M = $[\text{Rh}(\text{CO})_2\text{Cl}]_2$, PtCl_2 , PdCl_2 , $\text{Pd}(\text{PhCN})_2\text{Cl}_2$, $[\text{RuCl}_2(\text{CO})_3]_2$; R = H, Me, $^{\text{n}}\text{Hex}$, CH_2Bn , Ph, $^{\text{t}}\text{Bu}$.^{26-27,29}

A major improvement for the synthesis of substituted naphthalenes was made by Shibata and coworkers who discovered that *in situ* generated Ph_3PAu^+ resulted in the high yielding formation of products **66** at ambient temperature (Scheme 1-19).³⁰ Generally, the 6-*endo* product **66-endo** was favored >20:1, yet in some cases, significant amounts of **66-exo** were formed ($\text{R}^1 = \text{CH}_2\text{N}(\text{Me})\text{Ts}$, I). Only geminally substituted nucleophilic alkene substrates were reported ($\text{R}^3 = \text{Me}$, Ph), presumably due to the stability of the carbocation intermediates. Uemura and coworkers have applied the gold cyclization methodology to dienynes possessing a planar chiral (η^6 -arene) CrCO_3 auxiliary (e.g. **67**) for stereoselective formation of axial chiral biaryl complexes (Scheme 1-20).^{31a-b} The major stereoisomeric product from these reactions has an *anti* relationship between the metal fragment and the *ortho* substituent of the biaryl junction. This route is a nice complement to the palladium-catalyzed coupling of these complexes that, in most cases, gives predominately the *syn* isomer (e.g. **68**).^{31c}



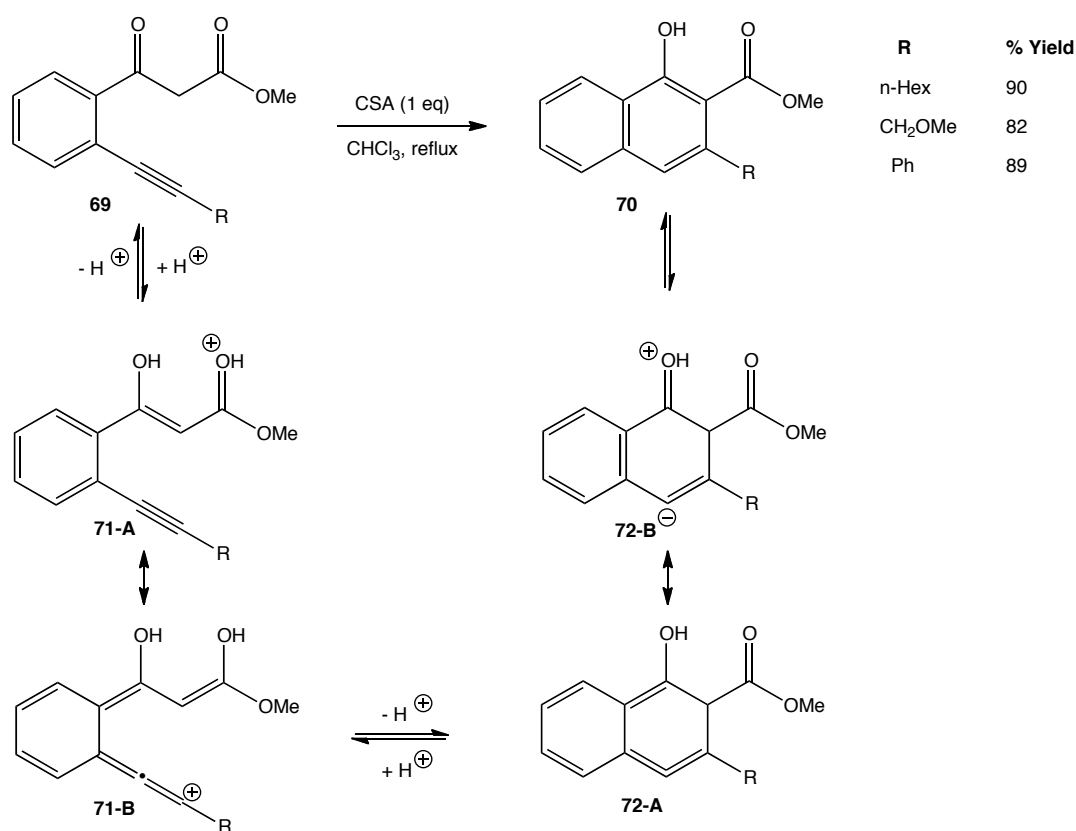
Scheme 1-19. Ambient temperature gold catalyzed cycloaromatization of geminal and tri-substituted terminal alkene **Type II-internal** dienynes. $\text{R}^1 = \text{Ph}$, CH_2OMe , CH_2OSiR_3 , CH_2OH , CH_2NMeTs , ^nBu , I; $\text{R}_2 = \text{H}$, Me; $\text{R}^3 = \text{Me}$, Ph.³⁰



Scheme 1-20. Complementary methods for synthesis of stereoisomeric pairs of biaryl complexes.³¹

Towards a metal free route to naphthalenes, Ciufolini and Weiss have described the use of camphorsulfonic acid (CSA) as a trigger for cyclization of *ortho*-alkynylphenyl- β -ketoesters **69** (Scheme 1-21).³² A variety of alkyne substitution was tolerated to give 1,2,3-substituted naphthalenes **70** in high yield. The reaction is thought to proceed through charged intermediates due to the inability of thoroughly purified samples of **69** to give any product under photolytic or thermal conditions. The proposed mechanism initiates by protonation of the tautomeric dienyne form of **69** giving cationic intermediate **71**. This structure has significant positive charge build-up on the terminal alkyne carbon due to resonance delocalization. Intramolecular nucleophilic attack of the enol and deprotonation gives allenic intermediate **72-A** that can be represented as a resonance hybrid with zwitterionic **72-B**. Proton exchange would then lead to the naphthalene product **70**. In support of this mechanism, calculations performed

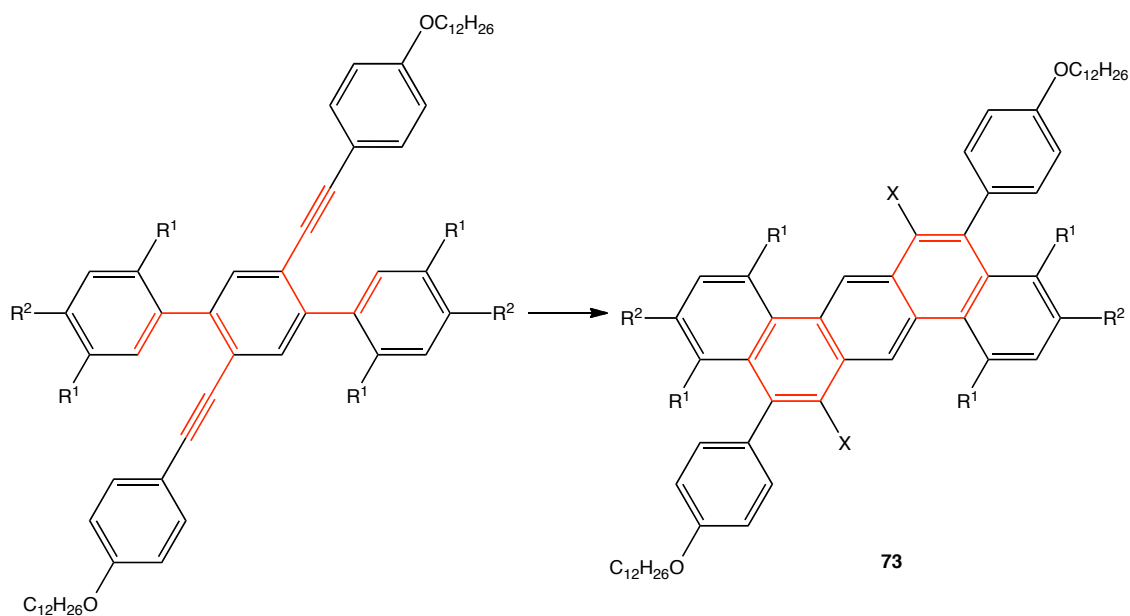
at the MNDO level of theory show the reaction from a structurally simplified enol form of **69** to the zwitterionic intermediate **72-B** is exothermic by $-3.7 \text{ kcal}\cdot\text{mol}^{-1}$.



Scheme 1-21. Acid catalyzed tautomeric dienyne **71-A** cycloaromatization.³²

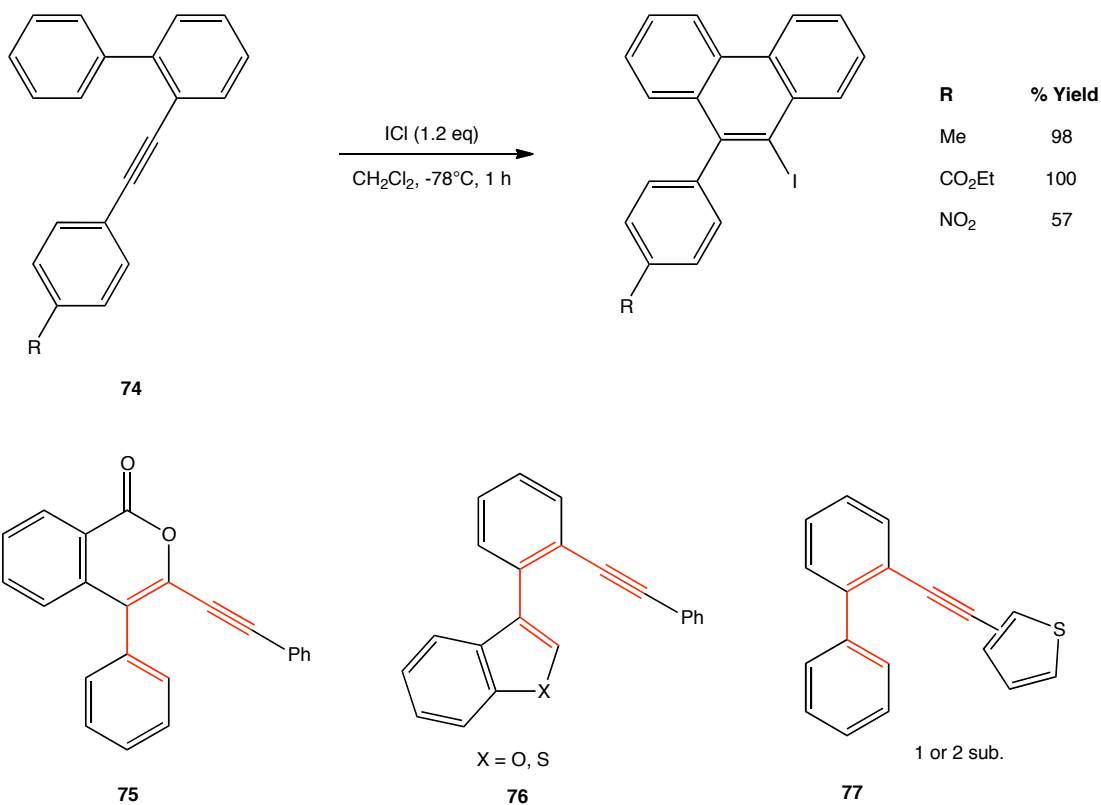
A significant amount of research has been directed towards triggering a Friedel-Crafts type cyclization of **Type III** dienynes to give substituted phenanthrenes which are useful building blocks for polycyclic aromatics.³³ Swager and coworkers first demonstrated the utility of such a transformation in the preparation of compound **73** with the ultimate goal of making fused polycyclic aromatic polymers (Scheme 1-22).³⁴ The reactions were extremely high yielding (> 90%) but required an alkyne substituted with an electron-donating group (*p*-phenyl-OC₁₂H₂₆) for cyclization to occur. When a cyclohexyl or phenyl substituted alkyne was used, the reaction

failed. Also interesting was the observation that the reaction only proceeded in polar non-nucleophilic solvents (i.e. CH_2Cl_2) and not in non-polar or etheral solvents. The solvent dependence suggested formation of carbocation intermediates.



Scheme 1-22. TFA and $\text{I}(\text{py})_2\text{BF}_4$ triggered cycloaromatizations in the formation of extended polyaromatic platforms. Conditions: $\text{CF}_3\text{CO}_2\text{H}$ ($\text{X} = \text{H}$) or $\text{I}(\text{py})_2\text{BF}_4$ ($\text{X} = \text{I}$); $\text{R}^1 = \text{OMe}, \text{Me}, \text{H}$; $\text{R}^2 = \text{H}, \text{OMe}$.³⁴

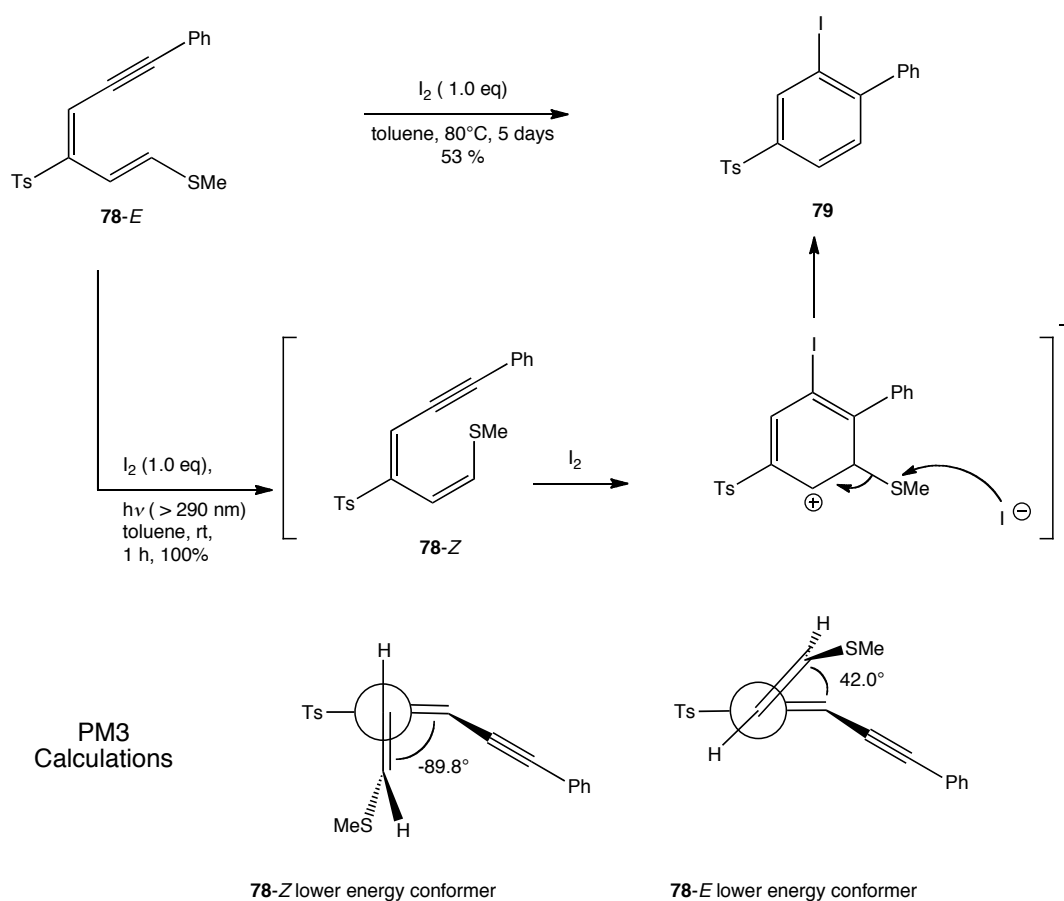
Larock and coworkers demonstrated that through the use of ICl as an electrophilic trigger even a *para*-substituted nitro phenyl substituted alkyne **74** ($\text{R} = \text{NO}_2$) would proceed to product albeit in moderate yield (Scheme 1-23).^{35a} These researchers also showed an expanded substrate scope by using several alternative alkene and alkyne components (i.e. **75** – **77**). In later studies, it was also shown that other stoichiometric electrophiles could also affect the cyclization.^{35b}



Scheme 1-23. Expanded alkyne substituent scope via use of ICl as the cyclization triggering reagent.³⁵

Ogura and coworkers have discovered an interesting photolytic dienyne cycloaromatization involving I_2 as an electrophilic trigger (Scheme 1-24).³⁶ Reaction of the *E*-vinyl methyl sulfide **78-E** with I_2 under thermal conditions proceeded very slowly, yet, photolyzing the reaction mixture gave quantitative yield of product **79** within 1 h. It was believed that the photolytic acceleration was due to an initial isomerization of **78-E** to **78-Z** as the latter is believed to cyclize faster. Proof of **78-Z** as an intermediate came from isolation of the species from the reaction mixture then independent cyclization with I_2 in the dark. The reason for the enhanced rate of cyclization of **78-Z** compared to **78-E** was not clear. Energy minimization calculations using PM3 level of theory showed the distance between the terminal alkene and alkyne carbons is larger for **78-Z** than **78-E** which does not correlate with the reactivity. One

major difference observed from the computational study was a significant difference in the central diene dihedral angle, calculated to be $+42.0^\circ$ for **78-E** and -89.8° for **78-Z**. From the discussion of this parameter, the authors seemed to suggest that better orbital alignment between the terminal alkene and alkyne π systems may be responsible for the increased reactivity.

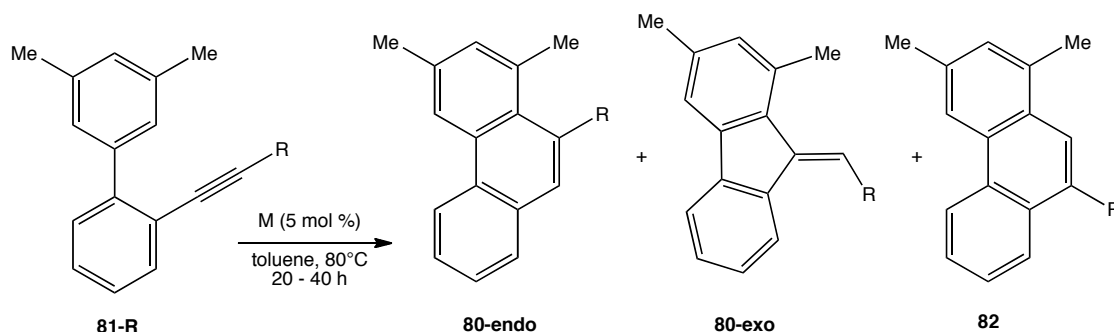


Scheme 1-24. Photolytic activation of cycloaromatization with iodine electrophilic triggering.³⁶

The earliest in-depth look at metal catalysis for the formation of phenanthrenes via dienyne cyclization was performed by Fürstner and coworkers over several publications.³⁷ Fürstner's work has been applied to many different systems.³⁸ Summarized in Table 1-2, are

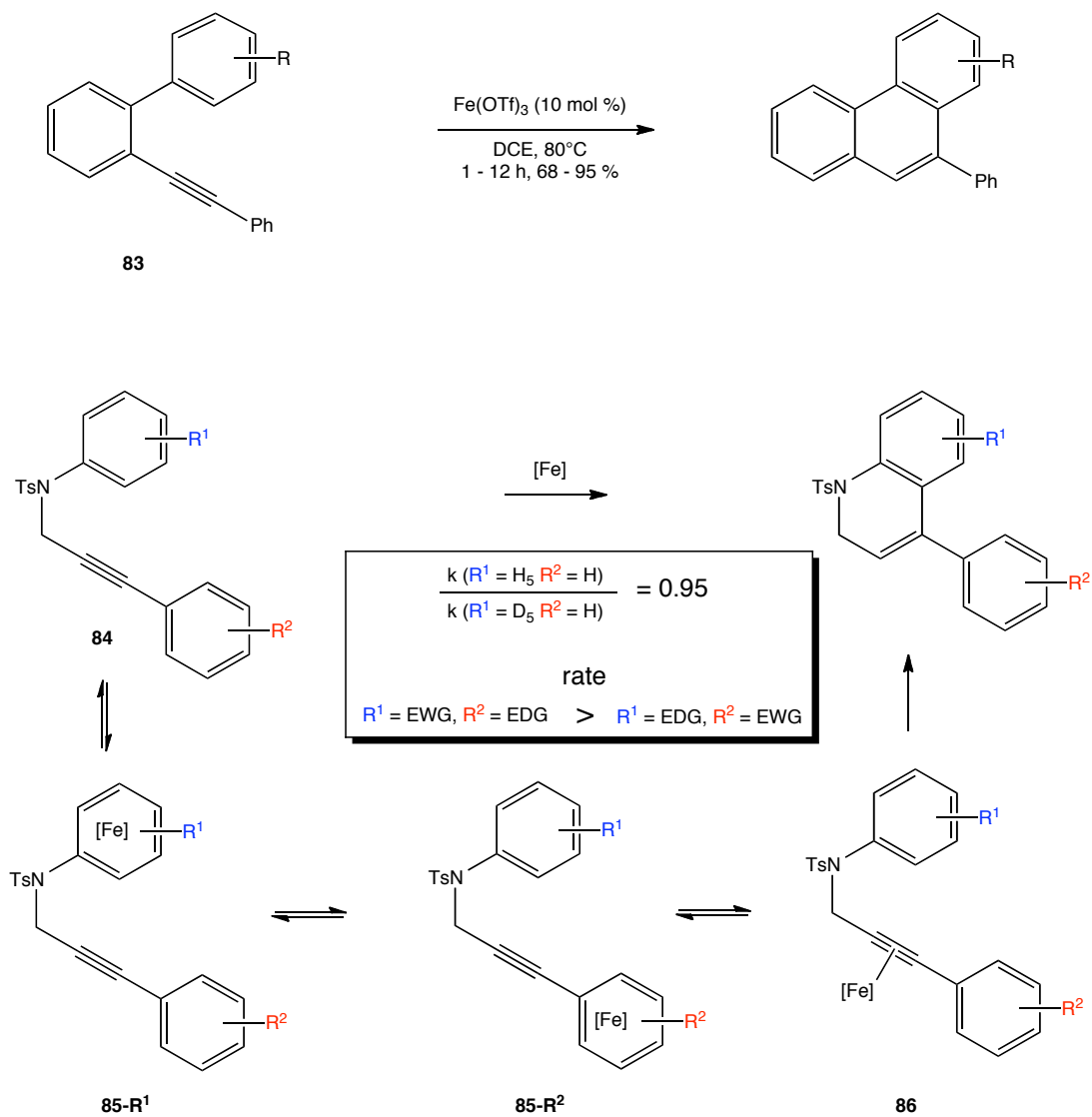
some key findings from their study. For cyclization of terminal and simple alkyl substituted alkynes, PtCl_2 was determined to be the most general high yielding catalyst although AuCl_3 and GaCl_3 also proved effective.^{37a} In general the reaction proceeds to the 6-*endo* product **80-endo** although use of an electron-withdrawing alkyne substituent **81-CO₂Me** gave almost exclusively the *exo* product **80-exo**. Reactions of alkynyl halides failed under PtCl_2 catalysis, but use of InCl_3 gave the halogenated **80-endo** in high yield with no detectable amount of the other regioisomer.^{37b} As an extension of the InCl_3 catalysis, these researchers used the methodology to prepare a biaryl natural product, *O*-methyldehydroisopiline. A surprising find came while testing halogenated alkynes **81-Br, I** with gold(I) chloride that resulted in the rearranged product **82**.^{37c} These researchers explained this unexpected reactivity to the formation of a gold vinylidene complex that then, presumably, proceeded to product through an initial 6π electrocyclicization (see Section VI).

Table 1-2. Summary of Fürstner and coworkers study of metal catalysis for the formation of phenanthrenes from diene cycloaromatization. (a) Yield not reported.³⁷



| M | R (% Yield) | % 80-endo | : | % 80-exo | : | % 82 |
|-----------------|-------------------------------------|-----------|---|----------|---|------|
| PtCl_2 | H (64) | 97 | | 3 | | 0 |
| | Me (89) | 100 | | 0 | | 0 |
| | CO ₂ Me (-) ^a | 5 | | 95 | | 0 |
| InCl_3 | Br (77) | 100 | | 0 | | 0 |
| | Cl (90) | 100 | | 0 | | 0 |
| AuCl | Br (77) | 0 | | 0 | | 100 |
| | I (76) | 0 | | 0 | | 100 |

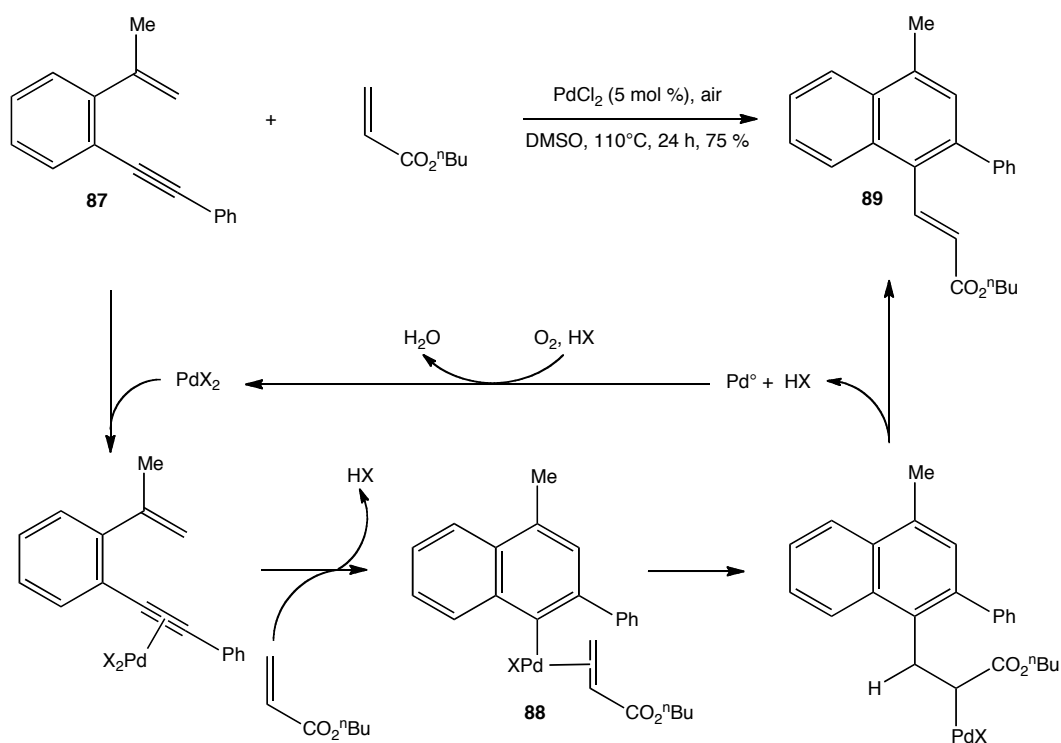
More recently, Takaki and coworkers have reported iron(III) triflate catalysis of *ortho* alkynyl substituted biphenyl arenes **83** (Scheme 1-25).³⁹ These studies were done in parallel with cyclization of arene-tethered alkynes **84**. The kinetic isotope effect (KIE) for the nucleophilic arene of **84** ($R^1 = H(D)_5 / R_2 = H_5$) was calculated to be 0.95 suggesting a Friedel-Crafts mechanism. Contrary to the KIE mechanistic implications, the rate of the reaction was observed to *increase* when the nucleophilic arene was substituted with an electron withdrawing group (EWG) while the alkyne phenyl substituent possessed an electron-donating group (EDG). To explain this, a pre-rate determining step equilibrium between Fe-arene complexes **85-R¹** and **85-R²** was invoked where only **85-R²** could deliver the metal to the alkyne to form the activated electrophilic complex **86**. Despite these interesting mechanistic studies, the dienyne substrates **83** do not seem to follow the arene electronic trend. Use of an EWG on the nucleophilic arene **83** ($R = NO_2, CN, CF_3$) increases the reaction time to > 6 h, where an unsubstituted arene ($R = H$) goes to completion within 1 h.



Scheme 1-25. Use of iron catalysis for diene cycloaromatization. R = 4-CN, 4-CO₂Me, 4-NO₂, 4-CF₃, 3,5-F₂, H, 4-OMe.³⁹

Although in most cases the metal-vinyl species **56** (E = Pt, Pd, Au, etc., Scheme 1-16) is lost by protonation, Loh and Feng were able to intercept this species with an alkene demonstrating the multi-component potential of the diene 6-*endo* cyclization (Scheme 1-26).⁴⁰ Using PdCl₂ to catalyze the cyclization of **87** allowed for metallated adduct **88** to enter into the Heck catalytic cycle to give the tri-substituted naphthalene **89**. Although many oxidants were

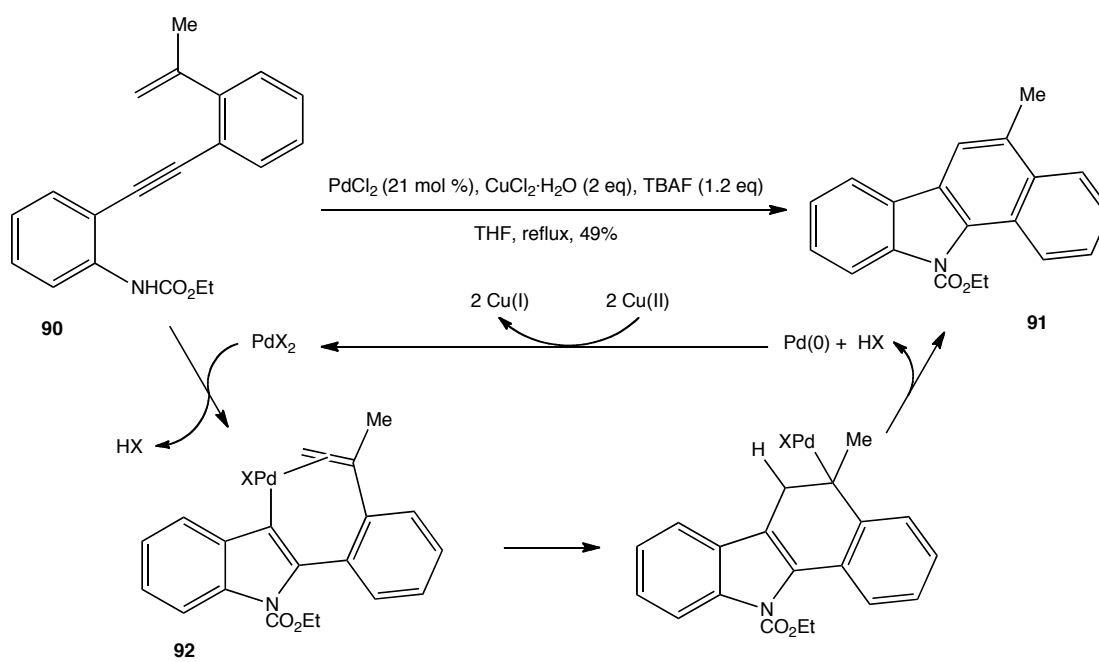
screened, none were able to substantially boost the yield much higher than by simple use of atmospheric oxygen. Although most examples utilized geminal-substituted alkenes, one case employed the use of a tri-substituted alkene that gave rise to a tetra-substituted naphthalene in 61% yield.



Scheme 1-26. One pot 6-*endo* cycloaromatization / Heck coupling.⁴⁰

The examples covered thus far have all used the terminal alkene as the nucleophile for attack on the activated alkyne. It is also possible to intercept the alkyne with an external or tethered nucleophile creating a species that can cyclize by other mechanisms. Yasuhara and coworkers were the first to implement this strategy for dienynes with the cyclization of *ortho*-alkynyl carbamates **90** to the substituted indole **91** under PdCl_2 catalysis (Scheme 1-27).^{41a} Initial attack of the carbamate gives vinyl palladium species **92** that proceeds through a

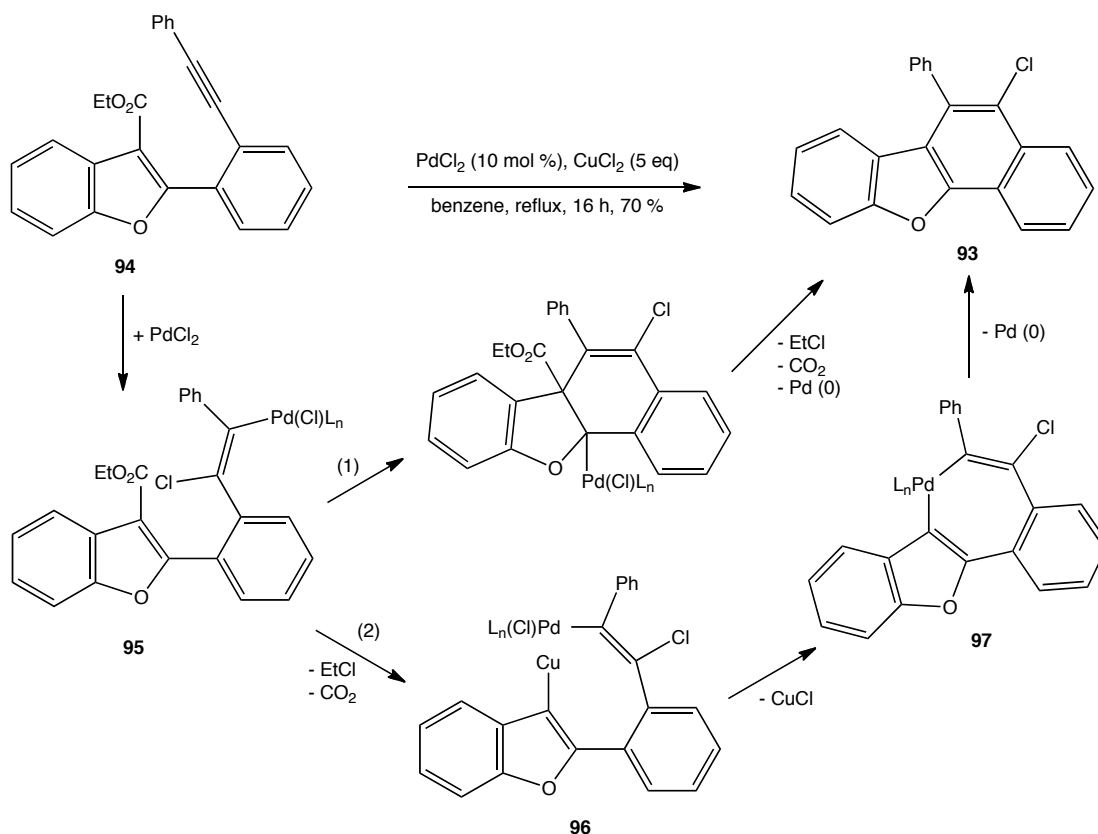
successive 1,2-insertion and β -hydride elimination to proceed to **91**. The role of TBAF (tetrabutylammonium fluoride) appears to be that of a mild base.^{41b}



Scheme 1-27. Capture of activated alkyne by tethered nucleophile coupled with Heck coupling to give cycloaromatized product.^{41a}

A related transformation reported by Li and coworkers towards the synthesis of polycyclic aromatic furan **93**, involved initial trans 1,2-insertion across the alkyne of the substrate **94** to give **95** (Scheme 1-28).⁴² The authors do not comment on how this insertion occurred, but it may be reasonable to propose a nucleophilic attack of the chloride on the palladium alkyne complex. From **95**, two possible pathways to **93** were proposed: (1) 1,2-insertion into the furan ring followed by decarboxylation with elimination of ethyl chloride and palladium to give the product **93** and (2) decarboxylation with elimination of ethyl chloride to form a vinyl copper species **96** that can transmetallate with palladium to proceed to product through metallacycle **97**. CuCl_2 has multiple roles in the reaction by providing a source of

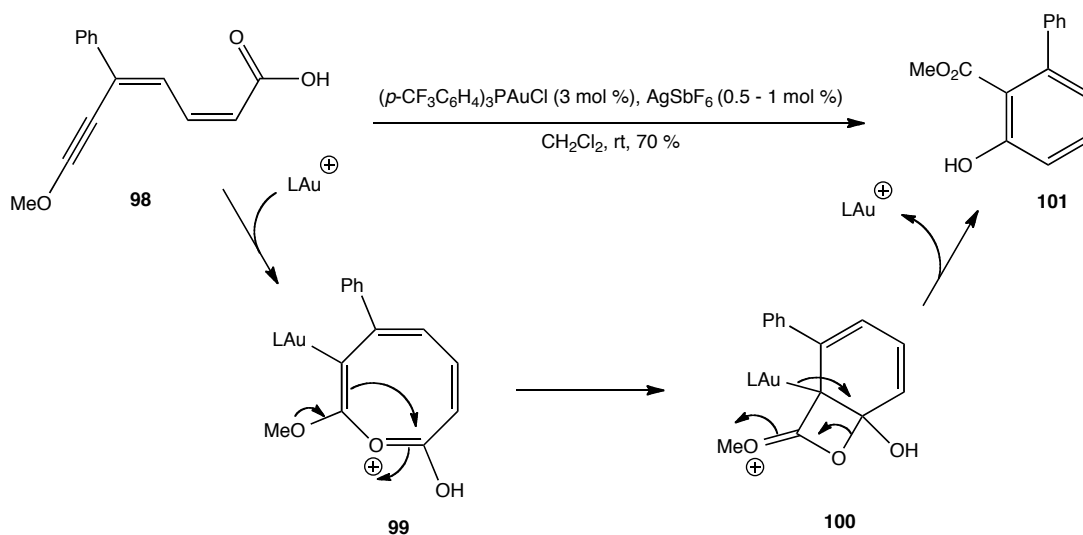
chloride, oxidizing the Pd(0) back to the active Pd(II), and potentially inducing decarboxylation. Use of LiCl in place of CuCl₂ resulted in no observation of product thus confirming at least one of the latter two roles of the reagent.



Scheme 1-28. Intermolecular capture of coordinated alkyne leading to aromatized product.⁴²

Aguilar and coworkers recently reported an impressive use of gold catalysis to induce an aromatization initiated by intramolecular nucleophilic attack of a pendent carboxylic acid.⁴³ The unusual *Z,Z* – dienyne substrate **98** can be prepared in a single step from a dialkynyl chromium carbene species.⁴⁴ Activation of the alkyne by the *in situ* generated cationic gold catalyst was proposed to induce an intramolecular nucleophilic attack of the carboxylate to give **99** which then ring closes to form bicyclic compound **100** (Scheme 1-29). Regeneration of the

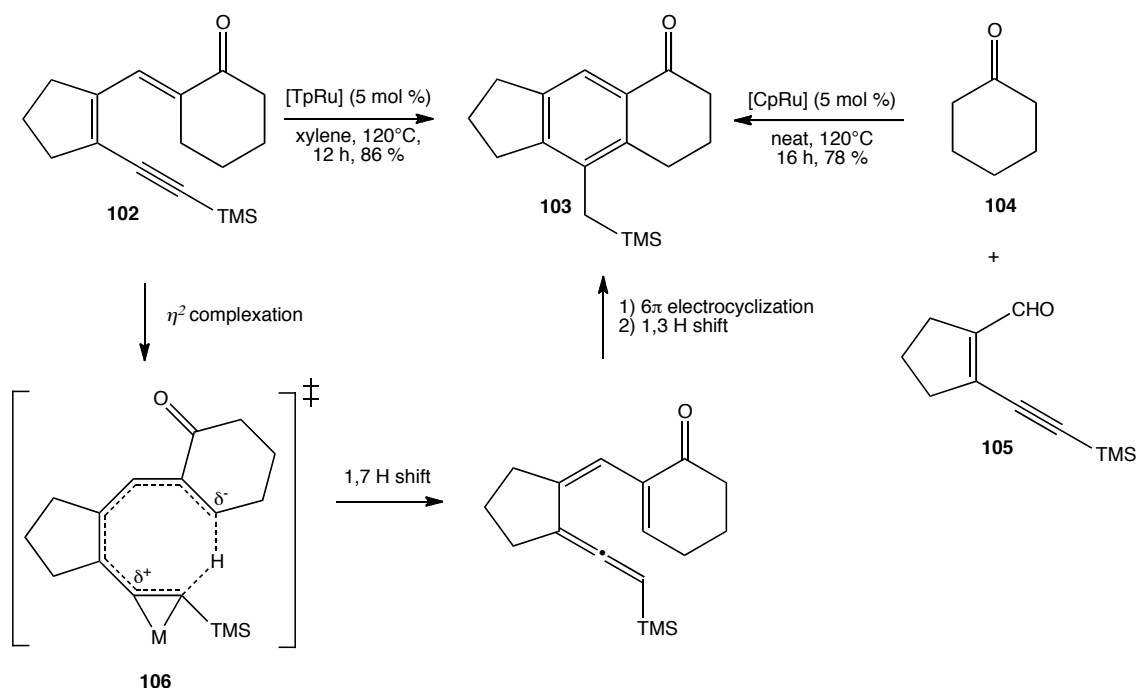
AuL⁺ species gives a 1,2,3-trisubstituted arene **101**. The reaction was dependent on the alkoxyalkyne substrate and use of aryl-substituted alkynes resulted in a 6 π electrocyclicization from an intermediate analogous to **99** that ultimately led to *meta*-substituted arenes after loss of CO₂.



Scheme 1-29. Gold catalyzed cycloaromatization of the *Z,Z*-dienyne **98**.⁴³

Liu and coworkers have demonstrated the use of ruthenium complexes to activate the alkyne for a [1,7]-H shift that ultimately leads to cycloaromatized product.^{5b} Dienyne structure activity studies show the reaction was most efficient with substrates containing an electron donating alkyne substituent and an electron-withdrawing terminal alkene substituent. Substrates without this substitution showed little enhancement with metal complexes over the non-catalyzed thermal reaction. A particularly successful dienyne, **102**, possess both of these characteristics and gives the aromatized product **103** in high yield (Scheme 1-30). The observation that dienynes containing an α,β -unsaturated ketone work well for the reaction, led these researchers to consider developing a one-pot Aldol condensation / cycloaromatization methodology as demonstrated by the reaction of cyclohexanone **104** with aldehyde **105**. The

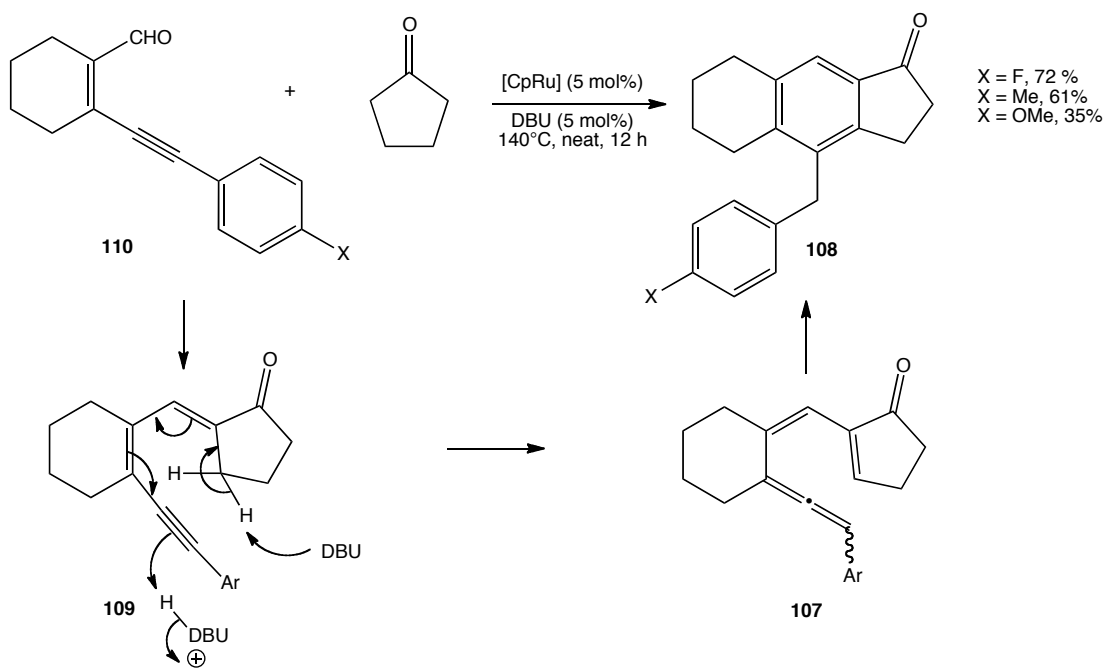
mechanism of this reaction is believed to proceed through an asynchronous transition state **106** for the [1,7]-H shift followed by a 6π electrocyclicization and [1,3]-H shift to give **103**. Consistent with the non-symmetrical nature of **106** are the observed structure activity relationships that are hypothesized to stabilize the developing charge in the transition state. The role of η^2 -complexation is two-fold: (1) distorting the geometry of the alkyne away from linearity thus facilitating the shift by proximity and (2) polarizing the π system to stabilize the positive charge build-up in **106**.



Scheme 1-30. [1,7]-H shift facilitated by η^2 -complexation. $[\text{TpRu}] = [\text{TpRu}(\text{PPh}_3)(\text{NCMe})_2]\text{PF}_6$, $[\text{CpRu}] = \text{CpRu}(\text{PPh}_3)_2\text{Cl}$.^{5b}

As alluded to in a footnote in Liu's initial publication, the [1,7]-H shift is facilitated by catalytic use of base (i.e. 2,6-lutidine, DBU). In later studies conducted by Liu and Yang regarding the tandem Aldol / aromatization reaction, the η^2 -complexation mechanism seems to have been abandoned or modified for a protonation / reprotonation sequence resulting in rate

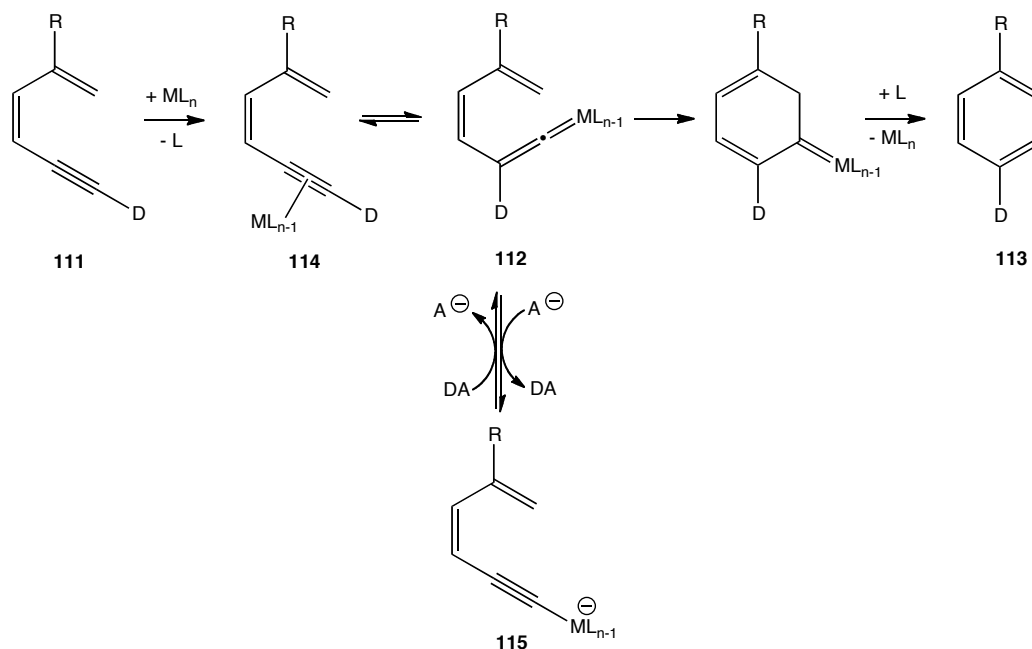
enhancement for the formation of allene **107** (Scheme 1-31).⁴⁵ Consistent with this mechanism, the highest yields of product **108** were obtained by use of electron deficient phenyl substituents on the alkyne as this would be expected to lower the pK_a of the allylic protons. The primary role of the metal catalyst in this system appears to be facilitating the Aldol reaction as a control experiment from dienyne **109** ($X = H$) gave near identical yields when the reaction was conducted with and without the metal (70% and 55%, respectively) whereas removal of the metal from the tandem Aldol reaction with aldehyde **110** resulted in a significantly lower yield (18% vs. 65% with metal).



Scheme 1-31. Formal [1,7]-H shift cycloaromatization pathway catalyzed by base. [CpRu] = CpRu(PPh₃)₂Cl.⁴⁵

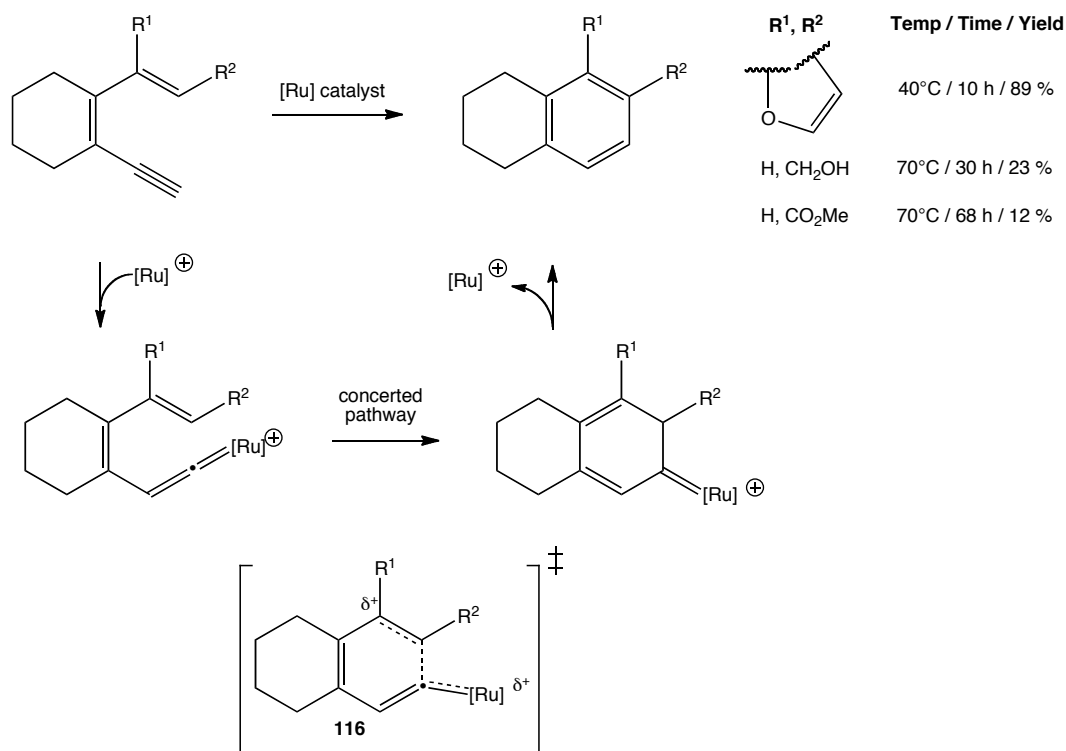
VI. Metal Vinylidene Triggered

Reaction of a dienyne possessing a terminal alkyne (i.e. **111**, Scheme 1-32) with certain transition metal complexes can result in the formation of a metal vinylidene complex **112**.⁴⁶ This reactive intermediate provides a common cycloaromatization route for dienynes by proceeding through a 6π electrocyclization and formal [1,2]-H transfer / demetallation to provide aromatic product **113**. Complex **112** is in equilibrium with the η^2 -alkyne complex **114** and many times it is difficult to determine which species is the true intermediate in the direct reaction pathway. As shown in Scheme 1-32, use of a deuterated terminal alkyne represents a common mechanistic experiment to determine if a metal vinylidene was formed as migration of the D-atom from the terminal to internal alkyne carbon should be observed. Depending on the metal and ligand environment, the vinylidene hydrogen can be relatively acidic and deprotonated with weak bases (e.g. basic alumina, for $ML_n = [Ru(PPh_3)_2Cp]^+$) to form a metal acetylide **115**. Thus use of a protic solvent often times results in partial loss of the isotopic label in **113**.



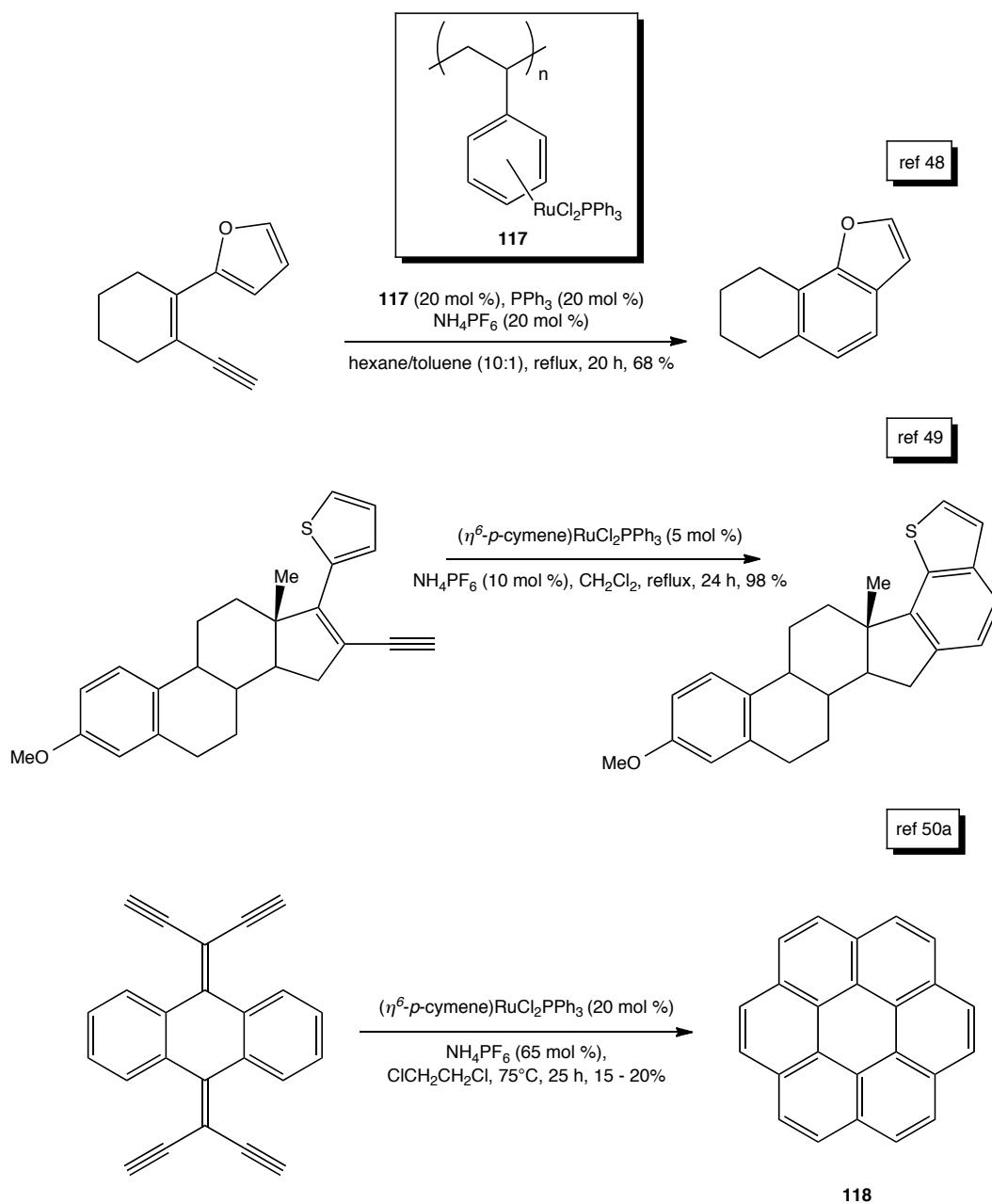
Scheme 1-32. General mechanism of dienyne cycloaromatization involving a metal vinylidene intermediate.

Merlic and Pauly were the first to demonstrate the feasibility of the metal vinylidene cycloaromatization pathway for dienyne (Scheme 1-33).⁴⁷ A variety of terminal alkene modified dienyne were shown to cyclize in relatively high yield under Ru(II) catalysis. It was observed that electron-rich terminal alkene substrates and electron deficient metal complexes provided the most efficient cyclizations. This substrate/catalyst dependence allowed these researchers to consider an asynchronous transition state **116** that would be stabilized by nucleophilic alkenes and electron-poor metals.



Scheme 1-33. First example of metal vinylidene diyne cycloaromatization. Conditions: (η^6 -*p*-cymene)RuCl₂PPh₃ (5 mol%), NH₄PF₆ (5 - 15 mol%), CH₂Cl₂ or ClCH₂CH₂Cl.⁴⁷

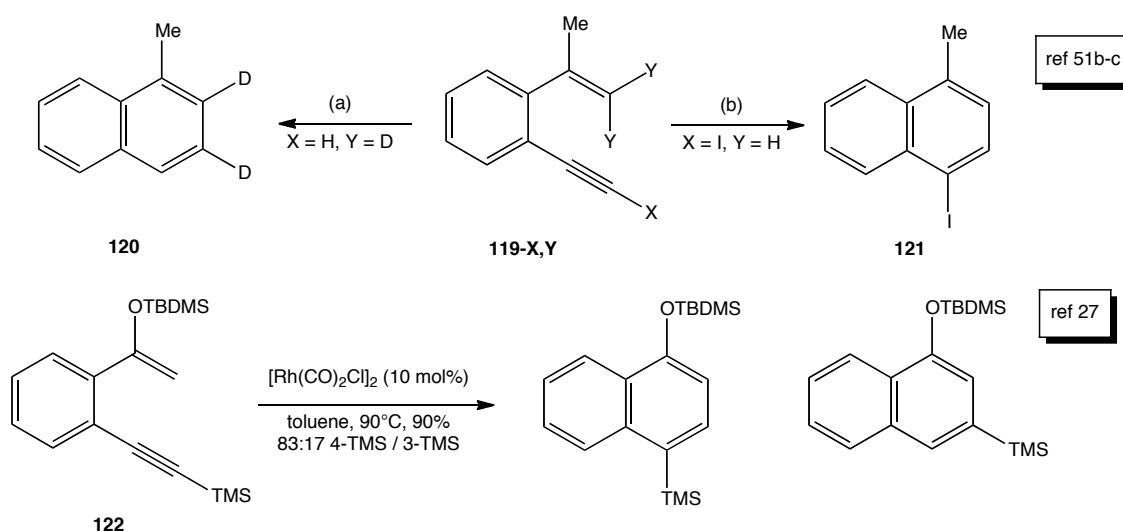
Merlic and Pauly's pioneering work has sparked many developments and applications with the same or related ruthenium systems. Kobayashi and Akiyama demonstrated use of a polystyrene ruthenium catalyst **117** for diyne cycloaromatizations along with many other metal catalyzed reactions (Scheme 1-34).⁴⁸ Thiemann and coworkers have used Merlic's system for synthesis of polyaromatic steroid derivatives.⁴⁹ The research group of Scott as well as Liu have also utilized the potential of ruthenium vinylidenes in the synthesis of coronene (**118**) and heteroatom derivatives of coronene.⁵⁰



Scheme 1-34. Applications of metal vinylidene diene cycloaromatizations.⁴⁸⁻⁵⁰

Iwasawa and coworkers have developed use of $(\text{CO})_5\text{W}\cdot\text{THF}$ as a cyclization promoter in either stoichiometric or catalytic amounts.⁵¹ In addition to the standard acetylenic deuterium labeling experiment (Scheme 1-32), it was shown that by allowing the geminal dideuterio diene **119-H,D** to react with $(\text{CO})_5\text{W}\cdot\text{THF}$ resulted in incorporation of the D label into the 2

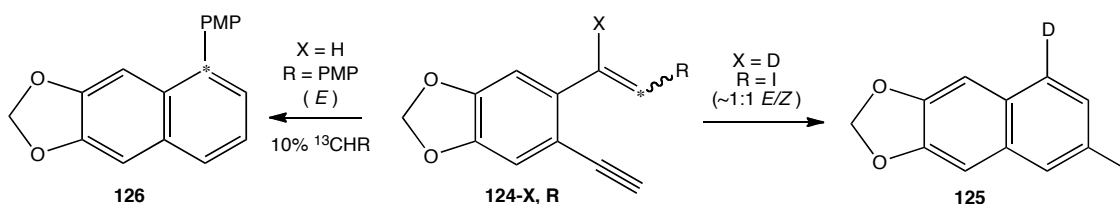
and 3 positions of the product naphthalene **120**, thus indicating a 1,2-shift for the alkene hydrogens (Scheme 1-35).^{51b} One of the most impressive features of the tungsten system was the ability to form the intermediate metal vinylidene with an iodoalkyne substrate **119-I,H** thus allowing formation of an aromatic iodide **121**.^{51c-d} Dankwardt has also shown and proposed that silyl substituted alkynes (e.g. **122**) undergo 1,2-shifts through a vinylidene mechanism.²⁷



Scheme 1-35. Vinylidene cycloaromatizations resulting in 1,2-shift of non-hydrogen substituents. (a) (CO)₅W·THF (1 eq), THF, 1 day, rt. (b) (CO)₅W·THF (1 eq), THF, 15 h, rt.^{27, 51b-c}

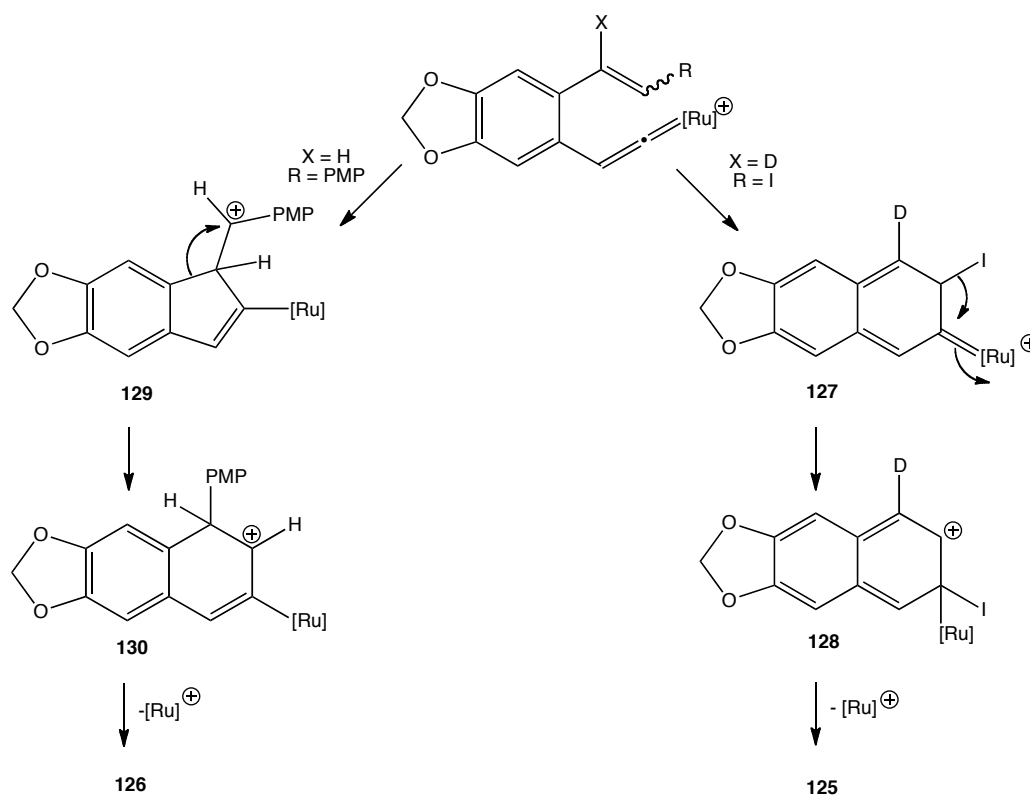
Liu and coworkers have uncovered many impressive skeletal rearrangements from studies on the formation of cationic vinylidenes resulting from use of [TpRu(PPh₃)(NCMe)₂]PF₆ (**123**, Tp = *tris*-pyrazolylborate) and vinyl substituted dienynes (Scheme 1-36).⁵² In their initial findings, the reactions of vinyl substituted dienynes **124** with **123** were found to undergo formal 1,2-shifts, but in opposite directions depending on the terminal alkene substituent.^{52a} Reaction of the vinyl iodide **124-D, I** with catalytic amounts of the metal complex resulted in a 1,2-shift of the iodine to the 7-position of the naphthalene **125** in 80% yield. The reaction also works with the vinyl bromide, but the yields are substantially lower for most substrates. Use of an electron-

rich aryl group as a substituent on the terminal alkene carbon **124-H**, **PMP** (PMP = *p*-methoxyphenyl) resulted in a 1,2-shift of the aryl group to the 5-position of the naphthalene to yield **126** as the major product in 73% yield. To provide some mechanistic insight, isotopic labeling experiments with ^{13}C enriched aryl substituted **124-H**, **PMP** were performed and resulted in the incorporation of the label into the 1-position of **126**, ruling out a direct 1,2-aryl shift.



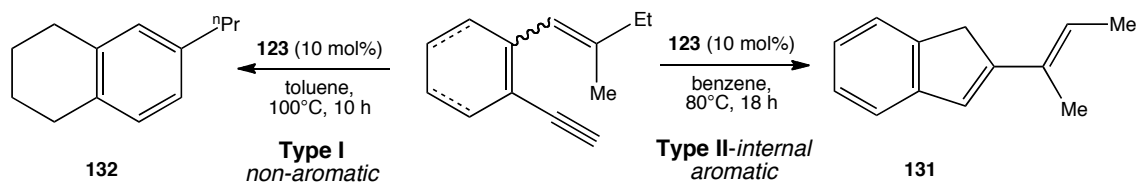
Scheme 1-36. Isotopic labeling experiments probing mechanism of $[\text{TpRu}(\text{PPh}_3)(\text{NCMe})_2]\text{PF}_6$ (**123**) catalyzed cycloaromatization / formal 1,2 – substituent shifts. Conditions: **123** (8 - 10 mol %), toluene, 110°C , 6 - 8 h. * = ^{13}C enriched carbon, PMP = *para*-methoxyphenyl.^{52a}

The proposed mechanisms for these transformations are shown in Scheme 1-37. The halogen-rearranged product **125** was hypothesized to occur through a simple 1,2-halide shift from cyclized intermediate **127** to give **128** followed by regeneration of the catalyst. The aryl shift was postulated to occur by initial 5-*endo-dig* cyclization to give carbocation intermediate **129**, the formation of which was facilitated by the strong electron-donating *para*-methoxy aryl group. A 1,2-shift of the ring carbon-carbon bond then gives **130** thus validating the carbon isotopic labeling results. Loss of ruthenium from this species would then give the observed product **126**.



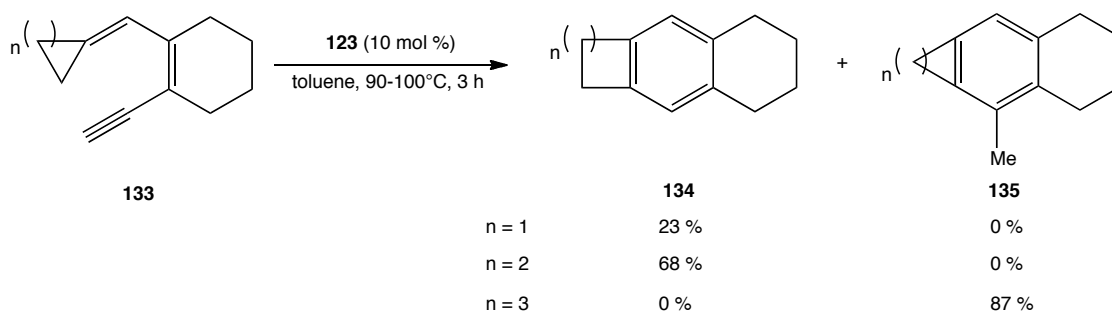
Scheme 1-37. Proposed mechanistic pathways for formation of the 1,2-halide and aryl shift products.^{52a}

The reactivity of dienynes with geminal disubstituted terminal alkenes with **123** were found to be very sensitive to the electronic and structural environment of the substrate. For example, reaction of a **Type II-internal** dienyne resulted in a non-aromatization pathway to indene **131** (Scheme 1-38).^{52b} Simply changing to a **Type I** dienyne reverses the reactivity back to a cycloaromatization pathway to give **132**.^{52c} The formation of **131** was believed to involve a non-classical carbocation species and the reader is referred to the cited reference for a full discussion of the mechanism. A mechanistic proposal for the formation of **132** was not given.



Scheme 1-38. Dependence of electronic nature of alkene of reaction pathway.^{52b-c}

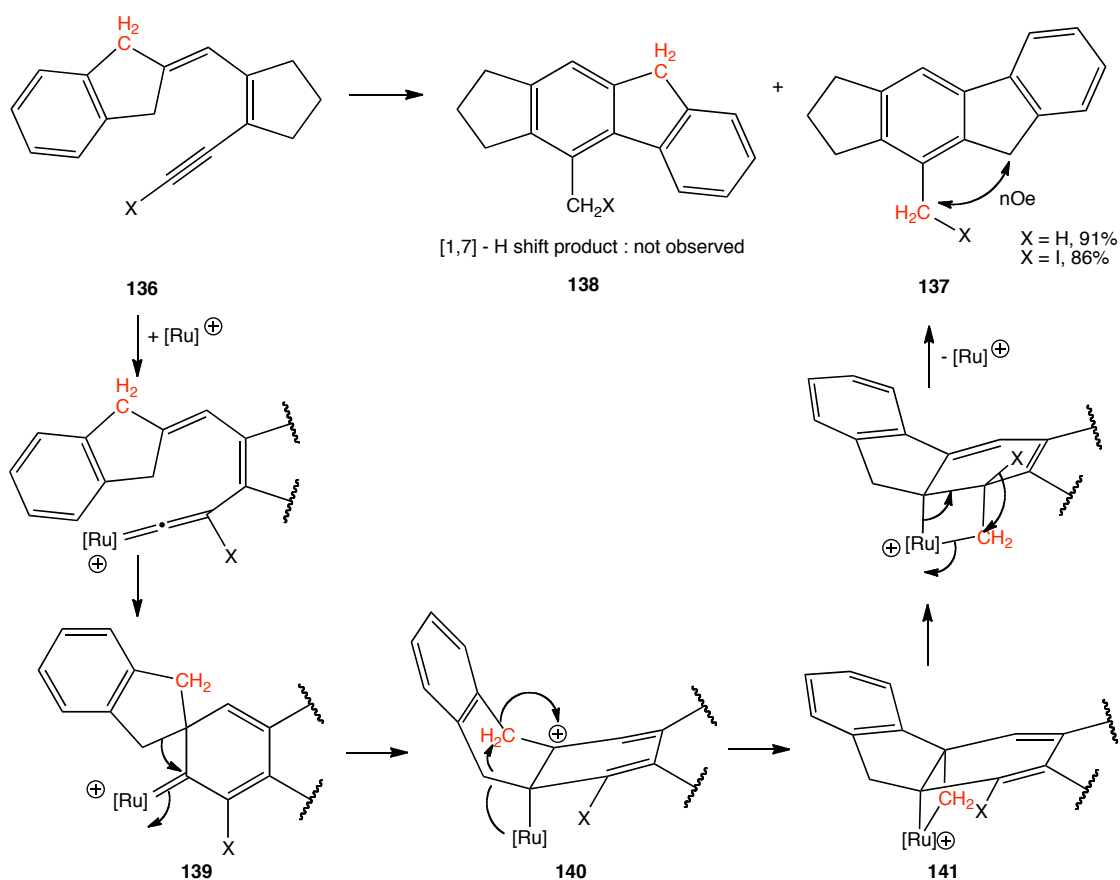
Cyclic alkylidene substrates open up yet another reaction pathway for dienynes under catalysis by **123** (Scheme 1-39).^{52c} Use of cyclopropylidene ($n = 1$) and cyclobutylidene ($n = 2$) dienynes **133** resulted in a 1,2-alkyl shift to afford **134** presumably formed by a similar mechanism to **125**. Increasing the cyclic alkylidene chain to a 5-membered ring ($n = 3$) results in formation of **135**.



Scheme 1-39. Changing reactivity of alkylidene substituted dienynes as the carbon tether size increases.^{52c}

One mechanistic possibility that would lead to **135** would initiate from a [1,7]-H shift of a methylene hydrogen (see Scheme 1-30). This mechanism was ruled out by use of substrates such as **136** that give an alternative product **137** to one originating from a [1,7]-H shift (**138**, Scheme 1-40). The relative connectivity of the ortho substituents in **137** was verified by nOe of the acyclic benzylic position. Use of the iodo and deuterated alkynyl substrates ($X = I$ & D , resp.) as well as deuteration of both cyclopentylidene methylene positions in **136** confirmed a

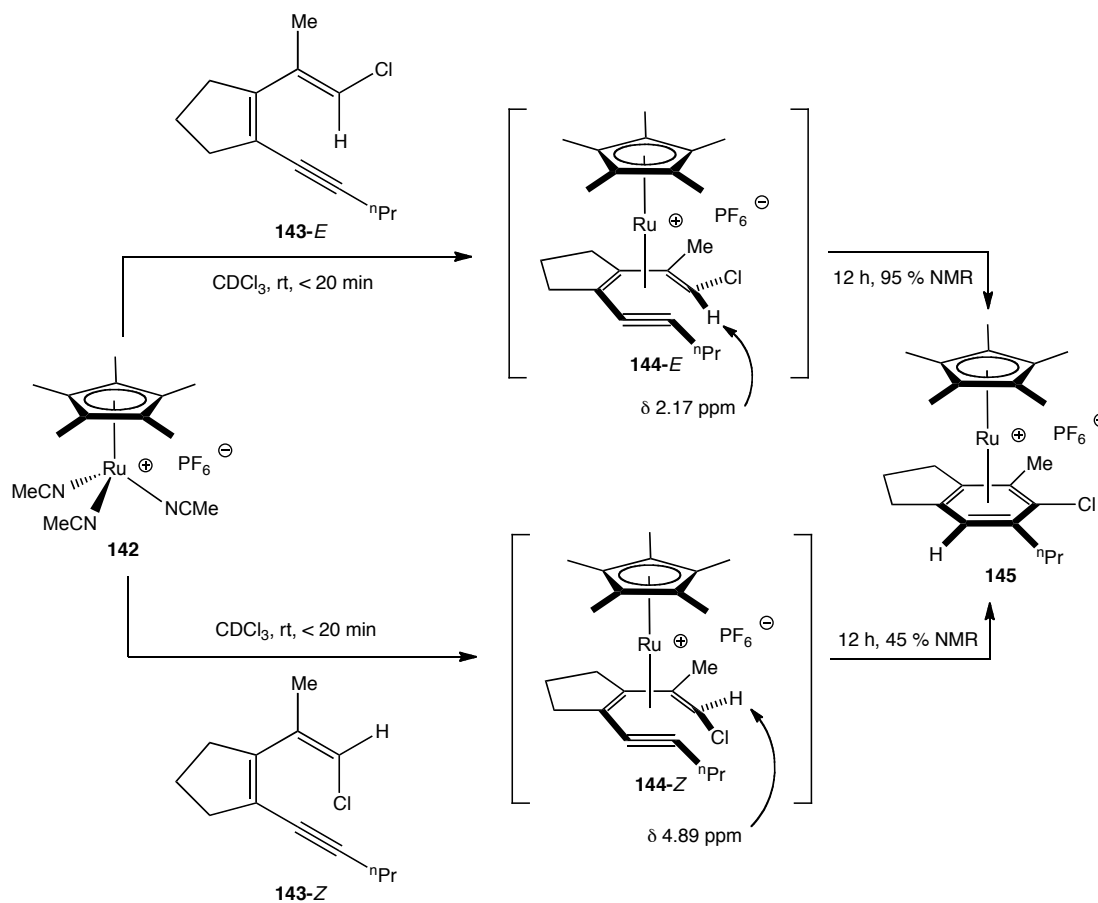
bond scission of the *trans*-methylene (red). To account for this unusual reactivity, Liu has put forth the mechanism shown in Scheme 1-40. From the vinylidene 6π electrocyclization product **139**, 1,2-alkyl shift gives cationic complex **140**. This species is proposed to undergo a metal-assisted 1,2-phenyl shift to give metallacycle **141**. [1,5]-alkyl shift of the metallacycle's methylene followed by 1,2-migration of the original alkyne substituent X and loss of the metal gives **137**.



Scheme 1-40. Proposed mechanism for 1,3-methylene migration. Conditions: **123** (10 mol %), toluene, 100°C, 1.5 h.^{52c}

VII. η^6 -Coordination of π System

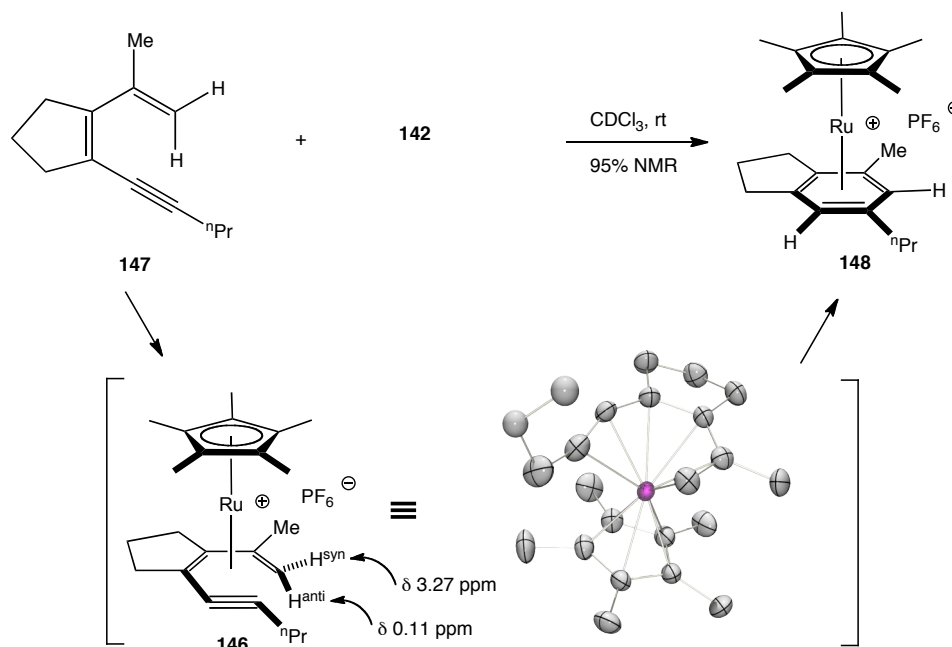
O'Connor and coworkers discovered that use of cationic cyclopentadienyl ruthenium complexes cyclize **Type I** dienyne in high yield to form η^6 – arene complexes.⁵³ Reaction of $[\text{Cp}^*\text{Ru}(\text{NCMe})_3]\text{PF}_6$ (**142**) with both dienyne **143-E** and **143-Z** led to immediate formation of a different transient metal-dienyne complex **144** as observed by NMR spectroscopy for each isomer (Scheme 1-41).^{53b} This *in situ* formed complex slowly converted to product **145** over the course of 12 h. These species displayed key ^1H NMR resonances at δ 2.17 (s, 1H) for **144-E** and δ 4.89 (s, 1H) for **144-Z** that provide good correlation by chemical shift to the H^{anti} and H^{syn} of related ruthenium η^4 -diene complexes, respectively. Furthermore, integration of the free acetonitrile resonance for the reaction with **143-E** indicated ~ 9 H relative to **144-E**, providing evidence that all components of the dienyne π system may be involved in the coordination sphere consistent with an η^6 -dienyne structure. As demonstrated by the yields for the reaction of **143-E** and **143-Z**, the *trans*-stereoisomer gives cleaner formation of the product **145**.



Scheme 1-41. NMR observation of transient species in $[\text{Cp}^*\text{Ru}(\text{NCMe})_3]\text{PF}_6$ (**142**) triggered cycloaromatization of 1-chlorodienynes.^{53b}

Unequivocal proof for the η^6 -coordination mode came from single-crystal X-ray characterization of a crystalline sample obtained at low-temperature of the analogous transient species **146** from the reaction of diene **147** with **142** (Scheme 1-42). Consistent with the structures of **144-E** and **144-Z**, **146** showed both an upfield and downfield vinyl CH resonance corresponding to H^{anti} and H^{syn} , respectively. The solid-state structure of **146** contained some very impressive bond metrics such as a distorted alkyne triple bond ($\angle\text{C}^{\text{sp}2}\text{C}\equiv\text{C}$: $151.8(4)^\circ$ and $\angle\text{C}\equiv\text{C}\text{C}^{\text{sp}3}$: $156.8(4)^\circ$), a decreased non-bonded distance between the terminal alkyne and

alkene carbons of 2.80 Å, and a Ru - H^{anti} distance of 2.20 Å (in range of a metal-agostic interaction).

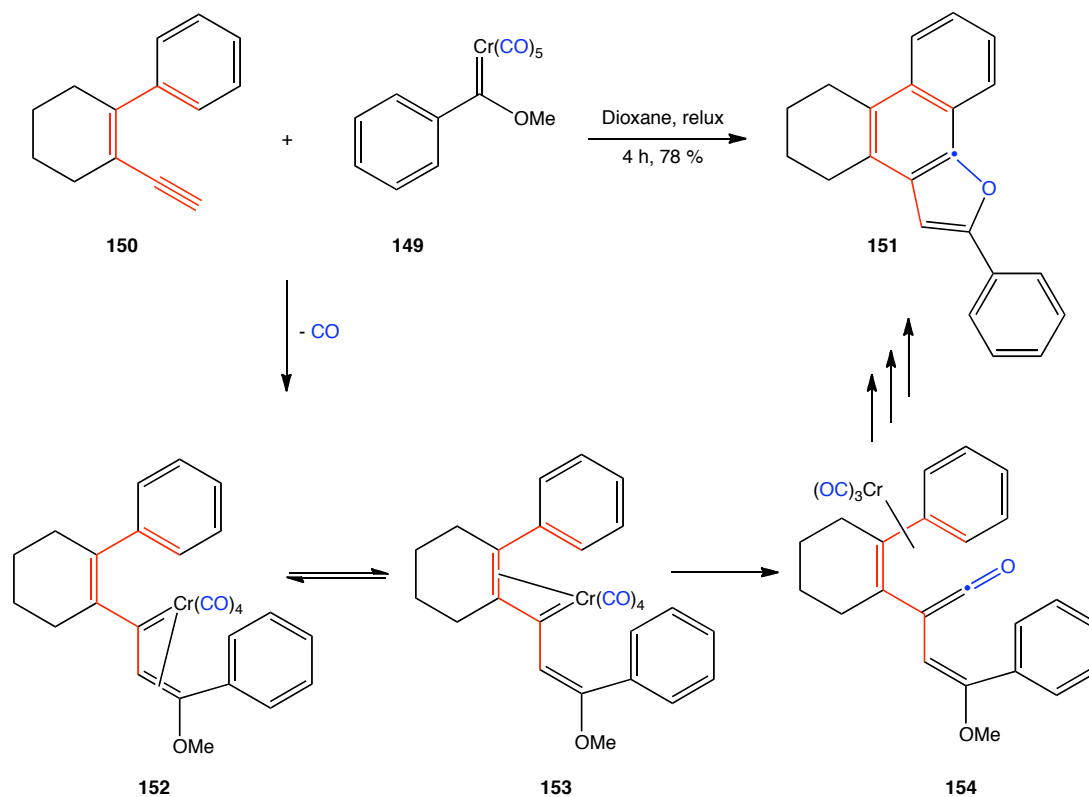


Scheme 1-42. X-ray characterization of η^6 -dienyne.^{53b}

Although these researchers were not able to definitively show **146** lies on the direct reaction coordinate to **148** therefore differentiating this mode of activation from other possibilities (i.e. η^2 -alkyne coordination), the proximity of the terminal carbons of the π system and the short Ru-H^{anti} distance seems to be indicative of a reaction intermediate. While the transformation gives the cyclized product in high yield at ambient temperature, a stoichiometric amount of ruthenium complex is required and removal of the metal fragment from the aromatized product is not always trivial.

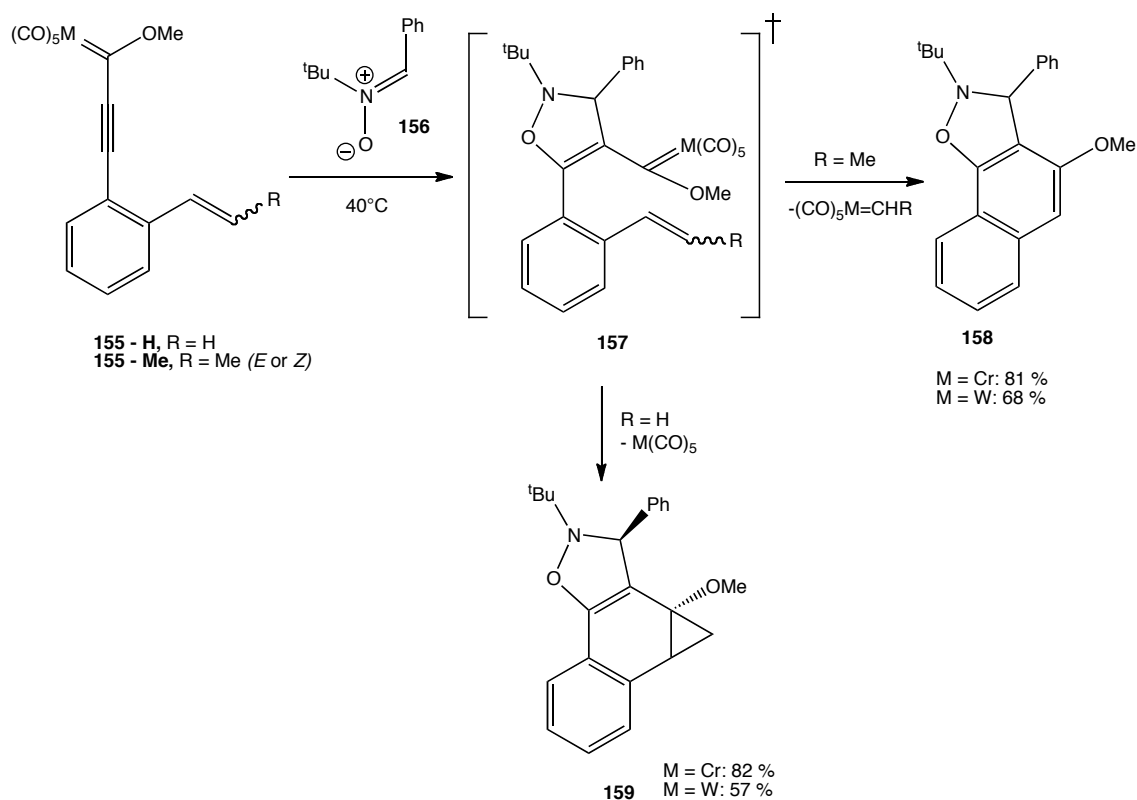
VIII. Metal carbene Induced

Herndon and coworkers have extensively studied the use of chromium pentacarbonyl Fischer carbene complexes (e.g. **149**) to induce cycloaromatization of dienyne using the common Dötz reaction platform (Scheme 1-43).^{54,55} In their initial report, 1-aryl-2-alkynyl-cyclohexenes **150** were found to react with metal carbene **149** to give cycloaromatized products of type **151** in high yield.^{53a} Although the example shown in Scheme 1-43 demonstrates use of a **Type II-terminal** dienyne, **Type I** dienyne were also shown to be effective substrates as well.^{54b} One substrate limitation was use of **Type II-internal** dienyne.^{54c} This can be explained by analysis of the potential equilibrium between the possible η^3 -vinylcarbene intermediates, **152** and **153**, formed during the reaction. It is known that electron-donating substituents in the coordination sphere of the η^3 -vinylcarbene inhibit the CO insertion step. Therefore **153** with a less electron-rich alkene should be expected to insert faster to give ketene **154** that proceeds to the observed product **151**. If the central alkene of the dienyne is inhibited from forming a complex with the Cr metal center, as the case with a **Type II-internal** dienyne, then only **152** would be able to react further either by cycloaromatization if a γ -vinyl or aryl group is present in the chromium carbene **149** or through other pathways such as CH insertion. Although **Type II-internal** dienyne were not viable substrates, other heterocyclic aromatic systems were able to perform the cycloaromatization if there isn't a competing cyclization component on the Fischer carbene.^{54d,55}



Scheme 1-43. Reaction of a metal carbene with the dienynyl alkyne resulting in an overall cycloaromatization.^{54a}

Barluenga and coworkers have also found success for dienyne cycloaromatization by incorporating a tungsten or chromium pentacarbonyl carbene moiety pendent to the alkyne (Scheme 1-44).⁵⁷ Fischer carbenes are activating groups for polar cycloaddition reactions due to the metal's electron-withdrawing nature. Treatment of **155** with nitrene **156** initially results in formation of cycloadduct **157**. The carbene is now brought into range of the proximal alkene inducing further reactivity. When either the *E* or *Z* disubstituted alkene **155-Me** was used, the only observed product was cycloaromatized **158** resulting from a metathesis reaction. Reaction of monosubstituted alkene **155-H** resulted in cyclopropane formation to give **159**. The authors postulate that use of the more substituted alkene raises the activation barrier to **159**, presumably due to sterics, therefore making the pathway to **158** favored.



Scheme 1-44. Use of pendent Fischer carbenes for metathesis cycloaromatization.⁵⁷

IX. Conclusions and Future Outlook

In summary, the *cis*-1,3-dien-5-yne structural unit represents a valuable synthon in the construction of highly substituted benzenoid systems. This review has covered the main mechanisms of activation to achieve both formal cycloaromatization via the two main thermal pathways as well as other pathways providing access to new systems. Table 1-3 summarizes these methodologies by dienyne structure (see Figure 1-1) and the activating reagent. From analysis of the references from this table, it is apparent that there is an abundance of systems designed to promote **Type II-internal** over *terminal* dienyne cyclizations. This may be due to a generally easier synthesis of the former substrate thus facilitating a scope study. It may also be

reasonable to state that much of the chemistry that was only studied for **Type II-internal** dienyne could also be applicable to **Type II-terminal** dienyne as shown by several of the systems that are able to utilize both types of substrates (e.g. metal-vinylidene induced). While much progress has been made by catalytic and stoichiometric promoters, many of the reactions covered still require elevated temperatures and less processes exist that provide cyclization pathways for **Type I** dienyne. Future development will no doubt augment the methodologies that are able to overcome these challenges.

Table 1-3. Organization of references covered in this review for dienyne cycloaromatization activation methodologies classified by dienyne **Type** (see Figure 1-1) and promoter / catalytic reagent.

| Dienyne | Type I | Type II- <i>internal</i> | Type II- <i>terminal</i> | Type III |
|--|-----------------------|--|------------------------------|--------------------------------|
| Photolytic | 7 | 9; 10 | 8a-d; 13a-b | 11 |
| Internally Activated (e.g. vinyl triflate) | 21a-b; 23a-b | 21c | 19 | |
| Acid / Electrophile (i.e. TfOH, I ₂) | 36 | 32 | | 34a-c; 35a-b |
| Base | 18; 20; 45 | 15; 16a-c; 18 | | 16b-c |
| Metal (temp < 50°C) | 47; 43; 51c-d; 53a-b; | 24, 26; 27; 30; 31a-b; 51a-d; 57 | 47 | 30; 37a,c; 51b |
| Metal (temp ≥ 50°C) | 5b; 25; 47; 52c; 54b | 24; 27; 28a-b; 29; 40; 41a; 52a-b; 54d; 56 | 37c; 47; 48; 49; 50a-b; 54a; | 27; 37a-c; 38a-d; 39; 42; 50b; |

X. References

1. For review: Zimmermann, G.; *Eur. J. Org. Chem.* **2001**, 457.
2. Hopf, H.; Musso, H. *Angew. Chem. Int. Ed.* **1969**, *8*, 680.
3. (a) Christl, M.; Braun, H.; Muller, G. *Angew. Chem., Int. Ed. Engl.* **1992**, *31*, 473. (b) Roth, W.R.; Hopf, H.; Horn, C. *Chem. Ber.* **1994**, *127*, 1765. (c) Prall, M.; Krüger, A.; Schreiner, P.R.; Hopf, H. *Chem. Eur. J.* **2001**, *7*, 4386. (d) Engels, B.; Schöneboom, J.C.; Münster, A.F.; Groetsch, S.; Christl, M. *J. Am. Chem. Soc.* **2002**, *124*, 287. (e) Balcioglu, N.; A. Özgür Özsar, A. *J. Mol. Struct.-Theochem.* **2004**, *677*, 125. (f) Litovitz, A.E.; Carpenter, B.K.; Hopf, H. *Org. Lett.* **2005**, *7*, 507. (e) Mackie, I.D.; Johnson, R.P. *J. Org. Chem.* **2009**, *74*, 499.

4. Spangler, C.W. *Chem. Rev.* **1976**, *76*, 187.
5. (a) Aitken, R.A.; Boeters, C.; Morrison, J.J. *J. Chem. Soc., Perkin Trans. 1* **1997**, 2625. (b) Lian, J.; Lin, C.; Chang, H.; Chen, P.; Liu, R. *J. Am. Chem. Soc.* **2006**, *128*, 9661.
6. For an acid catalyzed variant: Jacobi, P.A.; Kravitz, J.I. *Tetrahedron Letters*, **1988**, *29*, 6873.
7. Kaplan, L.; Walch, S.P.; Wilzbach, K.E. *J. Am. Chem. Soc.* **1968**, *90*, 5646.
8. (a) Tinnemans, A.H.A.; Laarhoven, W.H. *Tetrahedron Lett.* **1973**, *14*, 817. (b) Tinnemans, A.H.A.; Laarhoven, W.H. *J. Chem. Soc., Perkin Trans. 2* **1976**, 1111. (c) Tinnemans, A.H.A.; Laarhoven, W.H. *J. Chem. Soc., Perkin Trans. 2* **1976**, 1115. (d) van Arendonk, R.J.F.M.; Fornier de Violet, P.; Laarhoven, W.H. *Rec. Trav. Chim.* **1981**, *100*, 256.
9. op den Brouw, P.M.; Laarhoven, W.H. *J. Chem. Soc., Perkin Trans. 2* **1982**, 795.
10. Sajimon, M.C.; Lewis, F.D. *Photochem. Photobiol. Sci.* **2005**, *4*, 629.
11. Lewis, F.D.; Karagiannis, P.C.; Sajimon, M.C.; Lovejoy, K.S.; Zuo, X.; Rubin, M.; Gevorgyan, V. *Photochem. Photobiol. Sci.* **2006**, *5*, 369.
12. van Arendonk, R.J.F.M.; Laarhoven, W.H. *Rec. Trav. Chim.* **1981**, *100*, 263.
13. (a) Kaafarani, B.R.; Neckers, D.C. *Tetrahedron Lett.* **2001**, *42*, 4099. (b) Kaafarani, B.R.; Wex, B.; Bauerb, J.A.K.; Neckers, D.C. *Tetrahedron* **2002**, *43*, 8227.
14. (a) Reischl, W.; Okamura, W.H. *J. Am. Chem. Soc.* **1982**, *104*, 6115. (b) Brinker, U.H.; Wilk, G.; Gomann, K. *Angew. Chem. Int. Ed.* **1983**, *22*, 868.
15. Porter, N.A.; Hogenkamp, D.J.; Khouri, F.F. *J. Am. Chem. Soc.* **1990**, *112*, 2402.
16. (a) Xu, J.; Wang, Y.; Burton, D.J.; *Org. Lett.* **2006**, *8*, 2555. (b) Wang, Y.; Xu, J.; Burton, D.J. *J. Org. Chem.* **2006**, *71*, 7780. (c) Wang, Y.; Burton, D.J. *Org. Lett.* **2006**, *8*, 5295. (d) Wang, Y.; Burton, D.J.; *J. Fluorine Chem.* **2007**, *128*, 1052.
17. Although not technically a dienyne cycloaromatization, deuterium labeling studies performed during the base catalyzed conversion of *ortho*-alkynylphenyl ketones to naphthols have also provided evidence for allene intermediates. Makra, F.; Rohloff, J.C.; Muehidorf, A.V.; Link, J.O.; *Tetrahedron Lett.* **1995**, *36*, 6815.
18. Zhou, H.; Xing, Y.; Yao, J.; Chen, J. *Org. Lett.* **2010**, *12*, 3674.
19. Himbert, G.; Henn, L.; Hoge, R. *J. Orgmet. Chem.* **1980**, *184*, 317.
20. Abell, A.D.; Massy-Westropp, R.A.; Reynolds, G.D.; *Aust. J. Chem.* **1985**, *38*, 1129.
21. (a) Hanack, M.; Michel, U. *Angew. Chem. Int. Ed.* **1979**, *18*, 870. (b) Hanack, M.; Holweger, W. *J. Chem. Soc.; Chem. Comm.* **1981**, 713. (c) Bleckmann W.; Hanack, M. *Chem. Ber.* **1984**, *117*, 3021.

22. Depke, G.; Hanack, M.; Hummer, W.; Schwarz, H. *Angew. Chem. Int. Ed.* **1983**, *22*, 11983.
23. (a) Hanack, M.; Rieth, R. *J. Chem. Soc.; Chem. Commun.* **1985**, 1487. (b) Hanack, M.; Rieth, R. *Chem. Ber.* **1987**, *120*, 1659.
24. Liu, L.; Zhang, J. *Angew. Chem. Int. Ed.* **2009**, *48*, 6093.
25. Torii, S.; Okumoto, H.; Nishimura, A.. *Tetrahedron Lett.* **1991**, *32*, 4167.
26. Imamura, K.; Yoshikawa, E.; Gevorgyan, V.; Yamamoto, Y. *Tetrahedron Lett.* **1999**, *40*, 4081.
27. Dankwardt, J.W. *Tetrahedron Lett.* **2001**, *42*, 5809.
28. (a) Belmont, P.; Andrez, J.; Allan, C.S.M. *Tetrahedron Lett.* **2004**, *45*, 2783. (b) Godet, T.; Belmont, P. *SynLett* **2008**, 2513.
29. Herndon, J.W.; Zhang, Y.; Wang, K. *J. Organomet. Chem.* **2001**, *634*, 1.
30. Shibata, T.; Ueno, Y.; Kanda, K. *SynLett.* **2006**, 0411.
31. (a) Michon, C.; Liu, S.; Hiragushi, S.; Uenishi, J.; Uemura, M. *SynLett.* **2008**, 1321. (b) Michon, C.; Liu, S.; Hiragushi, S.; Uenishi, J.; Uemura, M. *Tetrahedron*, **2008**, *64*, 11756. (c) Uemura, M.; Kamikawa, K. *J. Chem. Soc., Chem. Commun.* **1994**, 2697.
32. Ciufolini, M.A.; Weiss, T.J. *Tetrahedron Lett.* **1994**, *35*, 1127.
33. For representative examples of applied uses of polycyclic aromatics: (a) Cram, D. J. *Nature* **1992**, *356*, 29. (b) Praefcke, K.; Kohne, B.; Singer, D. *Angew. Chem., Int. Ed. Engl.* **1990**, *29*, 177. (c) Veber, D. F.; Strachan, R. G.; Bergstrand, S. J.; Holly, F. W.; Homnick, C. F.; Hirschmann, R.; Torchiana, M. L.; Saperstein, R. *J. Am. Chem. Soc.* **1976**, *98*, 2367.
34. (a) Goldfinger, M.B.; Swager, T.M. *J. Am. Chem. Soc.* **1994**, *116*, 7895. (b) Goldfinger, M.B.; Crawford, K.B.; Swager, T.M. *J. Am. Chem. Soc.* **1997**, *119*, 4578. (c) Goldfinger, M.B.; Crawford, K.B.; Swager, T.M. *J. Org. Chem.* **1998**, *63*, 1676.
35. (a) Yao, T.; Campo, M.A.; Larock, R.C. *Org. Lett.* **2004**, *6*, 2677. (b) Marino, T.Y.; Campo, A.; Larock, R.C. *J. Org. Chem.* **2005**, *70*, 3511.
36. Matsumoto, S.; Takase, K.; Ogura, K. *J. Org. Chem.* **2008**, *73*, 1726.
37. (a) Fürstner, A.; Mamane, V. *J. Org. Chem.* **2002**, *67*, 6264. (b) Fürstner, A.; Mamane, V. *Chem. Commun.* **2003**, 2112. (c) Mamane, V.; Hannen, P.; Fürstner, A. *Chem. Eur. J.* **2004**, *10*, 4556.
38. (a) Storch, J.; Cermák, J.; Karban, J. *Tetrahedron Lett.* **2007**, *48*, 6814. (b) Storch, J.; Sykora, J.; Cermák, J.; Karban, J.; Císarová, I.; Ruzicka, A. *J. Org. Chem.* **2009**, *74*, 3090. (c) Storch, J.; Cermák, J.; Karban, J.; Císarová, I.; Sykora, J. *J. Org. Chem.* **2010**, *75*, 3137. (d) Liu, R-S.; Lush, S-F.; Diao, E.W-G.; Sohel, S.M.A.; Lin, M-Y.; Lee, T-J.; Chen, T-A. *Chem. Eur. J.* **2010**, *16*, 1826.

39. Komeyama, K.; Igawa, R.; Takaki, K. *Chem. Commun.* **2010**, *46*, 1748.
40. Loh, T-P.; Feng, C. *J. Am. Chem. Soc.* **2010**, *132*, 17710.
41. (a) Yasuhara, A.; Takeda, Y.; Suzuki, N.; Sakamoto, T. *Chem. Pharm. Bull.* **2002**, *50*, 235. (b) Yasuhara, A.; Kanamori, Y.; Kaneko, M.; Numata, A.; Kondo, Y. Sakamoto, T. *J. Chem. Soc., Perkin Trans. 1.* **1999**, 529.
42. Huang, X-C.; Wang, F.; Liang, Y.; Li, J-H. *Org. Lett.* **2009**, *11*, 1139.
43. García- García, P.; Fernández-Rodríguez, M.A.; Aguilar, E. *Angew. Chem. Int. Ed.* **2009**, *48*, 5534.
44. Barluenga, J.; García- García, P.; Saa, D.; Fernández-Rodríguez, M.A.; Bernardo de la Rúa, R.; Ballesteros, A.; Aguilar, E.; Tomás, M. *Angew. Chem. Int. Ed.* **2007**, *46*, 2610.
45. Yang, C.; Liu, R. *Tetrahedron Lett.* **2007**, *48*, 5887.
46. For reviews: (a) Bruce, M. I. *Adv. Organomet. Chem.* **1983**, *22*, 59. (b) Davies, S. G.; McNally, J. P.; Smallridge, A. J. *Adv. Organomet. Chem.* **1990**, *30*, 1. (c) Bruce, M. I. *Chem. Rev.* **1991**, *91*, 197.
47. Merlic, C. A.; Pauly, M. E. *J. Am. Chem. Soc.* **1996**, *118*, 11319.
48. Akiyama, R.; Kobayashi, S. *Angew. Chem. Int. Ed.* **2002**, *41*, 2602.
49. Watanabe, M.; Mataka, S.; Thiemann, T. *Steroids* **2005**, *70*, 856.
50. (a) Donovan, P.M.; Scott, L.T. *J. Am. Chem. Soc.* **2004**, *126*, 3108. (b) Shen H-C.; Tang, J-M.; Chang, H-K.; Yang, C-W.; Liu, R-S. *J. Org. Chem.* **2005**, *70*, 10113.
51. (a) Maeyama, K.; Iwasawa, N. *J. Am. Chem. Soc.* **1998**, *120*, 1928. (b) Maeyama, K.; Iwasawa, N. *J. Org. Chem.* **1999**, *64*, 1344. (c) Miura, T.; Iwasawa, N. *J. Am. Chem. Soc.* **2002**, *124*, 518. (d) Miura, T.; Murata, H.; Kiyota, K.; Kusama, H.; Iwasawa, N. *J. Mol. Catal. A-Chem.* **2004**, *213*, 59.
52. (a) Shen, H.; Pal, S.; Lian, J.; Liu, R. *J. Am. Chem. Soc.* **2003**, *125*, 15762. (b) Madhushaw, R.J.; Lo, C-Y.; Hwang, C-W.; Su, M-D.; Shen, H-C; Pal, S.; Shaikh, I.R.; Liu, R-S. *J. Am. Chem. Soc.* **2004**, *126*, 15560. (c) Lian, J-J.; Odedra, A.; Wu, C-J.; Liu, R-S. *J. Am. Chem. Soc.* **2005**, *127*, 4186.
53. (a) O'Connor, J.M.; Friese, S.J.; Tichenor, M. *J. Am. Chem. Soc.* **2002**, *124*, 3506. (b) O'Connor, J.M.; Friese, S.J.; Rodgers, B.L.; Rheingold, A.L.; Zakharov, L. *J. Am. Chem. Soc.* **2005**, *127*, 9346.
54. (a) Hemdon, J.W.; Hayford, A. *Organometallics* **1995**, *14*, 1556. (b) Herndon, J.W.; Zhang, Y.; Wang, H.; Wang, K. *Tetrahedron Lett.* **2000**, *41*, 8687. (c) Jackson, T.J.; Hemdon, J.W. *Tetrahedron* **2001**, *57*, 3859. (d) Zhang, Y.; Candelaria, D.; Herndon, J.W. *Tetrahedron Lett.* **2005**, *46*, 2211.

55. For review of Dötz reaction: Wulff, W.D. In *Comprehensive Organic Synthesis*; Trost, B.M., Fleming, I., Paquette, L.A., Eds.; Pergamon: Oxford, U.K., 1991; Vol. 5, pp 1065 – 1113.
56. Roy, P.; Ghorai, B.K. *Tetrahedron Lett.* **2011**, *52*, 251.
57. Barluenga, J.; Andina, F.; Aznar, F.; Valdéz, C. *Org. Lett.* **2007**, *9*, 4143.

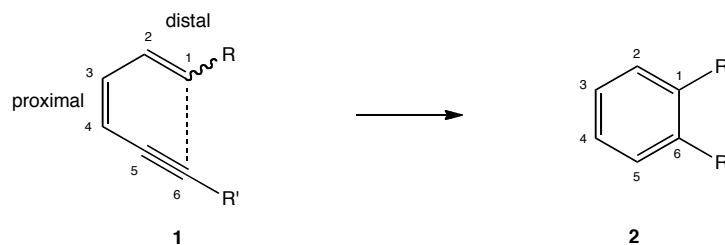
XI. Acknowledgments.

The material of Chapter 1, in full, is currently being prepared for submission for publication with the following authors: Hitt, D.M.; O'Connor, J.M. The dissertation author was the primary investigator and author of this material.

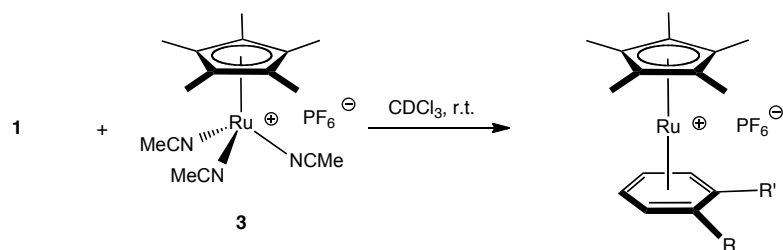
CHAPTER 2: Dienyne Cycloaromatization Triggered by Ruthenium C-H Bond Activation

I. Introduction.

Cycloaromatizations of polyunsaturated molecules constitute a valuable area of research in the synthesis of highly substituted aromatic systems. A structural motif that has generated a large subset of this research is the *cis*-1,3-dien-5-yne unit **1**, in which the most common cyclization mode generates an aromatic product **2** with bond formation occurring between the terminal atoms of the conjugated system (C¹-C⁶, Scheme 2-1). Thermally, known as the Hopf cyclization¹, this reaction has found little use in synthesis due to the high temperatures needed, but several methodologies have been developed which accomplish the formal Hopf cyclization using either a metal or non-metal promoter / catalyst.²⁻⁴ The majority of these methodologies can be classified into two main mechanisms: (1) activation of the alkyne via umpolung coordination for nucleophilic attack of the distal alkene (C¹=C²)² and (2) isomerization of the alkyne to an allene or metal vinylidene thus inducing a 6 π electrocyclization.³ Previous studies in the O'Connor laboratory have contributed to this area of research in the development of cationic cyclopentadienyl ruthenium(II) complexes (e.g. [Cp**Ru*(NCMe)₃]PF₆ **3**) as stoichiometric promoters that appear to operate by η^6 -metal coordination of the dienyne π system prior to cyclization (Scheme 2-2).⁵



Scheme 2-1. The Hopf cycloaromatization.¹

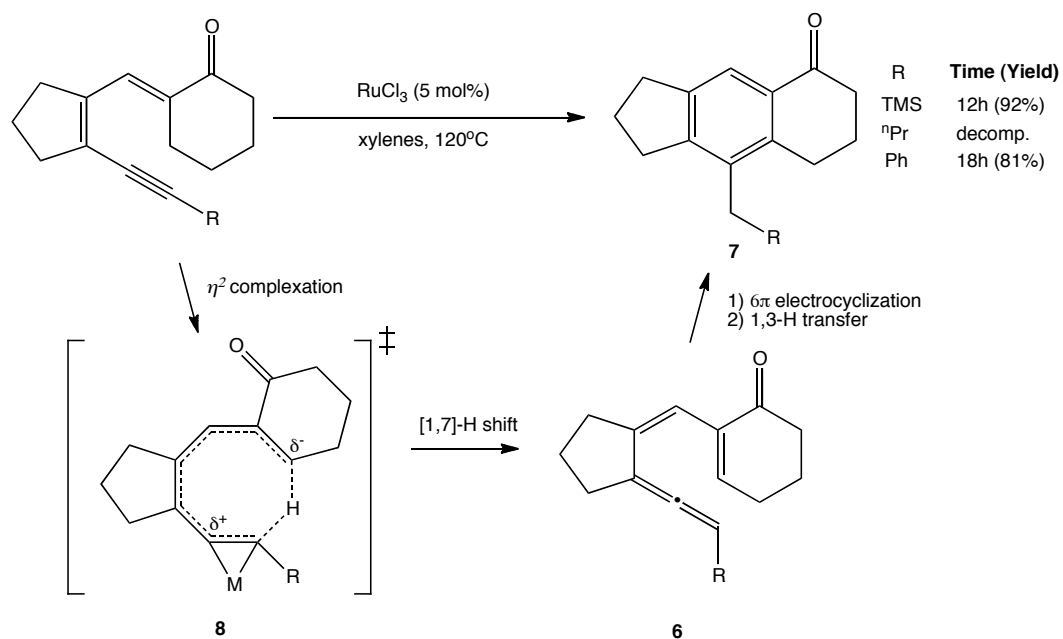


Scheme 2-2. Triggering the formal Hopf cycloaromatization with $[\text{Cp}^*\text{Ru}(\text{NCMe})_3]\text{PF}_6$ **3**.⁵

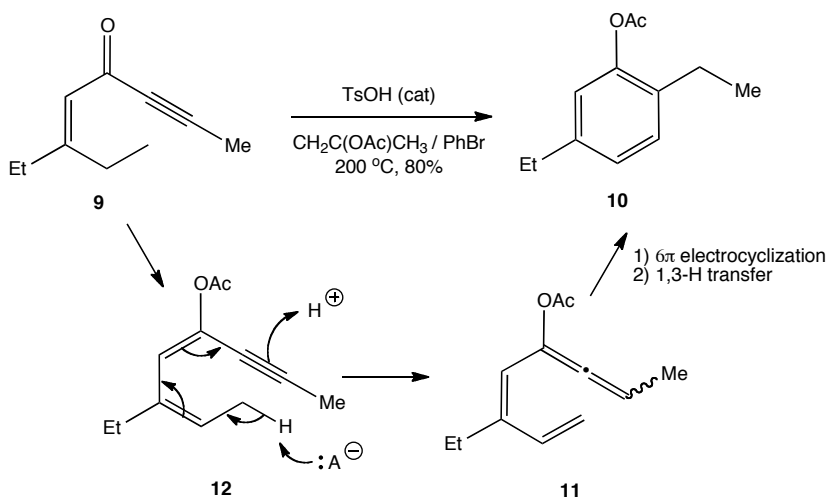
In continuing studies with these systems, we have recently uncovered a different cyclization route using substrates containing an allylic alkyl group (e.g. **4**, Scheme 2-3). The aromatic product **5** results from bond formation between the allylic carbon (C^*) and the internal alkyne carbon (C^5), thus resulting in a net addition of the allylic CH bond across the alkyne. Examples of related transformations in the literature are rare.⁶⁻⁸ Among the synthetically useful methodologies, Liu and coworkers have reported metal-catalyzed aromatizations with dienyne in which they propose an asynchronous [1,7]-hydrogen shift of a metal bound η^2 -alkyne intermediate followed by a 6π electrocyclization of allene **6** and subsequent isomerization to give arene product **7** (Scheme 2-4).^{7a} Support for transition state **8** comes from rate enhancement for substrates containing an electron-rich TMS substituted alkyne and an electron withdrawing vinyl carbonyl. Jacobi and coworkers have reported conversion of 1-en-4-yn-3-one **9** at elevated temperatures under acid catalysis to arene **10** (Scheme 2-5).⁸ Analogous to Liu's work, conjugated allene **11** is proposed to form after initial formation of the 4-dienynyl acetyl ether **12** and proton transfer. We herein report our findings using cationic ruthenium complexes to promote novel dienyne cyclizations.



Scheme 2-3. Cycloaromatization resulting from allylic alkyl addition to internal alkyne carbon.



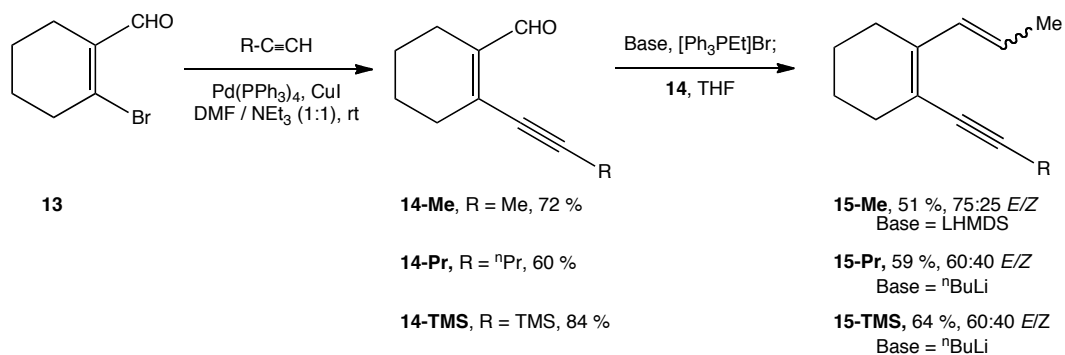
Scheme 2-4. Metal catalyzed cycloaromatization via [1,7]-H shift.⁷



Scheme 2-5. Acid catalyzed cycloaromatization of *in situ* generated dienyne **12**.⁸

II. Initial Observation and Optimization.

We prepared three dienyne substrates differing in alkyne substitution as a starting point for our study using the route shown in Scheme 2-6. Synthesis began from the known 2-bromocyclohex-1-enecarbaldehyde **13** that was prepared in one step from cyclohexanone.⁹ Sonogashira coupling of **13** with the appropriate alkyne to afford **14** followed by Wittig olefination provided dienynes **15** in good yield as mixtures of *E* and *Z* isomers.



Scheme 2-6. Synthesis of dienynes with varying alkyne substitution.

Consistent with previous work, the reaction of **15-Me** (entry 1, Table 2-1) with $[\text{Cp}^*\text{Ru}(\text{NCMe})_3]\text{PF}_6$ (**3**)¹⁰ resulted in the rapid formation (< 15 min) of $[\text{Cp}^*\text{Ru}(\eta^6\text{-6,7-dimethyltetraline})]\text{PF}_6$ **16-Me** in 68% NMR yield.⁵ Also observed by ¹H NMR spectroscopy were several Cp*Ru - dienyne complexes which were stable over the course of several days. Heating the reaction mixture for 24 h at 50°C was successful at converting the transient compounds but, surprisingly, the yield of **16-Me** remained unchanged and the formation of allyl addition products, $[\text{Cp}^*\text{Ru}(\eta^6\text{-5-ethyltetraline})]\text{PF}_6$ (**17-Me**, 10% NMR Yield) and 5-ethyltetraline¹¹ (**18-Me**, 8% NMR yield) was observed. Reaction of the sterically larger *n*-propyl substituted alkyne **15-Pr** (entry 2) under similar conditions also gave a mixture of **16**, **17**, and **18**, but the ratio of the allyl addition products (**17-Pr** and **18-Pr**¹²) to the formal Hopf product (**16-Pr**) had increased.

Structural assignments of the observed metal complexes were made primarily through interpretation of the ¹H NMR (CDCl₃) spectra. **16-Me, Pr** and **17-Me, Pr** all exhibit an upfield shift of the aromatic hydrogen resonances (δ 6.0 - 5.0) and Cp* methyl hydrogen resonances between δ 2.0 and 1.7, both of which are well known characteristics for $[\text{Cp}^*\text{Ru}(\eta^6\text{-arene})]\text{X}$ complexes. Complexes **16-Me, Pr** show uncoupled aromatic hydrogen resonances, **16-Me**: δ 5.52 (s, 2H) and **16-Pr**: δ 5.54 (s, 1H), 5.43 (s, 1H), as well as uncoupled methyl resonances, **16-Me**: δ 2.08 (s, 6H) and **16-Pr**: δ 2.09 (s, 3H), both consistent with the 1,2,4,5-arene substitution pattern of **16**. The ¹H NMR spectra of **17-Me, Pr** exhibited a triplet and doublet resonances for the aromatic hydrogens, **17-Me**: δ 5.77 (t, $J = 5.7$ Hz, 1H), 5.61 (d, $J = 5.7$ Hz, 2H) and **17-Pr**: δ 5.70 (t, $J = 5.7$ Hz, 1H), 5.58 (d, $J = 5.7$ Hz, 1H), 5.53 (d, $J = 5.7$ Hz, 1H) consistent with the 1,2,3-substitution pattern of **17**.

Due to the catalytic turnover observed in the reactions with **15-Me, Pr**, we tested the reactivity of **15-TMS** with a larger excess (4.1 eq **15-TMS**) compared to entries 1-2. Upon mixing **3** and **15-TMS** at ambient temperature, rapid quantitative formation (< 15 min) of two Cp*Ru - dienyne complexes in a 6:4 ratio was observed by the appearance of Cp* resonances in the ¹H NMR spectrum at δ 1.90 and 1.71 and TMS resonances at δ 0.37 and 0.064 for the

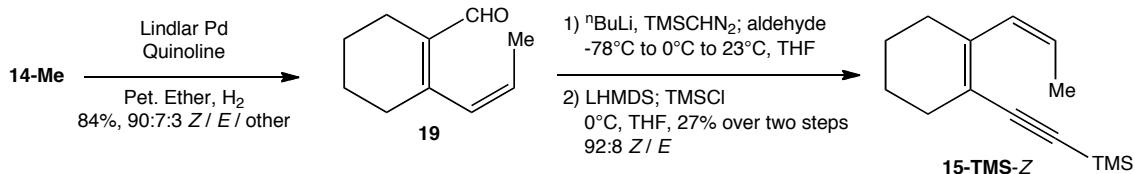
major species **I** and minor species **II**, respectively.¹³ We were pleased to find that **I** and **II** slowly converted to **17-TMS** and **18-TMS** in 57 and 31% NMR yields, respectively, over the course of 21h with no observation of **16-TMS** (entry 3). Another interesting observation for the reaction of **15-TMS** was the complete selectivity for reaction of the *cis*-stereoisomer **15-TMS-Z** (> 95% conversion **15-TMS-Z**, < 5% conversion **15-TMS-E**).

The ¹H NMR spectrum of **17-TMS** exhibits aromatic hydrogen signals with an identical coupling pattern but resonating slightly upfield compared to **17-Me, Pr**: δ 5.66 (t, $J = 6.0$ Hz, 1H), 5.54 (d, $J = 6.0$ Hz, 1H), and 5.39 (d, $J = 6.0$ Hz, 1H). The TMS resonance at δ 0.065 (s, 9H) is consistent with the TMS bound to a benzylic carbon as opposed to an aromatic carbon which exhibits TMS resonances δ 0.3 to 0.4 downfield of **17-TMS**.^{5a,14} Similar to **17-TMS**, the free arene **18-TMS** also exhibits a similar coupling pattern but slight upfield shift of the aromatic hydrogens as compared to **18-Me, Pr**.¹¹⁻¹² The structure of **17-TMS** and **18-TMS** is further supported by photolytic removal of the metal fragment from **17-TMS** to give **18-TMS** followed by desilylation with K₂CO₃ in MeOH affording known 5-methyltetraline.¹⁵

Table 2-1. Initial screening of dienyne substrates with varying alkyne substitution for reaction with $[\text{Cp}^*\text{Ru}(\text{NCMe})_3]\text{PF}_6$ **3**. (a) 1.05 - 1.5 eq **15-Me**. Reaction vessel kept at ambient temperature for 5 days then heated at 50°C for 24 h. (b) 1.05 - 1.5 eq **15-Pr**. Reaction vessel kept at ambient temperature for 13 days then heated at 50°C for 24 h. (c) 4.1 eq **15-TMS**. Reaction vessel kept at ambient temperature for 21 h.

| Entry | Substrate | % NMR yield 16 | % NMR yield 17 | % NMR yield 18 |
|----------------|---|-----------------------|-----------------------|-----------------------|
| 1 ^a | 15-TMS (R = Me, 75:25 <i>E/Z</i>) | 68 | 10 | 8 |
| 2 ^b | 15-Pr (R = ⁿ Pr, 60:40 <i>E/Z</i>) | 57 | 14 | 29 |
| 3 ^c | 15-Me (R = TMS, 60:40 <i>E/Z</i>) | 0 | 57 | 31 |

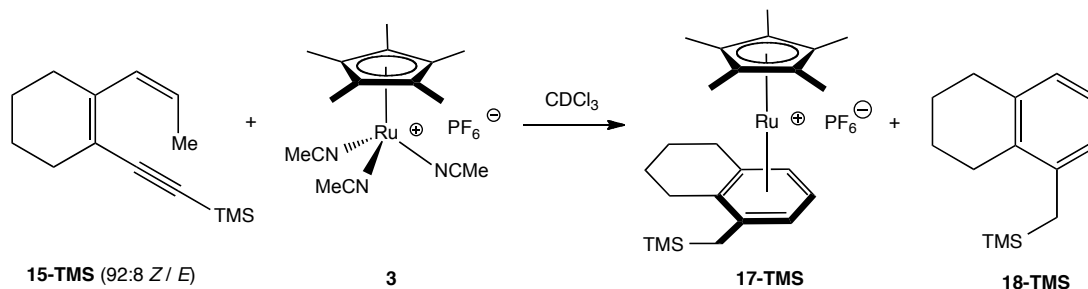
The selectivity observed with the *cis* stereoisomer **15-TMS-Z**, prompted us to prepare an enriched sample of this compound and test its reactivity with **3**. To this end, Lindlar hydrogenation of **14-Me** gave 90% *Z* enriched sample of **19**. Conversion to a 92% enriched sample of **15-TMS-Z** was accomplished by treatment of the aldehyde mixture with lithiated trimethylsilyldiazomethane followed by silylation of the terminal alkyne.



Scheme 2-7. Synthesis of **15-TMS-Z** enriched sample.

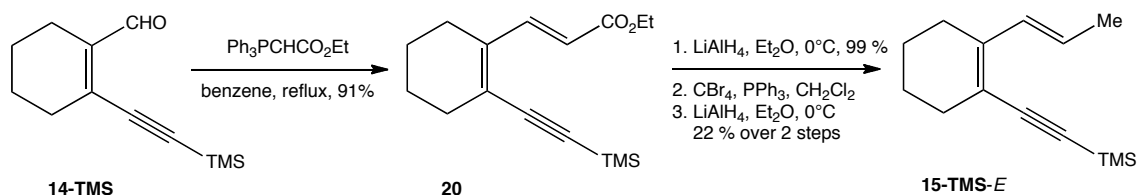
On an equimolar scale, initial formation (< 30 min) of **I** and **II** was observed in 90% NMR yield (67:33 **I** / **II**) that slowly converted to η^6 -arene **17-TMS** over the course of 24 h in 91% NMR yield (entry 1, Table 2-2). It was also found that the reaction could be accelerated if run at 50°C with no detrimental effect on yield (entry 2). Performing the reaction at 50°C with the **15-TMS-Z** enriched sample using a catalytic amount of **3** (20 mol%, entry 3) resulted in similar yields of **17-TMS** and free arene **18-TMS** when compared to the 6:4 *E/Z* **15-TMS** sample.

Table 2-2. Exploratory experiments with *Z* enriched sample of **15-TMS**.



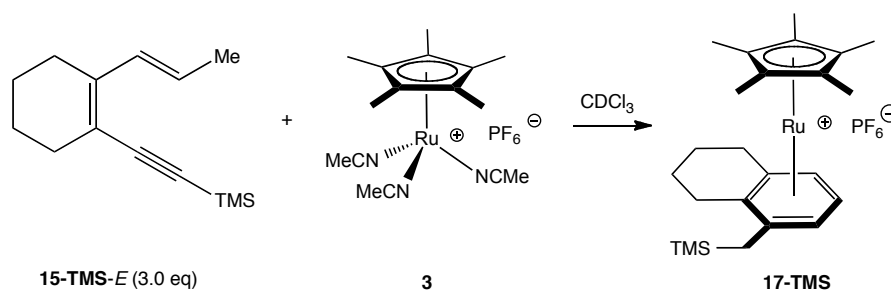
| Entry | 15-TMS eq. | Temp. (°C) | Time (h) | <i>E</i> / <i>Z</i> % conv. | % NMR yield 17-TMS | % NMR yield 18-TMS |
|-------|-------------------|------------|----------|-----------------------------|---------------------------|---------------------------|
| 1 | 1.0 | r.t. | 24 | 100 / 100 | 91 | - |
| 2 | 1.2 | 50 | 6 | 0 / 100 | 89 | 11 |
| 3 | 5.0 | 50 | 6 | 0 / 40 | 53 | 33 |

To obtain a better sense of the reactivity of *trans*-dienyne, we also synthesized **15-TMS-E** as shown in Scheme 2-8. Aldehyde **14-TMS** was olefinated with the stabilized ylide to give **20** as a single geometric isomer. LAH reduction of the **20** gave the primary alcohol that was then brominated and reduced with LAH to give pure **15-TMS-E**.



Scheme 2-8. Synthetic route to geometrically pure **15-TMS-E**.

Within 30 min of the reaction of **15-TMS-E** with **3**, a new Cp*Ru - diene complex **III** was formed in large excess to **I** and **II**. This compound was characterized by Cp* and TMS resonances at δ 1.78 and 0.38 in the ^1H NMR spectrum among several other distinguishable signals.¹⁶ At later reaction times, as the yield of **17-TMS** increased, the yield of **III** decreased while **I** and **II** increased. Over the course of 49 hours, the reaction reached 29% conversion of **15-TMS-E** (full conversion of **3**) and 66% NMR yield of **17-TMS**. These results suggest that **III** forms from **15-TMS-E** exclusively, as the former was only observed in trace amounts in the previous experiments using stereoisomeric mixtures of **15-TMS**. It is unclear whether **III** is converted directly to **17-TMS** or is first isomerized to **15-TMS-Z** as we were unable to observe the latter by ^1H NMR spectroscopy at intermediate reaction times. This experiment demonstrates that compound **15-TMS-E**, although less reactive than **15-TMS-Z**, is a viable substrate.

Table 2-3. Yields of transient species and **17-TMS** for the reaction *trans*-dienyne **15-TMS-E**.

| Time (h) | 15-TMS-E (% conv.) | NMR yield | | | |
|----------|--------------------|-----------|-----------|------------|---------------|
| | | I | II | III | 17-TMS |
| 0.5 | 35 | 6 | 1 | 44 | 0 |
| 7.5 | 27 | 19 | 4 | 37 | 18 |
| 24.5 | 27 | 0 | 0 | 11 | 56 |
| 49 | 29 | 0 | 0 | 0 | 66 |

III. Structure of Transient Complexes.

All attempts to isolate **I**, **II**, and **III** have failed to date, but some conclusions can be made about the coordination environment. The ^1H NMR spectra of **I** and **II** suggest these compounds are very similar in structure. Both contain three vinyl hydrogens in a spin-coupled system as observed by resonances at δ 6.02 (t, $J = 5.5$ Hz), 5.01 (d, $J = 5.5$ Hz), 4.81 (d, $J = 5.5$ Hz) for **I** and δ 4.61 (d, $J = 5$ Hz), 4.47 (dd, $J = 7$ Hz, 5 Hz), 4.33 (d, $J = 7$ Hz) for **II**. Also both complexes have a weakly / non-coupled vinyl hydrogen at δ 3.50 (s) for **I** and δ 5.18 (d, $J = 1.5$ Hz) for **II**. The upfield shift observed for many of the vinyl hydrogen chemical shifts is typical for metal coordinated alkenes. Transient species **II** exhibited an additional key resonance at δ 2.74 (s, 3H) corresponding to a metal-coordinated MeCN.¹⁷ Consistent with the assignment of the coordinated MeCN for **II** was the observation that added CD_3CN decreases the intensity of this resonance in the ^1H NMR spectrum.

To gain further insight into the possible differences and similarities in the structure of **I** and **II**, a VT NMR experiment was performed in which equimolar amounts of **15-TMS** (92:8 *Z*/*E*) and **3** (0.08 mmol scale, 0.09 M in CDCl₃) were allowed to react at 22°C and then cooled to -30°C. Upon cooling, the **I** / **II** ratio was observed to change from 35:65 to 5:95. Upon warming the sample back to 22°C, the ratio reverted back to 35:65 suggesting a reversible process. From this experiment and the observed MeCN resonance for **II**, we postulate that **I** and **II** interconvert by reversible coordination of an MeCN ligand (eq 1). Consistent with such an equilibrium, the **I** / **II** ratio decreased at lower temperatures based on a smaller entropic term. Unfortunately, attempts to perform Van't Hoff analysis on the system were thwarted by an inability to integrate the free MeCN resonance accurately.



Using our findings from the VT NMR equilibrium experiment, **15-TMS** (7:3 *E*/*Z*) was allowed to react with **3** (0.3 eq) and CD₃CN (4 eq) in CDCl₃, resulting in almost exclusive formation of **II** and only trace amounts of **III**. The sample was kept at -15°C and HSQC / HMBC NMR data were acquired (see Section VII. Experimental). Based on the results from these acquisitions, we propose a ruthenium η⁴-bound structure for **II** as shown in Figure 2-1. The three coupled vinyl hydrogen resonances exhibit one-bond correlations with a ¹³C resonance at δ 78.4 and two accidental isochronous resonances at δ 83.6.¹⁸ The chemical shifts of these carbons are in good agreement with known [Cp**Ru*(η⁴-diene)NCMe]X complexes (Table 2-4). Furthermore, the one bond correlation of the vinyl hydrogen resonance at δ 5.18 and carbon resonance at δ 120.6 (C^{exo}) supports the presence of these atoms outside the metal coordination sphere. HMBC correlations of the δ 5.18 ¹H resonance with the C³ at δ 78.4 and

TMS group at δ 0.11 provides good evidence that the C³-C⁴ bond has formed and supports the assigned connectivity of the TMS group.

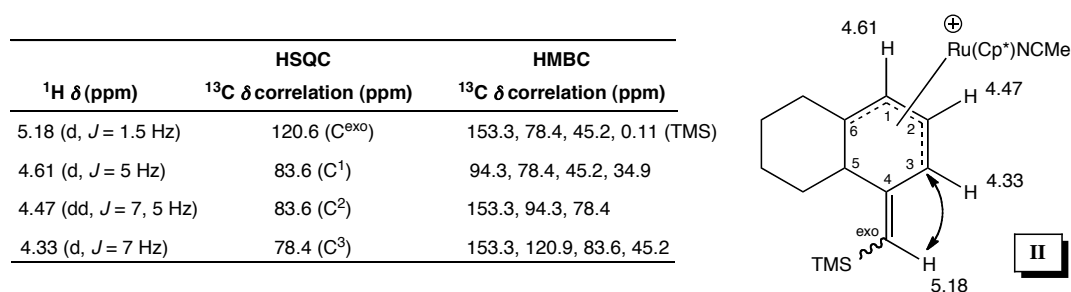


Figure 2-1. HSQC / HMBC correlations and proposed structure for **II**.

Table 2-4. NMR chemical shift values for known [Cp*Ru(η^4 -diene)NCMe]X complexes.^{17a}

| R | X | δ NCCMe ₃ (ppm) | δ CHCH ₂ (ppm) | δ CH (ppm) | δ CH (ppm) | δ CH (ppm) |
|----|------------------------------|-----------------------------------|----------------------------------|-------------------|-------------------|-------------------|
| H | PF ₆ ⁻ | 2.60 | 53.34 | 94.0 | | |
| Et | BF ₄ ⁻ | 2.64 | 51.85 | 80.55 | 89.97 | 94.92 |

Structural assignments for **I** and **III** are more speculative based on the limited amount of spectral data. Based on the ¹H NMR similarities and the observed equilibrium with **II**, several structures for **I** can be proposed. Interaction of the π system of the *exo*-TMS-methylene with the metal would result in a saturated metal center with no change in oxidation state (structure **I-A**, Figure 2-2). This structure would be consistent with the upfield shift of the *exo* vinyl hydrogen from δ 5.18 in **II** to δ 3.50 in **I**. This type of coordination is unknown in literature, however, η^6 -coordination of tetramethylfulvene by transition metal complexes is well known to occur.¹⁹ A Cp*Ru⁺ example, **21**, shows methylene ¹H resonances between δ 4.8 – 4.3 depending on the anion used.²⁰ Also conceivable would be either the agostic complex **I-B** or the metal hydride **I-**

C. Often times, it is difficult to differentiate these coordination modes by NMR spectroscopy due to a rapid isomerization on the NMR time scale, but for both agostic and hydride complexes originating from cationic cyclopentadienyl ruthenium systems, an ^1H NMR resonance is typically observed between δ -8.0 to -11.0 for the hydrogen interacting with the metal (see **22-24**).²¹ We have not observed such a resonance for **I**, suggesting that neither the **I-B** or **I-C** represents an accurate description of the coordination mode.

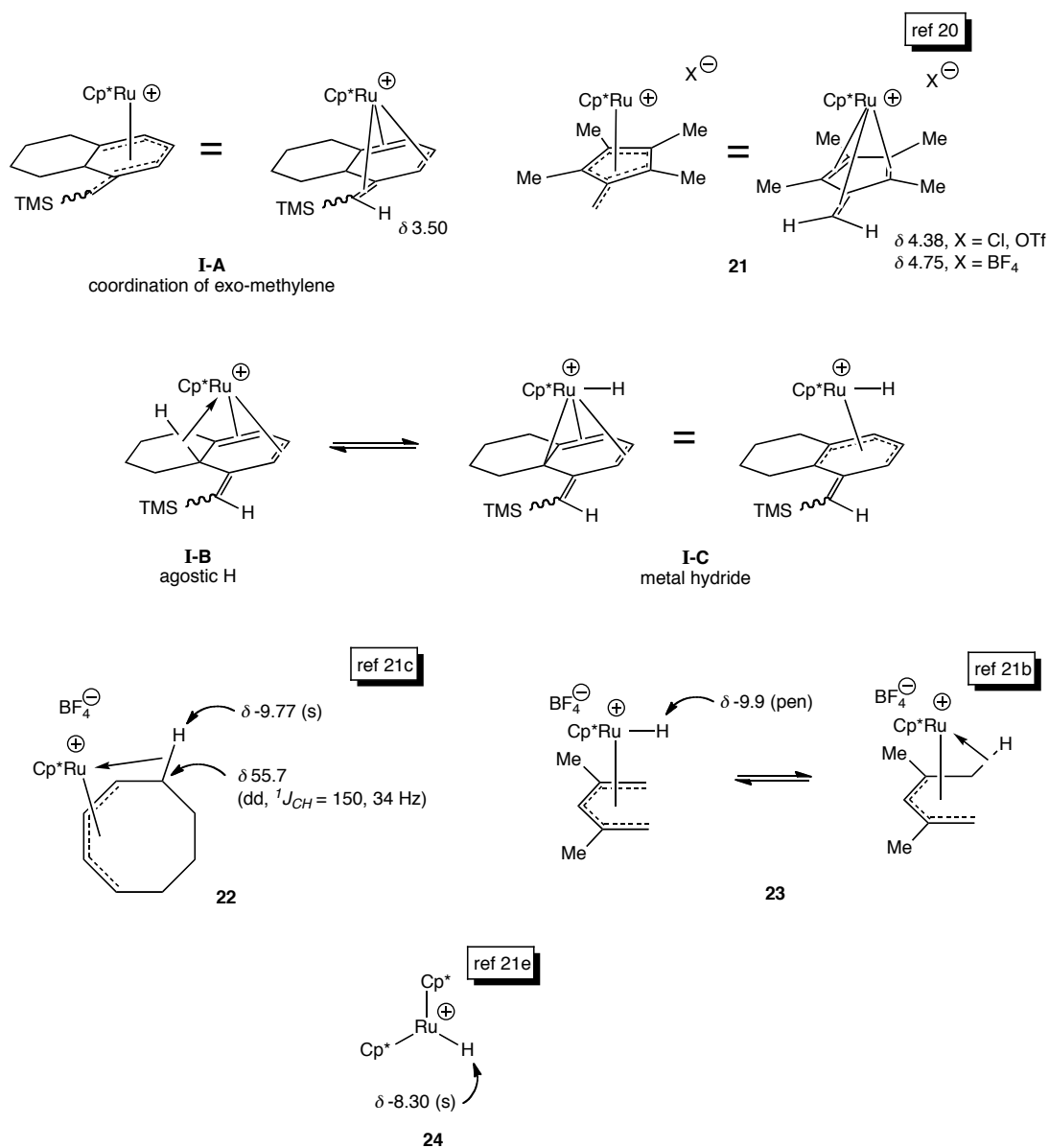


Figure 2-2. Possible structures for **I** and comparison with analogous known compounds.

For **III**, we are considering two structures: η^4 -diene **III-A** and η^4 -enyne **III-B**. Consistent with our data on **III**, both **A** and **B** would account for the inability to observe the H^{int} resonance by ^1H NMR spectroscopy, as this peak would be expected to come upfield in a very convoluted region of the spectrum. The H^{ext} chemical shift assignment is in good agreement with other $\text{Cp}^*\text{Ru}(\eta^4\text{-diene})$ complexes at δ 5.11 (d, $J = 10$ Hz).^{17,22} Also of note is the downfield shift of the TMS resonance from δ 0.21 in **15-TMS-E** to δ 0.38 in **III**. This may favor a structure like **III-B** where there is a greater perturbation of the alkyne hybridization. We have not observed a coordinated MeCN resonance in the ^1H NMR spectrum for **III**, but this could be due to fast exchange.

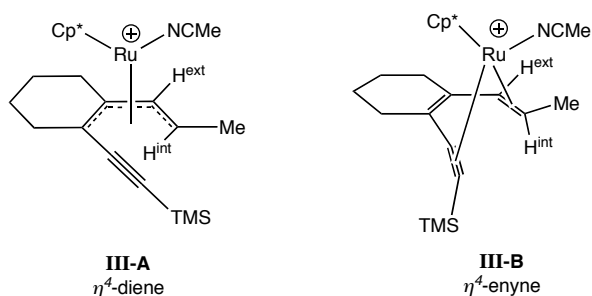


Figure 2-3. Possible structures for **III**.

IV. Attempts to Increase Catalytic Activity of System.

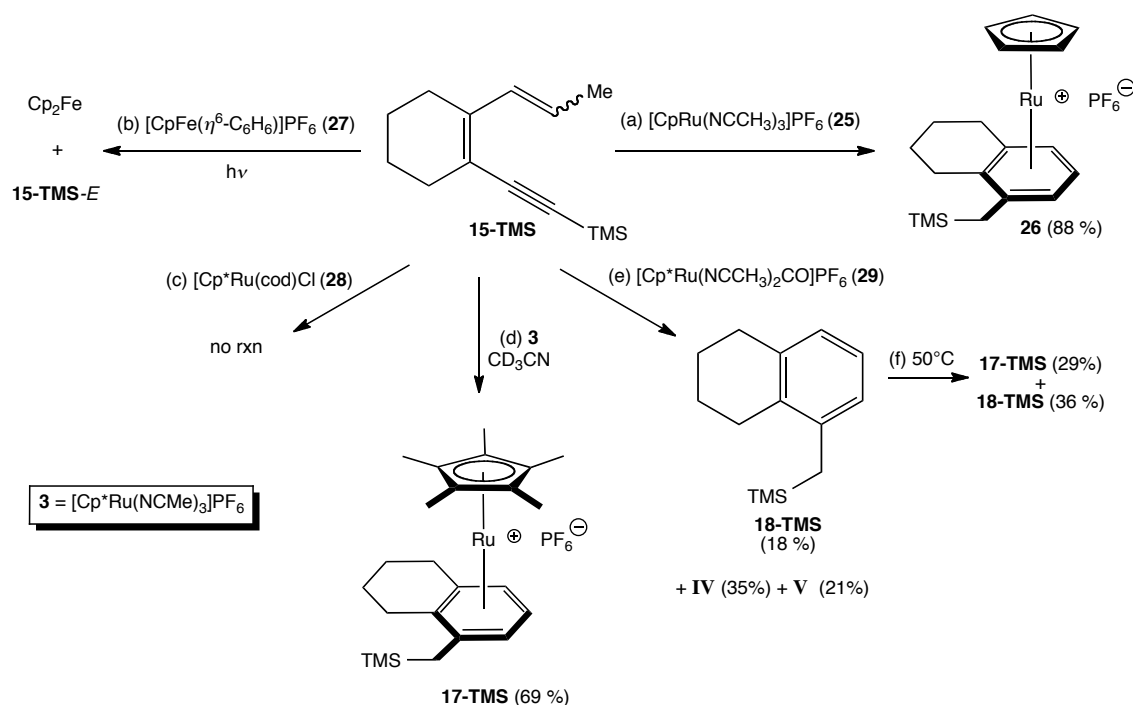
In an attempt to harness the catalytic potential of the $[\text{Cp}^*\text{RuL}_3]\text{PF}_6$ / **15-TMS** reaction, we have tried several experiments envisioned to prolong the life of the active metal species. Attempted photolysis of a **15-TMS** / **17-TMS** / **18-TMS** mixture using both a Hanovia lamp and direct sunlight source in both acetone- d_6 and CDCl_3 only resulted in isomerization of **15-TMS-Z** to **15-TMS-E**. Dienyne **15-TMS** was also allowed to react with **3** in CD_3CN in an attempt to

prevent binding of the Cp*Ru⁺ fragment to the arene product (Scheme 2-9). Surprisingly, after 11 days at ambient temperature, the only product observed was the complexed arene **17-TMS**.

A preliminary screen of other possible metals systems that might have similar reactivity was also conducted. Similar to **3**, reaction of **15-TMS** (92:8 *Z*/*E*) with the sterically smaller and less electron-donating [CpRu(NCMe)₃]PF₆ (**25**) (1.2 eq) at ambient temperature resulted in the immediate formation of several CpRu - dienyne complexes which slowly converted to the η^6 bound allyl addition product **26** in 66% NMR yield over the course of 7 days. Conversion of the reaction mixture at 7 days was slightly increased by heating at 50°C that resulted in conversion of all transient compounds and an 88% NMR yield of **26**. Treating **15-TMS** with [CpFe(η^6 -benzene)]PF₆ (**27**) under photolytic conditions in acetone-*d*₆ in an attempt to form an analogous [CpFeL₃]PF₆ system *in situ* only resulted in disproportionation to ferrocene and isomerization of **15-TMS-Z** to **15-TMS-E**.

The reaction of **15-TMS** was also attempted with Cp*Ru(cod)Cl (**28**) and [Cp*Ru(CO)(NCMe)₂]PF₆ (**29**)²³ with the expectation that these complexes would provide two available coordination sites for the substrate thereby preventing η^6 -complexation. Attempted reaction of **15-TMS** with **28** resulted in no reaction even upon heating at 50°C for 18 h. Reaction of **29** with **15-TMS** at ambient temperature resulted in the initial quantitative formation of a single Cp*Ru - dienyne complex (**IV**). Over the course of 5 days, **IV** decreased to 35% NMR yield while formation of a second Cp*Ru - dienyne complex, **V**, and **18-TMS** were observed in 21 and 18 % NMR yield, respectively.²⁴ As expected, the reaction was able to suppress formation of **17-TMS**. Analogous to the reactions with **3**, the system showed complete selectivity for **15-TMS-Z** (> 91% conversion **15-TMS-Z**, < 5% conversion **15-TMS-E**). Also suspected of forming was the bis-CO complex [Cp*Ru(CO)₂NCMe]PF₆ (**30**) based on the similarities of the observed chemical shifts of the CH₃CN and Cp* hydrogen resonances (δ 2.50 and δ 1.99, respectively) compared with literature values reported in CD₂Cl₂.²⁵ In an attempt to convert **IV** and **V**, the reaction mixture was heated to 50°C for 54 h resulting in complete

conversion of **IV**, **V** and **15-TMS-Z** in addition to partial conversion of **15-TMS-E** (73%). The NMR yield of **18-TMS** increased to 36% but unfortunately this was accompanied by the formation of **17-TMS** in 29% NMR yield. The relative amount of the bis-CO complex **30** also increased but due to difficulty in acquiring an integral on the resonances for the starting metal complex **29**, the exact NMR yield could not be calculated.



Scheme 2-9. Additional experiments designed to produce a metal catalyzed cycloaromatization. (a) **15-TMS** (92:8 *Z* / *E*, 1 eq), **25** (1 eq), CDCl_3 , 7 days at rt then 24 h at 50°C . (b) **27**, **15-TMS** (7:3 *E* / *Z*, 4 eq), $\text{acetone-}d_6$, ~29 h direct sunlight. (c) **28**, **15-TMS** (6:4 *E* / *Z*, 10 eq), $\text{acetone-}d_6$, then 18 h at 50°C . (d) **15-TMS** (7:3 *E* / *Z*, 1 eq), **3** (1 eq), CD_3CN , 12 days at rt then 4 days at 50°C . (e) **15-TMS** (6:4 *E* / *Z*, 1 eq), **29** (1 eq), CDCl_3 , 5 days at rt (f) 54 h at 50°C .

V. Mechanistic Studies and Discussion.

The [1,7]-hydrogen shift / electrocyclization proposed by Liu (Scheme 2-4) provides one possible mechanistic pathway for cycloaromatization.^{7a} Although this mechanism rationalizes the selectivity of the *cis*-stereoisomer **15-TMS-Z**, there are considerable differences between Liu's thermal [1,7]-H shift system and the dienyne reaction with **3**. The former required temperatures in excess of 120°C and the reactivity was limited to substrates containing an α,β -unsaturated carbonyl (e.g. **31**) when metal catalysts similar to **3** (i.e. [TpRu(PPh₃)(NCMe)₂]PF₆, CpRu(PPh₃)₂Cl) were used. In general, conversion of substrates electronically similar to **15-TMS** (e.g. **32**) were unsuccessful.

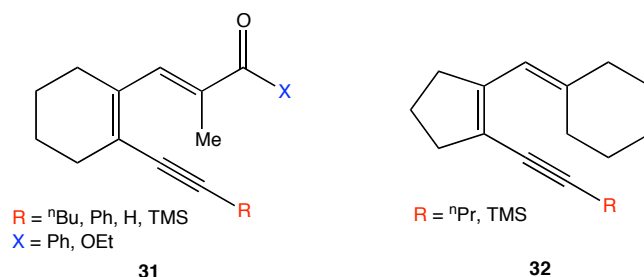
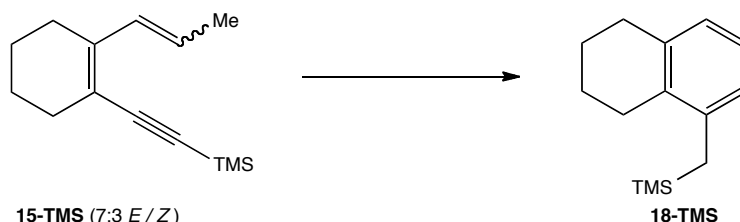


Figure 2-4. Dienyne substrates used for Liu's metal-catalyzed dienyne cyclization.^{7a}

In order to determine how **15-TMS** would perform under Liu's system, we matched the reported conditions as closely as possible and monitored the reaction progress by ¹H NMR spectroscopy (Table 2-5). Use of one of Liu's top performing catalysts - RuCl₃ - resulted in almost identical conversion and yield as were obtained without catalyst (entry 1 and 2). In Liu's initial report, it was mentioned in a footnote that use of base also had a beneficial effect. This was later studied in more detail and applied to these researchers previously developed tandem Aldol / cycloaromatization methodology.^{7b} To test this, **15-TMS** was thermalized in the presence of 2,6-lutidine and conversion to **18-TMS** was observed to occur in significantly lower yield than

was the case without added base (entry 3). Another successful catalyst in Liu's system, PtCl_2 in $\text{DMF-}d_7$, was also tested and resulted in a higher conversion of both geometric isomers but no observed formation of **18-TMS** (entry 4). To rule out a detrimental solvent effect, **15-TMS** was thermalized without a catalyst in $\text{DMF-}d_7$. The formation of product was observed but in lower yield than the thermal reaction in *o*-xylene (entry 2 and 5). Although not isolated from the PtCl_2 -catalyzed reaction mixture, formation of 6-methyl-7-trimethylsilyl-tetraline may have occurred in 36% NMR determined by a TMS resonance at δ 0.44 in the ^1H NMR spectrum. This product would be the result of a PtCl_2 -catalyzed 6-*endo* cyclization.^{2f}

Table 2-5. Performance of **15-TMS** under previously reported literature conditions. (a) Observed formation of TMS resonances at δ 0.44 and 0.09 in 36 and 28% NMR yield, respectively. May be observing formation of 6-methyl-7-TMS-tetraline.



| Entry | Catalysis | Condition | t (h) | Z / E % Conv. | Product Yield |
|-------|--|------------------------------------|-------|---------------|----------------|
| 1 | $\text{RuCl}_3 \cdot \text{H}_2\text{O}$ | <i>o</i> -xylene- d_{10} , 145°C | 19.5 | 35 / 0 | 103 |
| 2 | none | <i>o</i> -xylene- d_{10} , 145°C | 19.5 | 33 / 0 | 102 |
| 3 | 2,6-lutidine | <i>o</i> -xylene- d_{10} , 145°C | 19.5 | 48 / 10 | 53 |
| 4 | PtCl_2 | $\text{DMF-}d_7$, 145°C | 18.75 | 74 / 92 | 0 ^a |
| 5 | none | $\text{DMF-}d_7$, 145°C | 21.5 | 57 / 0 | 70 |

While the inability of Liu's conditions to promote the cycloaromatization of **15-TMS** tends to favor an alternative mechanism, it does not provide any firm evidence against the [1,7]-H shift / electrocyclization mechanism as shown in Scheme 2-4. Closer inspection of this mechanism shows that if **3** were acting as the catalyst, one and only one MeCN would need to

dissociate for formation of the reactive η^2 -alkyne intermediate. One would therefore expect an inverse first order rate dependence on [MeCN] for formation of **I** and **II**. This analysis assumes that the [1,7]-H shift is the rate-determining step in the pathway. During labeling experiments with dienyne substrates deuterated at the allylic positions, Liu reported that longer reaction times were required to reach full conversion versus the analogous protio substrate (D – 48 h vs. H – 24 h). Although qualitative, this result indicates the presence of a kinetic isotope effect (KIE) and suggests either the [1,7]-H shift or an isomerization step leading to **I** / **II** is rate limiting.

Based on the observed KIE by Liu and the high-energy nature of **8**, we felt our assumption on the rate-determining step of the reaction was valid and performed kinetic experiments with the overall goal of obtaining the rate dependence of [MeCN]. Shown in Figure 2-5 and Table 2-6 are the results obtained from these experiments. In a normalization run, **3** (0.014 M) was allowed to react with **15-TMS** (7:3 *E/Z*, 0.014 M) and CD₃CN (0.545 M) in a CDCl₃ / acetone-*d*₆ mixture and the formation of **II** was monitored by integration of the TMS resonance at δ 0.064 in the ¹H NMR spectrum. Compound **I** was not observed due to the large excess of CD₃CN used in the reaction. Doubling the concentration of CD₃CN reduced the initial rate by a factor of 4 equating to an inverse second order rate dependence on [MeCN]. For completeness, the concentrations of **15-TMS** and **3** were also varied in separate runs and both reactants were confirmed to be first order.

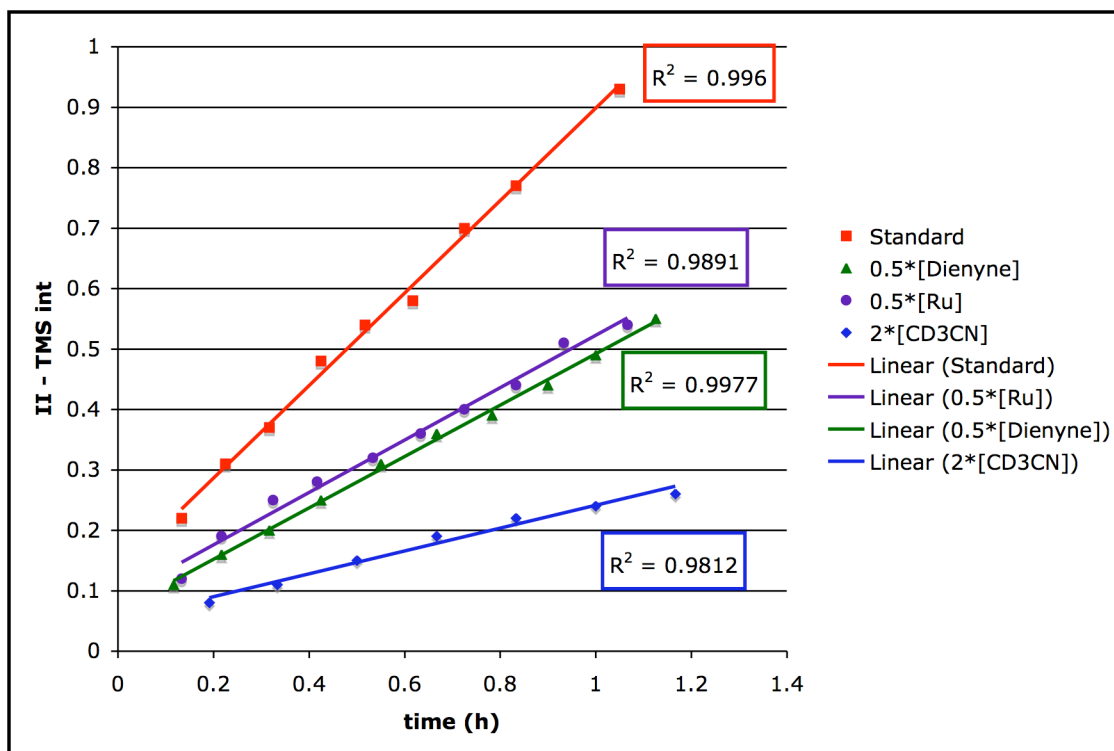


Figure 2-5. Plots for the formation of **II** vs. time and regression trend lines for the reaction of **15-TMS** and **3**. Normalized run (red square), varied concentration of **15-TMS** (purple circle), varied concentration of **3** (green triangle), and varied concentration of CD₃CN (blue diamond). Reaction was monitored to < 10 % conversion of **15-TMS**.

Table 2-6. Relative rates and calculated reaction orders for the conversion of **15-TMS** and **3** to **II**. (a) Relative rates were calculated as the slope of the least squares regression best-fit line for the increase in **II** over time (h) and normalized to standard run. (b) Errors represented as 95% confidence intervals.

| Plot | Symbol | Rel. Rate ^{a,b} | Reaction Order ^b |
|--------------------------|----------------|--------------------------|-----------------------------|
| Standard | Red Square | 1 ± 0.11 | |
| 2 * [CD ₃ CN] | Blue Diamond | 0.25 ± 0.04 | -2.0 ± 0.2 |
| 0.5 * [Dienyne] | Green Triangle | 0.56 ± 0.04 | 0.8 ± 0.1 |
| 0.5 * [Ru] | Purple Circle | 0.57 ± 0.06 | 0.8 ± 0.1 |

The results from the kinetic experiments rule out simple η^2 -alkyne coordination at the rate-determining step, but, as shown in Figure 2-6, other coordination modes consistent with an inverse second order MeCN rate law could be envisioned to trigger a [1,7]-H shift. One possibility would be an η^4 -enyne intermediate **33** that locks the alkyne and alkene into the reactive conformation. Although this coordination mode seems reasonable, X-ray structure analysis of a related [Cp*Ru(CO)(ene- η^4 -diyne)]PF₆ (**34**) show the two terminal alkyne carbons (*c* and *d*) are moved further apart by about 0.1 Å compared to the uncomplexed enediyne.²⁶ This would correspond by analogy to an increased distance between the two reactive groups in **33**. Also reasonable would be intermediate **35** resembling structurally characterized η^6 -dienyne **36**.^{5b} Complex **36** has a 2.80 Å distance between the terminal alkene and alkyne carbons. While this short distance would certainly assist the [1,7]-H shift, it is questionable if a CH₃ could replace the H^{int} position and still allow for the formation of an intermediate like **35**. Previous studies in the O'Connor laboratory have suggested η^6 -dienyne **36** as a possible intermediate in the formation of the formal Hopf product (see Scheme 2-2).²⁶ It may be reasonable to correlate the formation of the new alkyne insertion products **17-TMS** / **18-TMS** with the reasoning that **15-TMS** *cannot* form the η^6 -dienyne intermediate due to steric repulsion between the bulky TMS group and H^{int} (*E*) / CH₃ (*Z*). If **36** is an intermediate in formal Hopf dienyne cyclization and it was able to form from the reaction of **15-TMS** and **3**, we would expect that **15-TMS-E** would cyclize much faster than **15-TMS-Z**, but this is not the case.

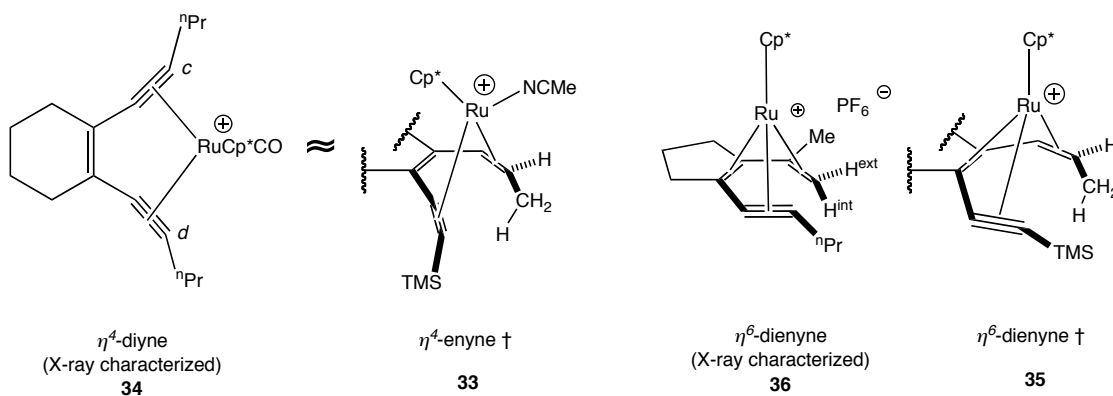
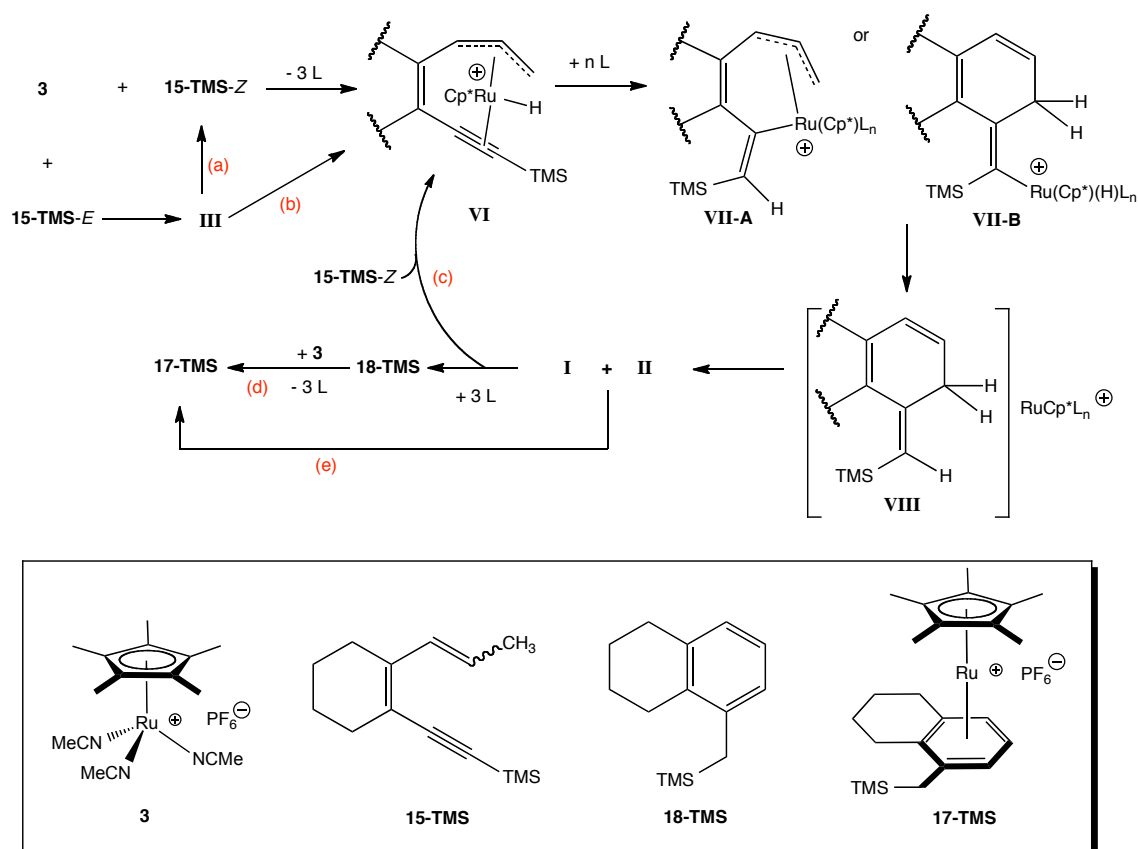


Figure 2-6. Comparison of X-ray characterized enediyne and dienyne Cp^*RuL_n complexes to possible intermediate structures for a [1,7]-H shift.

Another possible mechanism initiates by oxidative addition of the dienyne allylic C-H bond. This process is proposed to occur directly for **15-TMS-Z** by reaction with **3**, resulting in the formation of the allyl hydride complex **VI** (Scheme 2-10). The *trans*-isomer **15-TMS-E** initially forms the spectroscopically observed transient species **III** that slowly converts to **VI**. It cannot be determined if this is a sequential process that first results in isomerization to **15-TMS-Z**, pathway (a), or direct conversion to **VI**, pathway (b). From **VI**, an intramolecular insertion of the hydride or allyl across the alkyne gives vinyl complexes **VII-A** and **VII-B**, respectively. Sequential reductive elimination gives Ru-complexed *iso*-toluene **VIII**, which could potentially be a common intermediate for both the C-H metal insertion and [1,7]-H shift mechanisms. Isomerization of **VIII** gives the observed transient species, **I** and **II**, that exist as an equilibrating mixture. A formal [1,3]-H shift would then give the aromatized products, **17-TMS** and **18-TMS**. In the most direct catalytic pathway (c), **15-TMS-Z** would displace the cyclized product **18-TMS** from the coordination sphere of the post cyclization metal-arene adduct (*vide infra*) to regenerate hydride **VI**. This substitution probably does not occur from the η^6 -arene complex **17-TMS** as was shown that photolysis of latter in the presence of dienyne only results in isomerization of the distal alkene. Once liberated, the free arene **18-TMS** could then compete

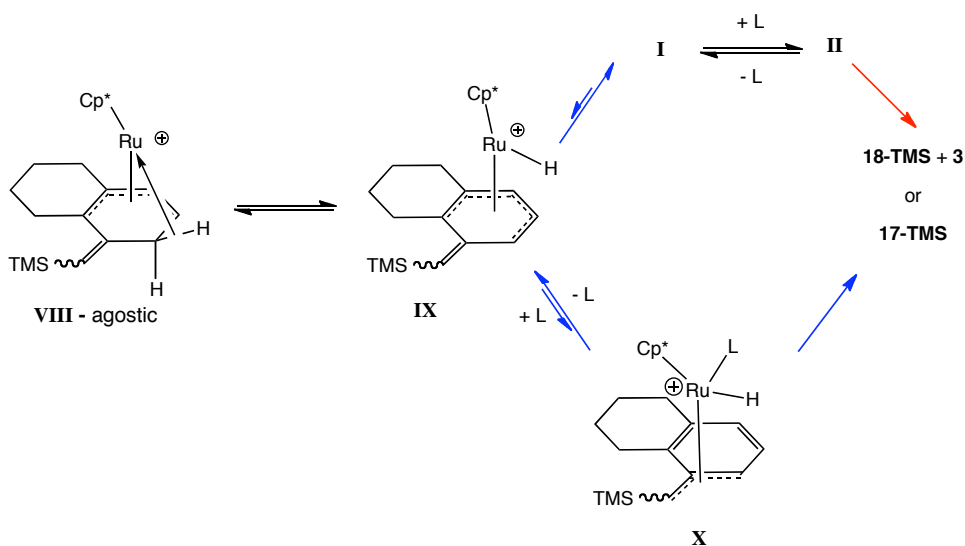
with the substrate for binding of any free **3** resulting in catalyst death by formation of **17-TMS** (d). Evidence against pathway (d) was seen during the reaction of **3** and **15-TMS** in CD_3CN that resulted in the slow conversion of substrate to **17-TMS** as the sole product (Scheme 2-9). If the pathway to **17-TMS** were by η^6 -complexation of **18-TMS**, a measurable amount of the arene should have been observable in the reaction with CD_3CN as arene binding would be inhibited due to a disfavorable equilibrium to open coordination sites on **3**. Therefore the most reasonable pathway to **17-TMS** would be by direct conversion from **I** and **II** (e).



Scheme 2-10. Proposed metal hydride C-H activation mechanism.

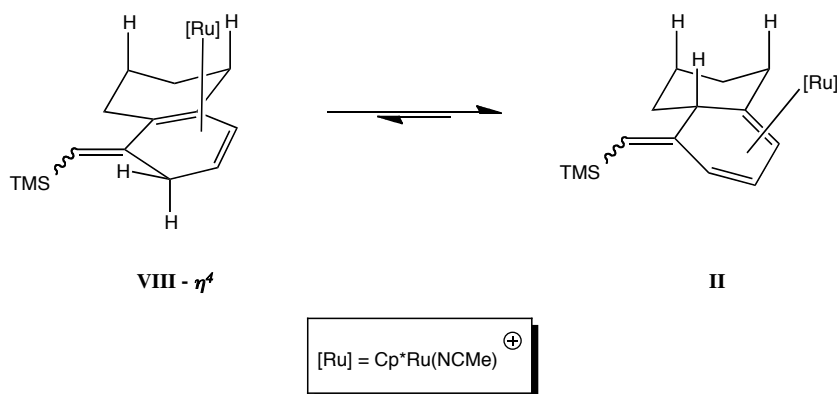
Assuming our proposed structures for **I** and **II** are correct, it is interesting that **VIII** converts to these complexes before proceeding to product. If the isomerization occurs through

a metal hydride mechanism, one explanation could be that the chelate-effect of the η^5 -pentadienyl coordination in the initially formed hydride **IX** disfavors formation of allyl hydride **X** and a lower energy option may be reductive elimination to the isomerized structures **I** and **II** (Scheme 2-11). From the NMR observed species, the reaction could either follow a direct path (red arrow), not involving the metal, or slowly move back through **IX** and **X** to products (blue arrows).



Scheme 2-11. Proposed mechanism for conversion of the observable transient complexes, **I** and **II** to aromatized products.

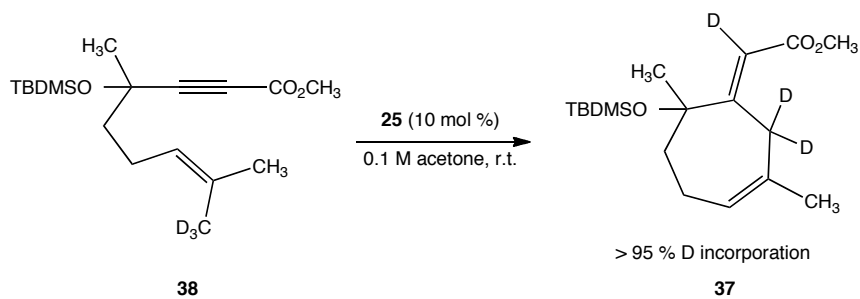
Thermodynamically, the positioning of the alkenes in **I** and **II** would be more favorable for coordination of a metal fragment than in **VIII**. As shown in Scheme 2-12, the metal encounters less congestion from the axial hydrogen atoms due to tilting of the planar η^4 -diene in **II**. Also, the diene portion in **VIII** is more electron-donating therefore more back-bonding from the metal would be expected in **I** and **II**. This may explain why a species consistent with the connectivity of **VIII** is not observed in the reaction mixture.



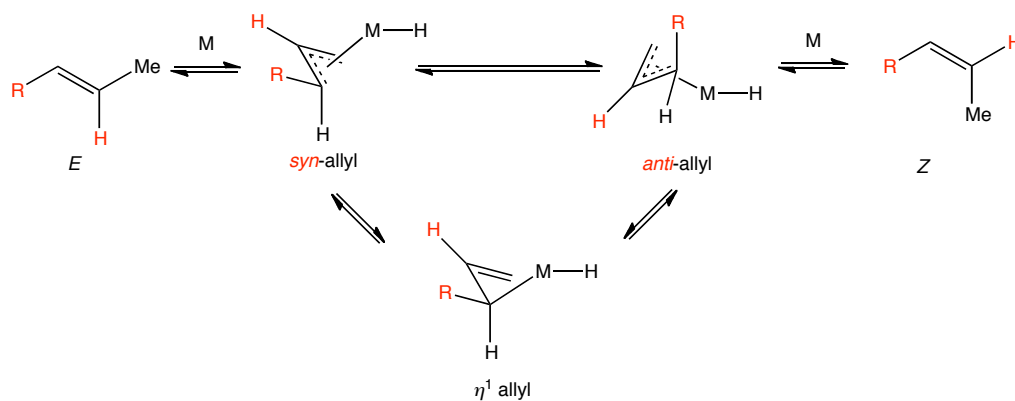
Scheme 2-12. Possible thermodynamic explanation for hydrogen shuttling from **VIII- η^4** to **II**.

In regards to the selectivity for **15-TMS-Z** and support of a mechanism involving **VI**, Trost and coworkers have proposed similar Ru-allyl hydrides and observed substantial selectivity for *cis*-allylic C-H bond activation over *trans*-allylic C-H bond activation during cycloisomerization of enynes to cycloheptenes.²⁷ Irrespective of a kinetic isotope effect, cycloheptene **37** was obtained with nearly quantitative deuterium incorporation in the indicated positions for the intramolecular competition reaction of enyne **38** catalyzed by **25** (Scheme 2-13). These researchers have provided two possible explanations for the selectivity: (1) van der Waals strain created between the substituents of the quaternary carbon and the cyclopentadienyl (Cp) ligand in the *syn*-allyl complex (derived from the *trans*-methyl) and/or (2) a slow π - σ - π isomerization pathway of the *syn*-allyl complex to the *anti*-allyl complex (see Scheme 2-14).

If the C-H metal insertion mechanism is operable for the dienyne cycloaromatization, then the selectivity for **15-TMS-Z** may be attributed to a relatively slow π - σ - π isomerization compared to the rate of cyclization of the *anti*-allyl complex (stereochemistry of **VI** as pictured in Scheme 2-10). Similar to the conversion of **38** to **37**, **15-TMS-E** must isomerize at some point on the reaction coordinate in order to make carbon-carbon bond formation feasible therefore making it less reactive than **15-TMS-Z**.²⁸



Scheme 2-13. Intramolecular competition study showing selective CH activation of the *cis*-allylic methyl with $[\text{CpRu}(\text{NCMe})_3]\text{PF}_6$ (**25**).²⁷



Scheme 2-14. π - σ - π isomerization.

As a final note, we probed the possibility of observing a metal hydride by mixing **15-TMS** with **3** at -75°C then monitoring the reaction mixture by ^1H NMR spectroscopy while gradually warming to ambient temperature. As the sample was warmed, the conversion of starting material to **I** and **II** was observed. There was no observation of any $\text{Ru}(\text{IV})\text{H}$ resonances in the spectral region between δ -8.0 to -11.0 ppm.²¹

VI. Conclusions and Future Outlook.

In conclusion, we have demonstrated a high yielding cycloaromatization of a *cis*-1,3-dien-5-yne resulting from the intramolecular addition of an allylic CH bond across the 5-yne. This dienyne cyclization route is fundamentally different to previous studies with identical metal systems that resulted in the formal Hopf product. The divergent pathway appears to be correlated to the alkyne substituent, becoming more pronounced as the steric bulk of the group increases. Exploratory studies with TMS substituted dienyne **15-TMS** show modest levels of catalysis with [Cp**Ru*(NCCH₃)₃]PF₆ **3**, non-detrimental rate enhancement under mild warming (50°C), and substrate selectivity for the *cis*-stereoisomer **15-TMS-Z**. Three potential intermediates (**I**, **II**, and **III**) have been identified for the reaction of **15-TMS**. An equilibrium between **I** and **II** was observed involving possible reversible coordination of an acetonitrile ligand and **III** appears to originate from the *trans*-stereoisomer **15-TMS-E**. Based on HSQC and HMBC data, a tentative structure was proposed for **II** in which the carbon bond for the cyclized product has formed. Speculative structures were also given for **I** and **III**. Initial rate kinetics have identified an inverse second order MeCN rate dependence for the formation of **II**, ruling out simple η^2 -coordination of the alkyne as the cyclization triggering event. We are currently considering two mechanistic models to account for the observed reactivity: (1) a [1,7]-hydrogen shift / 6 π electrocyclozation pathway and (2) an initial metal C-H bond activation followed by sequential 1,2-insertion, reductive elimination, and isomerization. In regards to the latter mechanism, we have conducted a low temperature NMR experiment but were unable to obtain any evidence for a metal hydride. Future studies are being directed towards differentiating these mechanisms as well as exploring the substrate scope and structure elucidation of transient complexes observed at intermediate reaction times.

VII. Experimental.

i. General Procedures.

All reactions directed toward the synthesis of dienyne substrates were performed in round bottom flasks equipped with magnetic teflon coated stir bars and rubber septa under a positive pressure of N₂, unless otherwise noted. Dienyne cyclization reactions were performed under an N₂ atmosphere in 5 mm J-young NMR tubes equipped with a teflon needle valve. Solutions of air- and moisture-sensitive reagents were transferred by syringe or stainless steel cannula. Air- and moisture-sensitive solids were handled in a glove box under an N₂ atmosphere. Organic solvent solutions were concentrated by rotary evaporation (ca. 10 – 160 torr) at 25 - 35°C, unless otherwise noted. High vacuum distillations were performed at 23°C (ca. 0.01 torr) using a receiver flask cooled to -75°C. Preparative thin layer chromatography (PTLC) was performed on glass plates pre-coated with silica gel (1 mm, 60 Å pore size, EMD Chemicals) and visualized by exposure with ultraviolet light. Flash column chromatography purification of synthetic intermediates and dienynes substrates was performed by literature procedure²⁹ using silica gel (60 Å, particle size 0.043 – 0.060 mm, EMD Chemicals).

ii. Materials.

Tetrahydrofuran (THF), ethyl ether and hexanes used for reaction solvents were dried either by a solvent dispensing system equipped with two neutral alumina columns under argon atmosphere or over sodium/benzophenone ketyl under an N₂ atmosphere. Chloroform-*d* and methylene chloride-*d*₂ were dried over calcium hydride under a nitrogen atmosphere. Acetone-*d*₆ was dried over 4 Å activated sieves for 5 h under an N₂ atmosphere. All other solvents were used as received from commercial suppliers. [Cp*Ru(NCMe)₃]PF₆ (**3**) was prepared according

to literature procedure.¹⁰ All other literature compounds were prepared according to the indicated reference or purchased from commercial suppliers and used as received.

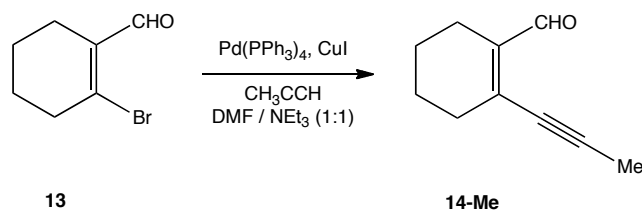
iii. Instrumentation.

NMR spectra were recorded on a Varian Mercury 300 (¹H, 300 MHz; ¹³C 75.5 MHz), Varian Mercury 400 (¹H, 400 MHz; ¹³C 100.7 MHz), Jeol ECA 500 (¹H, 500 MHz) or Varian VX 500 (¹H, 500 MHz; ¹³C 125 MHz) spectrometer. ¹H and ¹³C NMR chemical shifts are reported in parts per million (ppm). ¹H NMR chemical shifts were referenced to the residual protio resonance for CDCl₃ (δ 7.26). ¹³C NMR chemical shifts were referenced to CDCl₃ (δ 77.16). Infrared (IR) spectra were recorded on a JASCO FT-IR 4100 attenuated total reflectance (ATR) platform (3mm) using ZnSe plates (thin films). High-resolution mass spectra were obtained by the University of California, San Diego Mass Spectrometry Facility. Melting points are uncorrected and were recorded on an Electrothermal or Stanford Research Systems EZ-Melt apparatus.

iv. Preparation and characterization data for dienyne substrates and synthetic intermediates.

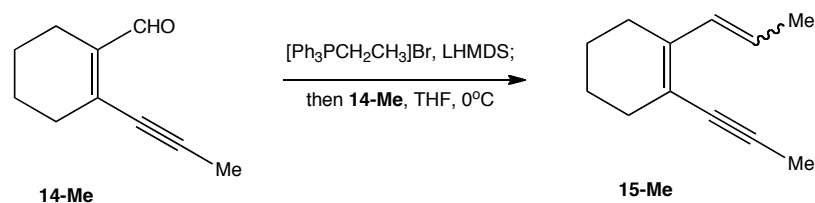
2-(Prop-1-yn-1-yl)cyclohex-1-enecarbaldehyde (14-Me). Pd(PPh₃)₄ (0.305 g, 0.246 mmol) and CuI (0.100 g, 0.529 mmol) were added to a propyne saturated stirring solution of **13** (1.00 g, 5.29 mmol) in NEt₃/DMF (1:1, 40 mL) at 23°C. After stirring at 23°C under a propyne atmosphere for 3 h, the reaction mixture was concentrated, diluted with 1M aq. HCl (100 mL), and extracted with Et₂O (100 mL). The organic extract was washed successively with 1M aq. HCl (2 x 50 mL) / H₂O (2 x 50 mL) / brine (50 mL), dried over anhydrous MgSO₄, concentrated, and purified by flash column chromatography (99:1 hexanes / EtOAc) to afford **14-Me** as a

yellow oil (0.564 g, 3.81 mmol, 72%). IR: 2221 (C≡C), 1668 (C=O) cm^{-1} . ^1H NMR (500 MHz, CDCl_3) δ : 1.58 – 1.67 (m, 4H, 4,5- CH_2), 2.04 (s, 3H, CH_3), 2.19 – 2.24 (m, 2H, 6- CH_2), 2.33 – 2.38 (m, 2H, 3- CH_2), 10.15 (s, 1H, CHO). ^{13}C NMR (100 MHz, CDCl_3) δ : 4.6 (CH_3), 21.1 (CH_2), 21.8 (CH_2), 21.9 (CH_2), 32.6 (CH_2), 77.1 (C≡C), 95.9 (C≡C), 141.0 (C=C), 141.8 (C=C), 193.1 (CHO). HRMS (EI): Calcd for ($\text{C}_{10}\text{H}_{12}\text{O}$): 148.0883, found 148.0882.

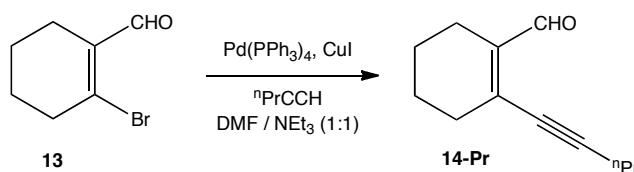


1-(Prop-1-en-1-yl)-2-(prop-1-yn-1-yl)cyclohex-1-ene (15-Me). Lithium bis(trimethylsilyl)amide (2.06 mL, 2.06 mmol, 1 M in THF) was added to a stirring mixture of ethyltriphenylphosphonium bromide (1.02 g, 2.74 mmol) in THF (3.3 mL) at 0°C. **14-Me** (203 mg, 1.37 mmol, 0.84 M in THF) was then added dropwise. After stirring at 0°C for 30 min, the reaction mixture was quenched with sat. aq. NH_4Cl (10 mL) and extracted with Et_2O (4 x 20 mL). The organic extracts were dried with anhydrous MgSO_4 , concentrated, and purified by flash column chromatography (hexanes) to afford **15-Me** as a colorless oil (113 mg, 0.705 mmol, 51%, 75:25 *E/Z*). ^1H NMR (400 MHz, CDCl_3) δ : 1.55 – 1.67 (m, 8H, *E/Z*-4,5- CH_2), 1.77 (dd, $^3J_{\text{HH}} = 7.5$ Hz, $^4J_{\text{HH}} = 1.5$ Hz, 3H, *Z*- $\text{CH}=\text{CHCH}_3$), 1.82 (d, $^3J_{\text{HH}} = 7.0$ Hz, 3H, *E*- $\text{CH}=\text{CHCH}_3$), 1.99 (s, 3H, *Z*- $\text{C}\equiv\text{CCH}_3$), 2.04 (s, 3H, *E*- $\text{C}\equiv\text{CCH}_3$), 2.15 – 2.25 (m, 4H, *E*-3,6- CH_2), 2.26 – 2.32 (m, 4H, *Z*-3,6- CH_2), 5.51 (dq, $^3J_{\text{HH}} = 11.5$ Hz, $^3J_{\text{HH}} = 7.0$ Hz, 1H, *Z*- $\text{CH}=\text{CHCH}_3$), 5.73 (dq, $^3J_{\text{HH}} = 15.6$ Hz, $^3J_{\text{HH}} = 7.0$ Hz, 1H, *E*- $\text{CH}=\text{CHCH}_3$), 6.28 (app. d, $^3J_{\text{HH}} = 12.5$ Hz, 1H, *Z*- $\text{CH}=\text{CHCH}_3$), 6.79 (d, $^3J_{\text{HH}} = 16.0$ Hz, 1H, *E*- $\text{CH}=\text{CHCH}_3$). ^{13}C NMR (100 MHz, CDCl_3) δ : 4.53 (*Z*- $\text{C}\equiv\text{CCH}_3$), 4.61 (*E*- $\text{C}\equiv\text{CCH}_3$), 15.7 (*Z*- $\text{CH}=\text{CHCH}_3$), 18.6 (*E*- $\text{CH}=\text{CHCH}_3$), 22.3 (*E*- CH_2), 22.4 (*Z*- CH_2), 22.6 (*E*- CH_2), 22.7 (*Z*- CH_2), 25.2 (*E*- CH_2), 29.8 (*Z*- CH_2), 30.9 (*Z*- CH_2), 31.1 (*E*- CH_2), 80.1 (*E*- $\text{C}\equiv\text{C}$), 80.7 (*Z*- $\text{C}\equiv\text{C}$), 89.3 (*Z*- $\text{C}\equiv\text{C}$), 89.9 (*E*- $\text{C}\equiv\text{C}$), 117.5 (*E*- $\text{C}=\text{C}$), 118.6 (*Z*- $\text{C}=\text{C}$), 124.4 (*E*- $\text{CH}=\text{CH}$), 125.6 (*Z*- $\text{CH}=\text{CH}$),

130.7 (*Z*-CH=CH), 131.8 (*E*-CH=CH), 138.9 (*E*-C=C), 140.2 (*Z*-CH=CH). HRMS (EI): Calcd for (C₁₂H₁₆): 160.1247, found 160.1246.

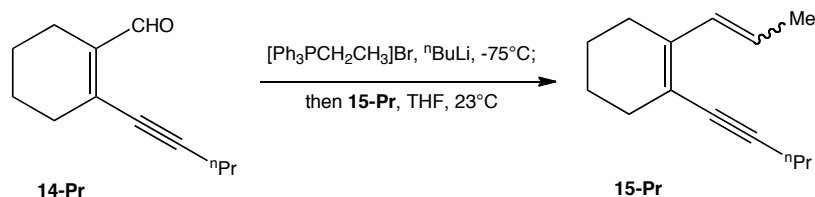


2-(Pent-1-yn-1-yl)cyclohex-1-enecarbaldehyde (14-Pr). Pd(PPh₃)₄ (0.549 g, 0.480 mmol) and Cul (0.151 g, 0.790 mmol) were added to an argon saturated stirring solution of **13** (1.00 g, 5.28 mmol) in NEt₃/DMF (1:1, 40 mL) at 23°C. After stirring at 23°C for 10 min, 1-pentyne (0.78 mL, 7.93 mmol) was added and the reaction was stirred at 23°C for 5 h before being diluted with 1M aq. HCl (50 mL) and extracted with hexanes (2 x 50 mL). The organic extracts were washed successively with 1M aq. HCl (50 mL) / water (100 mL) / brine (100 mL), dried over MgSO₄, concentrated, and purified by flash column chromatography (hexanes) to afford **14-Pr** as a yellow oil (0.560 g, 3.18 mmol, 60%). The product exhibited spectroscopic properties identical to those reported in literature.³⁰

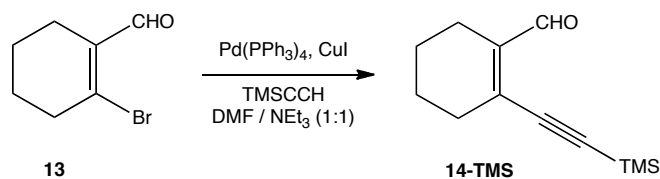


1-(Pent-1-yn-1-yl)-2-(prop-1-en-1-yl)cyclohex-1-ene (15-Pr). n-Butyllithium (2.27 mL, 3.63 mmol, 1.6 M in hexanes) was added dropwise to a stirring mixture of ethyltriphenylphosphonium bromide (1.35 g, 3.63 mmol) in THF (121 mL) at -78°C. After warming to 23°C, **14-Pr** (400 mg, 2.27 mmol, 0.39 M in THF) was added over 15 min. The reaction mixture was then stirred for 1 h at 23°C, quenched with sat. aq. NH₄Cl (100 mL) and extracted with Et₂O (100 mL). The organic extract was washed with brine (100 mL), dried with anhydrous MgSO₄, concentrated,

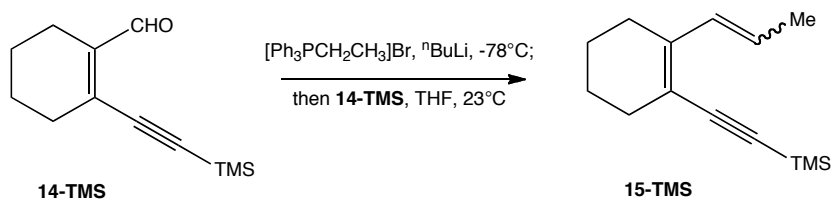
and purified by flash column chromatography (hexanes) to afford **15-Pr** as a yellow oil (251 mg, 1.33 mmol, 59%, 60:40 *E/Z*). ^1H NMR (400 MHz, CDCl_3) δ : 0.98 (t, $^3J_{\text{HH}} = 7.0$ Hz, 3H, *Z*- $\text{CH}_2\text{CH}_2\text{CH}_3$), 1.03 (t, $^3J_{\text{HH}} = 7.5$ Hz, 3H, *E*- $\text{CH}_2\text{CH}_2\text{CH}_3$), 1.50 – 1.67 (m, 12H, *E/Z*-4,5- CH_2 / *E/Z*- $\text{CH}_2\text{CH}_2\text{CH}_3$), 1.77 (dd, $^3J_{\text{HH}} = 7.4$ Hz, $^4J_{\text{HH}} = 2.0$ Hz, 3H, *Z*- $\text{CH}=\text{CHCH}_3$), 1.82 (d, $^3J_{\text{HH}} = 6.5$ Hz, 3H, *E*- $\text{CH}=\text{CHCH}_3$), 2.15 – 2.33 (m, 8H, *E/Z*-3,6- CH_2), 2.33 (t, $^3J_{\text{HH}} = 7.0$ Hz, 2H, *Z*- $\text{CH}_2\text{CH}_2\text{CH}_3$), 2.37 (t, $^3J_{\text{HH}} = 7.0$ Hz, 2H, *E*- $\text{CH}_2\text{CH}_2\text{CH}_3$), 5.50 (dq, $^3J_{\text{HH}} = 11.8$ Hz, $^3J_{\text{HH}} = 7.0$ Hz, 1H, *Z*- $\text{CH}=\text{CHCH}_3$), 5.73 (dq, $^3J_{\text{HH}} = 15.6$ Hz, $^3J_{\text{HH}} = 6.5$ Hz, 1H, *E*- $\text{CH}=\text{CHCH}_3$), 6.30 (app. d, $^3J_{\text{HH}} = 11.5$ Hz, 1H, *Z*- $\text{CH}=\text{CHCH}_3$), 6.81 (d, $^3J_{\text{HH}} = 16.0$ Hz, 1H, *E*- $\text{CH}=\text{CHCH}_3$). ^{13}C NMR (100 MHz, CDCl_3) δ : 13.6, 15.7, 18.7, 21.7, 21.8, 22.4, 22.5, 22.59, 22.64, 22.7, 25.2, 29.8, 31.0, 31.2, 81.1 (C \equiv C), 81.8 (C \equiv C), 93.9 (C \equiv C), 94.6 (C \equiv C), 117.6 (C=C), 118.7 (C=C), 124.3 (CH=CH), 125.6 (CH=CH), 130.8 (CH=CH), 132.0 (CH=CH), 138.8 (C=C), 140.1 (C=C). HRMS (EI): Calcd for (C $_{14}$ H $_{20}$): 188.1560, found 188.1559.



2-((Trimethylsilyl)ethynyl)cyclohex-1-enecarbaldehyde (14-TMS). $\text{Pd}(\text{PPh}_3)_4$ (2.84 g, 2.46 mmol) and CuI (0.779 g, 4.10 mmol) were added to an argon saturated stirring solution of **13** (5.16 g, 27.3 mmol) in NEt_3/DMF (1:1, 210 mL) at 23°C . After stirring at 23°C for 10 min, trimethylsilylacetylene (5.78 mL, 40.9 mmol) was added and the reaction was stirred at 23°C for 16 h, concentrated, diluted with CH_2Cl_2 (200 mL), filtered through celite, washed successively with aq. 1% HCl (200 mL) / brine (200 mL), dried over Na_2SO_4 , concentrated, and purified by flash silica column chromatography (98:2 hexanes / EtOAc) to afford **14-TMS** as an orange oil (4.76 g, 23.1 mmol, 84%). The product exhibited spectroscopic properties identical to those reported in literature.³¹

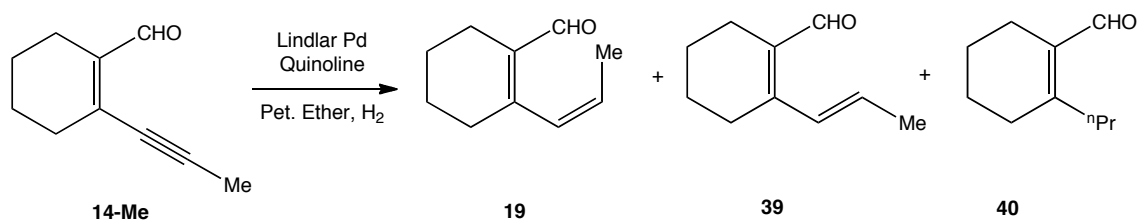


Trimethyl((2-(prop-1-en-1-yl)cyclohex-1-en-1-yl)ethynyl)silane (15-TMS). *n*-Butyllithium (0.87 mL, 1.39 mmol, 1.6 M in hexanes) was added dropwise to a stirring mixture of ethyltriphenylphosphonium bromide (0.517 g, 1.39 mmol) in THF (46 mL) at -78°C . After warming to 23°C , **14-TMS** (190 mg, 0.870 mmol, 0.39 M in THF) was added and the reaction mixture was then stirred for 30 min at 23°C , quenched with sat. aq. NH_4Cl (100 mL) and extracted with Et_2O (1 x 200 mL, 1 x 50 mL). The organic extract was washed with brine (100 mL), dried with anhydrous MgSO_4 , concentrated, and purified by flash column chromatography (hexanes) to afford **15-TMS** as a yellow oil (122 mg, 0.559 mmol, 64%, 59:41 *E/Z*). Spectral properties reported with **15-TMS-E** and **15-TMS-Z**.



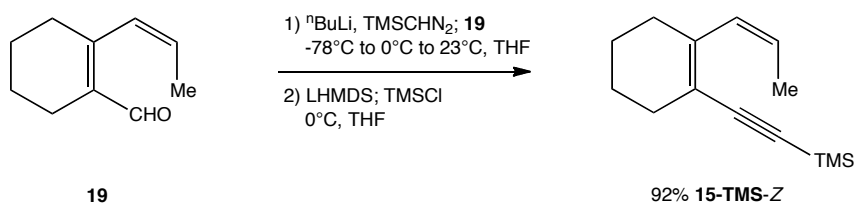
(Z)-2-(Prop-1-en-1-yl)cyclohex-1-enecarbaldehyde (19). H_2 was bubbled through a stirring mixture of quinoline (0.020 mL, 0.17 mmol) and Lindlar Pd (192 mg, 0.09 mmol Pd) in pet. ether (28 mL) at 23°C for 5 min. **14-Me** (252 mg, 1.70 mmol, 2M in EtOAc) was then added. After stirring at 23°C under a hydrogen atmosphere for 1.25 h, the reaction mixture was filtered through celite, concentrated, and purified by flash column chromatography (98:2 hexanes / EtOAc) to afford a mixture of **19**, **39**, **40**, and **14-Me** as a colorless oil (214 mg, 1.42 mmol, 84%) in a 89 : 7 : 2 : 2 NMR ratio, respectively. IR: $1666 (\text{C}=\text{O}) \text{ cm}^{-1}$. ^1H NMR (500 MHz, CDCl_3) for **19** δ : 1.59 (dd, $^3J_{\text{HH}} = 6.8 \text{ Hz}$, $^4J_{\text{HH}} = 2.0 \text{ Hz}$, 3H, $\text{CH}=\text{CHCH}_3$), 1.62 – 1.70 (m, 4H, 4,5- CH_2), 2.17

– 2.28 (m, 4H, 3,6-CH₂), 5.82 (dq, ³J_{HH} = 11.6 Hz, ³J_{HH} = 6.8 Hz, 1H, CH=CHCH₃), 5.99 (app. d, ³J_{HH} = 11.7 Hz, 1H, CH=CHCH₃), 9.76 (s, 1H, CHO); observable for **39** δ: 1.88 (d, ³J_{HH} = 6.8 Hz, 3H, CH=CHCH₃), 6.04 (dq, ³J_{HH} = 15.1 Hz, ³J_{HH} = 6.8 Hz, 1H, CH=CHCH₃), 6.97 (d, ³J_{HH} = 15.6 Hz, 1H, CH=CHCH₃), 10.28 (s, 1H, CHO); observable for **40** δ: 0.94 (t, ³J_{HH} = 7.3 Hz, 3H, CH₂CH₂CH₃), 2.49 (t, ³J_{HH} = 7.8 Hz, 2H, CH₂CH₂CH₃), 10.11 (s, 1H, CHO). ¹³C NMR (125 MHz, CDCl₃) for **19** δ: 14.7 (CH=CHCH₃), 21.7 (CH₂), 21.9 (CH₂), 22.1 (CH₂), 31.8 (3-C), 127.9 (CH=CHCH₃), 130.1 (CH=CHCH₃), 135.0 (1-C), 155.5 (2-C), 193.7 (CHO). HRMS (EI): Calcd for **19**, **39** (C₁₀H₁₄O): 150.0139, found 150.1042; Calcd for **40** (C₁₀H₁₆O): 152.1196, found 152.1193.



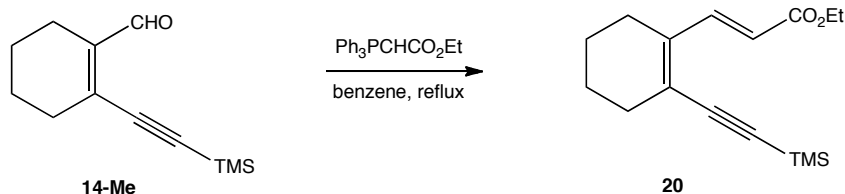
92% Z -Trimethyl((2-(prop-1-en-1-yl)cyclohex-1-en-1-yl)ethynyl)silane (15-TMS). *n*-Butyllithium (1.35 mL, 2.13 mmol, 1.6 M in hexanes) was added dropwise to a stirring solution of (trimethylsilyl)diazomethane (1.07 mL, 2.13 mmol, 2 M in Et₂O) in THF (5.2 mL) at -78°C. After stirring at -78°C for 45 min, **19** (214 mg, 1.42 mmol, 1M in THF) was added dropwise. After stirring at -78°C for 1 h, the reaction was warmed to 0°C for 30 min then to 23°C for 1 hr before quenching with sat. aq. NH₄Cl (10 mL). The quenched reaction mixture was extracted with Et₂O (3 x 20 mL) and the organic extracts were washed with brine, dried over anhydrous MgSO₄, concentrated, and purified by flash column chromatography (hexanes) to afford alkyne product as a colorless oil (67 mg, 0.458 mmol, 32%). Lithium bis(trimethylsilyl)amide (0.916 mL, 0.916 mmol, 1 M in THF) was added to a stirring mixture of the alkyne product (67 mg, 0.458 mmol) in THF (4.6 mL) at 0°C. After stirring at 0°C for 10 min, chlorotrimethylsilane (0.174 mL, 1.37 mmol) was added. After stirring at 0°C for 1 h, the reaction mixture was quenched with sat. aq. NH₄Cl (10 mL) and extracted with Et₂O (3 x 20 mL). The organic extracts were washed

with brine, dried with anhydrous MgSO_4 , concentrated, and purified by flash column chromatography (hexanes) to afford **15-TMS** as a colorless oil (83 mg, 0.308 mmol, 83%). IR: 2135 ($\text{C}\equiv\text{C}$) cm^{-1} . ^1H NMR (500 MHz, CDCl_3) for **15-TMS-Z** δ : 0.17 (s, 9H, TMS), 1.57 – 1.64 (m, 4H, 4,5- CH_2), 1.76 (dd, $^3J_{\text{HH}} = 7.5$ Hz, $^4J_{\text{HH}} = 1.7$ Hz, 3H, $\text{CH}=\text{CHCH}_3$), 2.22 – 2.31 (m, 4H, 3,6- CH_2), 5.53 (dq, $^3J_{\text{HH}} = 12.0$ Hz, $^3J_{\text{HH}} = 7.5$ Hz, 1H, $\text{CH}=\text{CHCH}_3$), 6.25 (app. d, $^3J_{\text{HH}} = 12.0$ Hz, 1H, $\text{CH}=\text{CHCH}_3$). ^{13}C NMR (100MHz, CDCl_3) for **15-TMS-Z** δ : 0.4 (TMS), 16.0 (CHCH_3), 22.3 (CH_2), 22.6 (CH_2), 30.0 (CH_2), 30.5 (CH_2), 97.4 ($\text{C}\equiv\text{C}$), 106.6 ($\text{C}\equiv\text{C}$), 118.0 ($\text{C}=\text{C}$), 126.7 ($\text{CH}=\text{CH}$), 130.5 ($\text{CH}=\text{CH}$), 143.3 ($\text{C}=\text{C}$). HRMS (EI): Calcd for ($\text{C}_{14}\text{H}_{22}\text{Si}$): 218.1485, found 218.1484.

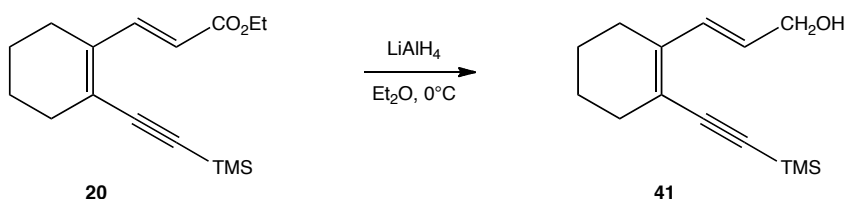


(E)-Ethyl 3-(2-((trimethylsilyl)ethynyl)cyclohex-1-enyl)acrylate (20).

Ethyl (triphenylphosphoranylidene)acetate (1.87 g, 5.37 mmol) and **14-TMS** (1.00 g, 4.85 mmol) were refluxed in benzene (4.8 mL) for 2 h, concentrated, and purified by flash column chromatography (95:5 hexanes / EtOAc) to afford **20** as a yellow solid (1.22 g, 4.41 mmol, 91%). Mp: 44 - 46°C; IR: 2139 ($\text{C}\equiv\text{C}$), 1710 ($\text{C}=\text{O}$) cm^{-1} . ^1H NMR (400 MHz, CDCl_3) δ : 0.24 (s, 9H, TMS), 1.31 (t, $^3J_{\text{HH}} = 7.0$ Hz, 3H, CH_2CH_3), 1.59 – 1.71 (m, 4H, 4,5- CH_2), 2.20 – 2.26 (m, 2H, 6- CH_2), 2.30 – 2.36 (m, 2H, 3- CH_2), 4.22 (q, $^3J_{\text{HH}} = 7.0$ Hz, 2 H, CH_2CH_3), 5.88 (d, $^3J_{\text{HH}} = 16.1$ Hz, 1H, $\text{CH}=\text{CHCO}_2\text{Et}$), 8.06 (d, $^3J_{\text{HH}} = 16.1$ Hz, 1H, $\text{CH}=\text{CHCO}_2\text{Et}$). ^{13}C NMR (100MHz, CDCl_3) δ : 0.1 (TMS), 14.5 (CH_2CH_3), 21.9 (CH_2), 22.0 (CH_2), 25.0 (CH_2), 31.3 (CH_2), 60.4 (CH_2CH_3), 102.3 ($\text{C}\equiv\text{C}$), 104.3 ($\text{C}\equiv\text{C}$), 117.7 ($\text{CH}=\text{CH}$), 127.8 ($\text{C}=\text{C}$), 139.9 ($\text{C}=\text{C}$), 144.2 ($\text{CH}=\text{CH}$), 167.6 (CO_2Et). HRMS (EI): Calcd for ($\text{C}_{16}\text{H}_{24}\text{O}_2\text{Si}$): 276.1540, found 276.1543.



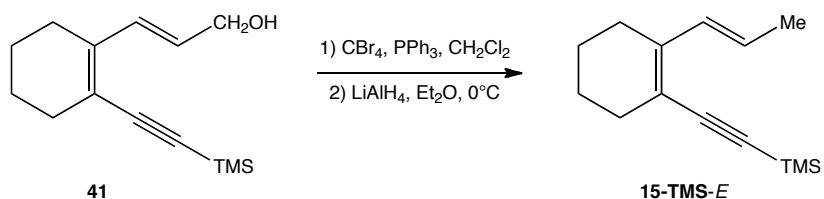
(E)-3-(2-((Trimethylsilyl)ethynyl)cyclohex-1-en-1-yl)prop-2-en-1-ol (41). Lithium aluminum hydride (103 mg, 2.71 mmol) was added to a stirring solution of **20** (250 mg, 0.904 mmol) in Et₂O (9 mL) at 0°C. After stirring at 0°C for 10 min, the reaction mixture was quenched by sequential addition of H₂O (0.40 mL) / 1.3 M aq. NaOH (0.80 mL) / H₂O (1.2 mL), filtered through anhydrous K₂CO₃, and concentrated to afford **41** as a colorless oil (209 mg, 0.891 mmol, 99%). IR: 3332 (OH), 2134 (C≡C) cm⁻¹. ¹H NMR (400 MHz, CDCl₃) δ: 0.21 (s, 9H, TMS), 1.35 (bs, 1H, OH), 1.56 – 1.70 (m, 4H, 4,5-CH₂), 2.20 – 2.30 (m, 4H, 3,6-CH₂), 4.25 (d, ³J_{HH} = 6.0 Hz, 2H, CH₂OH), 5.90 (dt, ³J_{HH} = 15.6 Hz, ³J_{HH} = 6.0 Hz, 1H, CH=CHCH₂), 7.00 (d, ³J_{HH} = 15.6 Hz, 1H, CH=CHCH₂). ¹³C NMR (100MHz, CDCl₃) δ: 0.3 (TMS), 22.1 (CH₂), 22.4 (CH₂), 25.3 (CH₂), 30.8 (CH₂), 64.3 (CH₂OH), 99.5 (C≡C), 105.3 (C≡C), 120.2 (C=C), 128.2 (CH=CH), 132.0 (CH=CH), 140.9 (C=C). HRMS (EI): Calcd for (C₁₄H₂₂OSi + Na): 257.1332, found 257.1334.



(E)-Trimethyl((2-(prop-1-en-1-yl)cyclohex-1-en-1-yl)ethynyl)silane

(15-TMS-E). Triphenylphosphine (234 mg, 0.892 mmol) was added slowly to a stirring solution of **41** (209 mg, 0.892 mmol) and carbon tetrabromide (296 mg, 0.892 mmol) in CH₂Cl₂ (9 mL) at 23°C. After stirring at 23°C for 1 h, the reaction mixture was concentrated, dissolved in Et₂O (9 mL), and cooled to 0°C. Lithium aluminum hydride (102 mg, 2.68 mmol) was then added to the stirring solution. After stirring at 0°C for 45 min, the reaction mixture was quenched by

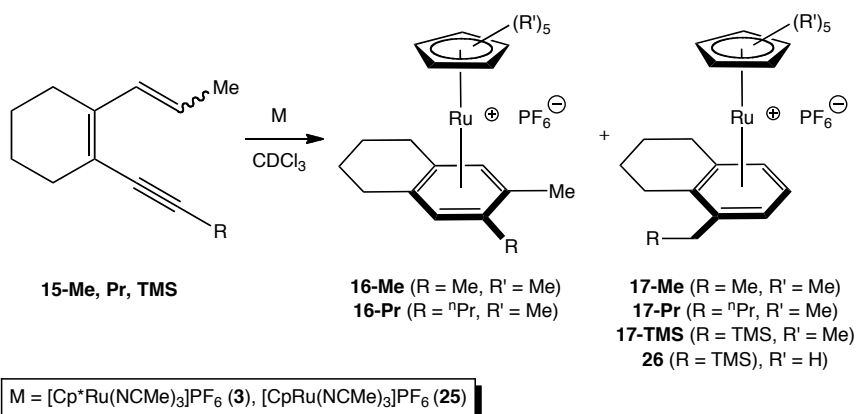
sequential addition of H₂O (0.10 mL) / 1.3 M aq. NaOH (0.20 mL) / H₂O (0.30 mL), filtered through anhydrous K₂CO₃, concentrated, and purified by flash column chromatography (99.5:0.5 hexanes / EtOAc) to afford **15-TMS-E** as a colorless oil (43 mg, 0.197 mmol, 22% over two steps). IR: 2134 (C≡C) cm⁻¹. ¹H NMR (400 MHz, CDCl₃) δ: 0.21 (s, 9H, TMS), 1.55 – 1.67 (m, 4H, 4,5-CH₂), 1.83 (d, ³J_{HH} = 6.5 Hz, 3H, CH=CHCH₃), 2.18 – 2.28 (m, 4H, 3,6-CH₂), 5.79 (dq, ³J_{HH} = 15.6 Hz, ³J_{HH} = 6.5 Hz, 1H, CH=CHCH₃), 6.82 (d, ³J_{HH} = 16.1 Hz, 1H, CH=CHCH₃). ¹³C NMR (100MHz, CDCl₃) δ: 0.3 (TMS), 18.9 (CHCH₃), 22.3 (CH₂), 22.5 (CH₂), 25.4 (CH₂), 30.6 (CH₂), 98.5 (C≡C), 106.0 (C≡C), 116.9 (C=C), 125.7 (CH=CH), 131.9 (CH=CH), 142.0 (C=C). HRMS (EI): Calcd for (C₁₄H₂₂Si): 218.1485, found 218.1487.



v. Preparation and characterization data for cycloaromatized products.

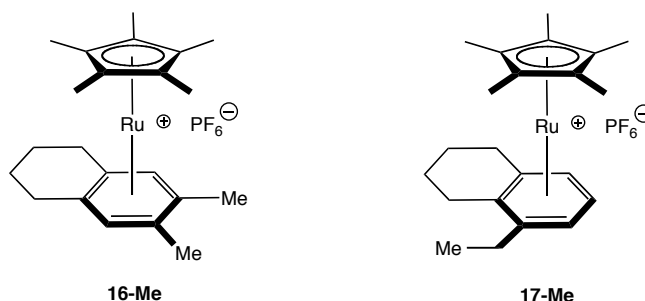
General Procedure Ru(η^6 – arene) complexes. CDCl₃ was distilled into a Teflon sealed J-young tube containing diene substrate **15** and 1,3,5-tri-*tert*-butylbenzene (0.5 – 1 mg) using Schlenk techniques. After the resulting solution had been degassed (3x freeze / pump / thaw), reaction vessel was taken into glove box and contents poured into vial containing metal reagent ([Cp**Ru*(CH₃CN)₃]PF₆ (**3**) or [Cp*Ru*(CH₃CN)₃]PF₆ (**25**) at 23°C. After 5 min of mixing at 23°C, the reaction mixture was transferred back to J-young tube and reacted for the indicated time and temperature until judged to completion by ¹H NMR spectroscopy. The post reaction mixture was concentrated, chromatographed (5.75 inch glass pipette filled with 2.5 cm of Aldrich activated neutral Brockmann I, standard grade aluminum oxide 150 mesh) with CH₂Cl₂ (6 mL) then 95:5 CH₂Cl₂ / acetone (20 mL), and crystallized by vapor diffusion (Et₂O into conc. CH₂Cl₂

solution of chromatographed material) to afford the Ru(η^6 – arene) products (**16-17**, **26**) as air stable solids.



86:14 (η^5 -Pentamethylcyclopentadienyl)(η^6 -6,7-dimethyltetralinyl)ruthenium (II) hexafluorophosphate (**16-Me**) / (η^5 -pentamethylcyclopentadienyl)(η^6 -5-ethyltetralinyl)ruthenium (II) hexafluorophosphate (**17-Me**). **15-Me** (75:25 *E* / *Z*, 3.4 mg, 0.021 mmol), **3** (11 mg, 0.021 mmol), CDCl₃ (0.73 mL). 5 days at 23°C then 24 h at 50°C. white solid (7mg, 0.013 mmol, 62%). ¹H NMR (500 MHz, CDCl₃) δ : 1.23 (t, ³J_{HH} = 7.5 Hz, 3H, **17-Me** -CH₂CH₃), 1.62 – 1.85 (m, 8H, **16-Me/17-Me** -2,3-CH₂), 1.79 (s, 15H, **16-Me**-Cp*), 1.84 (s, 15H, **17-Me**-Cp*), 2.08 (s, 6H, **16-Me**-ArCH₃), 2.16 (dq, ²J_{HH} = 14.6 Hz, ³J_{HH} = 8.0 Hz, 1H, **17-Me**-C(*H*)H'CH₃), 2.32 – 2.47 (m, 2H, **17-Me**), 2.38 (dt, ²J_{HH} = 16.6 Hz, ³J_{HH} = 7.5 Hz, 2H, **16-Me**-1,4-CH^{syn}), 2.59 (dt, ²J_{HH} = 17.2 Hz, ³J_{HH} = 5.7 Hz, 1H, **17-Me**-C(*H*)H'), 2.68 – 2.83 (m, 2H, **17-Me**), 2.71 (dt, ²J_{HH} = 17.2 Hz, ³J_{HH} = 5.2 Hz, 2H, **16-Me**-1,4-CH^{anti}), 5.54 (s, 2H, **16-Me**-ArH), 5.61 (d, ³J_{HH} = 5.7 Hz, 2H, **17-Me**-6,8-ArH), 5.77 (t, ³J_{HH} = 5.7 Hz, 1H, **17-Me**-7-ArH). ¹³C NMR (125 MHz, CDCl₃) δ : 9.7 (**16-Me**-CpCH₃), 10.2 (**17-Me**-CpCH₃), 14.1 (**17-Me**-CH₂CH₃), 16.2 (**16-Me**-ArCH₃), 21.5 (**17-Me**-CH₂), 21.8 (**16-Me**-2,3-CH₂), 22.0 (**17-Me**-CH₂), 23.3 (**17-Me**-CH₂), 23.9 (**17-Me**-CH₂), 25.6 (**16-Me**-1,4-CH₂), 27.1 (**17-Me**-CH₂), 87.2 (**17-Me**-C^{Ar}H), 87.3 (**17-Me**-C^{Ar}H), 87.4 (**17-Me**-C^{Ar}H), 89.3 (**16-Me**-C^{Ar}H), 93.5 (**16-Me**-Cp*), 94.4 (**17-Me**-Cp*), 98.6 (**16-Me**-C^{Ar}), 99.3 (**17-Me**-C^{Ar}), 101.1 (**16-Me**-C^{Ar}), 101.6 (**17-Me**-C^{Ar}), 103.0 (**17-Me**-C^{Ar}). HRMS (EI):

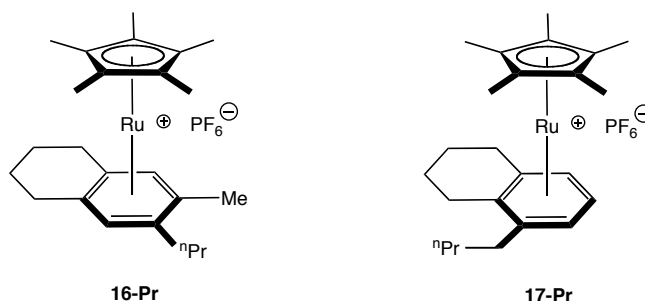
Calcd for (C₂₂H₃₁Ru – PF₆): 391.1496, found 391.1498. Anal. Calcd for C₂₂H₃₁F₆PRu: C, 48.80; H, 5.77. Found: C, 48.80; H, 5.61.



70:30 (η^5 – pentamethylcyclopentadienyl)(η^6 – 6-methyl-7-propyltetralinyl)ruthenium (II) hexafluorophosphate (16-Pr) / (η^5 – pentamethylcyclopentadienyl)(η^6 – 5-butyltetralinyl)ruthenium (II) hexafluorophosphate (17-Pr). 15-Pr (60:40 *E* / *Z*, 22 mg, 0.12 mmol), **3 (60 mg, 0.12 mmol), CDCl₃ (0.79 mL). 68 h at 50°C. white solid (34 mg, 0.060 mmol, 51%). ¹H NMR (500 MHz, CDCl₃) δ : 0.92 (t, ³J_{HH} = 6.9 Hz, 3H, **17-Pr**-(CH₂)₃CH₃), 0.98 (t, ³J_{HH} = 7.7 Hz, 3H, **16-Pr**-(CH₂)₂CH₃), 1.35 – 1.86 (m, 14H, **16-Pr**-3xCH₂ / **17-Pr**-4xCH₂), 1.78 (s, 15H, **16-Pr**-Cp*), 1.83 (s, 15H, **17-Pr**-Cp*), 2.00 – 2.13 (m, 2H, **16-Pr**-C(*H*)H', **17-Pr**-C(*H*)H'), 2.09 (s, 3H, **16-Pr**-ArCH₃), 2.31 - 2.47 (m, 6H, **16-Pr**-C(*H*)H', **16-Pr**-CH₂, **17-Pr**-C(*H*)H', **17-Pr**-CH₂), 2.54 – 2.61 (m, 1H, **17-Pr**-C(*H*)H'), 2.69 – 2.82 (m, 3H, **16-Pr**-1,4-CH^{anti}, **17-Pr**-C(*H*)H'), 5.43 (s, 1H, **16-Pr**-ArH), 5.53 (d, ³J_{HH} = 6.3 Hz, 1H, **17-Pr**-ArH), 5.54 (s, 1H, **16-Pr**-ArH), 5.58 (d, ³J_{HH} = 6.3 Hz, 1H, **17-Pr**-ArH), 5.70 (t, ³J_{HH} = 6.3 Hz, 1H, **17-Pr**-7-ArH). ¹³C NMR (125 MHz, CDCl₃) δ : 9.8 (**16-Pr**-CpCH₃), 10.1 (**17-Pr**-CpCH₃), 13.9 (**16-Pr**-(CH₂)₂CH₃), 14.0 (**17-Pr**-(CH₂)₃CH₃), 15.8 (**16-Pr**-ArCH₃), 21.5 (**17-Pr**-CH₂), 21.77 (**16-Pr**-CH₂), 21.79 (**16-Pr**-CH₂), 22.0 (**17-Pr**-CH₂), 22.7 (**17-Pr**-CH₂), 23.4 (**17-Pr**-CH₂), 23.5 (**16-Pr**-CH₂), 25.5 (**16-Pr**-CH₂), 25.6 (**16-Pr**-CH₂), 27.0 (**17-Pr**-CH₂), 30.4 (**17-Pr**-CH₂), 32.1 (**17-Pr**-CH₂), 32.4 (**16-Pr**-CH₂), 87.0 (**17-Pr**-C^{Ar}H), 87.2 (**17-Pr**-C^{Ar}H), 87.7 (**17-Pr**-C^{Ar}H), 88.1 (**16-Pr**-C^{Ar}H), 89.5 (**16-Pr**-C^{Ar}H), 93.7 (**16-Pr**-Cp*), 94.5 (**17-Pr**-Cp*), 97.8 (**16-Pr**-C^{Ar}), 99.3 (**17-Pr**-C^{Ar}), 101.2 (**16-Pr**-9,10-C^{Ar}), 101.6 (**17-Pr**-C^{Ar}), 101.9 (**17-Pr**-**

C^{Ar}), 102.0 (**16-Pr- C^{Ar}**). HRMS (EI): Calcd for $(C_{24}H_{35}Ru - PF_6)$: 419.1809, found 419.1814. Anal.

Calcd for $C_{24}H_{35}F_6PRu$: C, 50.61; H, 6.19. Found: C, 50.45; H, 6.26.



(η^5 -Pentamethylcyclopentadienyl)(η^6 -5-(trimethylsilylmethyl)tetralinyl)ruthenium (II)

hexafluorophosphate (17-TMS). 15-TMS (92:8 *Z/E*, 10.8 mg, 0.050 mmol), **3** (5.7 mg, 0.0113

mmol), $CDCl_3$ (0.80 mL). 26 h at 23°C. white solid (5 mg, 0.0083 mmol, 74%). mp. 207 –

210°C. 1H NMR (400 MHz, $CDCl_3$) δ : 0.06 (s, 9H, TMS), 1.54 – 1.93 (m, 5H, 2,3- CH_2 ,

$C(H)H^TMS$), 1.55 (d, $^2J_{HH} = 13.1$ Hz, 1H, $C(H)HTMS$), 1.83 (s, 15H, Cp^*), 2.26 (ddd, $^2J_{HH} =$

16.6 Hz, $^3J_{HH} = 8.5$ Hz, $^3J_{HH} = 5.0$ Hz, 1H, 1/4- CH^{syn}), 2.40 – 2.49 (m, 2H, 1/4- CH^{syn} , 1/4- CH^{anti}),

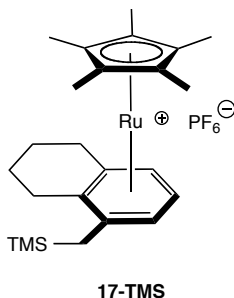
2.80 (ddd, $^2J_{HH} = 17.1$ Hz, $^3J_{HH} = 8.5$ Hz, $^3J_{HH} = 5.02$ Hz, 1H, 1/4- CH^{anti}), 5.39 (d, $^3J_{HH} = 6.0$ Hz,

1H, ArH), 5.54 (d, $^3J_{HH} = 6.0$ Hz, 1H, ArH), 5.66 (t, $^3J_{HH} = 6.0$ Hz, 1H, 7-ArH). ^{13}C NMR (125

MHz, $CDCl_3$) δ : -1.2 (TMS), 10.1 ($CpCH_3$), 20.5 (CH_2), 21.7 (CH_2), 22.2 (CH_2), 24.6 (CH_2), 27.2

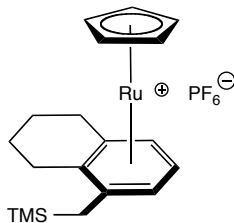
(CH_2), 86.3 ($C^{Ar}H$), 86.4 ($C^{Ar}H$), 86.8 ($C^{Ar}H$), 94.1 (Cp^*), 97.5 (C^{Ar}), 101.1 (C^{Ar}), 104.3 (C^{Ar}).

HRMS (EI): Calcd for $(C_{24}H_{37}RuSi - PF_6)$: 449.1735, found 449.1738.



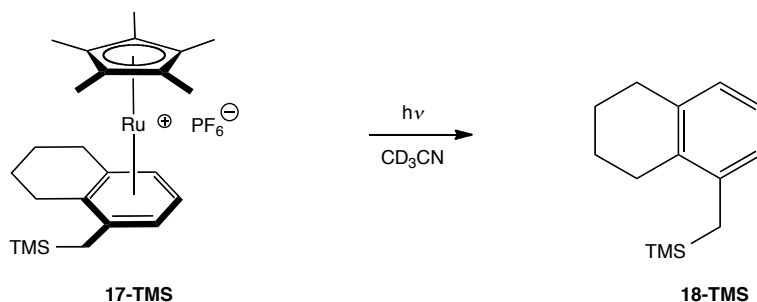
(η^5 -Cyclopentadienyl)(η^6 -5-(trimethylsilylmethyl)tetralinyl)ruthenium (II)

hexafluorophosphate (26). **15-TMS** (92:8 *Z* / *E*, 4 mg, 0.018 mmol), **25** (8 mg, 0.018 mmol), CDCl_3 (0.93 mL). 7 days at 23°C then 24 h at 50°C. colorless solid (5 mg, 0.0094 mmol, 52 %). m.p. 190 - 192°C. ^1H NMR (500 MHz, CDCl_3) δ : 0.07 (s, 9H, TMS), 1.66 – 1.96 (m, 4H, 2,3- CH_2), 2.00 (d, $^2J_{\text{HH}} = 13.8$ Hz, 1H, C(*H*)H'TMS), 2.19 (d, $^2J_{\text{HH}} = 13.8$ Hz, 1H, C(*H*)HTMS), 2.58 – 2.89 (m, 4H, 1,4- CH_2), 5.17 (s, 5H, Cp), 5.92 – 5.95 (m, 2H, 6,8-ArH), 5.97 – 6.01 (m, 1H, 7-ArH). ^{13}C NMR (100 MHz, CDCl_3) δ : -1.3 (TMS), 22.2 (CH_2), 22.6 (CH_2), 23.3 (CH_2), 27.2 (CH_2), 29.4 (CH_2), 81.1 (Cp), 84.0 (C^{ArH}), 84.3 (C^{ArH}), 84.4 (C^{ArH}), 100.2 (C^{Ar}), 102.8 (C^{Ar}), 106.0 (C^{Ar}). HRMS (EI): Calcd for ($\text{C}_{19}\text{H}_{27}\text{RuSi} - \text{PF}_6$): 379.0953, found 379.0959.



26

5-(Trimethylsilylmethyl)tetraline (18-TMS). A solution of **17-TMS** (63 mg, 0.105 mmol) in CD_3CN (0.80 mL) was subjected to direct sunlight under air. After 42 days, the reaction mixture was concentrated, chromatographed (5.75 inch glass pipette filled with 2.5 cm of Aldrich activated neutral Brockmann I, standard grade aluminum oxide 150 mesh) with CH_2Cl_2 (6 mL), and purified by high vacuum distillation to afford **18-TMS** as a colorless oil. ^1H NMR (300 MHz, CDCl_3) δ : 0.01 (s, 9H, TMS), 1.69 – 1.85 (m, 4H, 2,3- CH_2), 2.06 (s, 2H, CH_2TMS), 2.57 (t, $^3J_{\text{HH}} = 6.5$ Hz, 2H, ArCH_2), 2.76 (t, $^3J_{\text{HH}} = 6.5$ Hz, 2H, ArCH_2), 6.76 – 6.84 (m, 2H, 6,8-ArH), 6.97 (t, $^3J_{\text{HH}} = 7.5$ Hz, 1H, 7-ArH). ^{13}C NMR (100 MHz, CDCl_3) δ : -1.1 (TMS), 23.1 (CH_2), 23.2 (CH_2), 23.8 (CH_2), 27.5 (CH_2), 30.5 (CH_2), 125.0 (C^{ArH}), 125.4 (C^{ArH}), 126.3 (C^{ArH}), 133.9 (C^{Ar}), 137.5 (C^{Ar}), 139.1 (C^{Ar}). HRMS (EI): Calcd for ($\text{C}_{14}\text{H}_{22}\text{Si}$): 218.1485, found 218.1486.



vi. Procedures for VT, kinetic, and exploratory experiments.

Observation of 5-methyltetraline. Anhydrous K_2CO_3 (2 mg, 0.015 mmol) was added to a stirring solution of **18-TMS** (1 mg, 0.005 mmol) in THF / CH_3OH (1 mL, 1:1) at 23°C . After 2 h at 23°C , the reaction mixture was filtered and concentrated. ^1H NMR (CDCl_3) of resulting mixture showed reaction to be at partial conversion and observation of 5-methyltetraline.¹⁵

VT NMR equilibrium experiment for I and II. CDCl_3 (0.85 mL) was distilled into a Teflon sealed J-young tube containing **15-TMS** (92:8 *Z* / *E*, 16.5 mg, 0.076 mmol) and 1,3,5-tri-*tert*-butylbenzene (0.5 – 1 mg) using Schlenk techniques. After the resulting solution had been degassed (3x freeze / pump / thaw), reaction vessel was taken into glove box and contents poured into vial containing **3** (38 mg, 0.076 mmol) at 23°C . After 5 min of mixing at 23°C , the reaction mixture was transferred back to J-young tube, removed from box, and cooled to -40°C . After 1 h at -40°C , the reaction vessel was loaded into NMR at 23°C , probe was cooled and experiment started.

Sample preparation for VT NMR HMBC and HSQC acquisition for II. CDCl_3 (0.85 mL) was distilled into a Teflon sealed J-young tube containing **15-TMS** (7:3 *E* / *Z*, 40.0 mg, 0.183 mmol) using Schlenk techniques. After the resulting solution had been degassed (3x freeze / pump /

thaw), reaction vessel was taken into glove box and contents poured into vial containing **3** (27.7 mg, 0.0549 mmol) at 23°C. After 5 min of mixing at 23°C, the reaction mixture filtered and transferred back to J-young tube, removed from box, and maintained at -75°C until NMR experiment was performed.

General procedure for the attempted photolytic catalysis of 15-TMS in presence of 17-TMS. Indicated solvent was distilled into a Teflon sealed J-young tube containing a **15-TMS-Z** / **15-TMS-E** / **17-TMS** mixture and 1,3,5-tri-*tert*-butylbenzene (0.5 – 1 mg) using Schlenk techniques. After the resulting solution had been degassed (3x freeze / pump / thaw), reaction vessel was placed in the presence of light source for 13 days.

a. Photolysis in CDCl₃. **15-TMS** (2.5 mg, 0.0114 mmol, 7:3 *Z* / *E*), **17-TMS** (1 mg, 0.00167 mmol).

b. Photolysis in acetone – d₆. **15-TMS** (3 mg, 0.0137 mmol, 7:3 *Z* / *E*), **17-TMS** (1 mg, 0.00167 mmol).

Reaction of 15-TMS with 3 in CD₃CN. **15-TMS** (3.6 mg, 0.0165 mmol, 7:3 *E* / *Z*) was reacted with **3** (9.0mg, 0.0178 mmol) in CD₃CN (0.93 mL) using the general procedure for preparation of Ru(η^6 – arene) products. After 12 days at 23°C, **17-TMS** was observed in 60% NMR yield and after 4 days at 50°C, **17-TMS** was observed in 69% NMR yield based on conversion of **15-TMS**.

Attempted reaction of 15-TMS with 28. **15-TMS** (10.6 mg, 0.049 mmol, 6:4 *E* / *Z*) was reacted with **28** (1.8 mg, 0.0005 mmol) in d₆-acetone (0.86 mL) using the general procedure for preparation of Ru(η^6 – arene) products. After 18 h at 50°C, no reaction was observed by ¹H NMR spectroscopy.

Reaction of 15-TMS with 29. **15-TMS** (7 mg, 0.032 mmol, 6:4 *E* / *Z*) was reacted with [Cp**Ru*(CO)(NCMe)₂]*PF*₆ **29** (16.4 mg, 0.033 mmol) in CDCl₃ (0.87 mL) using the general procedure for preparation of Ru(*η*⁶ – arene) products. Reaction mixture was kept at 23°C for 5 days then 50°C for 54 h.

General Procedure for Thermal Reactions of 15-TMS. A mixture of **15-TMS** (7:3 *E* / *Z*), 1,3,5-tri-*tert*-butylbenzene (0.5 – 1 mg), and catalyst (if applicable) in indicated solvent were degassed (3x freeze / pump / thaw) and flame sealed in a Wilmad 504-PP NMR tube under 10 mtorr vacuum on Schlenk line. The contents were then heated at 145°C.

a. RuCl₃. **15-TMS** (40 mg, 0.183 mmol), RuCl₃·H₂O (1.9 mg, 0.0092 mmol), *o*-xylene-*d*₁₀ (0.37 mL).

b. uncatalyzed in *o*-xylene. **15-TMS** (40 mg, 0.183 mmol), *o*-xylene-*d*₁₀ (0.37 mL).

c. 2,6-lutidine. **15-TMS** (40 mg, 0.183 mmol), 2,6-lutidine (0.011 mL, 0.092 mmol), *o*-xylene-*d*₁₀ (0.37 mL).

d. PtCl₂. **15-TMS** (57 mg, 0.261 mmol), PtCl₂ (7 mg, 0.026 mmol), DMF-*d*₇ (0.51 mL).

e. uncatalyzed in DMF. **15-TMS** (40 mg, 0.183 mmol), DMF-*d*₇ (0.36 mL).

General experimental for kinetic runs. Stock solutions of **3** (25 mg/mL in *d*₆ – acetone), **15-TMS** (7:3 *E* / *Z*, 8 mg/mL in CDCl₃) and 1,3,5-tri-*tert*-butylbenzene (2.1 mg/mL in CDCl₃) were prepared and used for additions. **3** was added to a J-young tube containing combined reagents at 23°C in glove box. Integral of **II** TMS resonance at δ 0.064 was normalized by setting ¹Bu resonance of internal standard to unity.

a. normalized run. **3** (0.184 mL, 0.0092 mmol), **15-TMS** (0.250 mL, 0.0092 mmol), 1,3,5-tri-*tert*-butylbenzene (0.238 mL, 0.0023 mmol), CD₃CN (0.019 mL, 0.3663 mmol).

Table 2-7. Observed change in the **II** TMS resonance integral at different times for normalized kinetic run.

| time (hr) | II TMS int |
|-----------|------------|
| 0.133 | 0.22 |
| 0.225 | 0.31 |
| 0.317 | 0.37 |
| 0.425 | 0.48 |
| 0.517 | 0.54 |
| 0.617 | 0.58 |
| 0.725 | 0.7 |
| 0.833 | 0.77 |
| 1.05 | 0.93 |

b. Varied [CD₃CN]. **3** (0.184 mL, 0.0092 mmol), **15-TMS** (0.250 mL, 0.0092 mmol), 1,3,5-tri-tert-butylbenzene (0.238 mL, 0.0023 mmol), CD₃CN (0.038 mL, 0.7326 mmol).

Table 2-8. Observed change in the **II** TMS resonance integral at different times for kinetic run with increased CD₃CN concentration.

| time (hr) | II TMS int |
|-----------|------------|
| 0.192 | 0.08 |
| 0.333 | 0.11 |
| 0.5 | 0.15 |
| 0.667 | 0.19 |
| 0.833 | 0.22 |
| 1 | 0.24 |
| 1.167 | 0.26 |

c. Varied [3]. **3** (0.092 mL, 0.0046 mmol), **15-TMS** (0.250 mL, 0.0092 mmol), 1,3,5-tri-tert-butylbenzene (0.238 mL, 0.0023 mmol), CD₃CN (0.019 mL, 0.7326 mmol), acetone-*d*₆ (0.092 mL).

Table 2-9. Observed change in the **II** TMS resonance integral at different times for kinetic run with decreased **3** concentration.

| time (hr) | II TMS int |
|-----------|------------|
| 0.133 | 0.12 |
| 0.217 | 0.19 |
| 0.325 | 0.25 |
| 0.417 | 0.28 |
| 0.533 | 0.32 |
| 0.633 | 0.36 |
| 0.725 | 0.4 |
| 0.833 | 0.44 |
| 0.933 | 0.51 |
| 1.067 | 0.54 |

d. Varied [15-TMS]. **3** (0.184 mL, 0.0092 mmol), **15-TMS** (0.125 mL, 0.0046 mmol), 1,3,5-tri-tert-butylbenzene (0.238 mL, 0.0023 mmol), CD₃CN (0.019 mL, 0.7326 mmol), CDCl₃ (0.125 mL).

Table 2-10. Observed change in the **II** TMS resonance integral at different times for kinetic run with decreased **15-TMS** concentration.

| time (hr) | II TMS int |
|-----------|------------|
| 0.117 | 0.11 |
| 0.217 | 0.16 |
| 0.317 | 0.2 |
| 0.425 | 0.25 |
| 0.55 | 0.31 |
| 0.667 | 0.36 |
| 0.783 | 0.39 |
| 0.9 | 0.44 |
| 1 | 0.49 |
| 1.125 | 0.55 |

Attempted observation of metal hydride species at low temperature. A solution of **15-TMS** (7:3 *E/Z*, 13.6 mg, 0.062 mmol) in CD₂Cl₂ (0.4 mL) was added dropwise to an NMR tube equipped with a rubber septum containing a solution of **3** (6 mg, 0.012 mmol) in CD₂Cl₂ (0.4 mL) at -75°C. A ¹H NMR spectrum of this mixture at -80°C confirmed no reaction had occurred. The sample was then monitored by ¹H NMR spectroscopy while slowly warming to 23°C.

vii. ¹H and ¹³C NMR spectra for unknown compounds.

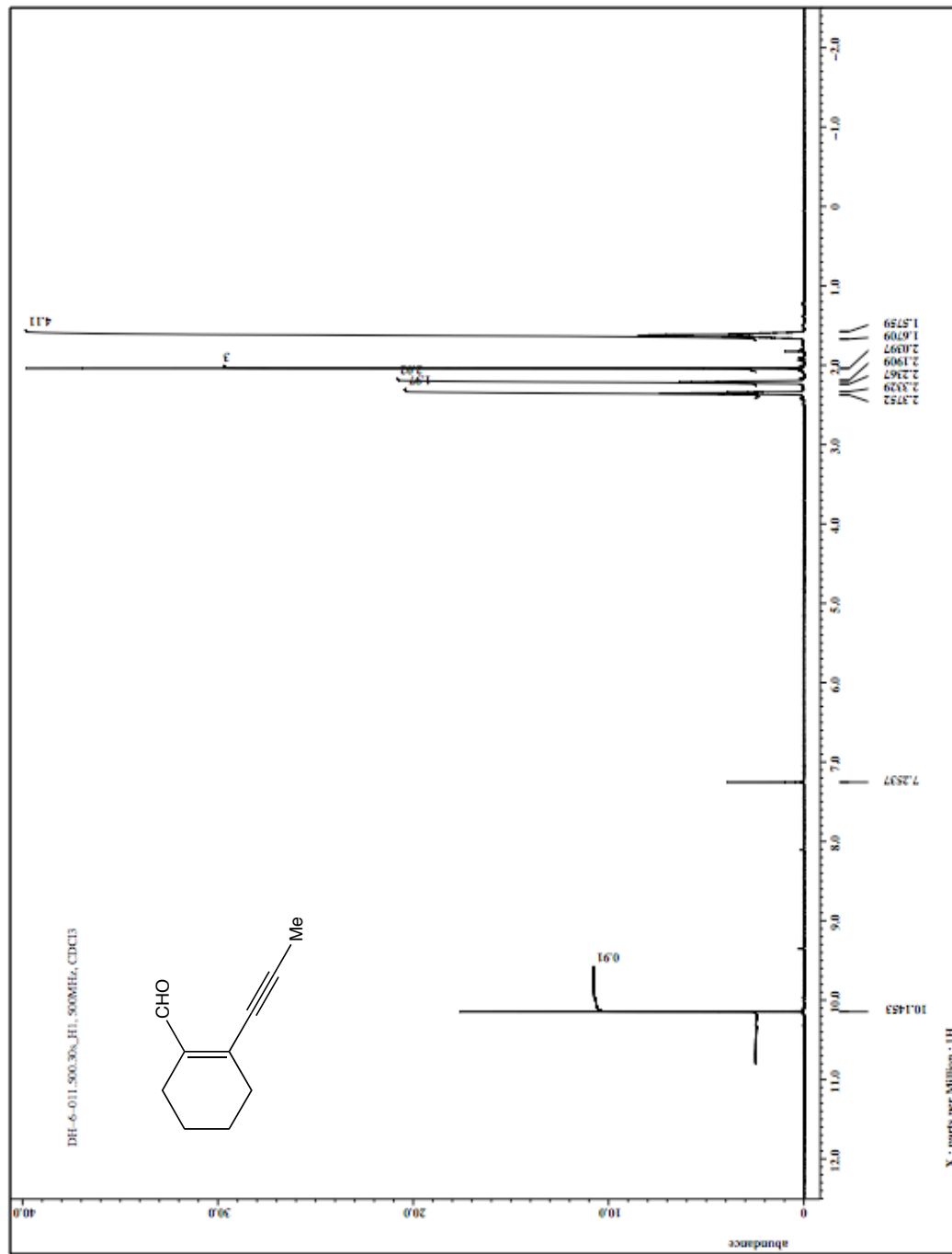


Figure 2-7. 14-Me ^1H NMR spectrum (500 MHz, CDCl_3).

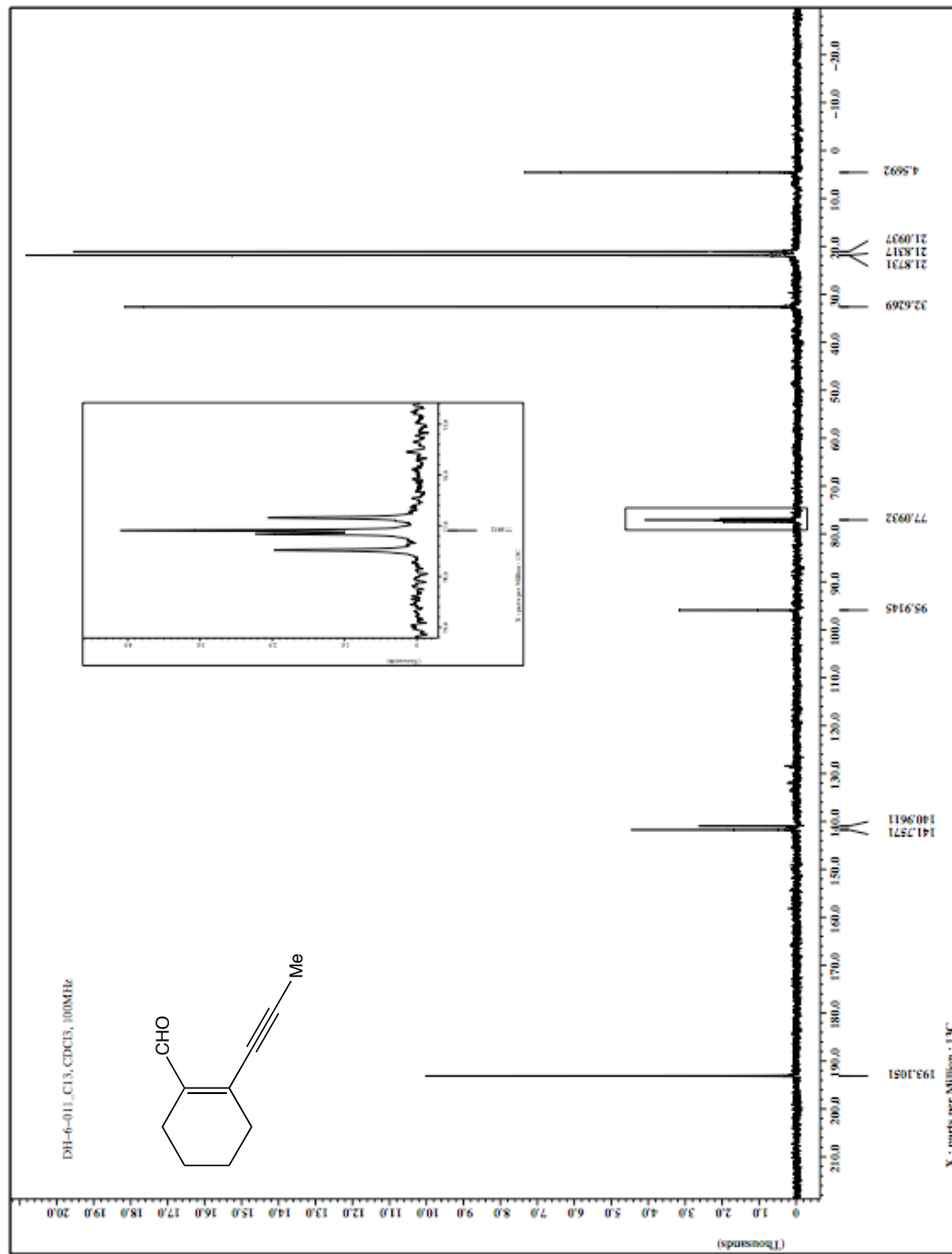


Figure 2-8. 14-Me ¹³C NMR spectrum (100 MHz, CDCl₃).

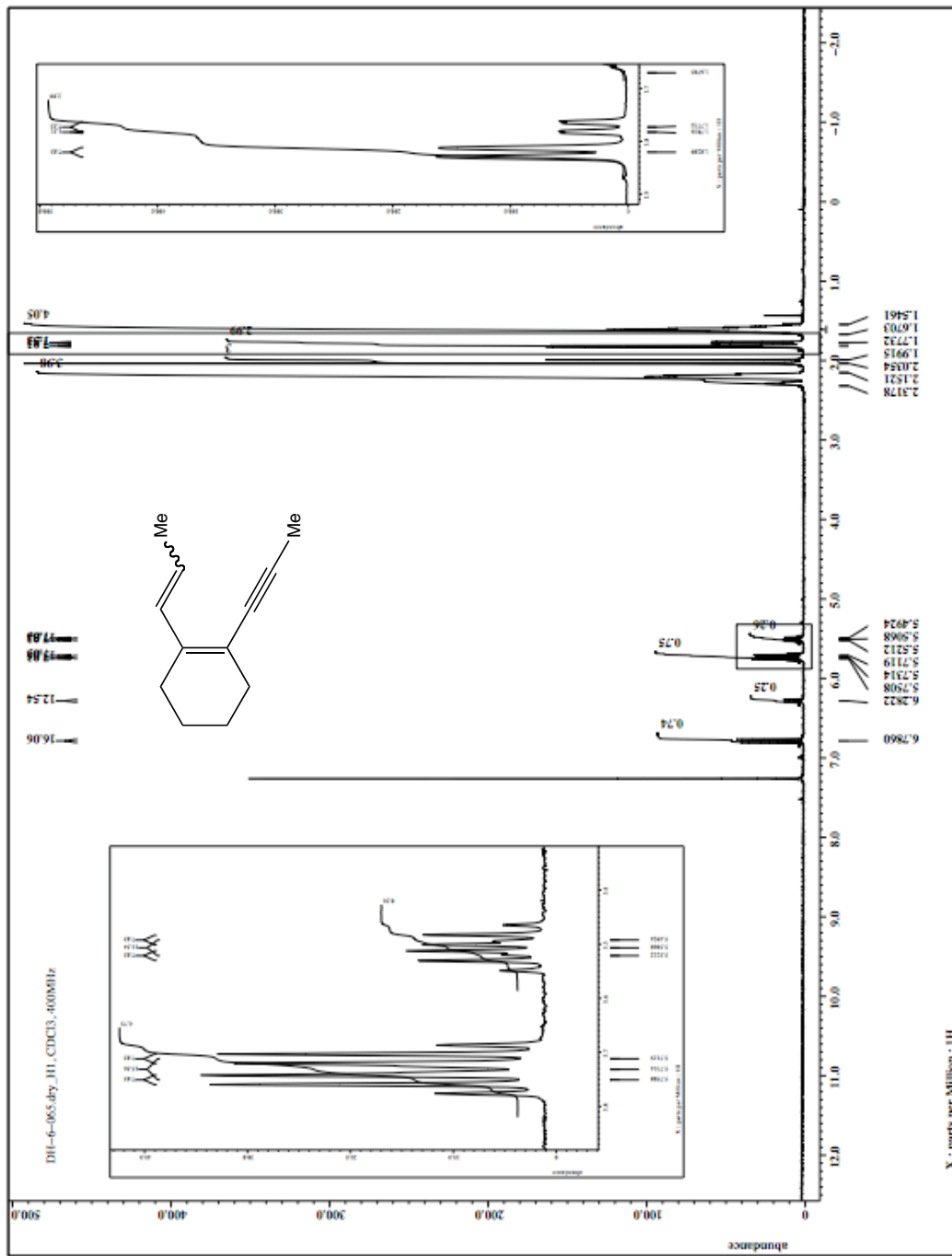


Figure 2-9. 15-Me (75:25 *E/Z*) ^1H NMR spectrum (400 MHz, CDCl_3).

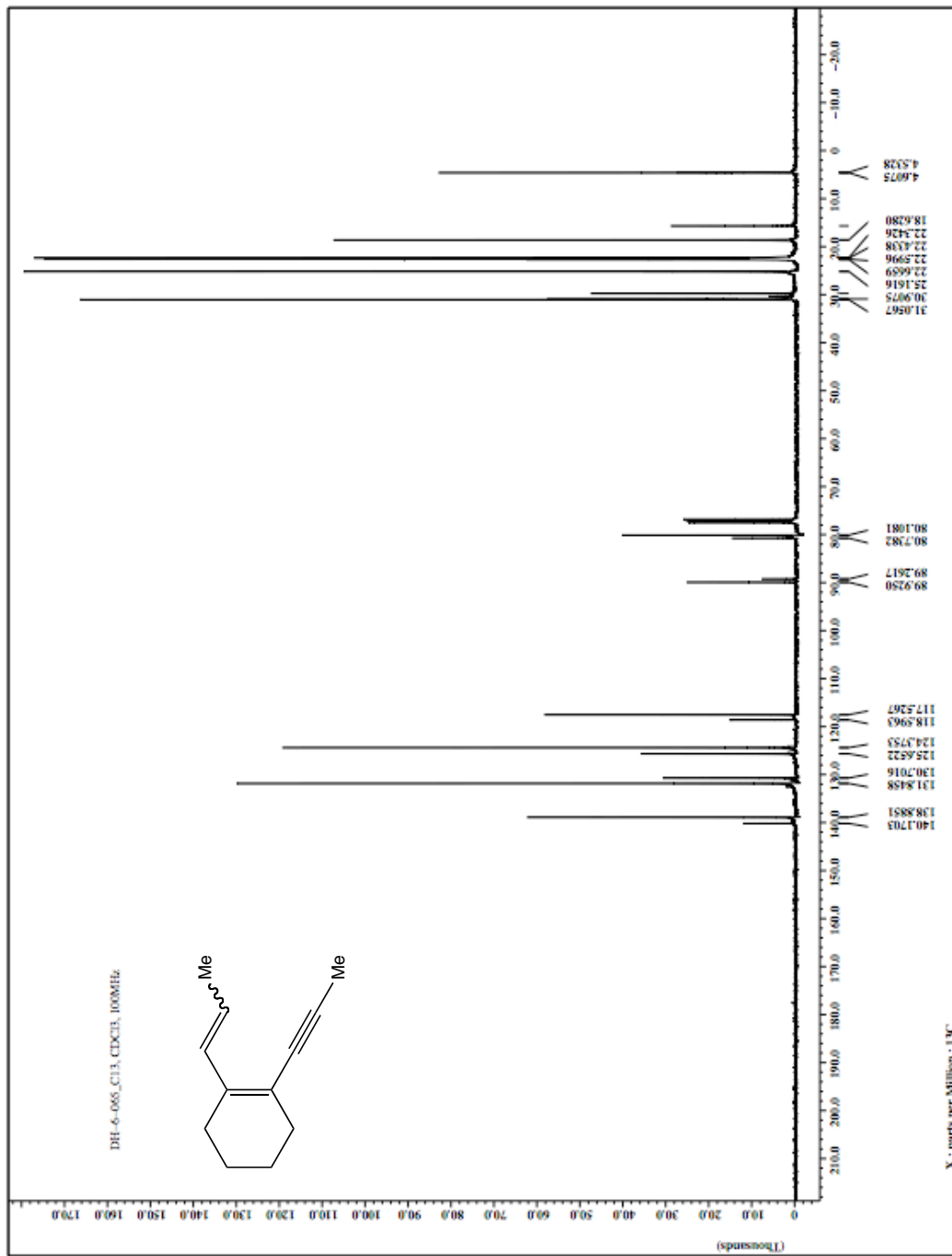


Figure 2-10. 15-Me (75:25 *E/Z*) ¹³C NMR spectrum (100 MHz, CDCl₃).

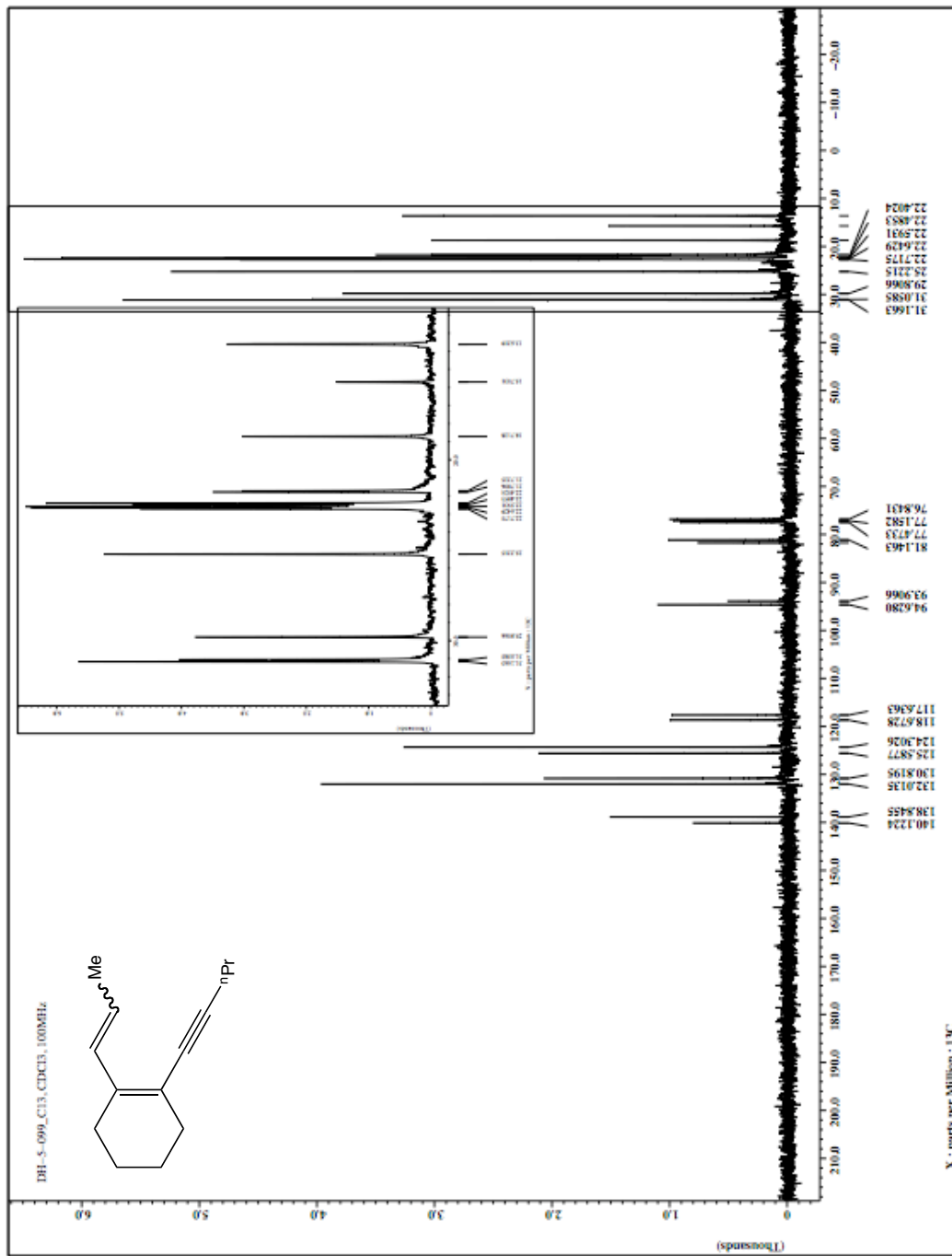


Figure 2-12. 15-Pr (6:4 *E/Z*) ^{13}C NMR spectrum (100 MHz, CDCl_3).

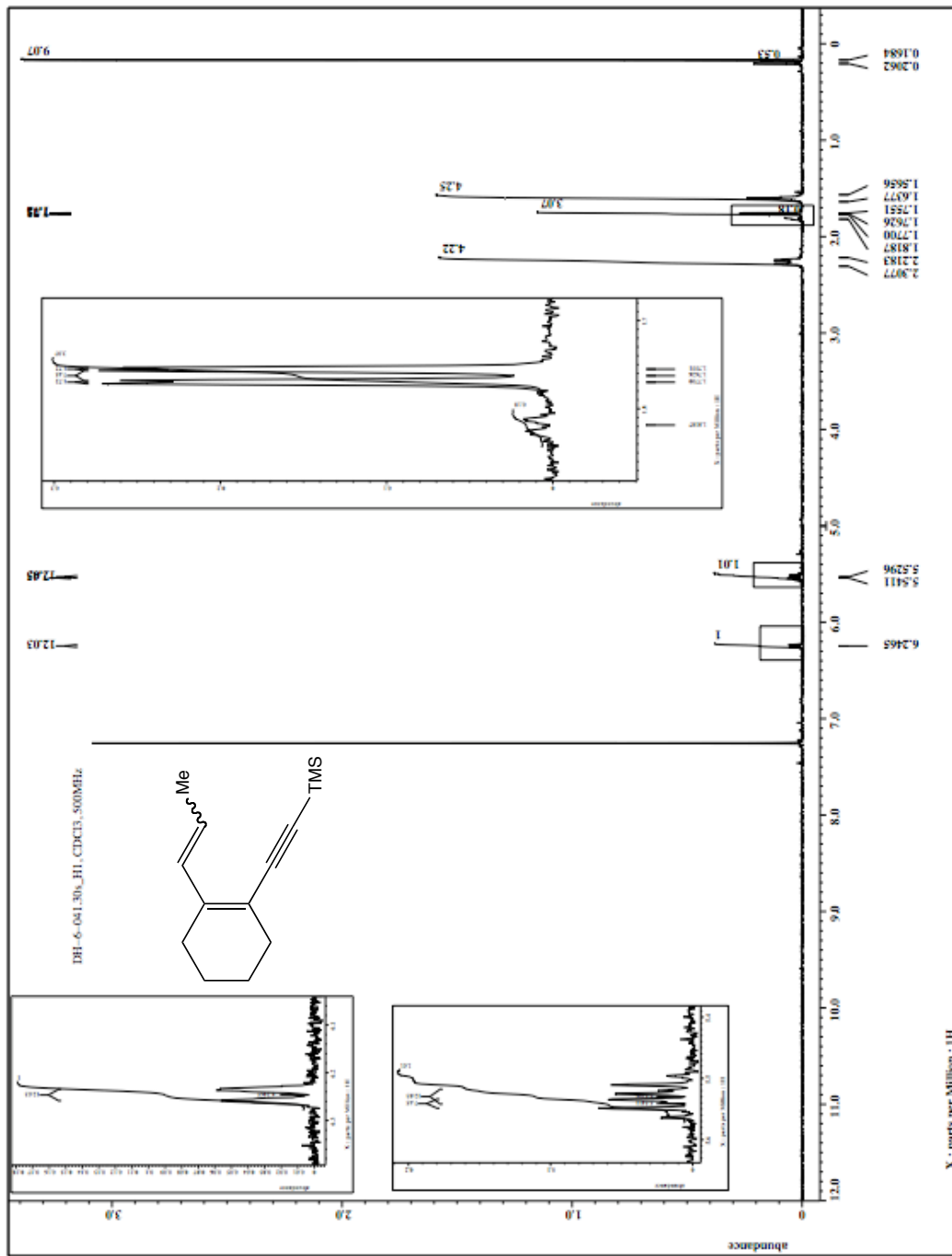


Figure 2-13. 15-TMS (92:8 Z/E) ¹H NMR spectrum (500 MHz, CDCl₃).

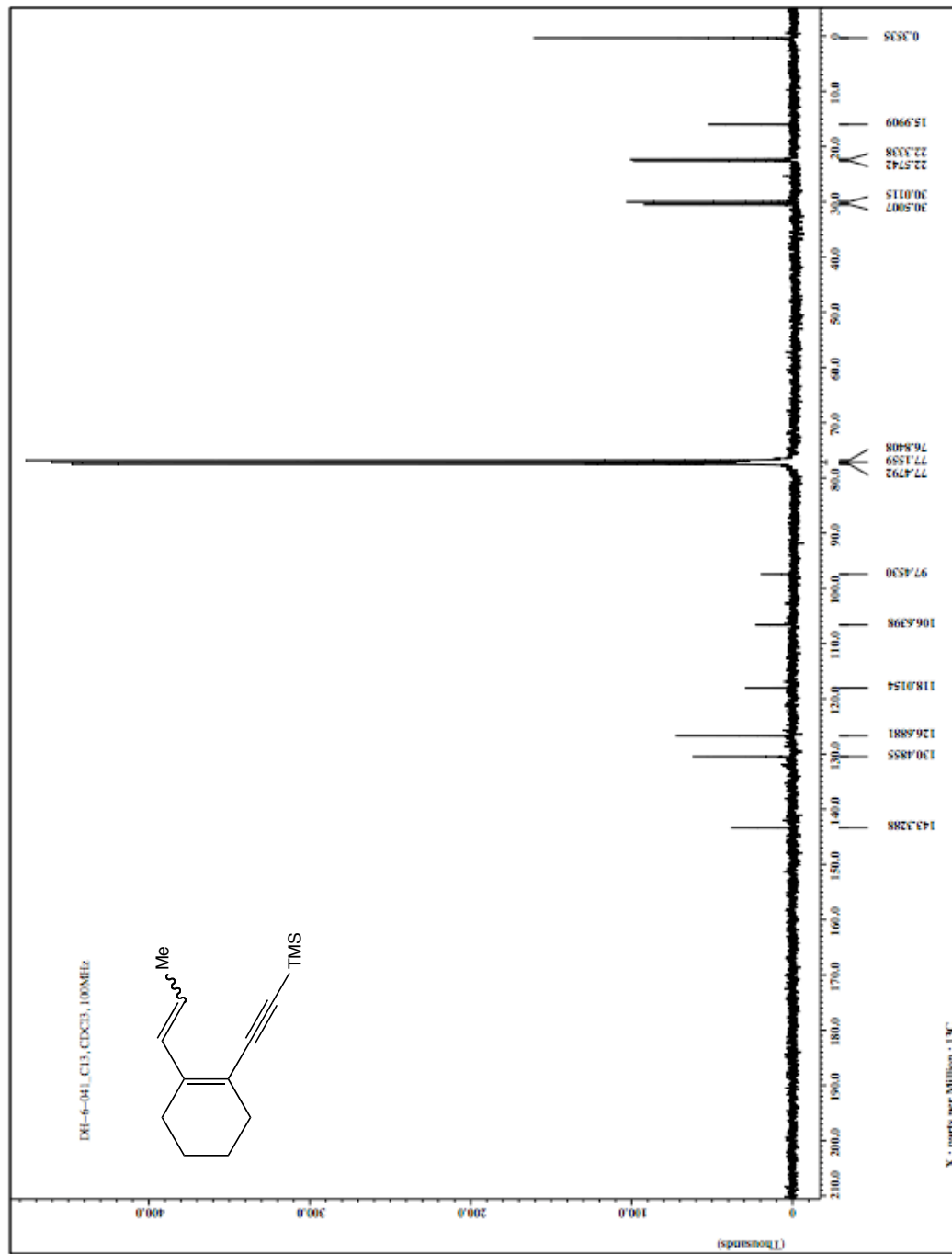


Figure 2-14. 15-TMS (92:8 Z/E) ^{13}C NMR spectrum (100 MHz, CDCl_3).

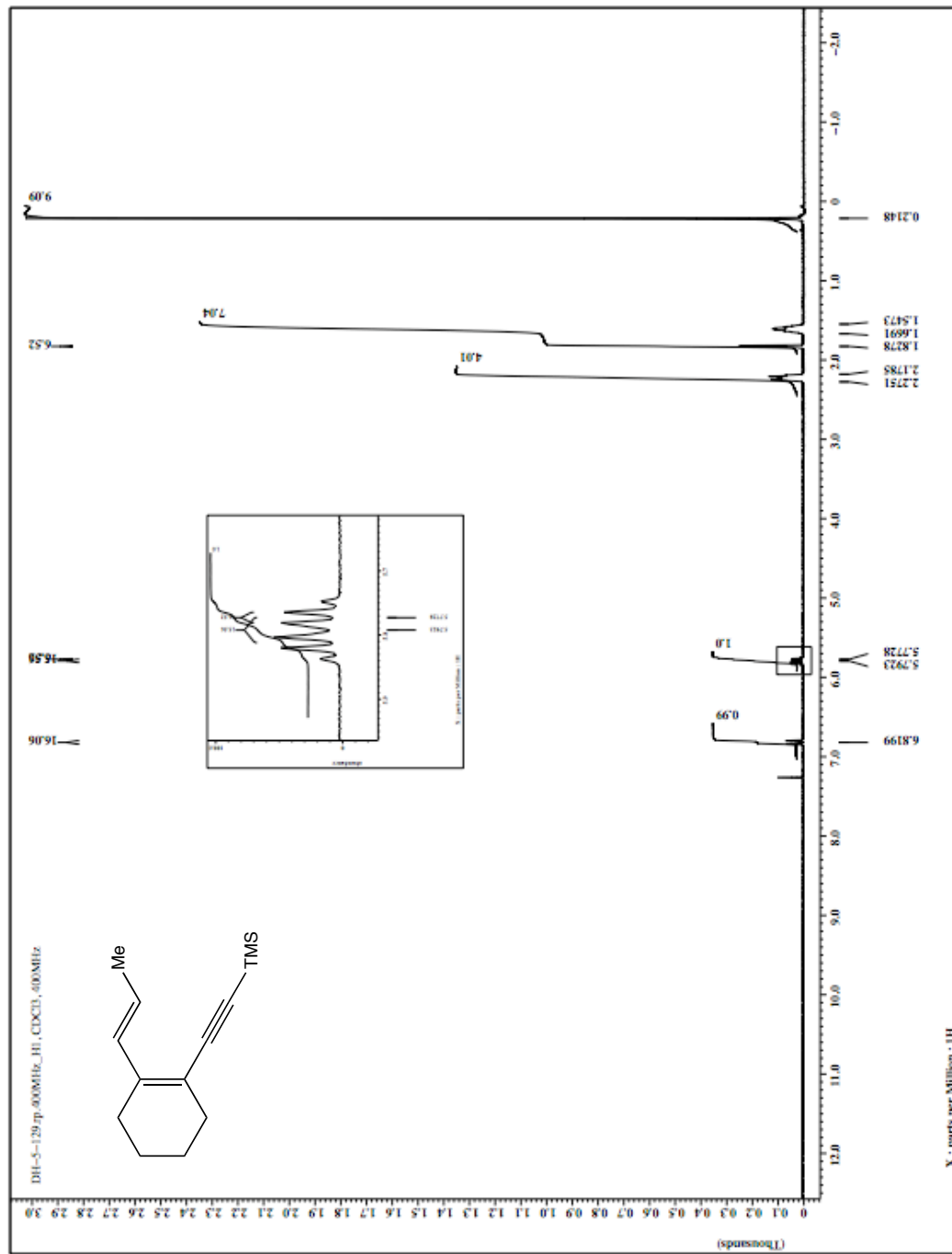


Figure 2-15. 15-TMS-*E*¹H NMR spectrum (400 MHz, CDCl₃).

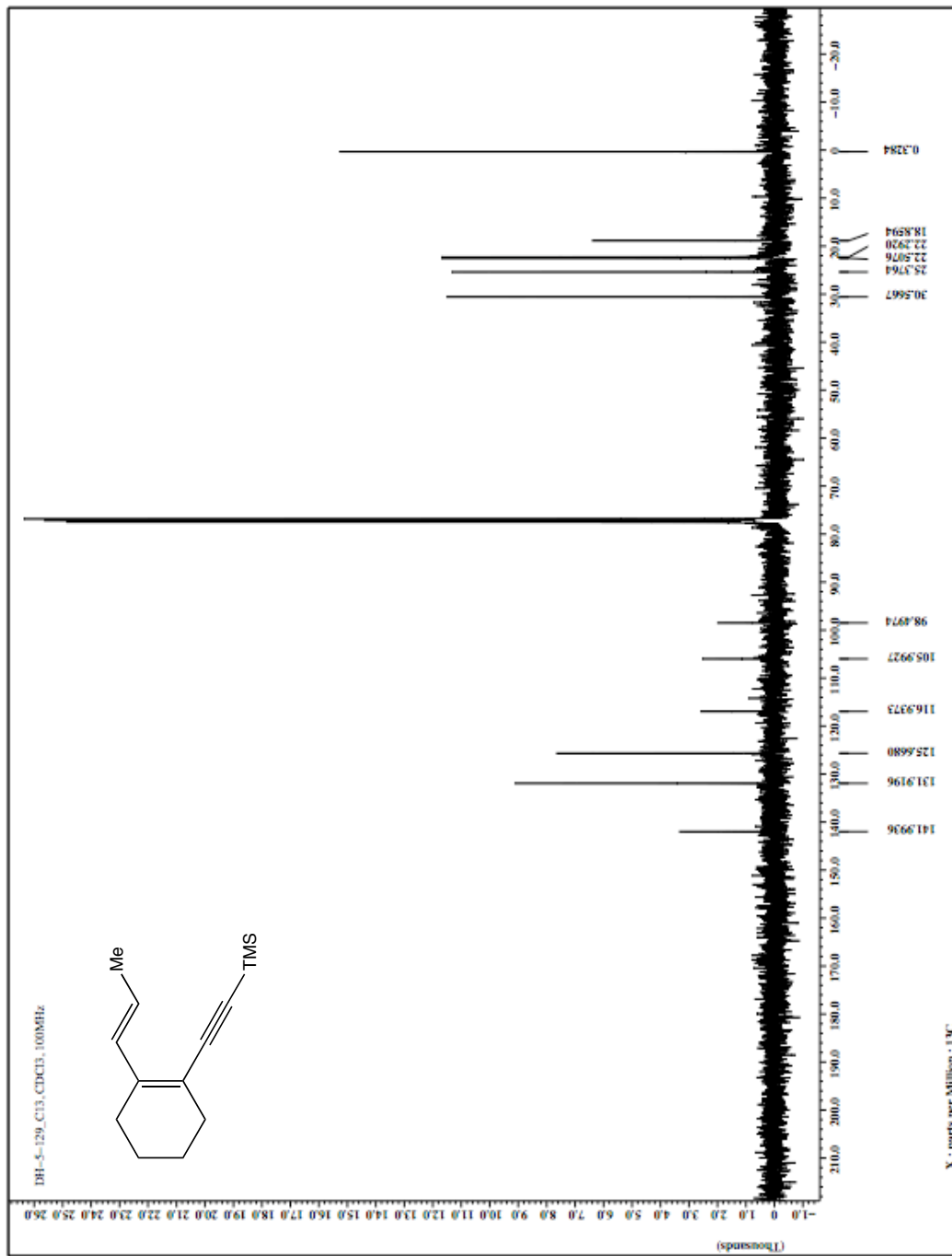


Figure 2-16. 15-TMS-E ^{13}C NMR spectrum (100 MHz, CDCl_3).

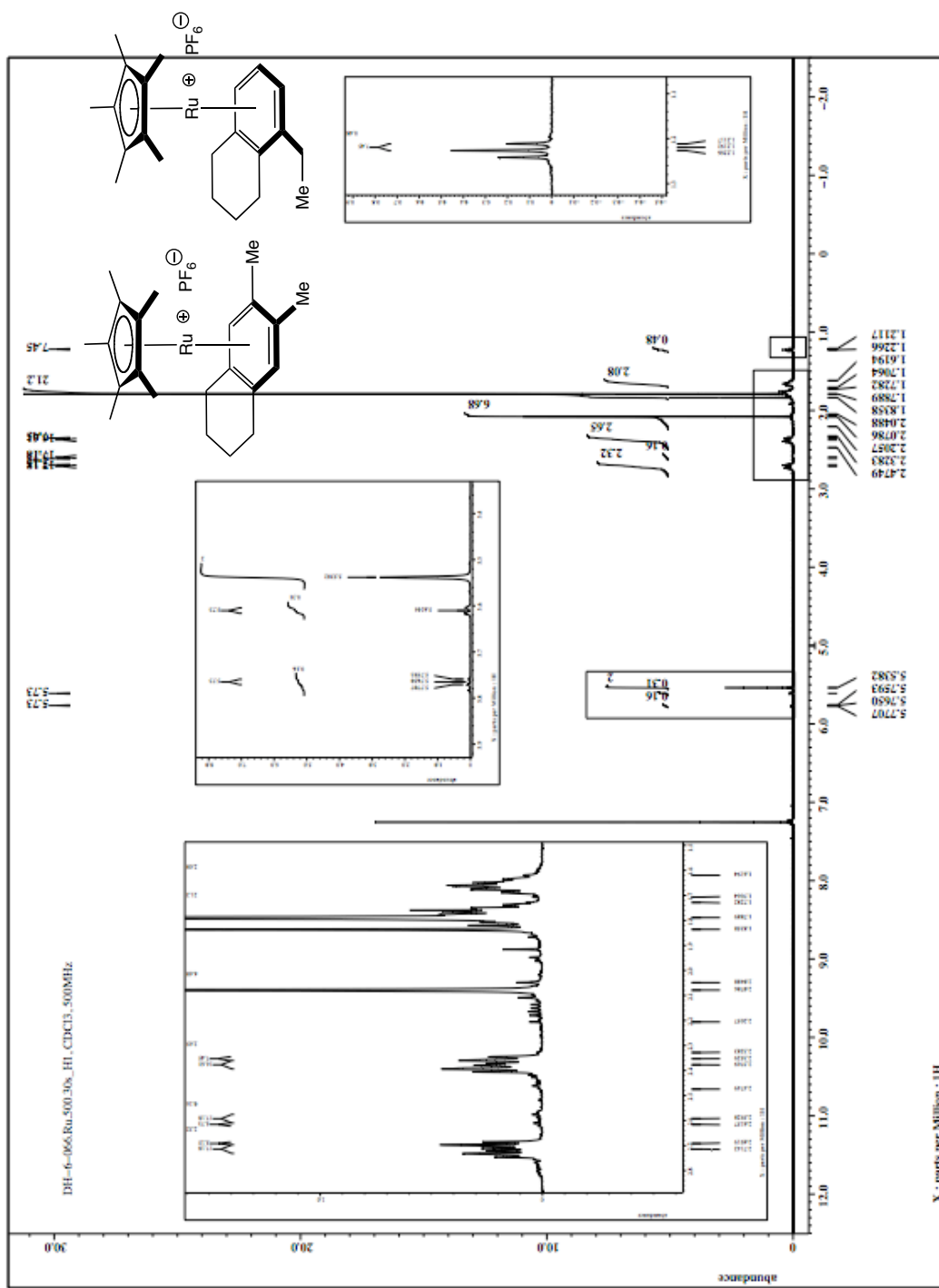




Figure 2-18. 86:14 16-Me / 17-Me ^{13}C NMR spectrum (125 MHz, CDCl_3).

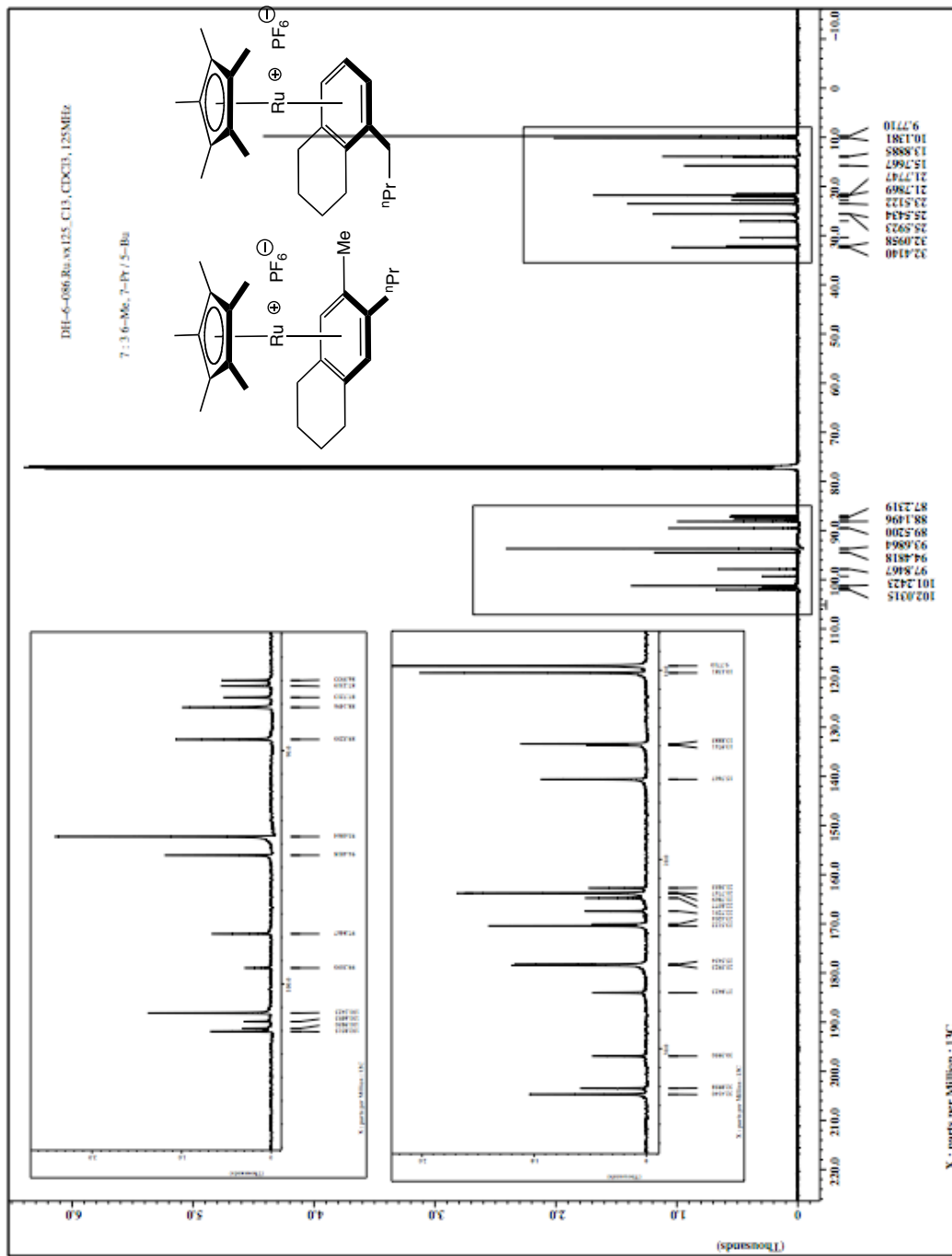


Figure 2-20. 69:31 16-Pr / 17-Pr ^{13}C NMR spectrum (125 MHz, CDCl_3).

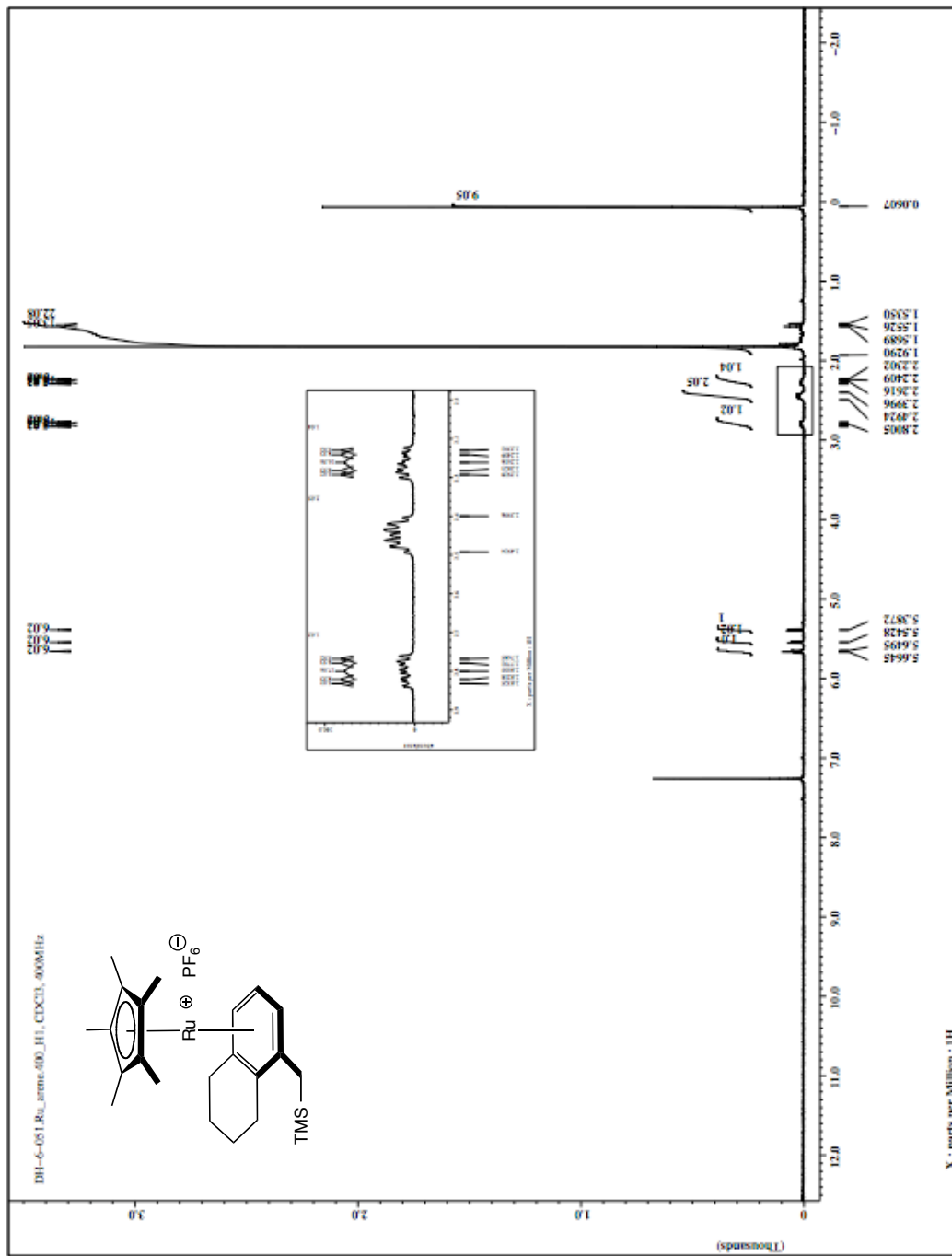


Figure 2-21. 17-TMS ¹H NMR spectrum (400 MHz, CDCl₃).

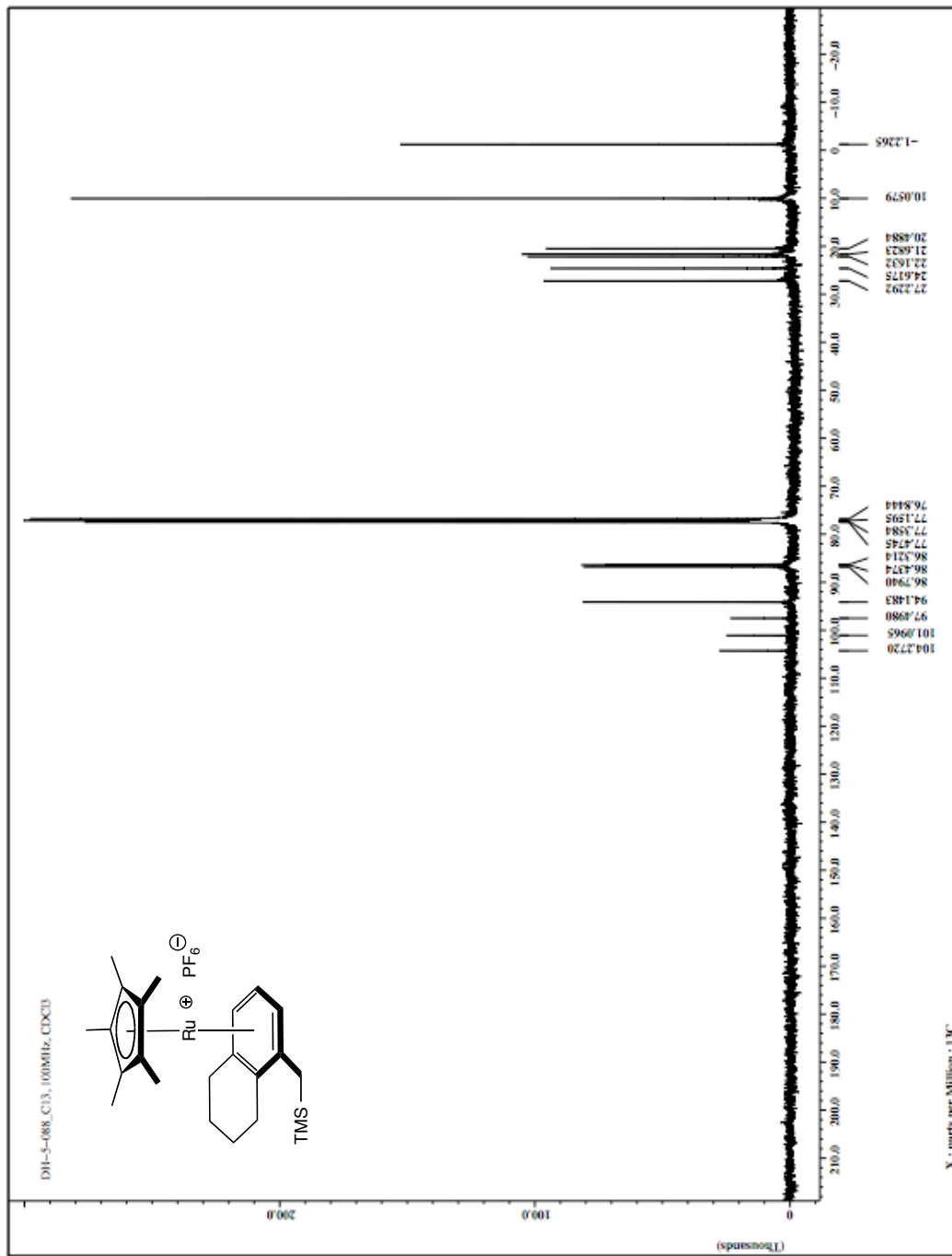


Figure 2-22. 17-TMS ^{13}C NMR spectrum (100 MHz, CDCl_3).

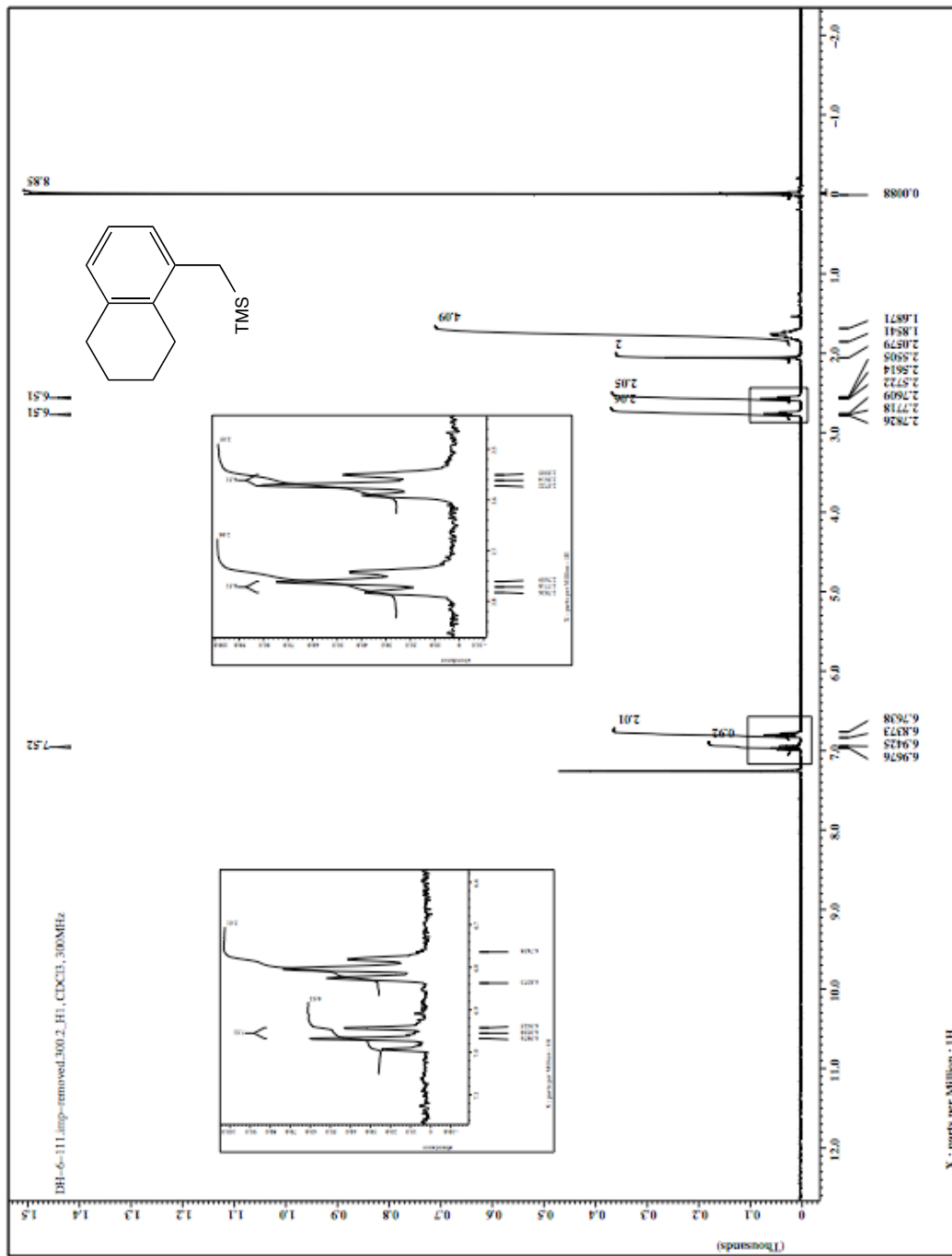


Figure 2-23. 18-TMS ^1H NMR (300 MHz, CDCl_3).

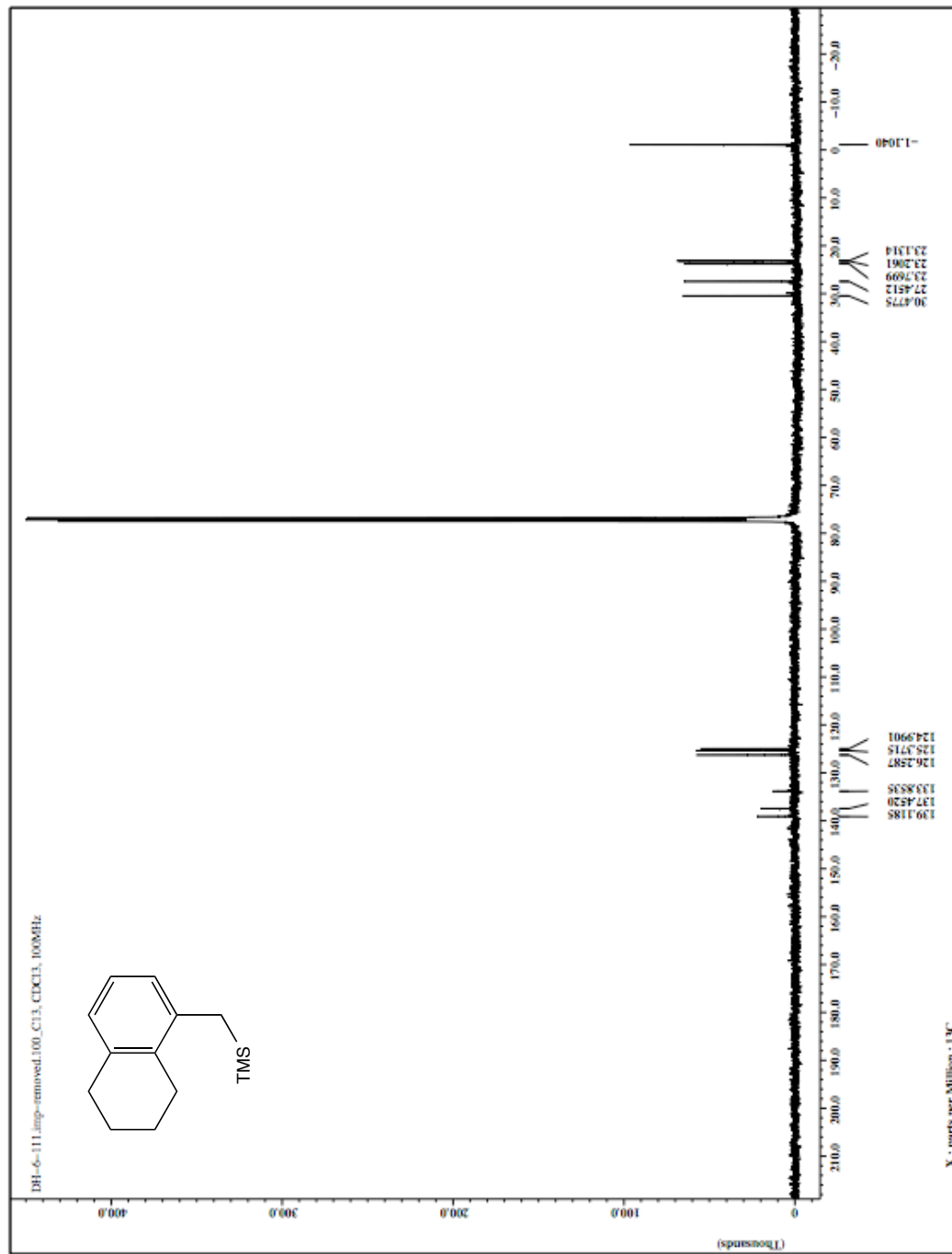


Figure 2-24. 18-TMS ^{13}C NMR spectrum (100 MHz, CDCl_3).

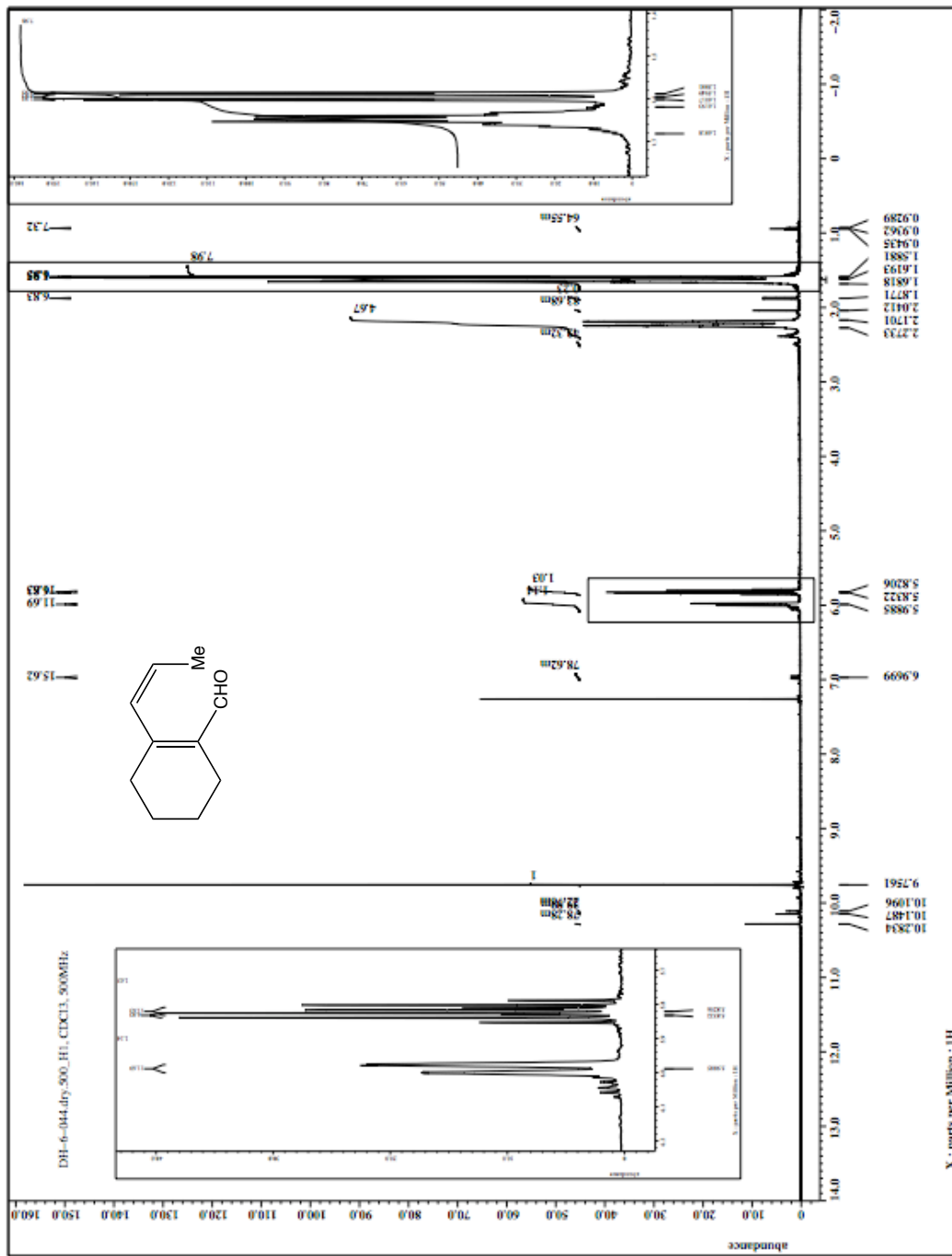


Figure 2-25. 89:7:2:2 19 / 39 / 40 / 14-Me ¹H NMR spectrum (500 MHz, CDCl₃).

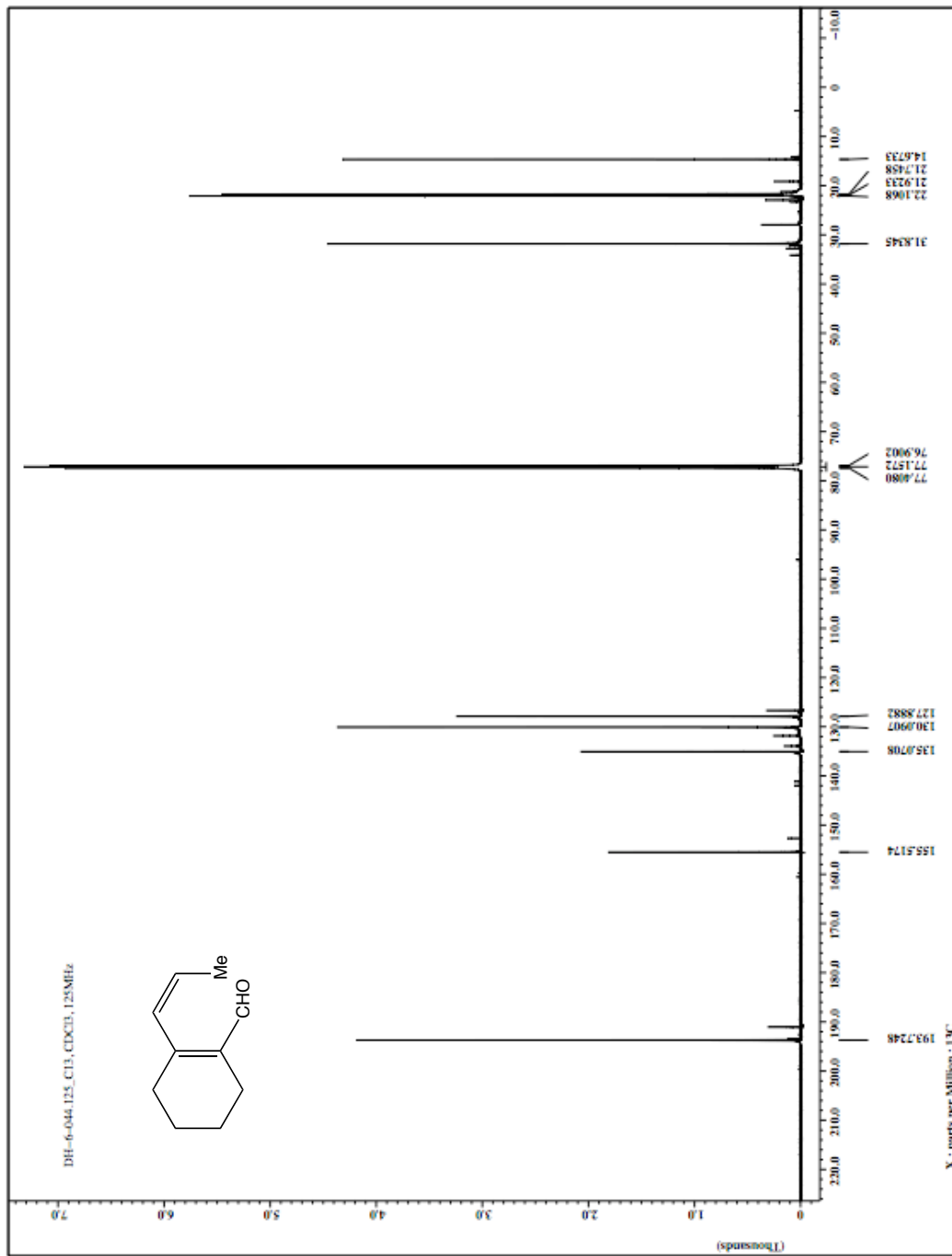


Figure 2-26. 89:7:2:2 19 / 39 / 40 / 14-Me ^{13}C NMR spectrum (125 MHz, CDCl_3).

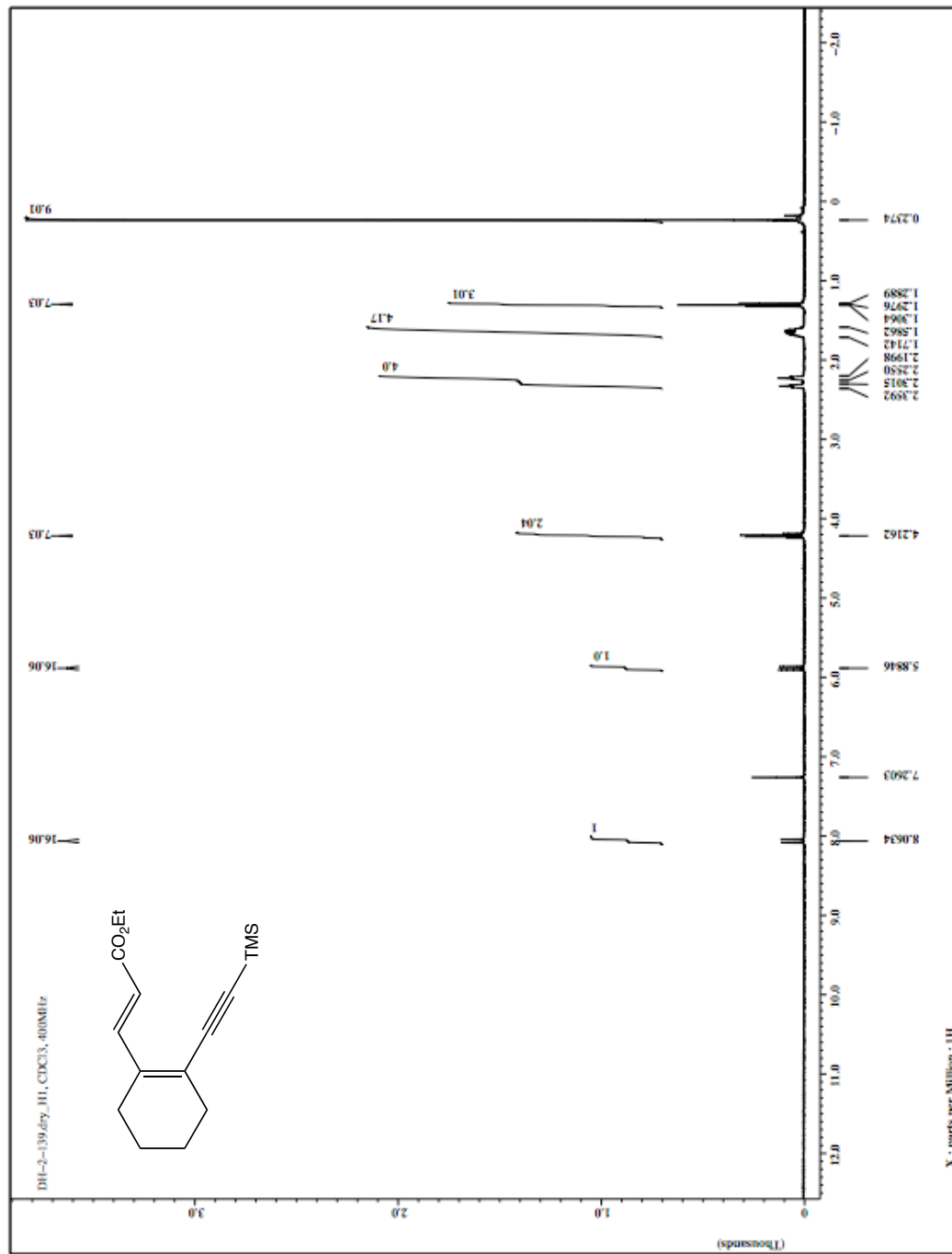


Figure 2-27. 20 ¹H NMR spectrum (400 MHz, CDCl₃).

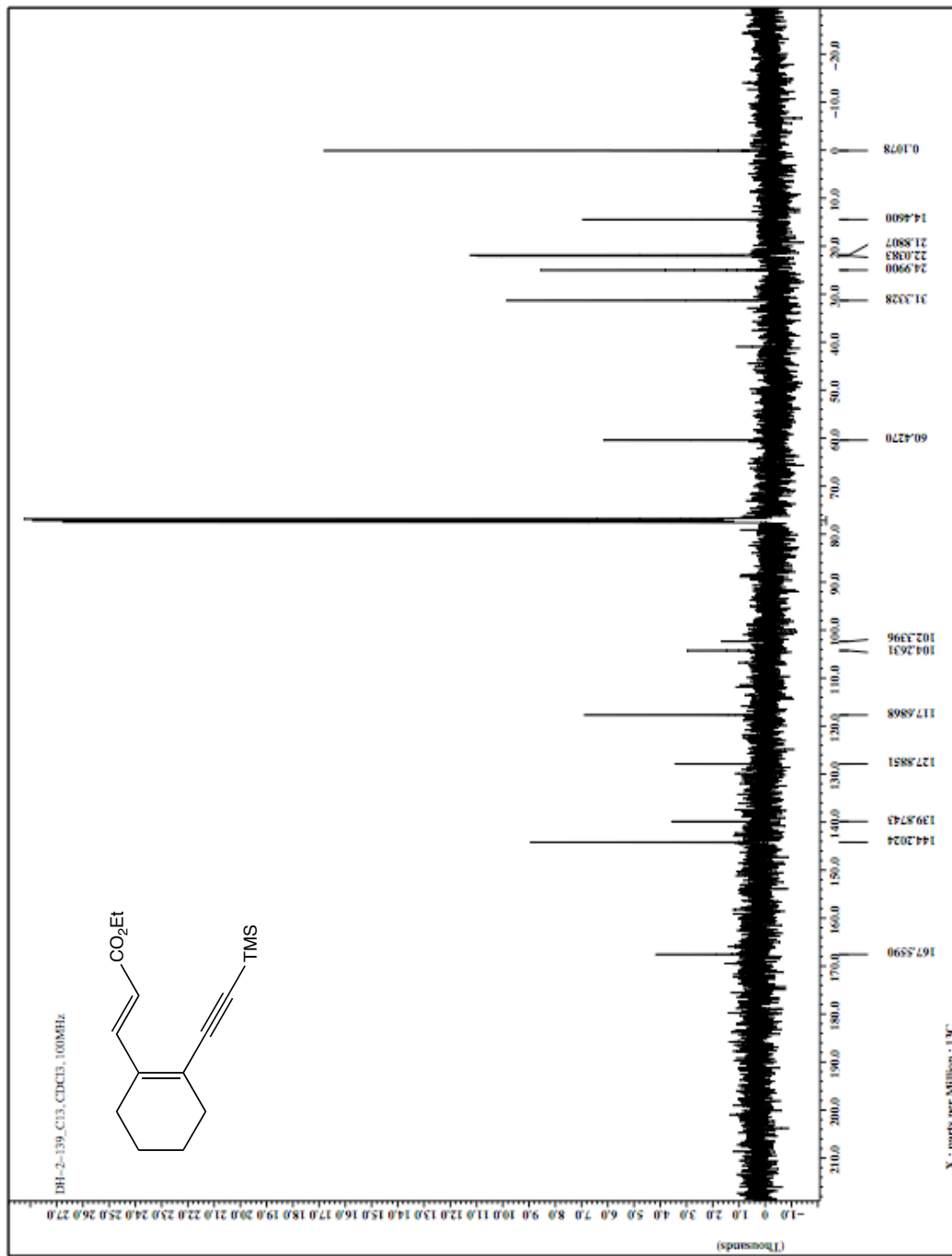


Figure 2-28. ^{13}C NMR spectrum (100 MHz, CDCl_3).

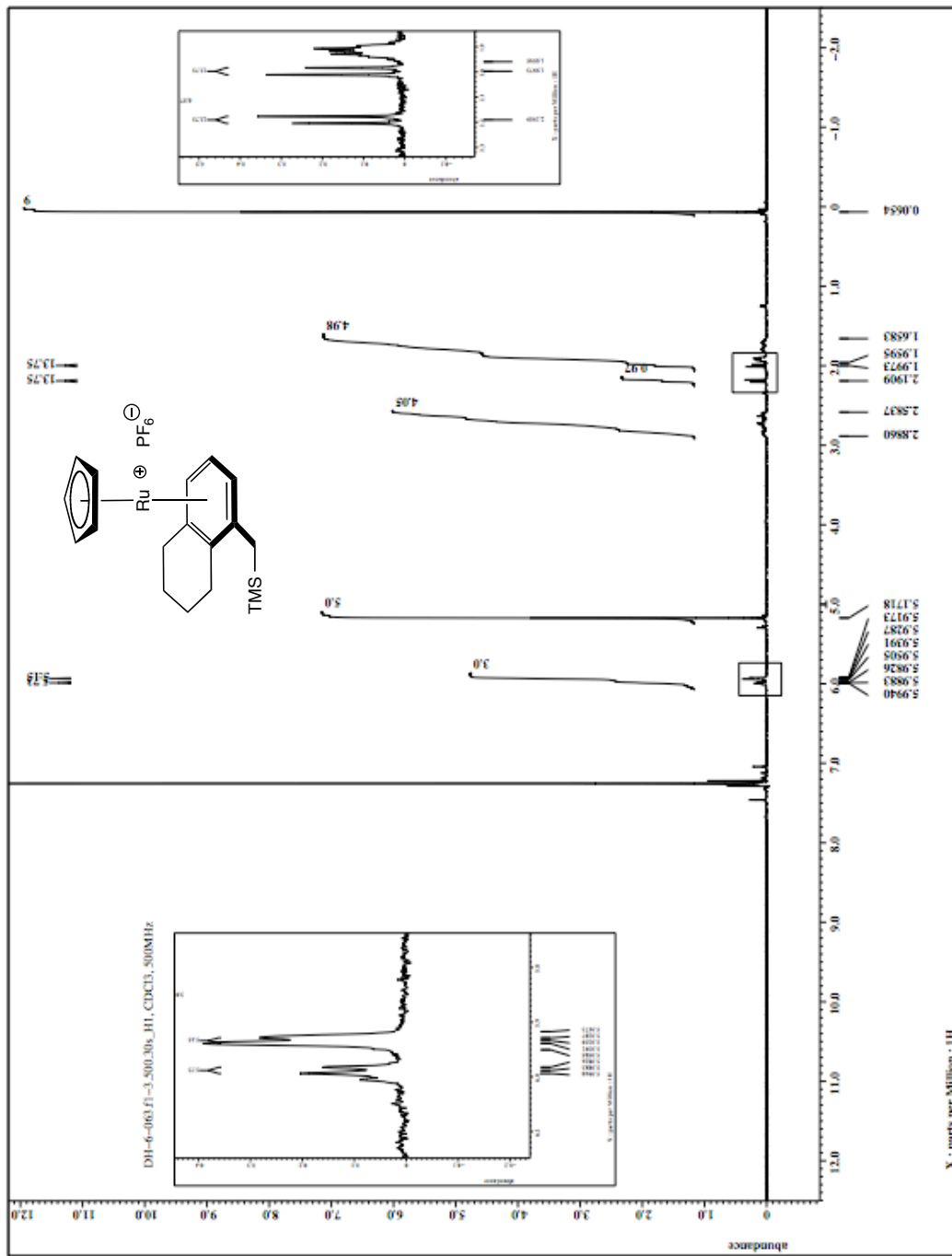


Figure 2-29. 26 ¹H NMR spectrum (500 MHz, CDCl₃).

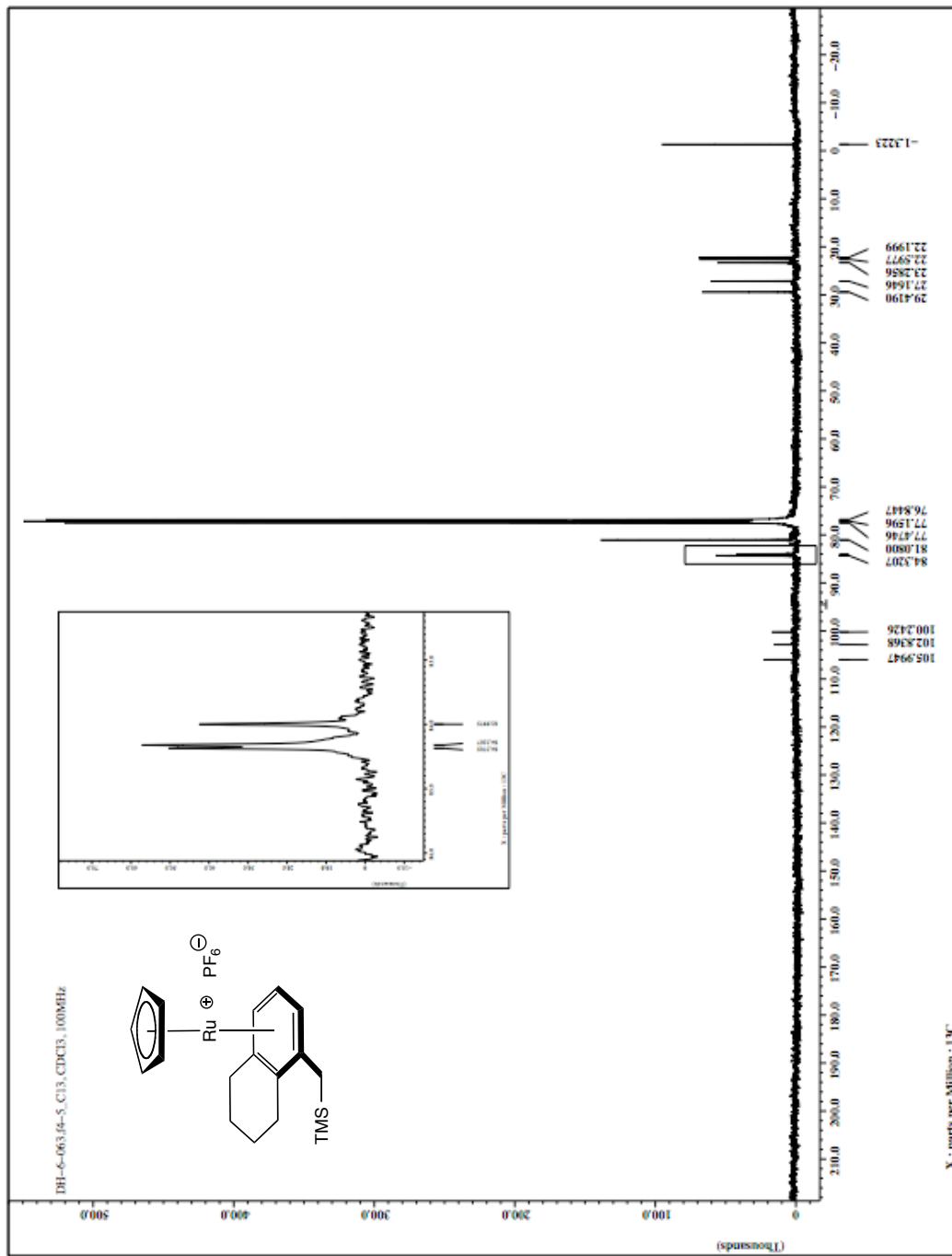


Figure 2-30. 26 ^{13}C NMR spectrum (100 MHz, CDCl_3).

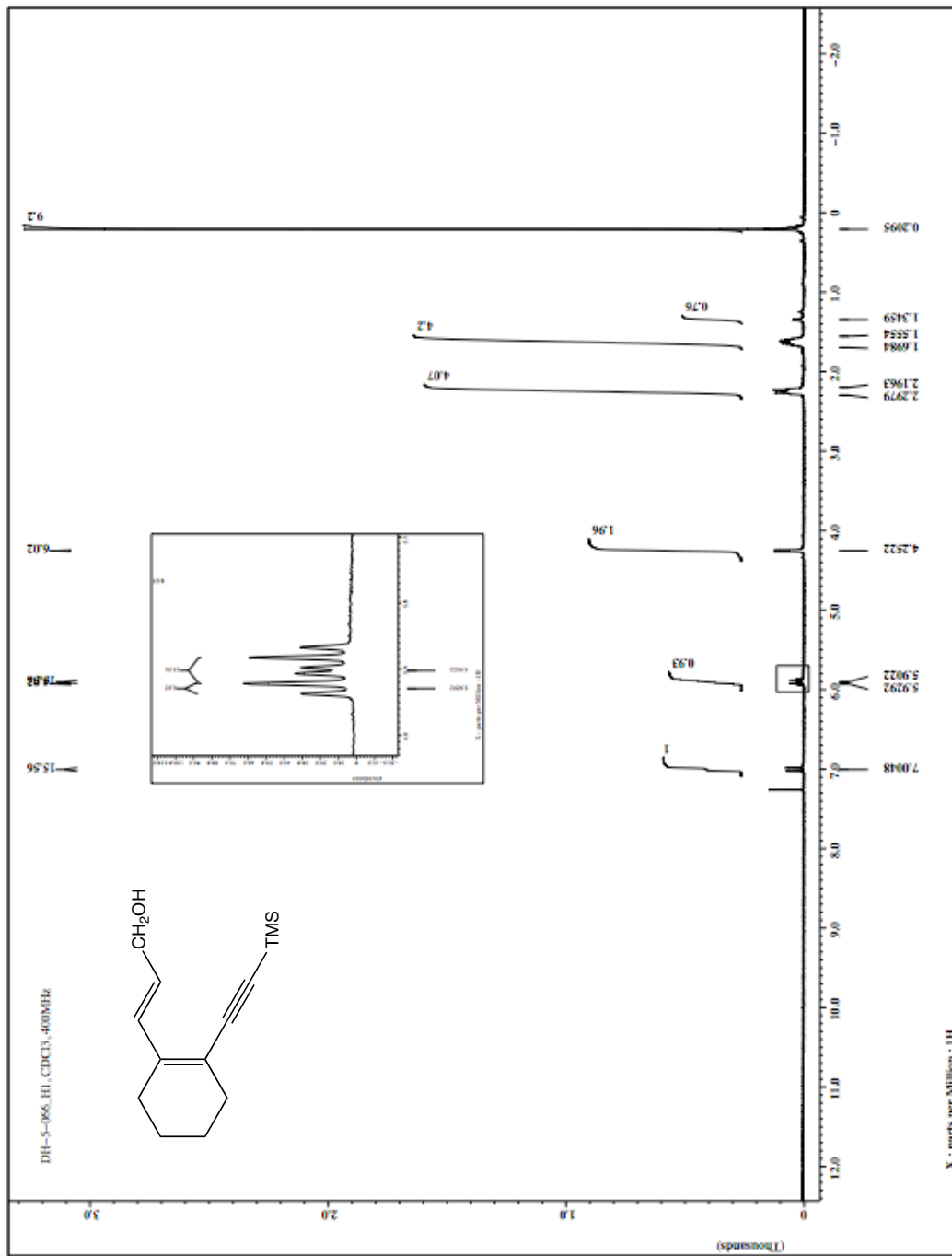


Figure 2-31. $^1\text{H NMR}$ spectrum (400 MHz, CDCl_3).

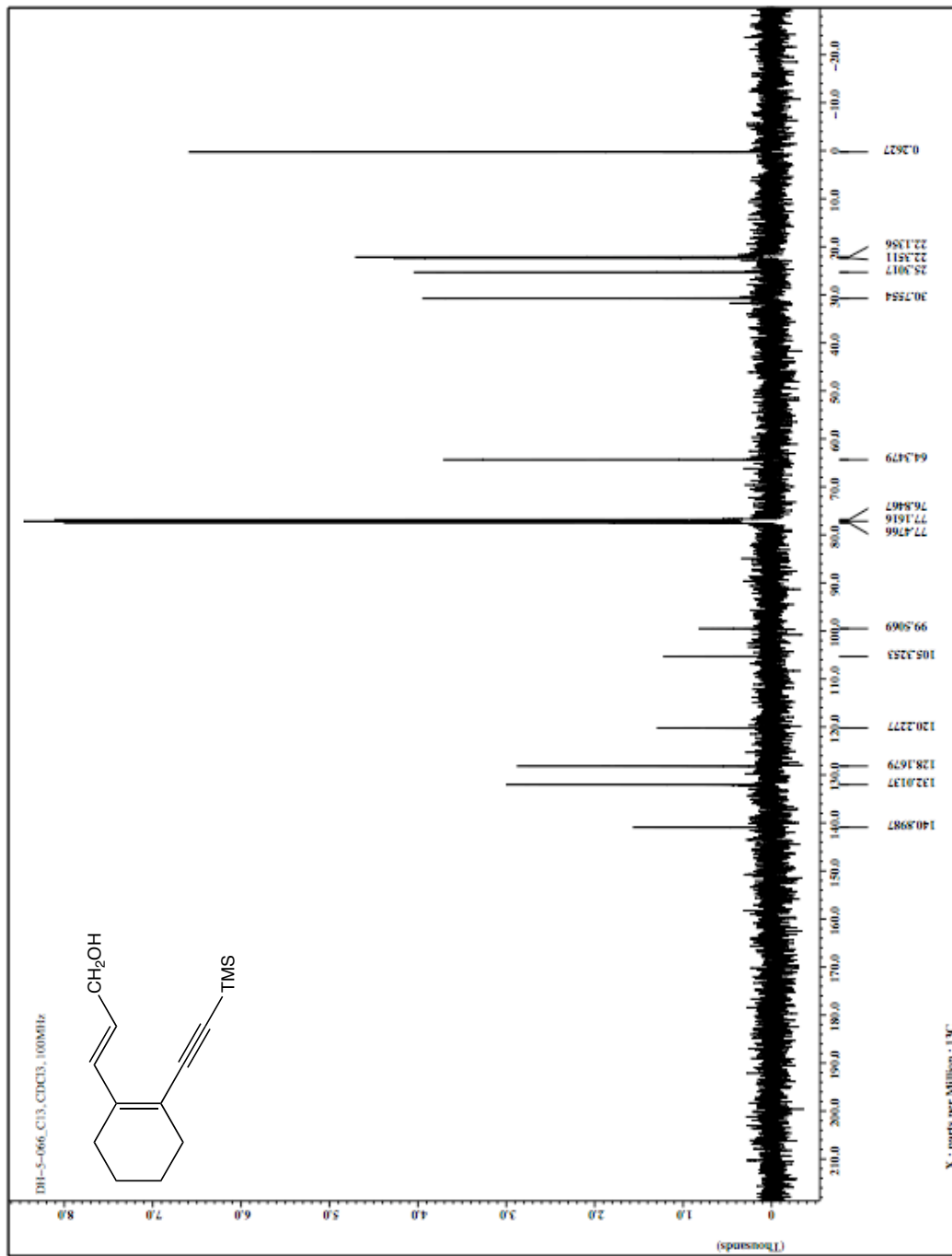


Figure 2-32. 41 ^{13}C NMR spectrum (100 MHz, CDCl_3).

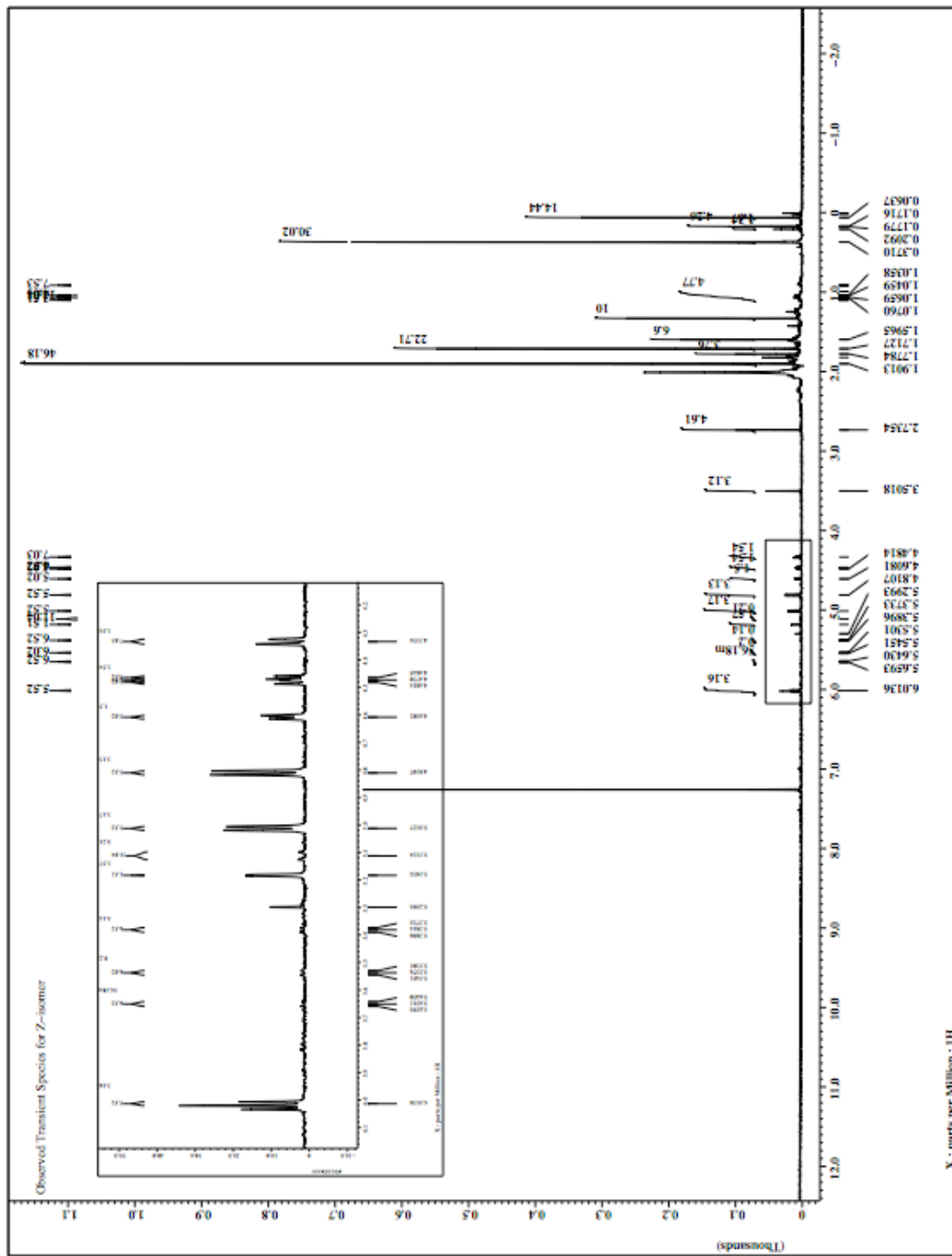


Figure 2-33. I / II ^1H NMR spectrum (400 MHz, CDCl_3).

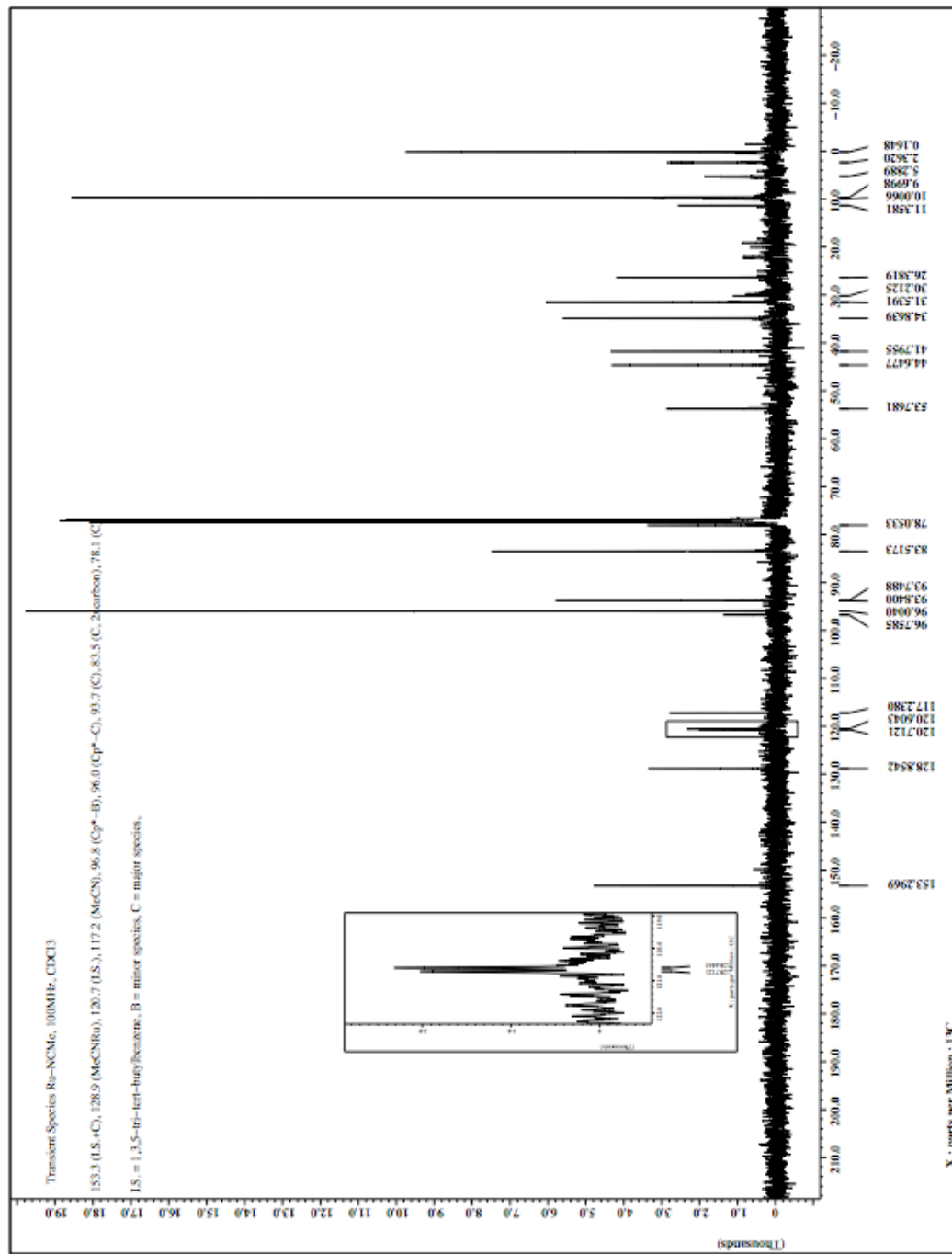


Figure 2-34. II ¹³C NMR spectrum (100 MHz, CDCl₃).

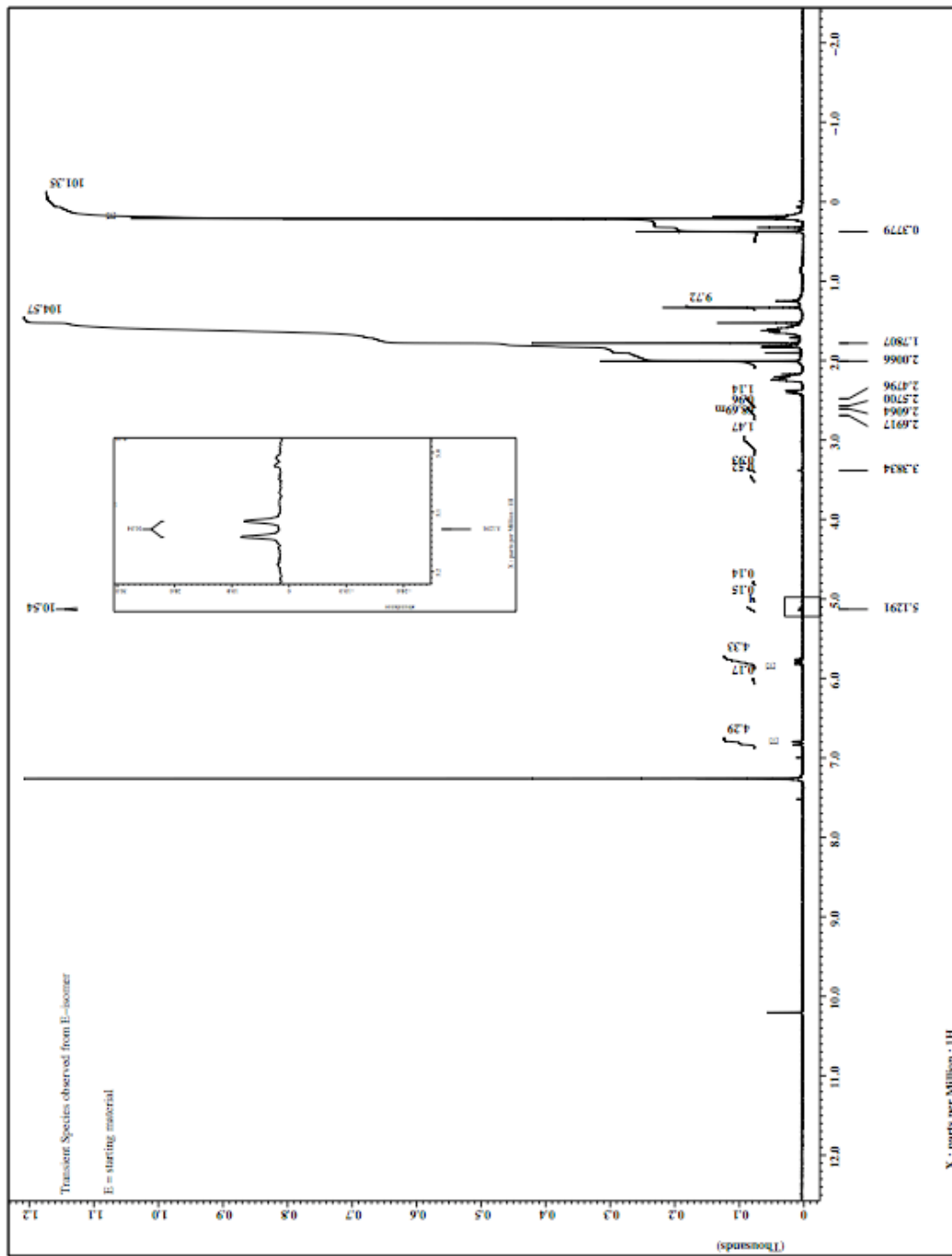


Figure 2-35. **III** ^1H NMR spectrum (400 MHz, CDCl_3).

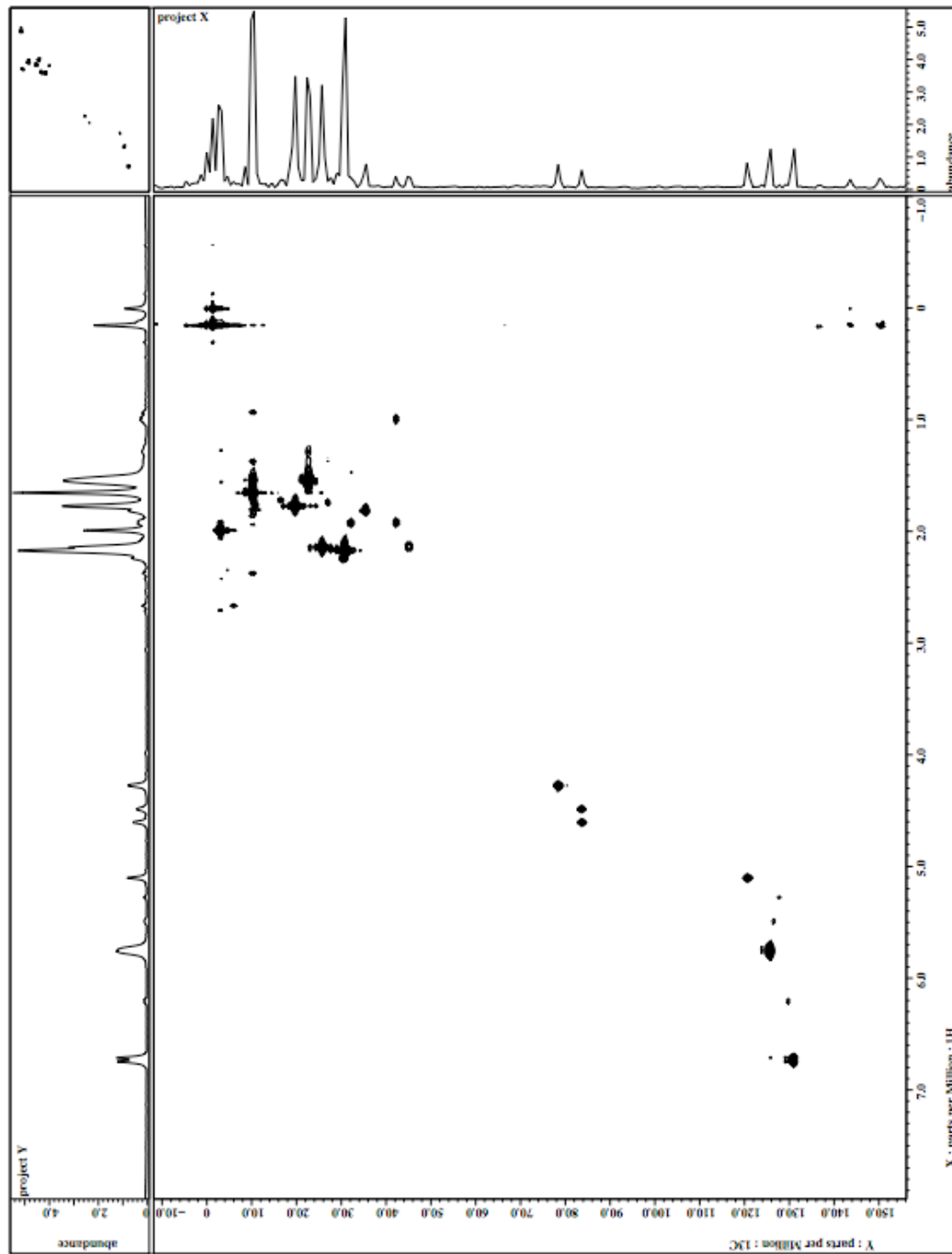


Figure 2-36. II HSQC spectrum (500 MHz, CDCl_3).

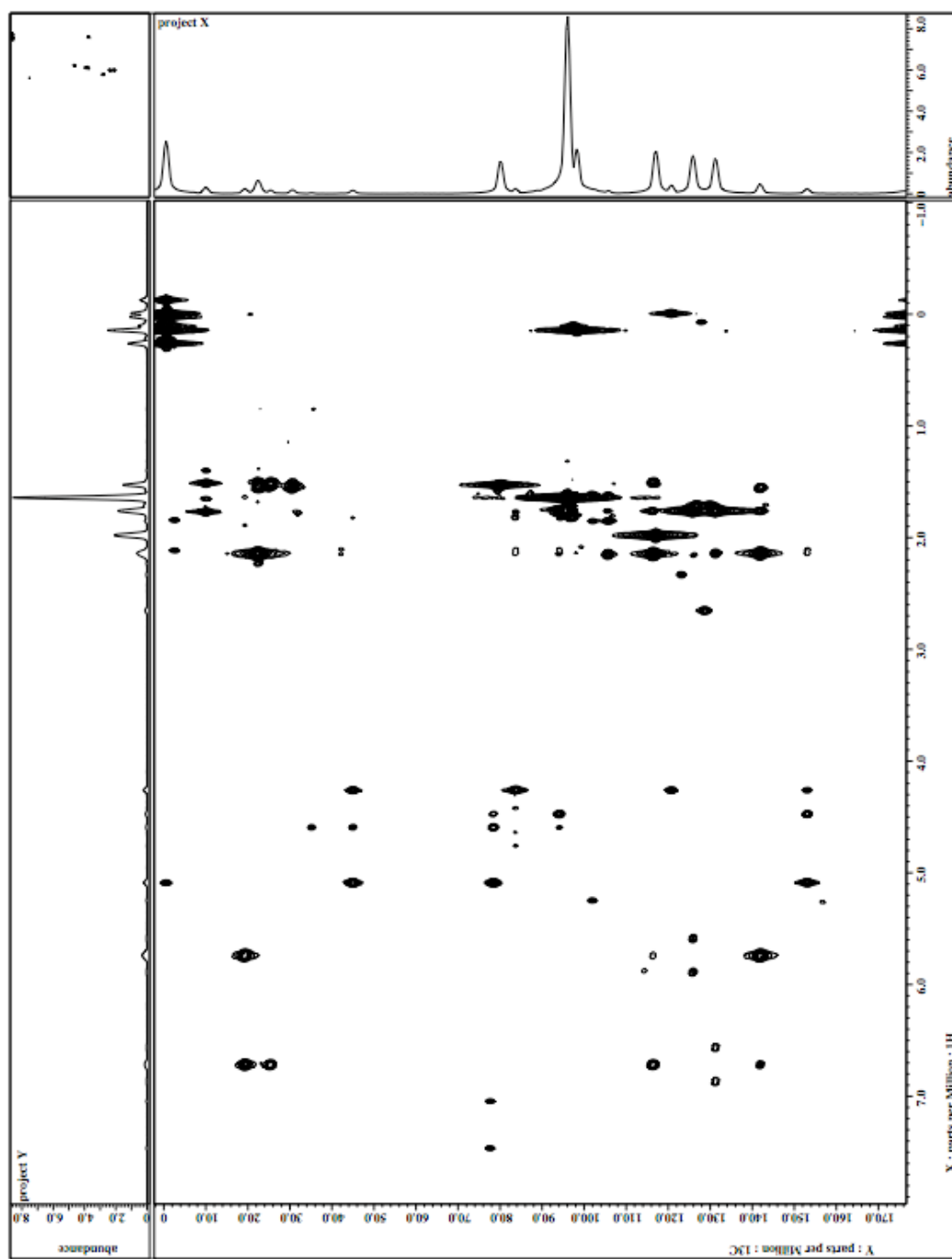


Figure 2-37. II HMBC spectrum (500 MHz, CDCl_3).

VIII. References.

1. (a) Hopf, H.; Musso, H. *Angew. Chem. Int. Ed.* **1969**, *8*, 680. For review: (b) Zimmermann, G. *Eur. J. Org. Chem.* **2001**, 457.
2. Representative examples of umplong activation: (a) Torii, S.; Okumoto, H.; Nishimura, A. *Tetrahedron Lett.* **1991**, *32*, 4167. (b) Goldfinger, M.B.; Crawford, K.B.; Swager, T.M. *J. Am. Chem. Soc.* **1997**, *119*, 4578. (c) Goldfinger, M.B.; Crawford, K.B.; Swager, T.M. *J. Org. Chem.* **1998**, *63*, 1676. (d) Imamura, K.; Yoshikawa, E.; Gevorgyan, V.; Yamamoto, Y. *Tetrahedron Lett.* **1999**, *40*, 4081. (e) Dankwardt, J.W. *Tetrahedron Lett.* **2001**, *42*, 5809. (f) Fürstner, A.; Mamane, V. *J. Org. Chem.* **2002**, *67*, 6264-6267. (g) Belmont, P.; Andrez, J.; Allan, C.S.M. *Tetrahedron Lett.* **2004**, *45*, 2783. (h) Yao, T.; Campo, M.A.; Larock, R.C. *Org. Lett.* **2004**, *6*, 2677. (i) Shibata, T.; Ueno, Y.; Kanda, K. *SynLett.* **2006**, 0411. (j) Michon, C.; Liu, S.; Hiragushi, S.; Uenishi, J.; Uemura, M. *SynLett.* **2008**, 1321. (k) Matsumoto, S.; Takase, K.; Ogura, K. *J. Org. Chem.* **2008**, *73*, 1726. (l) Mukherjee, A.; Pati, K.; Liu, R. *J. Org. Chem.* **2009**, *74*, 6311.
3. Representative examples of 6π electrocyclizations: (a) Himbert, G.; Henn, L.; Hoge, R. *J. Organomet. Chem.* **1980**, *184*, 317. (b) Porter, N.A.; Hogenkamp, D.J.; Khouri, F.F. *J. Am. Chem. Soc.* **1990**, *112*, 2402. (c) Makra, F.; Rohloff, J.C.; Muehldorf, A.V.; Link, J.O. *Tetrahedron Lett.* **1995**, *36*, 6815. (d) Merlic, C.A.; Pauly, M.E. *J. Am. Chem. Soc.* **1996**, *118*, 11319. (e) Maeyama, K.; Iwasawa, N. *J. Am. Chem. Soc.* **1998**, *120*, 1928. (f) Dankwardt, J.W. *Tetrahedron Lett.* **2001**, *42*, 5809. (g) Akiyama, R.; Kobayashi, Shu. *Angew. Chem. Int. Ed.* **2002**, *41*, 2602. (h) Shen, H.; Pal, S.; Lian, J.; Liu, R. *J. Am. Chem. Soc.* **2003**, *125*, 15762. (i) Donovan, P.M.; Scott, L.T. *J. Am. Chem. Soc.* **2004**, *126*, 3108. (j) Watanabe, M.; Mataka, S.; Thiemann, T. *Steroids* **2005**, *70*, 856. (k) Wang, Y.; Xu, J.; Burton, D.J. *J. Org. Chem.* **2006**, *71*, 7780. (l) Joo, J.M.; Yuan, Y.; Lee, C. *J. Am. Chem. Soc.* **2006**, *128*, 14818. (m) Wang, Y.; Burton, D.J. *Org. Lett.*, **2006**, *8*, 5295. (n) Zhou, H.; Xing, Y.; Yao, J.; Chen, J. *Org. Lett.* **2010**, *12*, 3674.
4. Other examples of dienyne cycloaromatizations: (a) Hanack, M.; Olweger, W. *J. Chem. Soc. Chem. Comm.* **1981**, 713. (b) Ciufolini, M.A.; Weiss, T.J. *Tetrahedron Lett.* **1994**, *35*, 1127. (c) Hemdon, J.W.; Hayford, A. *Organometallics* **1995**, *14*, 1556. (d) Tovar, J.D.; Swager, T.M. *J. Organometallic Chem.* **2002**, *653*, 215. (e) Lian, J.; Odedra, A.; Wu, C.; Liu, R. *J. Am. Chem. Soc.* **2005**, *127*, 4187. (f) Barluenga, J.; Andina, F.; Aznar, F.; Valdés, C. *Org. Lett.* **2007**, *9*, 4143. (g) Umeda, R.; Fukuda, H.; Miki, K.; Rahman, S.M.A.; Sonoda, M.; Tobe, Y. *C.R. Chimie*, **2009**, *12*, 378. (h) Liu, L.; Zhang, J. *Angew. Chem. Int. Ed.* **2009**, *48*, 6093.
5. (a) J.M. O'Connor, S.J. Friese, and M. Tichenor. *J. Am. Chem. Soc.* **2002**, *124*, 3506. (b) J.M. O'Connor, S.J. Friese, B.L. Rodgers, A.L. Rheingold, L. Zakharov. *J. Am. Chem. Soc.* **2005**, *127*, 9346.
6. Aitken, R.A.; Boeters, C.; Morrison, J.J. *J. Chem. Soc., Perkin Trans. 1* **1997**, 2626.
7. (a) Lian, J.; Lin, C.; Chang, H.; Chen, P.; Liu, R. *J. Am. Chem. Soc.* **2006**, *128*, 9661. (b) Yang, C.; Liu, R. *Tetrahedron Lett.* **2007**, *48*, 5887.
8. Jacobi, P.A.; Kravitz, J.I. *Tetrahedron Letters*, **1988**, *29*, 6873.

9. Waddell, M.; Bekele, T.; Lipton, M. *J. Org. Chem.* **2006**, *71*, 8372.
10. Steinmetz, B.; Schenk, W. *Organometallics*. **1999**, *18*, 943.
11. G.L. Thompson, W.E. Heyd, L.A. Paquette. *J. Am. Chem. Soc.* **1974**, *96*, 3177.
12. M. Adamczyk, D.S. Watt, D.A. Netzel. *J. Org. Chem.* **1984**, *49*, 4226.
13. ¹H NMR (400MHz, CDCl₃) **I**: δ 6.02 (t, *J* = 5.5 Hz, 1H), 5.01 (d, *J* = 5.5 Hz, 1H), 4.81 (d, *J* = 5.5 Hz, 1H), 3.50 (s, 1H), 1.90 (s, 15H, Cp*), 1.07 (td, *J* = 12.0, 4.0 Hz, 1H), 0.37 (s, 9H, TMS). **II**: δ 5.18 (d, *J* = 1.5 Hz, 1H), 4.61 (d, *J* = 5.0 Hz, 1H), 4.47 (dd, *J* = 6.7, 5.0 Hz, 1H), 4.33 (d, *J* = 7.0 Hz, 1H), 2.74 (s, 3H, Ru←NCCH₃), 1.71 (s, 15H, Cp*), 1.11 - 0.99 (m, 1H), 0.064 (s, 9H, TMS). (Figure 2-33)
14. K. Kamikawa, M. Furusyo, T. Uno, Y. Sato, A. Konoo, G. Bringmann, and M. Uemura. *Org. Lett.* **2001**, *3*, 3667.
15. Y. Yoshimi, A. Ishise, H. Oda, Y. Moriguchi, H. Kanezaki, Y. Nakaya, K. Katsuno, T. Itou, S. Inagaki, T. Morita and M. Hatanaka. *Tetrahedron Letters*, **2008**, *49*, 3400.
16. ¹H NMR (400MHz, CDCl₃) **III**: δ 5.11 (d, *J* = 10.5 Hz, 1H), 2.69 – 2.60 (m, 1H), 2.57 – 2.48 (m, 1H), 1.78 (s, 15H, Cp*), 0.38 (s, 9H, TMS) (Figure 2-35).
17. (a) Beydoun, K.; Zhang, H-J.; Sundararaju, B.; Demerseman, B.; Achard, M.; Xib, Z.; Bruneau, C. *Chem. Commun.* **2009**, 6580. (b) Mauthner, K.; Mereiter, K.; Schmid, R.; Kirchner, K. *Organometallics*, **1994**, *13*, 5054.
18. ¹³C NMR (125 MHz, CDCl₃) **II** sp² carbons + methine: δ 153.3 (C⁴), 120.9 (C^{exo}), 96.0 (Cp*), 94.3 (C⁶), 83.6 (C², C¹), 78.4 (C³), 45.2 (C⁵) ppm. 1D ¹³C NMR acquired from low temperature equilibrium experiment shows resonance at δ 83.6 ppm is ~ 2 x peak height over other vinyl CH resonances (Figure 2-34).
19. Kreindlin, A.Z.; Rybinskaya, M.A. *Russian Chemical Reviews*, **2004**, *73*, 417.
20. (a) Kölle, U.; Grub, J. *J. Organomet. Chem.* **1985**, *289*, 133. (b) Kreindlin, A.Z.; Petrovskii, P.V.; Rybinskaya, M.I.; Yanovskii, A.I.; Struchkov, Y.T. *J. Organomet. Chem.* **1987**, *319*, 229.
21. (a) Lange, G.; Reimelt, O.; Jessen, L.; Heck, J. *Eur. J. Inorg. Chem.* **2000**, 1941. (b) Bosch, H.W.; Hung, H.U.; Nietlispach, D.; Salzer, A. *Organometallics*, **1992**, *11*, 2087. (c) Bouachir, F.; Chaudret, B.; Dahan, F.; Agbossou, F.; Tkatchenko, I. *Organometallics*, **1991**, *10*, 455. (e) Bouachir, F.; Chaudret, B.; Tkatchenkob, I. *J. Chem. Soc., Chem. Comm.* **1986**, 94. (e) Liles, D.C.; Shaver, A.; Singleton, E.; Wiege, M.B. *J. Organomet. Chem.* **1985**, *288*, C33.
22. Albers, M.O.; Oosterhuizen, H.E.; Robinson, D.J.; Shaver, A.; Singleton, E. *J. Organomet. Chem.* **1985**, *282*, C49.
23. Rüba, E.; Mereiter, K.; Soldouzi, K. M.; Gemel, C.; Schmid, R.; Kirchner, K. *Organometallics* **2000**, *19*, 5384.
24. ¹H NMR (400MHz, CDCl₃) **IV**: δ 5.09 (d, *J* = 10 Hz, 1H), 4.18 (dq, *J* = 8.9 Hz, 6.5 Hz, 1H),

- 1.77 (s, Cp*), 1.53 (d, $J = 6.5$ Hz, 3 H, CH₃), 0.35 (s, 9 H, TMS). **V**: δ 4.68 (d, $J = 6$ Hz, 1H), 4.34 (s, 1H), 3.57 (s, 1H), 3.03 (td, $J = 6.5$ Hz, 1.5 Hz, 1H), 1.84 (s, Cp*).
25. Kulawiec, R.J.; Faller, J.W.; Crabtree, R.H. *Organometallics*, **1990**, *9*, 745.
26. Friese, S.; PhD. Dissertation, University of California, San Diego **2004**.
27. (a) Trost, B.M.; Toste, F.D. *J. Am. Chem. Soc.* **1999**, *121*, 9728. (b) Trost, B.M.; Toste, F.D. *J. Am. Chem. Soc.* **2002**, *124*, 5025.
28. Reductive elimination from the *syn*-allyl complex derived from **15-TMS-E** would result in a highly strained *Z,E*-cyclohexadiene product.
29. Still, W.C.; Khan, M.; Mitra, A. *J. Org. Chem.* **1978**, *43*, 2923.
30. Hohmann, M.; Krause, N. *Chem. Ber.* **1995**, *128*, 851.
31. Kato, Y.; Miki, K.; Nishino, F.; Ohe, K.; Uemura, S. *Org. Lett.* **2003**, *5*, 2619.

IX. Acknowledgements.

The material of Chapter 2, in part, is currently being prepared for submission for publication with the following authors: Hitt, D.M.; O'Connor, J.M. The dissertation author was the primary investigator and author of this material.

**CHAPTER 3: Stereoselective η^6 -Arene Complexation during Ruthenium Mediated
Dienyne and Eneidyne Cycloaromatization Reactions.**

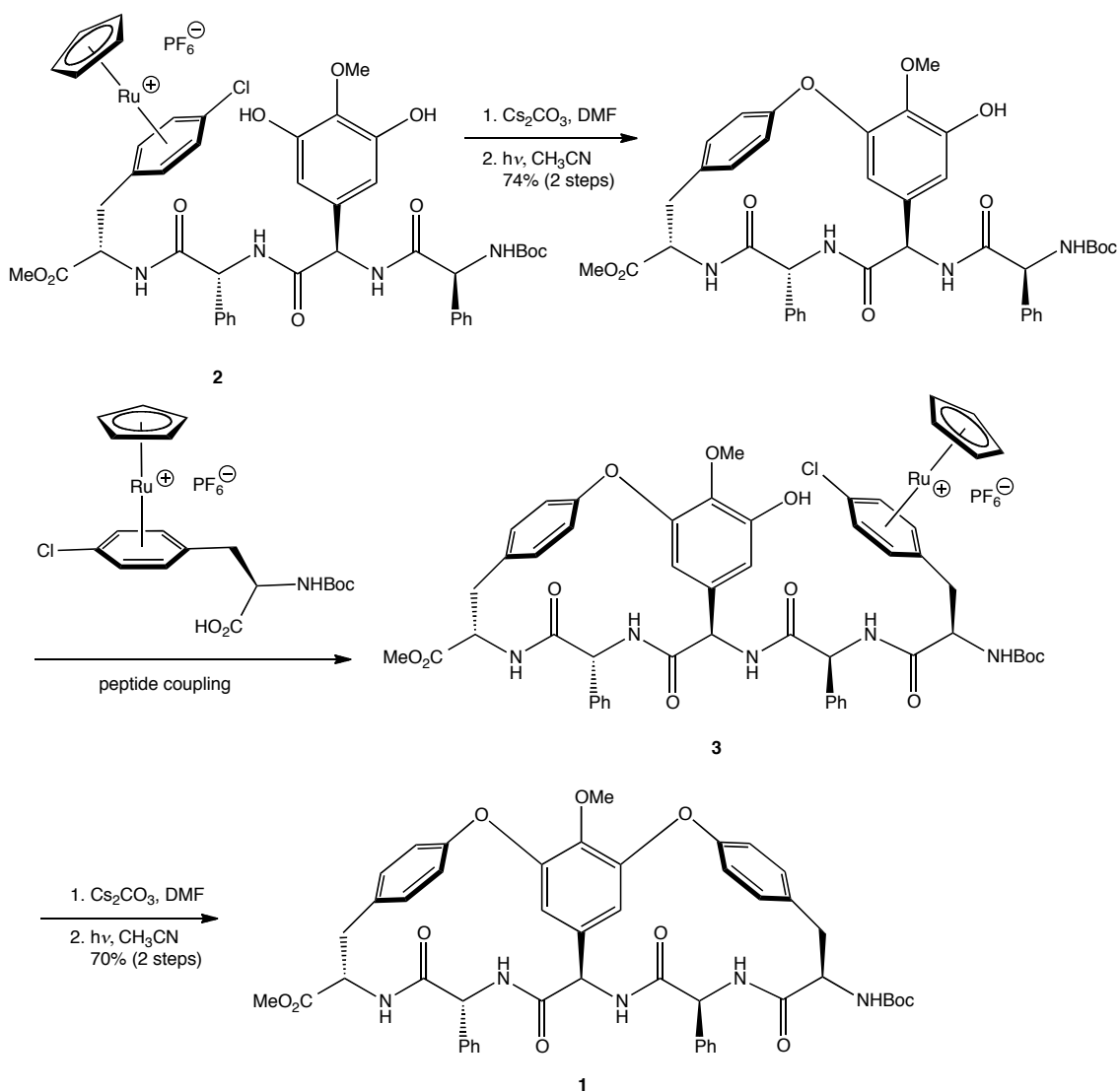
I. Introduction.

Complexation of the π system of an aromatic compound by a transition metal results in a large modification of the molecule's reactivity. For this reason, metal η^6 -arene complexes have been utilized as activating groups to access chemical transformations normally only obtainable under harsh conditions such as nucleophilic substitution,¹ dearomatization,² and aromatic CH lithiation.³ Historically, the most commonly used and studied metal-ligand system for these processes is the d^6 – 12 valence electron chromium tricarbonyl $[\text{Cr}(\text{CO})_3]$ fragment. A convenient isolobal alternative to the use of $\text{Cr}(\text{CO})_3$ are the cationic cyclopentadienyl (Cp) and pentamethylcyclopentadienyl (Cp*) ruthenium (II) d^6 metal fragments of group 8.⁴ Cp and Cp* ruthenium (II) η^6 -arene complexes are, in general, air-stable crystalline solids that are amenable to bench-top chemistry and, unlike $\text{Cr}(\text{CO})_3$, ruthenium arene complexes provide a facile photolytic method for removal and *recycling* of the metal-ligand system.⁵

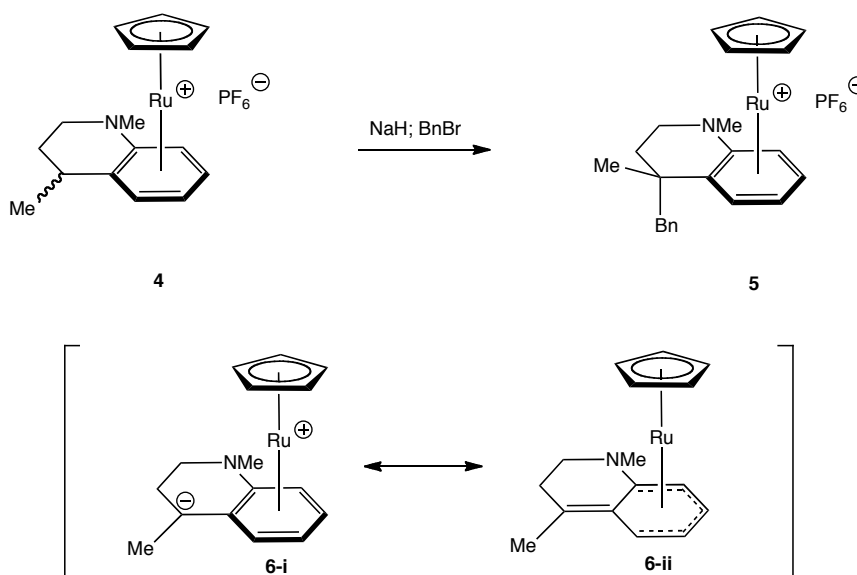
Some common examples of CpRu-arene coordination applications are shown in Scheme 3-1 and Scheme 3-2. Similar to $(\eta^6\text{-arene})\text{Cr}(\text{CO})_3$ complexes, the ruthenium-arene is highly activated for $\text{S}_{\text{N}}\text{Ar}$ reactions. Pearson and coworkers have demonstrated the utility of this enhanced reactivity by using $[\text{CpRu}(\eta^6\text{-arene})]\text{PF}_6$ as activating groups for synthesis of a biaryl ether peptidomacrocycle **1** common to several antibiotics such as vancomycin, ristocetin-A, and teicoplanin.⁶ The use of exceedingly mild conditions to induce the intramolecular cyclization of **2** and **3** allowed for construction of **1** with minimal epimerization to the sensitive α -stereocenters in the peptide.

The alkylation of $[\text{CpRu}(\eta^6\text{-}N,4\text{-dimethyltetrahydroquinoline})]\text{PF}_6$ (**4**) to give complex **5** highlights several useful features of η^6 -complexation.⁷ First, deprotonation of the benzylic hydrogen was accomplished by the moderately strong base, sodium hydride (as opposed to an alkyllithium), due to the resonance stabilized conjugate base **6**. The increased acidity of the benzylic hydrogen atoms effected by the related Cp* Ru^+ metal fragment has been

experimentally compared to that of a *para* substituted nitro group.⁸ Secondly, complexation creates a substantial steric bias to the approach of the nucleophile, causing substitution to occur exclusively *anti* to the metal fragment. This facial selectivity is general and has been used for stereoselective hydrogenations, Diels-Alder reactions, and various types of nucleophilic additions.⁹



Scheme 3-1. Use of cationic CpRu-arene complexes in the synthesis of core structure of peptidomacrocyclic antibiotics.⁶



Scheme 3-2. Stereoselective alkylation via benzylic deprotonation of a CpRu-arene.⁷

In addition to a carbon stereocenter, the complexes shown in Scheme 3-2 have another element of chirality resulting from η^6 -complexation to the different faces of the non-symmetrically substituted arene. This asymmetry is termed *planar chirality* and the absolute stereochemical assignment is typically designated according to the Schlägl system based on the clockwise or counterclockwise rotational direction from the highest priority to the next highest priority substituent analyzed from the face of the arene *anti* to the metal.¹⁰ Another convention uses a slight modification of the Cahn–Ingold–Prelog (CIP) rules where the chiral arene complex is viewed as having a κ^6 -coordination mode and analyzed from the aromatic carbon with the second highest priority substituent to the ruthenium.¹¹ Both systems use the R_p or S_p notation depending upon a clockwise or counterclockwise rotation, respectively. Application of the systems to complex **4** are shown in Figure 3-1 and for the purposes of the discussion in this chapter, the Schlägl system will be used.

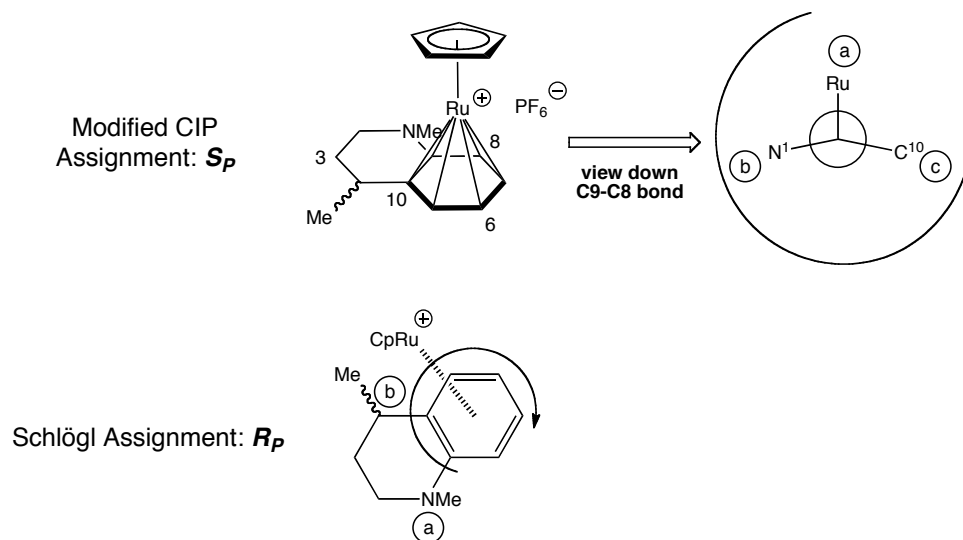
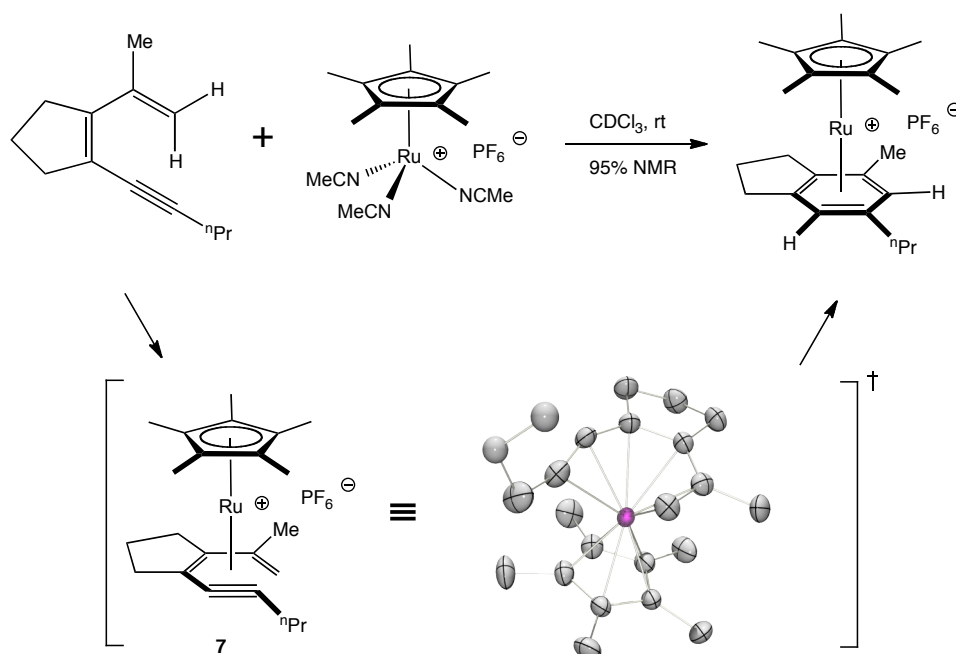


Figure 3-1. Comparison of the two stereochemical assignment conventions for planar chiral metal η^6 -arene complexes.

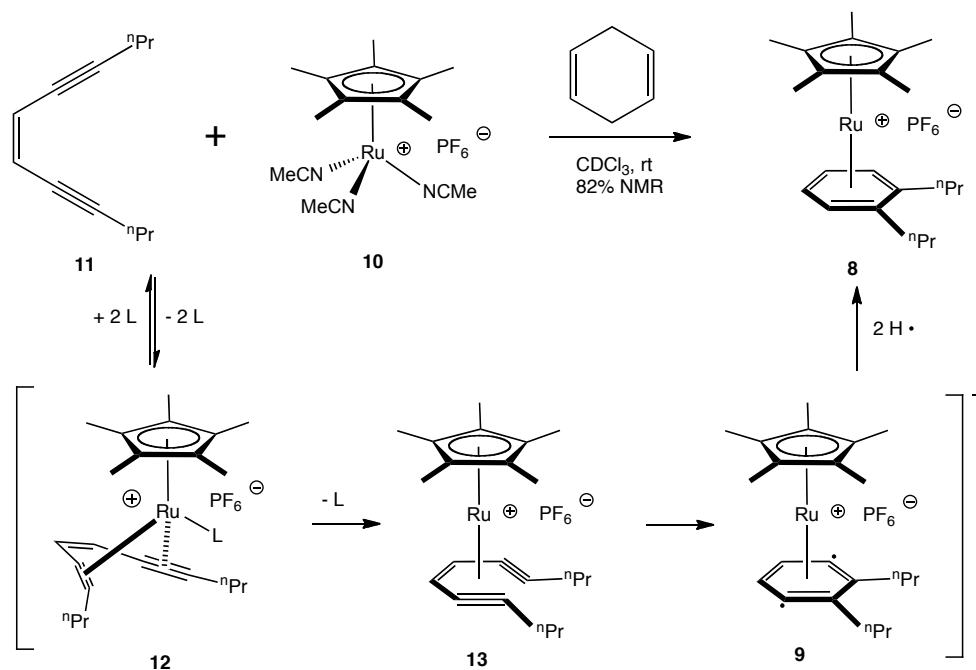
Interest in the O'Connor laboratory has been focused around cationic Cp and Cp*Ru(η^6 -arene) complexes since the discovery that these compounds are formed as products from the rapid and high yielding ambient temperature cycloaromatization of acyclic enediyne and dienyne substrates via reaction with cationic Cp and Cp* tris-acetonitrile ruthenium complexes (Scheme 3-3 and Scheme 3-4).¹² Formally, these transformations are known as the Bergman¹³ (enediyne) and Hopf¹⁴ (dienyne) cycloaromatizations. As discussed in Chapter 1, the ruthenium triggered Hopf cyclization may involve the intermediacy of the X-ray characterized η^6 -dienyne intermediate **7** that could be rationalized to accelerate the reaction by the induced proximity of the terminal carbon atoms of the reactive π system.

Shown in Scheme 3-4 is the current working mechanistic hypothesis for the ruthenium triggered Bergman reaction. Use of a deuterium atom donor (i.e. THF- d_8) leads to incorporation of the deuterium into the *para* positions of the product, **8**, supporting formation of *para*-benzyne diradical intermediate **9**. Reaction of cationic ruthenium complex **10** with enediyne **11** at low temperature led to observation of a transient C_s symmetric species by ¹H and ¹³C NMR

spectroscopy. Spectral similarities of this compound with an air-stable X-ray characterized intermediate model ($L = \text{CO}$) suggested the structure of the low temperature species to be η^4 -diyne intermediate **12** ($L = \text{MeCN}$). Also consistent with **12**, was an inverse second order rate dependence on the acetonitrile concentration for the reaction of a structurally similar enediyne with **10**.

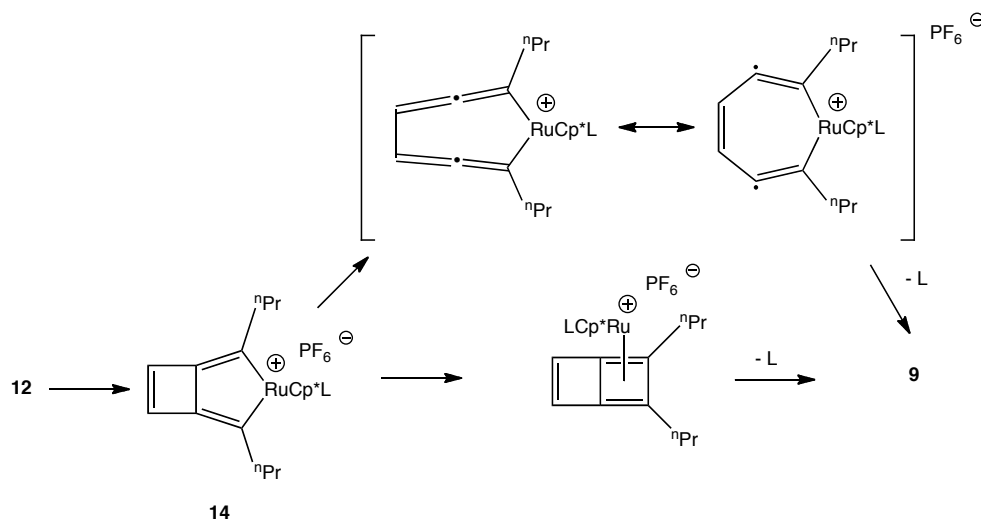


Scheme 3-3. Ruthenium triggered Hopf cycloaromatization.



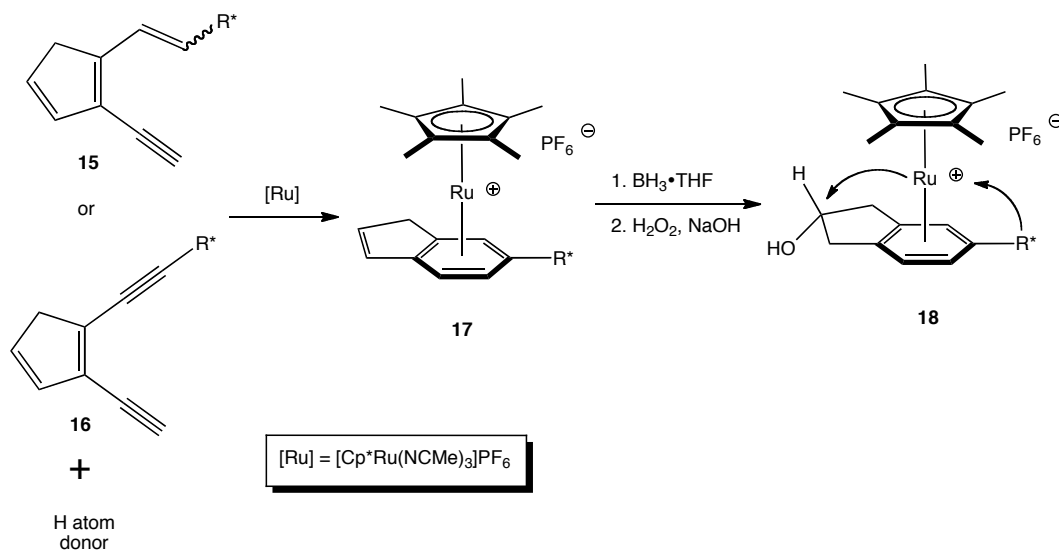
Scheme 3-4. Proposed intermediates for the ruthenium triggered Bergman cyclization.

By analogy to the ruthenium triggered Hopf cyclization, a pathway involving a similar η^6 -enediyne species **13** is favored for the cyclization. Coordination of all components of the enediyne π system would decrease the distance between the terminal alkyne carbon atoms thus accelerating the reaction.¹⁵ While a pathway proceeding through **13** was favored, a mechanism involving Ru(IV) metallacycle **14** could not be ruled out (Scheme 3-5).



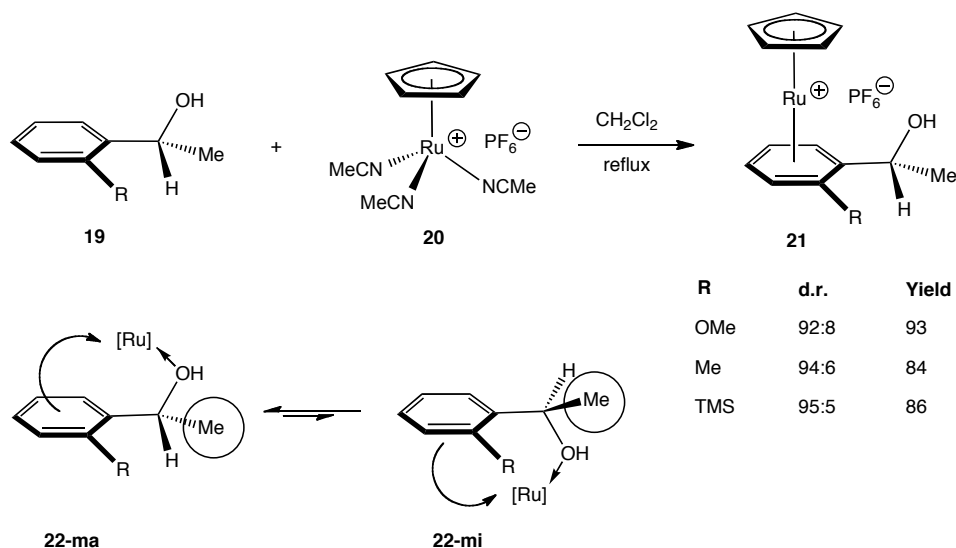
Scheme 3-5. Alternative intermediates not involving coordination of the central alkene.

Recognizing that the Ru η^6 -arene product of these reactions is chiral if the benzenoid portion is non-symmetric, we questioned if placement of a carbon stereocenter in the dienyne or enediyne substrates would result in facial selective coordination of the cationic ruthenium fragment. The synthetic utility of this process would be two-fold. First, the ability to easily synthesize structurally diverse dienyne and enediyne substrates would allow formation of highly substituted aromatic systems that would be difficult to obtain under traditional organic synthetic techniques. Second, the chiral relay system would effectively allow stereocontrol of functional groups distal to the original source of chirality as demonstrated by the hypothetical three-step reaction shown in Scheme 3-6. Use of dienyne **15** or enediyne **16** with a stereocenter containing substituent (R^*) could stereoselectively proceed to arene complex **17**. Any reaction of the pendent alkene could then be reliably predicted to occur from the face *anti* to the metal fragment as shown by the hydroboration / oxidation sequence to give **18**. Effectively the initial source of chirality has been used to influence the binding of the metal then facial selective attack of the alkene.



Scheme 3-6. Potential chiral relay system for a hydroboration / oxidation sequence created upon prior stereoselective binding of Cp^*Ru^+ induced by chiral substituent R^* .

Several methodologies exist that lead to metal η^6 -arene complexes with enhanced stereoselectivity starting from benzenoid precursors.¹⁶⁻¹⁷ Of particular relevance, Uemura and coworkers have shown ortho substituted secondary benzylic alcohols **19** react with $[CpRu(NCMe)_3]PF_6$ (**20**) to form η^6 -arene complexes stereoselectivity in favor of diastereomer **21** (Scheme 3-7).^{17b} These researchers proposed a pre-complexation equilibrium between intermediates **22-ma** and **22-mi** where by facial selectivity of the arene is created by minimizing the steric interactions between the ortho substituent and the stereocenter substituent.

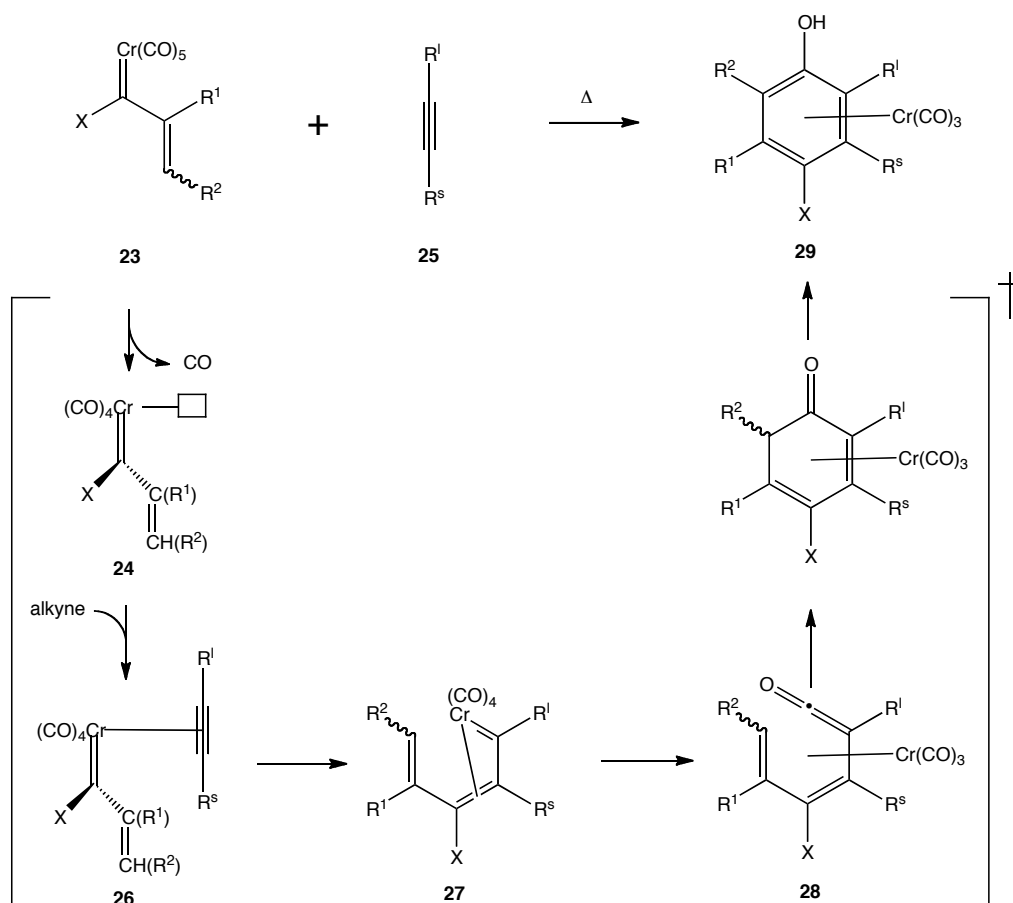


Scheme 3-7. Stereoselective CpRu η^6 -complexation of chiral arene.^{17b}

These systems are of potential synthetic utility as many provide excellent stereoselectivities and yields, but all require aromatic substrates. To our knowledge the only transformation capable of performing a one-pot cycloaromatization / facially selective η^6 -complexation is the thermal benzannulation of a vinyl or aryl substituted chromium carbene (e.g. **23**) with an alkyne collectively known as the Dötz reaction.¹⁸

The accepted mechanism of the Dötz reaction is shown in Scheme 3-8. The rate-determining step involves loss of CO to form the coordinatively unsaturated 16-electron complex **24**. Coordination of alkyne **25** to give **26** determines the placement of the alkyne substituents in the final product. Typically, high levels of regioselectivity are observed that can be predicted by inserting the alkyne carbon with the sterically smaller substituent (R^s) into the carbenoid carbon (CX). This insertion is thought to give η^3 -vinyl carbene complex **27**.¹⁹ Common substituents for position X are basic oxygen and nitrogen groups which stabilize and favor an *E* geometry across the α,β -double bond of **27**.²⁰ Recent work has also shown that **27** undergoes a reversible isomerization where the R^l and R^s substituents can be exchanged and sometimes result in a divergent reaction pathway to an indene product.²¹ The η^3 -vinyl carbene **27** undergoes a CO

insertion to give the chromium coordinated ketene **28** that proceeds through a 6π electrocyclicization and tautomerization to give the η^6 -bound phenol product **29**.

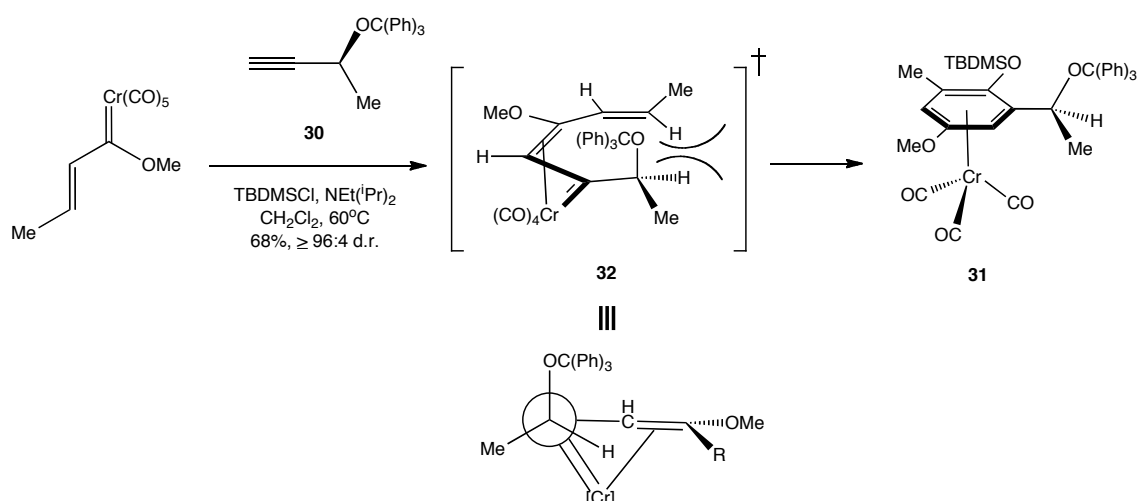


Scheme 3-8. Accepted mechanism of the Dötz reaction.

The stereoselectivity of the Dötz reaction has been systematically studied by incorporating carbon stereocenters into both alkyne substituents (R¹ and R^s),²² the vinyl substituents (R¹ and R²),²³ and the carbene substituent (X),²⁴ as well as use of atropisomers.²⁵ Several representative examples of these methodologies are presented below.

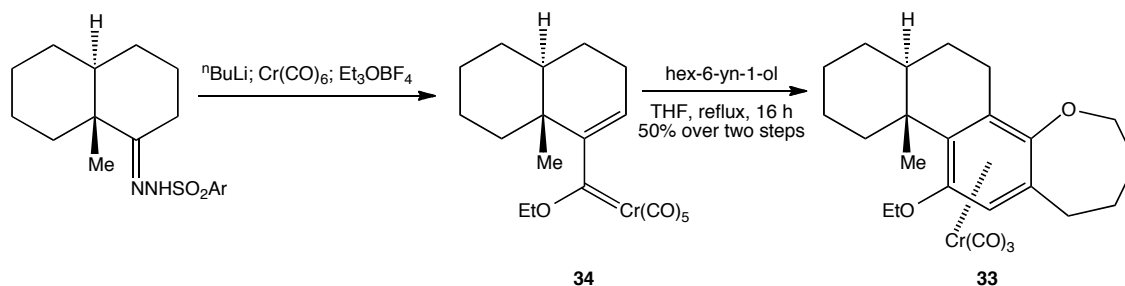
The earliest example by Wulff and coworkers utilized bulky chiral propargylic ethers (e.g. **30**, Scheme 3-9) to give high diastereomeric ratios in favor of chromium tricarbonyl arene

complex **31**.^{22a} The relative stereochemistry of **31** was assigned based on ¹³C and ¹H NMR spectral correlations with similar complexes that were characterized by X-ray diffraction. These researchers have proposed the observed stereochemistry to originate from the thermodynamically favored η^3 -vinyl carbene intermediate **32** that reduces steric interactions by keeping the largest stereocenter substituent (trityl ether) on the opposite face of the $\text{Cr}(\text{CO})_3$ while also placing the second largest substituent (methyl) away from the terminal vinyl hydrogen.



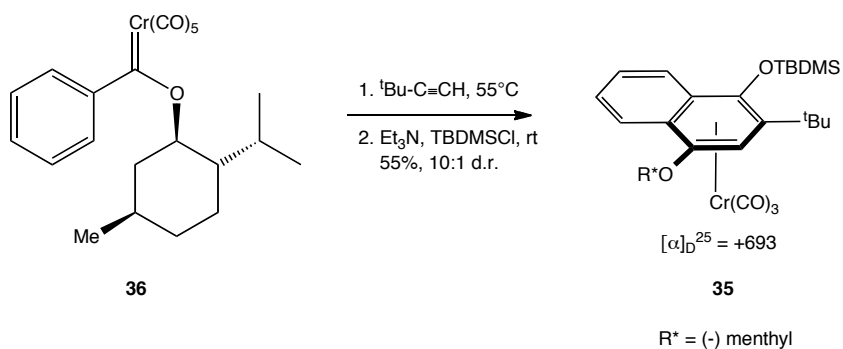
Scheme 3-9. Incorporation of alkyne stereocenter as secondary propargylic ethers for facially selective benzannulation.^{22a}

Quayle and coworkers were able to form **33** as a single diastereomer by incorporation of the chromium carbene into the conformationally locked *trans*-decalin **34** (Scheme 3-10).^{23a} The facial selectivity is consistent with the relative stereochemistry of the axial C-10 methyl group that directs the binding to the more sterically accessible α face.



Scheme 3-10. Stereoselectivity by facial steric differentiation of a rigid bicyclic substrate.^{23a}

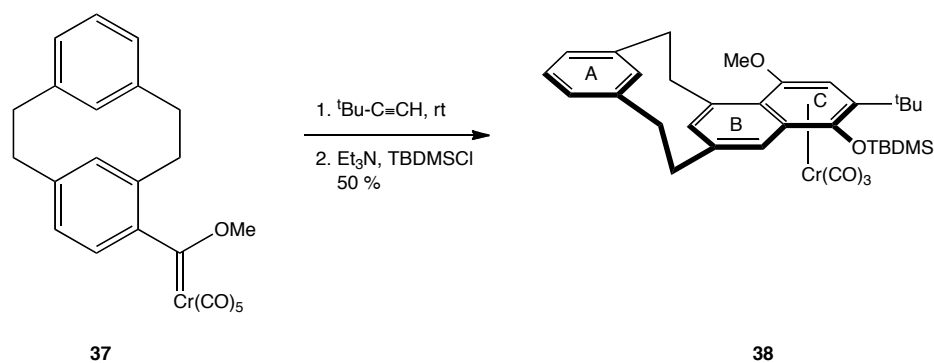
Dötz and coworkers were able to employ an auxiliary approach by use of several commercially available chiral alcohols as demonstrated by the synthesis of **35** in enantiomeric and high diastereomeric excess from the menthol derived chromium carbene **36** (Scheme 3-11).^{24a} Although an exact model of selectivity was not given, the η^3 -vinyl carbene intermediate (**27**, Scheme 3-8) was invoked as being involved in the stereo-differentiating step. The reaction is limited to aromatic substituents off the carbene as use of a vinyl substituent resulted in almost no diastereoselectivity.^{24b}



Scheme 3-11. Chiral auxiliary approach to stereoselective η^6 -complexation.^{24a}

Dötz has also provided a nice example of atropisomer-controlled diastereoselectivity via use of cyclophane chromium carbenes.^{25a} Benzannulation of **37** with *tert*-butyl acetylene resulted in the formation of X-ray characterized naphthalenophane complex **38** as a single

diastereomer (Scheme 3-12). Complex **38** exist with an *anti* relationship between the $\text{Cr}(\text{CO})_3$ and the conformationally restrained “A” ring due to minimization of steric interactions. The alkyne substituent is also key to obtaining high stereoselectivity as use of 3-hexyne gave a 2:1 mixture of stereoisomers. Later work has been focused on an intramolecular benzannulation from a *meta*-substituted arene that constructs the η^6 -cyclophane stereoselectively in a single step.^{25b,f}

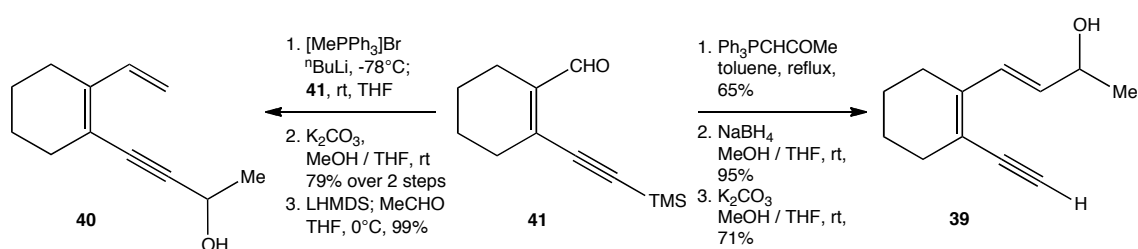


Scheme 3-12. Diastereoselective formation of an η^6 -bound naphthalenophane complex.^{25a}

The literature precedent describing the successful incorporation of stereoselective η^6 -arene complexation in the Dötz reaction provided good evidence that the same phenomena may be possible for the ruthenium-mediated enediyne and dienyne cycloaromatization. We were particularly interested with Wulff's model for stereoselectivity (see Scheme 3-9) and how similar steric interactions for η^3 -vinyl carbene **32** could be envisioned to exist in an η^6 -dienyne and enediyne. We therefore chose to focus on stereoselectivity induced from an allylic or propargylic stereocenter positioned on the terminus of the dienyne and enediyne π system. We herein report the first examples of facially selective metal η^6 -arene binding in metal-triggered Bergman and Hopf cycloaromatizations.

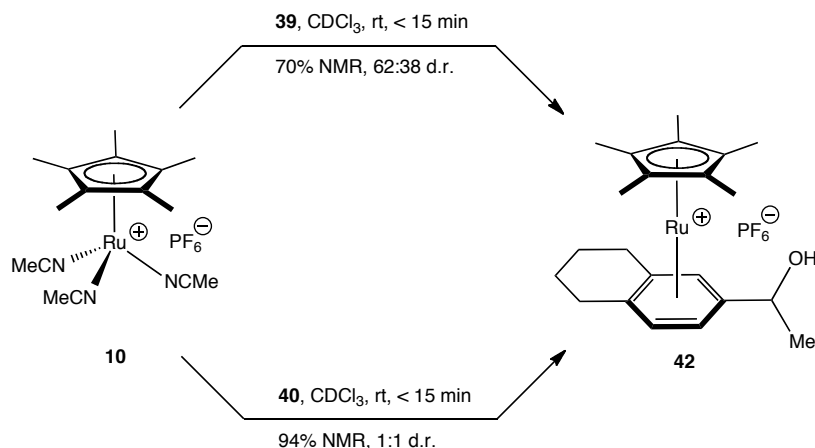
II. Dienyne Stereoselectivity: Discovery and Substrate Scope.

Dienynes **39** and **40** containing an allylic and propargylic stereocenter, respectively, were chosen as an ideal starting point for initial reactivity studies (Scheme 3-13). Synthesis of both substrates commenced from TMS substituted enynal **41** that is available in two steps from cyclohexanone.²⁶ Wittig olefination of **41** followed by sodium borohydride reduction and TMS removal gave secondary allylic alcohol **39**. In a similar fashion, olefination to the monosubstituted alkene followed by removal of the TMS gave the terminal alkyne. This product was then lithiated and quenched with acetaldehyde to give **40**.



Scheme 3-13. Synthetic route to dienynes **39** and **40**.

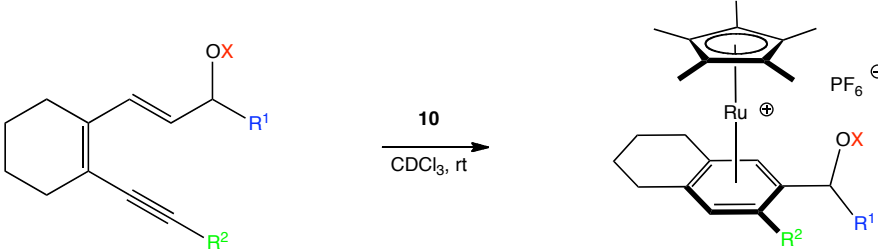
When **39** and **40** were reacted with a slight excess of [Cp*Ru(NCMe)₃]PF₆ (**10**,²⁷ 1.4 eq) in CDCl₃ and monitored by ¹H NMR spectroscopy, immediate formation of two [Cp*Ru(η^6 -arene)]PF₆ complexes consistent with the product structure **42** were observed (Scheme 3-14). While both substrates gave **42** in high yield, only **39** with the stereocenter located in the allylic position was stereoselective.



Scheme 3-14. Initial observation of stereoselectivity for the dienyne cycloaromatization reaction.

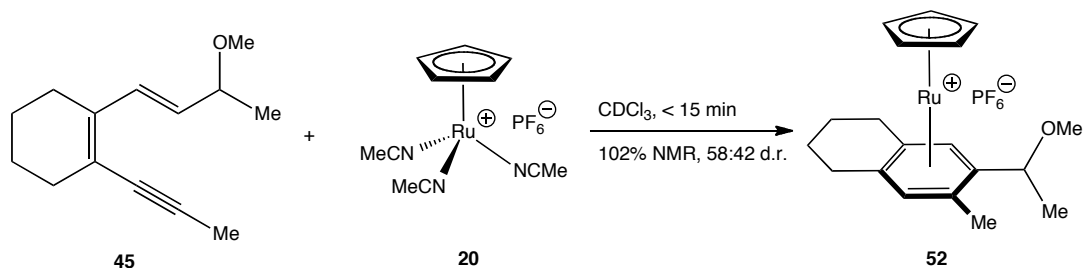
Optimistic about the observed diastereomeric ratio, dienynes (**43-47**) were prepared using a similar synthetic route to **39** and examined in reactions with Cp*Ru complex **10** to determine what dienyne structural features were important for the observed stereoselectivity (Table 3-1). All of dienynes allowed to react formed η^6 -arene products (**48-51**) except for **47**, which resulted in the decomposition of the substrate over the course of 23 h to NMR inactive material (entry 5). 1-Methoxyethyl allylic and methyl propargylic substitution (entry 3) was identified to give the highest observed d.r. In general, the reaction is adversely affected by increasing the steric size of the alkoxy, propargylic, or stereocenter substituent (entry 2, 4, and 5). The most dramatic effects were observed for the isopropyl-substituted dienyne **46** resulting in a much lower yield and essentially no stereoselectivity (entry 4) and the unsuccessful trimethylsilyl substituted dienyne **47** (entry 5). Based on the studies conducted in Chapter 2, it is not surprising why the reaction of **47** failed, as it is now known that increasing steric bulk in the propargylic position changes the reactivity of the cycloaromatization to a slower C-H bond activation / insertion mode.

Table 3-1. Exploring substrate scope with dienynes containing an allylic stereocenter. (a) Yield and d.r. determined by ^1H NMR spectroscopy. (b) Reaction stopped at 91% conversion of **44**. Yield based on conversion. (c) Product not isolated.



| Entry | Substrate | Product | X | R ¹ | R ² | Rxn Time | Yield (d.r.) ^a |
|-------|-----------|-----------|----|-----------------|----------------|----------|---------------------------|
| 1 | 43 | 48 | H | Me | Me | < 15 min | 97 (64:36) |
| 2 | 44 | 49 | Et | Me | Me | 3.5 h | 78 (63:37) ^b |
| 3 | 45 | 50 | Me | Me | Me | < 15 min | 94 (69:31) |
| 4 | 46 | 51 | H | ⁱ Pr | Me | < 15 min | 44 (52:48) ^c |
| 5 | 47 | - | H | Me | TMS | < 23 h | decomp. |

To probe the effect of changing the ligand environment on the metal complex, the best performing dienyne **45** (0.059 mmol) was allowed to react with $[\text{CpRu}(\text{NCMe})_3]\text{PF}_6$ **20** (0.088 mmol) under identical conditions as the reaction with **10** (Scheme 3-15). This resulted in the formation of **52** with a *lower* stereoselectivity compared to the formation of **50** clearly showing that either the smaller steric influence or electron-donating ability of the cyclopentadienyl ligand influences the product ratio.



Scheme 3-15. Probing the effect of the metal-ligand environment on the stereoselectivity.

III. Solid State Structure Determination of the η^6 -Arene Products.

The crystalline nature of the cationic cyclopentadienyl ruthenium arene complexes allowed for solid state X-ray structure determination to be obtained for isolated samples of the major and minor diastereomers of **50** and **52** and the minor diastereomers of **42** and **48**. This analysis confirmed the diastereotopic relationship between the major and minor isomers and also showed a conserved stereochemical relationship between the carbon stereocenter and the planar chirality of the metal binding for the major and minor diastereomers of each pair. This trend can be summarized using the following model: the major stereoisomer has the least sterically demanding group attached to the carbon stereocenter (hydrogen) directed towards the ortho substituent (R) on the aromatic ring when the oxygen substituent is rotated *syn* with the metal fragment as depicted in Figure 3-2.

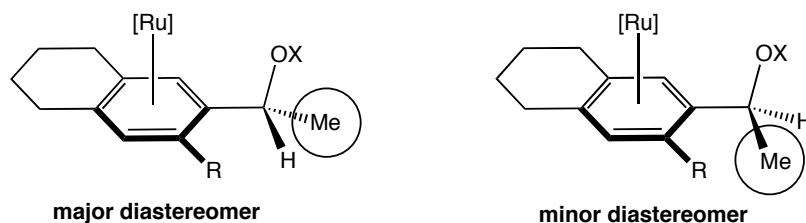
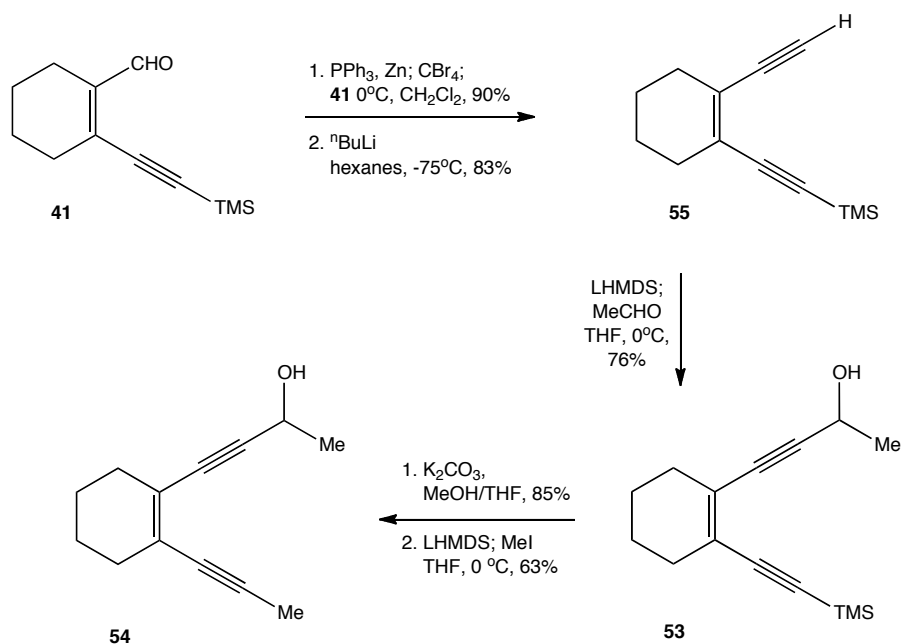


Figure 3-2. Conserved relative stereochemistry for the major and minor diastereomers from the metal-triggered dienyne cyclization reactions.

IV. Enediyne Stereoselectivity: Discovery and Substrate Scope.

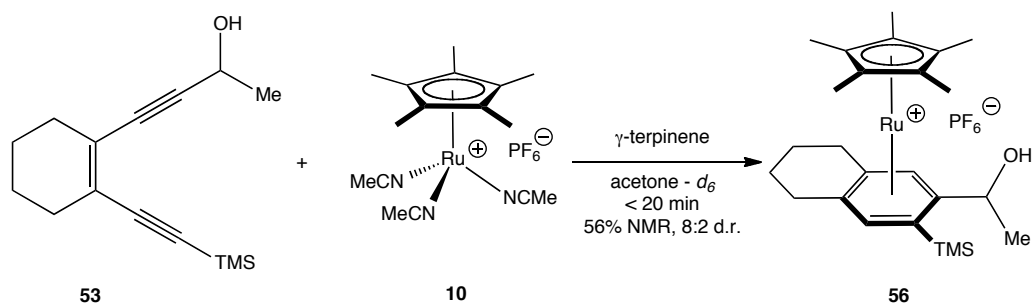
As a starting point for investigations into the potential stereoselectivity of the enediyne cycloaromatization reaction, we choose to prepare two cyclohexenediynes (**53** and **54**) that differed in substitution off the non-stereocenter alkyne (Scheme 3-16). Common intermediate **41** was converted to the asymmetrically substituted enediyne **55** using the Corey-Fuchs

protocol. Lithiation of this compound followed by quenching with acetaldehyde gave the TMS substituted alcohol **53**. This compound was desilylated, lithiated and quenched with methyl iodide to give the methyl substituted alcohol **54**.



Scheme 3-16. Synthetic route to model enediyne substrates for initial studies.

When **53** (0.005 mmol) was allowed to react with **10** (0.008 mmol) and γ -terpinene (0.027 mmol) in acetone-*d*₆ and monitored by ¹H NMR spectroscopy, immediate formation of two sets of resonances consistent with the product structure **56** were observed (Scheme 3-17). Integration of the presumed major **56-ma** and minor **56-mi** diastereomers' TMS resonances at δ 0.46 and 0.44, respectively, showed the compounds had been formed in a 8:2 ratio in a NMR yield of 56%. Performing the reaction in CDCl₃, THF-*d*₈, or a acetone-*d*₆ / THF-*d*₈ mixture showed no improvement in yield or ratio.



Scheme 3-17. Initial studies on enediyne cycloaromatization stereoselectivity.

On a preparative scale, **56-ma** was isolated pure after repeated chromatography, but **56-mi**, in our hands, proved impossible to isolate pure due to a facile TMS migration to give OTMS isomer **57-mi** (Figure 3-3). In an attempt to determine the relative stereochemistry of both diastereomers by X-ray analysis, **56-ma** and a **56-mi** / **57-mi** mixture were subjected to vapor diffusion crystallization conditions (ethyl ether / methylene chloride) that resulted in single crystals of the rearranged diastereomeric products, **57-ma** and **57-mi**. The relative stereochemistries from the X-ray experiments are shown in Figure 3-3 and major and minor diastereomers can be rationalized using the same model developed with the dienyne selectivity by orienting the oxygen *syn* to the metal (Figure 3-2). It is unclear if the isomerization of **56** to **57** is intra or intermolecular, but regardless of the mechanism, it is highly unlikely that the TMS migration affects either the carbon stereocenter or the planar chirality of the metal fragment and the stereochemical assignments of **56-ma** and **56-mi** are inferred to correlate with **57-ma** and **57-mi**, respectively.

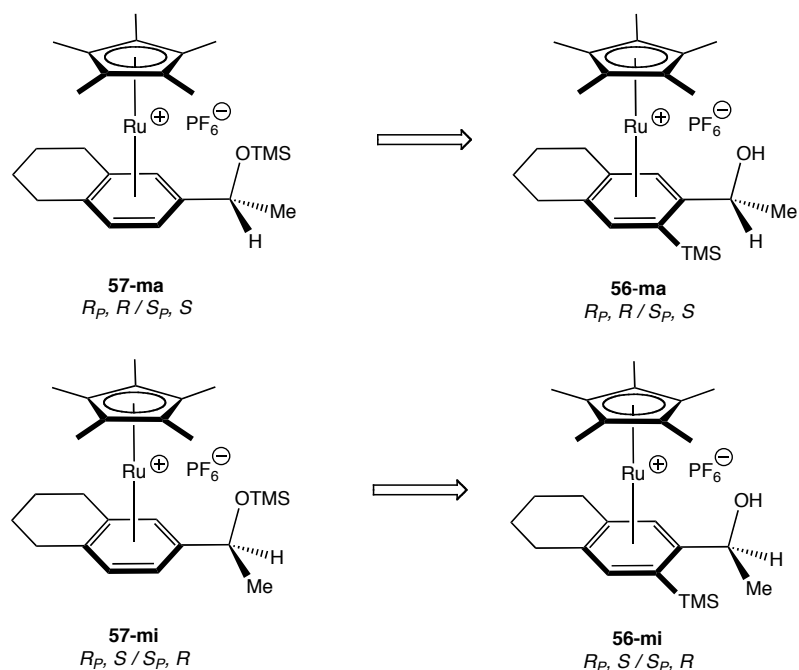
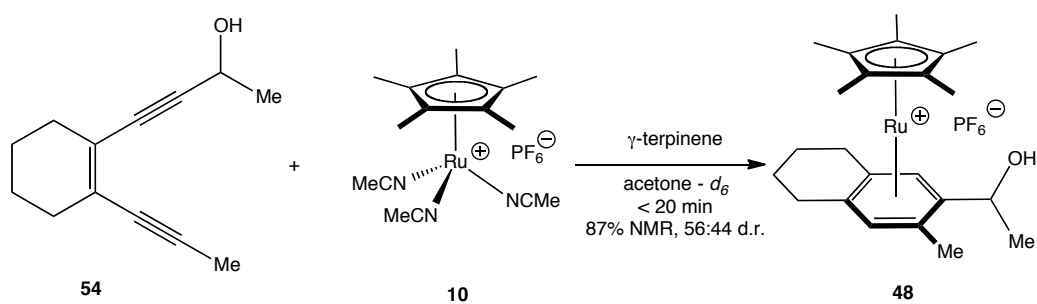


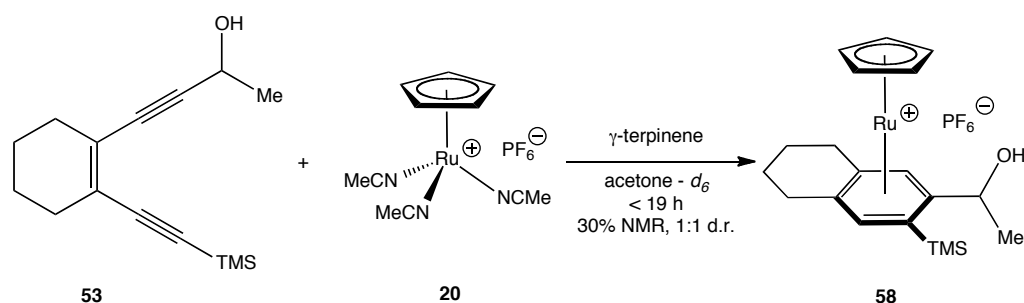
Figure 3-3. X-ray determined stereochemical assignments for **57-ma** / **57-mi** and inferred assignments for **56-ma** / **56-mi**.

Reaction of the methyl substituted enediyne **54** with **10** under the same conditions as the reaction with TMS substituted enediyne **53** resulted in formation of the previously isolated product **48** in a comparatively higher yield but *lower stereoselectivity* to formation of **56** (Scheme 3-18). Despite the low d.r., the major and minor isomers of **48** formed from the enediyne cyclization are consistent with those formed from the dienyne cyclization.



Scheme 3-18. Probing the effect of alkyne substitution on the stereoselectivity.

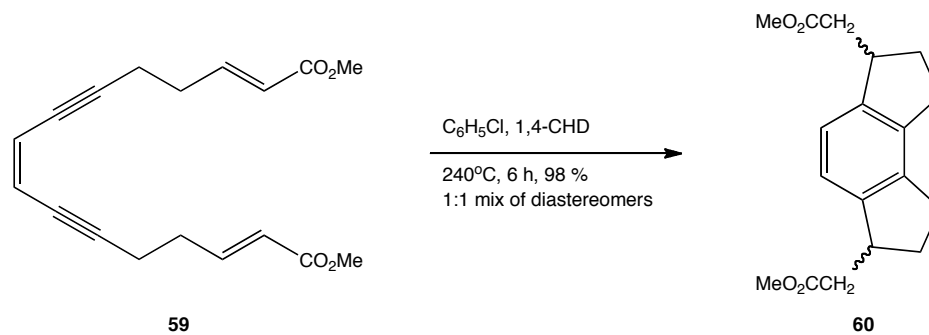
Reaction of the better performing enediyne **53** (0.018 mmol) with the sterically less demanding [CpRu(NCMe)₃]PF₆ complex **20** (0.020 mmol) and γ -terpinene (0.090 mmol) resulted in the formation of CpRu arene complex **58** in 30% NMR yield and no measurable stereoselectivity by NMR spectroscopy (Scheme 3-19). Also worth noting, was that the rate of cyclization was slower as determined by the ¹H NMR spectrum recorded after 30 min, which showed the reaction to be incomplete. Overall these results show a steric dependence on the stereoselectivity of the η^6 -complexation for the enediyne cyclization.²⁸



Scheme 3-19. Probing the effect of the metal-ligand environment on the stereoselectivity.

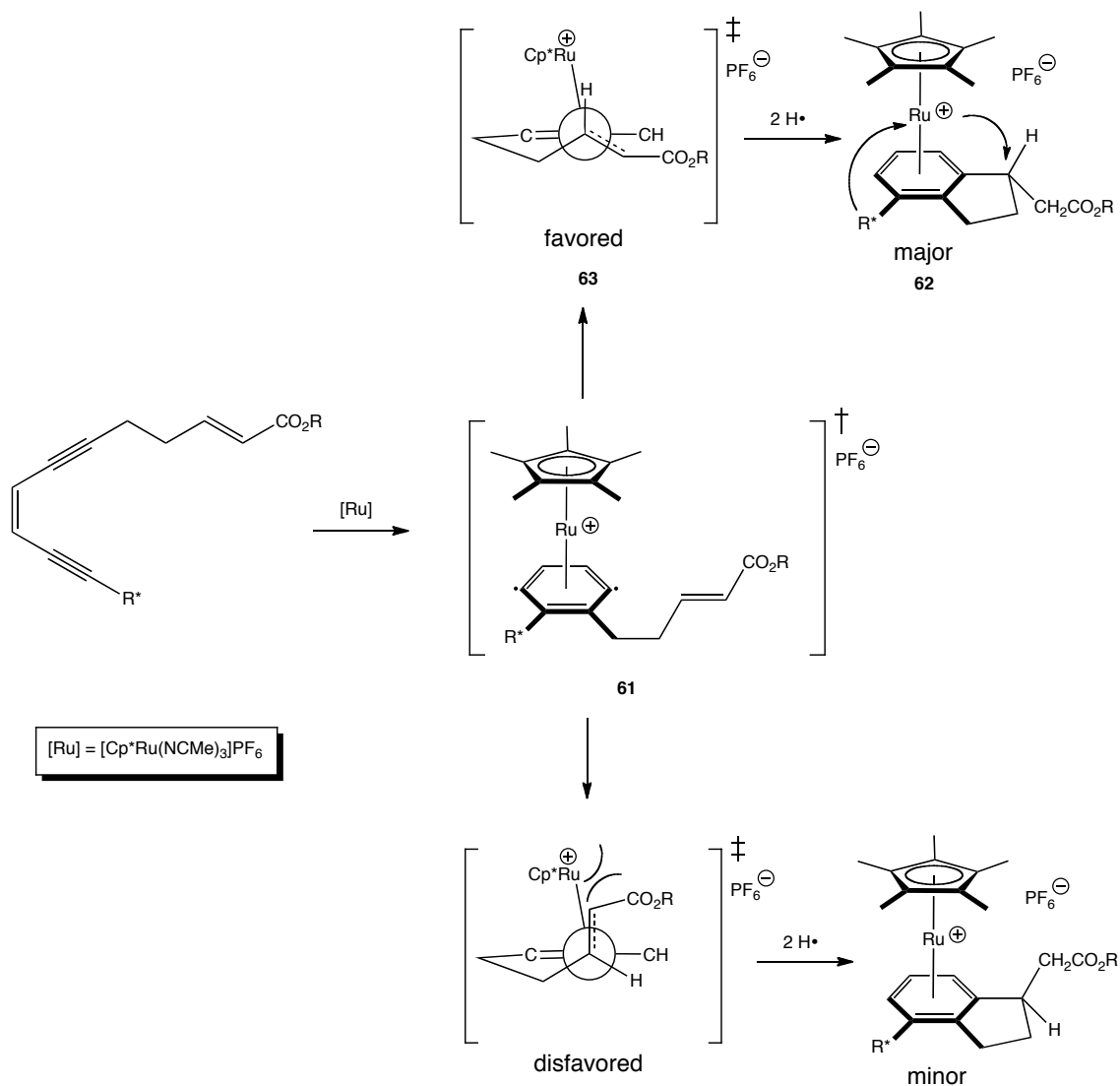
V. Stereoselective 5-*exo-trig* cyclization.

We also wanted to explore using the metal fragment as a stereocontrol element for capturing the proposed η^6 -*p*-benzyne intermediate intramolecularly with a tethered alkene in the enediyne cyclization. Grissom and coworkers have shown under thermal conditions that both positions of the *p*-benzyne can be trapped using enediyne **59** with an α,β -unsaturated ester tether in relatively high yield (Scheme 3-20).²⁹ One drawback of this reaction was that both the *cis* and *trans* stereoisomeric products of **60** were formed in an equal ratio.



Scheme 3-20. Capture of the *p*-benzyne radical by 5-*exo-trig* cyclization.²⁹

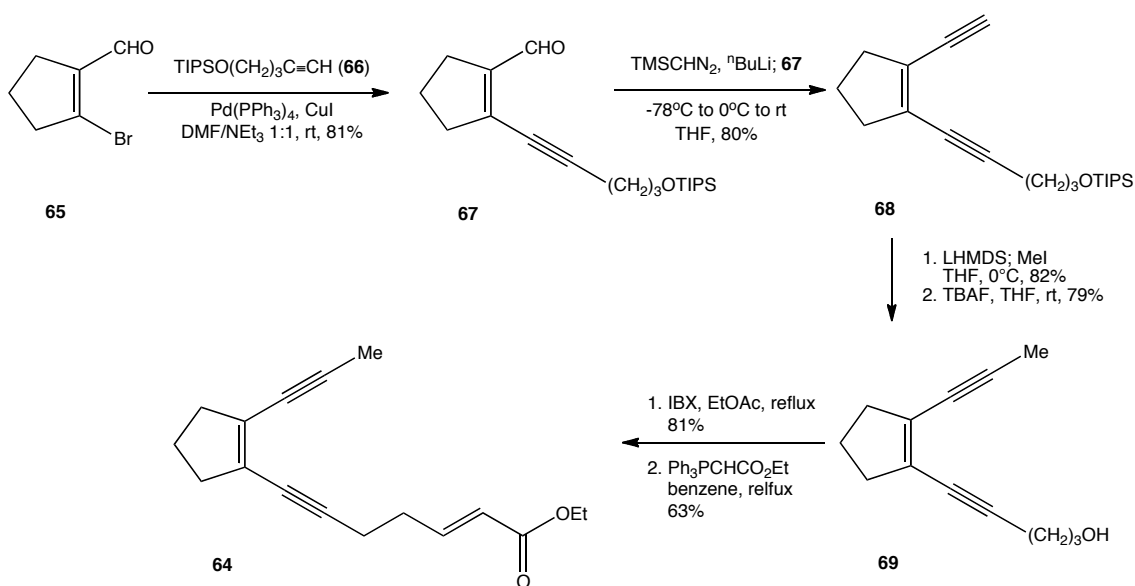
We hypothesized that η^6 -complexation of a metal fragment to one face of the *p*-benzyne (e.g. **61**) would favor the formation of stereoisomer **62** resulting from a lower energy transition state **63** (Scheme 3-21). Furthermore, with development of our substrate controlled stereoselective enediyne reaction it may be possible to set-up a chiral relay where the initial stereocenter would be able to control the newly formed stereocenter.



Scheme 3-21. Proposed method of stereocontrol for 5-*exo* capture of the *p*-benzyne radical.

To test our proposal we set out to synthesize enediyne **64** that contained a similar alkene tether to **59** (Scheme 3-22). As an initial point of investigation, we decided to first study selectivity of the relative stereochemistry of the metal complexation to the newly formed methine stereocenter and not to incorporate a stereocenter in the substrate as this would complicate analysis of the reaction if multiple stereoisomers were formed. Initiation of the synthesis started from vinyl bromide **65** that was prepared in one step from cyclopentanone by a literature

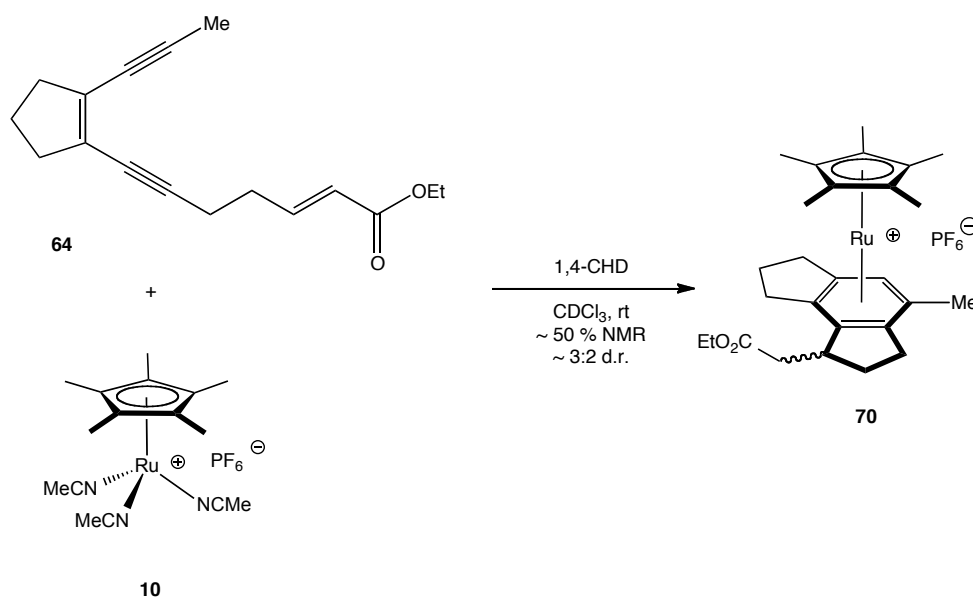
procedure.³⁰ Sonogashira coupling of **65** with TIPS protected 4-pentyn-1-ol (**66**)³¹ gave the enynal **67**. Conversion of this compound by treatment with lithiated trimethylsilyldiazomethane resulted in a vinylidene rearrangement to give terminal alkyne **68** that was then methylated from the acetylide and subsequently desilylated to unmask primary alcohol **69**. Oxidation of **69** followed by Wittig olefination gave the desired enediyne **64**.



Scheme 3-22. Synthetic route to enediyne substrate **64** with tethered alkene.

Reaction of **64** with **10** was first attempted in acetone- d_6 and γ -terpinene and although resonances consistent with product were observed, the reaction mixture was complicated and it was difficult to obtain an NMR yield or d.r. In an attempt to obtain a cleaner reaction, the conditions were changed to 1,4- CHD and CDCl_3 that resulted in slow formation of resonances consistent with the product **70** over the course of 64 h as observed by ^1H NMR spectroscopy (Scheme 3-23). The low reaction rate is attributed to the low solubility of **10** in CDCl_3 . Analysis of the reaction was difficult from the NMR spectrum due to overlapping peaks, but an approximate yield of 50% was determined based on 92% conversion of **64**. Although low, there

was a measurable d.r. of 3:2 based on rough integration of the Cp* resonances of the two products. Most importantly, there was no observation of new olefin resonances in the ^1H NMR spectrum indicating the radical cyclization had occurred. We have not pursued 5-*exo* stereoselectivity since this initial proof of concept, but there could be much potential in this approach. Modification of the tethered alkene and Cp ligand represent nice starting points for an optimization study.

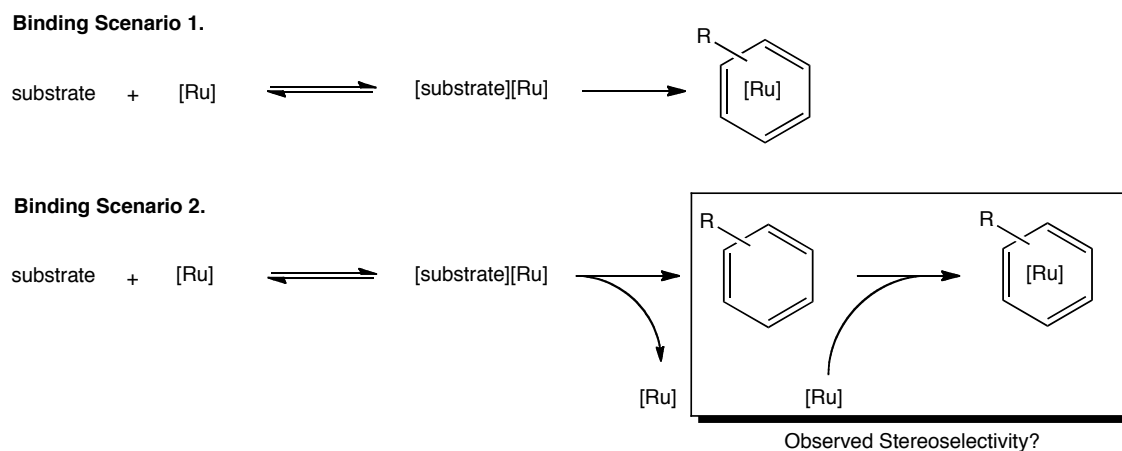


Scheme 3-23. Demonstration of Cp*Ru mediated enediyne cycloaromatization in combination with a 5-*exo* radical cyclization.

VI. Arene Binding Experiments.

Two basic mechanisms can be envisioned for the dienyne and enediyne cycloaromatizations: (i) the metal remains coordinated to the substrate throughout the reaction and is bound stereoselectively as a consequence of the cyclization (ii) the metal catalytically

cyclizes the substrate, dissociates from the arene product, and in a separate reaction binds stereoselectively. These scenarios are shown pictorial in Scheme 3-24.



Scheme 3-24. Basic mechanistic scenarios for formation of the ruthenium arene complex.

The final binding event shown in scenario 2 would be reminiscent of Uemura's work with ortho substituted benzylic alcohols (see Scheme 3-7) and in agreement with this mechanism are the relative stereochemistries observed for both the dienyne and enediyne cycloaromatizations. To distinguish between scenario 1 and 2, we preformed an arene binding experiment using the unbound aromatic product of complex **48** that was formed from the reaction of dienyne **43** and enediyne **54** with Cp*Ru complex **10**. This compound (**71**, Table 3-2) was prepared in one step by sodium borohydride reduction of commercially available 6-acetyl-7-methyl-tetraline. If the stereoselectivity were occurring by scenario 2, the observed diastereomeric ratio for binding arene **71** would be expected to correlate with what was observed for the enediyne and dienyne cyclizations.

Reaction of **71** under dienyne cyclization conditions (entry 1) resulted in slow complexation to form **48** in high yield and d.r. Presumably, the reduced rate is attributed to the low solubility of **10** in CDCl₃ in combination with the higher activation energy for binding a

tetrasubstituted arene. Subjecting **71** to enediyne cyclization conditions (entry 2) resulted in rapid formation of **48** but in low conversion as γ -terpinene competed with the arene for binding of **10** and a large amount of $[\text{Cp}^*\text{Ru}(\eta^6\text{-}p\text{-cymene})]\text{PF}_6$ was observed resulting from dehydrogenation of the hydrogen atom donor. Performing the reaction without γ -terpinene (entry 3) resulted in a similar yield and d.r. with high conversion of **71**. In all cases the major and minor diastereomeric products are consistent with the those formed from the cyclization reactions and, most importantly, binding of the free arene with **10** resulted in a significantly *higher* stereoselectivity than with the reactions of **10** with dienyne **43** (entry 1, Table 3-1) or enediyne **54** (Scheme 3-18), ruling out binding scenario 2. Overall these experiments represent an important study for the basic mechanism of ruthenium triggered enediyne and dienyne cycloaromatization reactions as we now have evidence for binding scenario 1.

Table 3-2. Arene binding experiments. (a) Yield and d.r. determined by ^1H NMR spectroscopy.

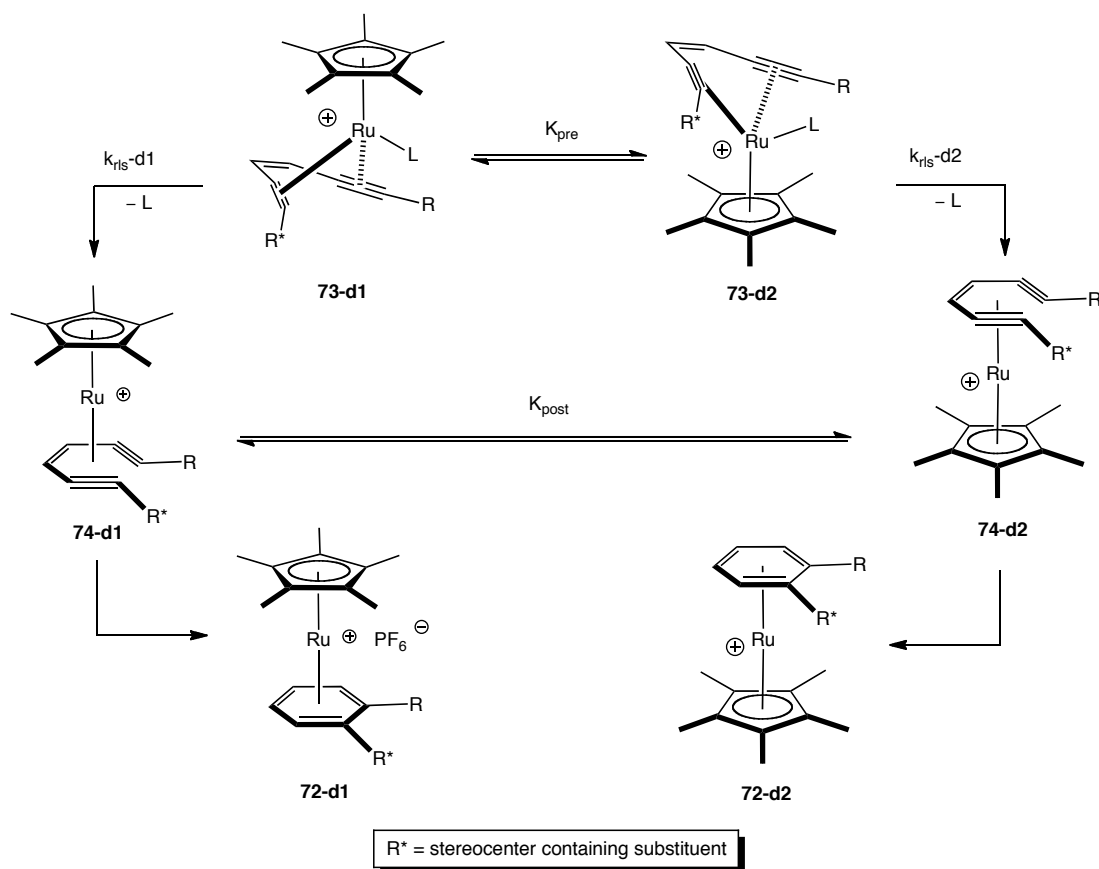
(b) Accompanied by formation of $[\text{Cp}^*\text{Ru}(\eta^6\text{-}p\text{-cymene})]\text{PF}_6$.

| Entry | Condition | Rxn Time | 71 % conv. | 48 Yield (d.r.) ^a | Cycloaromatization |
|-------|--|----------|-------------------|-------------------------------------|---------------------------|
| 1 | CDCl_3 , rt | 70 h | 48 | 99 (85:15) | w/ 43 : 97 (64:36) |
| 2 | d_6 -acetone, γ -terpinene (5 eq), rt | < 50 min | 36 | >99 (87:13) ^b | w/ 54 : 87 (56:44) |
| 3 | d_6 -acetone, rt | < 50 min | 95 | 91 (81:19) | w/ 54 : 87 (56:44) |

VII. Models for Stereoselectivity.

One difficulty when trying to predict a possible model of stereoselectivity for the enediyne and dienyne metal-triggered cycloaromatizations stems from the lack of mechanistic understanding for both reactions. In the discussion to follow, we present several possible pathways that may account for the relative stereochemistry of the products based on our working hypotheses as to how these reactions occur. A basic assumption made in all proposed models is that the metal remains bound to the face of the stereo-determining intermediate / transition state throughout the cyclization. Based on our arene binding experiments, we feel this assumption carries some merit.

In regards to the enediyne cycloaromatization, the two prevailing mechanistic hypotheses follow a pathway involving an η^6 -enediyne intermediate (Scheme 3-4) and a metallacycle intermediate (Scheme 3-5). Of these two, we tend to favor the former and the focus of the analysis will be based on this pathway. Summarized in Scheme 3-25 are several possible equilibria and competing irreversible steps that may be responsible for the stereoselectivity for the formation of the diastereomeric products **72-d1** and **72-d2**. Previous mechanistic studies by Friese and O'Connor on the metal-mediated enediyne cyclization have suggested that the rate-limiting step of the reaction occurs during the conversion of η^4 -diyne intermediate (e.g. **73**).^{12e} This conclusion is based on kinetic studies that showed an inverse second order dependence on the acetonitrile concentration and a build-up of these species at low temperature as observed by NMR spectroscopy.

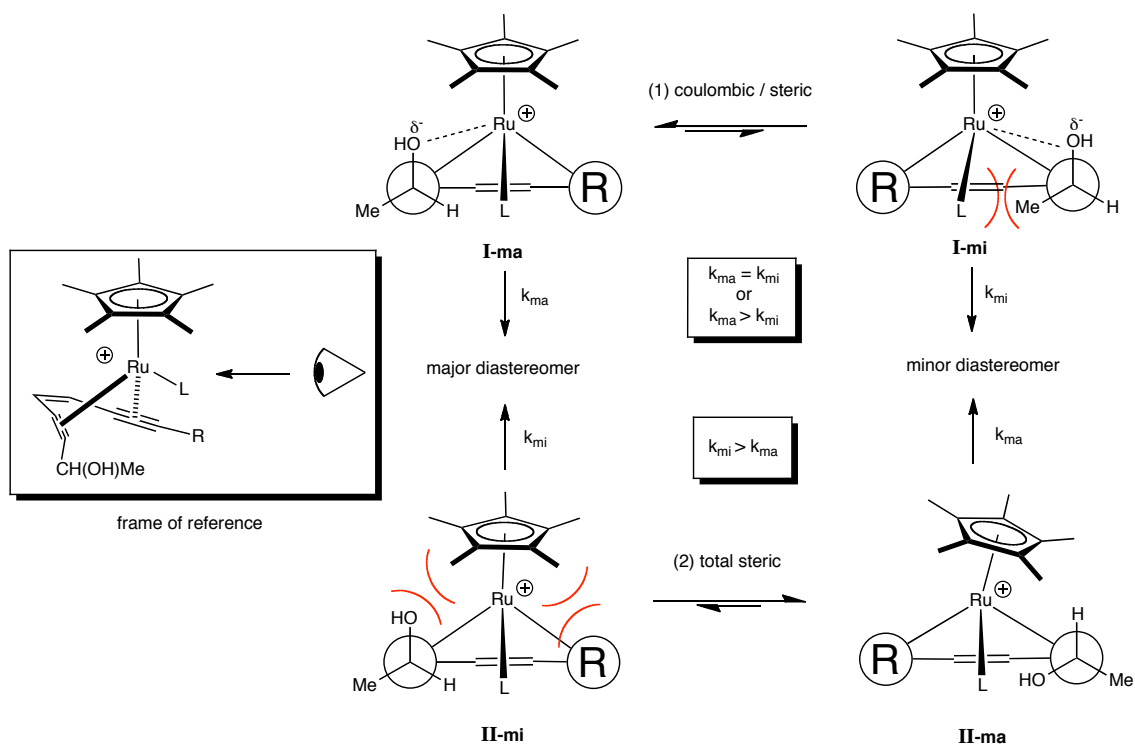


Scheme 3-25. Proposed pathways for conversion of diastereomeric η^4 -diyne complexes involving η^6 -enediynes intermediates.

As a starting point, one may consider the equilibrium between the diastereomeric η^4 -dienes **73-d1** and **73-d2** (K_{pre}). Two potential conformational models that would influence K_{pre} are shown in Scheme 3-26. The prevailing factor in both models is that the largest substituent on the stereocenter carbon (Me) will remain as distal to the Cp* and L as possible. In one scenario, there could be a combined columbic / steric influence (1) where the partial negatively charged hydroxy will align *syn* with the metal to provide some stabilization of the positive charge, thereby creating a favored (**I-ma**) and disfavored (**I-mi**) diastereomeric rotomer. The less stable **I-mi**, directs the bulky methyl group towards the other alkyne substituent and crowds

the L binding pocket. This model would require that **I-ma** and **I-mi** react at the same rate ($k_{ma} = k_{mi}$) or for **I-ma** to react faster ($k_{ma} > k_{mi}$).

If the hydroxy is not close enough to provide columbic stabilization, then the primary interaction would be steric in nature (2). In the more stable diastereomeric intermediate (**II-ma**), the metal ligand environment may be able to structurally distort by shifting the Cp* towards the stereocenter carbon when the R substituent is large (e.g. TMS) thereby minimizing strain. Due to the relative stereochemistry, the less stable diastereomeric intermediate **II-mi** would be expected to experience steric crowding of the Cp* from both the hydroxy substituent on the stereocenter carbon and the R substituent and therefore would have less freedom to shift the Cp* ligand. To explain the relative stereochemistry of the products, ground state destabilization of **II-mi** could be invoked thus lowering the activation barrier and causing this diastereomer to react faster ($k_{mi} > k_{ma}$). Both models are consistent with the observed substituent effects as in each case the destabilization is dictated by the steric bulk of the Cp* ligand and alkyne R group and less differentiation would be observed for spatially less demanding moieties.



Scheme 3-26. Proposed models of stereoselectivity based on equilibrium effects of the η^4 -diyne intermediate.

In favor of (2) are the observed non-bonded distances in the intermediate model η^4 -diyne CO complex shown in Figure 3-4.^{12e} This molecule crystallizes in a P-1 space group with two molecules in the asymmetric unit. Analysis of all the non-bonded distances between the propargylic carbon and atoms on the metal's ligands shows that the closest contacts, on average, are from the Cp* methyl group. It is expected that the non-bonded distance from the propargyl carbon to the MeCN methyl would be even larger than that calculated for the carbonyl oxygen because the methyl is a group extension to the nitrile and the Ru←CO bond would be predicted to be shorter than the Ru←NCCH₃ bond from metal back-bonding. It should be noted that the Ru – propargylic and propargylic – Cp* methyl carbon distances are very similar (3.41 and 3.5 Å, resp.). This result could lend some credence to the possibility of an electrostatic interaction from the hydroxy to ruthenium, but it should be kept in mind that the stabilizing /

destabilizing interactions are from substituents of the atoms being analyzed. The average for the closest Cp* methyl hydrogen – propargyl hydrogen contact was $1.1 \pm 0.3 \text{ \AA}$ shorter than the closest Ru – propargyl hydrogen contact.

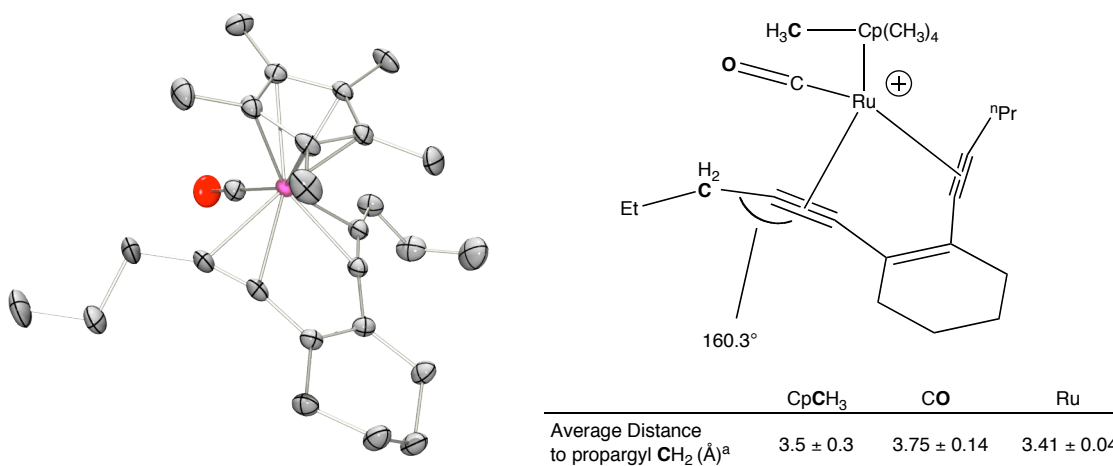
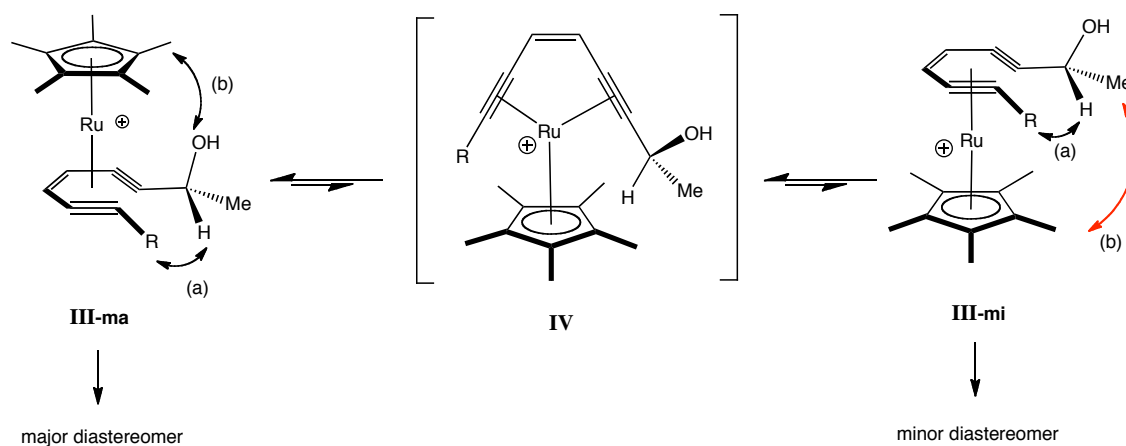


Figure 3-4. Enediyne structural changes induced by η^4 -coordination of the alkynes. (a) Average distance between atoms in bold for all molecules in asymmetric unit. Errors represented by 95% confidence intervals.^{12e}

The stereodetermining event may also occur due to a post rate-limiting step equilibrium between the η^6 -enediyne intermediates (**74-d1** and **74-d2**) before cyclization to product (Scheme 3-25). As a potential model, consider the equilibrium between diastereotopic intermediates **III-ma** and **III-mi** which is dictated by two steric interactions: (a) between the alkyne substituents and (b) between the carbon stereocenter substituents and the Cp* ligand (Scheme 3-27). If the R substituent were large, one could reason that interaction (a) would be higher priority, as the transition state leading to formation of the carbon-carbon bond would be stabilized by minimizing strain between the R group and the stereocenter substituents. Therefore, the secondary interaction (b) would control the facial selectivity of the metal and it follows that intermediate **III-ma** with the smaller hydroxy directed toward the Cp* methyl

substituents would be more stable and would lead to faster formation of the cyclized product. If the R substituent is small, the interaction (a) and (b) may have similar energetic contributions to the equilibrium leading to a lower observed diastereoselectivity as demonstrated by the methyl substituted enediyne **54**.

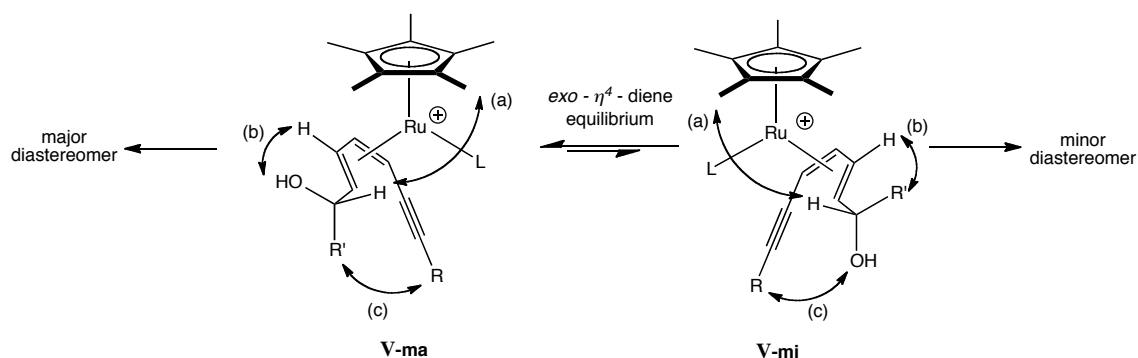
In order for this model to be plausible, the Cp*Ru⁺ metal fragment must be able to switch faces without proceeding back to the 18 electron η^4 -diyne acetonitrile complex (**73**). Otherwise the stereoselectivity would depend on the rate of conversion of **73** as this is believed to be the rate-limiting step. One potential pathway between **III-ma** and **III-mi** not involving **73** could occur if the metal slips to a 16 electron η^4 -diyne and moves through a planar intermediate or transition state **IV**.



Scheme 3-27. Proposed model of stereoselectivity based on a post rate-limiting step equilibrium between the two diastereomeric η^6 -enediyne intermediates.

For the stereoselectivity observed in the dienyne cycloaromatization, a plausible model that fits all the data would be an unbalanced equilibrium between the two diastereotopic *exo*- η^4 -diene complexes (Scheme 3-28). The *exo* orientation refers to the *syn* positioning 2,3-substituents of the diene with respect to the Cp* ligand and is more commonly observed for

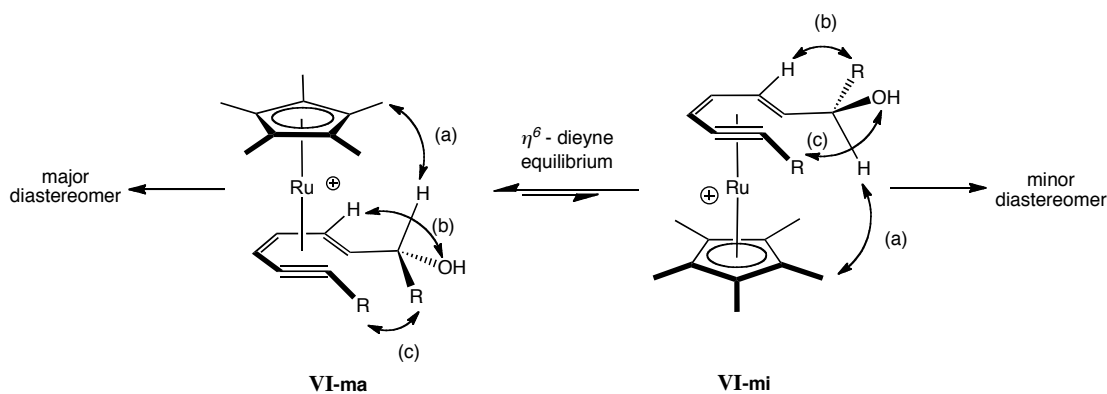
$\text{Cp}^*\text{Ru}(\eta^4\text{-diene})$ complexes than the *endo* orientation.³² The model considers three non-bonding interactions of the stereocenter substituents to be important for determining the facial selectivity: (a) with the Cp^* ligand, (b) 1,3-allylic strain with the 2-vinyl hydrogen, and (c) with the alkyne. The highest priority of these three is predicted to be (a). Therefore in both equilibrating diastereomers shown in Scheme 3-28, the sterically least demanding substituent (H) is directed towards the metal - ligand system. The next most critical would be (b). For the 1-alkoxyethyl dienyne **39**, **43**, **44**, and **45**, diastereomer **V-ma** provides the best possible spatial arrangement and leads to the major product observed with these substrates. When R' becomes larger than methyl, interaction (c) comes into play thus creating a competition with (b) and shifting the equilibrium towards diastereomer **V-mi**. This would explain the loss of stereoselectivity for isopropyl dienyne **46**. Also critical for cyclization is the propargylic substituent R as too much steric bulk in this position may not allow formation of the proposed η^6 -dienyne intermediate (Scheme 3-3).



Scheme 3-28. η^4 -Diene stereochemical model.

It is also reasonable to predict an unbalanced equilibrium between the two possible diastereotopic η^6 -dienynes as the stereodetermining event (Scheme 3-29). A reasonable model could utilize the same sterics interactions as presented in Scheme 3-28. Therefore the major

diastereomeric product would result from intermediate **VI-ma** providing that the R substituent isn't sterically larger than a methyl which increases the significance of interaction (c).



Scheme 3-29. η^6 -Dienyne stereochemical model.

VIII. Conclusions and Future Outlook.

In summary, we have demonstrated the first of examples of stereoselective metal η^6 -arene complexation for the ruthenium(II) mediated cycloaromatization of chiral dienyne and enediynes. We have identified: (1) several structural features of the metal system and substrate important for the observed stereoselectivity, (2) the relative stereochemistry of the major and minor diastereomeric products, and (3) performed arene binding experiments that rule out a mechanism resulting from simple η^6 -complexation of the benzenoid product. Future research will be focused on (I) further development of a mechanistic model to account for the stereoselectivity hopefully aided by a computational study, (II) possible identification of a different ligand system that will give higher diastereomeric ratios, and (III) further exploration of the correlation between the substrate's structural / electronic properties and the stereoselectivity. Studies directed at these goals currently being conducted in the lab are synthesis of a 1,3-di-*tert*-butylcyclopentadienyl ligand for the metal system toward aim (II) and

synthesis of a *sec*-butyl containing enediyne and dienyne to rule out / support a hydroxy-directed stereoselective model toward aims (I) and (III).

IX. Experimental.

i. General Procedures.

All reactions directed toward the synthesis of organic substrates were performed in round bottom flasks equipped with magnetic teflon coated stir bars and rubber septa under a positive pressure of N₂, unless otherwise noted. NMR scale ruthenium cyclization reactions were performed under an N₂ atmosphere in 5 mm J-young NMR tubes equipped with a teflon needle valve using freshly degassed solvents (freeze / pump / thaw procedure). Solutions of air- and moisture-sensitive reagents were transferred by syringe or stainless steel cannula. Air- and moisture-sensitive solids were handled in a glove box under N₂ atmosphere. Organic solvent solutions were concentrated by rotary evaporation (ca. 10 – 160 torr) at 25 - 35°C, unless otherwise noted. High vacuum distillations were performed at 23°C (ca. 0.010 torr) using a receiver flask cooled to -75°C. Preparative thin layer chromatography (PTLC) was performed on glass plates pre-coated with silica gel (1 mm, 60 Å pore size, EMD Chemicals) and visualized by exposure with ultraviolet light. Flash column chromatography purification of synthetic intermediates and substrates was performed by literature procedure³³ using silica gel (60 Å, particle size 0.043 – 0.060 mm, EMD Chemicals), activated neutral Brockmann I, standard grade aluminum oxide (150 mesh, Sigma-Aldrich), or reverse phase octadecylsilane bonded to silica gel (40 μm APD, 60 Å, J.T. Baker).

ii. Materials.

Tetrahydrofuran (THF), ethyl ether and hexanes used for reaction solvents were dried either by a solvent dispensing system equipped with two neutral alumina columns under argon atmosphere, over sodium/benzophenone ketyl under a N₂ atmosphere, or by 3 Å activated sieves by literature procedure.³⁴ Chloroform-*d* and methylene chloride-*d*₂ were dried over calcium hydride under a nitrogen atmosphere. Acetone-*d*₆ was dried over 4 Å activated sieves for 5 h under a N₂ atmosphere. All other solvents were used as received from commercial suppliers. [Cp⁺Ru(NCMe)₃]PF₆ (**10**) was prepared according to literature procedure.²⁷ All other literature compounds were prepared according to the indicated reference or purchased from commercial suppliers and used as received.

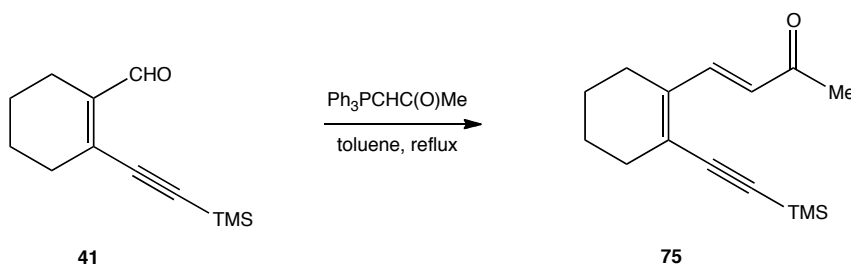
iii. Instrumentation.

NMR spectra were recorded on a Varian Mercury 300 (¹H, 300 MHz; ¹³C 75.5 MHz), Varian Mercury 400 (¹H, 400 MHz; ¹³C 100.7 MHz), Jeol ECA 500 (¹H, 500 MHz) or Varian VX 500 (¹H, 500 MHz; ¹³C 125 MHz) spectrometers. ¹H and ¹³C NMR chemical shifts (δ) are reported in parts per million (ppm). ¹H NMR chemical shifts were referenced to the residual protio resonance for CDCl₃ (δ 7.26). ¹³C NMR chemical shifts were referenced to CDCl₃ (δ 77.16). Infrared (IR) spectra were recorded on a Nicolet Avatar 360 FT-IR with KBr or NaCl plates as thin films or JASCO FT-IR 4100 attenuated total reflectance (ATR) platform (3mm) using ZnSe plates (thin films). High-resolution mass spectra were obtained by the University of California, San Diego Mass Spectrometry Facility. Melting points are uncorrected and were recorded on an Electrothermal or Stanford Research Systems EZ-Melt apparatus.

iv. Preparation and characterization data for synthetic intermediates, dienyne, enediyne, and arene substrates.

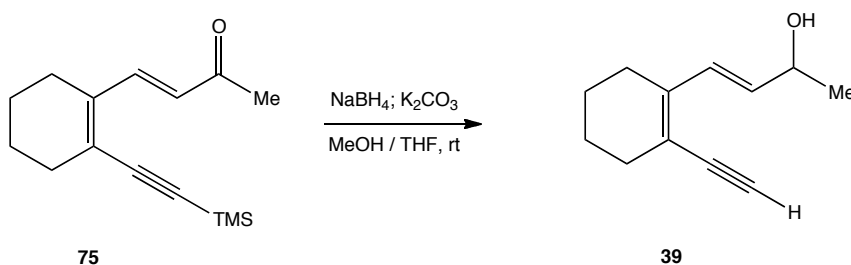
(*E*)-4-(2-((trimethylsilyl)ethynyl)cyclohex-1-enyl)but-3-en-2-one (75).

1-(triphenylphosphoranylidene)-2-propanone (640 mg, 2.01 mmol) and **41** (398 mg, 1.93 mmol) were refluxed in toluene (1 mL) for 1.5 h, concentrated, and purified by flash silica column chromatography (93:7 hexanes / EtOAc) to afford **75** as a yellow solid (307 mg, 1.24 mmol, 65%). mp. 45-50 °C. IR (KBr): 2137 (C≡C), 1691 (C=O) cm⁻¹. ¹H NMR (500 MHz, CDCl₃) δ: 0.23 (s, 9H, TMS), 1.59 – 1.70 (m, 4H, 4,5-CH₂), 2.20 – 2.24 (m, 2H, 6-CH₂), 2.30 – 2.35 (m, 2H, 3-CH₂), 2.31 (s, 3H, C(O)CH₃), 6.10 (d, ³J_{HH} = 16 Hz, 1H, CH=CHC(O)CH₃), 7.91 (d, ³J_{HH} = 16 Hz, 1H, CH=CH C(O)CH₃). ¹³C NMR (100MHz, CDCl₃) δ: 0.1 (TMS), 21.8 (CH₂), 21.9 (CH₂), 24.9 (CH₂), 26.3 (CH₃), 31.3 (CH₂), 102.8 (C≡C), 104.1 (C≡C), 127.1 (CH=CHC(O)CH₃), 128.7 (1-C), 140.2 (2-C), 143.7 (CH=CHC(O)CH₃), 199.5 (C(O)CH₃). HRMS (EI): Calcd for (C₁₅H₂₂OSi): 246.1434, found 246.1434.



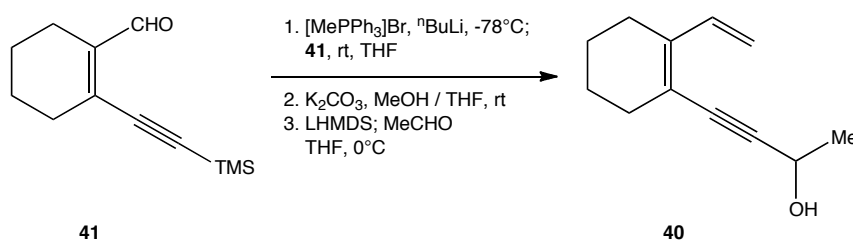
(*E*)-4-(2-ethynylcyclohex-1-enyl)but-3-en-2-ol (39). NaBH₄ (25 mg, 0.662 mmol) was added to a stirring solution of **75** (102 mg, 0.414 mmol) in MeOH / THF (4 mL, 1:1). After 10 min of stirring at 23°C, anhydrous K₂CO₃ (171 mg, 1.24 mmol) was added. After 16 h of stirring at 23°C, the reaction was then diluted with water (8 mL) and extracted with Et₂O. The organic extract was washed with brine (4 mL), dried over MgSO₄, concentrated, and purified by PTLC (8:2 hexanes / EtOAc) to afford **39** as a peach solid (52 mg, 0.30 mmol, 71%). m.p. 41 – 43 °C.

(KBr): 3299 (C^{sp}H), 2084 (C≡C) cm⁻¹. ¹H NMR (400 MHz, CDCl₃) δ: 1.30 (d, ³J_{HH} = 7 Hz, 3H, CH₃), 1.57 – 1.69 (m, 4H, 4,5-CH₂), 1.70 (s, 1H, OH), 2.19 – 2.30 (m, 4H, 3,6-CH₂), 3.25 (s, 1H, C≡CH), 4.42 (p, ³J_{HH} = 7 Hz, 1H, C(H)OH), 5.79 (dd, ³J_{HH} = 16 Hz, 7 Hz, 1H, CH=CHC(H)OH), 6.94 (d, ³J_{HH} = 16 Hz, 1H, CH=CHC(H)OH). ¹³C NMR (100 MHz, CDCl₃) δ: 22.1 (CH₂), 22.3 (CH₂), 23.5 (CH₂), 25.2 (CH₂), 30.8 (CH₃), 69.3 (C(H)OH), 82.3 (C≡CH), 83.8 (C≡CH), 119.0 (C=C), 129.8 (CH=CH), 133.6 (CH=CH), 141.3 (C=C). HRMS (EI): Calcd for (C₁₂H₁₆O): 176.1196, found 176.1194.



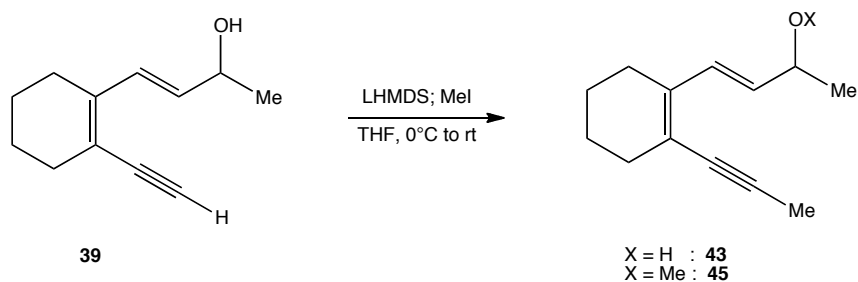
4-(2-Vinylcyclohex-1-en-1-yl)but-3-yn-2-ol (40). A 2.5 M solution of ⁿBuLi (0.940 mL, 2.34 mmol) in hexanes was added to a stirring heterogeneous mixture of [MePPh₃]₃Br (836 mg, 2.34 mmol) in THF (78 mL) at -78°C. The resulting yellow solution was warmed to 23°C and a solution of **41** (303 mg, 1.47 mmol) in THF (3.8 mL) was added over 15 min. After stirring at 23°C for 2 h, the reaction mixture was poured over sat. aq. NH₄Cl (150 mL) and extracted with Et₂O (200 mL). The organic extracts were washed with brine (150 mL), dried over Na₂SO₄, concentrated, purified by flash silica column chromatography (99:1 hexanes / EtOAc) to afford the TMS substituted dienyne as a clear oil. Anhydrous K₂CO₃ (610 mg, 4.41 mmol) was added to a stirring solution of the resulting product in MeOH / THF (15 mL, 1:1) at 23°C. After 4 h of stirring at 23°C, the reaction mixture was filtered through a fritted funnel, concentrated, diluted with aq. 1 M HCl (30 mL) and extracted with Et₂O (30 mL). The organic extracts were washed with 1 M HCl (20 mL), water (20 mL), brine (20 mL), dried over MgSO₄, concentrated, and purified by flash silica column chromatography (99:1 hexanes / EtOAc) to afford the terminal

alkyne as a clear oil (153 mg, 1.16 mmol). A 1 M solution of LHMDS (3.47 mL, 3.47 mmol) in THF was added to a stirring solution of the resulting product in THF (12 mL) at 0°C. After stirring at 0°C for 30 min, acetaldehyde (0.325 mL, 5.80 mmol) was added. After stirring at 0°C for 30 min, the reaction mixture was poured over sat. aq. NH₄Cl (30 mL) and extracted with Et₂O (30 mL). The organic extracts were washed with brine (30 mL), dried over MgSO₄, concentrated, purified by flash silica column chromatography (8:2 hexanes / EtOAc) to afford **40** as a clear oil (76 mg, 0.431 mmol, 29% over three steps). IR (NaCl): 3332 (OH), 2208 (C≡C) cm⁻¹. ¹H NMR (400 MHz, CDCl₃) δ: 1.51 (d, ³J_{HH} = 7 Hz, 3H, CH₃), 1.57 – 1.71 (m, 4H, 4,5-CH₂), 1.76 – 1.81 (m, 1H, OH), 2.19 – 2.29 (m, 4H, 3,6-CH₂), 4.67 – 4.77 (m, 1H, C(H)OH), 5.09 (d, ³J_{HH} = 11 Hz, 1H, CH=C(*H^{cis}*)H), 5.25 (d, ³J_{HH} = 17.5 Hz, 1H, CH=C(*H^{trans}*)H), 7.05 (dd, ³J_{HH} = 17.5 Hz, 11 Hz, 1H, CH=CH₂). ¹³C NMR (100 MHz, CDCl₃) δ: 22.1 (CH₂), 22.4 (CH₂), 24.5 (CH₂), 24.8 (CH₂), 30.9 (CH₃), 59.1 (CH(OH)), 84.1 (C≡C), 96.1 (C≡C), 113.3 (CH=CH₂), 119.4 (C=C), 136.9 (CH=CH₂), 140.9 (C=C). HRMS (EI): Calcd for (C₁₂H₁₆O): 176.1196, found 176.1195.



(E)-4-(2-(prop-1-ynyl)cyclohex-1-enyl)but-3-en-2-ol (43) and (E)-1-(3-methoxybut-1-enyl)-2-(prop-1-ynyl)cyclohex-1-ene (45). A 1M solution of LHMDS (16.5 mL, 16.5 mmol) in THF was added to a stirring solution of **39** (725 mg, 4.11 mmol) in THF (41 mL) at 0°C. After 20 min of stirring at 0°C, iodomethane (1.53 mL, 24.7 mmol) was added. After 24 h of stirring while gradually warming to 23°C, the reaction mixture was poured over sat. aq. NH₄Cl (80 mL) and extracted with Et₂O (80 mL). The organics extracts were washed with brine (100 mL), dried over MgSO₄, concentrated and purified by flash silica column chromatography with indicated mobile

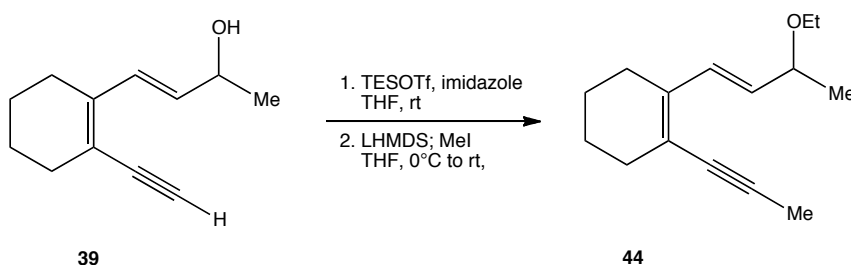
phases. (96:4 hexanes / EtOAc) to afford **45** as a yellow oil (425 mg, 2.08 mmol, 51%). ^1H NMR (500 MHz, CDCl_3) δ : 1.27 (d, $^3J_{\text{HH}} = 6$ Hz, 3H, $\text{CH}(\text{OCH}_3)\text{CH}_3$), 1.56 – 1.67 (m, 4H, 4,5- CH_2), 2.03 (s, 3H, $\text{C}\equiv\text{CCH}_3$), 2.18 – 2.25 (m, 4H, 3,6- CH_2), 3.27 (s, 3H, OCH_3), 3.83 (dq, $^3J_{\text{HH}} = 8$ Hz, 6 Hz, 1H, $\text{CH}(\text{OCH}_3)\text{CH}_3$), 5.54 (dd, $^3J_{\text{HH}} = 16$ Hz, 8 Hz, 1H, $\text{CH}=\text{CHC}(\text{OCH}_3)\text{H}$), 6.88 (d, $^3J_{\text{HH}} = 16$ Hz, 1H, $\text{CH}=\text{CHC}(\text{OCH}_3)\text{H}$). ^{13}C NMR (100 MHz, CDCl_3) δ : 4.8 ($\text{C}\equiv\text{CCH}_3$), 21.9 (CH_2), 22.3 (CH_2), 22.6 (CH_2), 25.2 (CH_2), 31.4 (CHCH_3), 56.1 (OCH_3), 78.7 ($\text{C}(\text{OCH}_3)\text{H}$), 79.9 ($\text{C}\equiv\text{C}$), 90.9 ($\text{C}\equiv\text{C}$), 120.6 ($\text{C}=\text{C}$), 130.4 ($\text{CH}=\text{CH}$), 132.3 ($\text{CH}=\text{CH}$), 138.2 ($\text{C}=\text{C}$). HRMS (EI): Calcd for ($\text{C}_{14}\text{H}_{20}\text{O}$): 204.1509, found 204.1506. (92:8 hexanes / EtOAc) to afford **43** as a yellow oil (168 mg, 0.883 mmol, 21%). IR (ZnSe): 3348 (OH) cm^{-1} . ^1H NMR (400 MHz, CDCl_3) δ : 1.31 (d, $^3J_{\text{HH}} = 6.5$ Hz, 3H, $\text{CH}(\text{OH})\text{CH}_3$), 1.50 (s, 1H, OH), 1.56 – 1.68 (m, 4H, 4,5- CH_2), 2.03 (s, 3H, $\text{C}\equiv\text{CCH}_3$), 2.16 – 2.26 (m, 4H, 3,6- CH_2), 4.39 – 4.47 (m, 1H, $\text{CH}(\text{OH})\text{CH}_3$), 5.73 (dd, $^3J_{\text{HH}} = 16$ Hz, 7 Hz, 1H, $\text{CH}=\text{CHC}(\text{OH})\text{H}$), 6.93 (d, $^3J_{\text{HH}} = 16$ Hz, 1H, $\text{CH}=\text{CHC}(\text{OH})\text{H}$). ^{13}C NMR (75 MHz, CDCl_3) δ : 4.8 ($\text{C}\equiv\text{CCH}_3$), 22.3 (CH_2), 22.5 (CH_2), 23.6 (CH_2), 25.2 (CH_2), 31.4 (CHCH_3), 69.6 ($\text{C}(\text{OH})\text{H}$), 79.8 ($\text{C}\equiv\text{C}$), 91.1 ($\text{C}\equiv\text{C}$), 120.9 ($\text{C}=\text{C}$), 130.5 ($\text{CH}=\text{CH}$), 132.4 ($\text{CH}=\text{CH}$), 138.1 ($\text{C}=\text{C}$). HRMS (EI): Calcd for ($\text{C}_{13}\text{H}_{18}\text{O}$): 190.1352, found 190.1349.



(E)-1-(3-ethoxybut-1-enyl)-2-(prop-1-ynyl)cyclohex-1-ene (44).

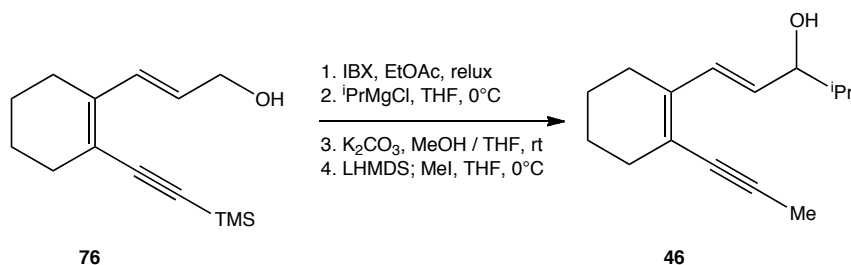
Triethylsilyl trifluoromethanesulfonate (0.41 mL, 1.812 mmol) was added to a stirring solution of **39** (106 mg, 0.604 mmol, 0.10 M) and imidazole (123 mg, 1.812 mmol, 0.30 M) in THF (6 mL) at 23°C. After 10 min of stirring at 23°C, the reaction was quenched with sat. aq. NH_4Cl (12 mL) and extracted with Et_2O (12 mL). The organic extracts were washed with saturated NH_4Cl (2 x

12 mL), dried over MgSO_4 , concentrated, and purified by flash alumina column chromatography (hexanes) to afford a clear oil. A 1M solution of LHMDS (0.56 mL, 0.56 mmol) in THF was added to a stirring solution of the resulting product in THF (2 mL) at 0°C . After 20 min of stirring at 0°C , iodomethane (0.058 mL, 0.93 mmol) was added. After 16 h of stirring while gradually warming to 23°C , the reaction mixture was poured over sat. aq. NH_4Cl (4 mL) and extracted with Et_2O (4 mL). The organics extracts were washed with brine (4 mL), dried over MgSO_4 , concentrated and purified by reverse phase C18 silica chromatography (9:1 MeOH / H_2O) to afford **44** as a clear oil (21 mg, 0.096 mmol, 16% over two steps). ^1H NMR (400 MHz, CDCl_3) δ : 1.20 (t, $^3J_{\text{HH}} = 7$ Hz, 3H, CH_2CH_3), 1.28 (d, $^3J_{\text{HH}} = 7$ Hz, 3H, $\text{CH}(\text{OEt})\text{CH}_3$), 1.56 – 1.68 (m, 4H, 4,5- CH_2), 2.03 (s, 3H, $\text{C}\equiv\text{CCH}_3$), 2.18 – 2.26 (m, 4H, 3,6- CH_2), 3.37 (dq, $^2J_{\text{HH}} = 9$ Hz, $^3J_{\text{HH}} = 7$ Hz, 1H, $\text{C}(\text{H}')\text{HCH}_3$), 3.51 (dq, $^2J_{\text{HH}} = 9$ Hz, $^3J_{\text{HH}} = 7$ Hz, 1H, $\text{C}(\text{H})\text{H}'\text{CH}_3$), 3.96 (p, $^3J_{\text{HH}} = 7$ Hz, 1H, $\text{CH}(\text{OEt})\text{CH}_3$), 5.58 (dd, $^3J_{\text{HH}} = 16$ Hz, 7 Hz, 1H, $\text{CH}=\text{CHCH}(\text{OEt})\text{CH}_3$), 6.88 (d, $^3J_{\text{HH}} = 16$ Hz, 1H, $\text{CH}=\text{CHCH}(\text{OEt})\text{CH}_3$). ^{13}C NMR (100 MHz, CDCl_3) δ : 4.8 ($\text{C}\equiv\text{CCH}_3$), 15.6 (CH_2CH_3), 22.2 (CH_2), 22.3 (CH_2), 22.6 (CH_2), 25.2 (CH_2), 31.3 ($\text{CH}(\text{OEt})\text{CH}_3$), 63.6 (CH_2CH_3), 76.8 ($\text{CH}(\text{OEt})\text{CH}_3$), 79.9 ($\text{C}=\text{C}$), 90.8 ($\text{C}=\text{C}$), 120.4 ($\text{C}=\text{C}$), 131.0 ($\text{CH}=\text{CH}$), 131.6 ($\text{CH}=\text{CH}$), 138.3 ($\text{C}=\text{C}$). HRMS (EI): Calcd for ($\text{C}_{15}\text{H}_{23}\text{O}$): 219.1743, found 219.1742.

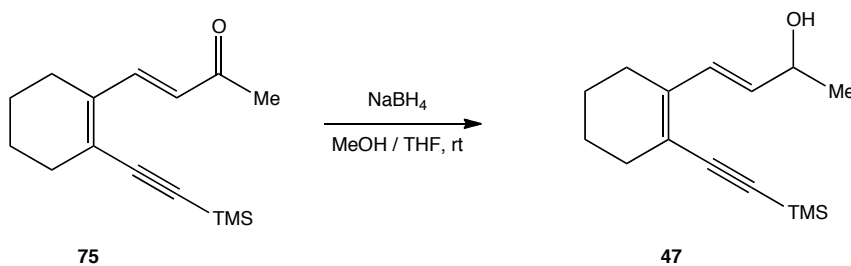


(E)-4-methyl-1-(2-(prop-1-ynyl)cyclohex-1-enyl)pent-1-en-3-ol (46). 2-Iodoxybenzoic acid⁹⁵ (373 mg, 1.33 mmol, 0.21 M) was added to a solution of **76**³⁶ (208 mg, 0.887 mmol) in EtOAc (6.5 mL), refluxed for 6 h, cooled to 23°C , filtered, and concentrated to afford a yellow oil (215 mg, 0.925 mmol). A 2M solution of $^i\text{PrMgCl}$ (0.93 mL, 1.85 mmol) in THF was added to a

stirring solution of the resulting product in THF (10 mL) at 0°C. After 20 min of stirring at 0°C, the reaction mixture was quenched with MeOH (3 mL), diluted with sat. aq. NH₄Cl (15 mL), and extracted with Et₂O (20 mL). The organic extracts were washed with water (2 x 10 mL), brine (10 mL), dried over MgSO₄, and concentrated to afford a yellow oil. Anhydrous K₂CO₃ (112 mg, 0.814 mmol) was added to a stirring solution of the resulting product in MeOH / THF (3 mL, 1:1) at 23°C. After 4 h of stirring at 23°C, the reaction mixture was filtered through a fritted funnel, concentrated, diluted with aq. 1 M HCl (5 mL) and extracted with Et₂O (5 mL). The organic extracts were washed with 1 M HCl (5 mL), water (5 mL), brine (5 mL), dried over MgSO₄, concentrated, and purified by flash silica column chromatography (96:4 hexanes / EtOAc) to afford the terminal alkyne as a yellow oil (44 mg, 0.215 mmol). A 1M solution of LHMDS (0.70 mL, 0.698 mmol) in THF was added to a stirring solution of the resulting product in THF (2 mL) at 0°C. After 20 min of stirring at 0°C, iodomethane (0.067 mL, 1.075 mmol) was added. After 1 h of stirring while gradually warming to 23°C, the reaction mixture was poured over sat. aq. NH₄Cl (4 mL) and extracted with Et₂O (4 mL). The organics extracts were washed with brine (4 mL), dried over MgSO₄, concentrated and purified by flash silica column chromatography (96:4 hexanes / EtOAc) to afford **46** as a clear oil (22 mg, 0.10 mmol, 11% over four steps). IR (ZnSe): 3332 (OH) cm⁻¹. ¹H NMR (400 MHz, CDCl₃) δ: 0.90 (d, ³J_{HH} = 7 Hz, 3H, CH(CH₃)CH₃), 0.96 (d, ³J_{HH} = 7 Hz, 3H, CH(CH₃)CH₃), 1.46 (m, 1H, OH), 1.56 – 1.69 (m, 4H, 4,5-CH₂), 1.76 (oct, ³J_{HH} = 7 Hz, 1H, CH(CH₃)₂), 2.03 (s, 3H, C≡CCH₃), 2.17 – 2.27 (m, 4H, 3,6-CH₂), 3.94 (t, ³J_{HH} = 7 Hz, 1H, CH(OH)CH), 5.70 (dd, ³J_{HH} = 16 Hz, 7.5 Hz, 1H, CH=CHCH(OH)CH), 6.93 (d, ³J_{HH} = 16 Hz, 1H, CH=CHCH(OH)CH). ¹³C NMR (100 MHz, CDCl₃) δ: 4.8 (C≡CCH₃), 18.3 (CH(CH₃)CH₃), 18.6 (CH(CH₃)CH₃), 22.3 (CH₂), 22.5 (CH₂), 25.3 (CH₂), 31.4 (CH₂), 34.2 (CH(CH₃)CH₃), 78.7 (CH(OH)CH), 79.8 (C≡C), 91.0 (C≡C), 120.7 (C=C), 129.8 (CH=CH), 132.2 (CH=CH), 138.3 (C=C). HRMS (EI): Calcd for (C₁₄H₂₀O + Na): 241.1563, found 241.1567.

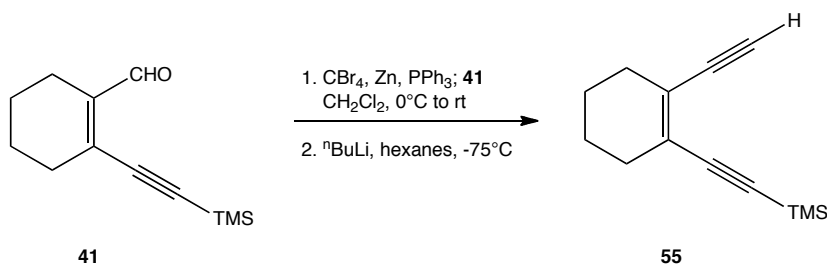


(*E*)-4-(2-((trimethylsilyl)ethynyl)cyclohex-1-enyl)but-3-en-2-ol (47). NaBH_4 (374 mg, 9.89 mmol) was added to a stirring solution of **75** (812 mg, 3.30 mmol) in MeOH / THF (66 mL, 1:1) at 23°C . After 10 min of stirring at 23°C , the reaction mixture was diluted with sat. aq. NH_4Cl (100 mL) and extracted with Et_2O (2 x 100 mL). The organic extracts were washed with brine (200 mL), dried over MgSO_4 , and concentrated to afford **47** as a pale yellow oil (775 mg, 3.12 mmol, 95%). IR (NaCl): 3345 (OH), 2135 ($\text{C}\equiv\text{C}$) cm^{-1} . ^1H NMR (400 MHz, CDCl_3) δ : 0.21 (s, 9H, TMS), 1.32 (d, $^3J_{\text{HH}} = 7$ Hz, 3H, CH_3), 1.50 – 1.68 (m, 5H, 4,5- CH_2 , OH), 2.19 – 2.28 (m, 4H, 3,6- CH_2), 4.41 (p, $^3J_{\text{HH}} = 7$ Hz, 1H, $\text{C}(\text{H})\text{OH}$), 5.79 (dd, $^3J_{\text{HH}} = 16$ Hz, 7 Hz, 1H, $\text{CH}=\text{CHC}(\text{H})\text{OH}$), 6.96 (d, $^3J_{\text{HH}} = 16$ Hz, 1H, $\text{CH}=\text{CHC}(\text{H})\text{OH}$). ^{13}C NMR (100 MHz, CDCl_3) δ : 0.3 (TMS), 22.1 (CH_2), 22.4 (CH_2), 23.4 (CH_2), 25.3 (CH_2), 30.7 (CH_3), 69.4 ($\text{CH}(\text{OH})$), 99.5 ($\text{C}=\text{C}$), 105.3 ($\text{C}\equiv\text{C}$), 120.1 ($\text{C}=\text{C}$), 130.2 ($\text{CH}=\text{CH}$), 133.3 ($\text{CH}=\text{CH}$), 141.0 ($\text{C}=\text{C}$). HRMS (EI): Calcd for ($\text{C}_{15}\text{H}_{24}\text{OSi}$): 248.1591, found 248.1589.



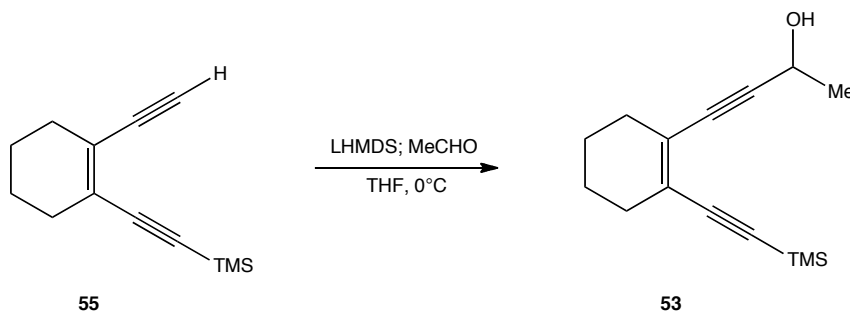
((2-Ethynylcyclohex-1-enyl)ethynyl)trimethylsilane (55). A solution of CBr_4 (9.09 g, 27.4 mmol) in CH_2Cl_2 (35 mL) was added over 15 min to a stirring heterogeneous mixture of Zn dust (3.58 g, 54.7 mmol) and PPh_3 (14.3 g, 54.7 mmol) in CH_2Cl_2 (140 mL) at 0°C . A solution of **41**

(2.82 g, 13.7 mmol) in CH_2Cl_2 (140 mL) was then added over 15 min to the stirring reaction mixture at 0°C . After 2 h of stirring while gradually warming to 23°C , the reaction mixture was filtered through celite, washed with water (300 mL), aq. 1 M HCl (300 mL), brine (300 mL), dried over Na_2SO_4 , concentrated, and purified by flash silica column chromatography (hexanes) to afford the intermediate geminal dibromide as a yellow solid (4.47 g, 12.3 mmol). A 2.5 M solution of $^n\text{BuLi}$ (16.7 mL, 35.9 mmol) in hexanes was added over 20 min to a stirring solution of the resulting product in hexanes (400 mL) at -75°C . After 1 h of stirring at -75°C , the reaction mixture was poured over sat. aq. NH_4Cl (400 mL) and extracted. The organic extracts were washed with brine (300 mL), dried over Na_2SO_4 , concentrated, and purified by flash silica column chromatography (hexanes) to afford **55** as a yellow oil (2.01 g, 9.93 mmol, 83%). The product exhibited spectroscopic properties identical to those reported in literature.³⁷



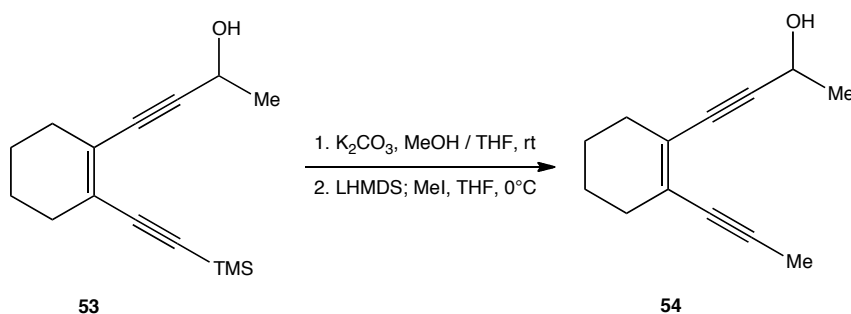
4-(2-((Trimethylsilyl)ethynyl)cyclohex-1-enyl)but-3-yn-2-ol (53). A 1 M solution of LHMDS (9.19 mL, 9.19 mmol) in THF was added to a stirring solution of **55** (620 mg, 3.06 mmol) in THF (31 mL) at 0°C . After stirring at 0°C for 30 min, acetaldehyde (0.860 mL, 15.32 mmol) was added. After stirring at 0°C for 30 min, the reaction mixture was poured over sat. aq. NH_4Cl (60 mL) and extracted with Et_2O (60 mL). The organic extracts were washed with brine (60 mL), dried over MgSO_4 , concentrated, purified by flash silica column chromatography (95:5 hexanes / EtOAc) to afford **53** as a yellow oil (573 mg, 2.33 mmol, 76%). IR (NaCl): 3364 (OH), 2140 ($\text{C}\equiv\text{C}$) cm^{-1} . ^1H NMR (400 MHz, CDCl_3) δ : 0.20 (s, 9H, TMS), 1.50 (d, $^3J_{\text{HH}} = 6.5$ Hz, 3H, $\text{CH}(\text{OH})\text{CH}_3$), 1.58 – 1.61 (m, 4H, 4,5- CH_2), 1.82 (d, $^3J_{\text{HH}} = 6.5$ Hz, 1H, OH), 2.17 – 2.24 (m, 4H, 3,6- CH_2),

4.70 (p, $^3J_{\text{HH}} = 6.5$ Hz, 1H, $\text{CH}(\text{OH})\text{CH}_3$). ^{13}C NMR (100 MHz, CDCl_3) δ : 0.2 (TMS), 21.8 (2 x CH_2), 24.6 (CH_2), 29.9 (CH_2), 30.0 ($\text{CH}(\text{OH})\text{CH}_3$), 59.0 ($\text{CH}(\text{OH})\text{CH}_3$), 84.7 ($\text{C}\equiv\text{C}$), 95.2 ($\text{C}\equiv\text{C}$), 98.2 ($\text{C}\equiv\text{C}$), 105.6 ($\text{C}\equiv\text{C}$), 126.7 ($\text{C}=\text{C}$), 127.0 ($\text{C}=\text{C}$). HRMS (EI): Calcd for ($\text{C}_{15}\text{H}_{22}\text{OSi}$): 246.1434, found 246.1432.

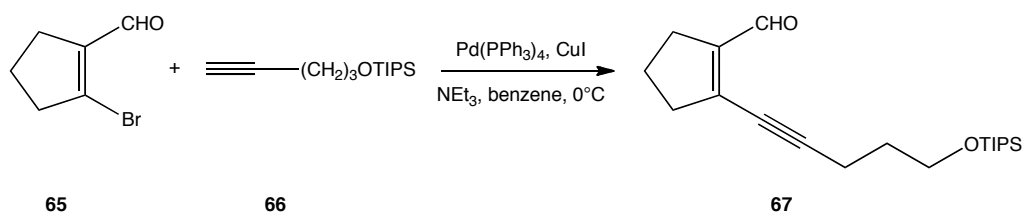


4-(2-(Prop-1-ynyl)cyclohex-1-enyl)but-3-yn-2-ol (54). Anhydrous K_2CO_3 (300 mg, 2.17 mmol) was added to a stirring solution of **53** (80 mg, 0.325 mmol) in THF / MeOH (4 mL, 1:1) at 23°C . After stirring at 23°C for 3 h, the reaction mixture was diluted with water (10 mL) and extracted with Et_2O (15 mL). The organic extract was washed with brine (10 mL), dried over MgSO_4 , and concentrated to give the desilylated product as a yellow oil (48 mg, 0.275 mmol, 85%). A 1 M solution of LHMDS (1.4 mL, 1.38 mmol) in THF was added to a stirring solution of the resulting product in THF (3 mL) at 0°C . After stirring at 0°C for 20 min, iodomethane (0.103 mL, 1.65 mmol) was added. After stirring for 4 h while slowly warming to 23°C , the reaction was poured over sat. aq. NH_4Cl (10 mL) and extracted with Et_2O (10 mL). The organics extracts were washed with brine (10 mL), dried over MgSO_4 , concentrated, and purified by flash silica column chromatography (95:5 hexanes / EtOAc) to afford **54** as a yellow oil (35 mg, 0.186 mmol, 63%). IR (ZnSe): 3348 (OH) cm^{-1} . ^1H NMR (400 MHz, CDCl_3) δ : 1.50 (d, $^3J_{\text{HH}} = 6$ Hz, 3H, $\text{CH}(\text{OH})\text{CH}_3$), 1.55 – 1.63 (m, 4H, 4,5- CH_2), 1.79 (d, $^3J_{\text{HH}} = 5.5$ Hz, 1H, OH), 2.02 (s, 3H, $\text{C}\equiv\text{CCH}_3$), 2.15 – 2.22 (m, 4H, 3,6- CH_2), 4.71 (app. p, $^3J_{\text{HH}} = 6$ Hz, 1H, $\text{CH}(\text{OH})\text{CH}_3$). ^{13}C NMR (100 MHz, CDCl_3) δ : 4.7 ($\text{C}\equiv\text{CCH}_3$), 22.0 (2 x CH_2), 24.7 (CH_2), 29.9 (CH_2), 30.5 ($\text{CH}(\text{OH})\text{CH}_3$), 59.1 ($\text{CH}(\text{OH})\text{CH}_3$),

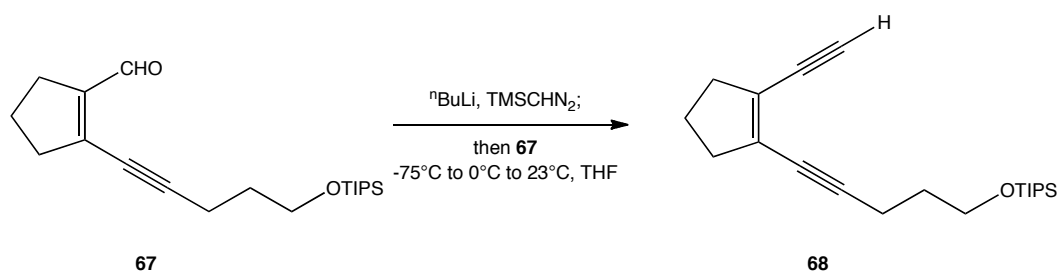
80.5 (C=C), 85.1 (C=C), 90.1 (C=C), 94.1 (C=C), 124.1 (C=C), 127.5 (C=C). HRMS (EI): Calcd for (C₁₃H₁₆O + Na): 211.1093, found 211.1097.



2-(5-((Triisopropylsilyl)oxy)pent-1-yn-1-yl)cyclopent-1-enecarbaldehyde (67). Pd(PPh₃)₄ (0.527 g, 0.460 mmol) and CuI (0.260 g, 1.37 mmol) were added to a stirring argon saturated solution of **65** (3.194 g, 18.25 mmol), **66** (4.608 g, 19.16 mmol), NEt₃ (12.73 mL, 91.25 mmol) in benzene (18.3 mL) at 0°C. After stirring for 20 h while gradually warming to 23°C, the reaction mixture was diluted with sat. aq. NH₄Cl (40 mL) and extracted with EtOAc (3 x 20 mL). The organic extracts were dried over MgSO₄, concentrated, and purified by flash silica column chromatography (99:1 hexanes / EtOAc) to afford **67** as a yellow oil (4.96 g, 14.8 mmol, 81%). IR (ZnSe): 1672 (C=O) cm⁻¹. ¹H NMR (400 MHz, CDCl₃) δ: 1.03 – 1.12 (m, 21H, TIPS), 1.80 (p, ³J_{HH} = 6.0 Hz, 2H, CH₂CH₂CH₂OTIPS), 1.94 (p, ³J_{HH} = 7.5 Hz, 2H, CH₂CH₂CH₂), 2.55 – 2.69 (m, 6H, CH₂CH₂CH₂OTIPS, CH₂CH₂CH₂), 3.79 (t, ³J_{HH} = 6.0 Hz, 2H, CH₂CH₂CH₂OTIPS), 10.02 (s, 1H, CHO). ¹³C NMR (100 MHz, CDCl₃) δ: 12.1 (SiCH(CH₃)₂), 16.5 (CH₂), 18.1 (SiCH(CH₃)₂), 22.2 (CH₂), 29.5 (CH₂), 31.8 (CH₂), 39.4 (CH₂), 61.8 (CH₂OTIPS), 75.2 (C≡C), 103.0 (C=C), 144.6 (C=C), 147.1 (C=C), 189.3 (C=O). HRMS (ESI): Calcd for (C₂₀H₃₄O₂Si + Na): 357.2220, found 357.2218.

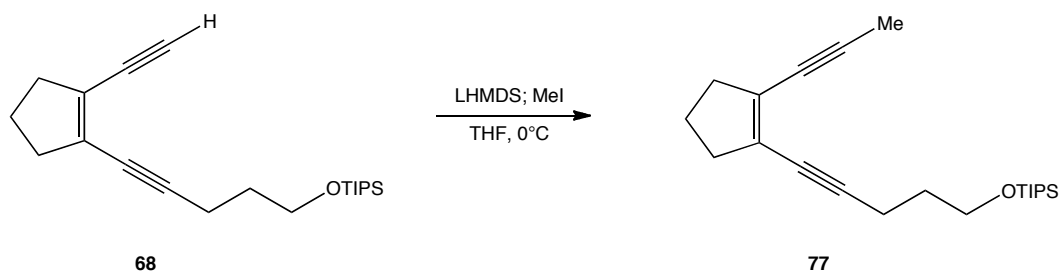


((5-(2-Ethynylcyclopent-1-en-1-yl)pent-4-yn-1-yl)oxy)triisopropylsilane (68). A 2.5 M solution of $^n\text{BuLi}$ (10 mL, 24.9 mmol) in hexanes was added to a stirring solution of TMSCHN_2 (12.4 mL, 24.8 mmol, 2 M in Et_2O) in THF (57 mL) at -75°C . After stirring for 45 min at -75°C , a solution of **67** (4.960 g, 14.8 mmol) in THF (17 mL) was added over the course of 20 min and the reaction mixture was stirred for 1 h at -75°C , then warmed to 0°C and stirred for 30 min, then warmed to 23°C and stirred 45 min before quenching with sat. aq. NH_4Cl (250 mL) and extracting with Et_2O (1 x 250 mL, 2 x 100 mL). The organic extracts were washed with brine (250 mL), dried over MgSO_4 , concentrated, and purified by flash silica column chromatography (hexanes) to afford **68** as an orange oil (3.91 g, 11.8 mmol, 80%). IR (ZnSe, thin film): 3312 (C^{spH}) cm^{-1} . ^1H NMR (400 MHz, CDCl_3) δ : 1.00 – 1.13 (m, 21H, TIPS), 1.79 (p, $^3J_{\text{HH}} = 6.0$ Hz, 2H, $\text{CH}_2\text{CH}_2\text{CH}_2\text{OTIPS}$), 1.91 (p, $^3J_{\text{HH}} = 7.0$ Hz, 2H, $\text{CH}_2\text{CH}_2\text{CH}_2$), 2.48 – 2.58 (m, 6H, $\text{CH}_2\text{CH}_2\text{CH}_2$, $\text{CH}_2\text{CH}_2\text{CH}_2\text{OTIPS}$), 3.28 (s, 1H, $\text{C}\equiv\text{CH}$), 3.80 (t, $^3J_{\text{HH}} = 6.0$ Hz, 2H, $\text{CH}_2\text{CH}_2\text{CH}_2\text{OTIPS}$). ^{13}C NMR (100 MHz, CDCl_3) δ : 12.1 ($\text{SiCH}(\text{CH}_3)_2$), 16.4 (CH_2), 18.2 ($\text{SiCH}(\text{CH}_3)_2$), 23.0 (CH_2), 32.1 (CH_2), 36.8 (CH_2), 37.5 (CH_2), 62.0 (CH_2OTIPS), 77.0 ($\text{C}=\text{C}$), 80.6 ($\text{C}=\text{C}$), 83.0 ($\text{C}\equiv\text{CH}$), 98.0 ($\text{C}=\text{C}$), 127.0 ($\text{C}=\text{C}$), 132.9 ($\text{C}=\text{C}$). HRMS (ESI): Calcd for ($\text{C}_{21}\text{H}_{34}\text{OSi} + \text{Na}$): 353.2271, found 353.2265.



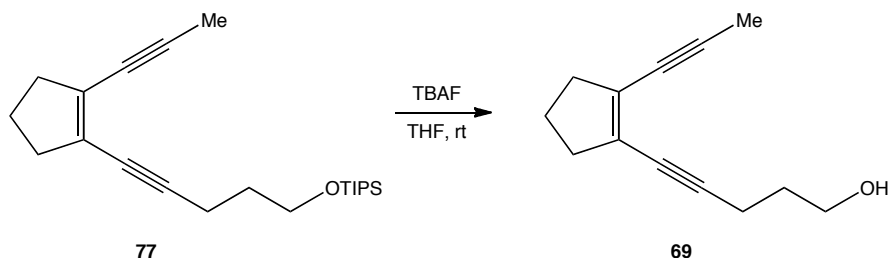
((5-(2-(Prop-1-yn-1-yl)cyclopent-1-en-1-yl)pent-4-yn-1-yl)oxy)triisopropylsilane (77). A 1M solution of LHMDS (23.7 mL, 23.7 mmol) in hexanes was added to a stirring solution of **68** (3.91 g, 11.83 mmol) in THF (85 mL) at 0°C . After stirring at 0°C for 15 min, iodomethane (2.21 mL,

35.5 mmol) was added and stirred for 45 min at 0°C before quenching with sat. aq. NH_4Cl (300 mL) and extracting with hexanes (1 x 300 mL, 1 x 150 mL). The organic extracts were washed with water (2 x 300 mL), brine (300 mL), dried with MgSO_4 , concentrated, and purified by flash silica column chromatography (hexanes) to afford **77** as a yellow oil (3.34 g, 9.70 mmol, 82%). IR (ZnSe): 2217 ($\text{C}\equiv\text{C}$) cm^{-1} . ^1H NMR (400 MHz, CDCl_3) δ : 1.00 – 1.13 (m, 21H, TIPS), 1.79 (tt, $^3J_{\text{HH}} = 7.0$ Hz, 6.0 Hz, 2H, $\text{CH}_2\text{CH}_2\text{CH}_2\text{OTIPS}$), 1.87 (p, $^3J_{\text{HH}} = 7.5$ Hz, 2H, $\text{CH}_2\text{CH}_2\text{CH}_2$), 2.04 (s, 3H, $\text{C}\equiv\text{CCH}_3$), 2.48 (t, $^3J_{\text{HH}} = 7.5$ Hz, 4H, $\text{CH}_2\text{CH}_2\text{CH}_2$), 2.52 (t, $^3J_{\text{HH}} = 7.0$ Hz, 2H, $\text{CH}_2\text{CH}_2\text{CH}_2\text{OTIPS}$), 3.80 (t, $^3J_{\text{HH}} = 6.0$ Hz, 2H, $\text{CH}_2\text{CH}_2\text{CH}_2\text{OTIPS}$). ^{13}C NMR (100 MHz, CDCl_3) δ : 4.9 ($\text{C}\equiv\text{CCH}_3$), 12.1 ($\text{SiCH}(\text{CH}_3)_2$), 16.5 (CH_2), 18.1 ($\text{SiCH}(\text{CH}_3)_2$), 23.0 (CH_2), 32.3 (CH_2), 37.15 (CH_2), 37.19 (CH_2), 62.0 (CH_2OTIPS), 76.6 ($\text{C}\equiv\text{C}$), 77.5 ($\text{C}\equiv\text{C}$), 92.2 ($\text{C}\equiv\text{C}$), 96.5 ($\text{C}\equiv\text{C}$), 128.8 ($\text{C}\equiv\text{C}$), 128.9 ($\text{C}\equiv\text{C}$). HRMS (ESI): Calcd for ($\text{C}_{22}\text{H}_{36}\text{OSi} + \text{Na}$): 367.2428, found 367.2431.

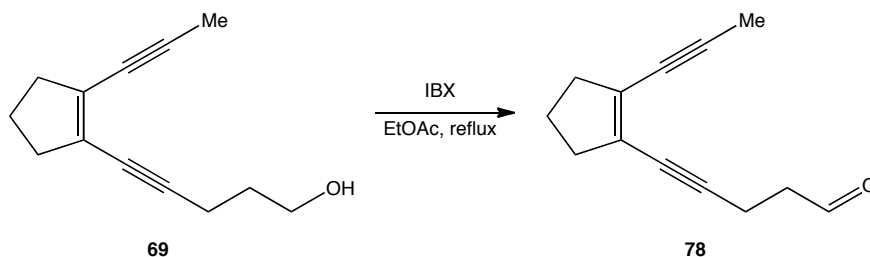


5-(2-(Prop-1-yn-1-yl)cyclopent-1-en-1-yl)pent-4-yn-1-ol (69). A 1 M solution of tetrabutylammonium fluoride (2.96 mL, 2.96 mmol) was added to a stirring solution of **77** (340 mg, 0.987 mmol) in wet THF (10 mL) at 23°C. After stirring at 23°C for 25 min, the reaction was concentrated, diluted with brine (25 mL) and extracted with Et_2O (1 x 25 mL, 1 x 10 mL). The organic extracts were dried over MgSO_4 , concentrated, and purified by flash silica column chromatography (85:15 hexanes / EtOAc) to afford **69** as a yellow oil (175 mg, 0.930 mmol, 94%). IR (ZnSe): 3312 (OH), 2215 ($\text{C}\equiv\text{C}$) cm^{-1} . ^1H NMR (400 MHz, CDCl_3) δ : 1.62 (bs, 1H, OH), 1.82 (p, $^3J_{\text{HH}} = 6.5$ Hz, 2H, $\text{CH}_2\text{CH}_2\text{CH}_2\text{OH}$), 1.88 (p, $J = 7.5$ Hz, 2H, $\text{CH}_2\text{CH}_2\text{CH}_2$), 2.05 (s, 3H, $\text{C}\equiv\text{CCH}_3$), 2.48 (t, $J = 7.5$ Hz, 4H, $\text{CH}_2\text{CH}_2\text{CH}_2$), 2.54 (t, $J = 7.0$ Hz, 2H, $\text{CH}_2\text{CH}_2\text{CH}_2\text{OH}$), 3.82

(t, $J = 6.0$ Hz, 2H, CH_2OH), ^{13}C NMR (75 MHz, CDCl_3) δ : 4.8 ($\text{C}\equiv\text{CCH}_3$), 16.5 (CH_2), 22.9 (CH_2), 31.3 (CH_2), 36.88 (CH_2), 36.95 (CH_2), 61.7 (CH_2OH), 76.5 ($\text{C}\equiv\text{C}$), 78.0 ($\text{C}\equiv\text{C}$), 92.5 ($\text{C}\equiv\text{C}$), 95.7 ($\text{C}\equiv\text{C}$), 128.6 ($\text{C}=\text{C}$), 129.4 ($\text{C}=\text{C}$). HRMS (ESI): Calcd for ($\text{C}_{13}\text{H}_{17}\text{O}$): 189.1274, found 189.1276.

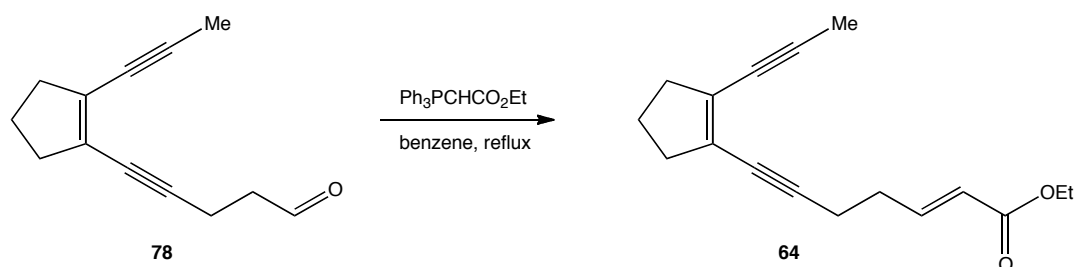


5-(2-(Prop-1-yn-1-yl)cyclopent-1-en-1-yl)pent-4-ynal (78). A solution of **69** (104 mg, 0.552 mmol) in EtOAc (4 mL) and 2-iodoxybenzoic acid³⁵ (232 mg, 0.829 mmol) was refluxed for 2.5 h, cooled to 23°C, filtered, concentrated, diluted in Et_2O , filtered twice more, and concentrated to afford **78** as a yellow oil (83 mg, 0.446 mmol, 81%). IR (ZnSe): 2216 ($\text{C}\equiv\text{C}$), 1723 ($\text{C}=\text{O}$) cm^{-1} . ^1H NMR (300 MHz, CDCl_3) δ : 1.87 (p, $^3J_{\text{HH}} = 7.5$ Hz, 2H, $\text{CH}_2\text{CH}_2\text{CH}_2$), 2.05 (s, 3H, $\text{C}\equiv\text{CCH}_3$), 2.48 (t, $^3J_{\text{HH}} = 7.5$ Hz, 4H, $\text{CH}_2\text{CH}_2\text{CH}_2$), 2.80 – 2.67 (m, 4H, $\text{CH}_2\text{CH}_2\text{CHO}$), 9.84 (m, 1H, CHO). ^{13}C NMR (100 MHz, CDCl_3) δ : 4.9 ($\text{C}\equiv\text{CCH}_3$), 13.4 (CH_2), 22.9 (CH_2), 29.8 (CH_2), 36.9 (CH_2), 37.1 (CH_2), 42.7 (CH_2CHO), 76.4 ($\text{C}\equiv\text{C}$), 78.5 ($\text{C}\equiv\text{C}$), 92.8 ($\text{C}\equiv\text{C}$), 94.0 ($\text{C}\equiv\text{C}$), 128.3 ($\text{C}=\text{C}$), 130.1 ($\text{C}=\text{C}$), 200.8 ($\text{C}=\text{O}$). HRMS (ESI): Calcd for ($\text{C}_{13}\text{H}_{14}\text{O}+\text{Na}$): 209.0937, found 209.0938.



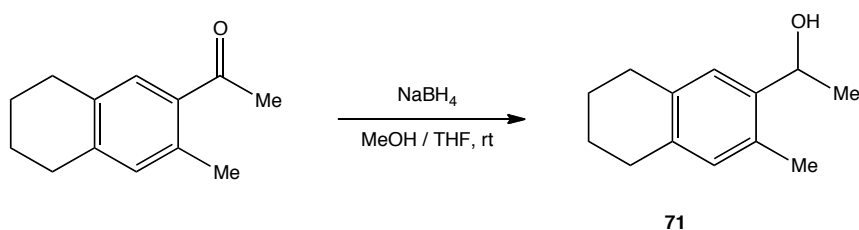
(E)-ethyl 7-(2-(prop-1-yn-1-yl)cyclopent-1-en-1-yl)hept-2-en-6-ynoate (64). A solution of ethyl (triphenylphosphoranylidene)acetate (64 mg, 0.183 mmol) and **78** (31 mg, 0.166 mmol) in benzene (2 mL) was refluxed for 1 h, concentrated under reduced pressure, and purified by

flash silica column chromatography (99:1 hexanes / EtOAc) to afford **64** as a pale yellow oil (27 mg, 0.105 mmol, 63%). IR (ZnSe): 2217 (C≡C), 1718 (C=O) cm^{-1} . ^1H NMR (400 MHz, CDCl_3) δ : 1.29 (t, $^3J_{\text{HH}} = 7.0$ Hz, 3H, OCH_2CH_3), 1.87 (p, $^3J_{\text{HH}} = 7$ Hz, 2H, $\text{CH}_2\text{CH}_2\text{CH}_2$), 2.05 (s, 3H, $\text{C}\equiv\text{CCH}_3$), 2.48 (t, $^3J_{\text{HH}} = 7.5$ Hz, 6H, $\text{CH}_2\text{CH}_2\text{CH}_2$, $\text{CH}_2\text{CH}_2\text{CH}=\text{CH}$), 2.57 (app t, $^3J_{\text{HH}} = 7.0$ Hz, 2H, $\text{CH}_2\text{CH}=\text{CHCO}_2\text{Et}$), 4.19 (q, $^3J_{\text{HH}} = 7.0$ Hz, 2H, OCH_2CH_3), 5.90 (dt, $^3J_{\text{HH}} = 15$ Hz, $^4J_{\text{HH}} = 1.5$ Hz, 1H, $\text{CH}=\text{CHCO}_2\text{Et}$), 7.01 (dt, $^3J_{\text{HH}} = 15.5$ Hz, 7.0 Hz, 1H, $\text{CH}=\text{CHCO}_2\text{Et}$). ^{13}C NMR (100MHz, CDCl_3) δ : 4.9 ($\text{C}\equiv\text{CCH}_3$), 14.4 (CH_2), 19.0 (OCH_2CH_3), 23.0 (CH_2), 31.7 (CH_2), 37.1 (CH_2), 37.2 (CH_2), 60.4 (OCH_2CH_3), 76.5 ($\text{C}\equiv\text{C}$), 78.5 ($\text{C}\equiv\text{C}$), 92.7 ($\text{C}\equiv\text{C}$), 94.7 ($\text{C}\equiv\text{C}$), 122.6 ($\text{CH}_2\text{CH}=\text{CHCO}_2\text{Et}$), 128.5 ($\text{C}=\text{C}$), 129.7 ($\text{C}=\text{C}$), 146.8 ($\text{CH}_2\text{CH}=\text{CHCO}_2\text{Et}$), 166.6 ($\text{CH}_2\text{CH}=\text{CHCO}_2\text{Et}$). HRMS (ESI): Calcd for ($\text{C}_{17}\text{H}_{20}\text{O}_2+\text{Na}$): 279.1356, found 279.1355.

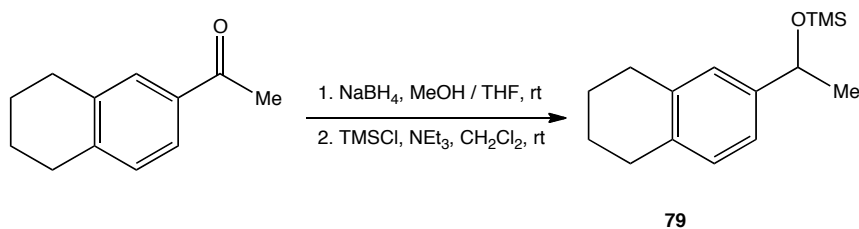


6-(1-Hydroxyethyl)-7-methyl-tetraline (71). NaBH_4 (130 mg, 3.43 mmol) was added to a stirring solution of 6-acetyl-7-methyl-tetraline (215 mg, 1.14 mmol) in THF / MeOH (12 mL, 1:1) at 23°C . After stirring for 30 min at 23°C , the reaction mixture was poured over acetone (5 mL), concentrated, diluted with H_2O (10 mL) and extracted with Et_2O (10 mL). The organic extracts were washed with brine (10 mL), dried over Na_2SO_4 , and concentrated to afford **71** as a pale yellow oil (210 mg, 1.10 mmol, 97%). IR (ZnSe): 3332 (OH) cm^{-1} . ^1H NMR (400 MHz, CDCl_3) δ : 1.47 (d, $^3J_{\text{HH}} = 6$ Hz, 3H, $\text{CH}(\text{OH})\text{CH}_3$), 1.69 (s, 1H, OH), 1.74 – 1.83 (m, 4H, 2,3- CH_2), 2.29 (s, 3H, ArCH_3), 2.69 – 2.79 (m, 4H, 1,4- CH_2), 5.08 (q, $^3J_{\text{HH}} = 6$ Hz, 1H, $\text{CH}(\text{OH})\text{CH}_3$), 6.86 (s, 1H, ArH), 7.21 (s, 1H, ArH). ^{13}C NMR (100 MHz, CDCl_3) δ : 18.5 (ArCH_3), 23.4 (CH_2), 23.5 (CH_2), 24.1 ($\text{CH}(\text{OH})\text{CH}_3$), 29.0 (CH_2), 29.2 (CH_2), 66.8 ($\text{CH}(\text{OH})\text{CH}_3$), 125.2 ($\text{C}^{\text{Ar}}\text{H}$), 131.1 ($\text{C}^{\text{Ar}}\text{H}$),

131.4 (C^{Ar}), 135.1 (C^{Ar}), 136.1 (C^{Ar}), 141.2 (C^{Ar}). HRMS (EI): Calcd for (C₁₃H₁₈O + Na): 213.1250, found 213.1251.



6-(1-(Trimethylsilyloxy)ethyl)-tetraline (79). NaBH₄ (671 mg, 17.76 mmol) was added to a stirring solution of 6-acetyl-tetraline (1.02 g, 5.92 mmol) in THF / MeOH (60 mL, 1:1) at 23°C. After stirring for 30 min at 23°C, the reaction mixture was then poured over acetone (50 mL), concentrated, diluted with H₂O (150 mL) and extracted with Et₂O (150 mL). The organic extracts were washed with brine (150 mL), dried over Na₂SO₄, and concentrated to afford a pale yellow oil. Chlorotrimethylsilane (0.090 mL, 0.920 mmol) was added to a stirring solution of the resulting oil (54 mg, 0.310 mmol) and triethylamine (0.130 mL, 0.920 mmol) in CH₂Cl₂ (3.1 mL) at 23°C. After 2 h of stirring at 23°C, the reaction mixture was poured over water (3 mL) and extracted. The organic extract was washed with water (3 mL), brine (3 mL), dried over MgSO₄, and concentrated to afford **79** as a yellow oil (69 mg, 0.277 mmol, 90% for second step). ¹H NMR (CDCl₃, 300 MHz) δ: 0.08 (s, 9H, TMS), 1.41 (d, ³J_{HH} = 6.5 Hz, 3H, CH(OTMS)CH₃), 1.73 – 1.84 (m, 4H, 2,3-CH₂), 2.69 – 2.83 (m, 4H, 1,4-CH₂), 4.79 (q, ³J_{HH} = 6.5 Hz, 1H, CH(OTMS)CH₃), 6.99 – 7.07 (m, 3H, ArH). ¹³C NMR (CDCl₃, 100 MHz) δ: 0.30 (TMS), 23.4 (2 x CH₂), 27.0 (CH(OTMS)CH₃), 29.2 (CH₂), 29.6 (CH₂), 70.6 (CH(OTMS)CH₃), 122.7 (C^{Ar}H), 126.1 (C^{Ar}H), 129.0 (C^{Ar}H), 135.7 (C^{Ar}), 136.9 (C^{Ar}), 143.6 (C^{Ar}). HRMS (EI): Calcd for (C₁₅H₂₄OSi): 248.1591, found 248.1588.



v. Procedures for NMR scale reactions

General procedure dienyne cyclizations. Ruthenium complex was added to a solution of dienyne and 1,3,5-tri-*tert*-butylbenzene (~0.5 – 1 mg) in CDCl₃ at 23°C in glove box.

Reaction of 39 with 10. 39 (4.3 mg, 0.024 mmol), 10 (18.5 mg, 0.037 mmol), CDCl₃ (0.55 mL).

Reaction of 40 with 10. 40 (3.4 mg, 0.019 mmol), 10 (14.2 mg, 0.028 mmol), CDCl₃ (1.09 mL).

Reaction of 43 with 10. 43 (6 mg, 0.032 mmol), 10 (24 mg, 0.047 mmol), CDCl₃ (0.75 mL).

Reaction of 44 with 10. 44 (8 mg, 0.037 mmol), 10 (22 mg, 0.044 mmol), CDCl₃ (0.72 mL).

Reaction of 45 with 10. 45 (2 mg, 0.0098 mmol), 10 (5.4 mg, 0.0108 mmol), CDCl₃ (0.80 mL).

Reaction of 46 with 10. 46 (2 mg, 0.0091 mmol), 10 (5.5 mg, 0.011 mmol), CDCl₃ (0.58 mL).

Distinguishable ¹H NMR (CDCl₃, 400 MHz) resonances for product 51 δ: 0.82 (d, ³J_{HH} = 7 Hz, 3H, CH(CH₃)CH'₃), 0.88 (d, ³J_{HH} = 7 Hz, 3H, CH(CH'₃)CH₃), 1.02 (d, ³J_{HH} = 7 Hz, 3H, CH(CH-₃)CH'₃), 1.06 (d, ³J_{HH} = 7 Hz, 3H, CH(CH'₃)CH₃), 1.82 (s, 15H, Cp*), 1.84 (s, 15H, Cp*), 2.10 (s, 3H, ArMe), 2.31 (s, 3H, ArMe), 4.09 (d, ³J_{HH} = 8 Hz, 1H, CH(OH)CH), 4.43 (d, ³J_{HH} = 4.5 Hz, 1H, CH(OH)CH), 5.26 (s, 1H, ArH), 5.467 (s, 1H, ArH), 5.476 (s, 1H, ArH), 5.75 (s, 1H, ArH).

Reaction of 47 with 10. 47 (1 mg, 0.0040 mmol), 10 (2.4 mg, 0.0048 mmol), CDCl₃ (0.95 mL).

Reaction of 45 with 20. 45 (12 mg, 0.059 mmol), 20 (38 mg, 0.088 mmol), CDCl₃ (1.2 mL).

General procedure for enediene cyclizations. Ruthenium complex was added to a solution of enediene, γ -terpinene, and 1,3,5-tri-*tert*-butylbenzene (~0.5 – 1 mg) in acetone-*d*₆ at 23°C in glove box.

Reaction of 53 with 10. **53** (1.3 mg, 0.0053 mmol), **10** (4.0 mg, 0.0079 mmol), γ - terpinene (4.3 μ L, 0.027 mmol), acetone- d_6 (0.934 mL).

Reaction of 54 with 10. **54** (2 mg, 0.011 mmol), **10** (8.0 mg, 0.016 mmol), γ - terpinene (8.8 μ L, 0.055 mmol), acetone- d_6 (0.57 mL).

Reaction of 53 with 20. **53** (4.4 mg, 0.018 mmol), **20** (8.7 mg, 0.020 mmol), γ - terpinene (14 μ L, 0.090 mmol), acetone- d_6 (0.85 mL).

Reaction of 64 with 10. **64** (16.4 mg, 0.0640 mmol), **10** (29.4 mg, 0.0582 mmol), 1,4-cyclohexadiene (0.009 mL, 0.0960 mmol), CDCl_3 (0.780 mL). Distinguishable ^1H NMR (CDCl_3 , 400 MHz) resonances for product **70** δ : 1.24 (t, $^3J_{\text{HH}} = 7$ Hz, 3H, ma- CH_2CH_3), 1.31 (t, $^3J_{\text{HH}} = 7$ Hz, 3H, mi- CH_2CH_3), 1.76 (s, 15H, ma-Cp*), 1.82 (s, 15H, mi-Cp*), 2.12 (s, 3H, ma-ArMe), 2.13 (s, 3H, mi-ArMe), 4.13 (q, $^3J_{\text{HH}} = 7$ Hz, 2H, ma- CH_2CH_3), 4.21 (q, $^3J_{\text{HH}} = 7$ Hz, 2H, mi- CH_2CH_3), 5.73 (s, 1H, mi-ArH), 5.76 (s, 1H, ma-ArH).

General procedure for arene binding experiments. **10** was added to a solution of arene **71**, hydrogen atom donor (if applicable), and 1,3,5-tri-*tert*-butylbenzene (~0.5 – 1 mg) in deuterated solvent at 23°C in glove box.

Reaction of 71 with 10 under dienyne cyclization conditions. **71** (6.5 mg, 0.034 mmol), **10** (25 mg, 0.051 mmol), CDCl_3 (0.80 mL).

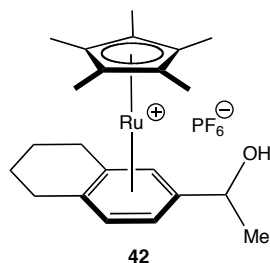
Reaction of 71 with 10 under enediyne cyclization conditions. **71** (2 mg, 0.011 mmol), **10** (8 mg, 0.016 mmol), γ - terpinene (8.8 μ L, 0.055 mmol), acetone- d_6 (0.43 mL).

Reaction of 71 with 10 without hydrogen atom donor. **71** (2 mg, 0.011 mmol), **10** (8 mg, 0.016 mmol), acetone- d_6 (0.64 mL).

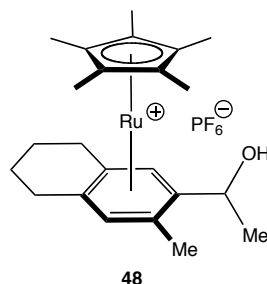
vi. Preparation and characterization data for Ru-arene complexes.

(η^5 -Pentamethylcyclopentadienyl)(η^6 -6-(1-hydroxyethyl)-tetralinyl)ruthenium(II)

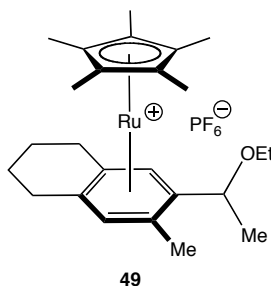
hexafluorophosphate (42). After 30 min at 23°C, the NMR scale reaction mixture of **39** with **10** was concentrated and purified by flash alumina column chromatography (95:5 CH₂Cl₂ / acetone) followed by crystallization (CH₂Cl₂ : ethyl ether) to afford a mixture of **42-ma** and **42-mi** as a colorless solid (4.2 mg, 0.008 mmol, 31%). **42-ma** and **42-mi** were isolated after repeated alumina chromatography. **(42-ma)**. decomp. 236 – 239°C. ¹H NMR (300 MHz, CDCl₃) δ : 1.55 (d, ³J_{HH} = 6.5 Hz, 3H, CH(OH)CH₃), 1.86 (s, 15H, Cp*), 1.59 – 1.94 (m, 4H, 2,3-CH₂), 2.31 – 2.46 (m, 3H, 1,4-CH^{syn}, OH), 2.66 – 2.88 (m, 2H, 1,4-CH^{anti}), 4.57 (dq, ³J_{HH} = 6.5 Hz, 4.5 Hz, 1H, CH(OH)CH₃), 5.51 (d, ³J_{HH} = 6 Hz, 1H, 7/8-C^{Ar}H), 5.59 (dd, ³J_{HH} = 6 Hz, ⁴J_{HH} = 1 Hz, 1H, 7/8-C^{Ar}H), 5.85 (s, 1H, 5-C^{Ar}H). ¹³C NMR (75 MHz, CDCl₃) δ : 10.2 (CpCH₃), 21.9 (2 x CH₂), 26.0 (CH₂), 26.1 (CH₂), 27.1 (CH(OH)CH₃), 66.7 (CH(OH)CH₃), 83.2 (C^{Ar}H), 83.9 (C^{Ar}H), 86.4 (C^{Ar}H), 95.0 (Cp*), 100.8 (C^{Ar}), 101.1 (C^{Ar}), 108.0 (C^{Ar}). HRMS (EI): Calcd for (C₂₂H₃₁ORu – PF₆): 407.1445, found 407.1453. **(42-mi)**. decomp. 254 - 258°C. ¹H NMR (400 MHz, CDCl₃) δ : 1.55 (d, ³J_{HH} = 6 Hz, 3H, CH(OH)CH₃), 1.88 (s, 15H, Cp*), 1.61 – 1.92 (m, 4H, 2,3-CH₂), 2.36 – 2.47 (m, 2H, 1,4-CH^{syn}), 2.53 (d, ³J_{HH} = 5 Hz, 1H, OH), 2.70 – 2.82 (m, 2H, 1,4-CH^{anti}), 4.59 (qd, ³J_{HH} = 6 Hz, 5 Hz, 1H, CH(OH)CH₃), 5.50 (d, ³J_{HH} = 6 Hz, 1H, 7/8-C^{Ar}H), 5.57 (s, 1H, 5-C^{Ar}H), 5.93 (d, ³J_{HH} = 6 Hz, 1H, 7/8-C^{Ar}H). ¹³C NMR (75 MHz, CDCl₃) δ : 10.3 (CpCH₃), 21.76 (CH₂), 21.83 (CH₂), 25.8 (CH₂), 26.3 (CH₂), 27.1 (CH(OH)CH₃), 66.6 (CH(OH)CH₃), 82.5 (C^{Ar}H), 84.5 (C^{Ar}H), 87.0 (C^{Ar}H), 95.0 (Cp*), 100.6 (C^{Ar}), 101.2 (C^{Ar}), 107.9 (C^{Ar}). HRMS (EI): Calcd for (C₂₂H₃₁ORu – PF₆): 407.1445, found 407.1449.



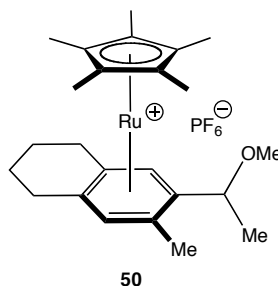
(η^5 -Pentamethylcyclopentadienyl)(η^6 -6-(1-hydroxyethyl)-7-methyl-tetralinyl)ruthenium (II) hexafluorophosphate (48**). After 19 h at 23°C, the NMR scale reaction mixture of **43** with **10** was concentrated and purified by flash silica column chromatography (95:5 CH₂Cl₂ / acetone) followed by crystallization (CH₂Cl₂ : ethyl ether) to afford both isolated and mixed samples of **48-ma** and **48-mi** (11.6 mg, 0.020 mmol, 63%). (**48-ma**). colorless solid. decomp. 274 – 276°C. IR (ZnSe): 3579 (OH) cm⁻¹. ¹H NMR (400 MHz, CDCl₃) δ : 1.48 (d, ³J_{HH} = 6.5 Hz, 3H, CH(OH)CH₃), 1.55 – 1.65 (m, 1H, 2/3-CH^{syn}), 1.81 (s, 15H, Cp*), 1.72 – 1.87 (m, 3H, 2,3-CH₂), 2.08 (s, 3H, ArCH₃), 2.33 – 2.41 (m, 2H, 1,4-CH^{syn}), 2.66 – 2.80 (m, 2H, 1,4-CH^{anti}), 2.82 (d, ³J_{HH} = 5.5 Hz, 1H, OH), 4.75 (dq, ³J_{HH} = 6.5 Hz, 5.5 Hz, 1H, CH(OH)CH₃), 5.45 (s, 1H, ArH), 5.87 (s, 1H, ArH). ¹³C NMR (100 MHz, CDCl₃) δ : 9.8 (CpCH₃), 15.7 (ArCH₃), 21.8 (CH₂), 21.9 (CH₂), 25.2 (CH(OH)CH₃), 25.6 (CH₂), 25.7 (CH₂), 63.7 (CH(OH)CH₃), 83.1 (C^{Ar}H), 88.7 (C^{Ar}H), 94.2 (Cp*), 95.6 (C^{Ar}), 100.5 (C^{Ar}), 101.1 (C^{Ar}), 106.5 (C^{Ar}). HRMS (EI): Calcd for (C₂₃H₃₃ORu – PF₆): 421.1602, found 421.1606. (**48-mi**): light brown plate crystals. decomp. 268 - 270 °C. IR (ZnSe): 3559 (OH) cm⁻¹. ¹H NMR (400 MHz, CDCl₃) δ : 1.56 (d, ³J_{HH} = 6.5 Hz, 3H, CH(OH)CH₃), 1.81 (s, 15H, Cp*), 1.64 – 1.84 (m, 4H, 2,3-CH₂), 2.27 (s, 3H, ArCH₃), 2.33 – 2.41 (m, 2H, 1,4-CH^{syn}), 2.64 (d, ³J_{HH} = 6.5 Hz, 1H, OH), 2.68 – 2.80 (m, 2H, 1,4-CH^{anti}), 4.68 (p, ³J_{HH} = 6.5 Hz, 1H, CH(OH)CH₃), 5.39 (s, 1H, ArH), 5.58 (s, 1H, ArH). ¹³C NMR (100 MHz, CDCl₃) δ : 10.0 (CpCH₃), 16.3 (ArCH₃), 21.76 (CH₂), 21.78 (CH₂), 22.2 (CH(OH)CH₃), 25.5 (CH₂), 25.7 (CH₂), 66.8 (CH(OH)CH₃), 85.2 (C^{Ar}H), 90.1 (C^{Ar}H), 94.0 (Cp*), 98.8 (C^{Ar}), 100.8 (C^{Ar}), 101.4 (C^{Ar}), 103.6 (C^{Ar}). HRMS (EI): Calcd for (C₂₃H₃₃ORu – PF₆): 421.1602, found 421.1607.**



(η^5 -Pentamethylcyclopentadienyl)(η^6 -6-(1-ethoxyethyl)-7-methyl-tetra-1,2,3,4-inyl)ruthenium (II) hexafluorophosphate (49). After 3.5 h at 23°C, the NMR scale reaction mixture of **44** with **10** was concentrated and purified by flash alumina column chromatography (CH_2Cl_2) to afford a mixture of **49-ma** and **49-mi** as a colorless solid (14 mg, 0.023 mmol, 63%). ^1H NMR (400 MHz, CDCl_3) δ : 1.22 (t, $^3J_{\text{HH}} = 7$ Hz, 3H, mi- CH_2CH_3), 1.30 (t, $^3J_{\text{HH}} = 7$ Hz, 3H, ma- CH_2CH_3), 1.38 (d, $^3J_{\text{HH}} = 6$ Hz, 3H, ma- $\text{CH}(\text{OH})\text{CH}_3$), 1.48 (d, $^3J_{\text{HH}} = 6.5$ Hz, 3H, mi- $\text{CH}(\text{OH})\text{CH}_3$), 1.80 (s, 15H, ma-Cp*), 1.81 (s, 15H, mi-Cp*), 1.56 – 1.86 (m, 8H, 2,3- CH_2), 2.10 (s, 3H, ma-Ar CH_3), 2.22 (s, 3H, mi-Ar CH_3), 2.31 – 2.46 (m, 4H, 1,4- CH^{syn}), 2.68 – 2.77 (m, 4H, 1,4- CH^{anti}), 3.45 (dq, $^2J_{\text{HH}} = 9$ Hz, $^3J_{\text{HH}} = 7$ Hz, 2H, C(H')H CH_3), 3.71 (dq, $^2J_{\text{HH}} = 9$ Hz, $^3J_{\text{HH}} = 7$ Hz, 1H, mi-C(H)H' CH_3), 3.84 (dq, $^2J_{\text{HH}} = 9$ Hz, $^3J_{\text{HH}} = 7$ Hz, 1H, ma-C(H)H' CH_3), 4.28 (q, $^3J_{\text{HH}} = 6.5$ Hz, 1H, mi- $\text{CH}(\text{OH})\text{CH}_3$), 4.30 (q, $^3J_{\text{HH}} = 6$ Hz, 1H, ma- $\text{CH}(\text{OH})\text{CH}_3$), 5.48 (s, 1H, mi-ArH), 5.61 (s, 1H, mi-ArH), 5.67 (s, 2H, ma-ArH). ^{13}C NMR (100 MHz, CDCl_3) δ : 9.8 (ma-Cp CH_3), 10.0 (mi-Cp CH_3), 15.65 (ma- CH_3), 15.74 (ma- CH_3), 16.0 (mi- CH_3), 16.3 (mi- CH_3), 17.8 (mi- CH_3), 20.6 (ma- CH_3), 21.8 (1 x ma- CH_2 , 2 x mi- CH_2), 21.9 (ma- CH_2), 25.4 (mi- CH_2), 25.6 (ma- CH_2), 25.8 (mi- CH_2), 25.9 (ma- CH_2), 63.7 (ma- CH_2CH_3), 64.2 (mi- CH_2CH_3), 70.3 (ma- $\text{CH}(\text{OH})\text{CH}_3$), 73.5 (mi- $\text{CH}(\text{OH})\text{CH}_3$), 83.3 (ma- C^{ArH}), 85.1 (mi- C^{ArH}), 89.2 (ma- C^{ArH}), 90.1 (mi- C^{ArH}), 94.0 (ma-Cp*), 94.2 (mi-Cp*), 95.5 (ma- C^{Ar}), 98.5 (mi- C^{Ar}), 100.0 (ma- C^{Ar}), 100.8 (mi- C^{Ar}), 101.7 (mi- C^{Ar}), 101.8 (ma- C^{Ar}), 103.0 (mi- C^{Ar}), 105.7 (ma- C^{Ar}). HRMS (EI): Calcd for ($\text{C}_{25}\text{H}_{37}\text{ORu} - \text{PF}_6$): 449.1915, found 449.1927.

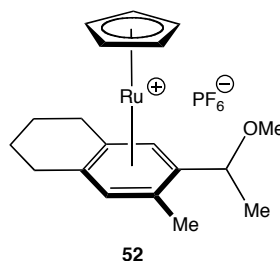


(η^5 -Pentamethylcyclopentadienyl)(η^6 -6-(1-methoxyethyl)-7-methyl-tetralinyl)ruthenium (II) hexafluorophosphate (50**). **10** (34 mg, 0.068 mmol) was added to a solution of **45** (12 mg, 0.058 mmol) in CDCl_3 (1 mL) at 23°C in glove box. After 30 min at 23°C , the reaction mixture was concentrated and purified by repeated PTLC (CH_2Cl_2 /acetone mixtures) followed by crystallization ($\text{EtOAc}/\text{CH}_2\text{Cl}_2$: hexanes) to afford isolated samples of **50-ma** and **50-mi** as colorless solids. (**50-ma**) decomp. $274 - 277^\circ\text{C}$. ^1H NMR (400 MHz, CDCl_3) δ : 1.39 (d, $^3J_{\text{HH}} = 6$ Hz, 3H, $\text{CH}(\text{OMe})\text{CH}_3$), 1.80 (s, 15H, Cp^*), 1.52 – 1.88 (m, 4H, 2,3- CH_2), 2.11 (s, 3H, ArCH_3), 2.27 – 2.47 (m, 2H, 1,4- CH^{syn}), 2.66 – 2.78 (m, 2H, 1,4- CH^{anti}), 3.47 (s, 3H, OCH_3), 4.20 (q, $^3J_{\text{HH}} = 6$ Hz, 1H, $\text{CH}(\text{OMe})\text{CH}_3$), 5.62 (s, 1H, ArH), 5.68 (s, 1H, ArH). ^{13}C NMR (100 MHz, CDCl_3) δ : 9.8 (Cp^*), 15.7 (CH_3), 19.9 (CH_3), 21.8 (CH_2), 21.9 (CH_2), 25.6 (CH_2), 25.8 (CH_2), 56.0 (OCH_3), 71.9 ($\text{CH}(\text{OMe})\text{CH}_3$), 83.2 (C^{ArH}), 89.1 (C^{ArH}), 94.1 (Cp^*), 95.9 (C^{Ar}), 100.0 (C^{Ar}), 101.7 (C^{Ar}), 105.3 (C^{Ar}). HRMS (EI): Calcd for ($\text{C}_{24}\text{H}_{35}\text{ORu} - \text{PF}_6$): 441.1726, found 441.1725. (**50-mi**) decomp. $196 - 197^\circ\text{C}$. ^1H NMR (400 MHz, CDCl_3) δ : 1.47 (d, $^3J_{\text{HH}} = 6$ Hz, 3H, $\text{CH}(\text{OMe})\text{CH}_3$), 1.81 (s, 15H, Cp^*), 1.62 – 1.87 (m, 4H, 2,3- CH_2), 2.21 (s, 3H, ArCH_3), 2.35 – 2.45 (m, 2H, 1,4- CH^{syn}), 2.68 – 2.78 (m, 2H, 1,4- CH^{anti}), 3.40 (s, 3H, OCH_3), 4.17 (q, $^3J_{\text{HH}} = 6$ Hz, 1H, $\text{CH}(\text{OMe})\text{CH}_3$), 5.41 (s, 1H, ArH), 5.63 (s, 1H, ArH). ^{13}C NMR (100 MHz, CDCl_3) δ : 10.0 (Cp^*), 16.4 (CH_3), 17.5 (CH_3), 21.8 (2 x CH_2), 25.4 (CH_2), 25.7 (CH_2), 56.1 (OCH_3), 75.9 ($\text{CH}(\text{OMe})\text{CH}_3$), 85.8 (C^{ArH}), 90.1 (C^{ArH}), 94.3 (Cp^*), 98.2 (C^{Ar}), 100.9 (C^{Ar}), 101.4 (C^{Ar}), 103.4 (C^{Ar}). HRMS (EI): Calcd for ($\text{C}_{24}\text{H}_{35}\text{ORu} - \text{PF}_6$): 441.1726, found 441.1727.**



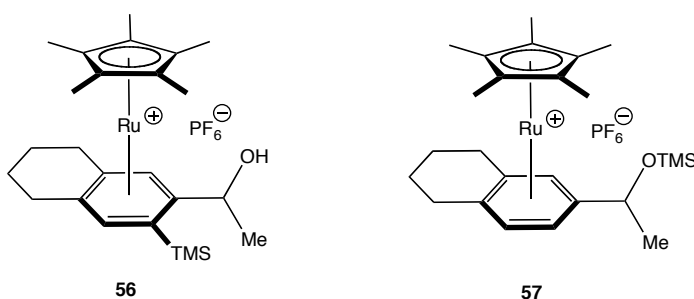
(η^5 -Cyclopentadienyl)(η^6 -6-(1-methoxyethyl)-7-methyl-tetralinyl)ruthenium(II)

hexafluorophosphate (52). After 30 min at 23°C, the NMR scale reaction mixture of **45** with **20** was concentrated and purified by flash silica column chromatography (CH_2Cl_2) followed by crystallization (CH_2Cl_2 : ethyl ether) to afford a mixture of **52-ma** and **52-mi** as a colorless solid. **52-ma** and **52-mi** were isolated after repeated flash silica column chromatography. (**52-ma**). mp 167 - 169°C. ^1H NMR (300 MHz, CDCl_3) δ : 1.40 (d, $^3J_{\text{HH}} = 6$ Hz, 3H, $\text{CH}(\text{OMe})\text{CH}_3$), 1.66 - 1.91 (m, 4H, 2,3- CH_2), 2.31 (s, 3H, ArCH_3), 2.53 - 2.84 (m, 4H, 1,4-CH), 3.49 (s, 3H, OCH_3), 4.34 (q, $^3J_{\text{HH}} = 6$ Hz, 1H, $\text{CH}(\text{OMe})\text{CH}_3$), 5.17 (s, 5H, Cp), 6.11 (s, 1H, ArH), 6.17 (s, 1H, ArH). ^{13}C NMR (75 MHz, CDCl_3) δ : 17.8 (CH_3), 20.7 (CH_3), 22.3 (CH_2), 22.4 (CH_2), 27.7 (CH_2), 28.3 (CH_2), 57.1 (OCH_3), 73.2 ($\text{CH}(\text{OMe})\text{CH}_3$), 81.4 (Cp), 81.5 (C^{ArH}), 87.8 (C^{ArH}), 98.2 (C^{Ar}), 101.4 (C^{Ar}), 102.7 (C^{Ar}), 106.4 (C^{Ar}). HRMS (EI): Calcd for ($\text{C}_{19}\text{H}_{25}\text{ORu} - \text{PF}_6$): 365.0976, found 365.0977. (**52-mi**). mp 188 - 189°C. ^1H NMR (400 MHz, CDCl_3) δ : 1.51 (d, $^3J_{\text{HH}} = 6$ Hz, 3H, $\text{CH}(\text{OMe})\text{CH}_3$), 1.69 - 1.89 (m, 4H, 2,3- CH_2), 2.36 (s, 3H, ArCH_3), 2.64 - 2.83 (m, 4H, 1,4-CH), 3.36 (s, 3H, OCH_3), 4.37 (q, $^3J_{\text{HH}} = 6$ Hz, 1H, $\text{CH}(\text{OMe})\text{CH}_3$), 5.19 (s, 5H, Cp), 6.12 (s, 1H, ArH), 6.14 (s, 1H, ArH). ^{13}C NMR (100 MHz, CDCl_3) δ : 18.3 (CH_3), 20.7 (CH_3), 22.2 (CH_2), 22.3 (CH_2), 27.8 (CH_2), 28.1 (CH_2), 57.2 (OCH_3), 74.4 ($\text{CH}(\text{OMe})\text{CH}_3$), 81.5 (Cp), 84.0 (C^{ArH}), 87.7 (C^{ArH}), 100.1 (C^{Ar}), 101.6 (C^{Ar}), 102.8 (C^{Ar}), 106.1 (C^{Ar}). HRMS (EI): Calcd for ($\text{C}_{19}\text{H}_{25}\text{ORu} - \text{PF}_6$): 365.0976, found 365.0979.



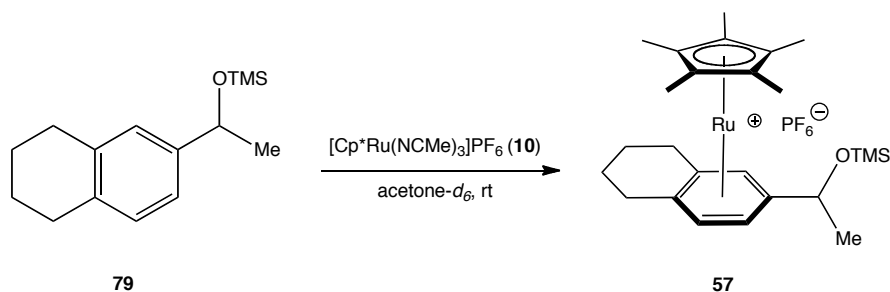
(η^5 -Pentamethylcyclopentadienyl)(η^6 -6-(1-hydroxyethyl)-7-trimethylsilyl-tetralinyl)ruthenium(II) hexafluorophosphate (56) and (η^5 -pentamethylcyclopentadienyl)(η^6 -6-(1-trimethylsiloxyethyl)-tetralinyl)ruthenium(II) hexafluorophosphate (57). **10** (50mg, 0.099mmol) was added to a solution of **53** (29mg, 0.119mmol) in THF/acetone (1:1, 2mL) at 23°C in glove box. After 30 min at 23°C, the reaction mixture was concentrated and purified by repeated flash silica column chromatography (CH₂Cl₂/acetone mixtures) followed by crystallization (CH₂Cl₂ : Et₂O) of separated fractions to afford isolated samples of **56-ma** and isomerized **57-mi** as colorless solids. **56-mi** was obtained as a mixture with **57-mi**. Only a small quantity of **57-ma** was isolated and spectroscopic assignments were verified by a separate arene binding reaction (*vide infra*). (**56-ma**) decomp 205 - 207°C. IR (ZnSe): 3572 (OH) cm⁻¹. ¹H NMR (400 MHz, CDCl₃) δ : 0.41 (s, 9H, TMS), 1.56 (d, ³J_{HH} = 6 Hz, 3H, CH(OH)CH₃), 1.60 – 1.69 (m, 1H, 2/3 - CH^{syn}), 1.85 (s, 15H, Cp*), 1.75 – 1.93 (m, 3H, 2,3-CH^{anti}, 2/3-CH^{syn}), 2.31 (dt, J_{HH} = 17 Hz, 5.5 Hz, 1H, 1/4-CH^{syn}), 2.48 (dt, J_{HH} = 17 Hz, 6 Hz, 1H, 1/4-CH^{syn}), 2.64 – 2.73 (m, 1H, 1/4-CH^{anti}), 2.85 (dt, J_{HH} = 17 Hz, 6 Hz, 1H, 1/4-CH^{anti}), 2.96 (d, ³J_{HH} = 6 Hz, 1H, OH), 4.69 (p, ³J_{HH} = 6 Hz, 1H, CH(OH)CH₃), 5.28 (s, 1H, ArH), 6.00 (s, 1H, ArH). ¹³C NMR (100MHz, CDCl₃) δ : 1.3 (TMS), 10.7 (CpCH₃), 21.8 (CH₂), 21.9 (CH₂), 25.1, 26.2, 27.1 (2 x CH₂, CH(OH)CH₃), 66.3 (CH(OH)CH₃), 84.1 (C^{Ar}H), 88.9 (C^{Ar}H), 92.8 (C^{Ar}), 94.9 (CpCH₃), 100.7 (C^{Ar}), 102.1 (C^{Ar}), 112.5 (C^{Ar}). HRMS (EI): Calcd for (C₂₅H₃₉ORuSi – PF₆): 485.1808, found 485.1807. (**56-mi**) ¹H NMR (300 MHz, CDCl₃) δ : 0.40 (s, 9H, TMS), 1.57 (d, ³J_{HH} = 6.5 Hz, 3H, CH(OH)CH₃), 1.60 – 1.69 (m, 1H, 2/3 - CH^{syn}), 1.83 (s,

15H, Cp*), 1.75 – 1.93 (m, 3H, 2,3-CH^{anti}, 2/3-CH^{syn}), 2.27 – 2.49 (m, 4H, 1,4-CH^{syn}), 2.66 (d, ³J_{HH} = 6.5 Hz, 1H, OH), 2.63 – 2.87 (m, 4H, 1,4-CH^{anti}), 4.59 (p, ³J_{HH} = 6.5 Hz, 1H, CH(OH)CH₃), 5.42 (s, 1H, ArH), 5.65 (s, 1H, ArH). (**57-mi**) decomp 245°C (brown on-set). ¹H NMR (300 MHz, CDCl₃) δ: 0.22 (s, 9H, TMS), 1.51 (d, ³J_{HH} = 6.5 Hz, 3H, CH(OTMS)CH₃), 1.86 (s, 15H, Cp*), 1.63 – 1.91 (m, 4H, 2,3-CH₂), 2.36 – 2.52 (m, 2H, 1,4-CH^{syn}), 2.69 – 2.84 (m, 2H, 1,4-CH^{anti}), 4.69 (q, ³J_{HH} = 6.5 Hz, 1H, CH(OTMS)CH₃), 5.55 (d, ³J_{HH} = 6.5 Hz, 1H, ArH), 5.68 (s, 1H, 5-ArH), 5.81 (d, ³J_{HH} = 6.5 Hz, 1H, ArH). ¹³C NMR (100 MHz, CDCl₃) δ: 1.1 (TMS), 10.4 (CpCH₃), 21.7 (CH₂), 21.8 (CH₂), 25.9, 26.3, 27.0 (2 x CH₂, CH(OTMS)CH₃), 67.7 (CH(OTMS)CH₃), 82.8 (C^{Ar}H), 83.9 (C^{Ar}H), 86.8 (C^{Ar}H), 94.7 (CpCH₃), 100.9 (C^{Ar}), 101.6 (C^{Ar}), 108.8 (C^{Ar}). HRMS (EI): Calcd for (C₂₅H₃₈ORuSi – H – PF₆): 484.1730, found 484.1734.



(η^5 -Pentamethylcyclopentadienyl)(η^6 -6-(1-trimethylsilyloxyethyl)-tetralinyl)ruthenium (II) hexafluorophosphate (**57**). **10** (21 mg, 0.042 mmol) was added to a solution of **79** (10 mg, 0.042 mmol) in acetone-*d*₆ (0.42 mL) at 23°C in glove box. After 15.5 h at 23°C, the reaction mixture was concentrated and purified by flash alumina column chromatography (CH₂Cl₂) followed by crystallization (CH₂Cl₂ : ethyl ether) to afford a mixture of **57-ma** and **57-mi** as a colorless solid (16 mg, 0.025 mmol, 61%). (**57-ma**) ¹H NMR (300 MHz, CDCl₃) δ: 0.24 (s, 9H, TMS), 1.50 (d, ³J_{HH} = 6 Hz, 3H, CH(OTMS)CH₃), 1.85 (s, 15H, Cp*), 1.60 – 1.90 (m, 4H, 2,3-CH₂), 2.34 – 2.47 (m, 2H, 1,4-CH^{syn}), 2.69 – 2.82 (m, 2H, 1,4-CH^{anti}), 4.67 (q, ³J_{HH} = 6 Hz, 1H, CH(OTMS)CH₃), 5.65 (s, 1H, 5-ArH), 5.68 (d, ³J_{HH} = 6 Hz, 1H, ArH), 5.74 (d, ³J_{HH} = 6 Hz, 1H, ArH). ¹³C NMR (100 MHz, CDCl₃) δ: 1.1 (TMS), 10.2 (CpCH₃), 21.8 (CH₂), 21.9 (CH₂), 25.8,

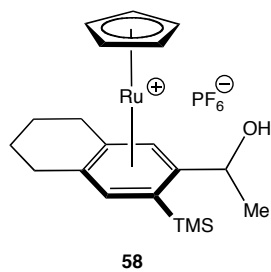
26.3, 27.2 (2 x CH₂, CH(OTMS)CH₃), 67.6 (CH(OTMS)CH₃), 83.0 (C^{Ar}H), 83.4 (C^{Ar}H), 86.8 (C^{Ar}H), 94.7 (CpCH₃), 100.3 (C^{Ar}), 101.4 (C^{Ar}), 108.8 (C^{Ar}). HRMS for mixture (ESI): Calcd for (C-²⁵H₃₉ORuSi – PF₆): 479.1841, found 479.1832.



(η^5 -Cyclopentadienyl)(η^6 -6-(1-hydroxyethyl)-7-trimethylsilyl-tetralinyl)ruthenium (II)

hexafluorophosphate (58). **20** (50 mg, 0.114 mmol) was added to a solution of **53** (53 mg, 0.215 mmol) and γ -terpinene (0.070 mL, 0.437 mmol) in acetone-*d*₆ (11 mL) at 23°C in glove box. After 16h at 23°C, the reaction mixture was concentrated and purified by repeated flash silica column chromatography (acetone/CH₂Cl₂ solvent mixtures) followed by crystallization (CH₂Cl₂/EtOAc : hexanes) to afford **58** as mixture of diastereomers as a colorless solid. ¹H NMR (300 MHz, CDCl₃) δ : 0.42 (s, 18H, TMS), 1.51 (d, ³J_{HH} = 6 Hz, 3H, dia1-CH(OH)CH₃), 1.56 (d, ³J_{HH} = 6 Hz, 3H, dia2-CH(OH)CH₃), 1.68 – 1.92 (m, 8H, 2,3-CH₂), 2.57 – 2.93 (m, 9H, 1,4-CH₂, dia2-OH), 3.11 (d, ³J_{HH} = 6 Hz, dia1-OH), 4.66 (p, ³J_{HH} = 6 Hz, 1H, dia1-CH(OH)CH₃), 4.77 (p, ³J_{HH} = 6 Hz, 1H, dia2-CH(OH)CH₃), 5.19 (s, 5H, dia2-Cp), 5.23 (s, 5H, dia1-Cp), 5.72 (s, 1H, dia1-ArH), 5.83 (s, 1H, dia2-ArH), 6.25 (s, 1H, dia2-ArH), 6.34 (s, 1H, dia1-ArH). ¹³C NMR (125 MHz, CDCl₃) δ : 0.80 (dia1-TMS), 1.25 (dia2-TMS), 22.18 (dia2-CH₂), 22.23 (dia1-CH₂), 22.3 (dia2-CH₂), 22.4 (dia1-CH₂), 25.0 (dia2-CH(OH)CH₃), 26.3 (dia1-CH(OH)CH₃), 27.9 (dia2-CH₂), 28.2 (dia1-CH₂), 28.3 (dia1,dia2-CH₂), 66.0 (dia1-CH(OH)CH₃), 67.8 (dia2-CH(OH)CH₃), 80.99 (dia2-Cp), 81.18 (dia1-Cp), 82.4 (dia1-C^{Ar}H), 84.4 (dia2-C^{Ar}H), 88.5 (dia1-C^{Ar}H), 89.2 (dia2-C^{Ar}H), 93.4 (dia1,dia2-C^{Ar}), 102.85 (dia1-C^{Ar}), 102.88 (dia2-C^{Ar}), 103.1 (dia1-C^{Ar}), 103.3 (dia2-

C^{Ar}), 111.9 (dia2- C^{Ar}), 114.6 (dia1- C^{Ar}). HRMS (EI): Calcd for ($C_{20}H_{29}ORuSi - PF_6$): 409.1058, found 409.1062.



vii. 1H and ^{13}C NMR spectra for characterized compounds.

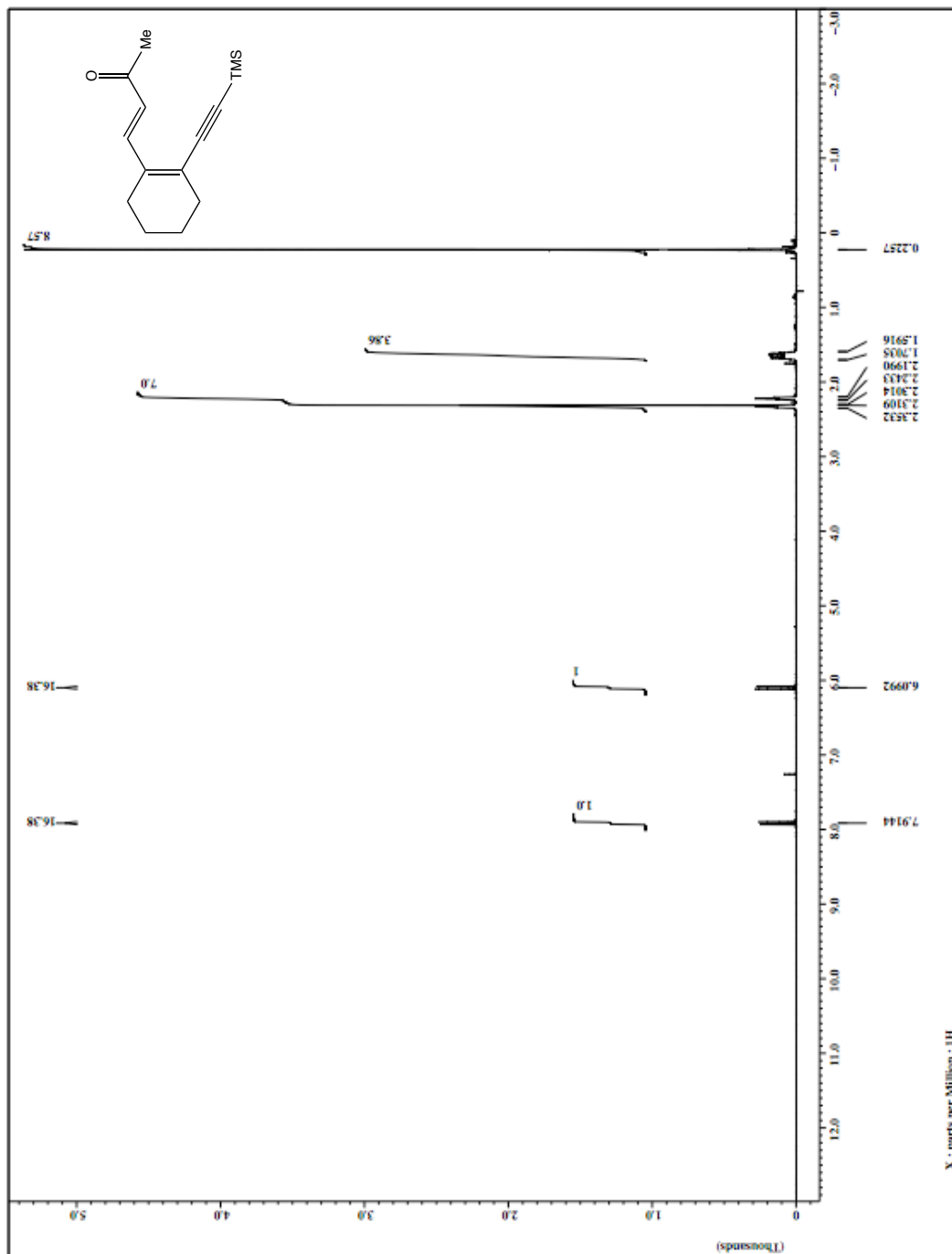


Figure 3-5. 75 ^1H NMR spectrum (500 MHz, CDCl_3).

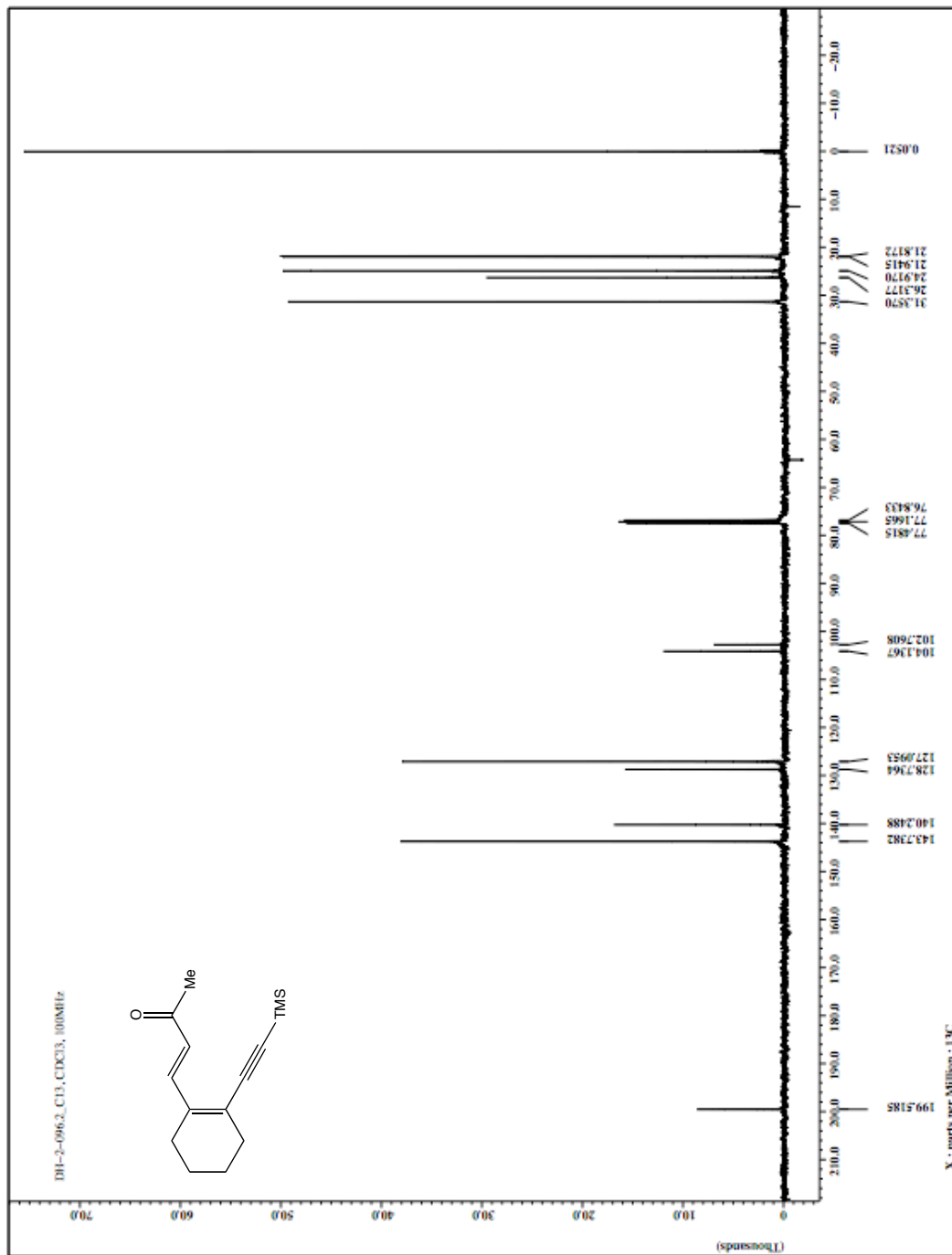


Figure 3-6. 75 ¹³C NMR spectrum (100 MHz, CDCl₃).

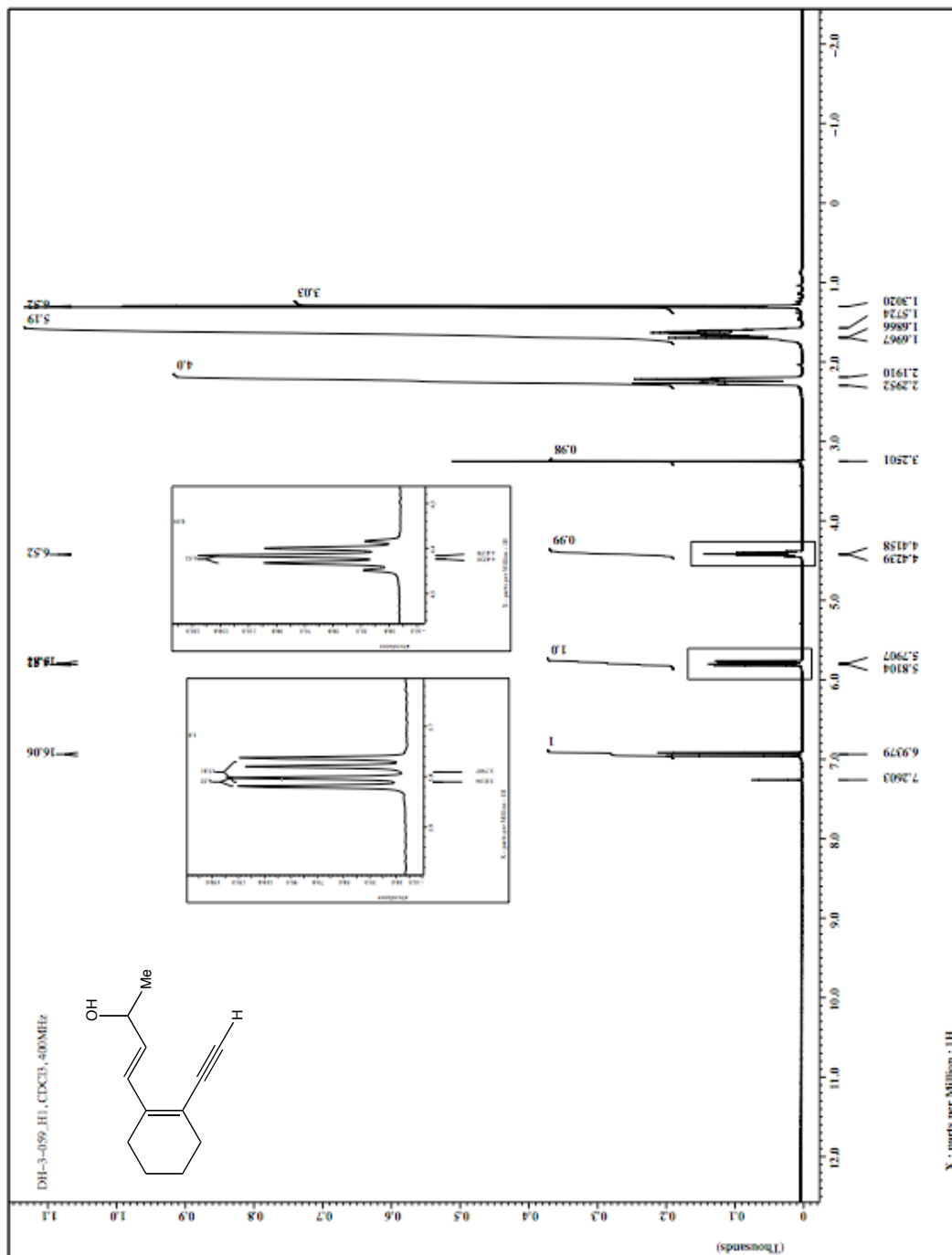


Figure 3-7. 39 ¹H NMR spectrum (400 MHz, CDCl₃).

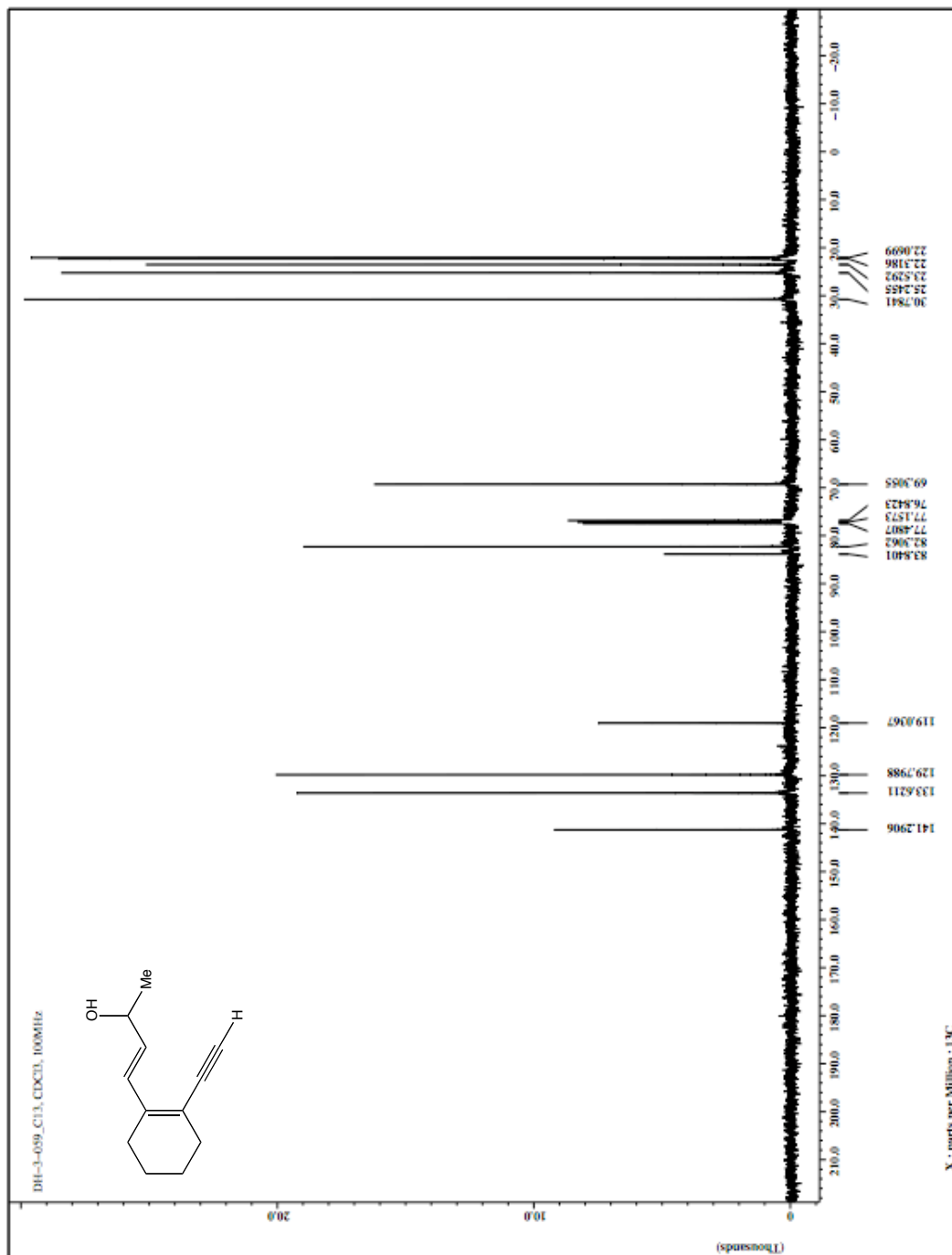


Figure 3-8. 39 ^{13}C NMR spectrum (100 MHz, CDCl_3).

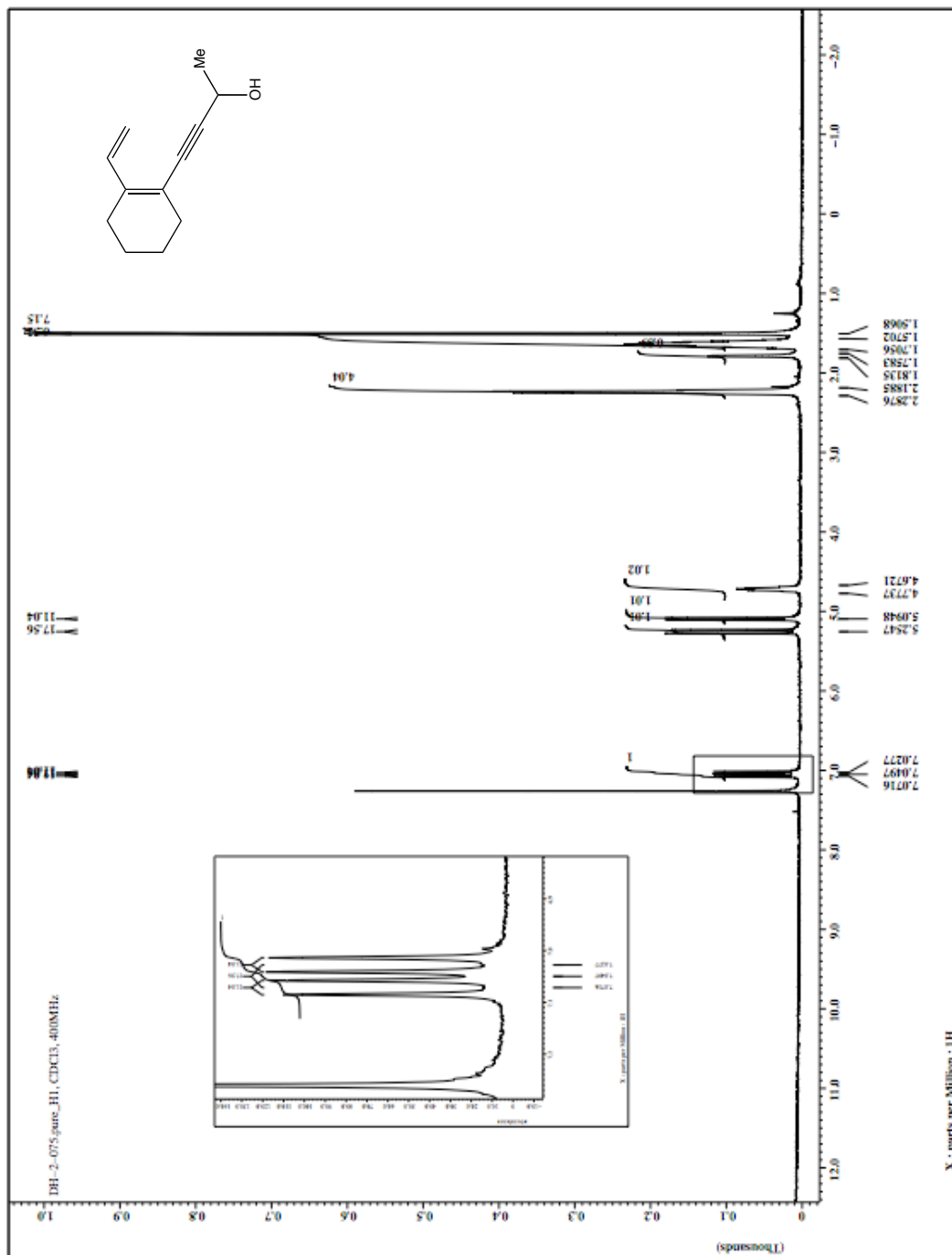


Figure 3-9. 40 ^1H NMR spectrum (400 MHz, CDCl₃).

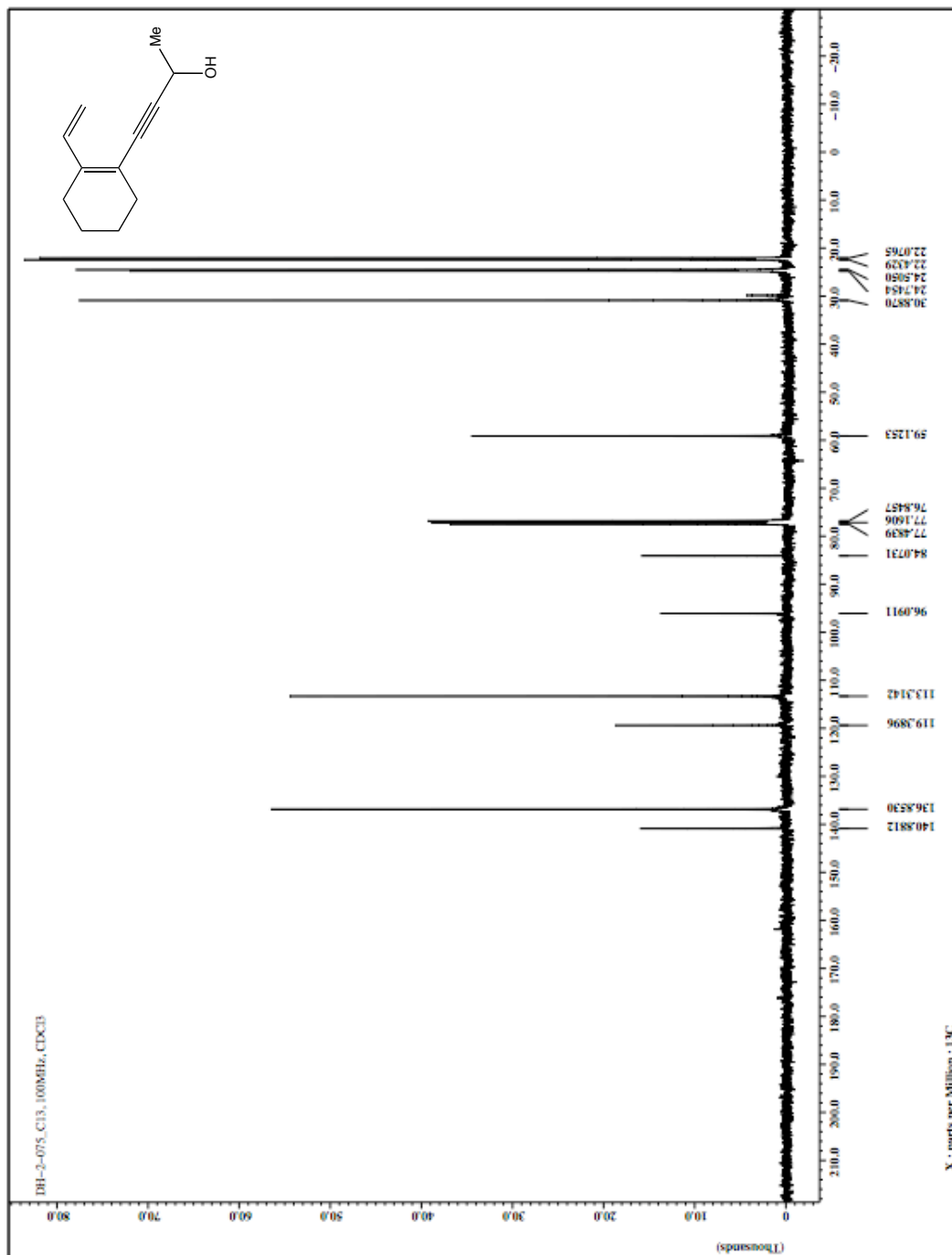


Figure 3-10. 40 ¹³C NMR spectrum (100 MHz, CDCl₃).

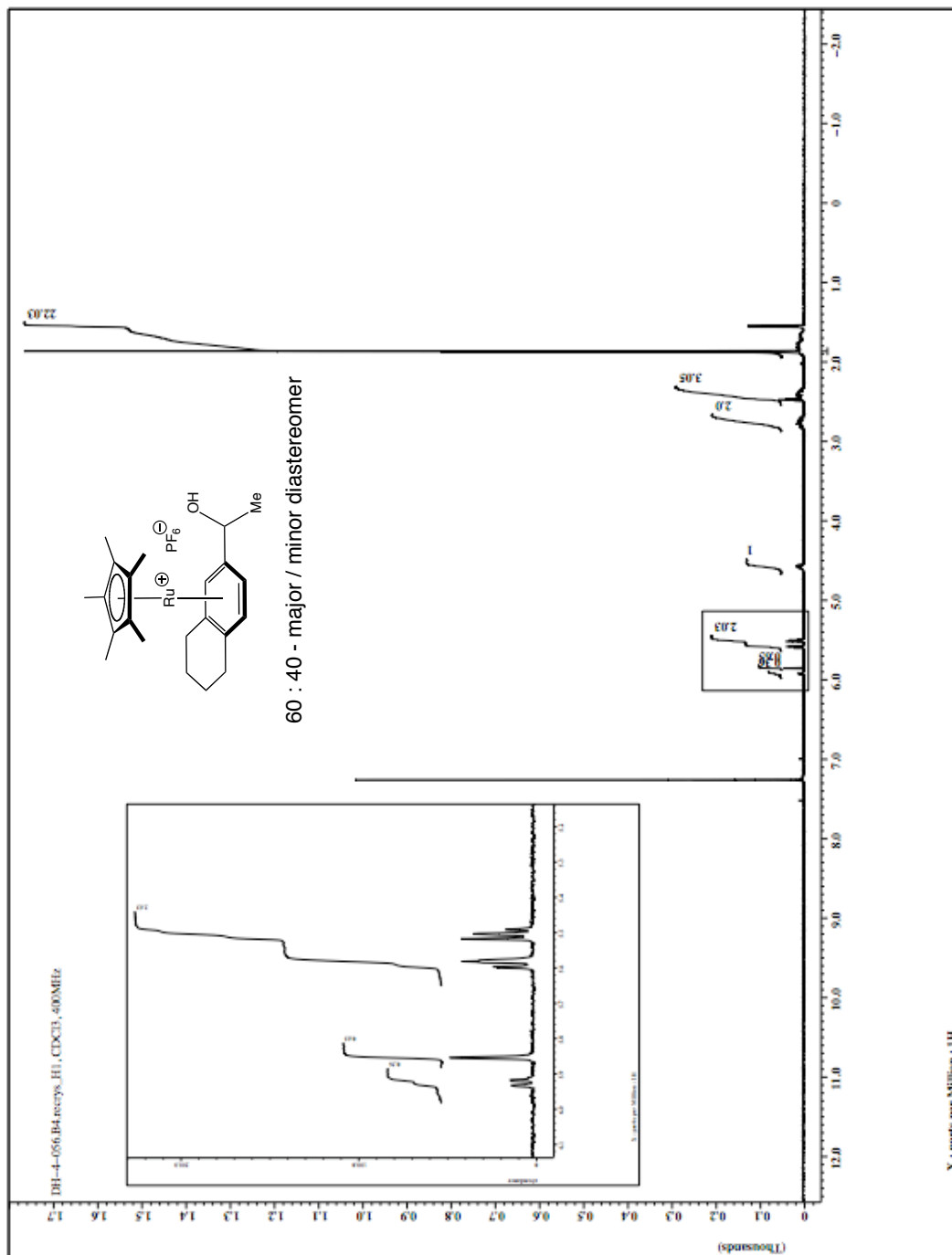


Figure 3-11. 42 ^1H NMR spectrum (400 MHz, CDCl₃).

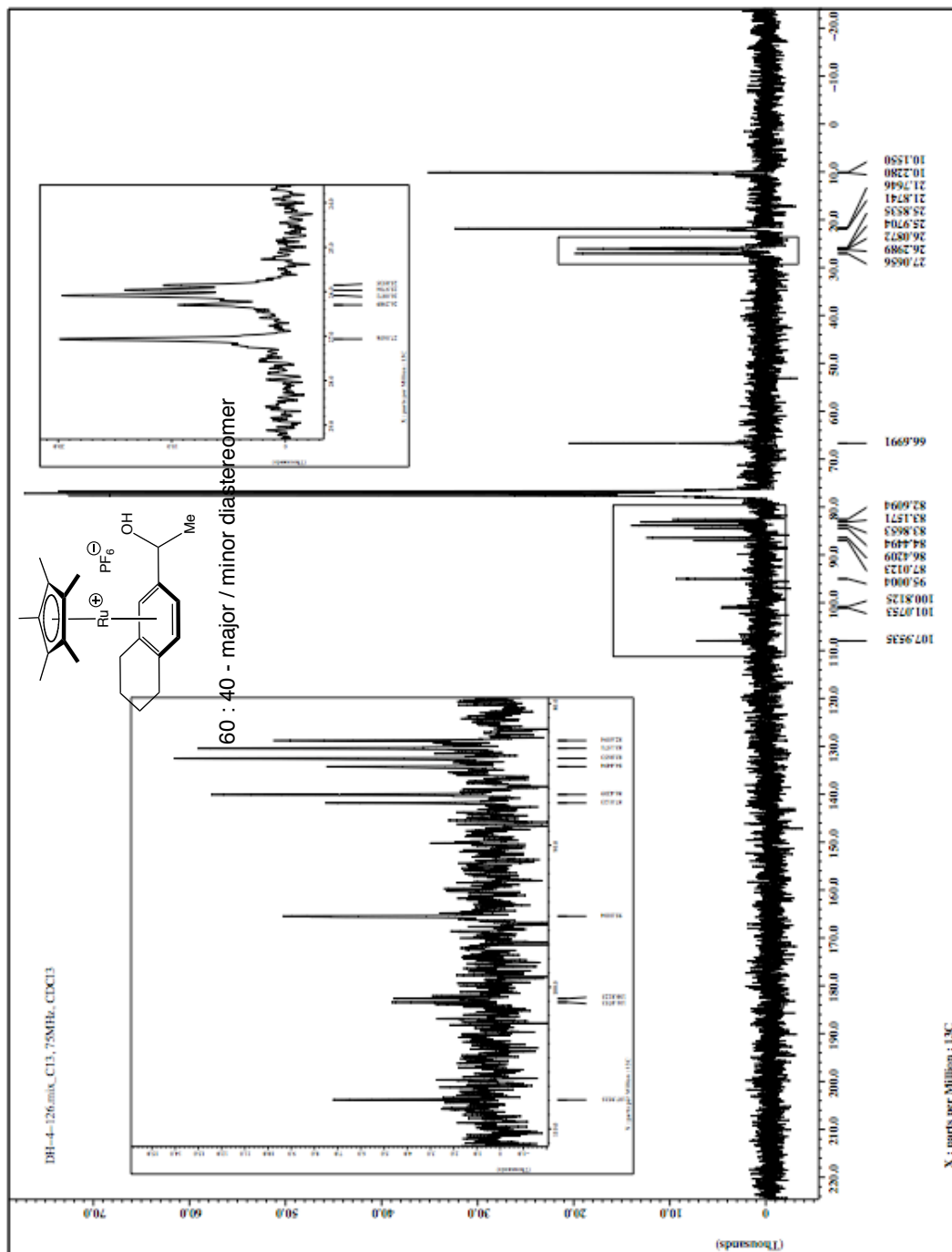


Figure 3-12. 42 ¹³C NMR spectrum (75 MHz, CDCl₃).

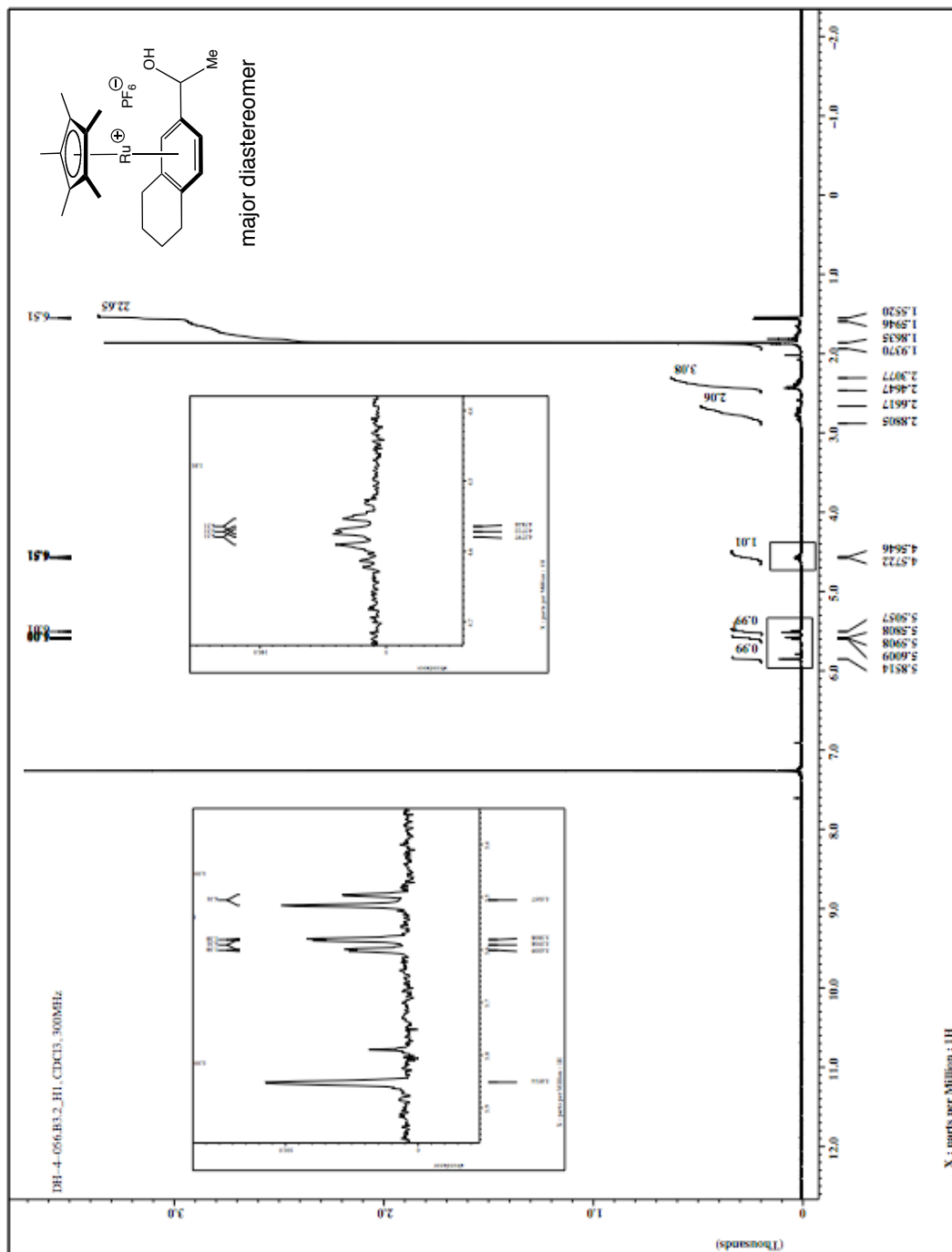


Figure 3-13. 42-ma ^1H NMR spectrum (300 MHz, CDCl_3).

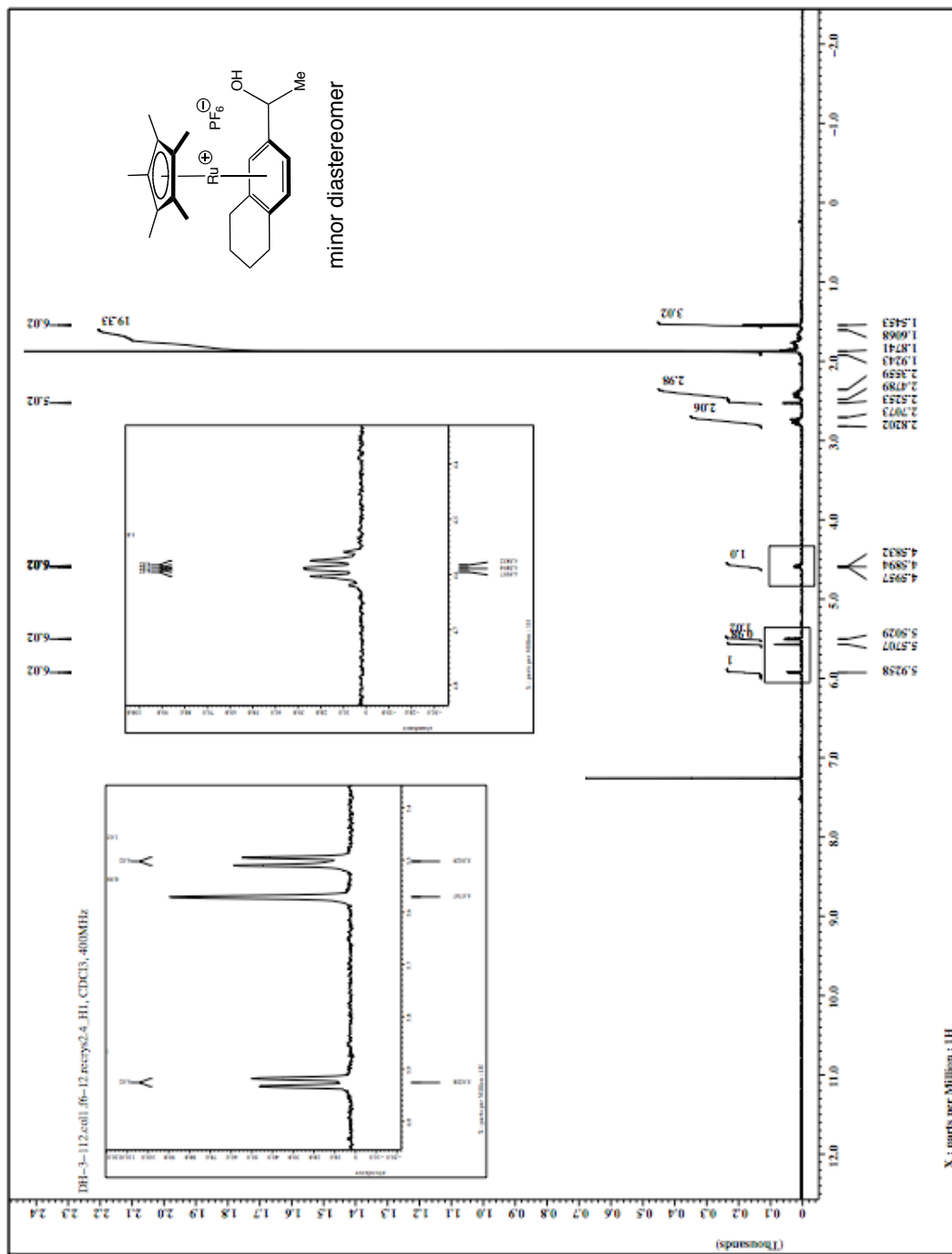


Figure 3-14. 42-mi ^1H NMR spectrum (400 MHz, CDCl_3).

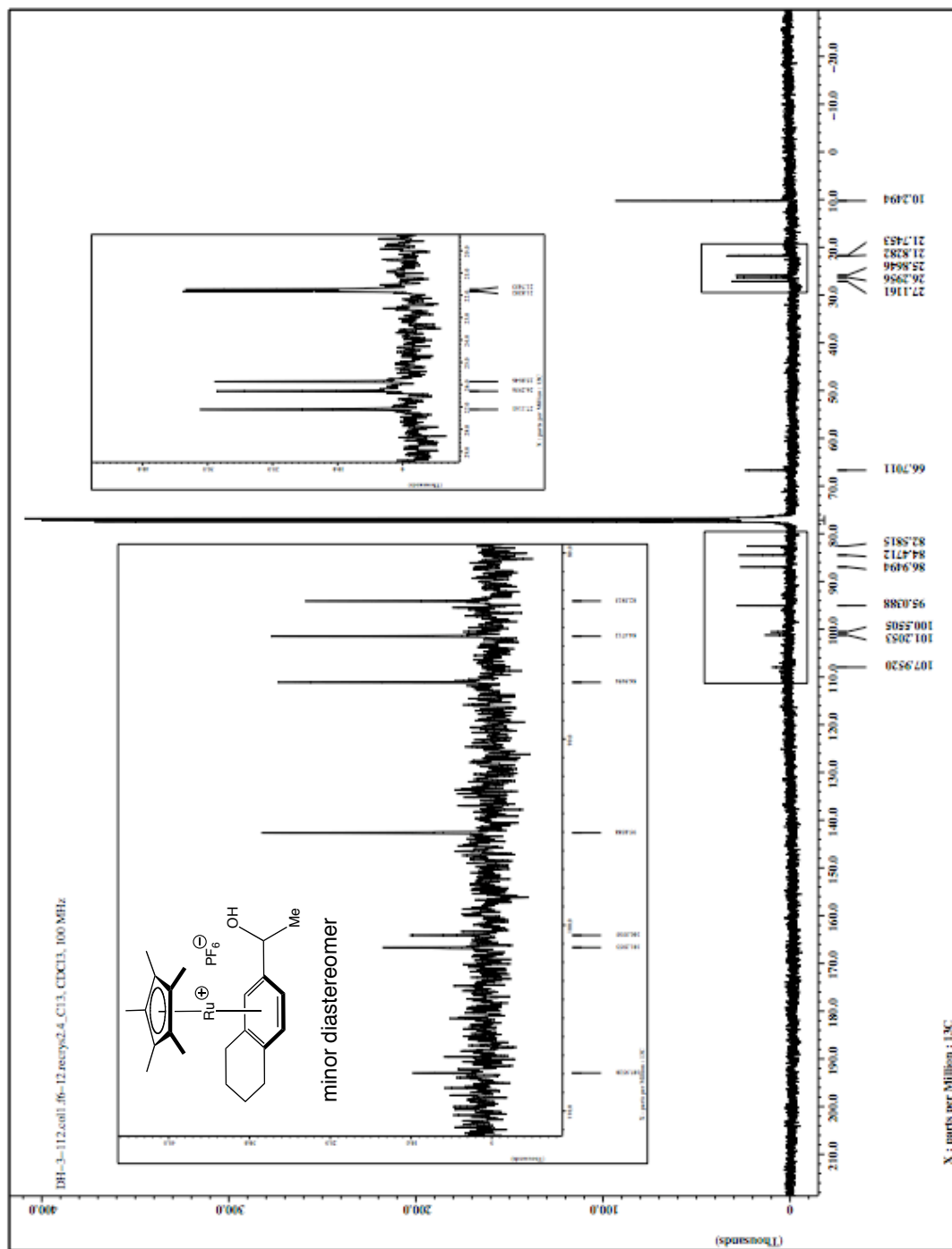


Figure 3-15. 42-mi ^{13}C NMR spectrum (100 MHz, CDCl_3).

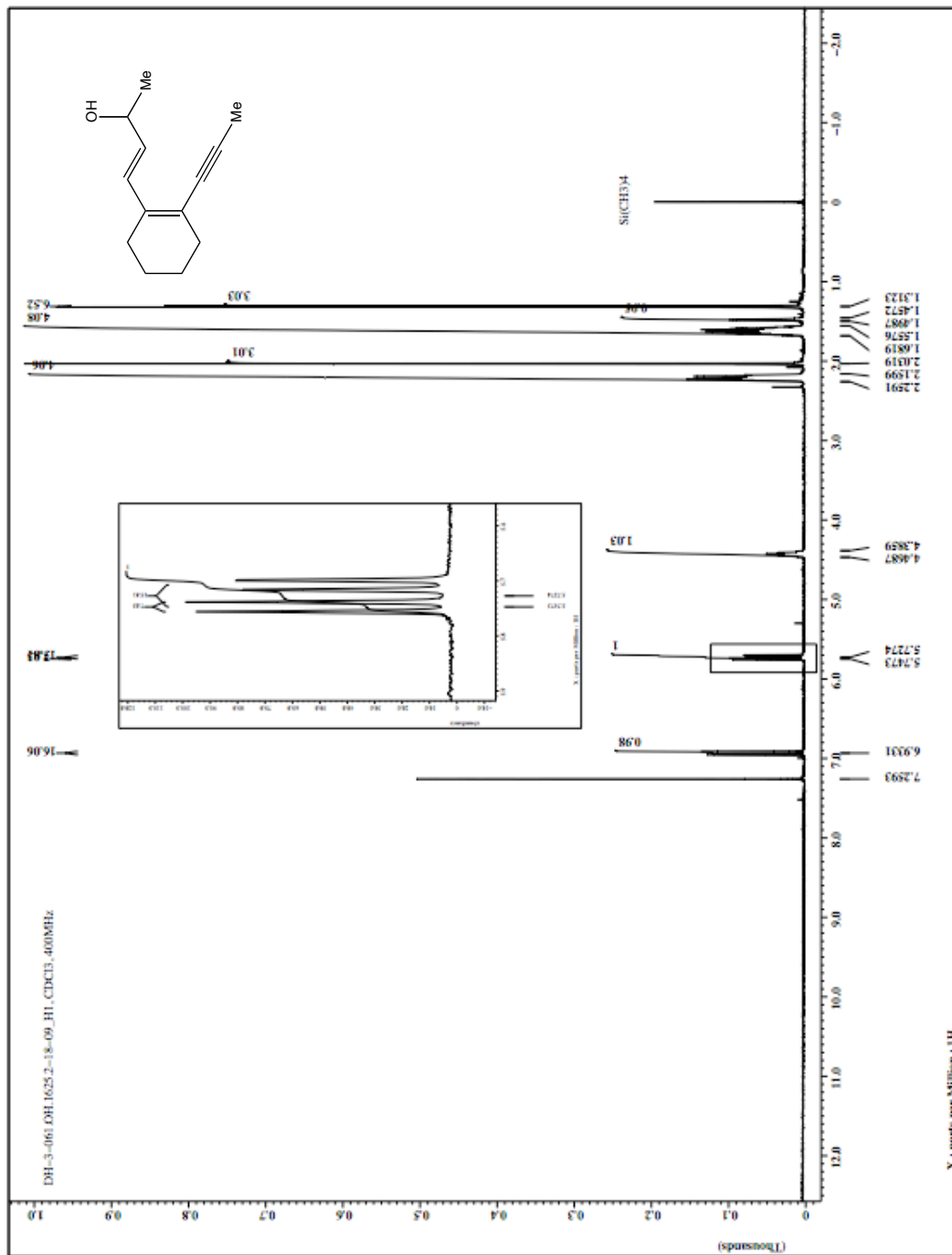


Figure 3-16. 43 ¹H NMR spectrum (400 MHz, CDCl₃).

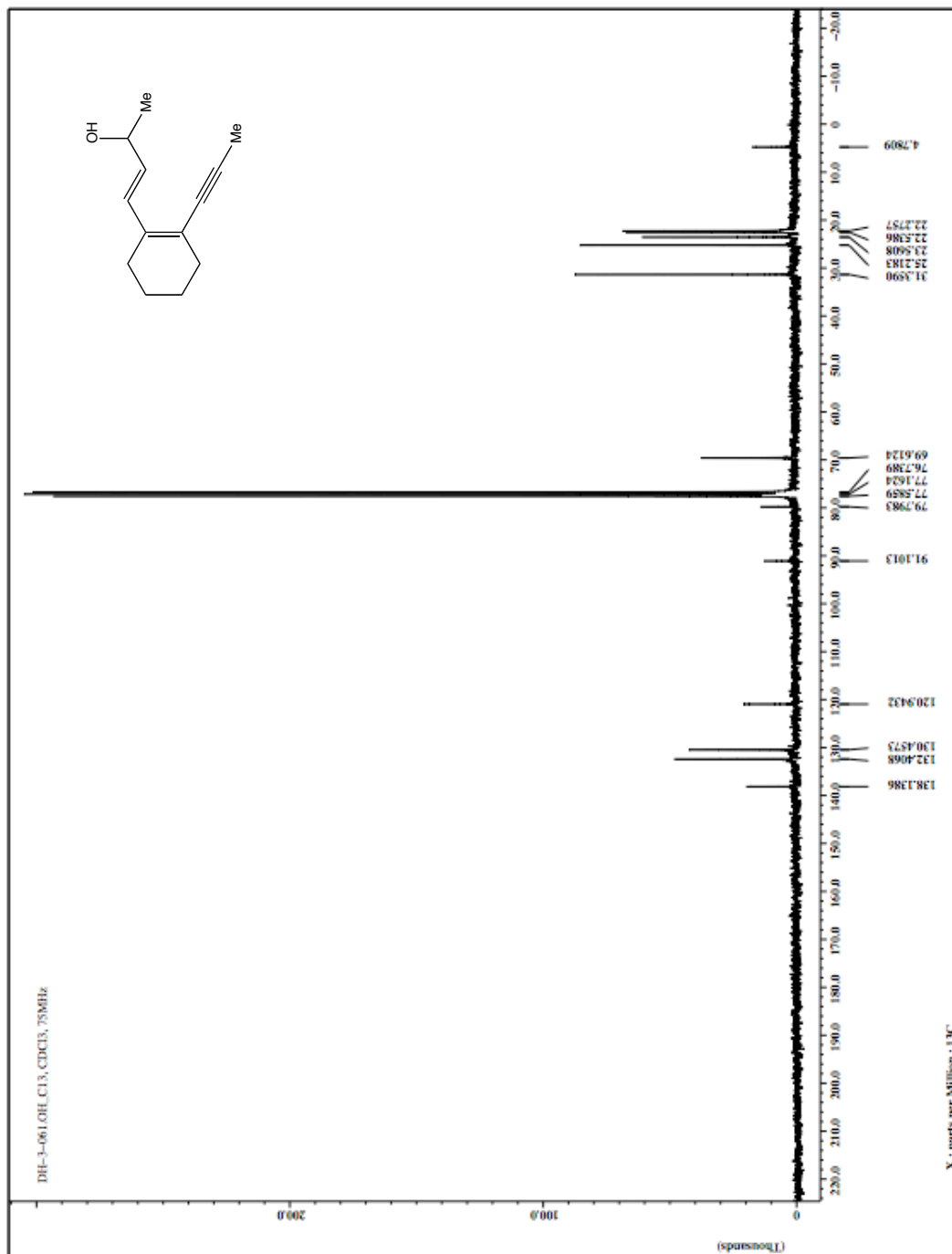


Figure 3-17. 43 ^{13}C NMR spectrum (75 MHz, CDCl_3).

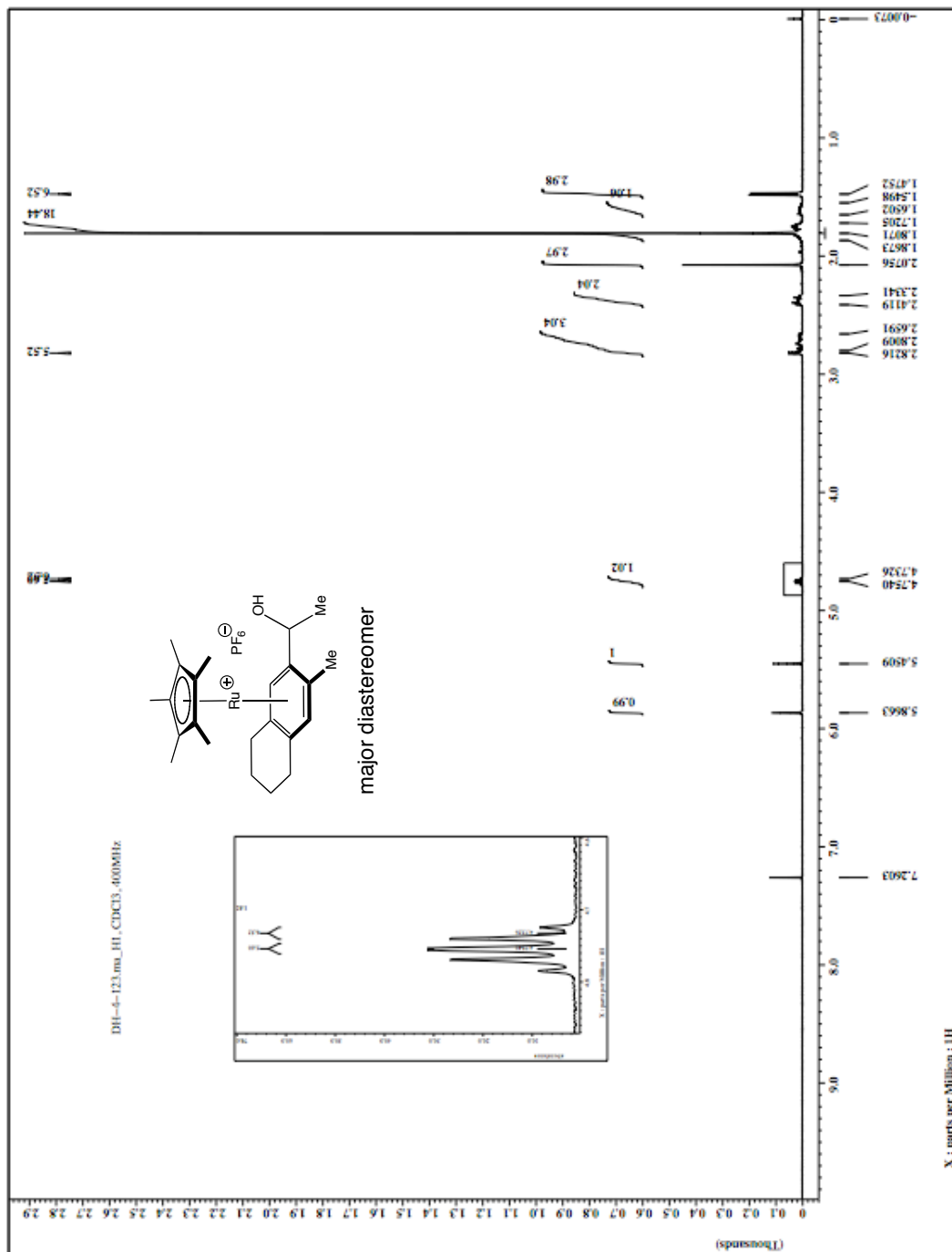


Figure 3-18. 48-ma ¹H NMR spectrum (400 MHz, CDCl₃).

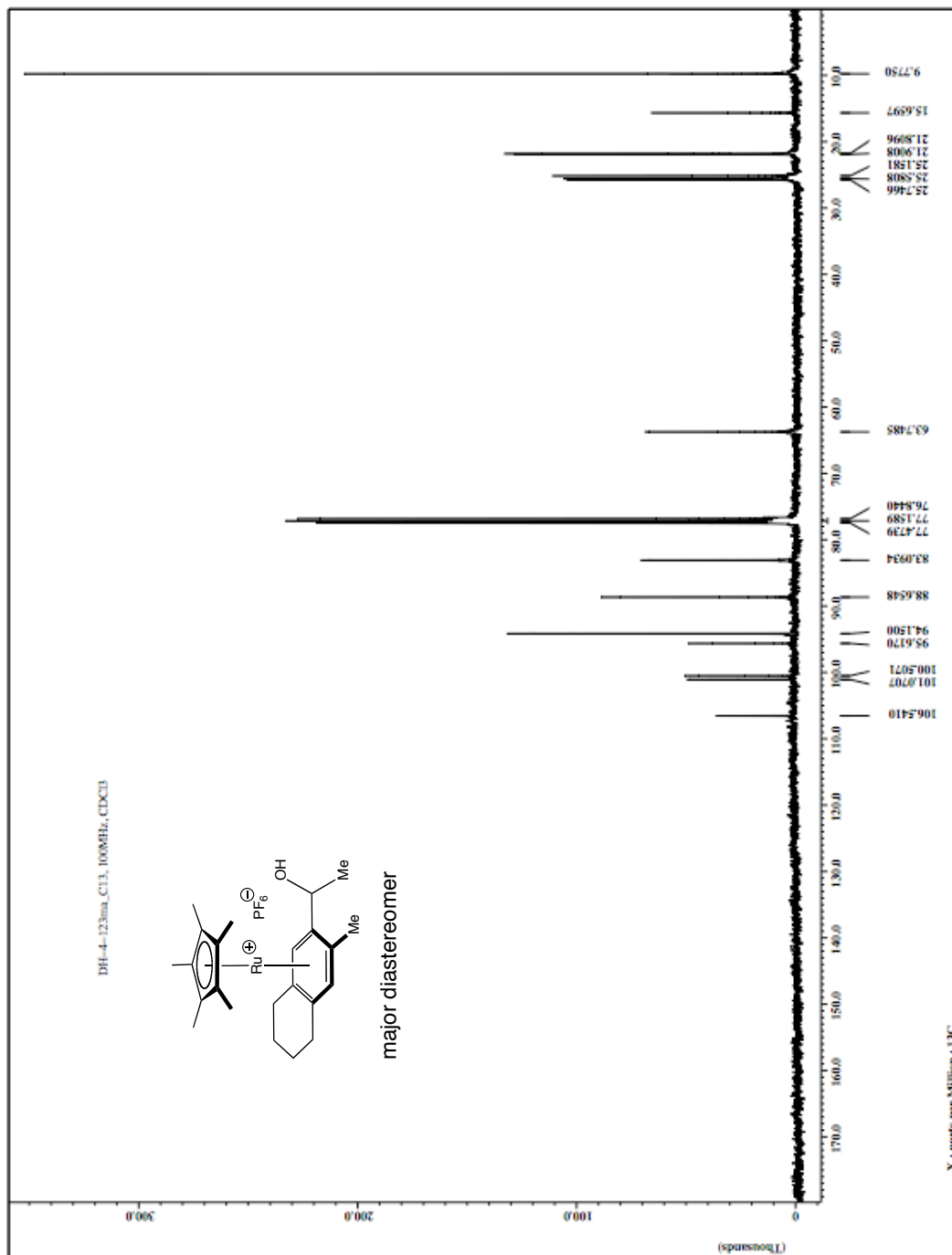


Figure 3-19. 48-ma ^{13}C NMR spectrum (100 MHz, CDCl_3).

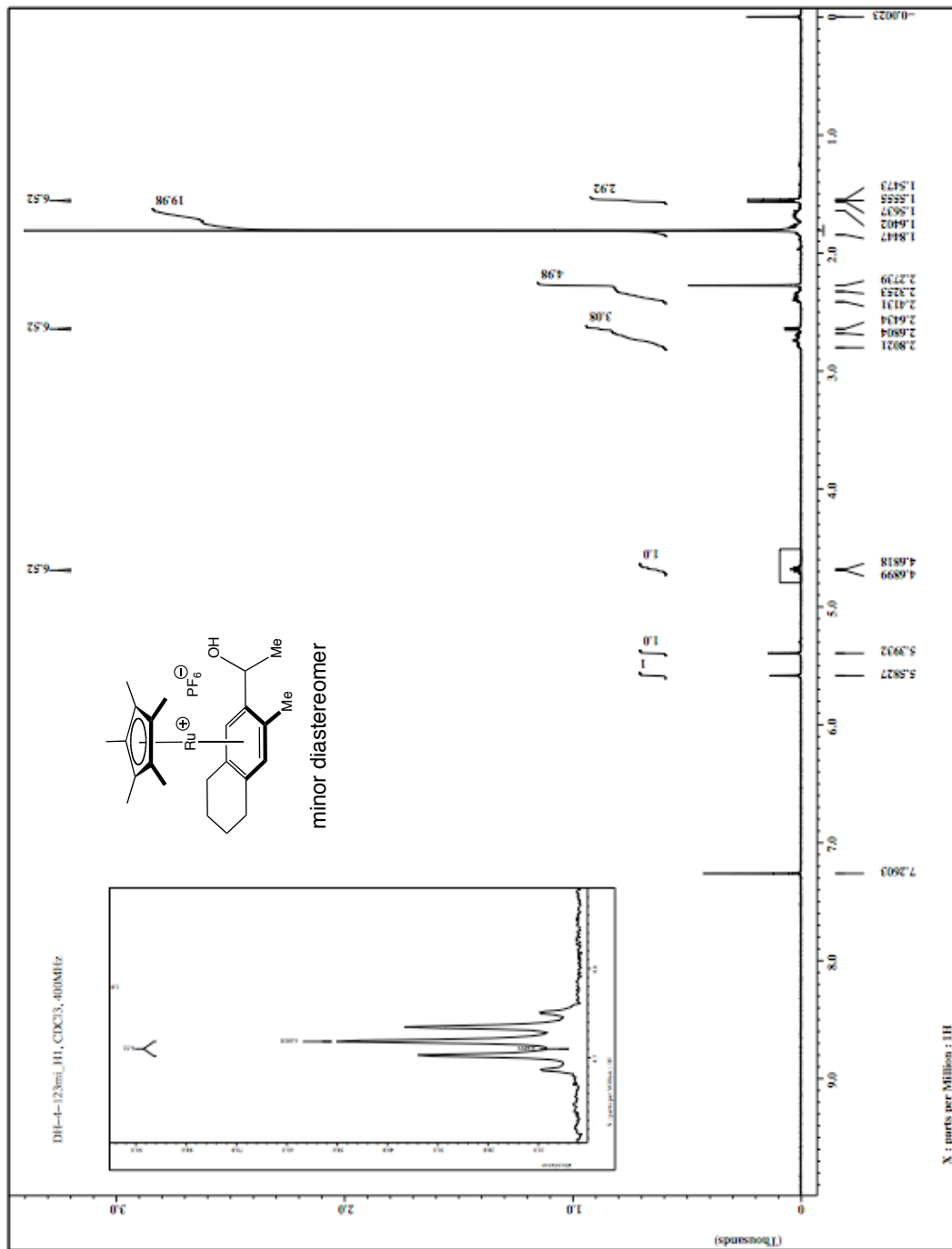


Figure 3-20. 48-mi ^1H NMR spectrum (CDCl_3 , 400MHz).

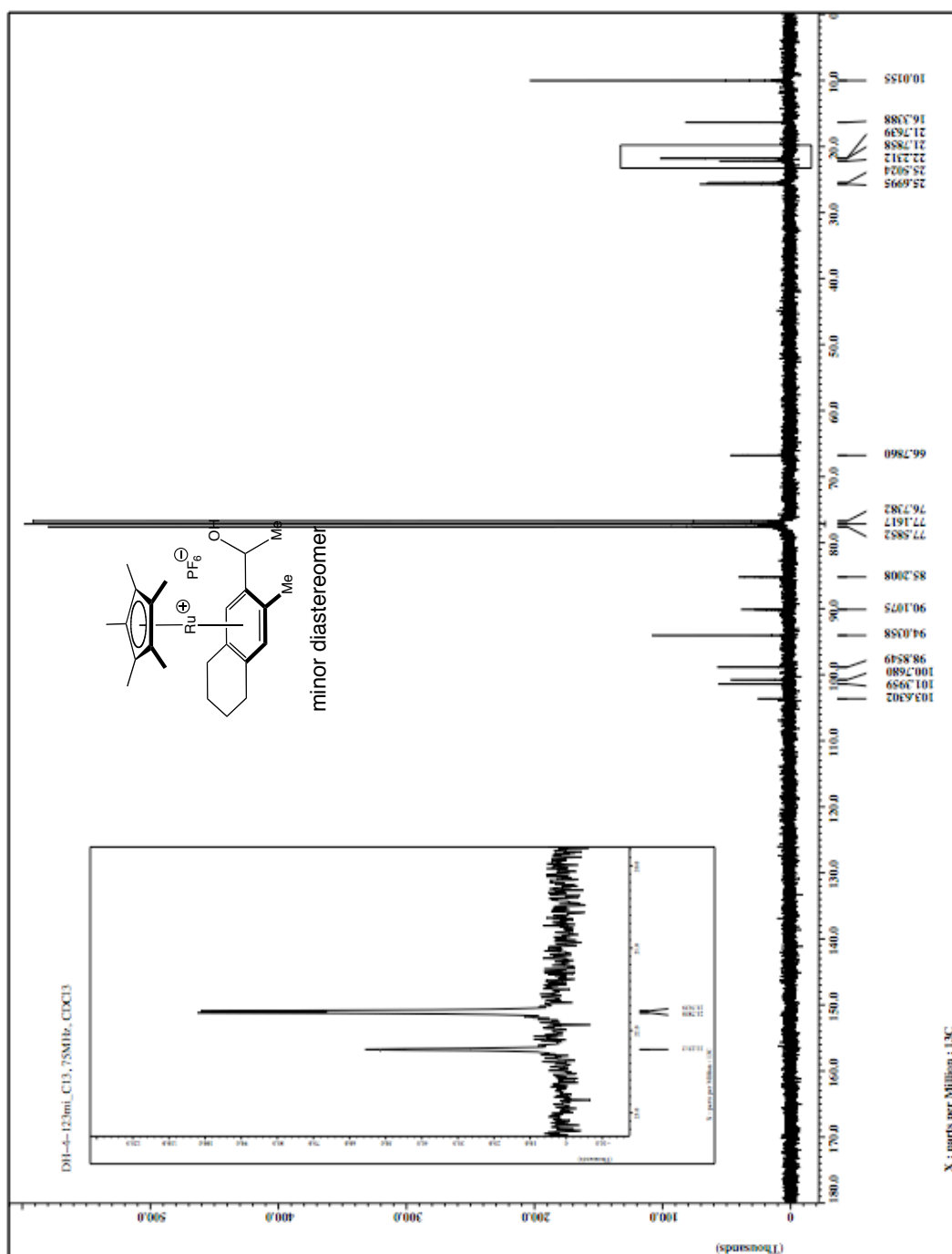


Figure 3-21. 48-mi ¹³C NMR spectrum (CDCl₃, 75 MHz).

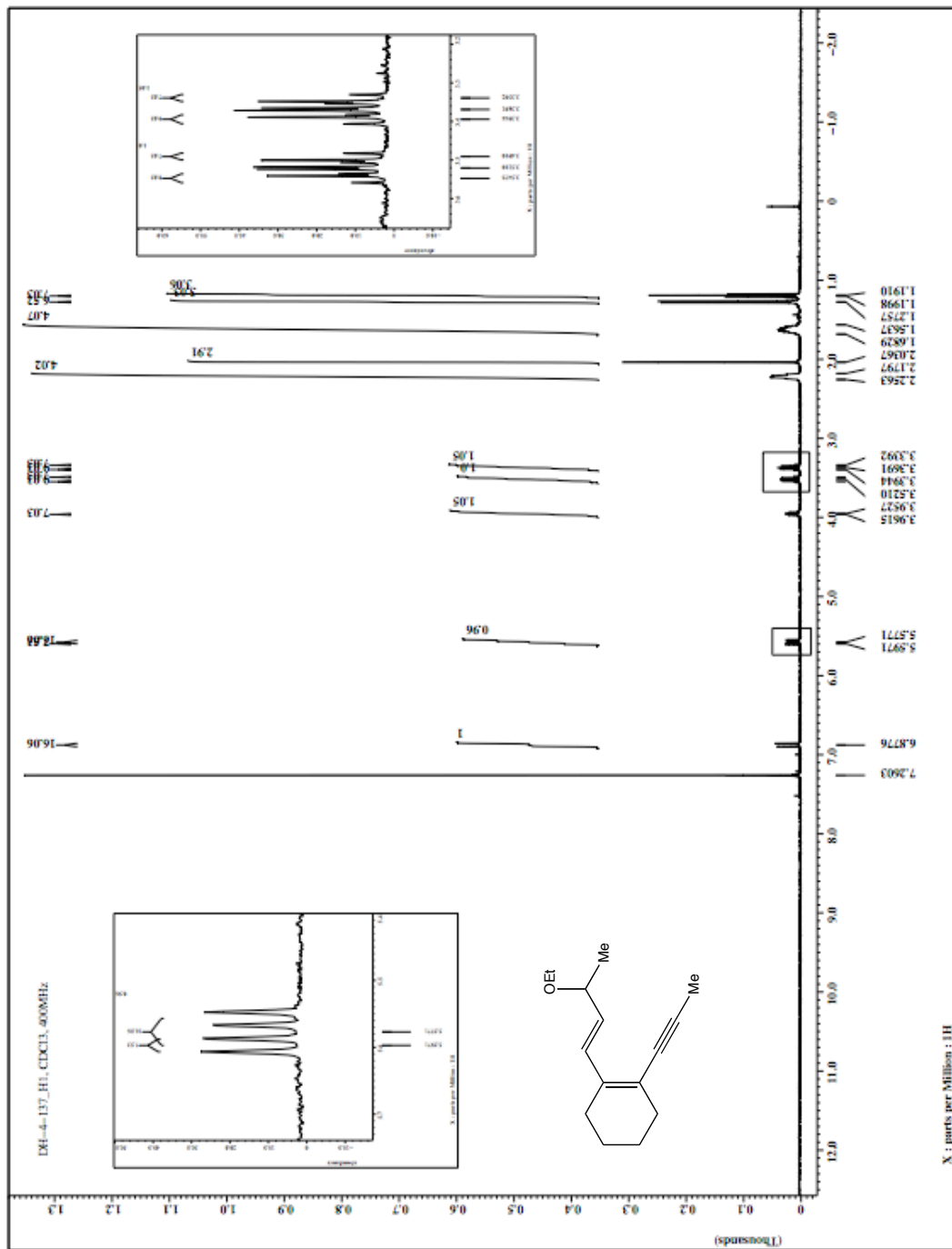


Figure 3-22. 44 ¹H NMR spectrum (CDCl₃, 400 MHz).

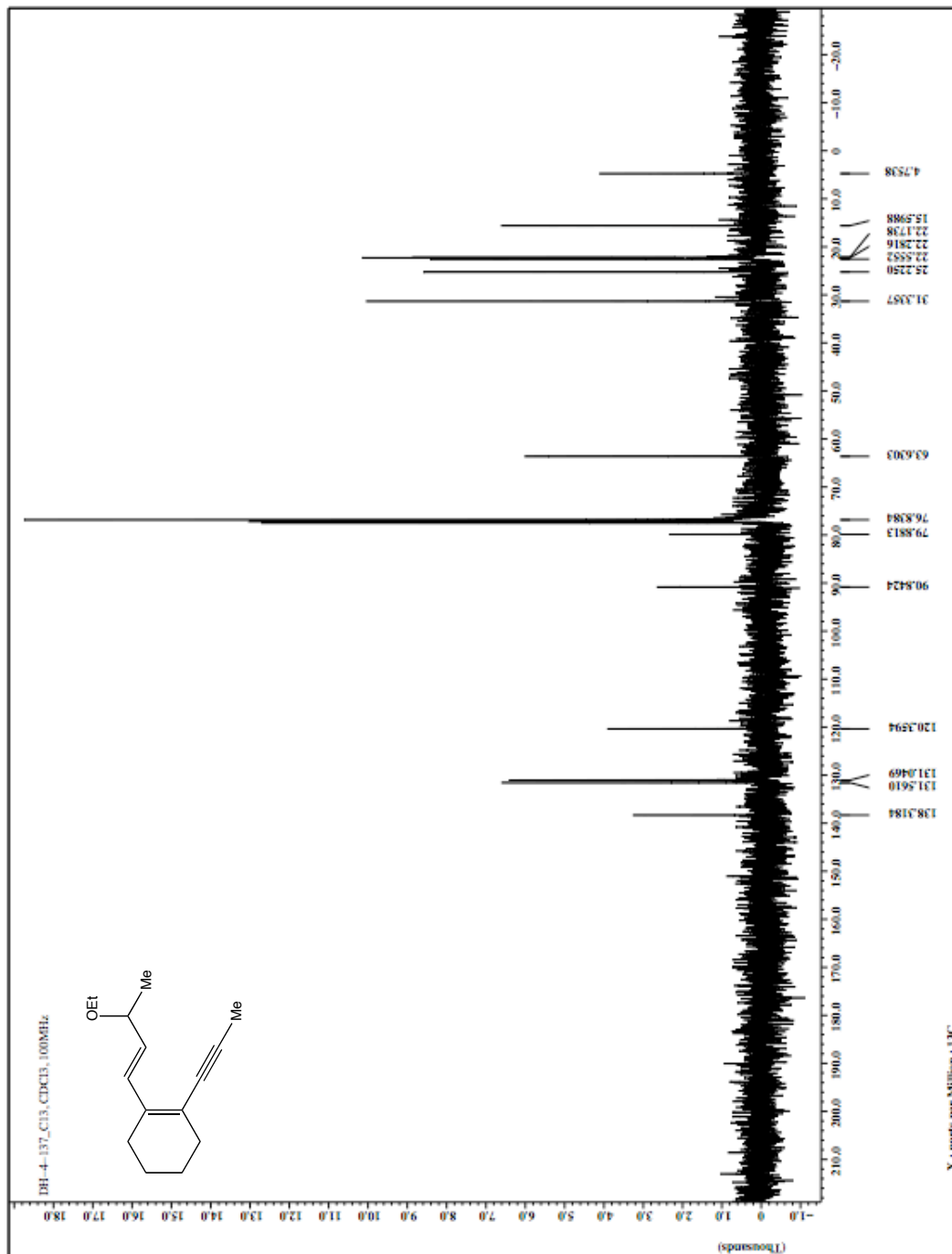


Figure 3-23. 44 ^{13}C NMR spectrum (CDCl_3 , 100 MHz).

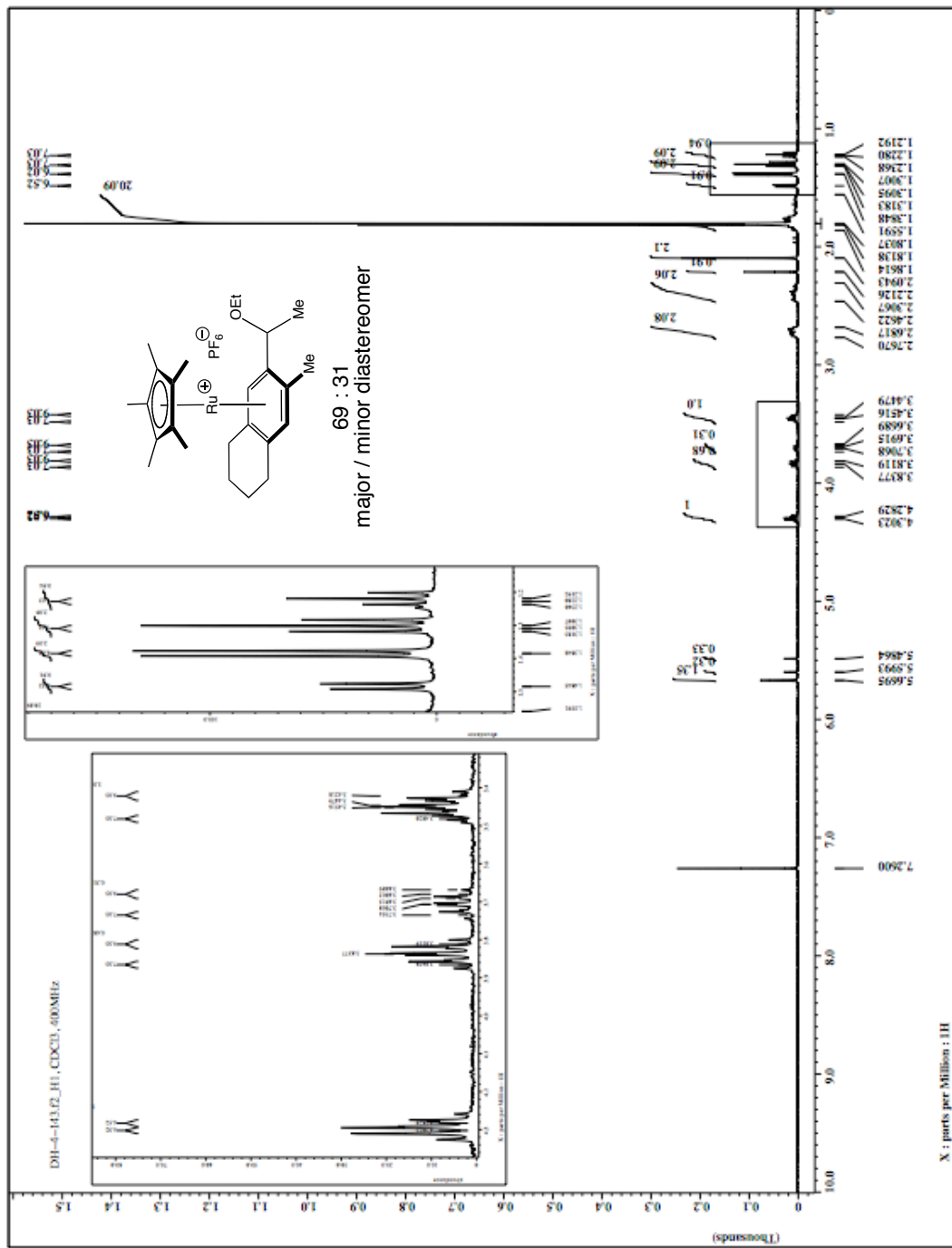


Figure 3-24. 49-ma > 49-mi ¹H NMR spectrum (CDCl₃, 400 MHz).

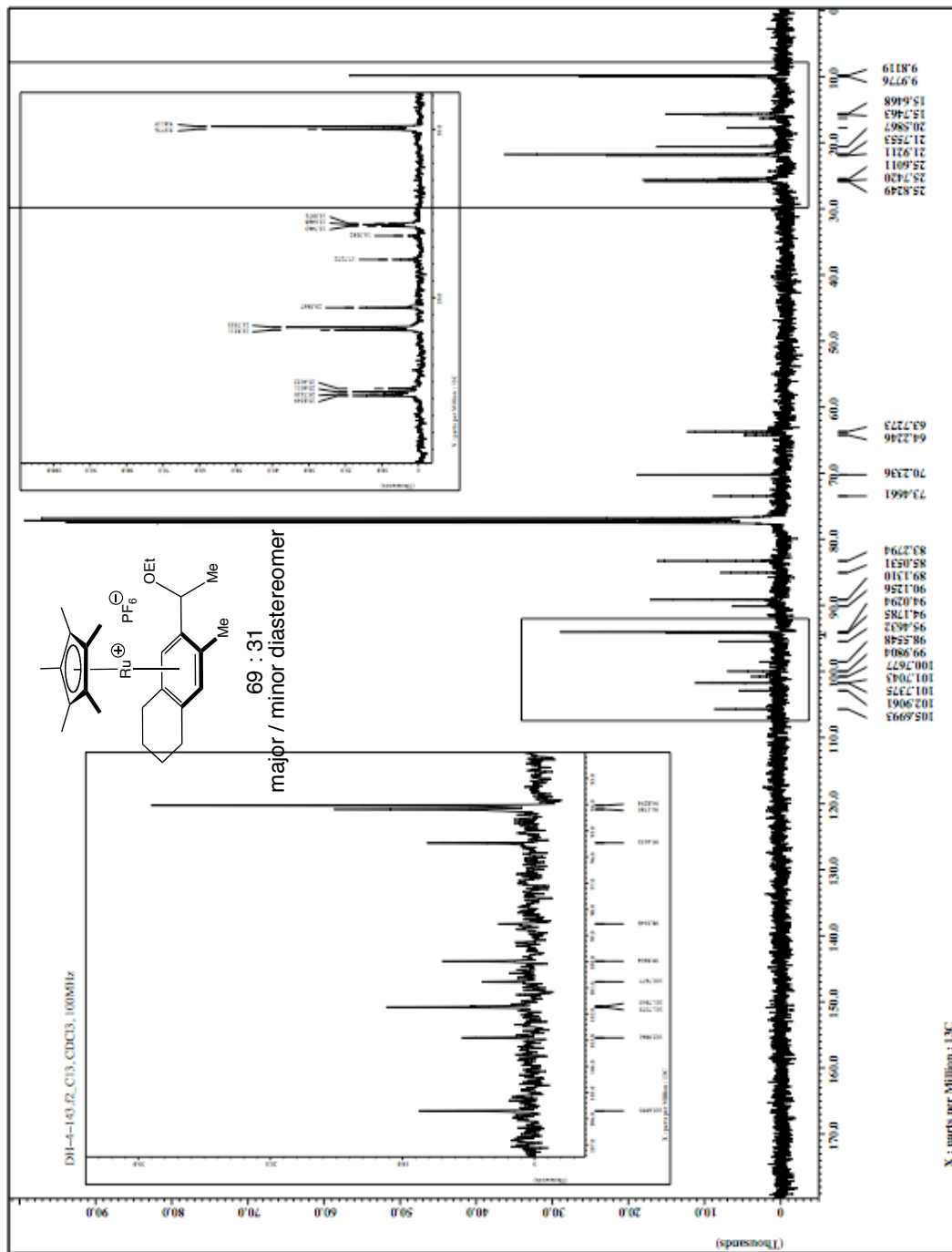


Figure 3-25. 49-ma > 49-mi ¹³C NMR spectrum (CDCl₃, 100 MHz).

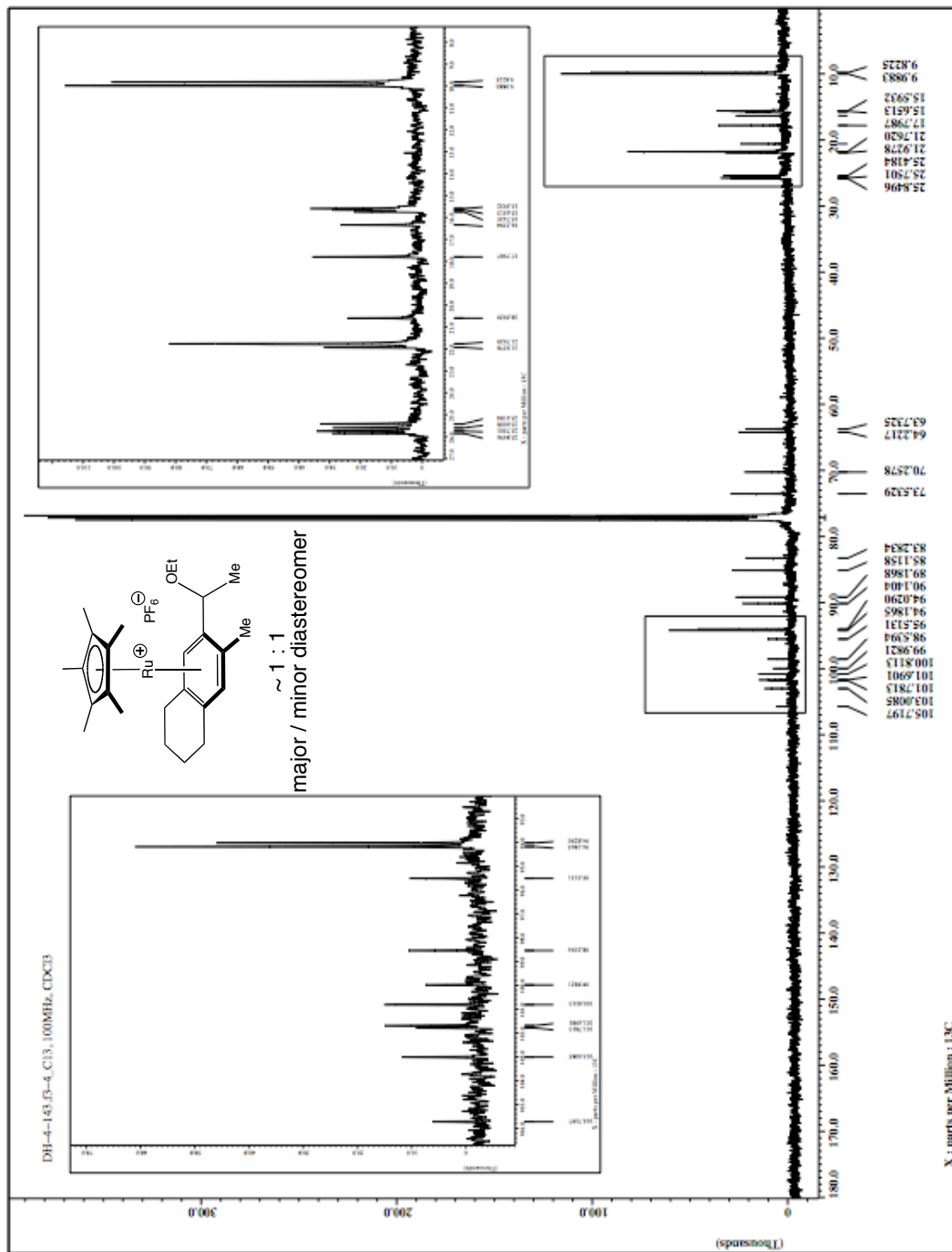


Figure 3-27. 49 ^{13}C NMR spectrum (CDCl_3 , 100 MHz).

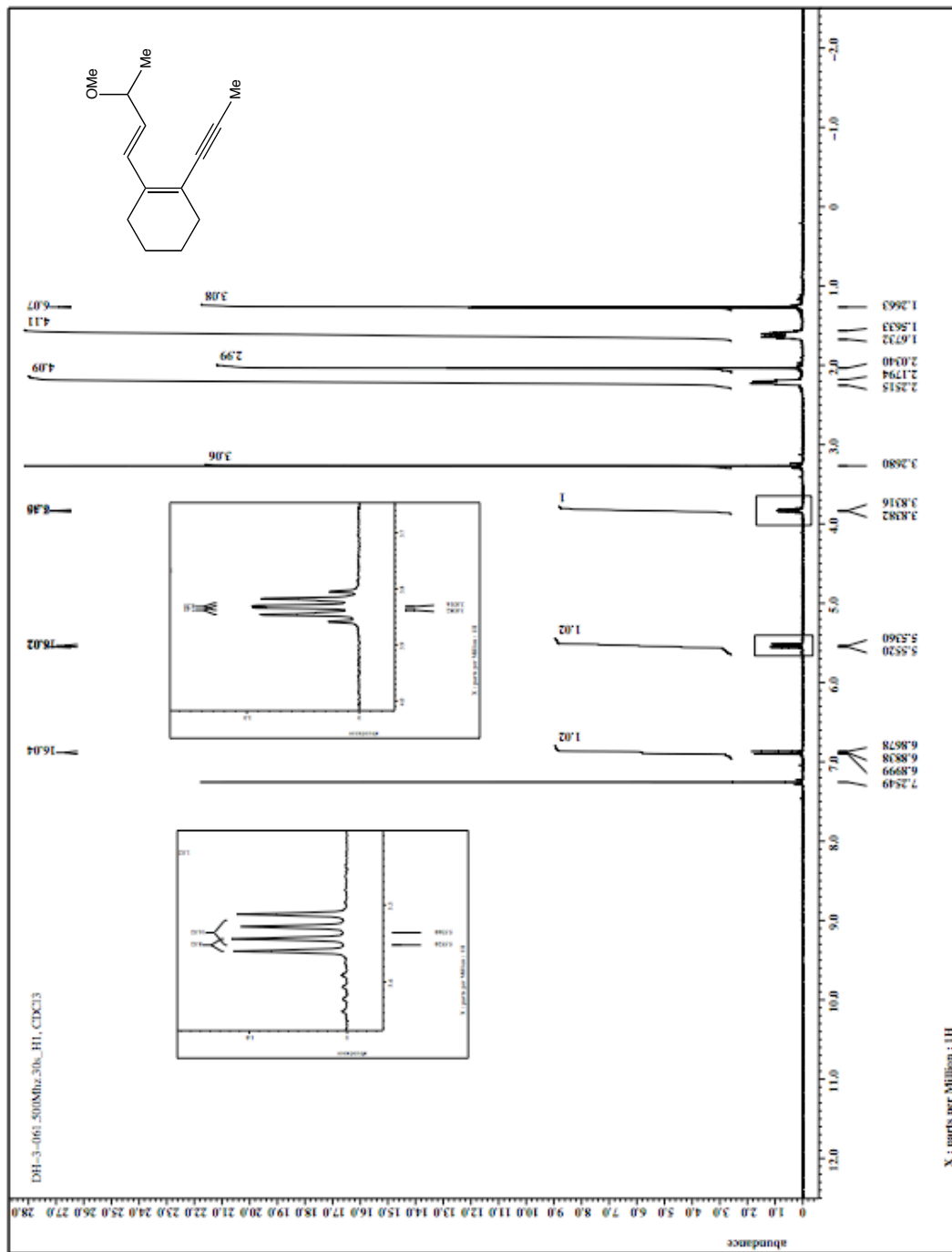


Figure 3-28. ¹H NMR spectrum (CDCl₃, 500 MHz).

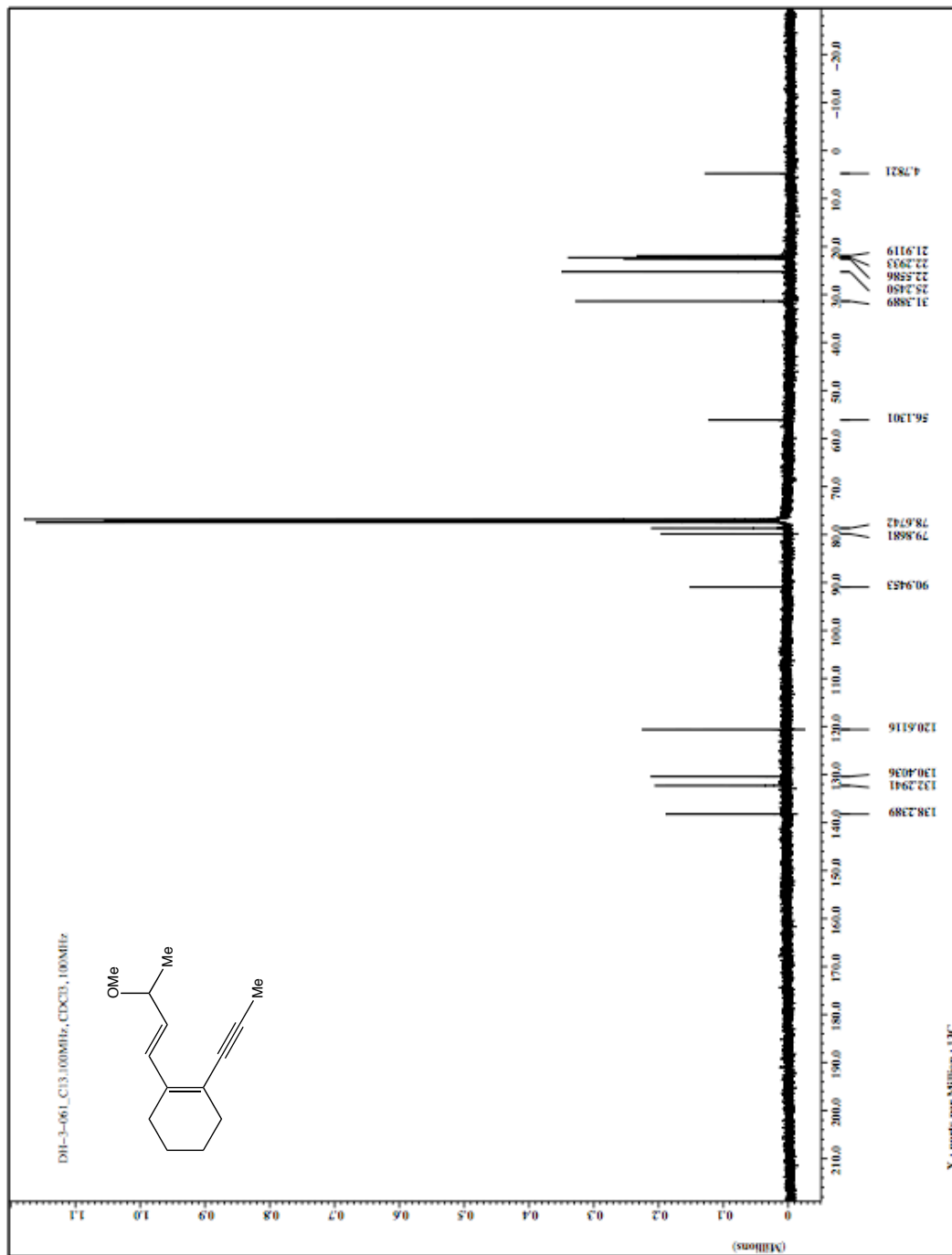


Figure 3-29. 45 ^{13}C NMR spectrum (CDCl_3 , 100 MHz).

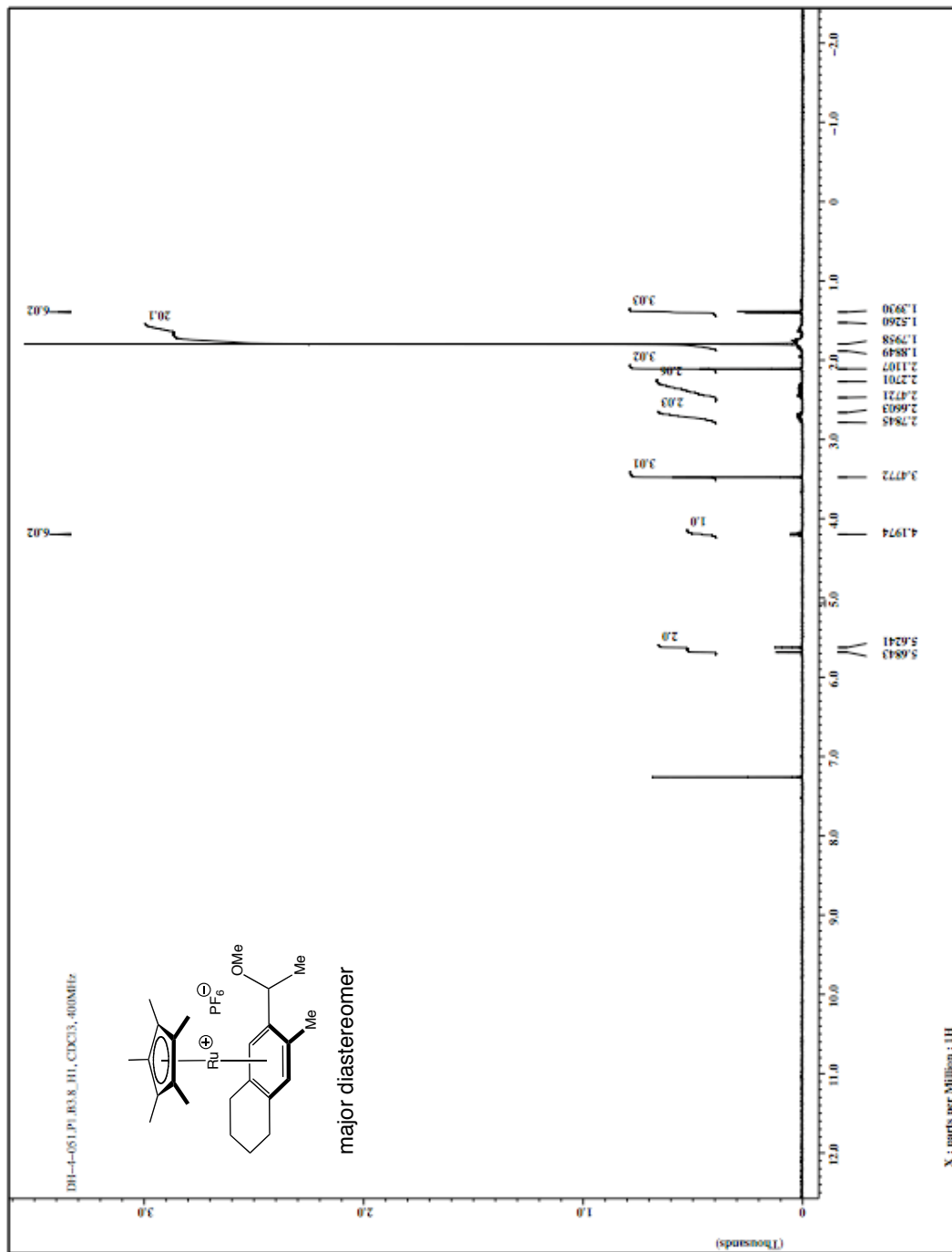


Figure 3-30. 50-ma ^1H NMR spectrum (CDCl_3 , 400 MHz).

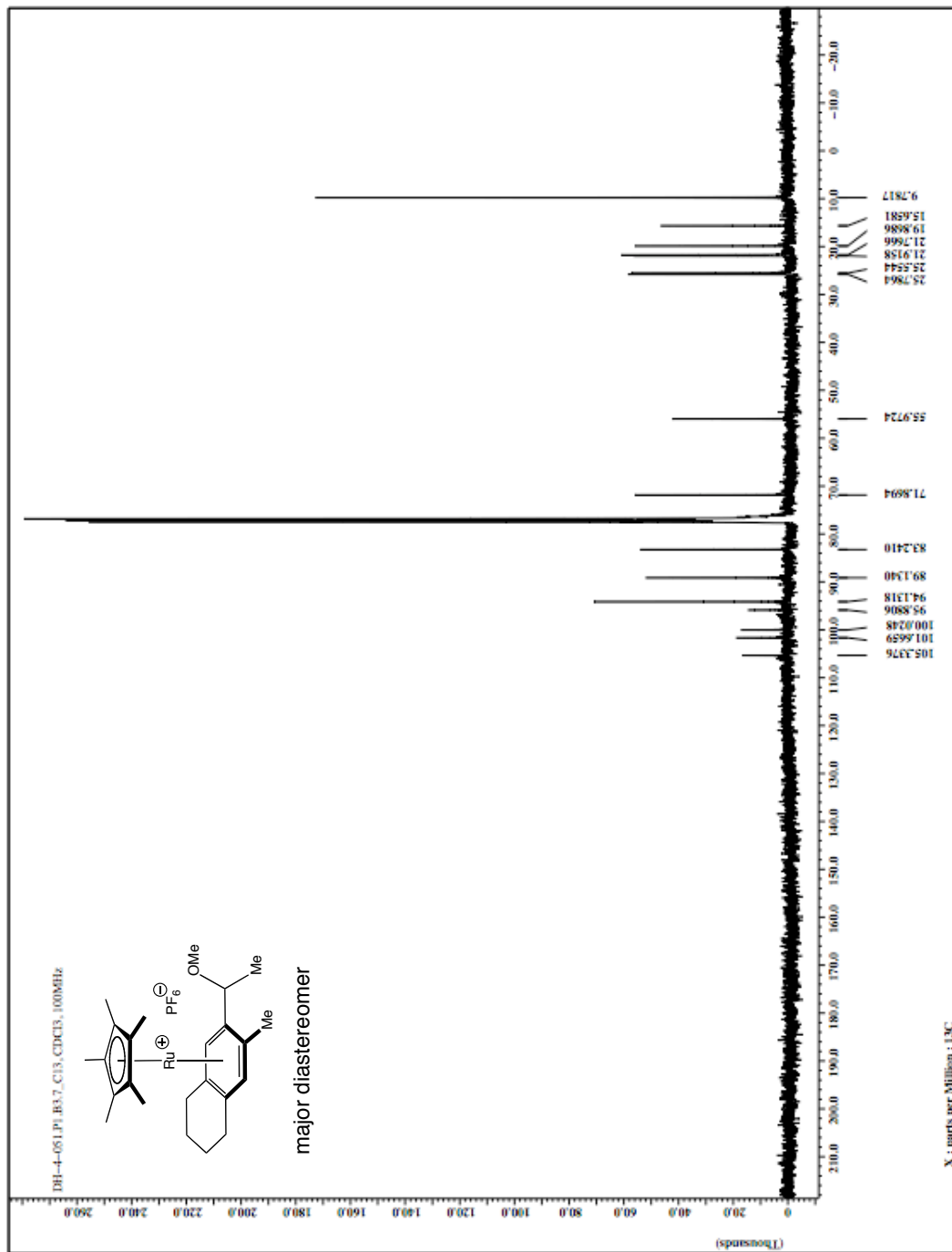


Figure 3-31. 50-ma ^{13}C NMR spectrum (CDCl_3 , 100 MHz).

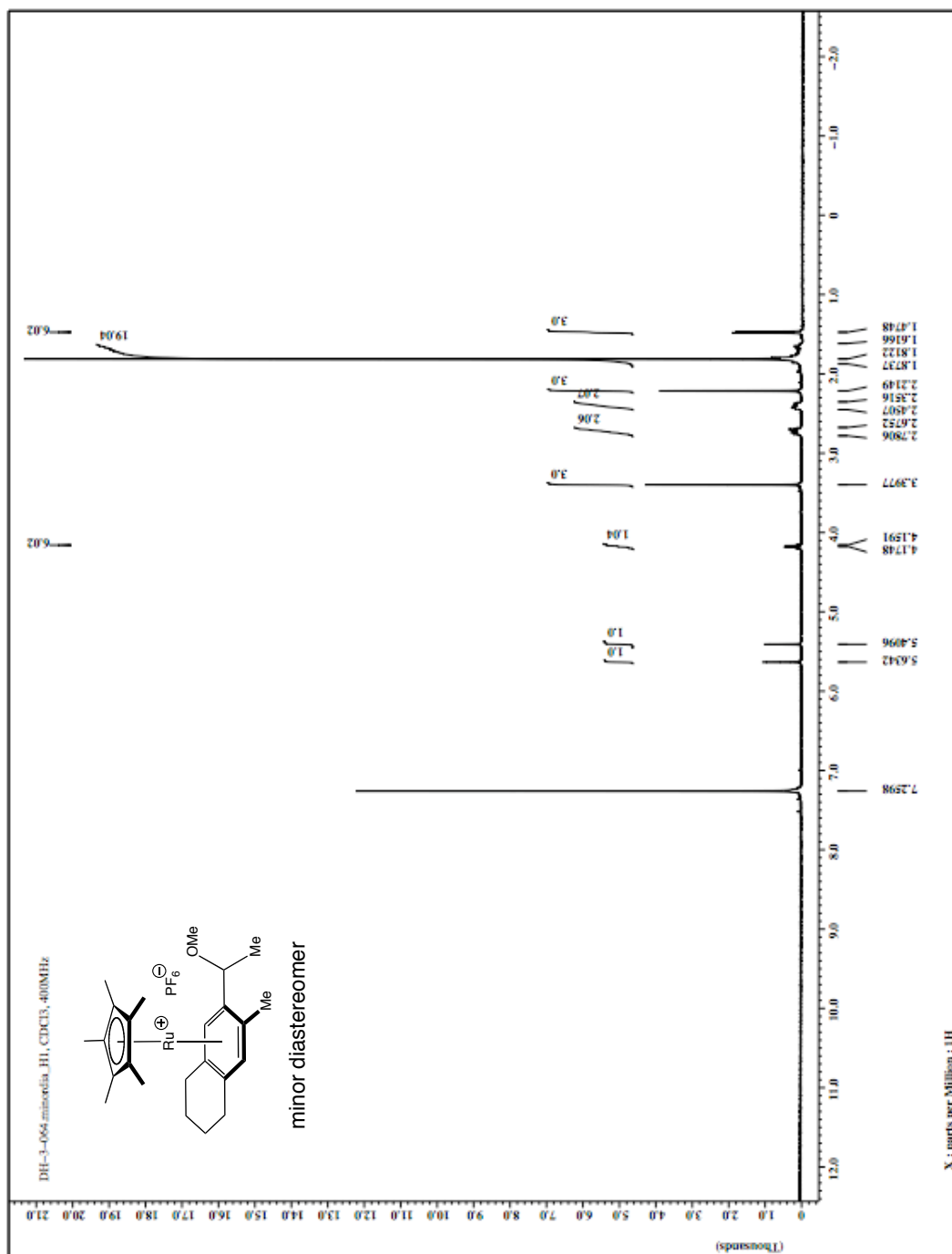


Figure 3-32. 50-mi ^1H NMR spectrum (CDCl_3 , 400 MHz).

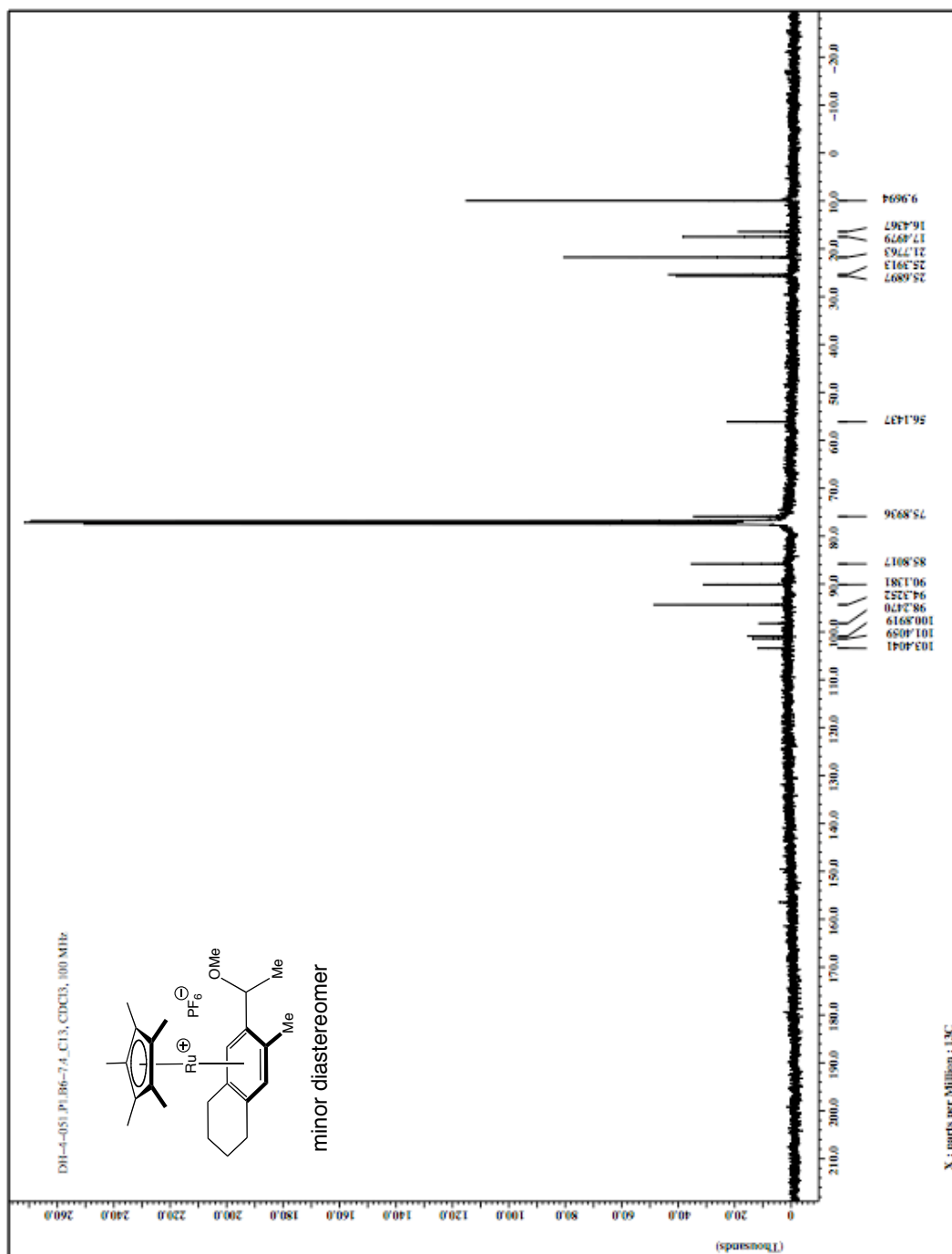


Figure 3-33. 50-mi ^{13}C NMR spectrum (CDCl_3 , 100 MHz).

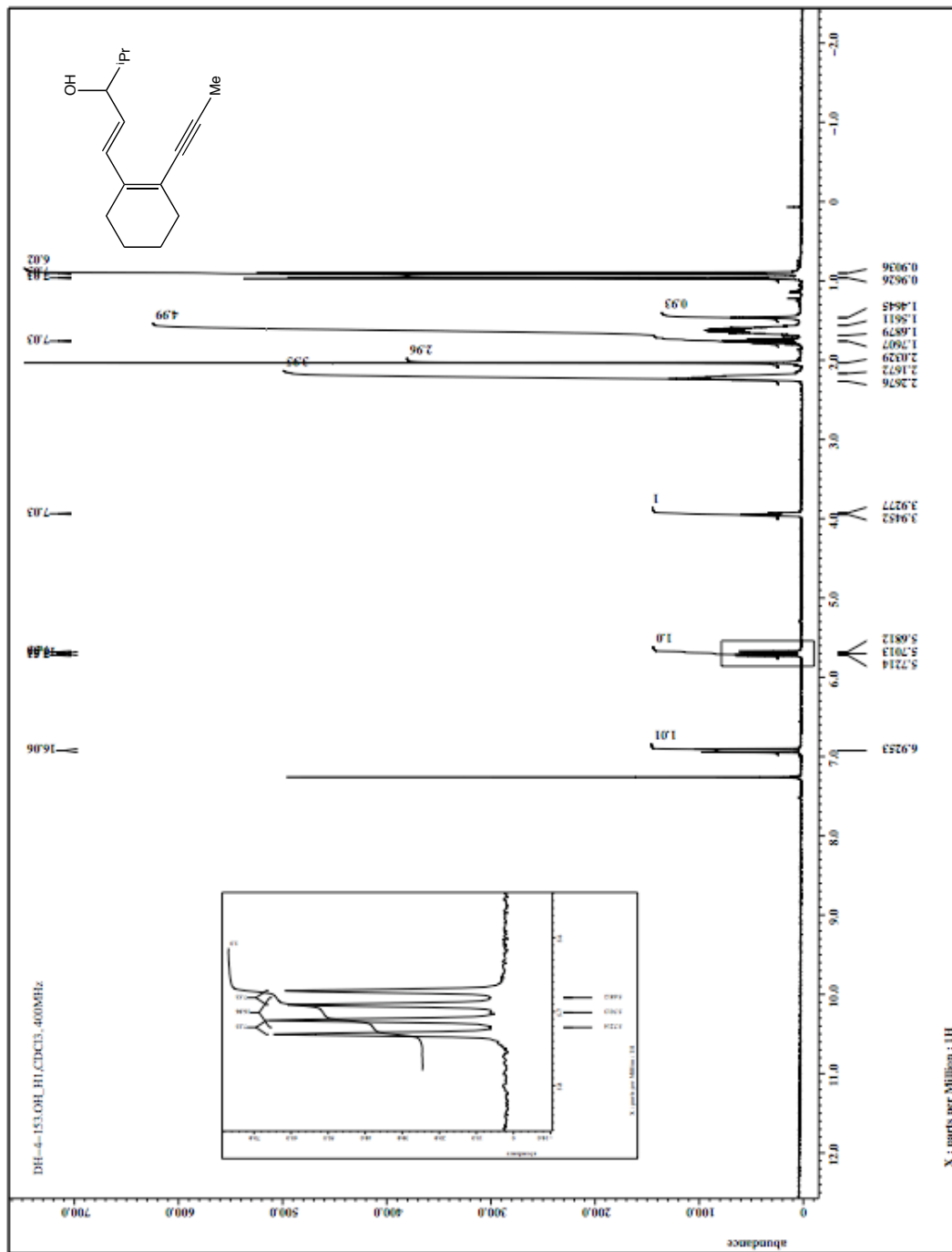


Figure 3-34. 46 ¹H NMR spectrum (CDCl₃, 400 MHz).

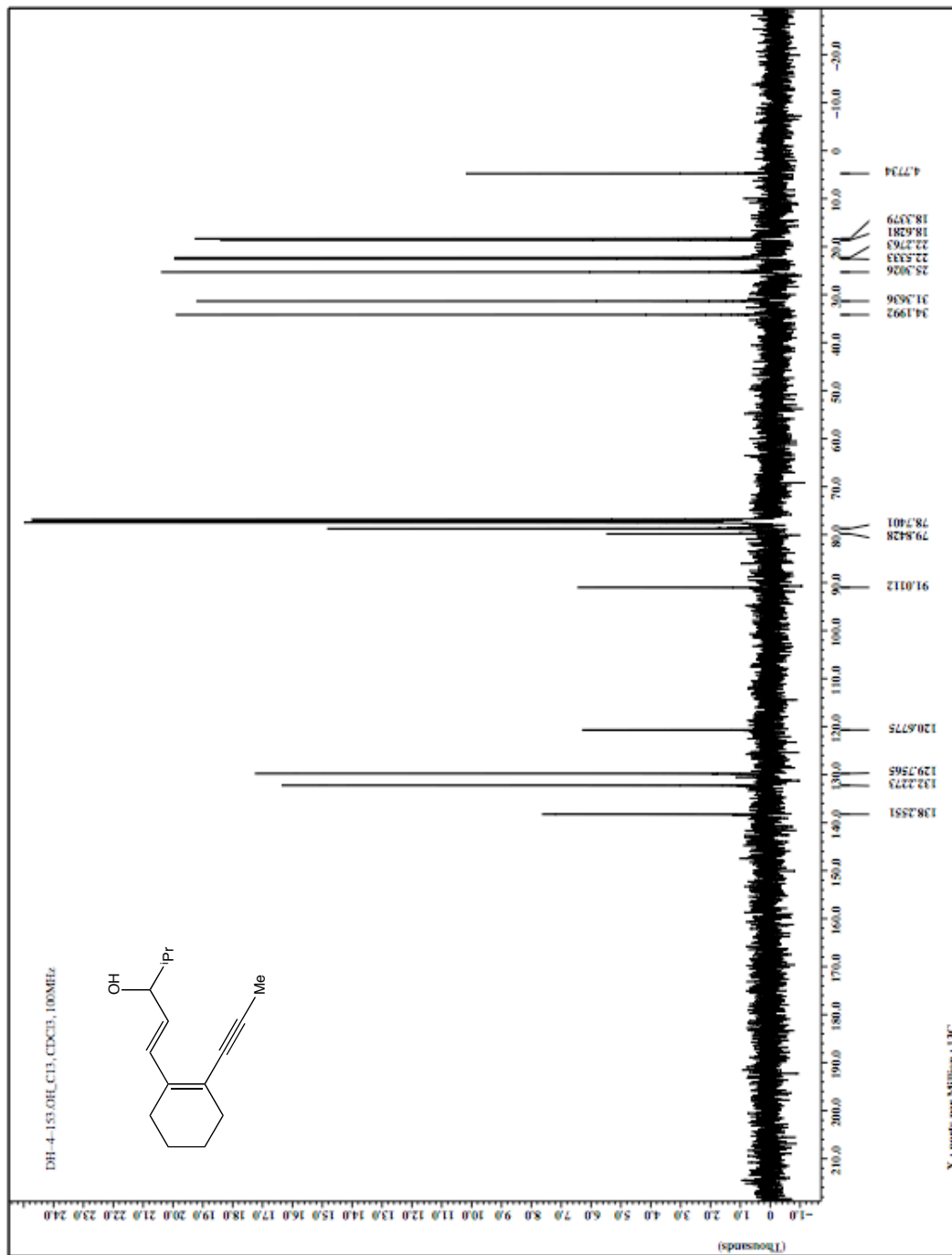


Figure 3-35. 46 ^{13}C NMR spectrum (CDCl₃, 100 MHz).

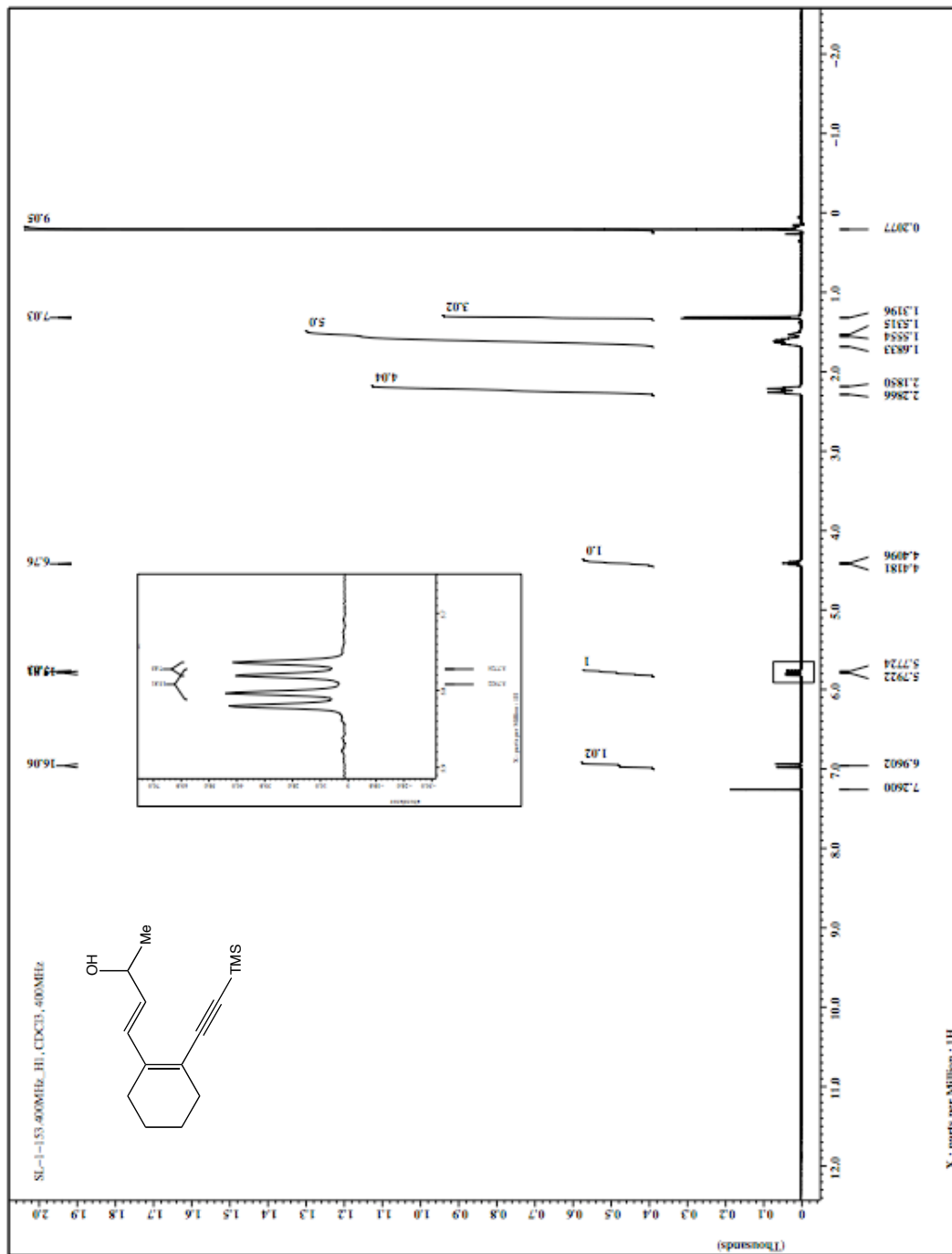


Figure 3-36. 47 ^1H NMR spectrum (CDCl₃, 400 MHz).

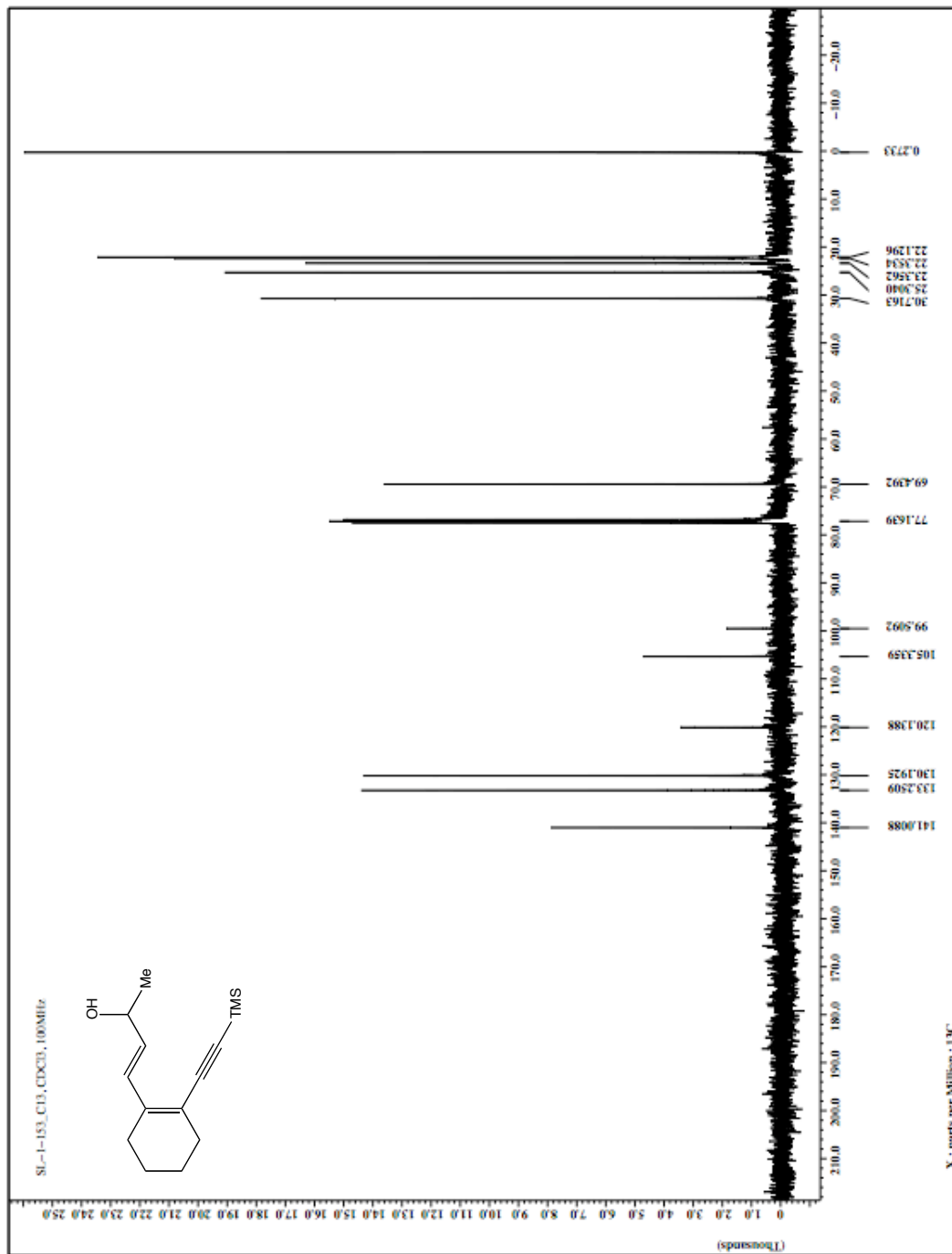


Figure 3-37. 47 ^{13}C NMR spectrum (CDCl_3 , 100 MHz).

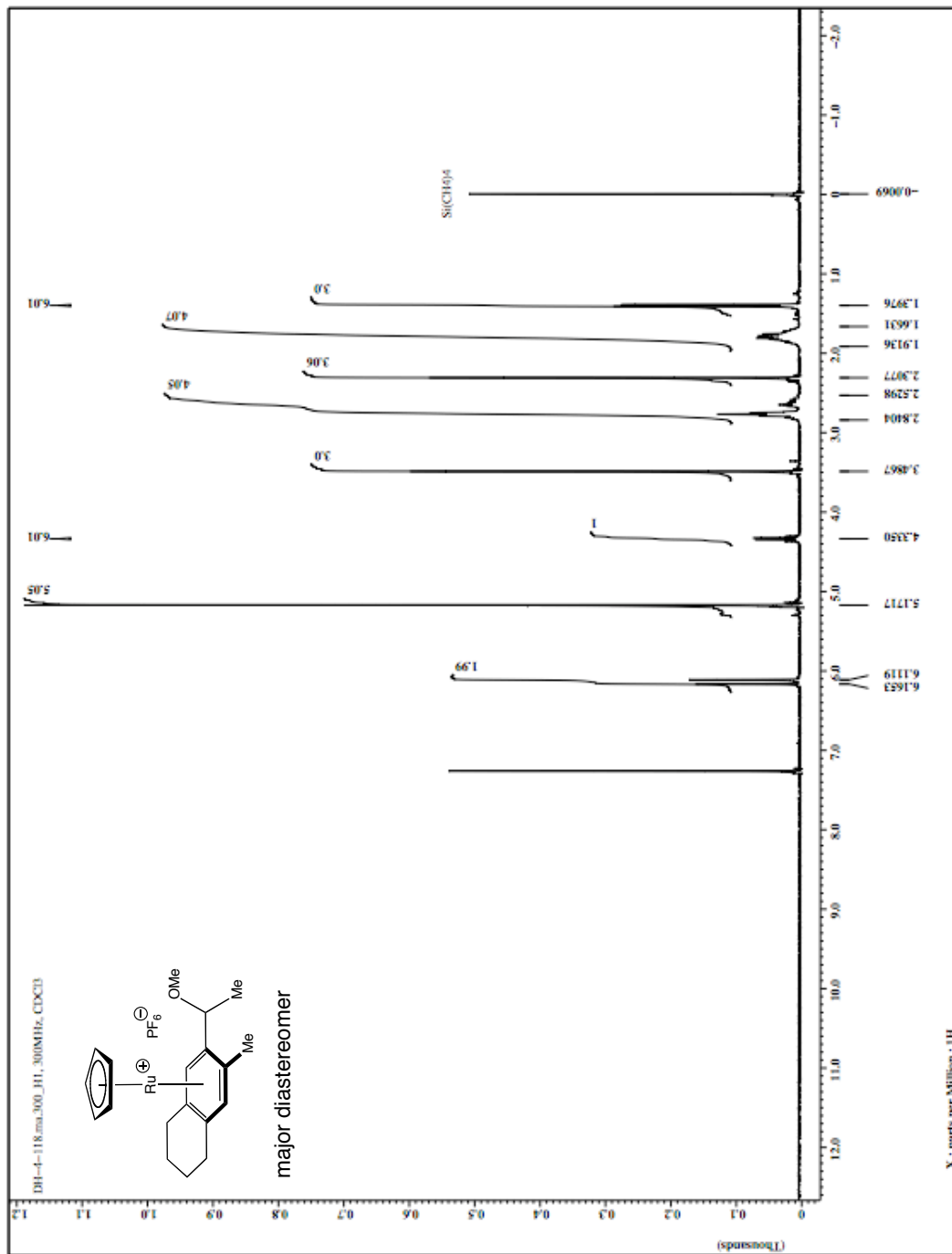


Figure 3-38. 52-ma ^1H NMR spectrum (CDCl_3 , 300 MHz).

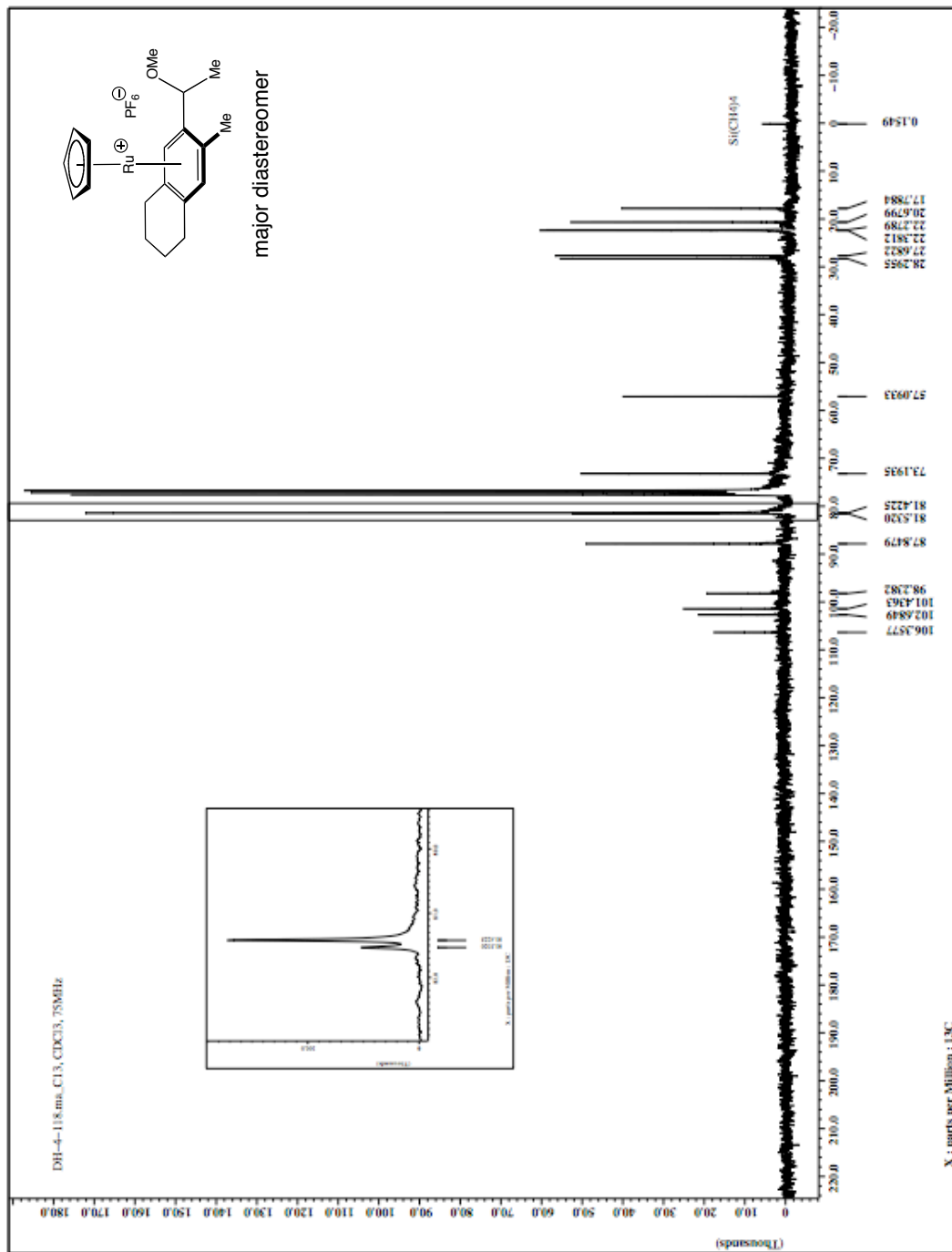


Figure 3-39. 52-ma ¹³C NMR spectrum (CDCl₃, 75 MHz).

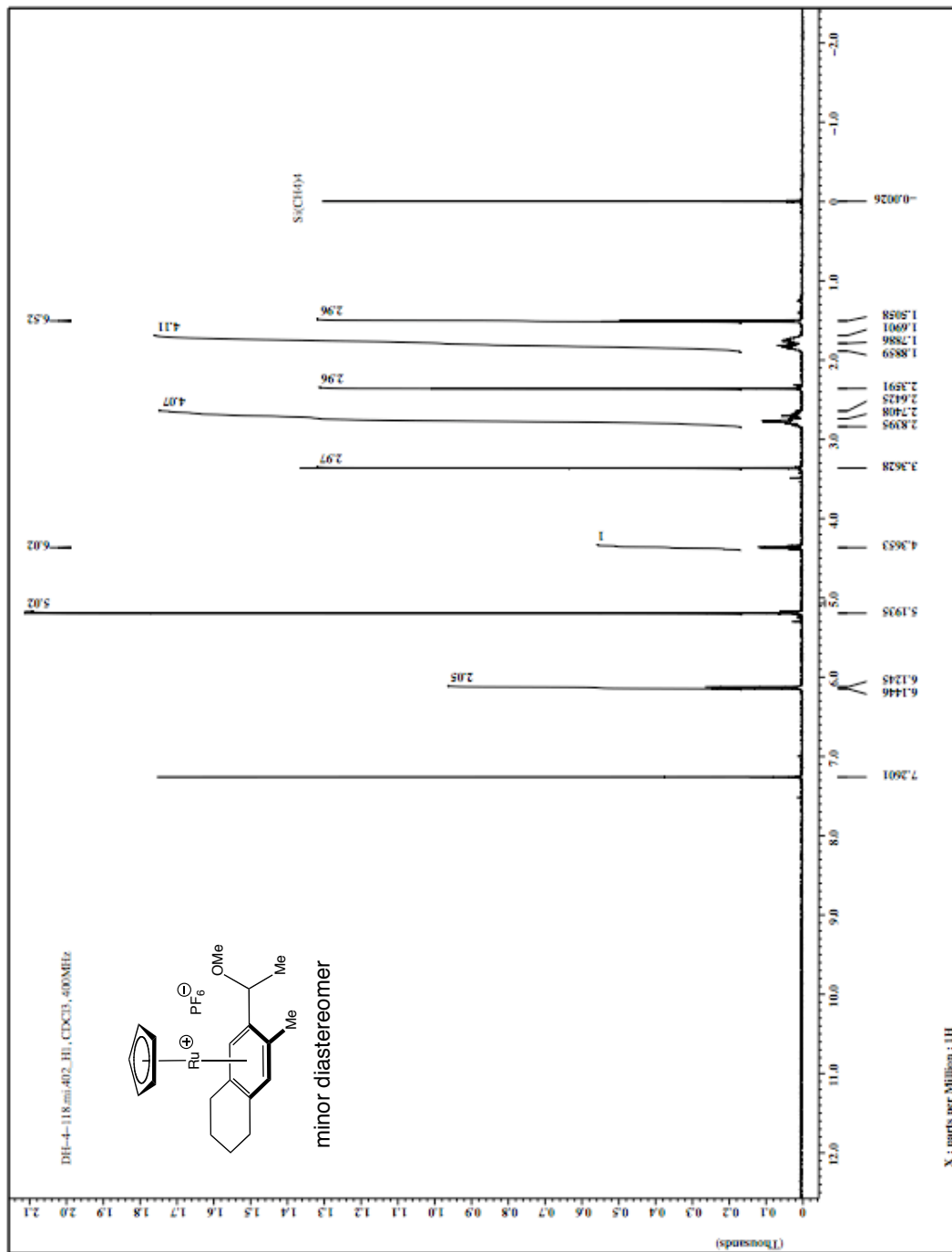


Figure 3-40. 52-mi ¹H NMR spectrum (CDCl₃, 400 MHz).

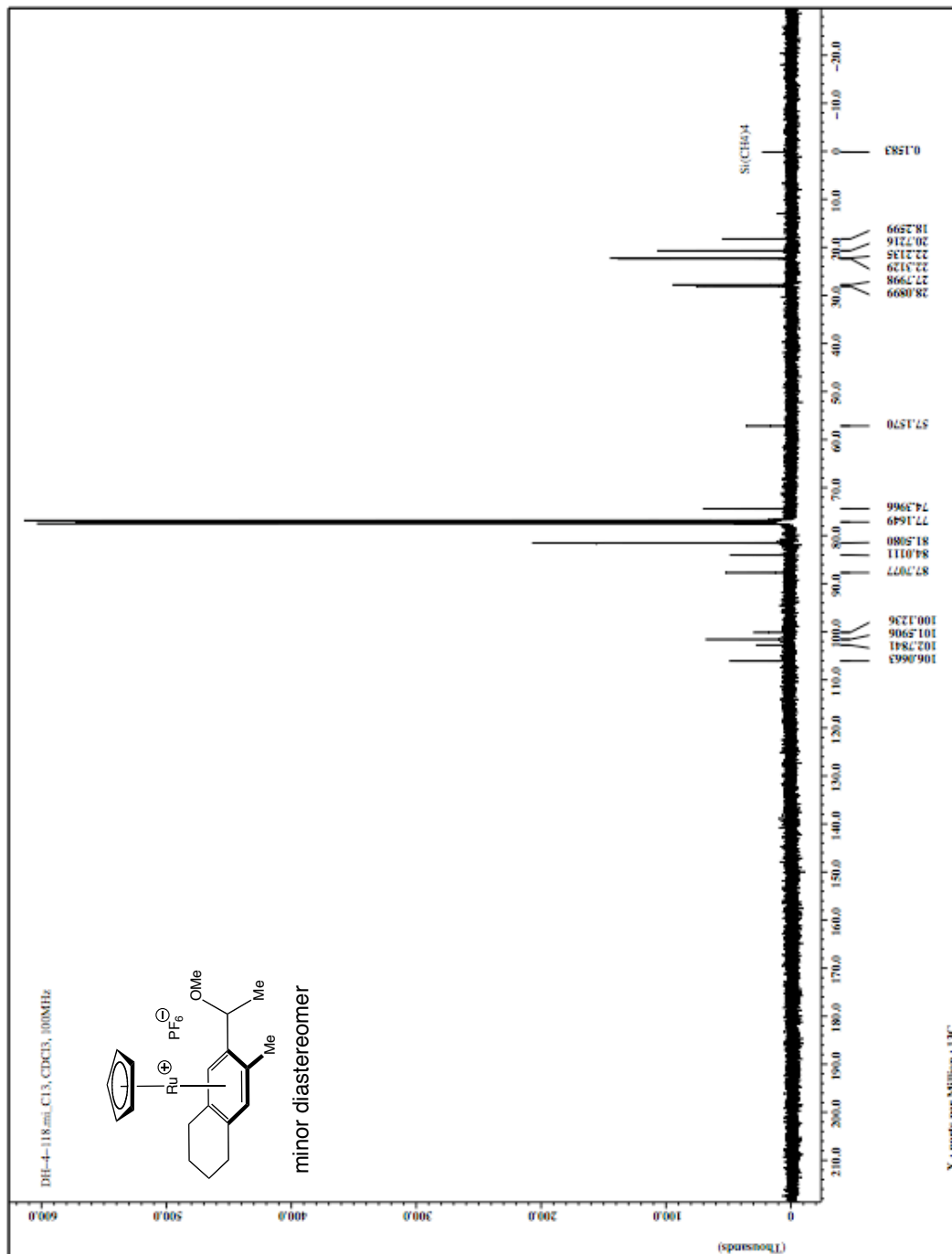


Figure 3-41. 52-mi ¹³C NMR spectrum (CDCl₃, 100 MHz).

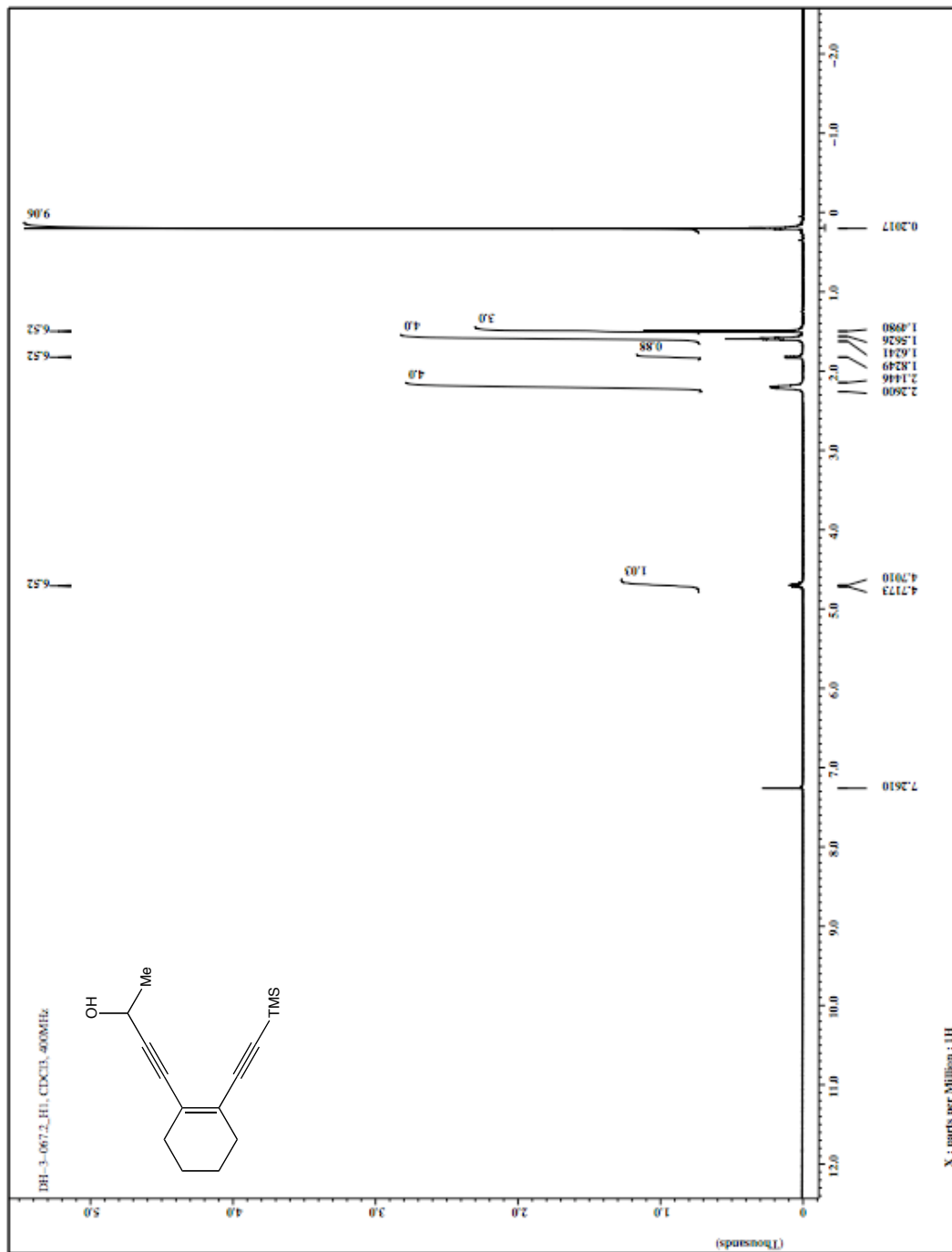


Figure 3-42. 53 ^1H NMR spectrum (CDCl₃, 400 MHz).

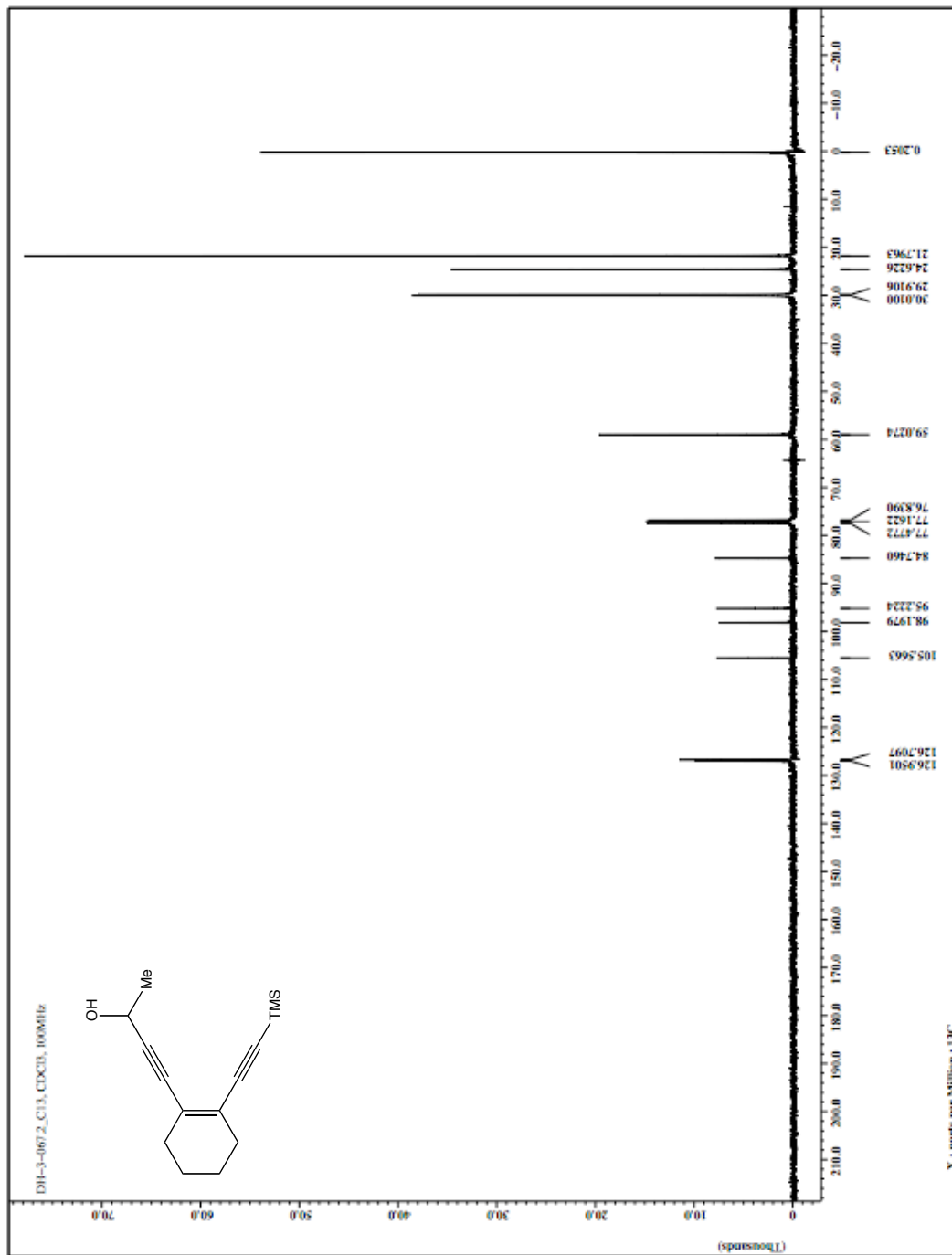


Figure 3-43. 53 ^{13}C NMR spectrum (CDCl_3 , 100 MHz).

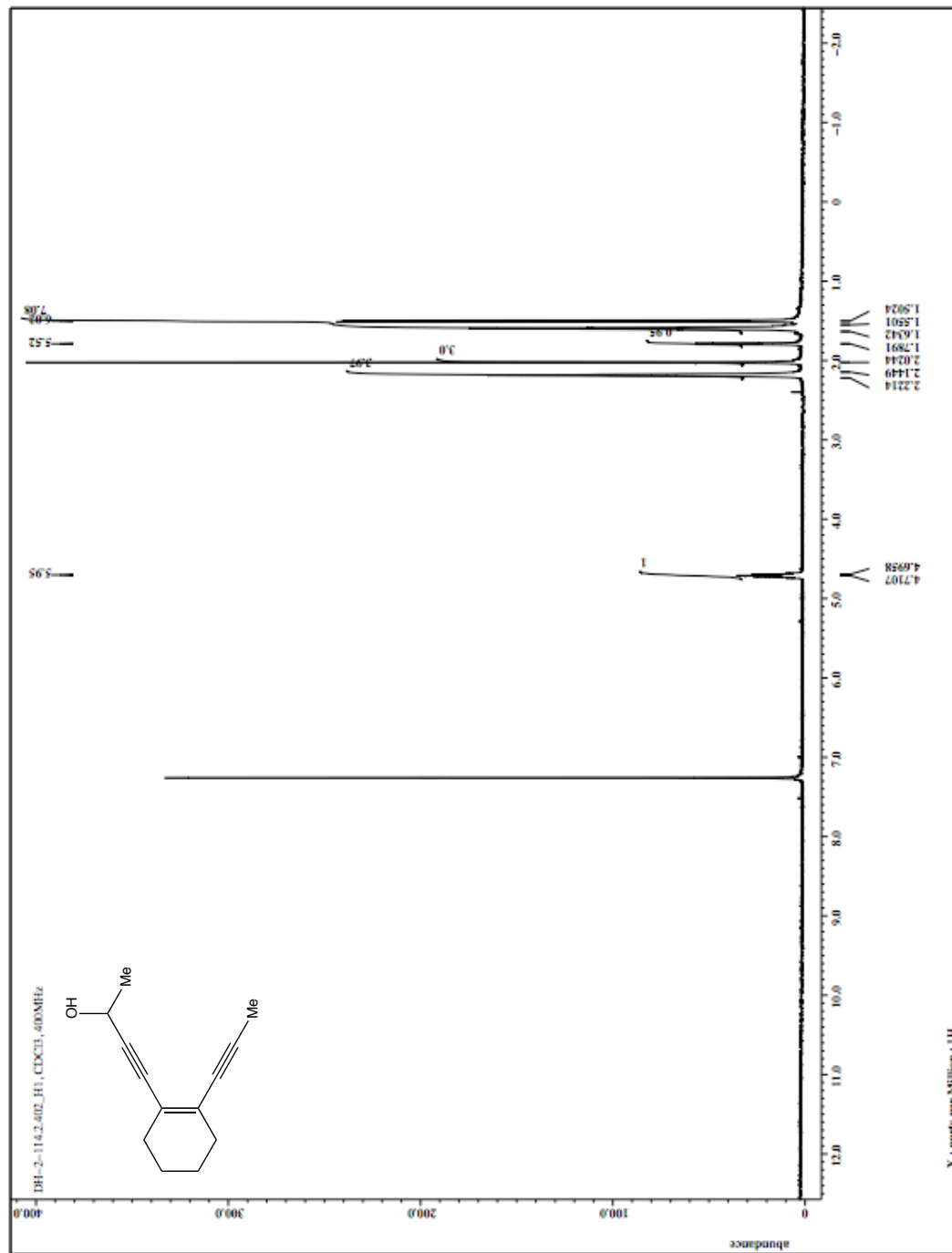


Figure 3-44. 54 ¹H NMR spectrum (CDCl₃, 400 MHz).

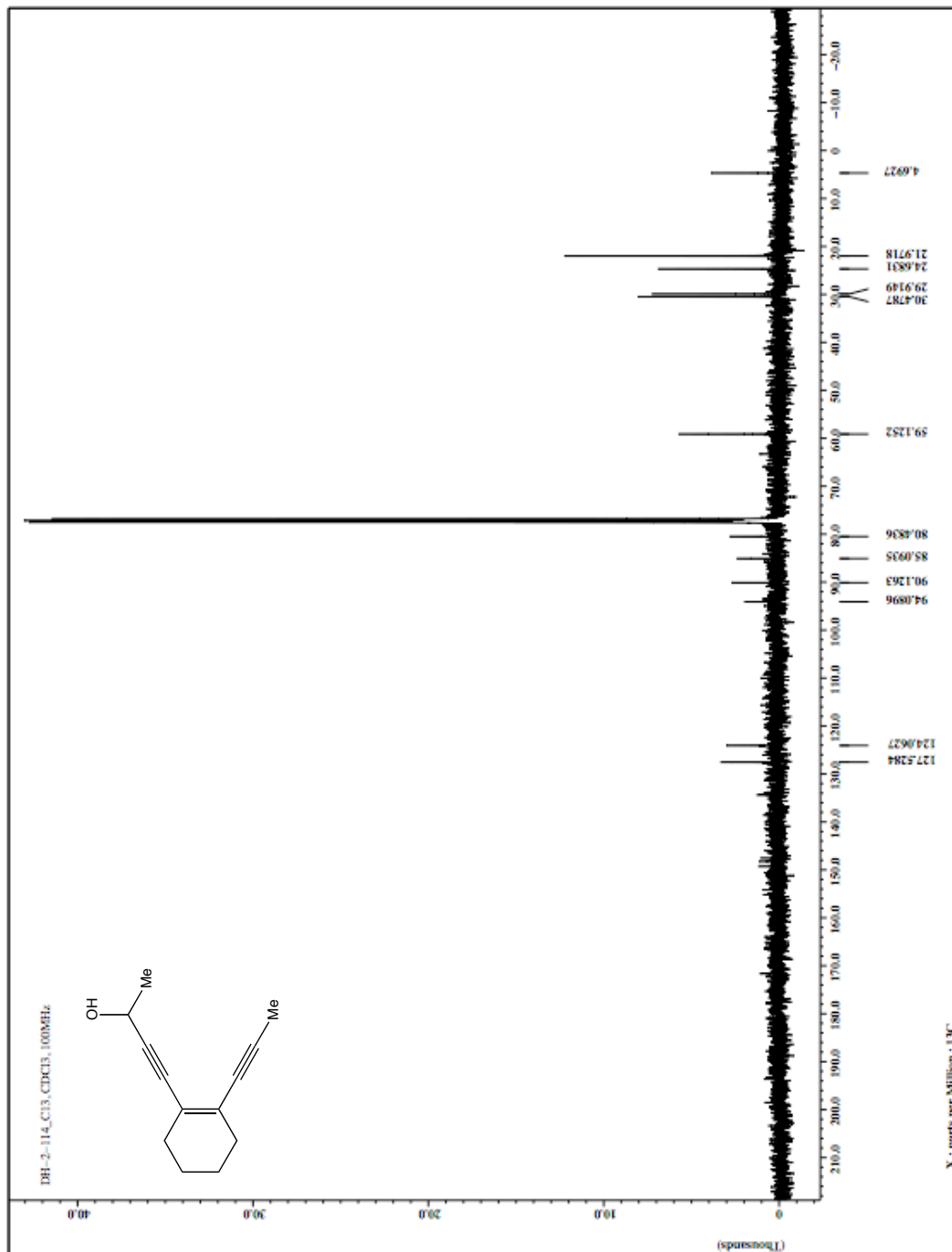


Figure 3-45. 54 ¹³C NMR spectrum (CDCl₃, 100 MHz).

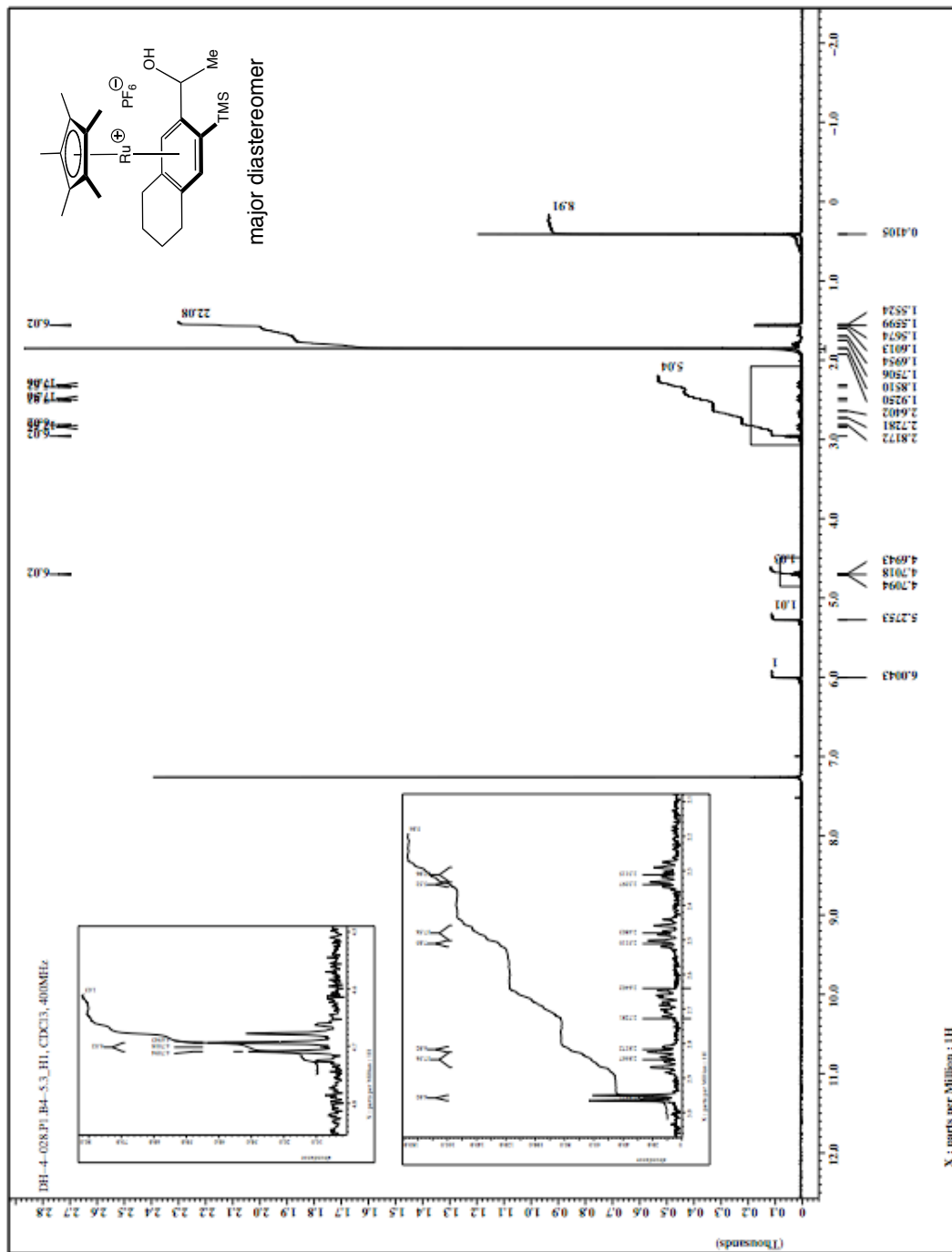


Figure 3-46. 56-ma ¹H NMR spectrum (CDCl₃, 400 MHz).

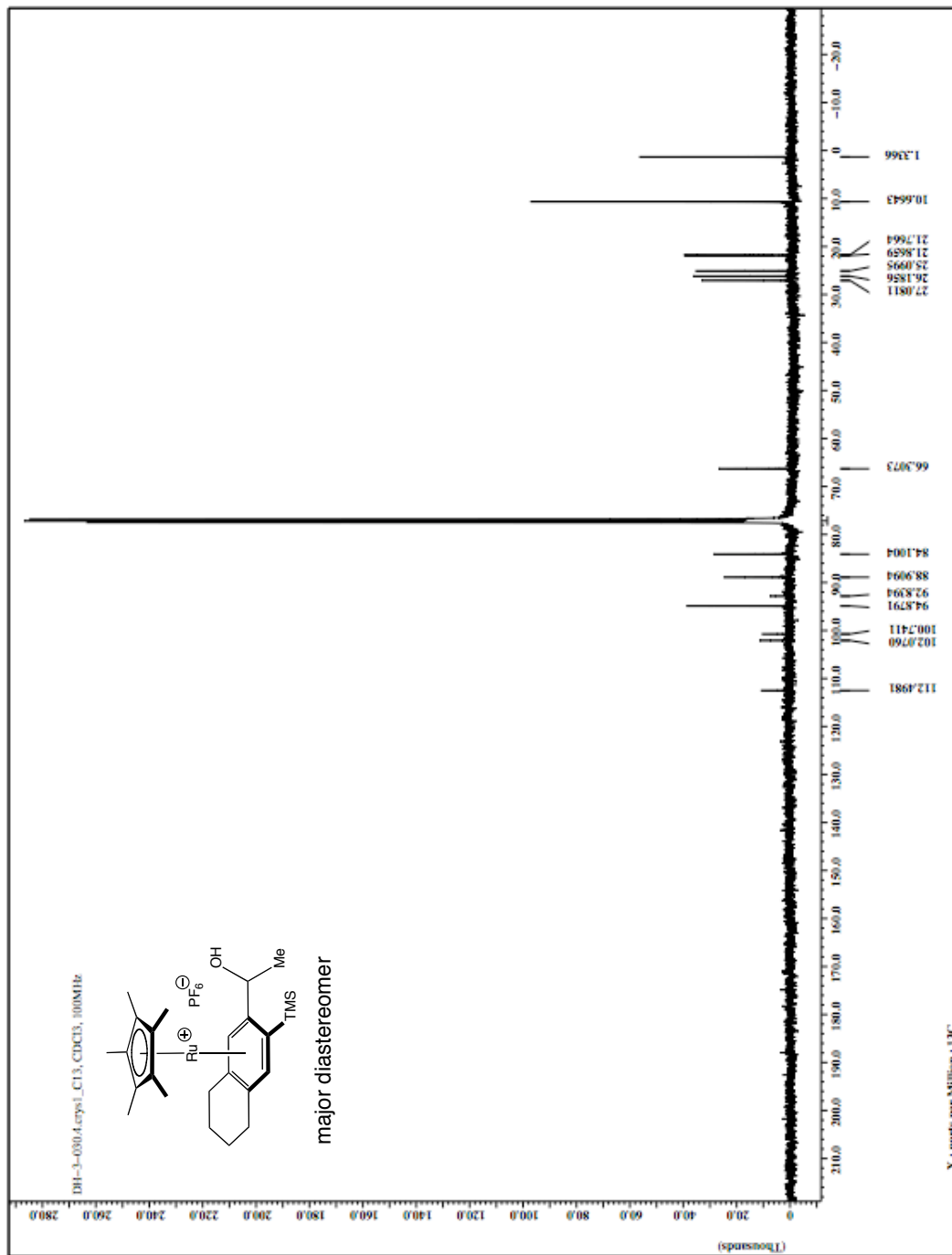


Figure 3-47. 56-ma ^{13}C NMR spectrum (CDCl_3 , 100 MHz).

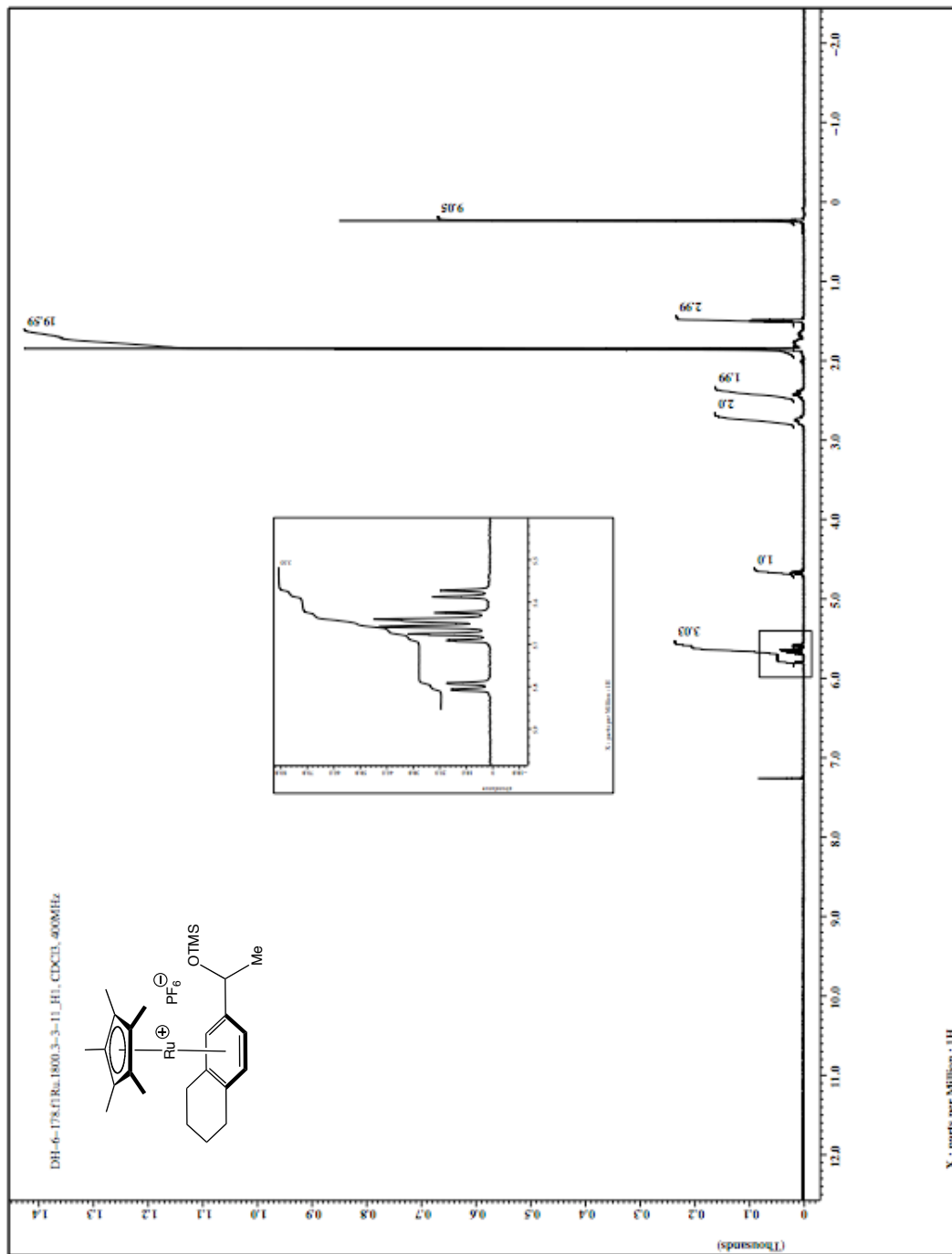


Figure 3-48. 57 ^1H NMR spectrum (CDCl_3 , 400 MHz).

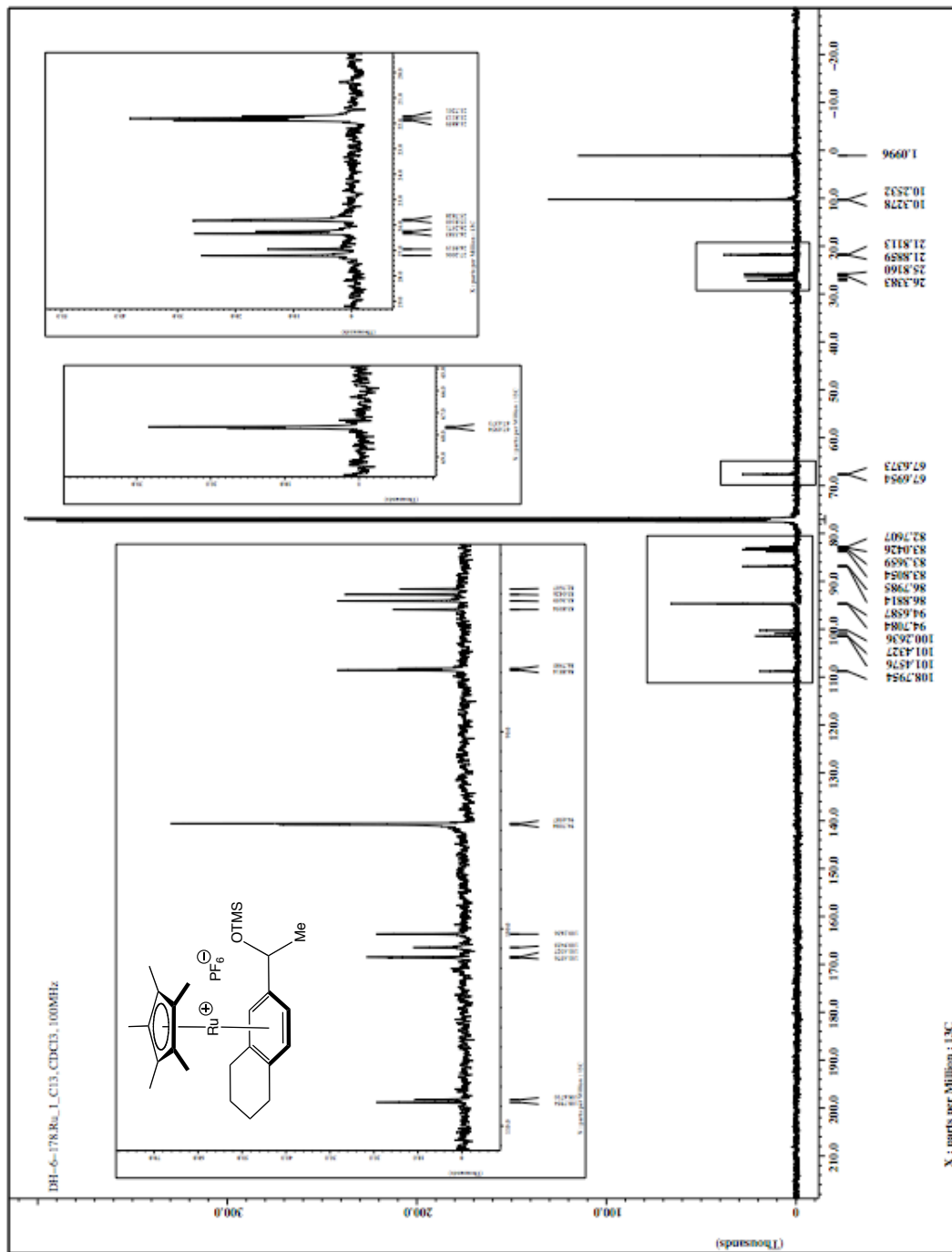


Figure 3-49. 57 ^{13}C NMR spectrum (CDCl_3 , 100 MHz).

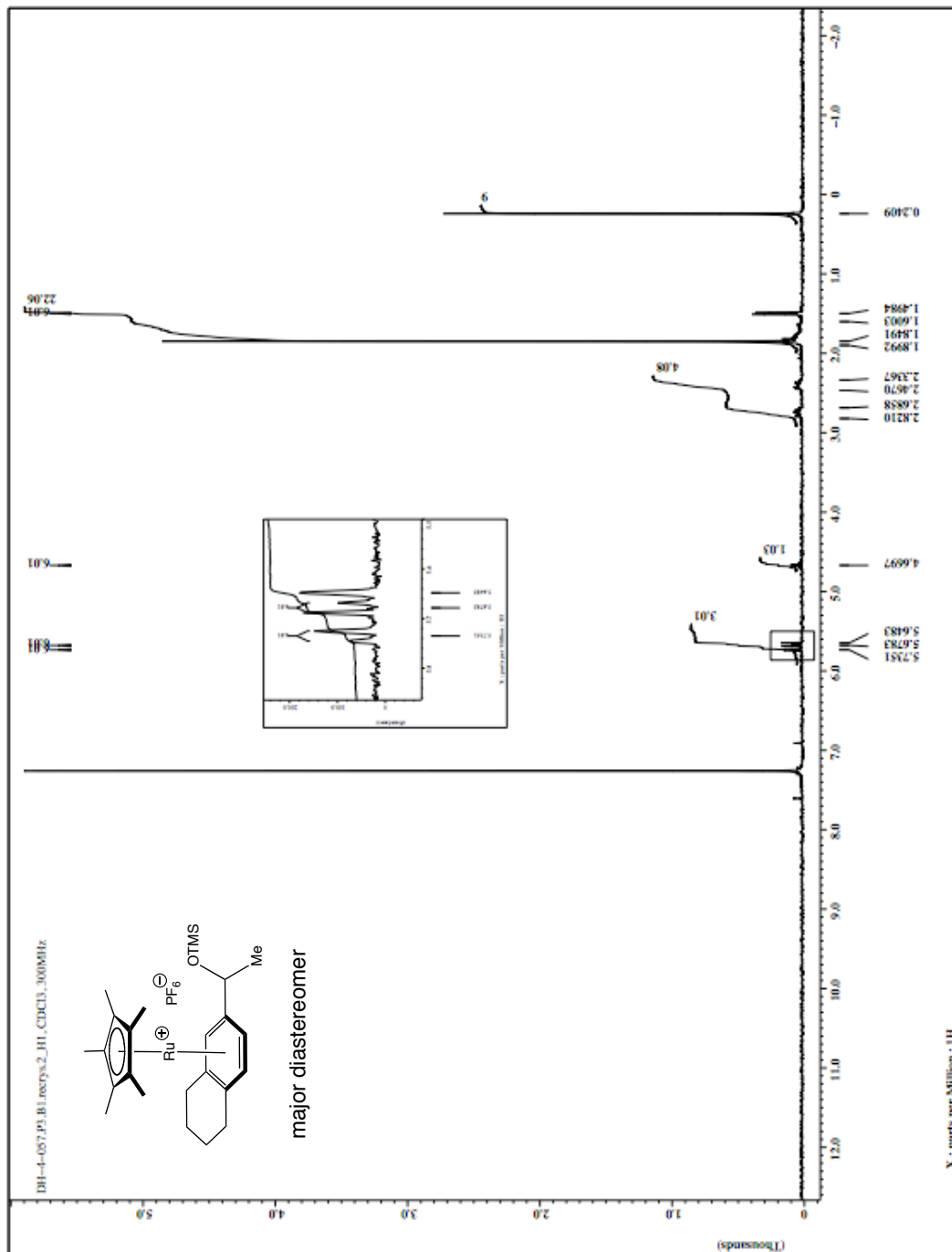


Figure 3-50. 57-ma ^1H NMR spectrum (CDCl_3 , 300 MHz).

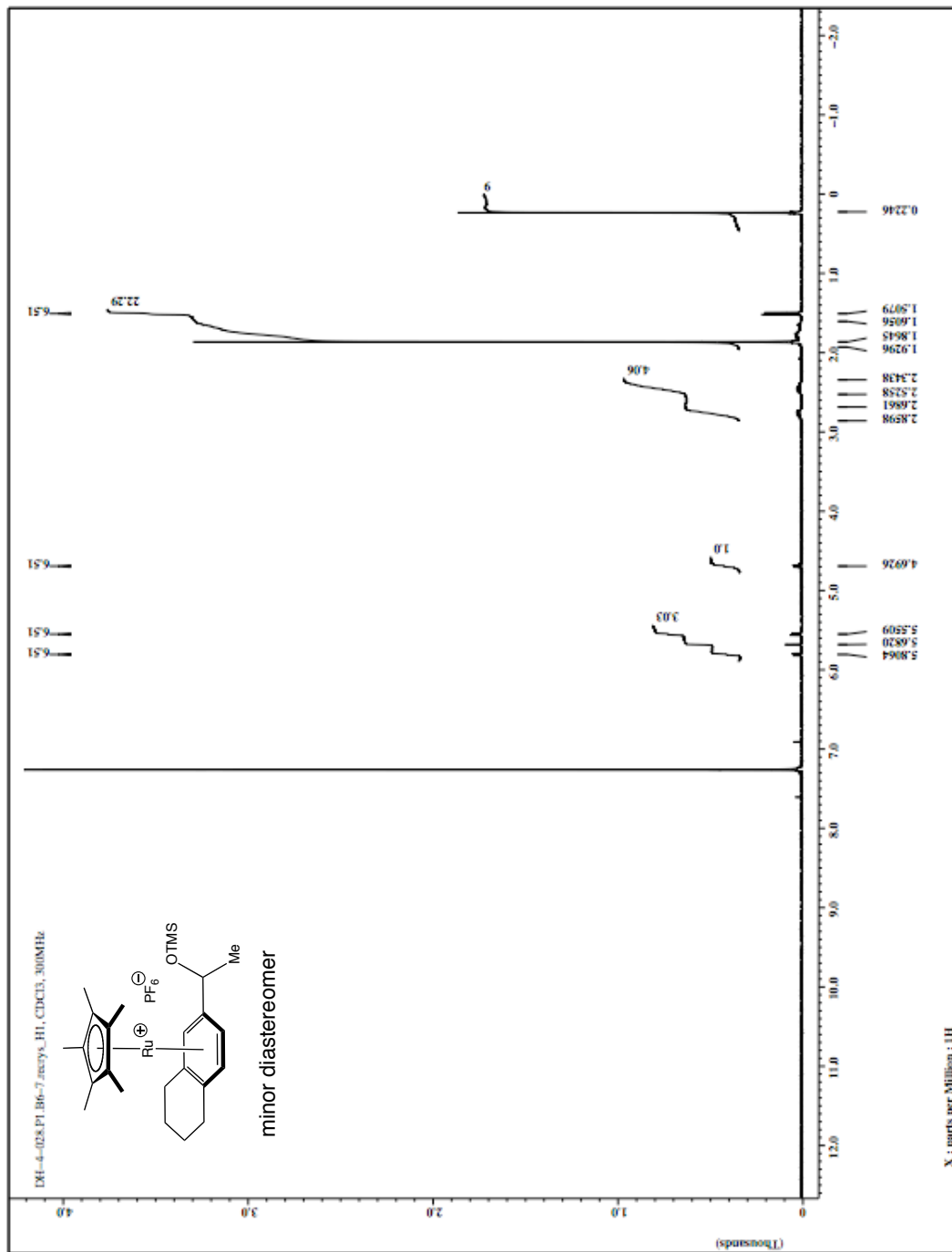


Figure 3-51. 57-mi ^1H NMR spectrum (CDCl_3 , 300 MHz).

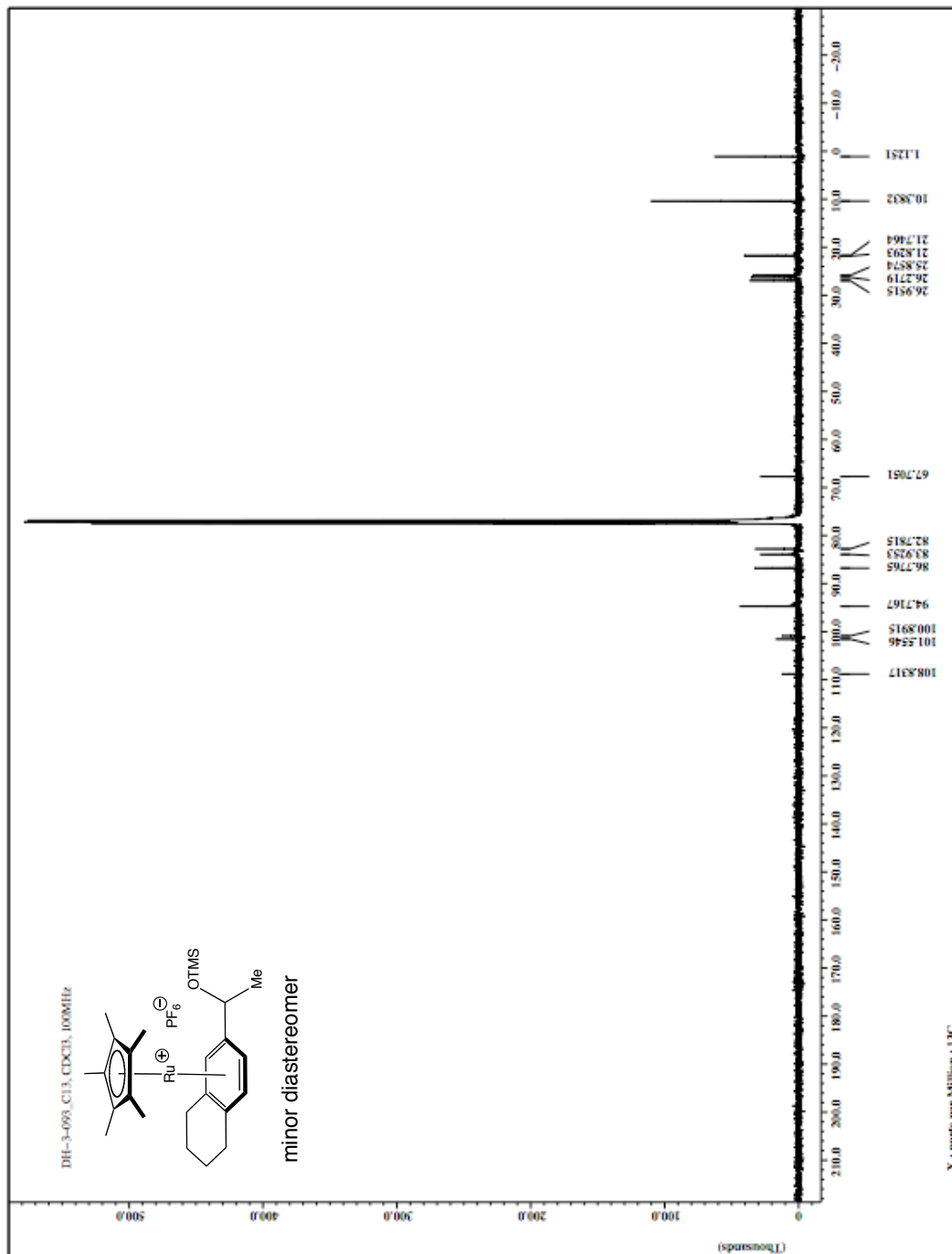


Figure 3-52. 57-mi ^{13}C NMR spectrum (CDCl_3 , 100 MHz).

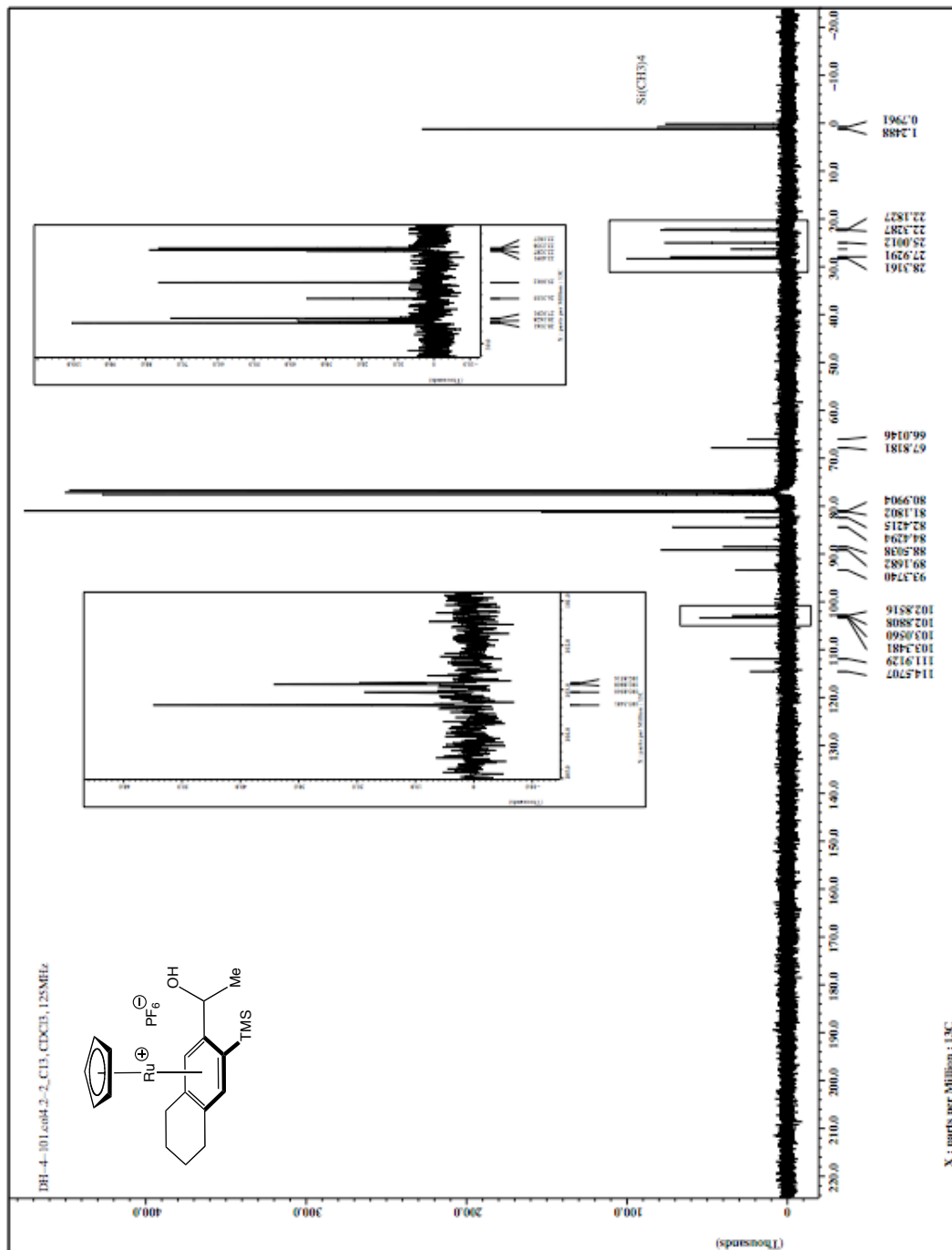


Figure 3-54. **58** ^{13}C NMR spectrum (CDCl_3 , 125 MHz).

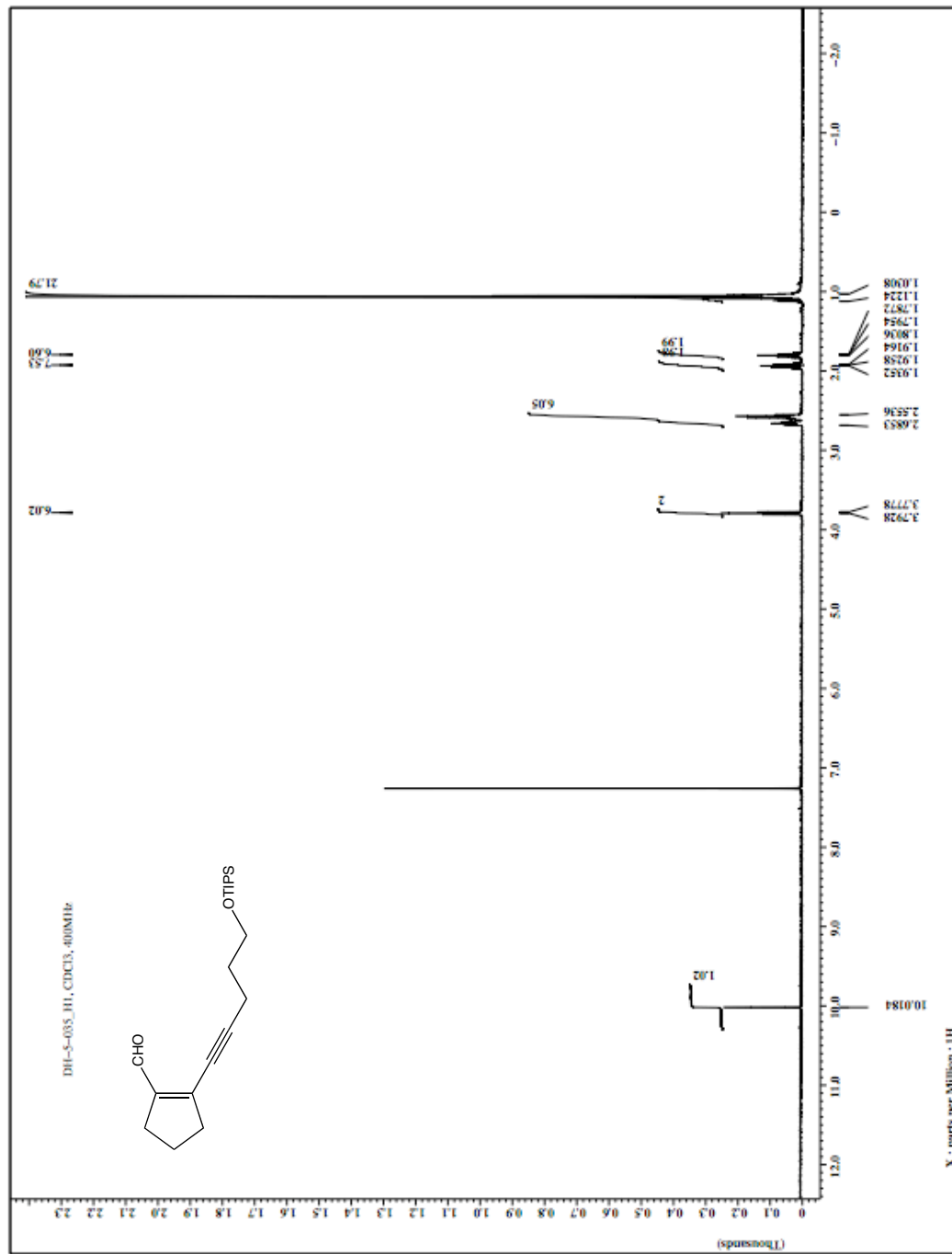


Figure 3-55. 67 ¹H NMR spectrum (CDCl₃, 400 MHz).

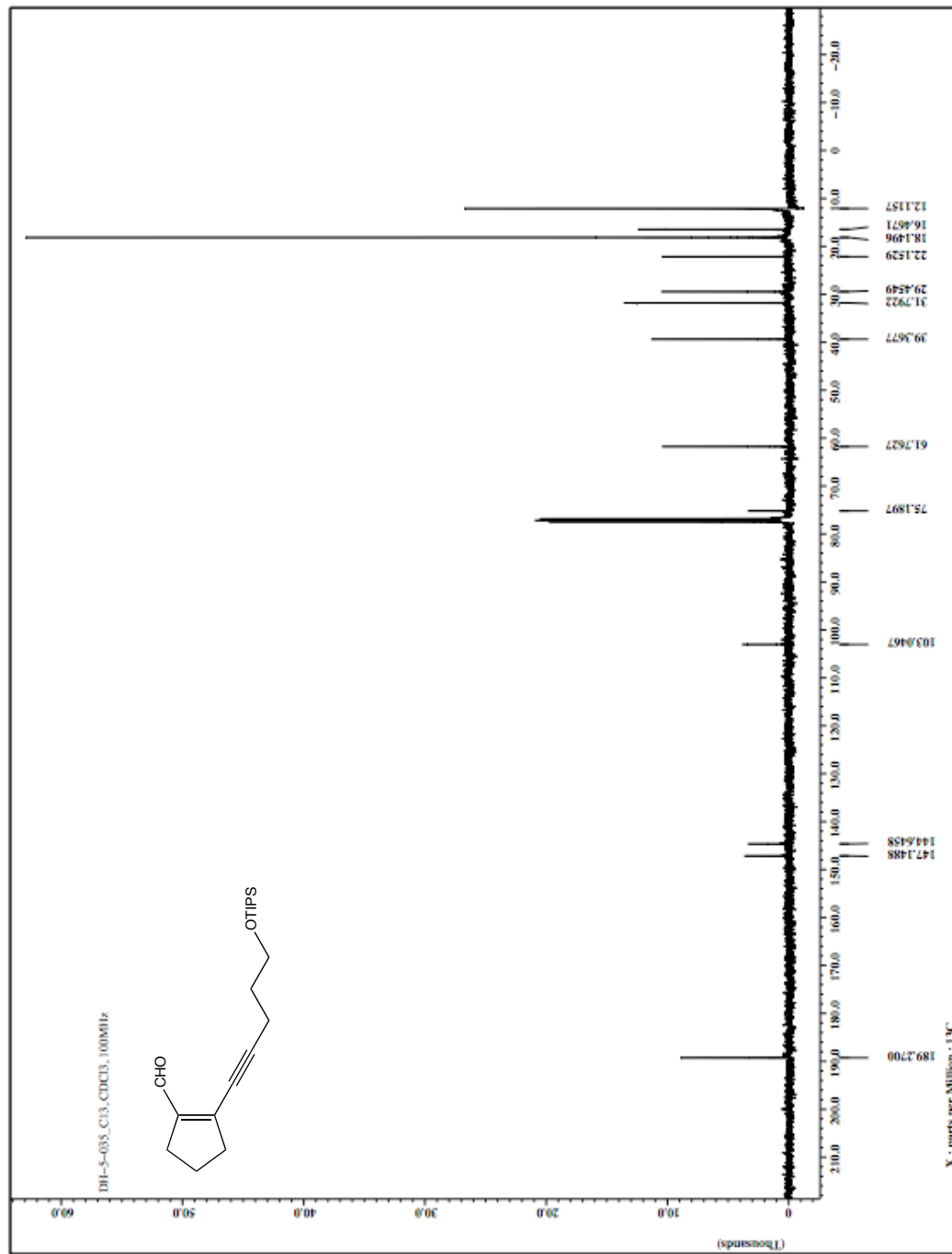


Figure 3-56. 67 ^{13}C NMR spectrum (CDCl_3 , 100 MHz).

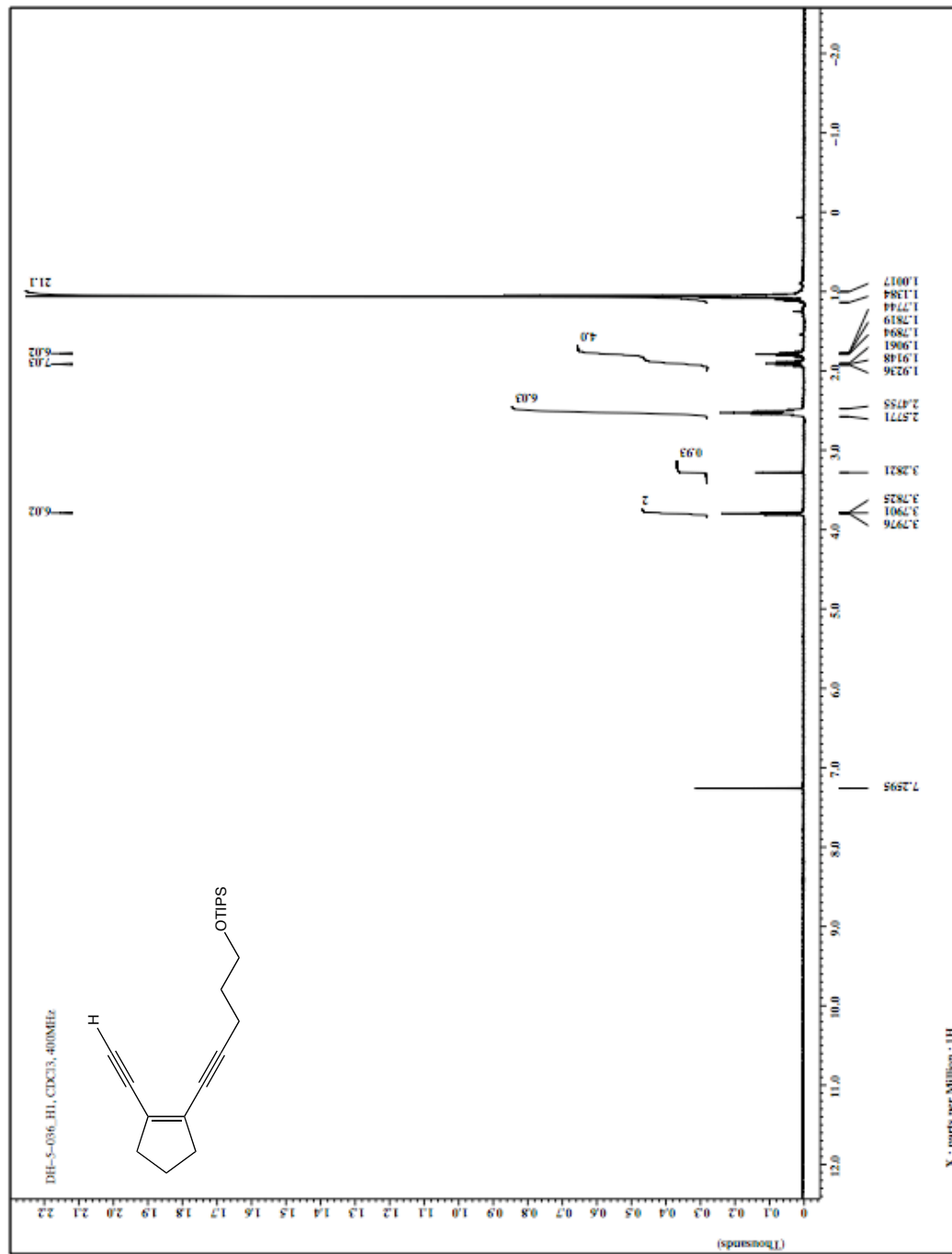


Figure 3-57. 68 ¹H NMR spectrum (CDCl₃, 400 MHz).

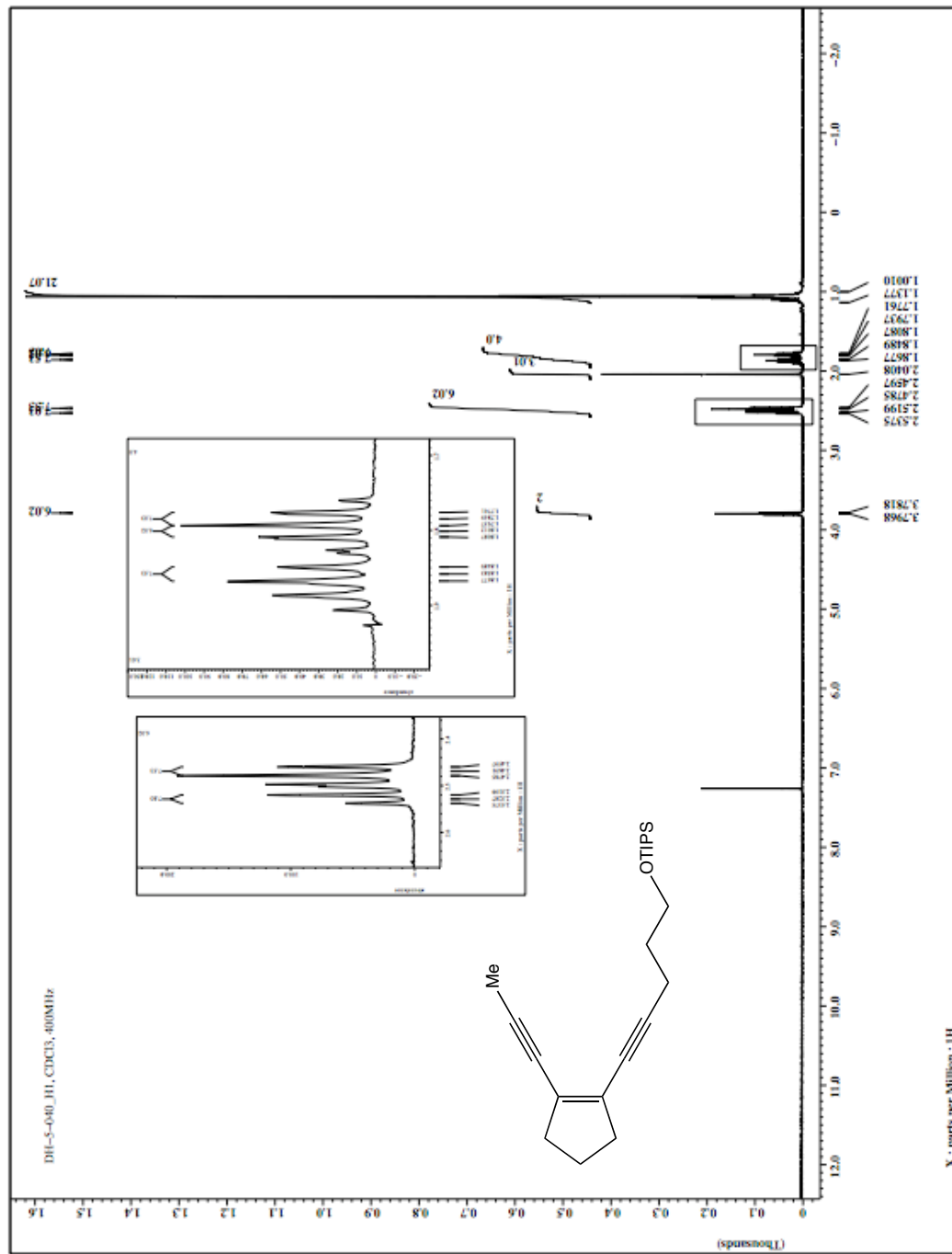


Figure 3-59. ^1H NMR spectrum (CDCl₃, 400 MHz).

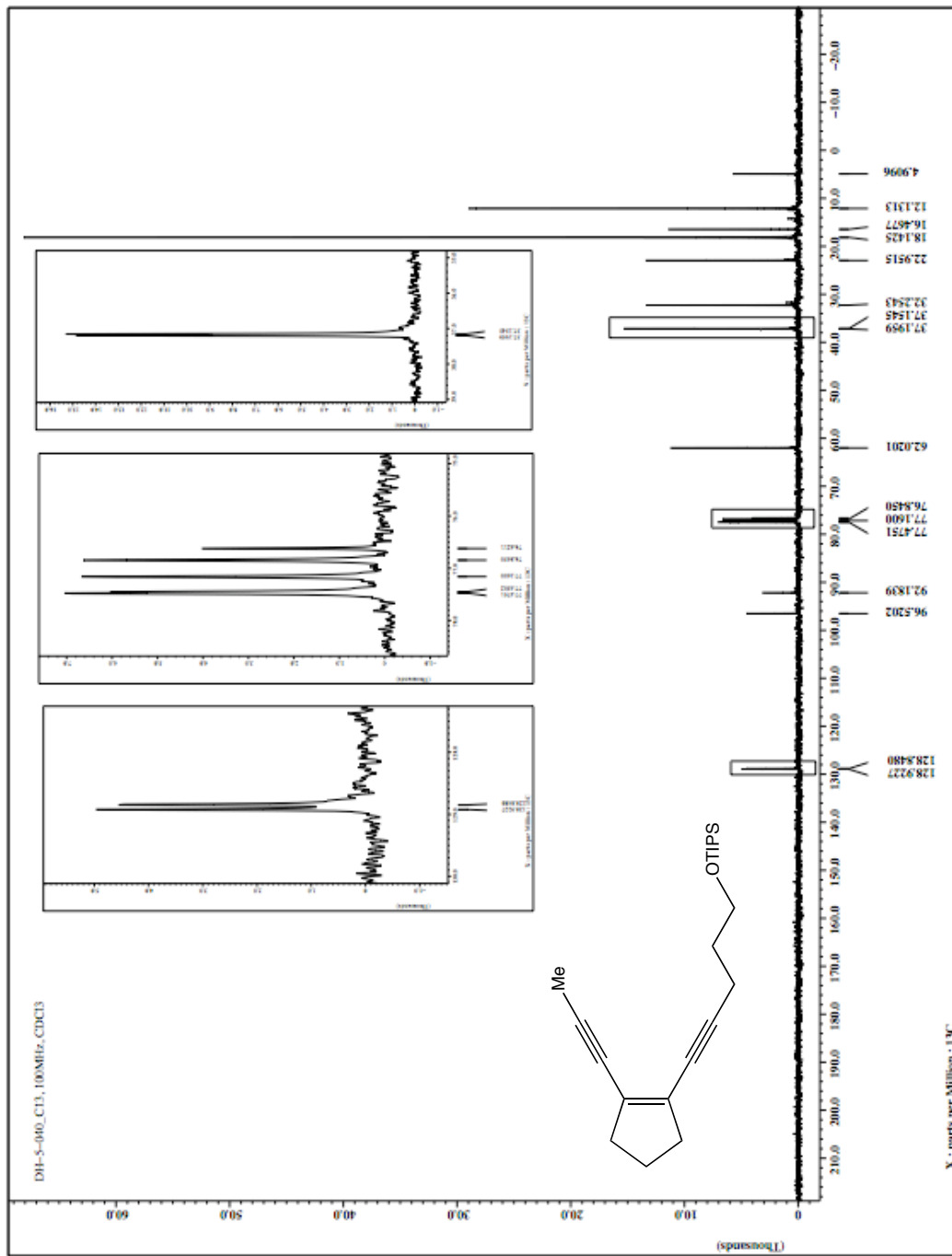


Figure 3-60. ^{13}C NMR spectrum (CDCl_3 , 100 MHz).

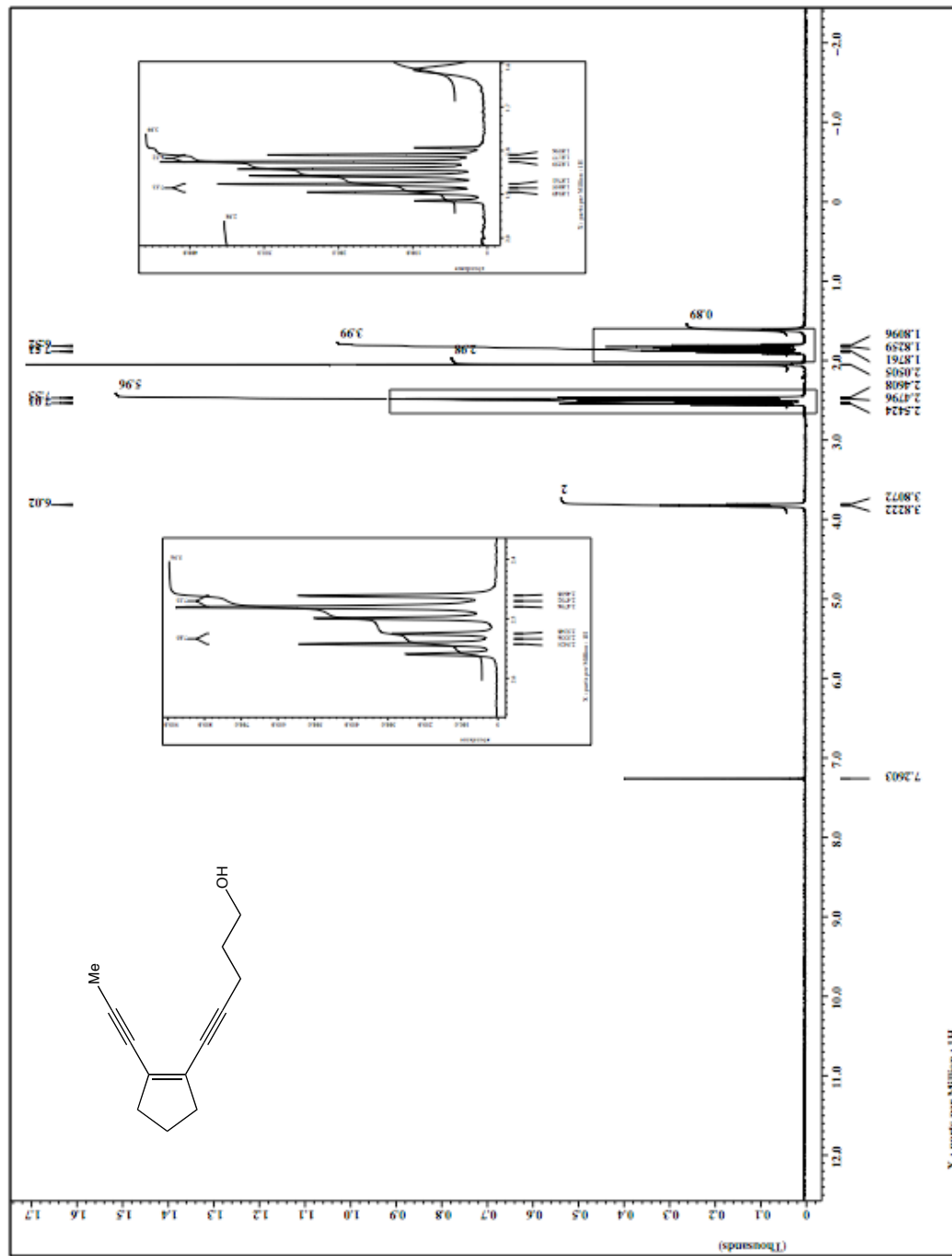


Figure 3-61. ⁶⁹ ¹H NMR spectrum (CDCl₃, 400 MHz).

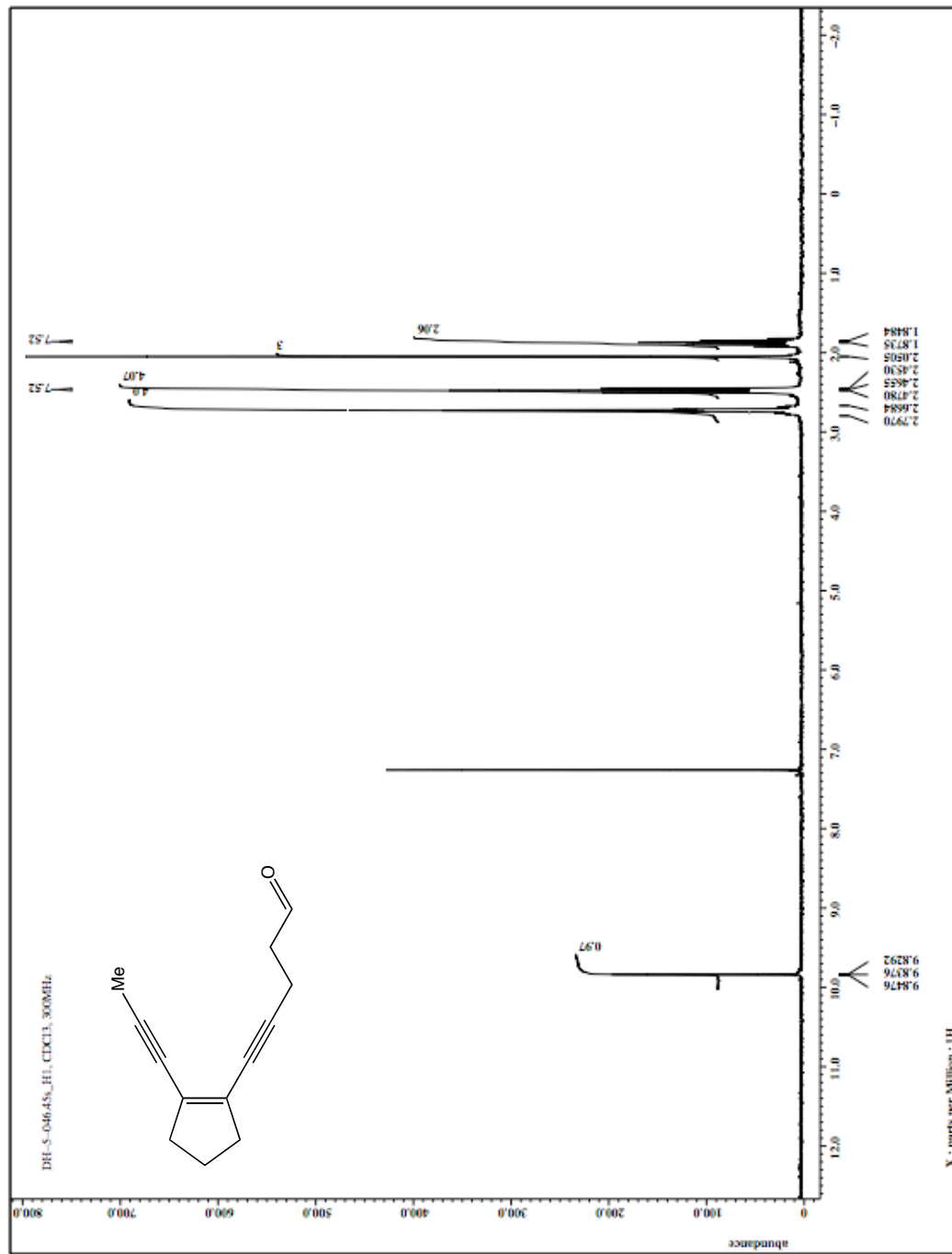


Figure 3-63. 78 ¹H NMR spectrum (CDCl₃, 300 MHz).

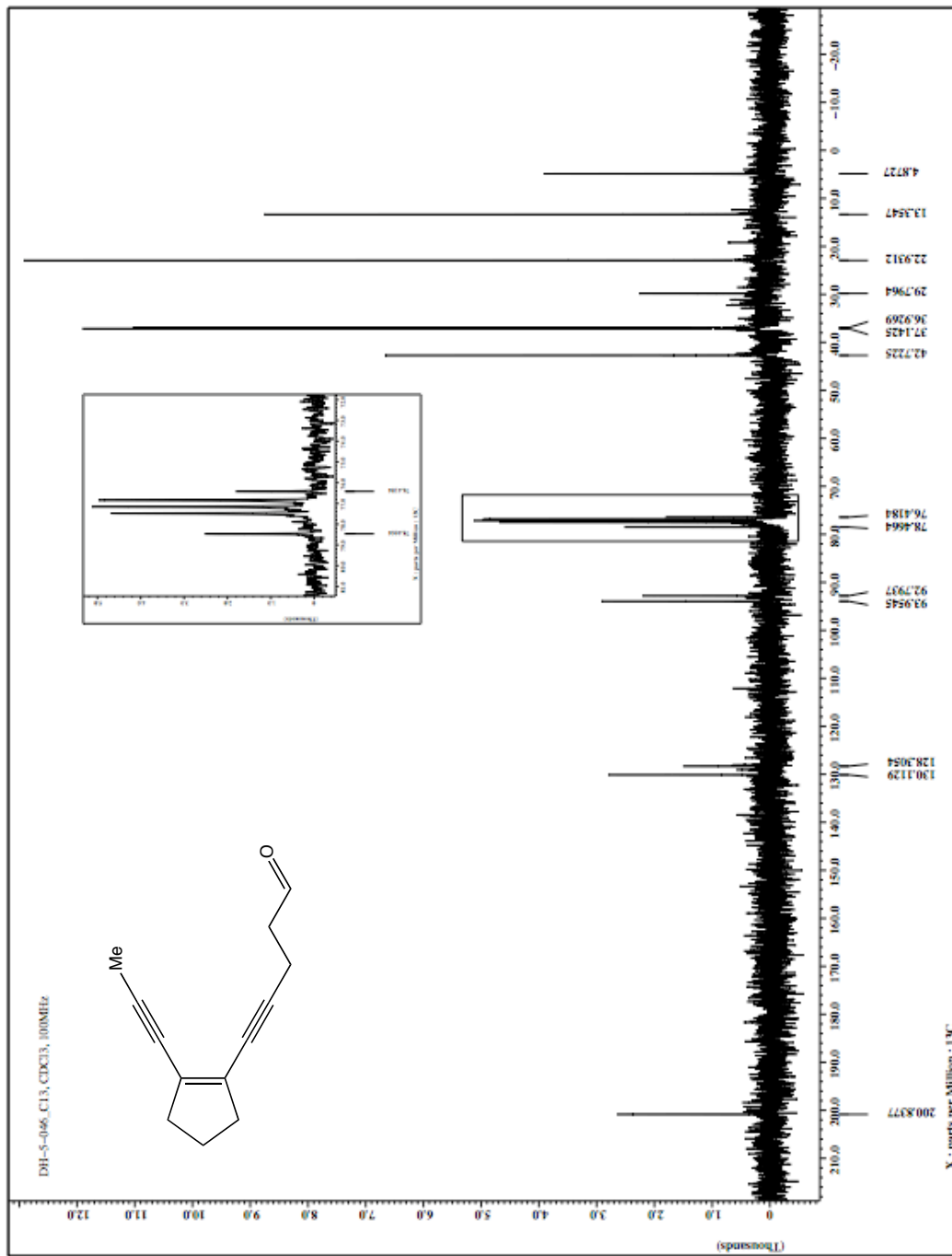


Figure 3-64. 78 ^{13}C NMR spectrum (CDCl_3 , 100 MHz).

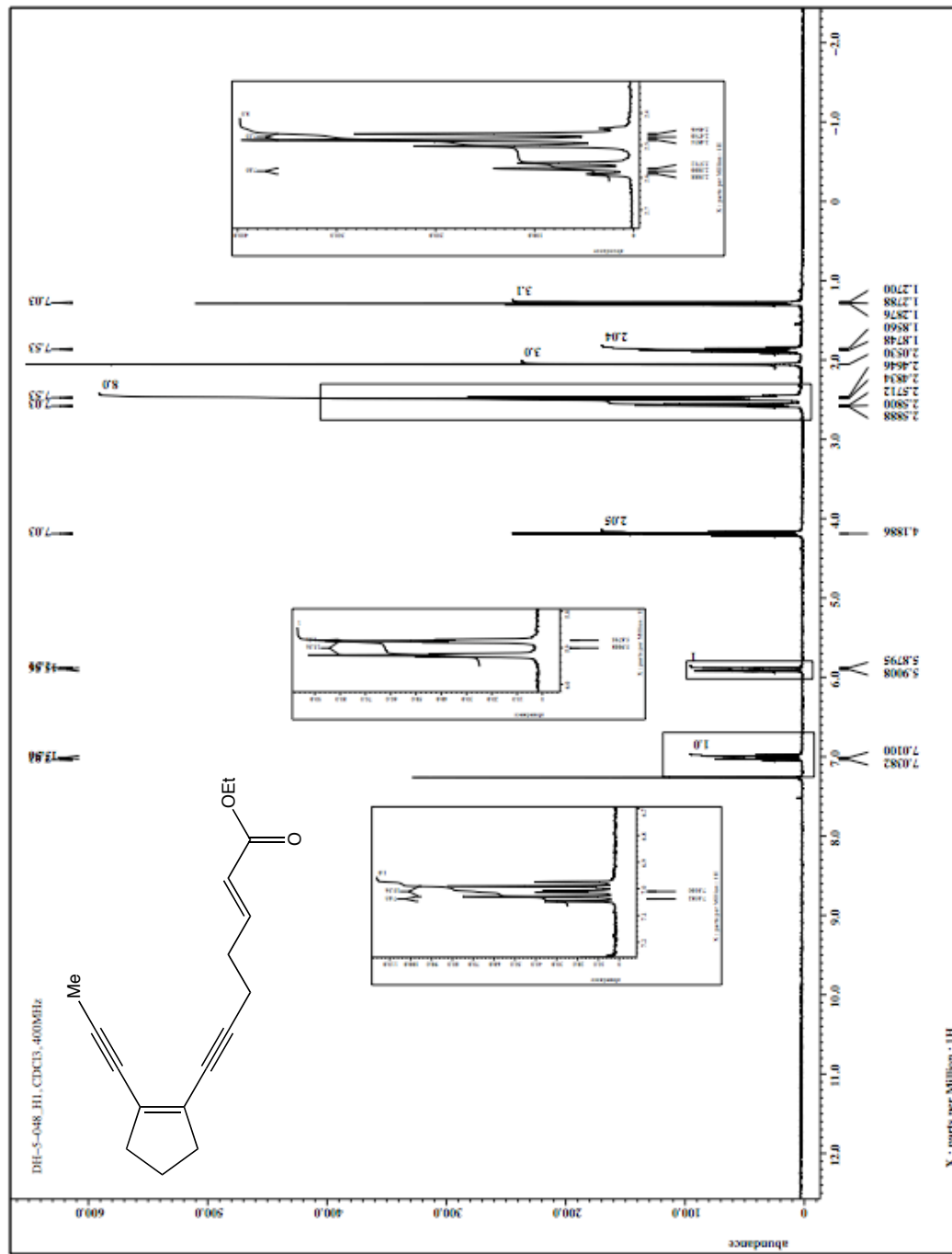


Figure 3-65. 64 ¹H NMR spectrum (CDCl₃, 400 MHz).

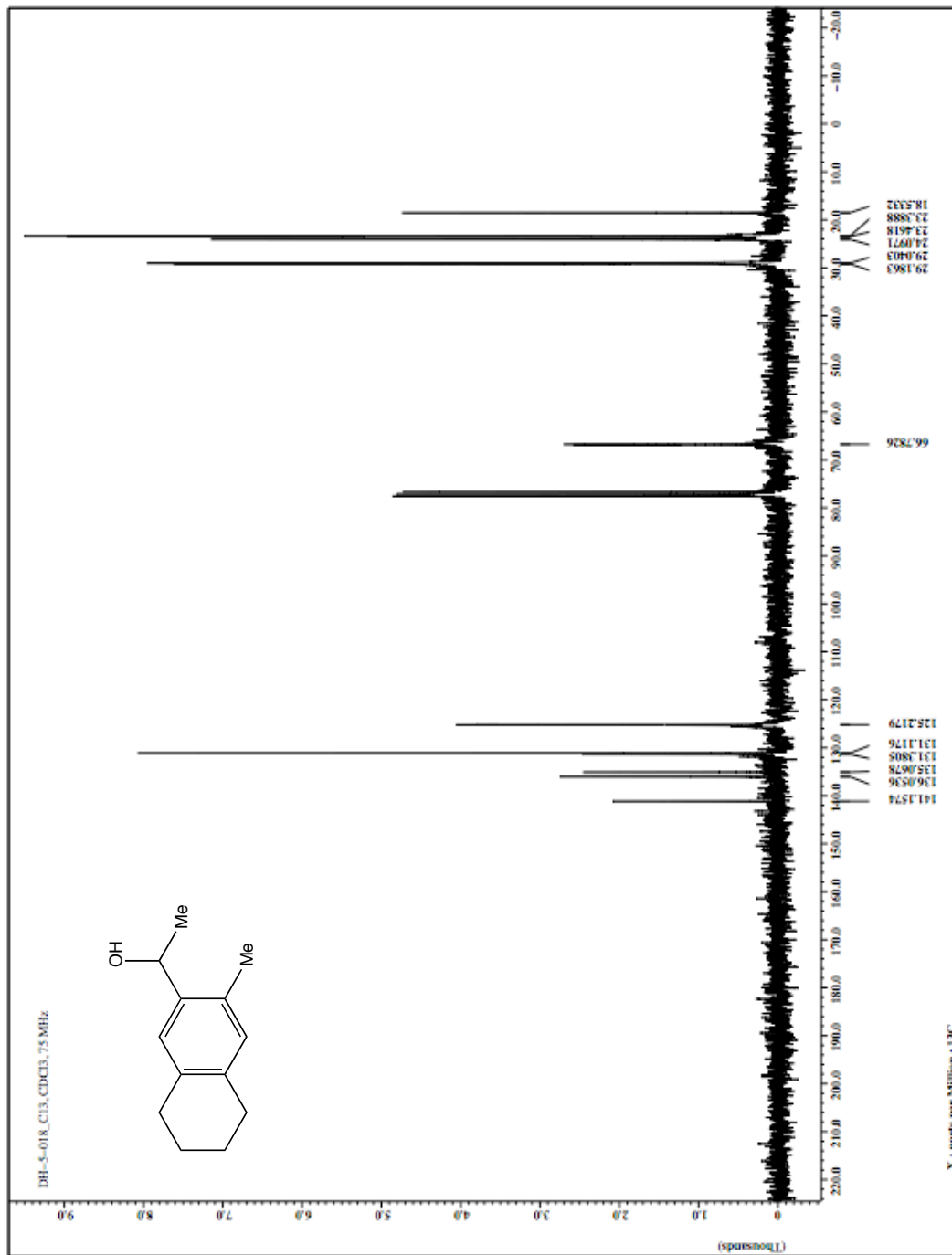


Figure 3-68. 71 ^{13}C NMR spectrum (CDCl_3 , 75 MHz).

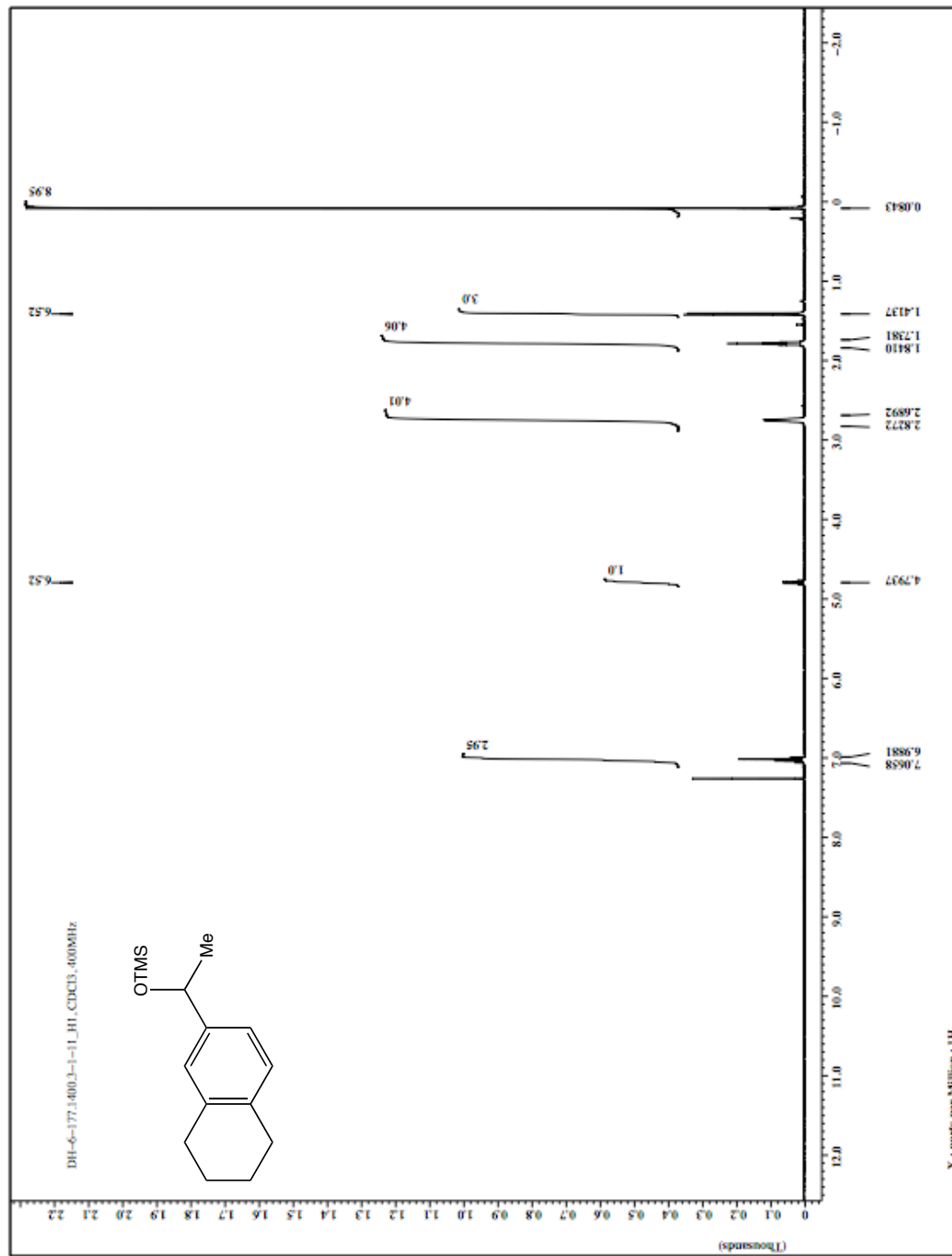


Figure 3-69. 79 ^1H NMR spectrum (CDCl_3 , 400 MHz).

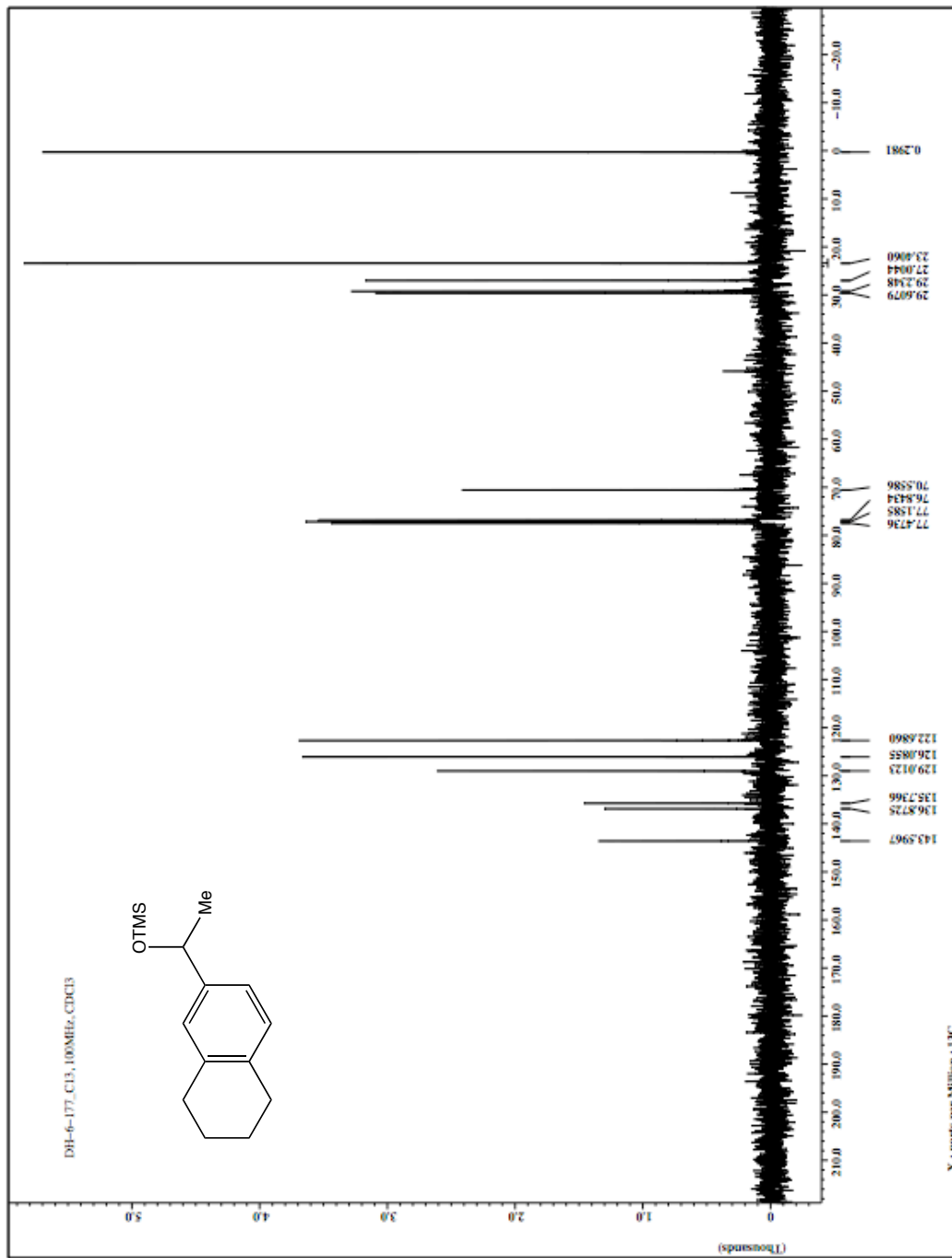


Figure 3-70. 79 ¹³C NMR spectrum (CDCl₃, 100 MHz).

viii. X-ray crystallographic summary and ORTEPS for characterized structures

General Experimental for X-Ray Structure Determinations.

A single crystal with general dimensions of $a \times b \times c$ was immersed in Paratone and placed on a Cryoloop. Data were collected on a Bruker SMART (APEX) CCD diffractometer, using a graphite monochromator with Mo or Cu $K\alpha$ radiation ($\lambda = 0.71073$ or 0.154056 \AA) at the defined temperature. The data were integrated using the Bruker SAINT software program and scaled using the SADABS software program. Solution by direct methods (SIR-2004) produced a complete heavy-atom phasing model consistent with the proposed structure. All non-hydrogen atoms were refined anisotropically by full-matrix least squares (SHELXL-97). All hydrogen atoms were placed using a riding model. Their positions were constrained relative to their parent atom using the appropriate HFIX command in SHELXL-97.

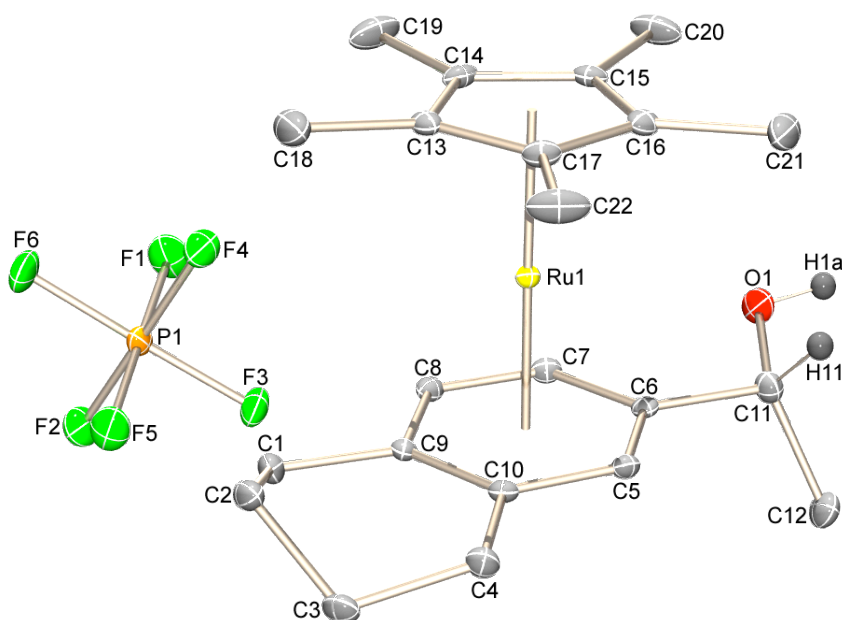


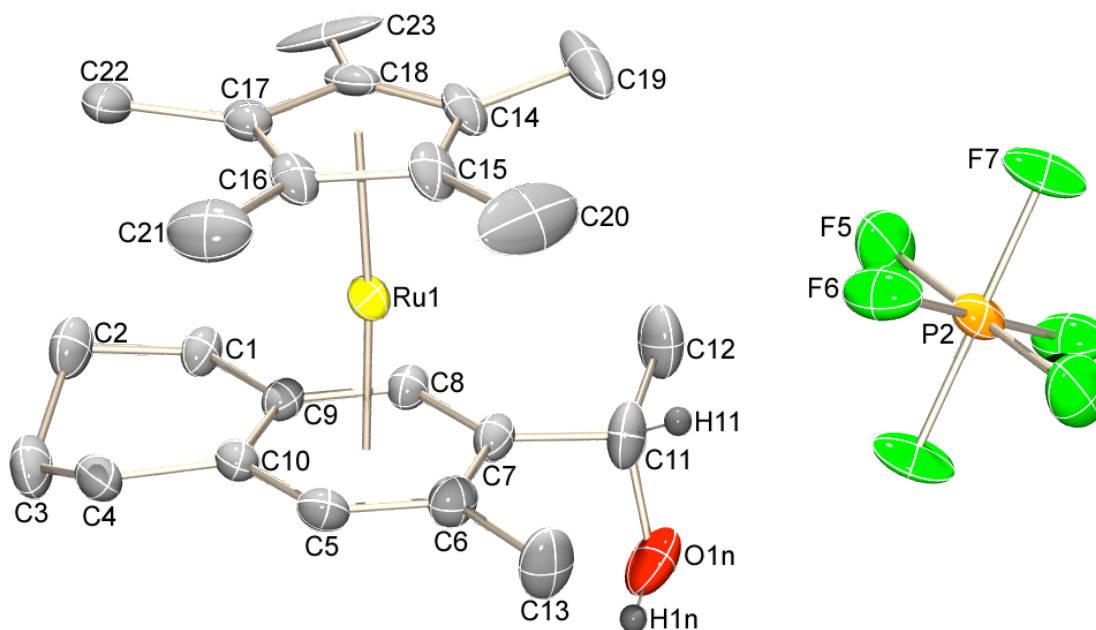
Figure 3-71. ORTEP of **42-mi**. Ellipsoids shown at 30 % probability. Most hydrogen atoms are omitted for clarity.

Table 3-3. Crystal data and structure refinement for **42-mi**.

| | | |
|---------------------------------|---|--------------------------------|
| Identification code | dh3112 | |
| Empirical formula | C ₂₂ H ₃₁ F ₆ O P Ru | |
| Formula weight | 557.51 | |
| Temperature | 100(2) K | |
| Wavelength | 0.71073 Å | |
| Crystal system | Triclinic | |
| Space group | P -1 | |
| Unit cell dimensions | a = 7.5848(7) Å | $\alpha = 98.4350(10)^\circ$. |
| | b = 11.1702(10) Å | $\beta = 92.0930(10)^\circ$. |
| | c = 13.4452(12) Å | $\gamma = 94.7740(10)^\circ$. |
| Volume | 1121.52(18) Å ³ | |
| Z | 2 | |
| Density (calculated) | 1.651 Mg/m ³ | |
| Absorption coefficient | 0.832 mm ⁻¹ | |
| F(000) | 568 | |
| Crystal size | 0.33 x 0.18 x 0.12 mm ³ | |
| Theta range for data collection | 1.53 to 25.36°. | |
| Index ranges | -9 ≤ h ≤ 9, -11 ≤ k ≤ 13, -16 ≤ l ≤ 15 | |
| Reflections collected | 7727 | |
| Independent reflections | 3804 [R(int) = 0.0154] | |
| Completeness to theta = 25.00° | 93.0 % | |
| Absorption correction | Semi-empirical from equivalents | |
| Max. and min. transmission | 0.9068 and 0.7709 | |
| Refinement method | Full-matrix least-squares on F ² | |
| Data / restraints / parameters | 3804 / 48 / 306 | |

Table 3-3. Crystal data and structure refinement for **42-mi**. (*continued*)

| | |
|--------------------------------------|------------------------------------|
| Goodness-of-fit on F ² | 1.060 |
| Final R indices [$I > 2\sigma(I)$] | R1 = 0.0238, wR2 = 0.0574 |
| R indices (all data) | R1 = 0.0253, wR2 = 0.0585 |
| Largest diff. peak and hole | 0.429 and -0.521 e.Å ⁻³ |

**Figure 3-72.** ORTEP of **48-mi**. Ellipsoids shown at 30 % probability. Most hydrogen atoms are omitted for clarity.**Table 3-4.** Crystal data and structure refinement for **48-mi**.

| | |
|---------------------|---|
| Identification code | dh4123mi2 |
| Empirical formula | C ₂₃ H ₃₃ F ₆ O P Ru |
| Formula weight | 571.53 |
| Temperature | 150(2) K |
| Wavelength | 0.71073 Å |

Table 3-4. Crystal data and structure refinement for **48-mi**. (*continued*)

| | | |
|-----------------------------------|---|------------------------------|
| Crystal system | Monoclinic | |
| Space group | C 2/c | |
| Unit cell dimensions | a = 32.28(2) Å | $\alpha = 90^\circ$. |
| | b = 9.476(7) Å | $\beta = 96.897(19)^\circ$. |
| | c = 15.462(11) Å | $\gamma = 90^\circ$. |
| Volume | 4696(6) Å ³ | |
| Z | 8 | |
| Density (calculated) | 1.617 Mg/m ³ | |
| Absorption coefficient | 0.797 mm ⁻¹ | |
| F(000) | 2336 | |
| Crystal size | 0.19 x 0.18 x 0.06 mm ³ | |
| Theta range for data collection | 1.27 to 26.38°. | |
| Index ranges | -39 ≤ h ≤ 40, -11 ≤ k ≤ 11, -19 ≤ l ≤ 19 | |
| Reflections collected | 36367 | |
| Independent reflections | 4742 [R(int) = 0.0785] | |
| Completeness to theta = 25.00° | 100.0 % | |
| Absorption correction | Semi-empirical from equivalents | |
| Max. and min. transmission | 0.9538 and 0.8634 | |
| Refinement method | Full-matrix least-squares on F ² | |
| Data / restraints / parameters | 4742 / 132 / 424 | |
| Goodness-of-fit on F ² | 1.091 | |
| Final R indices [I > 2σ(I)] | R1 = 0.0606, wR2 = 0.1402 | |
| R indices (all data) | R1 = 0.0797, wR2 = 0.1499 | |
| Extinction coefficient | 0.00028(7) | |
| Largest diff. peak and hole | 1.533 and -1.424 e.Å ⁻³ | |

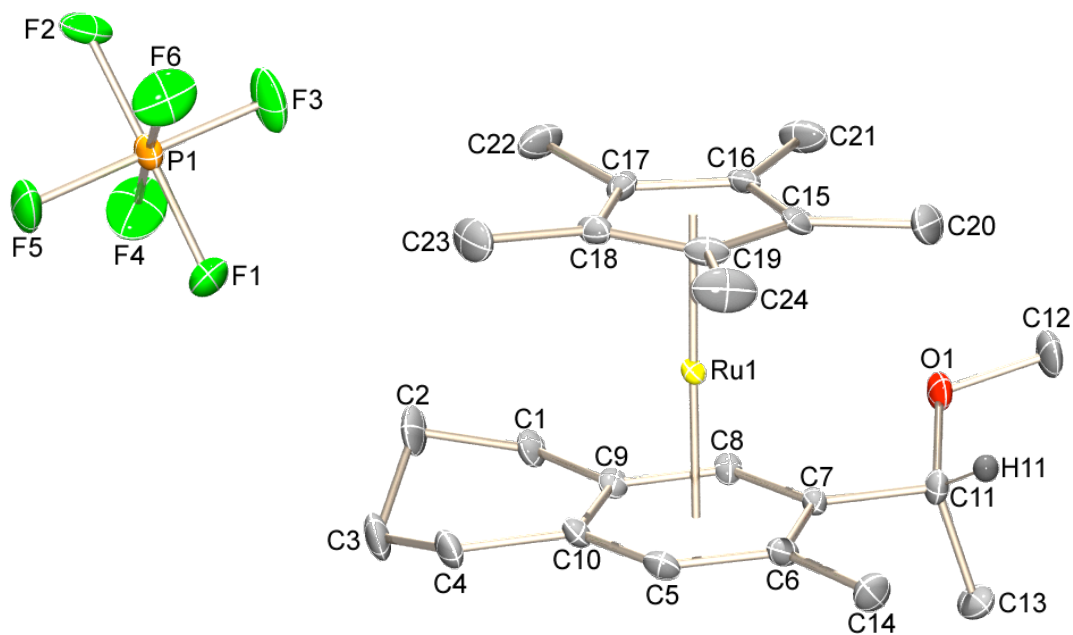


Figure 3-73. ORTEP of **50-ma**. Ellipsoids shown at 30% probability. Most hydrogen atoms are omitted for clarity.

Table 3-5. Crystal data and structure refinement for **50-ma**.

| | | |
|----------------------|---|-----------------|
| Identification code | dh4051 ma | |
| Empirical formula | C ₂₄ H ₃₅ F ₆ O P Ru | |
| Formula weight | 585.56 | |
| Temperature | 100(2) K | |
| Wavelength | 0.71073 Å | |
| Crystal system | Monoclinic | |
| Space group | P 2 ₁ /c | |
| Unit cell dimensions | a = 10.707(4) Å | α = 90°. |
| | b = 9.125(4) Å | β = 97.668(6)°. |
| | c = 25.935(10) Å | γ = 90°. |

Table 3-5. Crystal data and structure refinement for **50-ma**. (*continued*)

| | |
|-----------------------------------|---|
| Volume | 2511.2(17) Å ³ |
| Z | 4 |
| Density (calculated) | 1.549 Mg/m ³ |
| Absorption coefficient | 0.747 mm ⁻¹ |
| F(000) | 1200 |
| Crystal size | 0.14 x 0.10 x 0.08 mm ³ |
| Theta range for data collection | 1.58 to 28.54°. |
| Index ranges | -14<=h<=13, -10<=k<=11, -30<=l<=33 |
| Reflections collected | 19172 |
| Independent reflections | 5813 [R(int) = 0.1142] |
| Completeness to theta = 25.00° | 100.0 % |
| Absorption correction | Semi-empirical from equivalents |
| Max. and min. transmission | 0.9427 and 0.9026 |
| Refinement method | Full-matrix least-squares on F ² |
| Data / restraints / parameters | 5813 / 0 / 331 |
| Goodness-of-fit on F ² | 1.026 |
| Final R indices [I>2sigma(I)] | R1 = 0.0637, wR2 = 0.1567 |
| R indices (all data) | R1 = 0.0730, wR2 = 0.1669 |
| Largest diff. peak and hole | 1.125 and -1.809 e.Å ⁻³ |

Table 3-6. Crystal data and structure refinement for **50-mi.** (*continued*)

| | |
|-----------------------------------|---|
| Volume | 2476.0(13) Å ³ |
| Z | 4 |
| Density (calculated) | 1.571 Mg/m ³ |
| Absorption coefficient | 0.758 mm ⁻¹ |
| F(000) | 1200 |
| Crystal size | 0.09 x 0.04 x 0.02 mm ³ |
| Theta range for data collection | 2.29 to 28.22°. |
| Index ranges | -22<=h<=16, -10<=k<=10, -22<=l<=24 |
| Reflections collected | 23511 |
| Independent reflections | 5596 [R(int) = 0.1155] |
| Completeness to theta = 25.00° | 98.7 % |
| Absorption correction | Semi-empirical from equivalents |
| Max. and min. transmission | 0.9850 and 0.9349 |
| Refinement method | Full-matrix least-squares on F ² |
| Data / restraints / parameters | 5596 / 0 / 308 |
| Goodness-of-fit on F ² | 0.998 |
| Final R indices [I>2sigma(I)] | R1 = 0.0675, wR2 = 0.1273 |
| R indices (all data) | R1 = 0.1642, wR2 = 0.1606 |
| Largest diff. peak and hole | 0.723 and -0.588 e.Å ⁻³ |

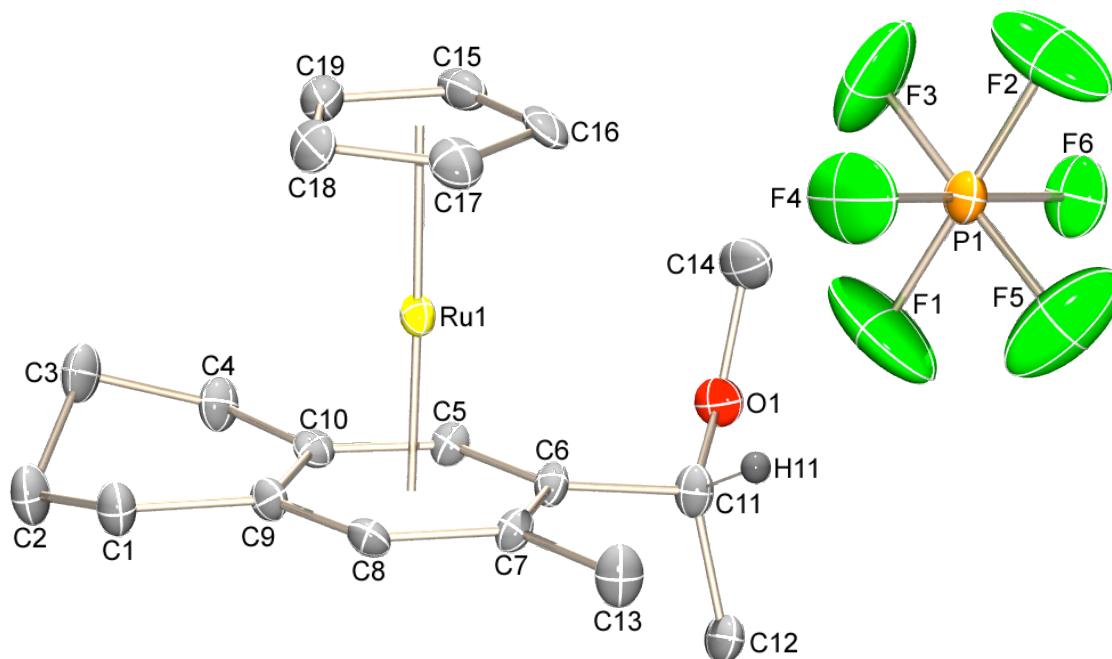


Figure 3-75. ORTEP of **52-ma**. Ellipsoids shown at 30% probability. Most hydrogen atoms are omitted for clarity.

Table 3-7. Crystal data and structure refinement for **52-ma**.

| | | |
|----------------------|---|-----------------------------|
| Identification code | dh4118ma | |
| Empirical formula | C ₁₉ H ₂₅ F ₆ O P Ru | |
| Formula weight | 515.43 | |
| Temperature | 100(2) K | |
| Wavelength | 1.54184 Å | |
| Crystal system | Monoclinic | |
| Space group | P n | |
| Unit cell dimensions | a = 10.2374(4) Å | $\alpha = 90^\circ$. |
| | b = 7.1600(3) Å | $\beta = 98.203(2)^\circ$. |
| | c = 13.6604(5) Å | $\gamma = 90^\circ$. |
| Volume | 991.06(7) Å ³ | |

Table 3-7. Crystal data and structure refinement for **52-ma**. (*continued*)

| | |
|-----------------------------------|---|
| Z | 2 |
| Density (calculated) | 1.727 Mg/m ³ |
| Absorption coefficient | 7.749 mm ⁻¹ |
| F(000) | 520 |
| Crystal size | 0.25 x 0.10 x 0.10 mm ³ |
| Theta range for data collection | 5.07 to 68.12°. |
| Index ranges | -12 ≤ h ≤ 8, -8 ≤ k ≤ 7, -16 ≤ l ≤ 15 |
| Reflections collected | 9329 |
| Independent reflections | 2688 [R(int) = 0.0333] |
| Completeness to theta = 67.00° | 98.3 % |
| Absorption correction | Semi-empirical from equivalents |
| Max. and min. transmission | 0.5113 and 0.2475 |
| Refinement method | Full-matrix least-squares on F ² |
| Data / restraints / parameters | 2688 / 2 / 256 |
| Goodness-of-fit on F ² | 1.057 |
| Final R indices [I > 2σ(I)] | R1 = 0.0256, wR2 = 0.0616 |
| R indices (all data) | R1 = 0.0269, wR2 = 0.0621 |
| Absolute structure parameter | 0.004(10) |
| Largest diff. peak and hole | 0.662 and -0.499 e.Å ⁻³ |

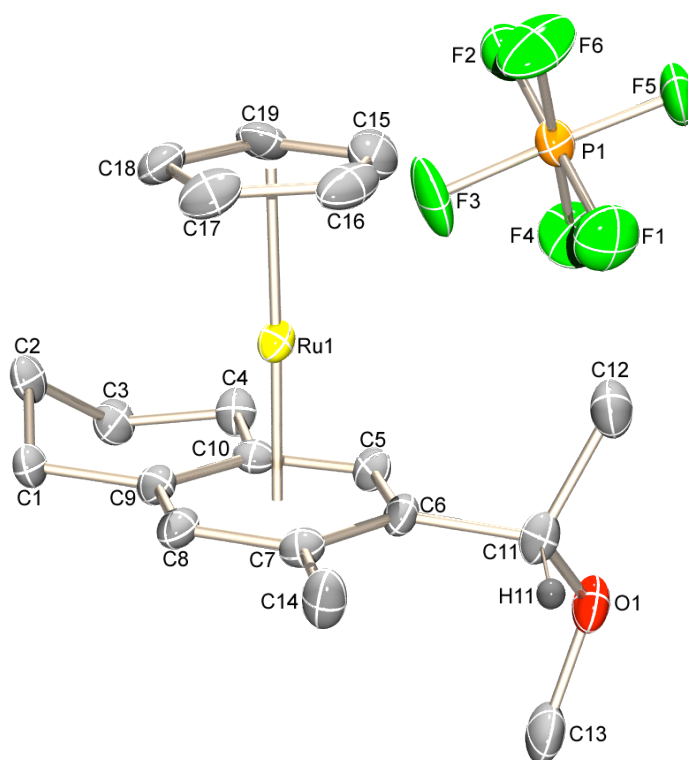


Figure 3-76. ORTEP of **52-mi**. Ellipsoids shown at 30% probability. Most hydrogen atoms are omitted for clarity.

Table 3-8. Crystal data and structure refinement for **52-mi**.

| | |
|---------------------|---|
| Identification code | dh4118mi3 |
| Empirical formula | C ₁₉ H ₂₅ F ₆ O P Ru |
| Formula weight | 515.43 |
| Temperature | 100(2) K |
| Wavelength | 0.71073 Å |
| Crystal system | Monoclinic |
| Space group | P 2 ₁ /c |

Table 3-8. Crystal data and structure refinement for **52-mi.** (*continued*)

| | | |
|--------------------------------------|---|----------------------------|
| Unit cell dimensions | a = 7.241(11) Å | $\alpha = 90^\circ$. |
| | b = 16.76(3) Å | $\beta = 92.37(2)^\circ$. |
| | c = 15.63(2) Å | $\gamma = 90^\circ$. |
| Volume | 1896(5) Å ³ | |
| Z | 4 | |
| Density (calculated) | 1.806 Mg/m ³ | |
| Absorption coefficient | 0.976 mm ⁻¹ | |
| F(000) | 1040 | |
| Crystal size | 0.25 x 0.10 x 0.10 mm ³ | |
| Theta range for data collection | 1.78 to 28.90°. | |
| Index ranges | -9<=h<=9, -20<=k<=22, -21<=l<=21 | |
| Reflections collected | 32776 | |
| Independent reflections | 4747 [R(int) = 0.0691] | |
| Completeness to theta = 25.00° | 99.6 % | |
| Absorption correction | Semi-empirical from equivalents | |
| Max. and min. transmission | 0.9087 and 0.7924 | |
| Refinement method | Full-matrix least-squares on F ² | |
| Data / restraints / parameters | 4747 / 0 / 273 | |
| Goodness-of-fit on F ² | 1.282 | |
| Final R indices [$I > 2\sigma(I)$] | R1 = 0.0762, wR2 = 0.1919 | |
| R indices (all data) | R1 = 0.0921, wR2 = 0.1981 | |
| Largest diff. peak and hole | 2.601 and -1.021 e.Å ⁻³ | |

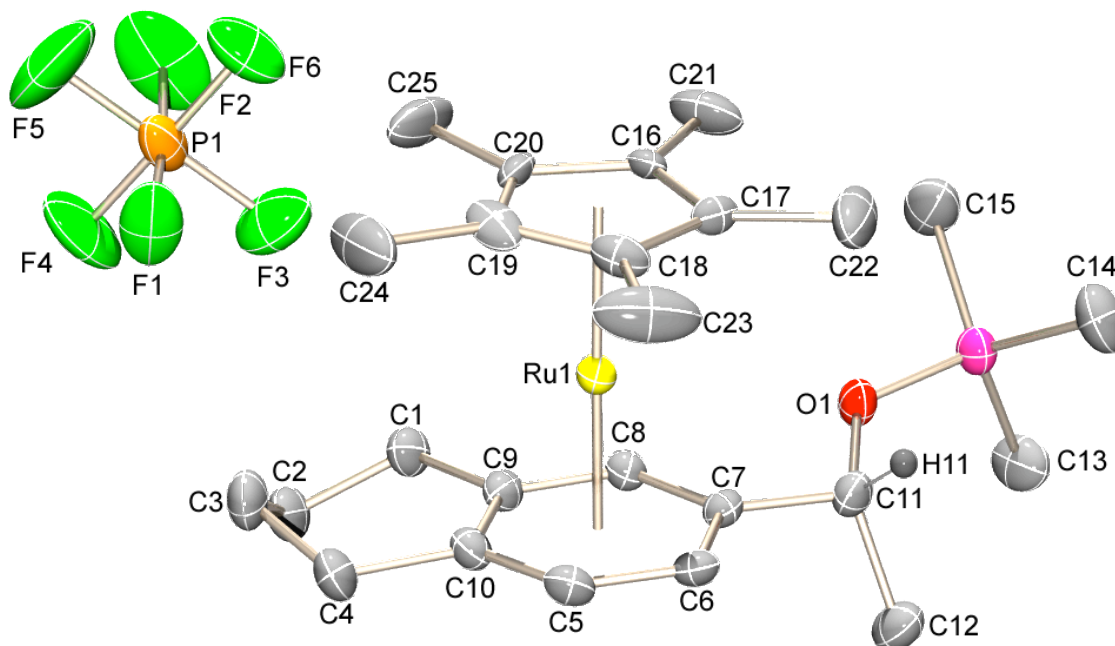


Figure 3-77. ORTEP of **57-ma**. Ellipsoids shown at 30% probability. Most hydrogen atoms are omitted for clarity.

Table 3-9. Crystal data and structure refinement for **57-ma**.

| | | |
|----------------------|--|-------------------------------|
| Identification code | dh3052 | |
| Empirical formula | C ₂₅ H ₃₈ F ₆ O P Ru Si | |
| Formula weight | 628.68 | |
| Temperature | 208(2) K | |
| Wavelength | 0.71073 Å | |
| Crystal system | Triclinic | |
| Space group | P -1 | |
| Unit cell dimensions | $a = 8.7255(18) \text{ \AA}$ | $\alpha = 99.999(3)^\circ$. |
| | $b = 10.908(2) \text{ \AA}$ | $\beta = 93.098(3)^\circ$. |
| | $c = 15.514(3) \text{ \AA}$ | $\gamma = 101.465(3)^\circ$. |
| Volume | $1419.1(5) \text{ \AA}^3$ | |

Table 3-9. Crystal data and structure refinement for **57-ma**. (*continued*)

| | |
|-----------------------------------|---|
| Z | 2 |
| Density (calculated) | 1.471 Mg/m ³ |
| Absorption coefficient | 0.706 mm ⁻¹ |
| F(000) | 646 |
| Crystal size | 0.05 x 0.02 x 0.02 mm ³ |
| Theta range for data collection | 1.94 to 28.13°. |
| Index ranges | -11 ≤ h ≤ 11, -13 ≤ k ≤ 14, -19 ≤ l ≤ 18 |
| Reflections collected | 10699 |
| Independent reflections | 5443 [R(int) = 0.0369] |
| Completeness to theta = 25.00° | 85.0 % |
| Absorption correction | Semi-empirical from equivalents |
| Max. and min. transmission | 0.9860 and 0.9655 |
| Refinement method | Full-matrix least-squares on F ² |
| Data / restraints / parameters | 5443 / 0 / 461 |
| Goodness-of-fit on F ² | 1.027 |
| Final R indices [I > 2σ(I)] | R1 = 0.0501, wR2 = 0.1059 |
| R indices (all data) | R1 = 0.0807, wR2 = 0.1213 |
| Largest diff. peak and hole | 0.713 and -0.662 e. Å ⁻³ |

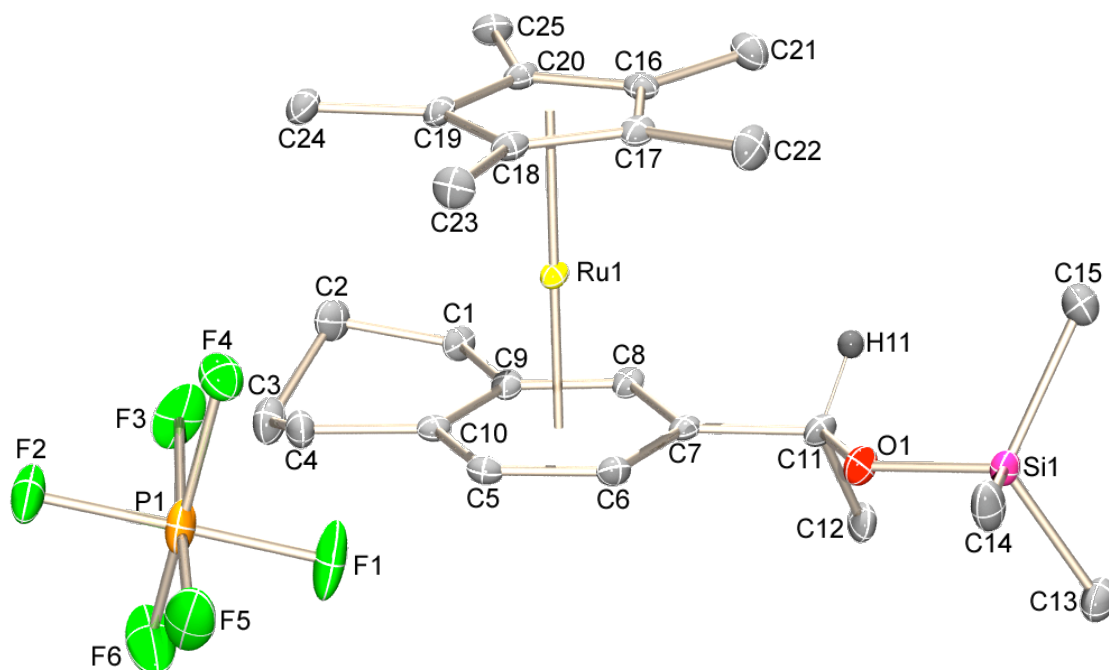


Figure 3-80. ORTEP of **57-mi**. Ellipsoids shown at 30% probability. Most hydrogen atoms are omitted for clarity.

Table 3-10. Crystal data and structure refinement for **57-mi**.

| | | |
|----------------------|--|------------------------------|
| Identification code | dh3093 | |
| Empirical formula | C ₂₅ H ₃₉ F ₆ O P Ru Si | |
| Formula weight | 629.69 | |
| Temperature | 90(2) K | |
| Wavelength | 1.54184 Å | |
| Crystal system | Triclinic | |
| Space group | P -1 | |
| Unit cell dimensions | $a = 10.0528(4)$ Å | $\alpha = 88.302(4)^\circ$. |
| | $b = 11.5254(5)$ Å | $\beta = 80.624(3)^\circ$. |
| | $c = 12.0865(5)$ Å | $\gamma = 79.656(4)^\circ$. |
| Volume | $1359.21(10)$ Å ³ | |

Table 3-10. Crystal data and structure refinement for **57-mi.** (*continued*)

| | |
|-----------------------------------|---|
| Z | 2 |
| Density (calculated) | 1.539 Mg/m ³ |
| Absorption coefficient | 6.168 mm ⁻¹ |
| F(000) | 648 |
| Crystal size | 0.15 x 0.10 x 0.05 mm ³ |
| Theta range for data collection | 3.71 to 68.47°. |
| Index ranges | -12<=h<=11, -13<=k<=11, -14<=l<=14 |
| Reflections collected | 12508 |
| Independent reflections | 4854 [R(int) = 0.0704] |
| Completeness to theta = 67.00° | 98.0 % |
| Absorption correction | Semi-empirical from equivalents |
| Max. and min. transmission | 0.7479 and 0.4581 |
| Refinement method | Full-matrix least-squares on F ² |
| Data / restraints / parameters | 4854 / 0 / 362 |
| Goodness-of-fit on F ² | 1.014 |
| Final R indices [I>2sigma(I)] | R1 = 0.0414, wR2 = 0.0859 |
| R indices (all data) | R1 = 0.0649, wR2 = 0.0948 |
| Largest diff. peak and hole | 0.955 and -0.899 e.Å ⁻³ |

X. References.

1. Semmelhack, M. F. In *Comprehensive Organometallic Chemistry II*. Abel, E. W.; Stone, F. G. A.; Wilkinson, G., Ed.; Pergamon: Oxford, New York, 1995; Vol. 12; p 979-1015.
2. Pape, A. R.; Kaliappan, K. P.; Kündig, E. P. *Chem. Rev.* **2000**, *100*, 2917.
3. Semmelhack, M. F. In *Comprehensive Organometallic Chemistry II*. Abel, E. W.; Stone, F. G. A.; Wilkinson, G., Ed.; Pergamon: Oxford, New York, 1995; Vol. 12; p 1017-1038.

4. (a) Pigge, F.C.; Coniglio, J.J. *Curr. Org. Chem.* **2001**, *5*, 757. (b) Le Bozec, H.; Touchard, D.; Dixneuf, P. H. *Adv. Organomet. Chem.* **1989**, *29*, 163. (c) Moriarty, R. M.; Gill, U. S.; Ku, Y. Y. *J. Organomet. Chem.* **1988**, *350*, 157.
5. McNair, A. M.; Schrenk, J. L.; Mann, K. R. *Inorg. Chem.* **1984**, *23*, 2633.
6. Pearson, A. J.; Chelliah, M. V. *J. Org. Chem.* **1998**, *63*, 3087.
7. Pigge, F. C.; Fang, S.; Rath, N. P. *Tetrahedron Lett.* **1999**, *40*, 2251.
8. Moutiers, G.; Peigneux, A.; Vichard, D.; Terrier, F. *Organometallics*, **1998**, *17*, 4469.
9. (a) Glatzhofer, D. T.; Liang, Y.; Khan, M. A. *Organometallics*, **1993**, *12*, 624. (b) Glatzhofer, D. T.; Liang, Y.; Funkhouser, G. P.; Khan, M. A. *Organometallics*, **1994**, *13*, 315. (c) Pigge, F. C.; Dhanya, R.; Hoefgen, E. R. *Angew. Chem. Int. Ed.* **2007**, *46*, 2887. (d) Moriarty, R. M.; Enache, L. A.; Gilardi, R.; Gould, G. L.; Wink, D. J. *Chem. Commun.* **1998**, 1155. (e) Kamikawa, K.; Norimura, K.; Furusyo, M.; Uno, T.; Sato, Y.; Konoo, A.; Bringmann, G.; Uemura M. *Organometallics*, **2003**, *22*, 1038.
10. (a) Schögl, K. *Top. Stereochem.* 1967, **1**, 39. (b) Bolm, C.; Muñoz, K. *Chem. Soc. Rev.* **1999**, *28*, 51.
11. (a) Solladié-Cavallo, A. In *Advances in Metal Organic Chemistry*, Liebeskind, L.S., Ed.; JAI: London, 1989, Vol 2; p 99. (b) Gibson, S. E.; Ibrahim, H. *Chem. Commun.* **2002**, 2465.
12. (a) O'Connor, J.M.; Friese, S.J.; Rodgers, B.L. *J. Am. Chem. Soc.* **2005**, *127*, 16342. (b) O'Connor, J.M.; Friese, S.J.; Rodgers, B.L. Rheingold, A.L.; Zakharov, L. *J. Am. Chem. Soc.* **2005**, *127*, 9346. (c) O'Connor, J.M.; Friese, S.J.; Tichenor, M. *J. Am. Chem. Soc.* **2002**, *124*, 3506. (d) O'Connor, J.M.; Lee, L.I.; Gantzel, P. *J. Am. Chem. Soc.* **2000**, *122*, 12057. (e) Friese, S.; PhD. Dissertation, University of California, San Diego **2004**.
13. Jones, R.R.; Bergman, R.G. *J. Am. Chem. Soc.* **1972**, *94*, 660.
14. Hopf, H.; Musso, H. *Angew. Chem. Int. Ed.* **1969**, *8*, 680.
15. The distance between the terminal carbon atoms of the alkynes has been correlated with rate enhancement in the thermal Bergman reaction. Nicolaou, K.C.; Smith, A.L. *Acc. Chem. Res.* **1992**, *25*, 497.
16. For reviews. (a) Paley, R.S. *Chem. Rev.* **2002**, *102*, 1493. (b) Bolm, C.; Muñoz, K. *Chem. Soc. Rev.* **1999**, *28*, 51.
17. For ruthenium examples. (a) Kamikawa, K.; Norimura, K.; Furusyo, M.; Uno, T.; Sato, Y.; Konoo, A.; Bringmann, G.; Uemura, M. *Organometallics* **2003**, *22*, 1038. (b) Kamikawa, K.; Furusyo, M.; Uno, T.; Sato, Y.; Konoo, A.; Bringmann, G.; Uemura, M. *Org. Lett.* **2001**, *3*, 3667.
18. For reviews. (a) Minatti, A.; Dötz, K.H. *Topics Organomet. Chem.* **2004**, *13*, 123. (b) Wulff, W.D. In *Advances in Metal-Organic Chemistry*. Liebeskind, L.S., Ed.; JAI Press LTD: Greenwich, CT, 1989; Vol. 1; p 209 – 393. (c) Wulff, W.D. In *Comprehensive Organic*

- Synthesis*. Trost, B.M.; Fleming, I., Ed.; Pergamon Press: New York, 1991; Vol. 5; p 1065 – 1113. (d) Dötz, K.H. *Angew. Chem., Int. Ed. Engl.* **1984**, *23*, 587.
19. Hofmann, P.; Hämmerle, M. *Angew. Chem., Int. Ed. Engl.* **1989**, *28*, 908.
20. Waters, M.L.; Brandvold, T.A.; Isaacs, L.; Wulff, W.D.; Rheingold, A.L. *Organometallics* **1998**, *17*, 4298.
21. Waters, M.L.; Bos, M.E.; Wulff, W.D. *J. Am. Chem. Soc.* **1999**, *121*, 6403.
22. (a) Hsung, R.P.; Wulff, W.D. *J. Am. Chem. Soc.*, **1994**, *116*, 6449. (b) Kretschik, O.; Nieger, M.; Dötz, K.H. *Organometallics*, **1996**, *15*, 3625. (c) Paetsch, D.; Dötz, K.H. *Tetrahedron Lett.* **1999**, *40*, 487. (d) Janes, E.; Nieger, M.; Saarenketo, P.; Dötz, K.H. *Eur. J. Org. Chem.* **2003**, 2276.
23. (a) Beddoes, R.L.; King, J.D.; Quayle, P. *Tetrahedron Lett.* **1995**, *36*, 3027. (b) Hsung, R.P.; Wulff, W.D.; Challener, C.A. *Synthesis*, **1996**, 773. (c) Pfeiffer, J.; Nieger, M.; Dötz, K.H. *Chem. Eur. J.* **1998**, *4*, 1843. (d) Dötz, K.H.; Jäkel, C.; Haase, W.-C. *J. Organomet. Chem.* **2001**, *617-618*, 119.
24. (a) Dötz, K.H.; Stinner, C.; Nieger, M. *J. Chem. Soc., Chem. Commun.* **1995**, 2535. (b) Dötz, K.H.; Stinner, C. *Tetrahedron: Asymmetry* **1997**, *8*, 1751. (c) Hsung, R.P.; Wulff, W.D.; Chamberlin, S.; Liu, Y.; Liu, R.-Y.; Wang, H.; Quinn, J.F.; Wang, S.L.B.; Rheingold, A.L. *Synthesis*, **2001**, 200.
25. (a) Longen, A.; Nieger, M.; Airola, K.; Dötz, K.H. *Organometallics*, **1998**, *17*, 1538. (b) Dötz, K.H.; Gerhardt, A. *J. Organomet. Chem.* **1999**, *578*, 223. (c) Tomuschat, P.; Kröner, L.; Steckhan, E.; Nieger, M.; Dötz, K.H. *Chem. Eur. J.* **1999**, *5*, 700. (d) Quast, L.; Nieger, M.; Dötz, K.H. *Organometallics*, **2000**, *19*, 2179. (e) Fogel, L.; Hsung, R.P.; Wulff, W.D. *J. Am. Chem. Soc.* **2001**, *123*, 5580. (f) Dötz, K.H.; Mittenzwey, S. *Eur. J. Org. Chem.* **2002**, 39.
26. Kato, Y.; Miki, K.; Nishino, F.; Ohe, K.; Uemura, S. *Org. Lett.* **2003**, *5*, 2619.
27. Steinmetz, B.; Schenk, W. *Organometallics*. **1999**, *18*, 943.
28. It should be noted that a CpRu⁺ fragment is also less electron donating than the Cp*Ru⁺ and this electronic effect on the stereoselectivity cannot be ruled out.
29. Grissom, J.W.; Calkins, T.L.; Huang, D.; McMillen, H. *Tetrahedron* **1994**, *50*, 4635.
30. Robertson, I.R.; Sharp, J.T. *Tetrahedron*. **1984**, *40*, 3095.
31. La Cruz, T.E.; Rychnovsky, S.D. *Chem. Commun.* **1994**, 168.
32. (a) Fagan, P.J., Mahoney, W.S.; Calabrese, J.C.; Williams, I.D. *Organometallics*, **1990**, *9*, 1843. (b) Gemel, C.; Kalt, D.; Mereiter, K.; Sapunov, V.N.; Schmid, R.; Kirchner, K. *Organometallics*, **1997**, *16*, 427. (c) Gemel, C.; Kirchner, K.; Schmid, R.; Mereiter, K. *Acta Cryst.* **1999**, *C55*, 2053. (d) Sánchez-Castro, M.E.; Paz-Sandoval, M.A. *Organometallics*, **2008**, *27*, 6083.
33. Still, W.C.; Khan, M.; Mitra, A. *J. Org. Chem.* **1978**, *43*, 2923.

34. Williams, D. B. G.; Lawton, M. *J. Org. Chem.* **2010**, *75*, 8351.
35. Frigerio, M.; Santagostino, M.; Sputore, S. *J. Org. Chem.* **1999**, *64*, 4537.
36. See Chapter 2, Section VII.
37. Nicolaou, K.C.; Montagnon, T.; Ulven, T.; Baron, P.S.; Zhong, Y.-L.; Sarabia, F. *J. Am. Chem. Soc.* **2002**, *124*, 5718.

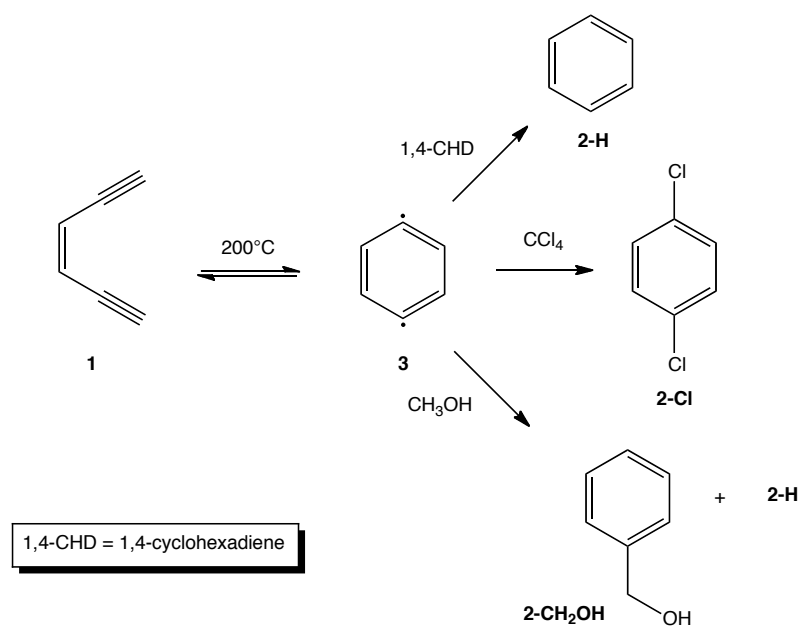
XI. Acknowledgements.

The material of Chapter 3, in part, is currently being prepared for submission for publication with the following authors: Hitt, D.M.; Holland, R.L.; O'Connor, J.M. The dissertation author was the primary investigator and author of this material.

CHAPTER 4: A Novel Route of Cycloaromatization for Conjugated Eneidyne

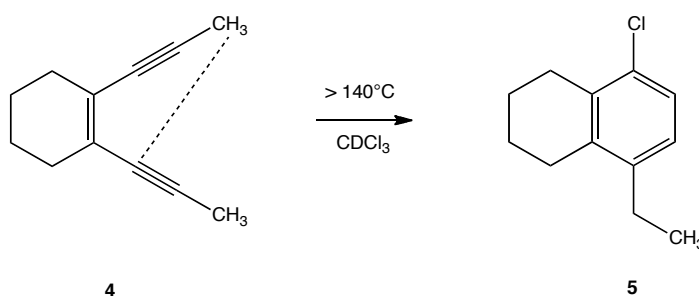
I. Introduction.

In 1972, Bergman and Jones reported that *cis*-1,5-hexadiyn-3-ene **1** cyclizes to a variety of benzenoid compounds **2** in the presence of a sufficient atom donor under thermal conditions (200°C, Scheme 4-1).¹ The currently accepted mechanism, as originally proposed by Bergman, involves the formation of a *para*-benzyne **3**. Radical species **3** was shown to be in equilibrium with the substrate by scrambling of a deuterium label between the acetylenic and vinylic positions. Since the initial report, the cycloaromatization has received considerable attention, mainly for the ability of the *para*-benzyne radical to attack and break the phosphate backbone of DNA providing applications as an anti-cancer therapeutic.² Due to the high temperatures needed to effect cyclization of non-cyclic enediynes, the reaction has found little use in synthesis.^{2b}



Scheme 4-1. Thermal cycloaromatization of conjugated enediyne **1** to atom abstraction products **2** through intermediacy of *para*-benzyne **3**.¹

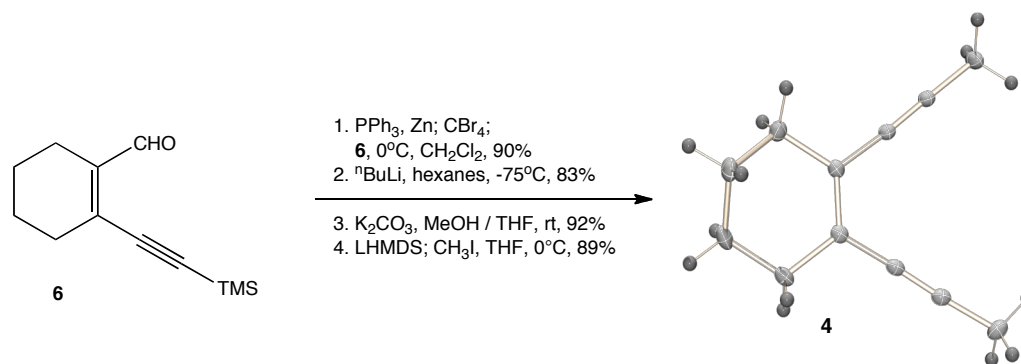
In continuation of previous work in the O'Connor laboratory with ruthenium triggered formal Bergman cycloaromatizations of enediyne, we desired to obtain a comparison in activation parameters for the metal mediated and thermal reactions.³ During our investigations, it was discovered that heating enediyne **4** in CDCl₃ at temperatures in excess of 140°C resulted in an unprecedented cycloaromatization resulting from bond formation between the propargylic and internal alkyne carbon atoms to give tetraline **5** (Scheme 4-2). Herein, we account the initial discovery and our current mechanistic hypothesis on this atypical cycloaromatization.



Scheme 4-2. Novel enediyne cycloaromatization pathway of **4** to 5-chloro-8-ethyl-tetraline **5**.

II. Results.

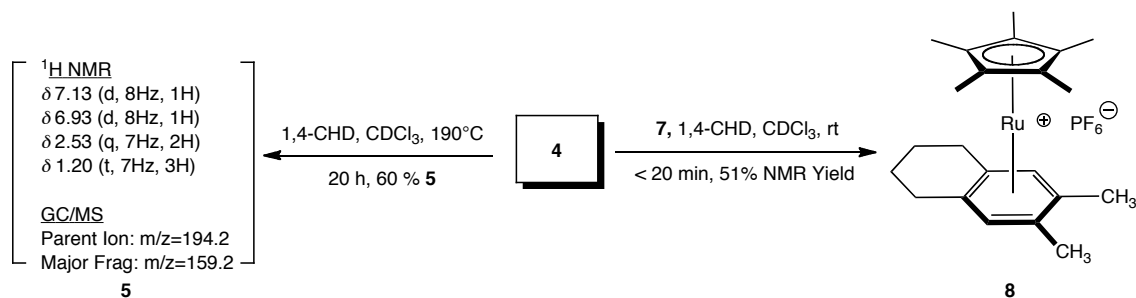
Synthesis of model enediyne **4** commenced from known **6** that was prepared in two steps from cyclohexanone.⁴ Aldehyde **6** was converted to the terminal alkyne by the Corey-Fuchs protocol then desilylated and methylated from the acetylide to give **4** as a crystalline solid, allowing for X-ray structure determination (Scheme 4-3).



Scheme 4-3. Synthetic route and ORTEP of model enediyne **4**.

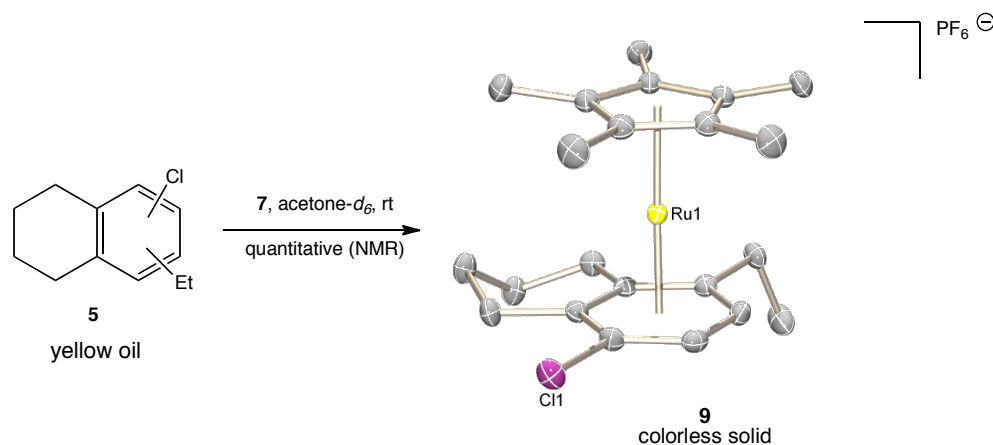
Treatment of **4** with [Cp**Ru*(NCMe)₃]PF₆ (**7**)⁵ and 1,4-cyclohexadiene (1,4-CHD) in CDCl₃ at ambient temperature led to rapid cycloaromatization giving η^6 -6,7-dimethyltetraline complex **8** in 51% NMR yield (Scheme 4-4). Consistent with the structure of **8**, uncoupled aromatic methyl and hydrogen resonances were observed at δ 2.08 and 5.52 in the ¹H NMR spectrum, respectively. The upfield shift of the aromatic hydrogen resonance is typical for η^6 -arene complexes.

We then examined the thermal reactivity of **4**. Heating a CDCl₃ solution of **4** and 1,4-cyclohexadiene at 190°C in a flame-sealed thick-walled NMR tube for 20 h yielded compound **5** with the spectral data shown in Scheme 4-4. The ¹H NMR spectrum of this compound exhibited two coupled doublets in the aromatic region and a coupled triplet and quartet in a 1:1:3:2 ratio, respectively, suggesting a 1,2 or 2,3 aromatic hydrogen substitution pattern and the presence of an ethyl group. GC/MS analysis of the reaction mixture showed a parent ion peak at 194.2 *m/z* with a major fragmentation peak at 159.2 *m/z* corresponding to loss of a chlorine atom. The parent ion peak would then correspond to the substrate mass + H + Cl. Three possible tetraline structures could fit this data: (1) 5-chloro-8-ethyl, (2) 5-chloro-6-ethyl, or (3) 6-chloro-5-ethyl.



Scheme 4-4. Expected and unexpected cycloaromatization of enediyne **4**.

In hopes of obtaining a crystalline material that might be suitable for X-ray analysis, **5** was allowed to react with **7** resulting in quantitative formation of arene complex **9** (Scheme 4-5). We were pleased to obtain single crystals upon slow diffusion of ethyl ether into a dichloromethane solution of **9**. The solid-state structure of **9** verified the connectivity of **5** to be 5-chloro-8-ethyl-tetraline. To rule out any possible structural rearrangements that might have occurred during complexation of **5**, **9** was subjected to sunlight in aerobic CH_3CN resulting in liberation of the free arene as verified by ^1H NMR spectroscopy.

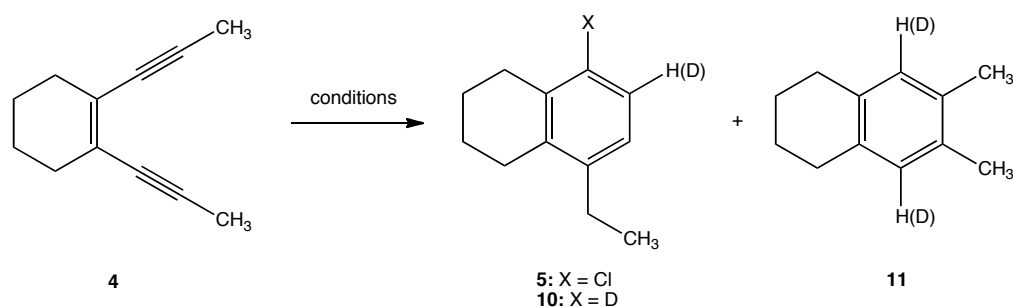


Scheme 4-5. Absolute structure determination of **5** through formation of crystalline Cp^*Ru -arene complex **9**.

To determine if this interesting cyclization was specific for halogenated solvents, the reaction was run in THF- d_6 (entry 1, Table 4-1). After 19 h at 200°C, two products, **10** and **11**, were observed in low yield based on the conversion of **4**. Compound **11** exhibited a singlet at δ 2.14 in the ^1H NMR spectrum that was assigned to the aromatic methyl of the Bergman cyclization product 5,8-dideutero-6,7-dimethyl-tetraline. Similar to **5**, the ^1H NMR spectrum of **10** exhibited triplet and quartet resonances at δ 1.16 and 2.55 ($J = 8$ Hz) in a $\sim 3:2$ ratio, respectively, suggesting the presence of an ethyl group. Also consistent with the integration of the ethyl hydrogen resonances, was a downfield uncoupled resonance at δ 6.91 integrating for ~ 1 H. Exact integration was not possible because the ethyl resonances were in a convoluted region of the spectrum. The observed ^1H NMR data are nearly identical to known 5-ethyltetraline and we therefore tentatively assign the structure of **10** as 5,6-dideutero-8-ethyl-tetraline.⁶ GC/MS of the reaction mixture showed a single chromatographic peak with a parent ion m/z of 162.3 consistent with the molecular formula of **10** and **11**. Based on the similarity in structure, it is reasonable to predict that these compounds have very similar retention times and could possibly come under the same peak in the GC/MS.

We also examined the role of the hydrogen atom donor, 1,4-CHD, by performing the reaction with and without this reagent at the same temperature (entries 2-3). Although the product was formed for the reaction without hydrogen atom donor, the rate of reaction and yield were much lower. Interestingly, ^1H NMR analysis of **5** obtained from entry 2, showed no incorporation of deuterium suggesting that the source of protio hydrogen may be from the substrate itself.

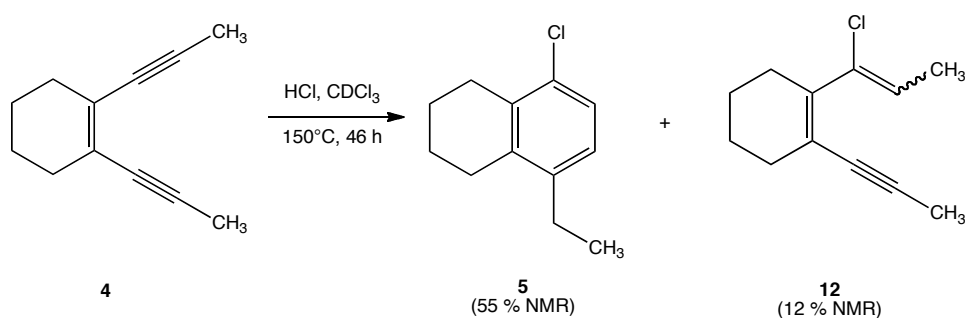
Table 4-1. Screening different reaction conditions to determine the role of solvent and hydrogen atom donor for the reaction of **4**. Conversion of **4** determined by ^1H NMR spectroscopy. Yields based on conversion of **4** and determined by ^1H NMR spectroscopy.



| Entry | conditions | Temp (°C) | time (h) | 4 % Conv. | 5 % Yield | 10 % Yield | 11 % Yield |
|-------|---------------------------|-----------|----------|------------------|------------------|-------------------|-------------------|
| 1 | THF- d_8 | 200 | 19 | 90 | - | 10 | 10 |
| 2 | CDCl_3 | 165 | 168 | 96 | 41 | - | 0 |
| 3 | CDCl_3 , 1,4-CHD | 165 | 26 | 97 | 69 | - | 0 |

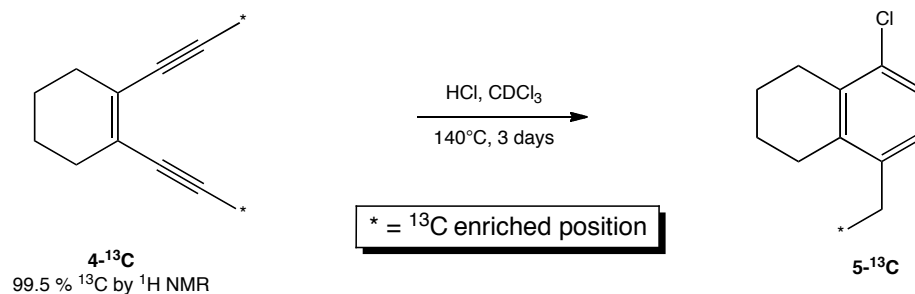
We also explored the possibility of promoting the cyclization with HCl. Indeed, when **4** was heated at 150°C for 46 h with ~ 0.5 eq. of HCl, formation of **5** was observed in 55% NMR yield with complete conversion of **4**. There was a great deal of baseline broadening in the aliphatic region of the ^1H NMR spectrum suggesting formation of soluble polymeric material that might explain the unaccounted mass balance. Accompanying the formation of **5**, was another compound (**12**) in 12% NMR yield that exhibited a downfield quartet resonance in the ^1H NMR spectrum at δ 5.72 ($J = 7$ Hz) along with an uncoupled resonance at δ 1.95 and a doublet at δ 1.62 ($J = 7$ Hz) integrating in a $\sim 1:3:3$ ratio, respectively. Based on these observed resonances, a vinyl chloride structure with unassigned alkene geometry was tentatively proposed for **12**. Treating **4** with HCl under identical conditions as the thermal reaction at ambient temperature resulted in no conversion of **4** after 24 h, but upon heating to 50°C , **12** was observed in 76% NMR yield (based on 9% conversion of **4**). The cyclized product **5** was not

observed at this temperature indicating formation of the addition product is faster than the cyclization.



Scheme 4-6. HCl promoted cycloaromatization of **4** and possible observation of addition product **12**.

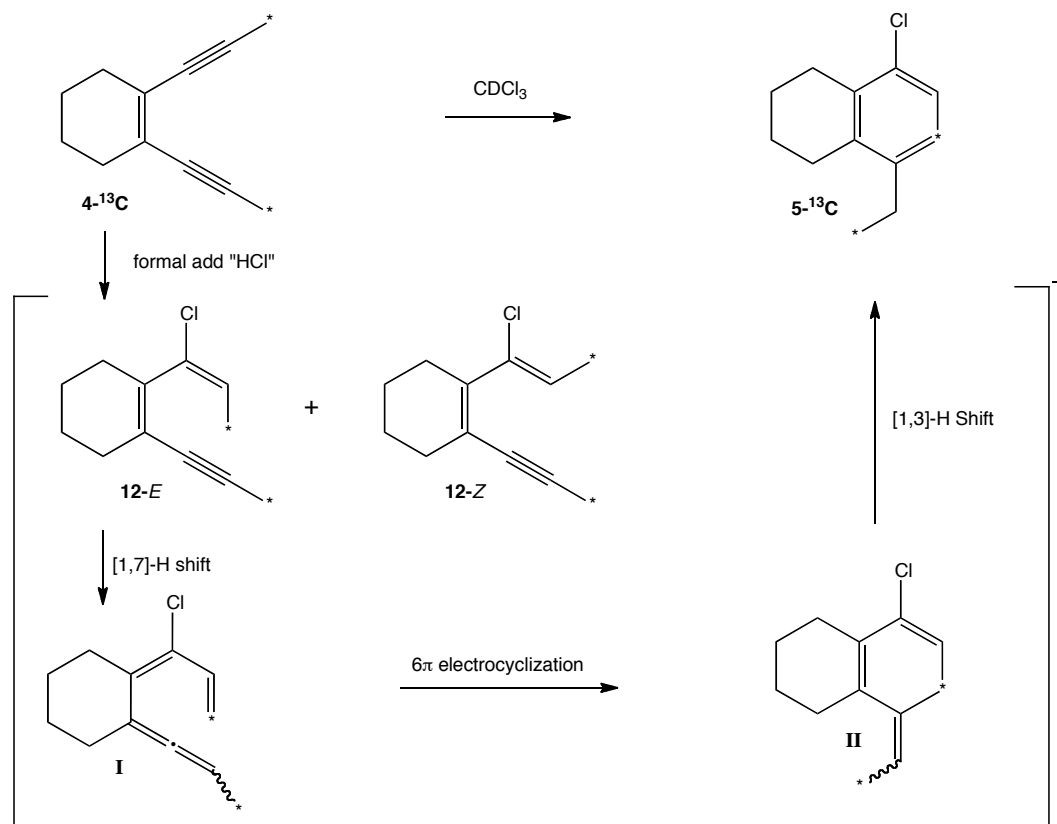
The most reasonable pathway for cyclization to **5** would involve bond formation between the propargylic methyl and internal alkyne carbon of the starting material **4**. To verify this connectivity, we prepared a ^{13}C -enriched sample of **4** using an identical synthetic route with $^{13}\text{CH}_3\text{I}$. The propargylic methyl groups of the enriched sample were determined to be $> 95\%$ ^{13}C by integration of the methyl doublet relative to the uncoupled residual ^{12}C methyl resonance at δ 2.02 in the ^1H NMR spectrum. Heating **4**- ^{13}C with HCl yielded a product with enrichment at δ 15.2 and 126.1 in the ^{13}C NMR spectrum, in excellent agreement with placement of the labeled carbons in **5**- ^{13}C (Scheme 4-7). Unfortunately, an NMR yield could not be obtained from this reaction due to baseline broadening in the ^1H NMR spectrum (possibly from polymerization) making it difficult to measure accurate integrals.



Scheme 4-7. ^{13}C labeling experiment demonstrating bond formation between the propargylic and internal alkyne carbon atoms.

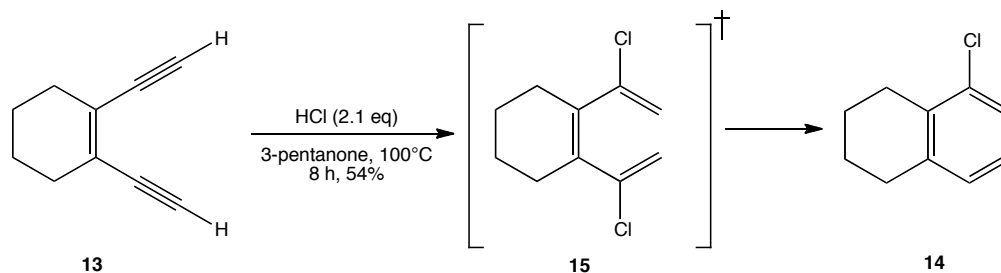
III. Discussion.

Shown in Scheme 4-8 is a proposed mechanism that would account for the formation of **5**. Formal addition of HCl across the alkyne would result in the formation of two possible geometric isomers, **12-E** and **12-Z**. If **12-E** is favored, then one could envision a [1,7]-shift of the allylic methyl hydrogen to give **I**. This pathway would seem unlikely for **12-Z** based on geometric grounds. From **I**, a 6π electrocyclization to give **II** followed by a formal [1,3]-hydrogen shift would lead to the observed product **5**, consistent with the ^{13}C labeling study.

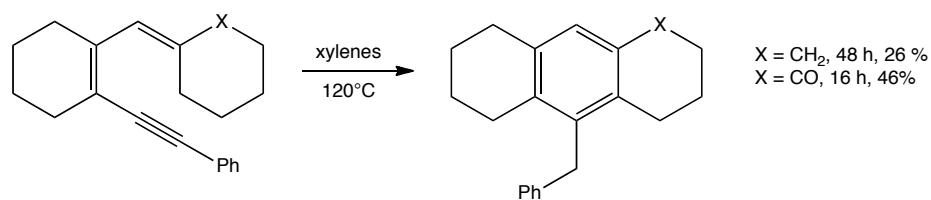


Scheme 4-8. Proposed mechanism for thermal cycloaromatization of enediyne **4** in CDCl_3 .

Liu and coworkers have shown HCl addition to 1,2-diethynylcyclohexene (**13**) ultimately results in cycloaromatization to give 5-chlorotetraline (**14**) presumably through the intermediacy of the double addition product **15** (Scheme 4-9).⁷ Interestingly, Liu did not try the reaction with enediynes containing internal alkynes (e.g. **4**). Pericyclic [1,7]-H shifts for dienynes are known.⁸ Most relevant to the current study was work done by Liu and coworkers that showed dienynes electronically similar to proposed intermediate **12** undergo cycloaromatization in xylenes at 120°C (Scheme 4-10).^{8b}

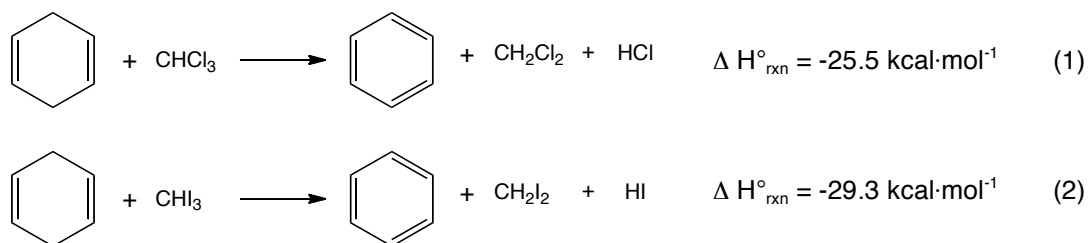


Scheme 4-9. Eneidyne cycloaromatization resulting from double HCl addition.⁷

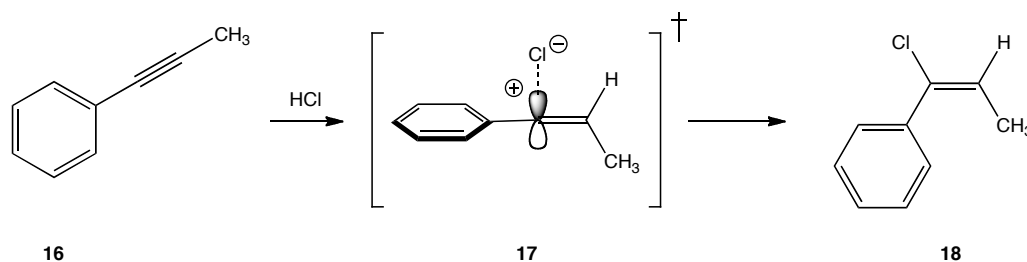


Scheme 4-10. Diene-yne cycloaromatization triggered by [1,7]-H shift.^{8b}

It has been demonstrated that direct addition of HCl to the reaction mixture triggers the cycloaromatization, but the rate enhancement with 1,4-CHD is more difficult to interpret. A significant mechanistic clue for the 1,4-CHD reactions was the observation of a multiplet centered at δ 5.30 in the ^1H NMR spectrum assigned to CH(D)Cl_2 , which forms in nearly equal yield to the aromatized product **5**. This species may result from the sequential abstraction of Cl from CDCl_3 then abstraction of hydrogen from 1,4-CHD, although it is not known what substrate derived species performs the initial homolysis. Although we are unsure to the mechanism of this pathway, another possibility being considered is the mildly exothermic generation of the electrophilic trigger, HCl, from the reaction of 1,4-CHD and CHCl_3 shown in equation 1.⁹ As a side note, a similar calculation for the reaction with CHI_3 showed the process to be more exothermic than the CHCl_3 reaction (equation 2) which suggests the process may be a general route for *in situ* generation of hydrogen halides.¹⁰



Preferential formation of the thermodynamically less stable **12-E** may not be intuitively obvious, but is well known in literature for electrophilic additions of HCl to alkynes.¹¹ As demonstrated with 1-phenylpropyne **16** (a commonly studied substrate for electrophilic alkyne additions), the intimate ion pair **17** formed subsequently after *syn*-protonation is inhibited from dissociation due to the low polarity of organic solvents commonly used for the reaction (Scheme 4-11).^{11d} Therefore, the overall addition of HCl gives the kinetic *syn* product **18**. Steric arguments between the *anti* substituent (CH₃ for **17**) and the nucleophile have also been used to explain the preference for the kinetic product.^{11c}



Scheme 4-11. Intimate ion-pair rationalization for preference of kinetic *syn* addition product formation.^{11d}

At this time, an exact proposed mechanism to account for the formation of the THF-*d*₈ derived product **10** (entry 1, Table 4-1) and formation of **5** from thermalysis in the absence of HCl or 1,4-CHD (entry 2, Table 4-1) is unknown, but we tend to favor a pathway involving a

dienyne intermediate (e.g. **12**) as shown in Scheme 4-8 and feel that this intermediate is most likely formed through radical species.

IV. Conclusions and Future Outlook.

In conclusion, we have uncovered a novel route of cycloaromatization for enediynes resulting from thermalysis in CDCl_3 . The product results from bond formation between the propargylic and internal alkyne carbons of the substrate and incorporation of chlorine in the aromatic ring. The reaction was found to be accelerated by use of 1,4-cyclohexadiene, a hydrogen atom donor, and HCl, a Brønsted acid. Although uncharacterized, preliminary experiments in $\text{THF-}d_6$ have provided some evidence for the formation of a similar product in low yield suggesting that the reaction may be general to other solvents as well. Our current mechanistic hypothesis involves formal addition of HCl to form a dienyne structure that then proceeds through a cascade of pericyclic reactions to ultimately give the aromatic product. Current work is being directed at studying the substrate scope and mechanism of this novel transformation. We are particularly interested in independent chemical synthesis and characterization of both geometric isomers of proposed intermediate dienyne **12**. While spectroscopic evidence has been obtained to support the formation of one of the isomers, examining the rate of cyclization of each isolated dienyne under the reaction conditions used for the cyclization will provide stronger support for these species' role as intermediates.

V. Experimental.

i. General Procedures.

All reactions directed toward the synthesis of organic substrates for cycloaromatizations were performed in round bottom flasks equipped with magnetic teflon coated stir bars and rubber septa under a positive pressure of N₂, unless otherwise noted. NMR scale ruthenium cyclization reactions were performed under a N₂ atmosphere in 5 mm J-young NMR tubes equipped with a teflon needle valve using freshly degassed solvents (freeze / pump / thaw procedure). Solutions of air- and moisture-sensitive reagents were transferred by syringe or stainless steel cannula. Air and moisture sensitive solids were handled in a glove box under a N₂ atmosphere. Organic solvent solutions were concentrated by rotary evaporation (ca. 10 – 160 torr) at 25 - 35°C, unless otherwise noted. High vacuum distillations were performed at 23°C (ca. 0.010 torr) using a receiver flask cooled to -75°C. Preparative thin layer chromatography (PTLC) was performed on glass plates pre-coated with silica gel (1 mm, 60 Å pore size, EMD Chemicals) and visualized by exposure with ultraviolet light. Flash column chromatography purification of synthetic intermediates and substrates was performed by literature procedure¹² using silica gel (60 Å, particle size 0.043 – 0.060 mm, EMD Chemicals) or activated neutral Brockmann I standard grade aluminum oxide (150 mesh, Sigma-Aldrich).

ii. Materials.

Tetrahydrofuran (THF), ethyl ether and hexanes used for reaction solvents were dried either by a solvent dispensing system equipped with two neutral alumina columns under argon atmosphere, over sodium/benzophenone ketyl under a N₂ atmosphere, or by 3 Å activated sieves by literature procedure.¹³ Chloroform-*d* was dried over calcium hydride under a nitrogen

atmosphere or by 3 Å activated sieves by literature procedure.¹³ Acetone-*d*₆ was dried over 4 Å activated sieves for 5 h under a N₂ atmosphere. Tetrahydrofuran-*d*₈ (THF-*d*₈) was dried over sodium/benzophenone ketyl under a N₂ atmosphere. All other solvents were used as received from commercial suppliers. [Cp*Ru(NCMe)₃]PF₆ (**7**) was prepared according to literature procedure.⁵ All other literature compounds were prepared according to the indicated reference or purchased from commercial suppliers and used as received.

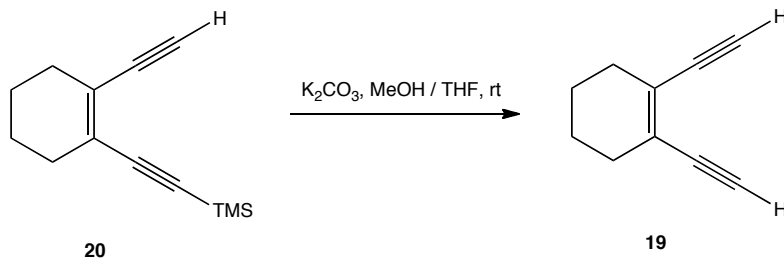
iii. Instrumentation.

NMR spectra were recorded on a Varian Mercury 300 (¹H, 300 MHz; ¹³C 75.5 MHz), Varian Mercury 400 (¹H, 400 MHz; ¹³C 100.7 MHz), Jeol ECA 500 (¹H, 500 MHz) or Varian VX 500 (¹H, 500 MHz; ¹³C 125 MHz) spectrometer. ¹H and ¹³C NMR chemical shifts (δ) are reported in parts per million (ppm). ¹H NMR chemical shifts were referenced to the residual protio resonance for CDCl₃ (δ 7.26). ¹³C NMR chemical shifts were referenced to CDCl₃ (δ 77.16). Infrared (IR) spectra were recorded on a Nicolet Avatar 360 FT-IR with KBr or NaCl plates (thin film) or JASCO FT-IR 4100 attenuated total reflectance (ATR) platform (3mm) ZnSe plate (thin film). High-resolution mass spectra were obtained by the University of California, San Diego Mass Spectrometry Facility. Melting points are uncorrected and were recorded on an Electrothermal or Standford Research Systems EZ-Melt apparatus.

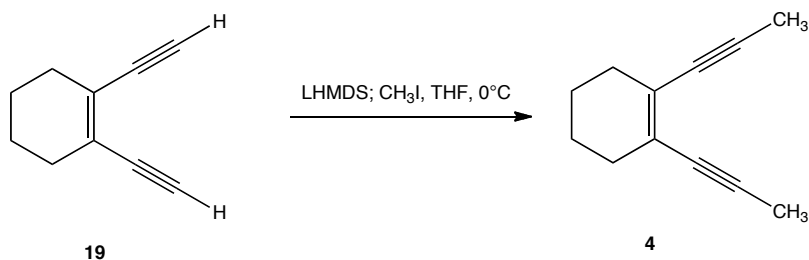
iv. Preparation and characterization data for synthetic intermediates and enediyne substrates.

1,2-Diethynylcyclohex-1-ene (19). Anhydrous K₂CO₃ (659 mg, 4.76 mmol) was added to a stirring solution of **20**¹⁴ (308 mg, 1.52 mmol) in THF / MeOH (14 mL, 1:1) at 23°C. After stirring at 23°C for 1 h, the reaction mixture was diluted with water (50 mL) and extracted with pentane

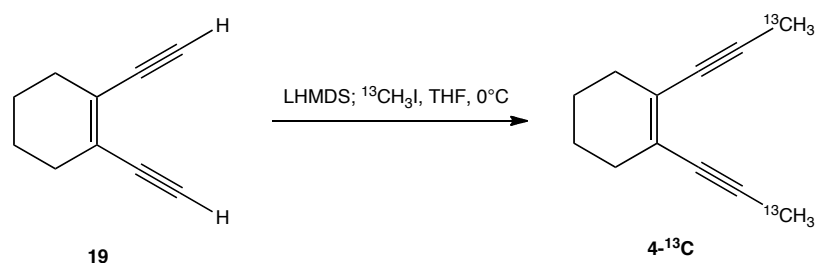
(3 x 50 mL). The organic extract was dried over MgSO_4 , concentrated, and purified by flash silica column chromatography (pentane) to afford **19** as a yellow oil (182 mg, 1.398 mmol, 92%). The product exhibited spectroscopic properties identical to those reported in literature.¹⁵



1,2-Di(prop-1-yn-1-yl)cyclohex-1-ene (4). A 1 M solution of LHMDS (3.00 mL, 3.00 mmol) in THF was added to a stirring solution of **19** (100 mg, 0.768 mmol) in THF (7.8 mL) at 0°C. After stirring at 0°C for 20 min, iodomethane (0.300 mL, 4.81 mmol) was added. After stirring for 4 h while slowly warming to 23°C, the reaction was poured over sat. aq. NH_4Cl (20 mL) and extracted with hexanes (2 x 20 mL). The organics extracts were successively washed with water (20 mL) / brine (20 mL), dried over MgSO_4 , concentrated, and purified by flash silica column chromatography (hexanes) to afford **4** as a yellow solid upon cooling to -20°C (108 mg, 0.683 mmol, 89%). mp: 31-34°C. ^1H NMR (400 MHz, CDCl_3) δ : 1.53 – 1.62 (m, 4H, 4,5- CH_2), 2.03 (s, 6H, CH_3), 2.12 – 2.21 (m, 4H, 3,6- CH_2). ^{13}C NMR (75 MHz, CDCl_3) δ : 4.79 (CH_3), 22.1 (4,5- CH_2), 30.4 (3,6- CH_2), 80.6 ($\text{C}\equiv\text{C}$), 89.4 ($\text{C}\equiv\text{C}$), 125.1 ($\text{C}=\text{C}$). HRMS (EI): Calcd for ($\text{C}_{12}\text{H}_{14}$): 158.1090, found 158.1088.



1,2-Di(3-¹³C-prop-1-yn-1-yl)cyclohex-1-ene (4-¹³C). A 1 M solution of LHMDS (4.82 mL, 4.82 mmol) in THF was added to a stirring solution of **19** (126 mg, 0.964 mmol) in THF (10 mL) at 0°C. After stirring at 0°C for 20 min, 99% ¹³C-iodomethane (0.361 mL, 5.78 mmol) was added. After stirring for 4 h while slowly warming to 23°C, the reaction was poured over sat. aq. NH₄Cl (30 mL) and extracted with hexanes (2 x 30 mL). The organics extracts were successively washed with water (30 mL) / brine (30 mL), dried over MgSO₄, concentrated, and purified by flash silica column chromatography (hexanes) to afford **4-¹³C** as a yellow solid upon cooling to -20°C (78 mg, 0.487 mmol, 51%). ¹H NMR (400 MHz, CDCl₃) δ: 1.53 – 1.62 (m, 4H, 4,5-CH₂), 2.03 (d, ¹J_{CH} = 131 Hz, 6H, ¹³CH₃), 2.12 – 2.21 (m, 4H, 3,6-CH₂). HRMS (EI): Calcd for (C-₁₀¹³C₂H₁₄): 160.1157, found 160.1159.



v. Procedures for NMR scale reactions.

General procedure enediyne cyclizations. A mixture of enediyne, 1,3,5-tri-*tert*-butylbenzene (0.5 – 1 mg), and acid / H-atom donor (if applicable) in indicated solvent were degassed (3x freeze / pump / thaw) and flame sealed in a Wilmad 504-PP or Wilmad 522-PP NMR tube under 0.010 torr vacuum. The contents were then heated at indicated temperature.

Reaction of 4 in CDCl₃ / 1,4-CHD @ 190°C. **4** (2.5 mg, 0.0158 mmol), 1,4-CHD (0.011 mL, 0.111 mmol), CDCl₃ (0.233 mL), 190°C.

Reaction of 4 in CDCl₃ / 1,4-CHD @ 165°C. **4** (5.5 mg, 0.035 mmol), 1,4-CHD (0.023 mL, 0.243 mmol), CDCl₃ (0.307 mL), 165°C.

Reaction of 4 in CDCl₃. **4** (2.8 mg, 0.018 mmol), CDCl₃ (0.281 mL), 165°C.

Reaction of 4 in THF-*d*₆. **4** (2 mg, 0.013 mmol), THF-*d*₆ (0.227 mL), 200°C.

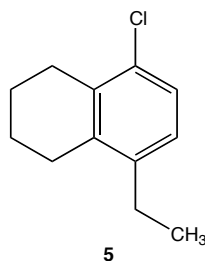
Reaction of 4 with HCl. **4** (9.0 mg, 0.0569 mmol), 12 M HCl (0.002 mL, 0.0284 mmol), CDCl₃ (0.450 mL), 150°C.

Reaction of 4-¹³C. **4-¹³C** (7.8 mg, 0.0487 mmol), 12 M HCl (0.010 mL, 0.142 mmol), CDCl₃ (0.250 mL), 140°C.

Reaction of 4 with 7. **7** (6 mg, 0.012 mmol) was added to a J-young tube containing a solution of **4** (1.7 mg, 0.011 mmol), 1,4-CHD (0.012 mL, 0.129 mmol) and 1,3,5-tri-*tert*-butylbenzene (1.5 mg) in CDCl₃ (0.78 mL) at 23°C in glove box.

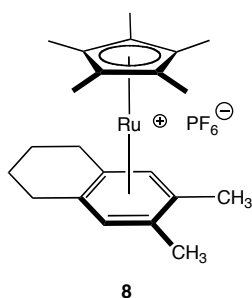
vi. Preparation and characterization data for cycloaromatized products.

5-Chloro-8-ethyl-tetraline (5). After 68 h at 150°C, the NMR scale reaction mixture of **4** with HCl was diluted CH₂Cl₂ (2 mL) and extracted with sat. aq. NaHCO₃ (2 x 2 mL). The aqueous phase was backwashed with CH₂Cl₂ (4 mL) and the combined organic extracts were washed with brine (4 mL), dried over MgSO₄, concentrated, and successively purified by silica column chromatography (5.75 inch glass pipette, hexanes) then high vacuum distillation to afford **5** as a colorless oil. ¹H NMR (400 MHz, CDCl₃) δ: 1.18 (t, ³J_{HH} = 7.5 Hz, 3H, CH₂CH₃), 1.74 – 1.83 (m, 4H, 2,3-CH₂), 2.56 (q, ³J_{HH} = 7.5 Hz, 2H, CH₂CH₃), 2.65 – 2.81 (m, 4H, 1,4-CH₂), 6.94 (d, ³J_{HH} = 8.0 Hz, 1H, 7-ArH), 7.15 (d, ³J_{HH} = 8.0 Hz, 1H, 6-ArH). ¹³C NMR (100 MHz, CDCl₃) δ: 14.5 (CH₃), 22.7 (CH₂), 22.8 (CH₂), 25.5 (ArCH₂), 26.7 (ArCH₂), 28.0 (ArCH₂), 126.1 (CH=CH), 126.2 (CH=CH), 132.3 (C=C), 134.8 (C=C), 137.3 (C=C), 140.9 (C=C).



(η^5 -Pentamethylcyclopentadienyl)(η^6 -6,7-dimethyl-tetralinyl)ruthenium (II)

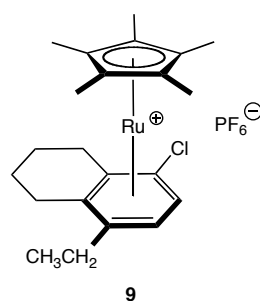
hexafluorophosphate (8). **7** (30 mg, 0.059 mmol) was added to a solution of **4** (10 mg, 0.065 mmol) in THF (1 mL) at 23°C in glove box. After 14 h at 23°C, the reaction mixture was concentrated, dissolved in minimum amount of CH₂Cl₂, and a brown solid was precipitated by addition of Et₂O. The resulting solid was purified by flash alumina column chromatography (2:8 then 7:3 EtOAc / hexanes) followed by crystallization (CH₂Cl₂ : ethyl ether) to afford **8** as a colorless solid. decomp. 260°C. ¹H NMR (400 MHz, CDCl₃) δ : 1.60 – 1.86 (m, 4H, 2,3-CH₂), 1.79 (s, 15H, Cp*), 2.08 (s, 6H, ArCH₃), 2.32 – 2.43 (m, 2H, 1,4-CH^{syn}), 2.66 – 2.77 (m, 2H, 1,4-CH^{anti}), 5.53 (s, 2H, ArH). ¹³C NMR (100 MHz, CDCl₃) δ : 9.8 (CpCH₃), 16.2 (ArCH₃), 21.8 (2,3-CH₂), 25.6 (1,4-CH₂), 89.2 (CpCH₃), 93.5 (C^{Ar}H), 98.6 (C^{Ar}), 101.1 (C^{Ar}). Anal. Calcd for C₂₂H₃₁F₆PRu: C, 48.80; H, 5.77. Found: C, 48.80; H, 5.61.



(η^5 -Pentamethylcyclopentadienyl)(η^6 -5-chloro-8-ethyl-tetralinyl)ruthenium (II)

hexafluorophosphate (9). **7** (14 mg, 0.028 mmol) was added to a solution of **4** (3.6 mg, 0.019 mmol) and 1,3,5-tri-*tert*-butylbenzene (0.5 – 1 mg) in acetone-*d*₆ (0.68 mL) at 23°C in glove box.

After 14 h at 23°C, the reaction mixture was concentrated and purified by flash alumina column chromatography (2:8 then 7:3 EtOAc / hexanes) followed by crystallization (CH₂Cl₂ : ethyl ether) to afford **9** as a colorless solid. decomp. 205 - 215°C. ¹H NMR (400 MHz, CDCl₃) δ: 1.24 (t, ³J_{HH} = 7.5 Hz, 3H, CH₂CH₃), 1.66 – 1.95 (m, 4H, 2,3-CH₂), 1.81 (s, 15H, Cp*), 2.23 (dq, ²J_{HH} = 14.6 Hz, ³J_{HH} = 7.5 Hz, 1H, C(H')HCH₃), 2.34 – 2.53 (m, 2H, 1,4-CH^{syn}), 2.39 (dq, ²J_{HH} = 14.6 Hz, ³J_{HH} = 7.5 Hz, 1H, C(H')HCH₃), 2.62 – 2.80 (m, 2H, 1,4-CH^{anti}), 5.92 (d, ³J_{HH} = 6.0 Hz, 1H, 7-ArH), 5.99 (d, ³J_{HH} = 6.0 Hz, 1H, 6-ArH). ¹³C NMR (100 MHz, CDCl₃) δ: 9.6 (CpCH₃), 14.0 (CH₂CH₃), 21.4 (2/3-CH₂), 21.5 (2/3-CH₂), 23.7 (1/4-CH₂), 24.0 (1/4-CH₂), 25.5 (CH₂CH₃), 87.9 (C^{Ar}H), 88.9 (C^{Ar}H), 95.3 (CpCH₃), 100.0 (C^{Ar}), 100.3 (C^{Ar}), 103.9 (C^{Ar}), 104.3 (C^{Ar}). Anal. Calcd for C₂₂H₃₀ClF₆PRu: C, 45.88; H, 5.25. Found: C, 45.85; H, 4.90.



vii. ¹H and ¹³C NMR spectra for unknown compounds.

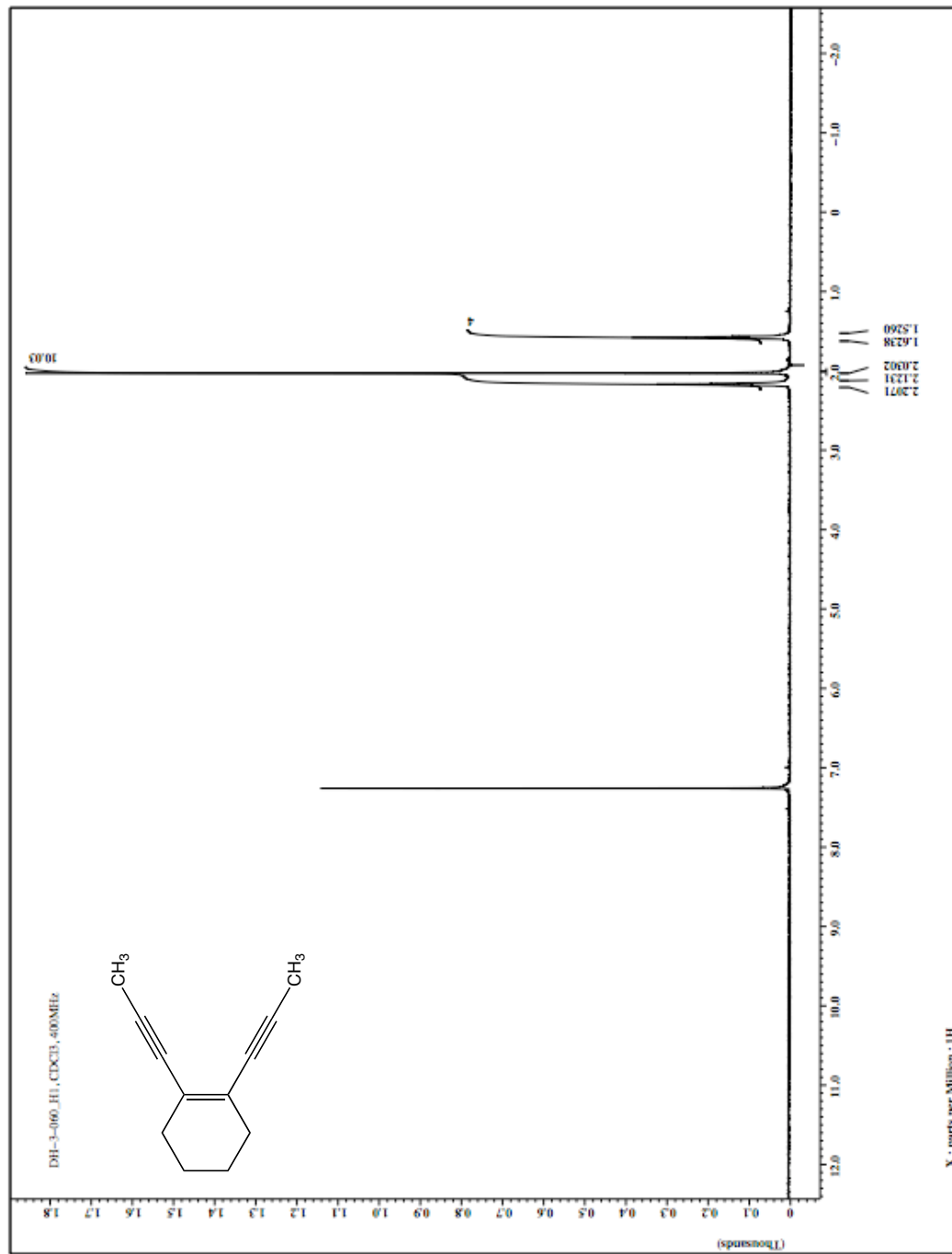


Figure 4-1. 4 ^1H NMR spectrum (CDCl_3 , 400 MHz).

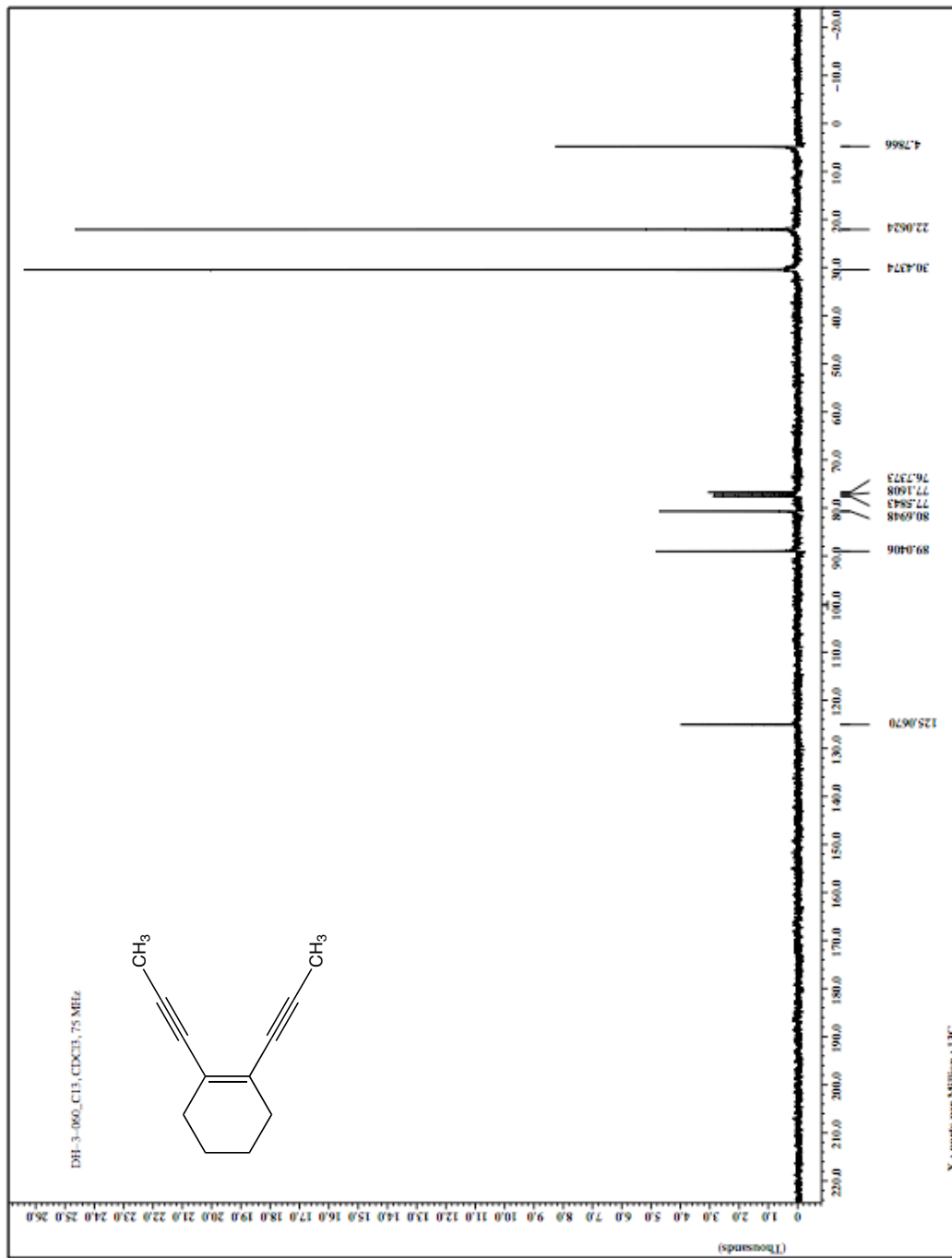


Figure 4-2. 4 ^{13}C NMR spectrum (CDCl_3 , 75 MHz).

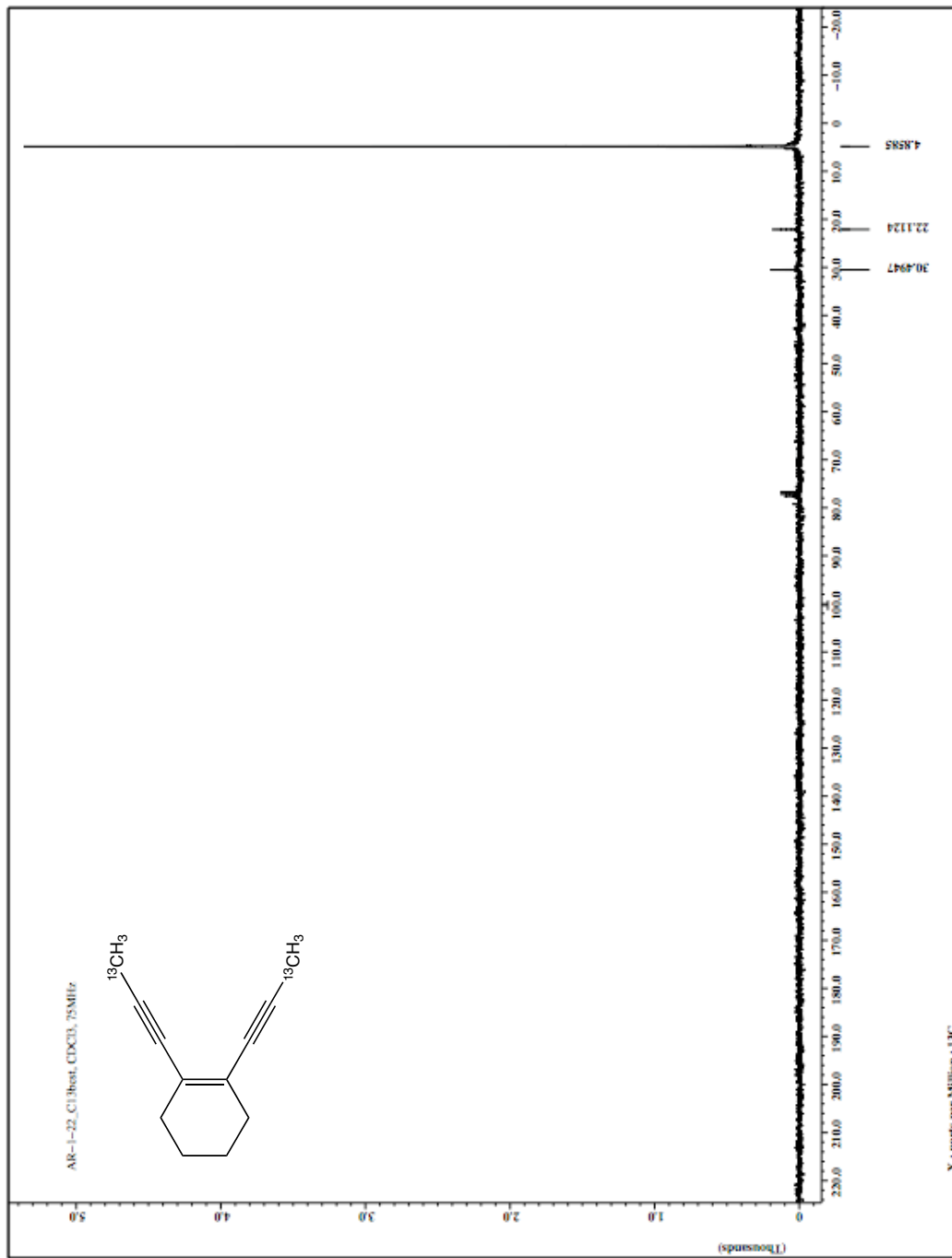


Figure 4-4. 4-¹³C ¹³C NMR spectrum (CDCl₃, 75 MHz).

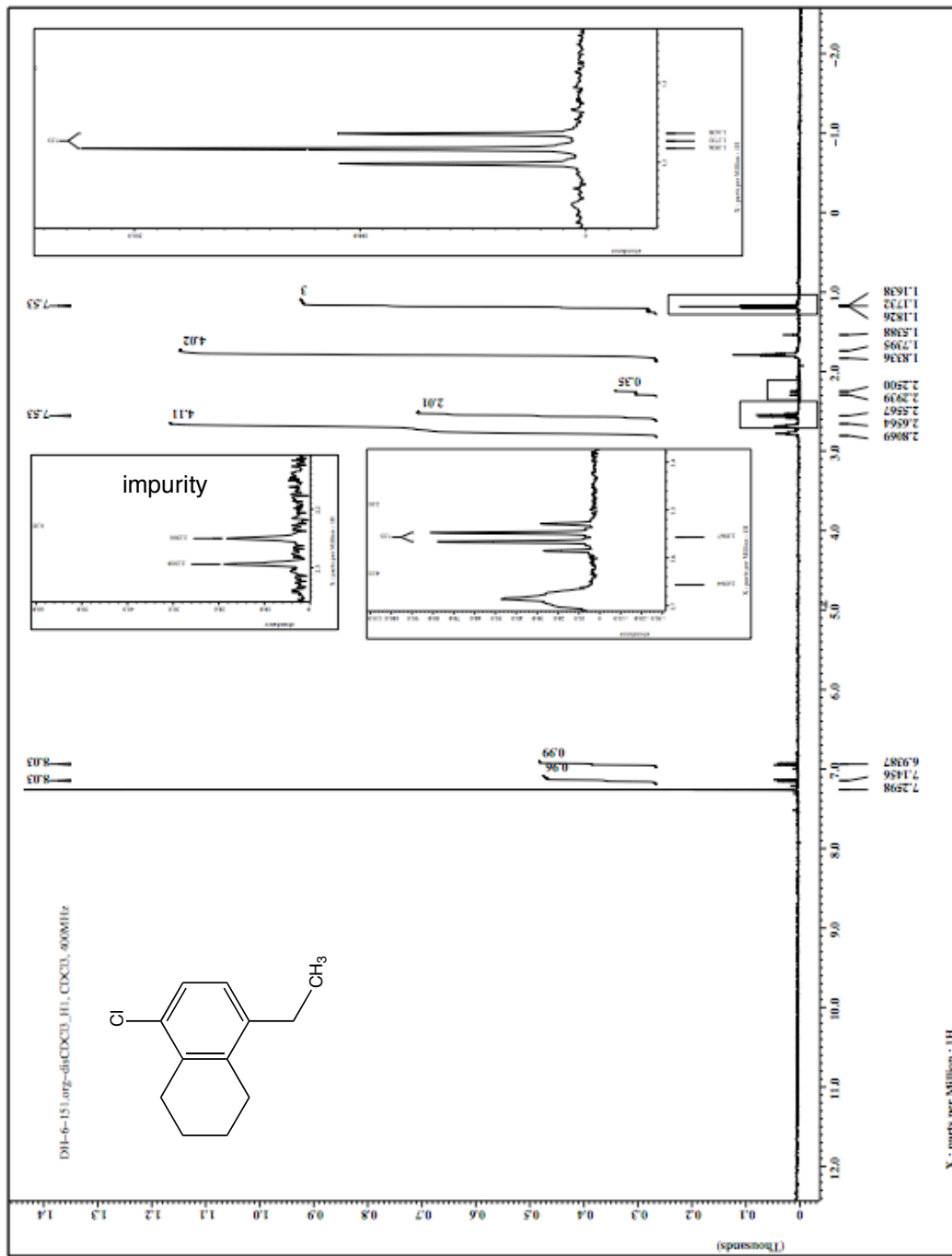


Figure 4-5. ^1H NMR spectrum (CDCl_3 , 400 MHz).

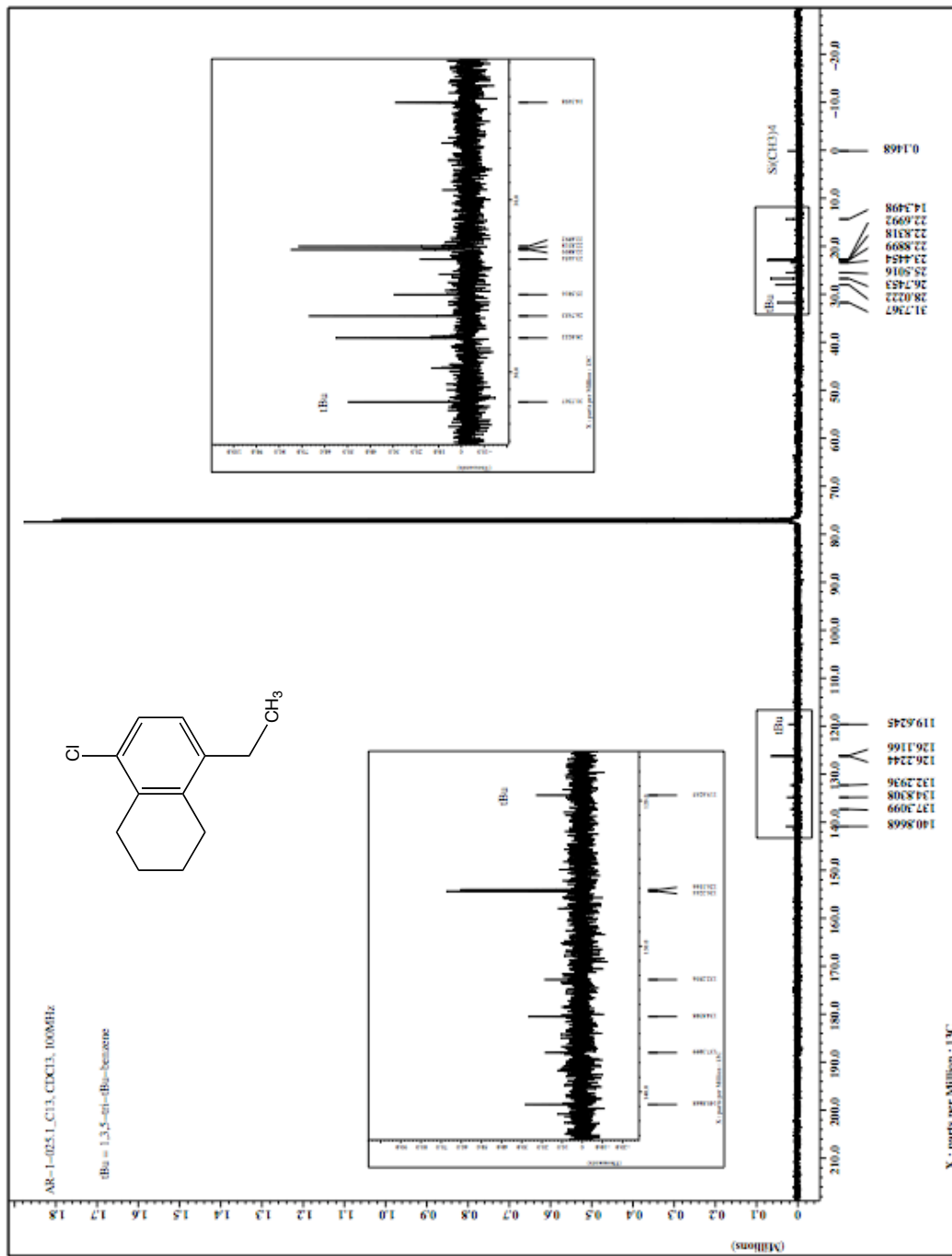


Figure 4-6. 5 ¹³C NMR spectrum (CDCl₃, 100 MHz).

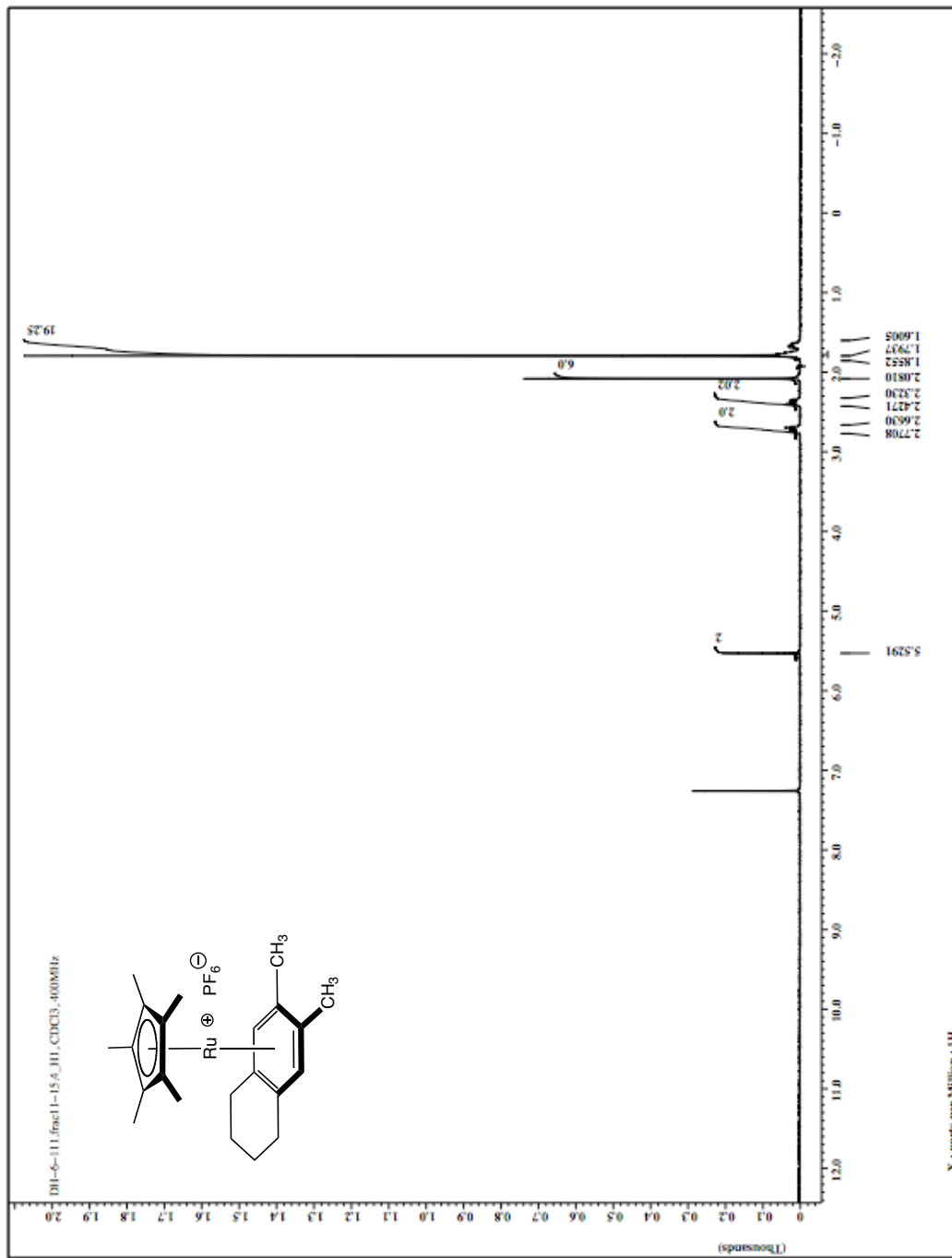


Figure 4-7. 8 ^1H NMR spectrum (CDCl_3 , 400 MHz).

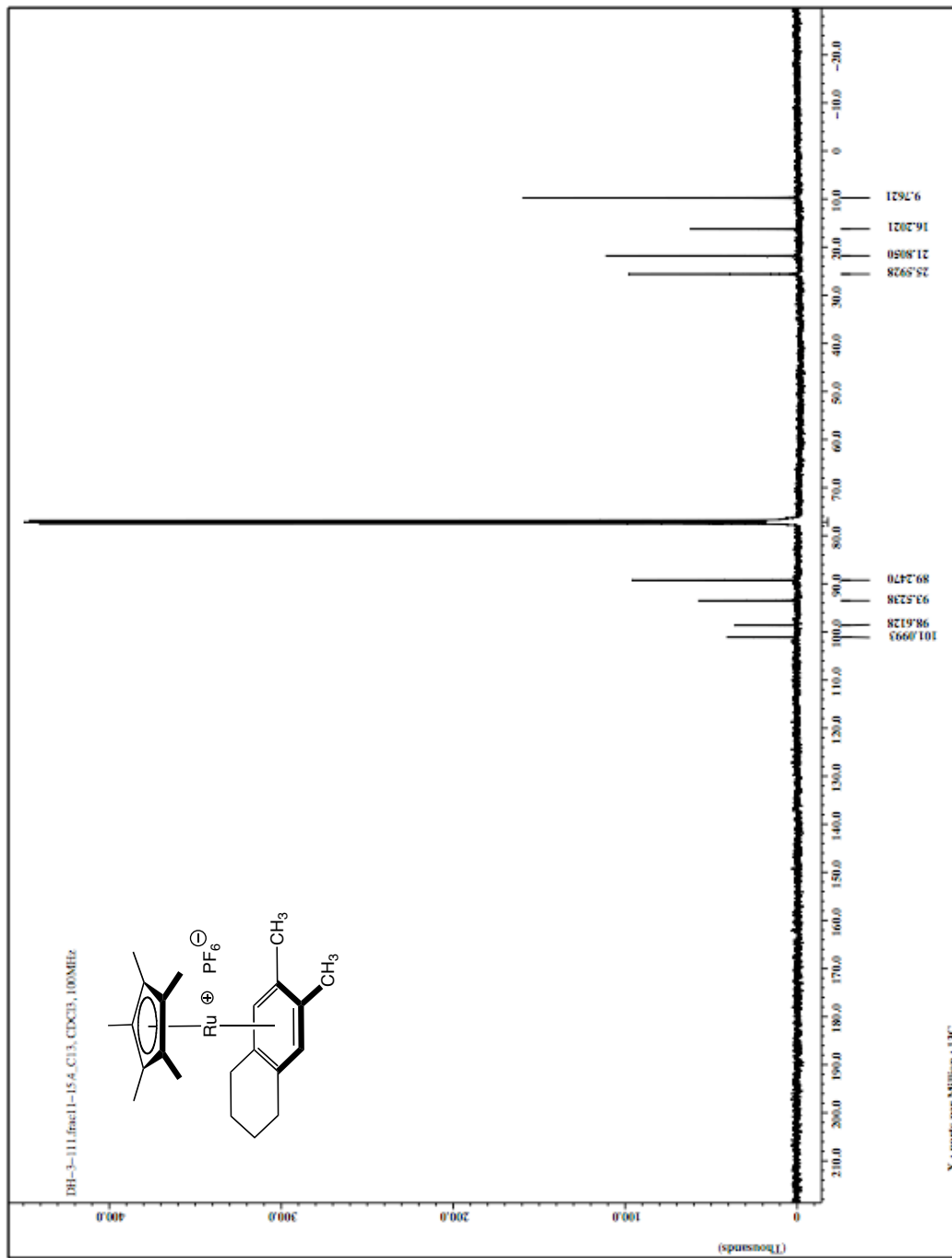


Figure 4-8. 8 ¹³C NMR spectrum (CDCl₃, 100 MHz).

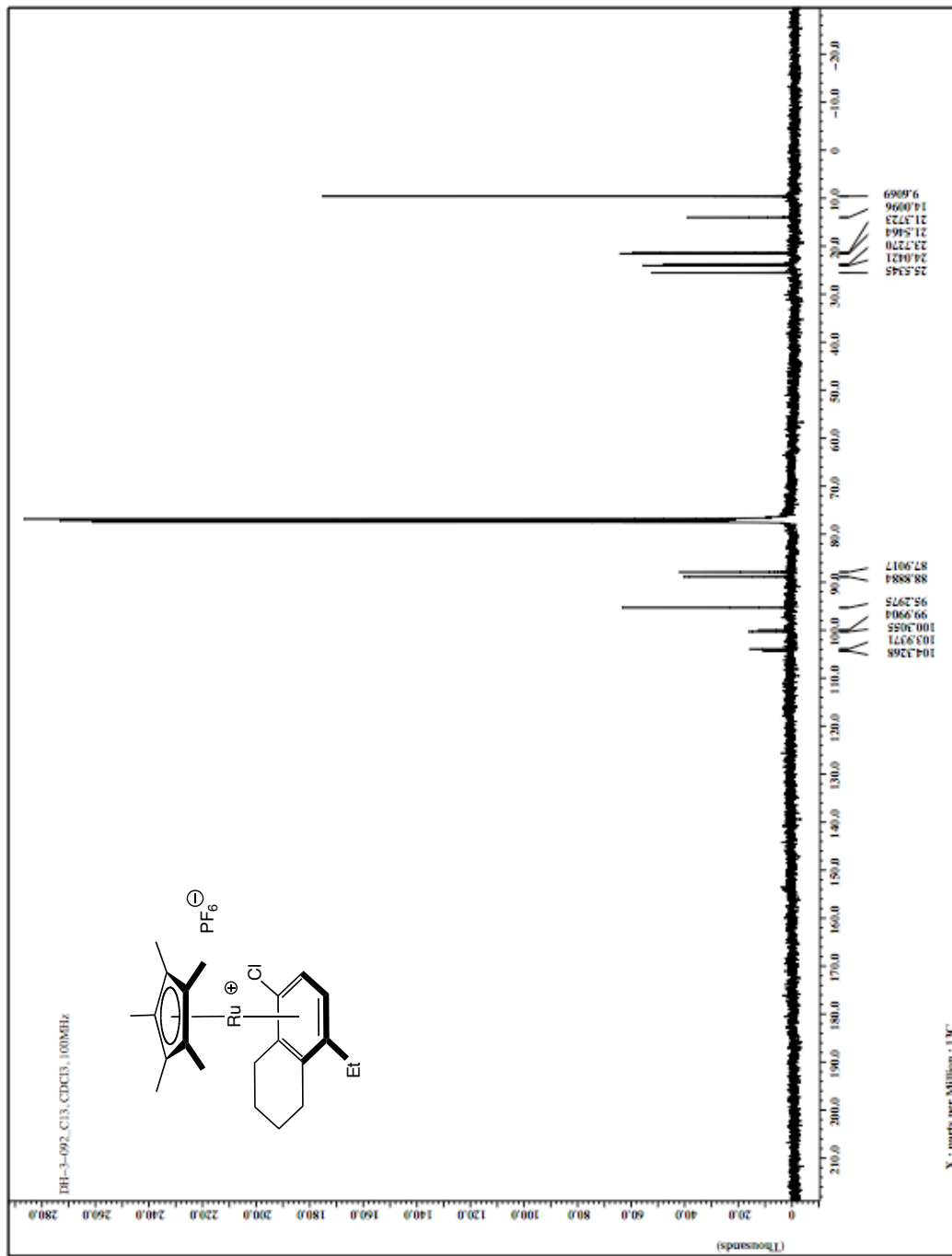


Figure 4-10. **9** ^{13}C NMR spectrum (CDCl_3 , 100 MHz).

viii. X-ray crystallographic summary and ORTEPS for characterized structures

General Experimental for X-Ray Structure Determinations.

A single crystal with general dimensions of $a \times b \times c$ was immersed in Paratone and placed on a Cryoloop. Data were collected on a Bruker SMART (APEX) CCD diffractometer, using a graphite monochromator with Mo or Cu $K\alpha$ radiation ($\lambda = 0.71073$ or 1.54178 \AA) at the defined temperature. The data were integrated using the Bruker SAINT software program and scaled using the SADABS software program. Solution by direct methods (SIR-2004) produced a complete heavy-atom phasing model consistent with the proposed structure. All non-hydrogen atoms were refined anisotropically by full-matrix leastsquares (SHELXL-97). All hydrogen atoms were placed using a riding model. Their positions were constrained relative to their parent atom using the appropriate HFIX command in SHELXL-97.

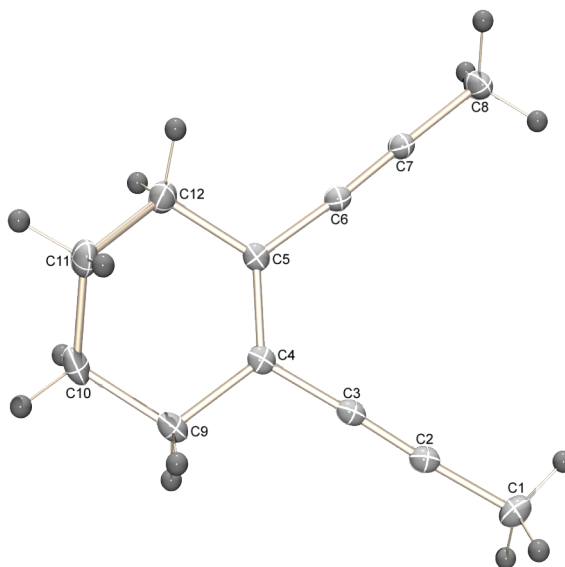


Figure 4-11. ORTEP of **4**. Ellipsoids shown at 30% probability.

Table 4-2. Crystal data and structure refinement for **4**.

Identification code

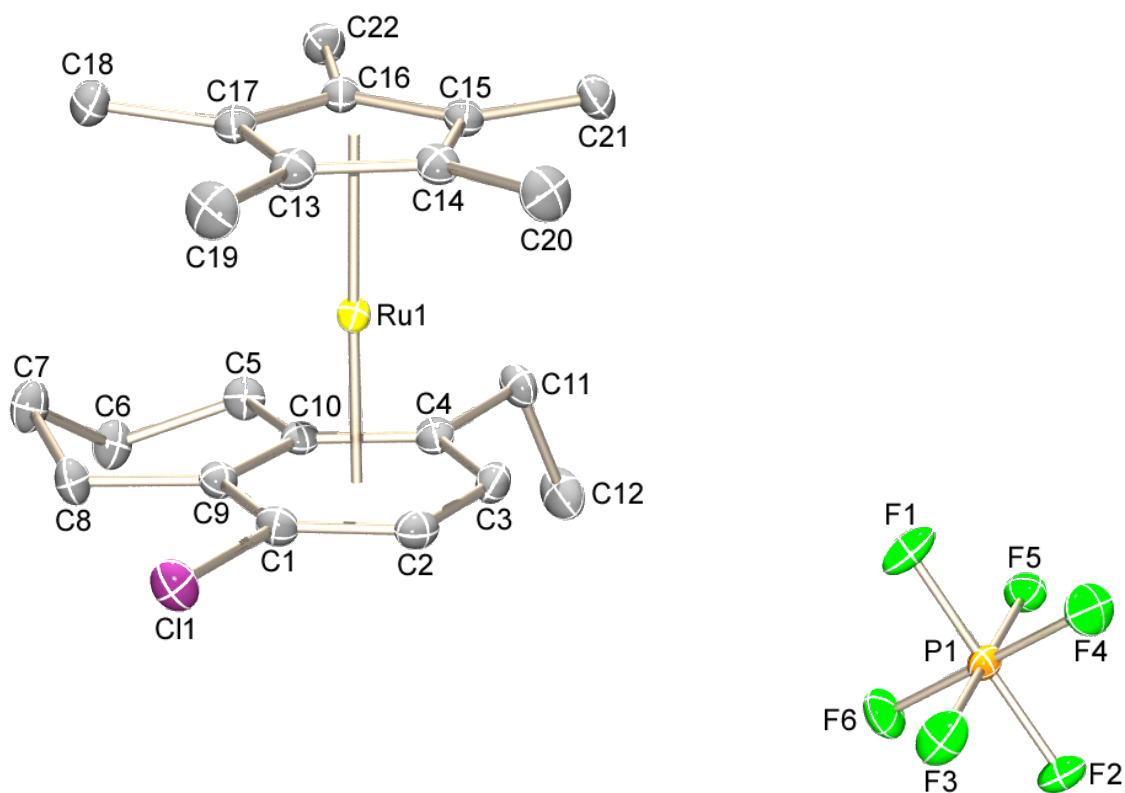
dh3089

Table 4-2. Crystal data and structure refinement for **4**. (*continued*)

| | | |
|-----------------------------------|---|-----------------|
| Empirical formula | C ₁₂ H ₁₄ | |
| Formula weight | 158.23 | |
| Temperature | 90(2) K | |
| Wavelength | 1.54178 Å | |
| Crystal system | Monoclinic | |
| Space group | C c | |
| Unit cell dimensions | a = 7.5706(7) Å | α = 90°. |
| | b = 12.0673(9) Å | β = 91.117(5)°. |
| | c = 10.5905(8) Å | γ = 90°. |
| Volume | 967.33(14) Å ³ | |
| Z | 4 | |
| Density (calculated) | 1.086 Mg/m ³ | |
| Absorption coefficient | 0.450 mm ⁻¹ | |
| F(000) | 344 | |
| Crystal size | 0.25 x 0.20 x 0.10 mm ³ | |
| Theta range for data collection | 6.90 to 68.29°. | |
| Index ranges | -8 ≤ h ≤ 9, -14 ≤ k ≤ 14, -12 ≤ l ≤ 12 | |
| Reflections collected | 3231 | |
| Independent reflections | 1245 [R(int) = 0.0097] | |
| Completeness to theta = 67.00° | 98.6 % | |
| Absorption correction | Semi-empirical from equivalents | |
| Max. and min. transmission | 0.9564 and 0.8958 | |
| Refinement method | Full-matrix least-squares on F ² | |
| Data / restraints / parameters | 1245 / 2 / 120 | |
| Goodness-of-fit on F ² | 1.060 | |

Table 4-2. Crystal data and structure refinement for **4**. (*continued*)

| | |
|--------------------------------------|------------------------------------|
| Final R indices [$I > 2\sigma(I)$] | R1 = 0.0272, wR2 = 0.0765 |
| R indices (all data) | R1 = 0.0275, wR2 = 0.0767 |
| Absolute structure parameter | 1.0(18) |
| Largest diff. peak and hole | 0.105 and -0.125 e.Å ⁻³ |

**Figure 4-12.** ORTEP of **9**. Ellipsoids shown at 30% probability. Hydrogen atoms omitted for clarity.**Table 4-3.** Crystal data and structure refinement for **9**.

| | |
|---------------------|--------------------|
| Identification code | dh3092 |
| Empirical formula | C22 H30 Cl F6 P Ru |
| Formula weight | 575.95 |

Table 4-3. Crystal data and structure refinement for **9**. (*continued*)

| | | |
|-----------------------------------|---|-------------------------------|
| Temperature | 100(2) K | |
| Wavelength | 0.71073 Å | |
| Crystal system | Monoclinic | |
| Space group | P 21/c | |
| Unit cell dimensions | a = 8.9350(6) Å | $\alpha = 90^\circ$. |
| | b = 14.4160(9) Å | $\beta = 93.2770(10)^\circ$. |
| | c = 17.5090(11) Å | $\gamma = 90^\circ$. |
| Volume | 2251.6(3) Å ³ | |
| Z | 4 | |
| Density (calculated) | 1.699 Mg/m ³ | |
| Absorption coefficient | 0.943 mm ⁻¹ | |
| F(000) | 1168 | |
| Crystal size | 0.50 x 0.25 x 0.10 mm ³ | |
| Theta range for data collection | 1.83 to 28.13°. | |
| Index ranges | -11 ≤ h ≤ 11, -18 ≤ k ≤ 18, -23 ≤ l ≤ 23 | |
| Reflections collected | 45885 | |
| Independent reflections | 5221 [R(int) = 0.0307] | |
| Completeness to theta = 25.00° | 100.0 % | |
| Absorption correction | Semi-empirical from equivalents | |
| Max. and min. transmission | 0.9116 and 0.6499 | |
| Refinement method | Full-matrix least-squares on F ² | |
| Data / restraints / parameters | 5221 / 0 / 286 | |
| Goodness-of-fit on F ² | 1.033 | |
| Final R indices [I > 2σ(I)] | R1 = 0.0236, wR2 = 0.0526 | |
| R indices (all data) | R1 = 0.0313, wR2 = 0.0565 | |

14. See Chapter 3, Section IX.
15. Odedra, A.; Wu, C-J.; Pratap, T.B.; Huang, C-W.; Ran, Y-F.; Liu, R-S. *J. Am. Chem. Soc.* **2005**, *127*, 3406.)

VII. Acknowledgements.

The material of Chapter 4, in part, is currently being prepared for submission for publication with the following authors: Hitt, D.M.; Raub, A.G.; O'Connor, J.M. The dissertation author was the primary investigator and author of this material.